THE APPLICATION OF HIGH POWER LASERS TO THE WELDING OF TEE SECTION JOINTS IN SHIP PRODUCTION

Volume II

Stephen John BROOKE, B.Sc.

Department of Naval Architecture and Shipbuilding
May 1987

University of Newcastle upon Tyne
Newcastle upon Tyne NE1 7RU

Thesis submitted for the degree of Doctor of Philosophy
Prepared in two volumes

CONTENTS

Volume I

Volume II

PAGE NUMBERING AS ORIGINAL

CHAPTER FIVE

WELD CLASSIFICATION - MECHANICAL TESTING

5.1 THE REQUIREMENTS SET BY CLASSIFICATION SOCIETIES

Virtually all ships are designed and constructed to rules set by a particular classification society or authoritative organisation, thus assuring the owner of a particular quality of design, materials and equipment used and workmanship. If any process or procedure used in the construction is changed, the new method must produce a product that is either of comparable or superior quality to the "conventional" product already accepted by the classification society.

Occasionally a change will be so radical that existing classification specifications are unable to accommodate the new process. In order for the procedural acceptance to be gained the properties of the new process must be compared against reliable source data for the conventional processes, classification rules where applicable or results of control sample tests for direct comparison.

Worldwide, one of the most recognised classification society is Lloyds Register of Shipping (Lloyds) based in London. Their ship design and construction rules were chosen as a basis for comparison for established merchant vessel welding standards not only because of their British origin but also for the ease of communication with their design

engineers. In addition there could be an early opportunity to familiarise shipyard based overseers with the process in anticipation of future formal procedural acceptance. A similar situation pertains for the Ministry of Defence (Navy) -(MOD(N)) with respect to British designed and built warships. Therefore the rules and representatives of both organisations were consulted in establishing a basis for classification of the welds.

Whilst Lloyds rules are essentially compiled within one document, "Rules and regulations for the classification of ships" [101] , those for the MOD(N) are assembled within relevant "Naval Engineering Standards" (NES) [102] [103] [104] . These are at present superceding and supplementing earlier standards published by Director General Ships (DG Ships) [124]. They refer in turn to relevant documents published by the British Standards Institution.

5.1.1 Standards for conventional testing of fillet welds

The majority of rules set by Lloyds and MOD(N) concentrate on the testing of butt welds either "as produced" or as wide "V" joints from which "all weld metal" test specimens may be extracted to test the welding consumables.

Apart from macrographic and hardness examination, acceptance for fillet welds is dependent on the use of recognised and listed consumables, employing labour with recognised qualifications. In

addition there are requirements for the deposition of welds with the required throat thickness, leg length and radius at the weld toe for a particular joint configuration and preparation.

The sizes quoted in the rules are stated to be required in order to help control distortion, reduce shrinkage, facilitate good workmanship and to provide a sound joint capable of withstanding all the likely service loading for the ship's life [102]. In addition to the normal dynamic and cyclic loading, in some instances "one shot" explosive loading needs consideration when post weld treatment such as mechanical grinding of the weld toe may be required.

As a narrow fully penetrating weld which has been designed to replace conventional twin fillet welds, the laser skid weld does not meet the conventional requirements with regard to weld profile and dependence on the "all weld metal" test for classification of the consumable material itself. Therefore the Author designed sets of alternative tests in order to ensure the compatibility, if not superiority, of the laser skid weld.

5.1.2 Alternative test procedure ratification by classification societies

Meetings were held with both LLoyds [105] and the MOD(N) [106] in order to discuss the applicability of existing rules and alternative test procedures to the laser skid weld. Whilst maintaining that their established rules should be adhered to whereever possible, they accepted

the then stated inconsistencies both with all-weld metal sample testing and Charpy impact testing when problems arose from the fracture deviating out of the weld zone.

Initially, for MOD(N), the Crack Tip Opening Displacement (CTOD) test was advised as an alternative. However, during later discussions [125] it was appreciated that CTOD testing remains a relatively expensive test to replace Charpy testing as a procedural method (£300 for a CTOD test compared with £30 for three Charpy specimens), so Charpy testing of samples extracted from the skid weld itself was proposed.

The laser skid weld (a fully penetrating joint with small reinforcing or "smoothing" beads) has been designed to replace twin fillet weld comprising fillets of regulated sizes, therefore concern was shown for the fatigue characteristics of the joint. However the existing rules do not state specific design limits with regard to fatigue properties. Therefore in the absence of any specific criteria reference was made to the design rules set by the British Standard Institution.

Normal process acceptance would also depend on showing that weld properties could be maintained for material chemical composition ranges within specified grades and for all joint configurations

After witnessing the production of samples for the first set of fatigue trials, Lloyds presented a set of discussion notes concerning testing for procedural acceptance [125] (Appendix C-1). They noted the

likely influence of practical process variables, assessed parameters affecting the joint properties, denoted limits for smoothing bead sizes and extent of defects. Concern was also shown with regard to joints containing reduced penetration, namely the effect of reducing transverse bending strength.

Although both Lloyds and MOD(N) made reference to the examination of metallurgical properties, hardness testing and micro examination, in order to gain direct comparison with conventional welds emphasis was placed on proving structural properties. Therefore a set of mechanical tests was designed in order to test weld tensile strength, ductility, toughness and fatigue resistance all described in this chapter.

Where acceptance criteria are not provided directly in the classification society rules, reference is made to the requirements placed on parent plate and for butt welds, table 5.01, and to the relevant British Standard.

5.1.3 Non-Destructive Testing

Prior to testing the welds to destruction, the Author used ultrasonic testing as a means of initial identification of any defects. Non-destructive testing (NDT) of conventional fillet welds is not normally required by classification rules due to difficulties in interpretation. It is possible to use radiography for examining the integrity of fillet welds by photographing from acute angles but

	BS4360 43A	MOD material mild steel (plate)	MOD material mild steel (all weld)	Lloyds grade A (plate)	Lloyds grade A (all weld) covered electrodes	Lloyds grade A (all weld) wire flux
Yield stress (N/mm^2) min.	245	245	310	235	305	305
Ultimate tensile stress (N/mm^2)	430/510	430/510	430/600	400/490	400/560	400/560
Elongation % min	22	22	22	22	22	22
Charpy V-notch (°C/J)	-	-	+20°/47	-	1:+20°/47 2:0°/47 3:-20°/47	1:+20°/34 2:0°/34 3:-20°/34

NOTES

Lloyds charpy V-notch test values are given for 3 grades of electrodes suitable for the respective working temperature limitations.

Table 5.01 - Material mechanical property specification as defined by classification bodies for parent plate and all weld metal test pieces.

resulting X-ray contrasts vary continually due to the radiused shape of the fillets. A similar situation exists for the other dominant shipyard NDT method, ultrasonic testing.

For fully penetrating tee joints the situation is slightly better when testing in way of the web plate. The best radiograph results are gained when the web can be cut off, just above the the weld, so that contrast within this region is consistent. However, this necessitates a "destructive" test procedure. A few laser skid welds were tested by this method which proved successful in showing any pores in the weld, but as a first method of establishing weld quality, the test was destructive and expensive.

Therefore, being relatively simple and inexpensive, ultrasonic testing was used as an initial test after first producing the weld to identify any potential defects in way of the web plate.

Samples were up-turned and gel brushed on the plate face plate surface. Using a narrow 5mm probe unit, the system was calibrated to the plate thickness prior to traversing the probe along the joint line. The position and depth of defects were identified from peaks on an oscilloscope trace. Large areas and isolated zones of "lack of fusion" could be identified. However, confirmation of the type of defect could usually only be made through subsequent destructive testing.

Evenso, this test enabled the Author to make an initial assessment of a weld's integrity prior to further, more expensive destructive testing.

5.2 CRUCIFORM TEST

The cruciform tensile test to destruction was designed to determine the relative tensile strength of joints subject to a static tensile load. After the test the fracture surfaces, whether in the weld or the parent plate, may be examined for flaws.

Although the test is not normally required by Lloyds or the MOD for conventional weld procedure acceptance the test is recommended by BS 4870:Part 1:1981: Approval testing of welding procedures" [126]. Minimum acceptance level is that the ultimate tensile strength (UTS) should be no less than that required for the parent material. The UTS requirements for both parent plate and all weld metal samples are summarised in table 5.01 for Lloyds and MOD(N).

5.2.1 Preparation of Test pieces for Cruciform Tests

Test pieces were cold cut from welds in each plate thickness to sizes defined by BS 709:1971 "Methods of testing fusion welded joints and weld metal in steel", [127] as shown in figure 5.01. For the first two samples tested one of the webs was produced by fillet welding using the MMA, process to weld the web on the opposite side of the face plate to the laser welded joint. However, as the MMA weld failed rather than the

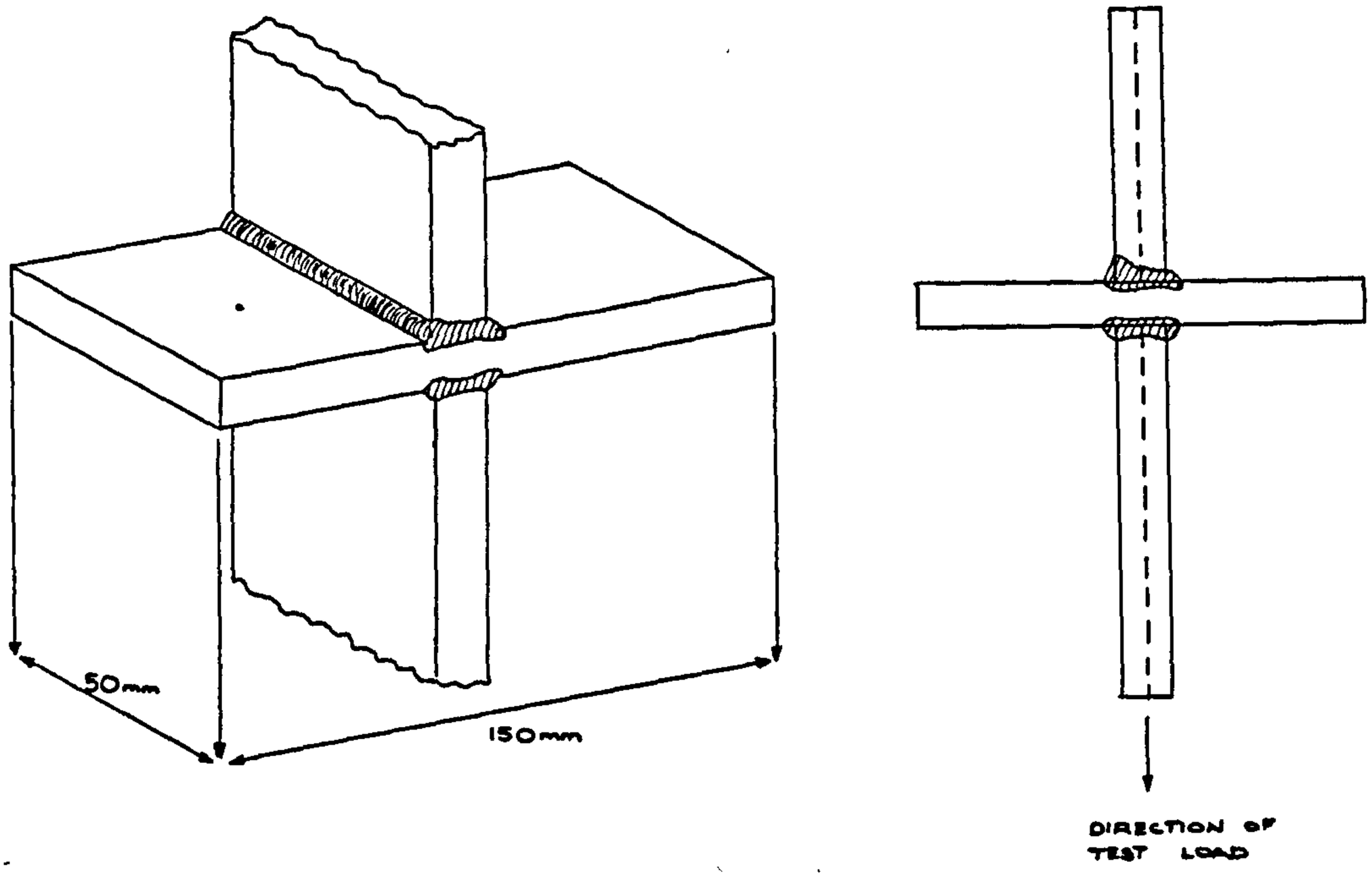

Figure 5.01 - Dimensions of test samples used for tensile testing

laser weld, all subsequent welds were produced with laser welds joining both webs to the face plate.

5.2.2 Cruciform Test Results

For the first test, when a laser weld was positioned opposite an MMA weld (4mm leg length), the MMA weld failed at the weld throat, the laser weld remaining intact. For the next sample the leg lengths of the opposing MMA weld were increased in size, with thicker plate and a prepared joint with a double bevel of 60 degrees and 5mm nose. This time the joint failed in the parent plate on the side of the laser weld. Therefore it was evident that, provided any possible heat treating effect as a result of welding the conventional joint had not affected the laser weld joint strength, the tensile strength of the laser skid was superior to that of the parent plate.

In order to ensure no heat treating effect of the secondary weld, all subsequent welds were produced by laser. Table C5.01 (Appendix C-2) shows a listing of each test detailing the point and type of failure Figure 5.02 summarises these results. Ultimate tensile stress has been plotted against carbon equivalent showing a proportional relationship for those welds failing in the parent plate. Figure 5.03 shows typical examples of the failed cruciform sections.

Of those that failed in the weld due to defects 50% reached stress levels above the minimum requirement set by classification societies.

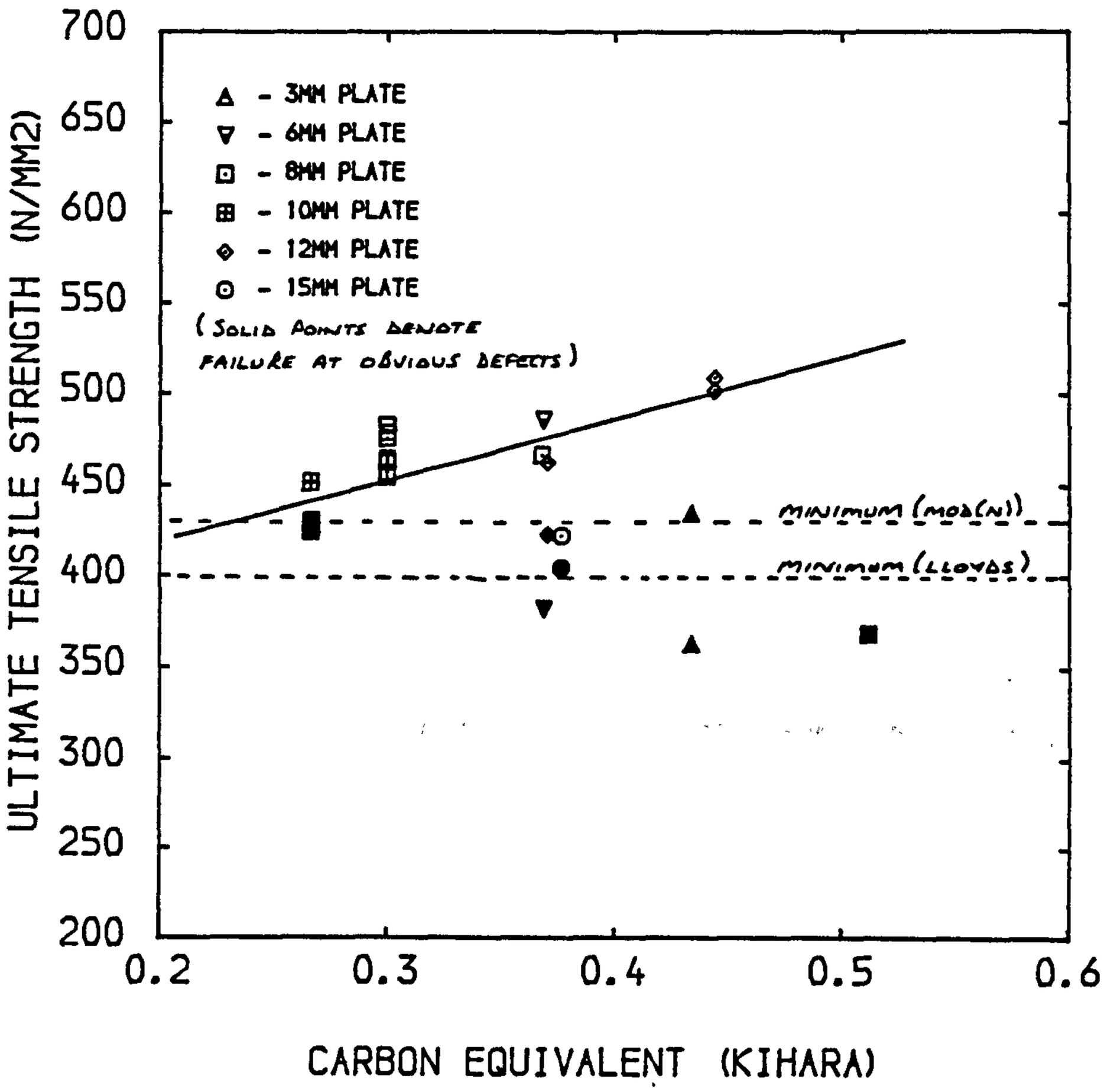

Figure 5.02 - Ultimate tensile strength of laser skid welds compared with parent plate carbon equivalent

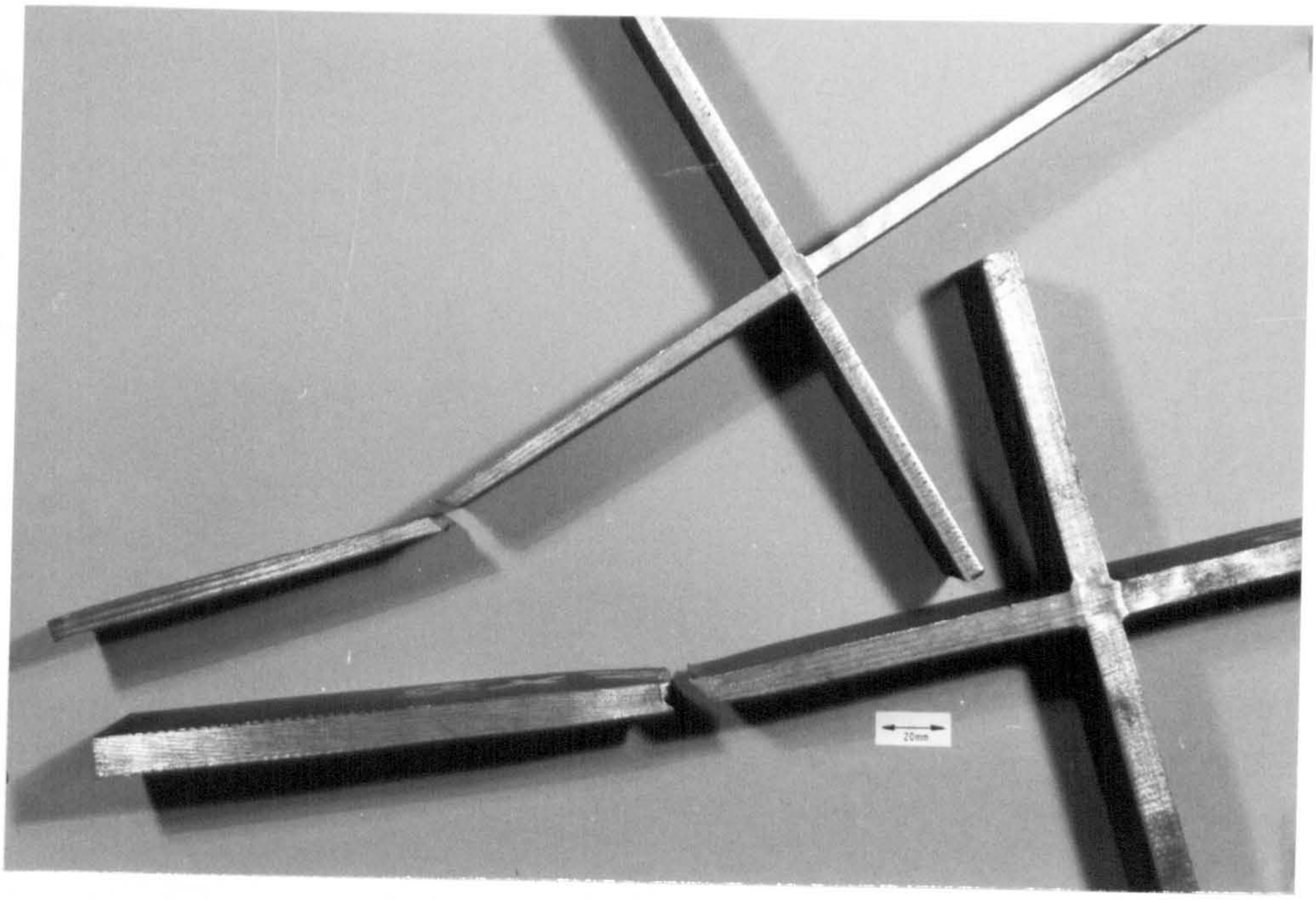

Figure 5.03 - Laser skid welded cruciform samples failed in the parent plate during tensile testing

Figure 5.04 - Defect (lack of fusion) identified in the skid weld during tensile testing

Where defects were suspected in the joints prior to testing, the test has also enabled the fault types to be confirmed and subsequntly identified.

For example, a laser weld in 8mm plate, whilst visually sound but showing zones of lack of fusion by ultrasonic scanning, tensile testing showed this fault in the weld centre where the incident beam has been set too high. Build-up of molten material has fused the joint both at the incident and emergent side but failed to fuse in the weld centre, figure 5.04.

The present tests on skid welded samples have shown the superior quality of the skid weld in tension over the minimum requirements as set by classification societies.

5.3 FILLET WELD FRACTURE TEST

The fillet weld fracture test as defined by B.S 709:1971 [127] requires that a weld fillet is broken open to permit examination of the fracture surfaces. The test is designed to ensure that fracture is most likely to occur through any flaws present e.g. cracks or porosity.

The test is normally conducted on a single fillet weld run made on either a tee or lap joint. If necessary, in order to promote failure through the weld material, a saw cut may be made on the fillet surface. A force is then applied perpendicularly to the upper edge of the web plate or attachment in order to fracture the weld through bending.

Unlike the single fillet, the fully penetrating laser skid weld shape does not provide any inherent points of discontinuity for a static load to initiate fracture. Therefore, either flaws in the weld material structure will form a discontinuity or the test will operate as a "bend" test similar to that used on plane butt welds [127] to reveal the ductility of the joint.

5.3.1 Fracture test specimen manufacture

Test specimens were cold cut from laser skid welded and MMA welded samples to dimensions as detailed in B.S. 709, figure 5.05. Initial tests were carried out on laser welds in 8mm thick plate, with the incident bead removed (by grinding) and with the emergent bead intact, also with the emergent bead removed and the incident bead intact. Further tests were conducted for each plate thickness as follows:

1. As welded; weld known to be sound from previous tests.
2. Saw cut placed in emergent bead.
3. Saw cut placed in incident bead.
4. As welded, but with suspected flaws.

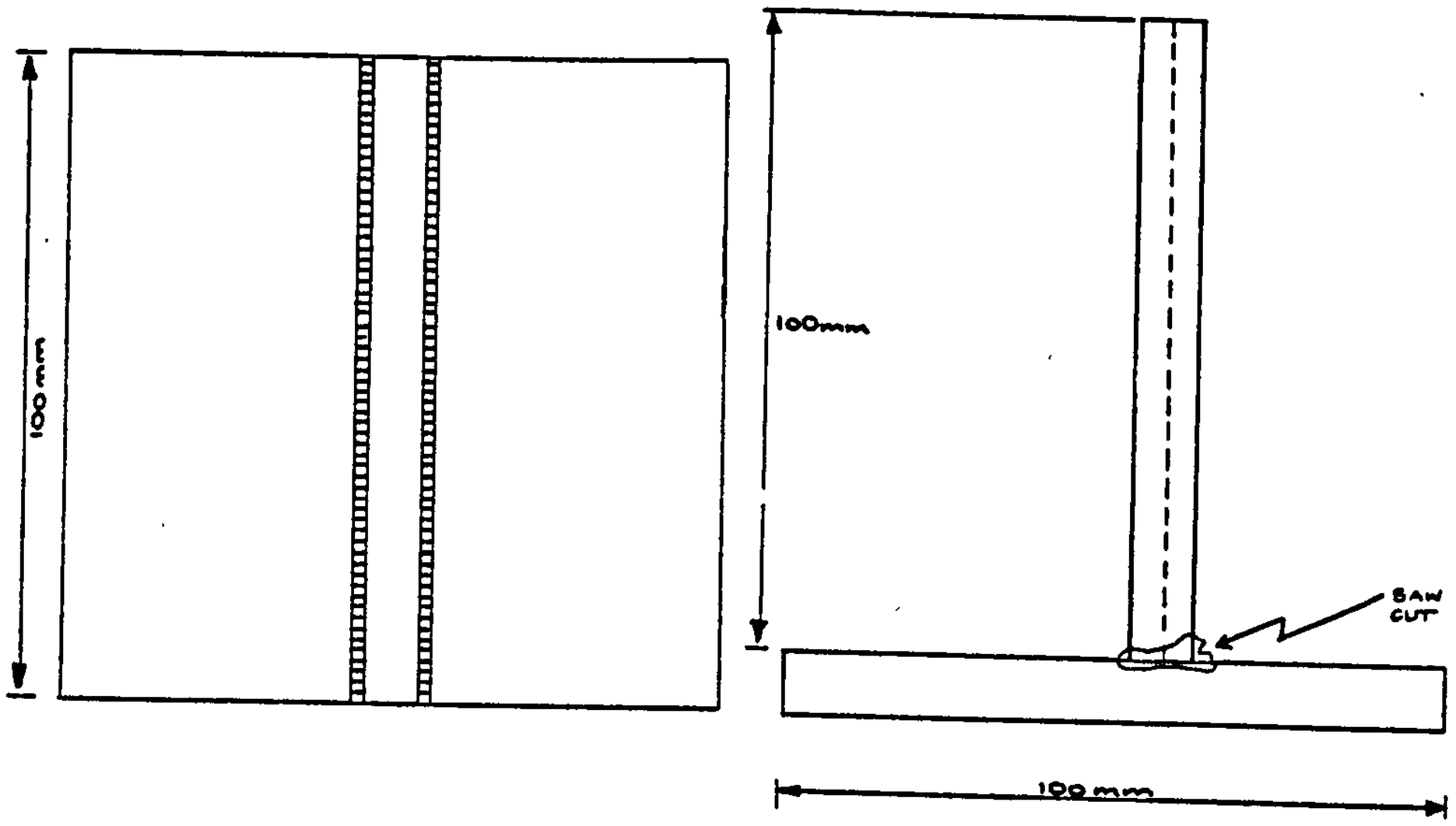

Figure 5.05 - Dimensions of the samples used for fillet fracture type testing

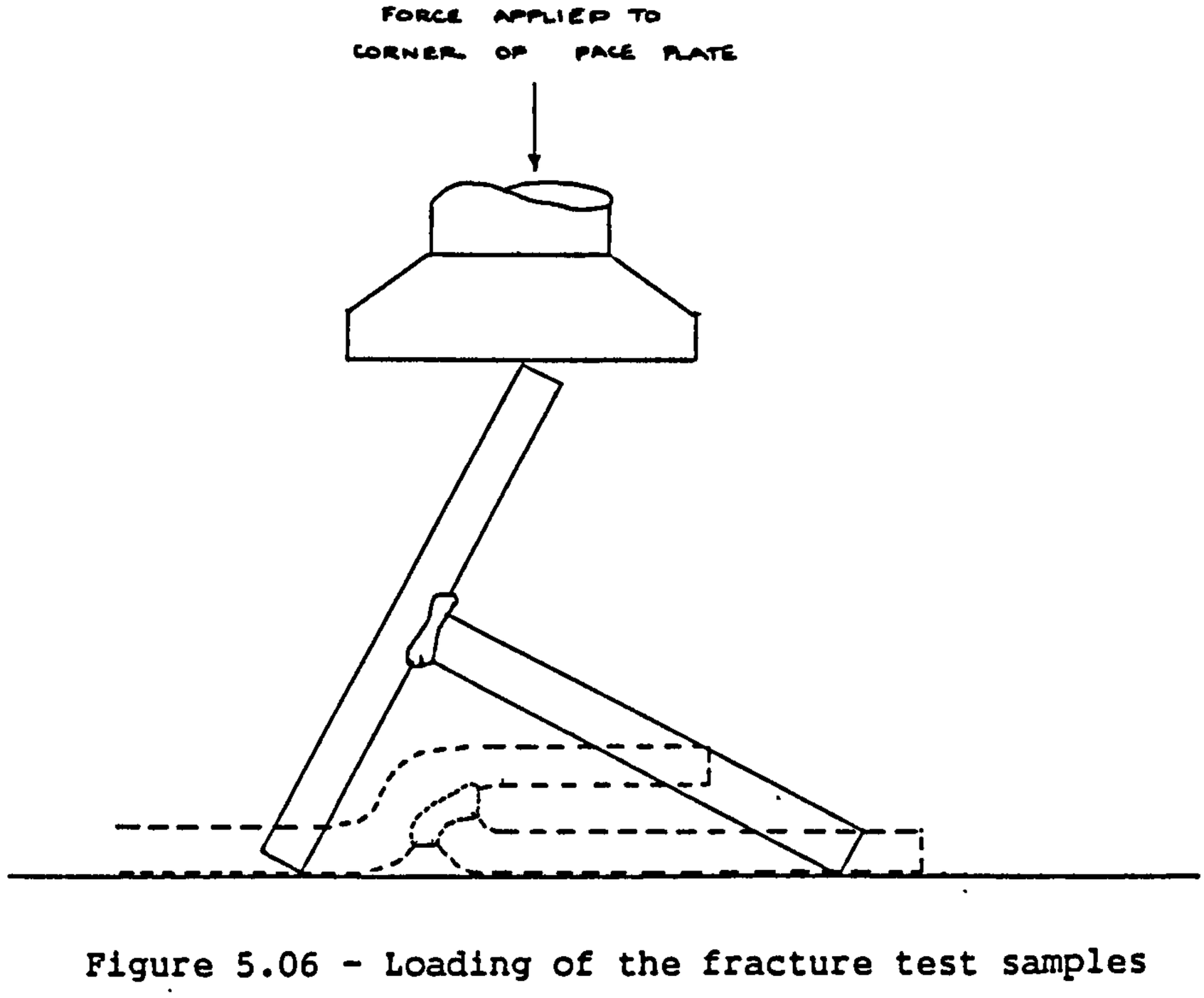

Figure 5.06 - Loading of the fracture test samples

5.3.2 Fracture testing details

Test specimens were placed in a hydraulically operated compressive testing machine (Amsler, 35t maximum capacity) with the load applied as shown in figure 5.06. The applied load was increased until the joint yielded, and then maintained until either the weld fractured or the web had been folded parallel to the face plate. The specimen was then removed for examination.

5.3.3 Fracture testing results and discussion

A summary of fracture and bend surfaces is detailed in table 5.02.

In every joint specimen, the web was forced over parallel to the face plate without the two parts becoming fully separating. No failure was observed in the welds shown to be satisfactory by previous visual and ultrasonic scanning (type 1 above). This emphasised both the overall strength and ductility of the fully penetrating joints, figure 5.07.

In the other, rather less satisfactory type 4 samples some failures occurred. The failure path either followed the track of a defect in the weld material or, if no defect was present, followed a principle shear stress failure path by ductile cleavage into the web plate material. Placing of a saw cut to provide failure initiation, by ensuring a stress concentration within the weld metal, helped to expose a number of occasional defects previously located but not identified by ultrasonic

Plate Th'ness	Satisfactory weld	Notch in emerg. bead	Notch in incid. bead	Faults in weld
3	No visual failure	Partial ductile failure into web; partial lack of fusion to face plate	Slight crack on surface	No visual failure
6	No visual failure	Saw cut in pores at failure initiation then ductile into web	Mainly ductile failure into web plate. Two zones of lack of fusion.	No visual failure
8	No visual failure	No visual failure	Ductile failure into web plate-part lack of fusion visable	Cracks formed at pores-rest intact
10	No visual failure	Small crack. Three zones of centre line cracking opened	Brittle failure five areas of centre line crack	Gross porosity and ductile failure.
12	No visual failure	Ductile failure into web plate	Partial ductile failure into web; partial ductile/brittle failure in weld	Slight cracking at weld toe
15	No visual failure	No visual failure	Ductile failure into web plate	Lack of fusion; ductile failure to web.

Table 5.02 - Fillet fracture test results

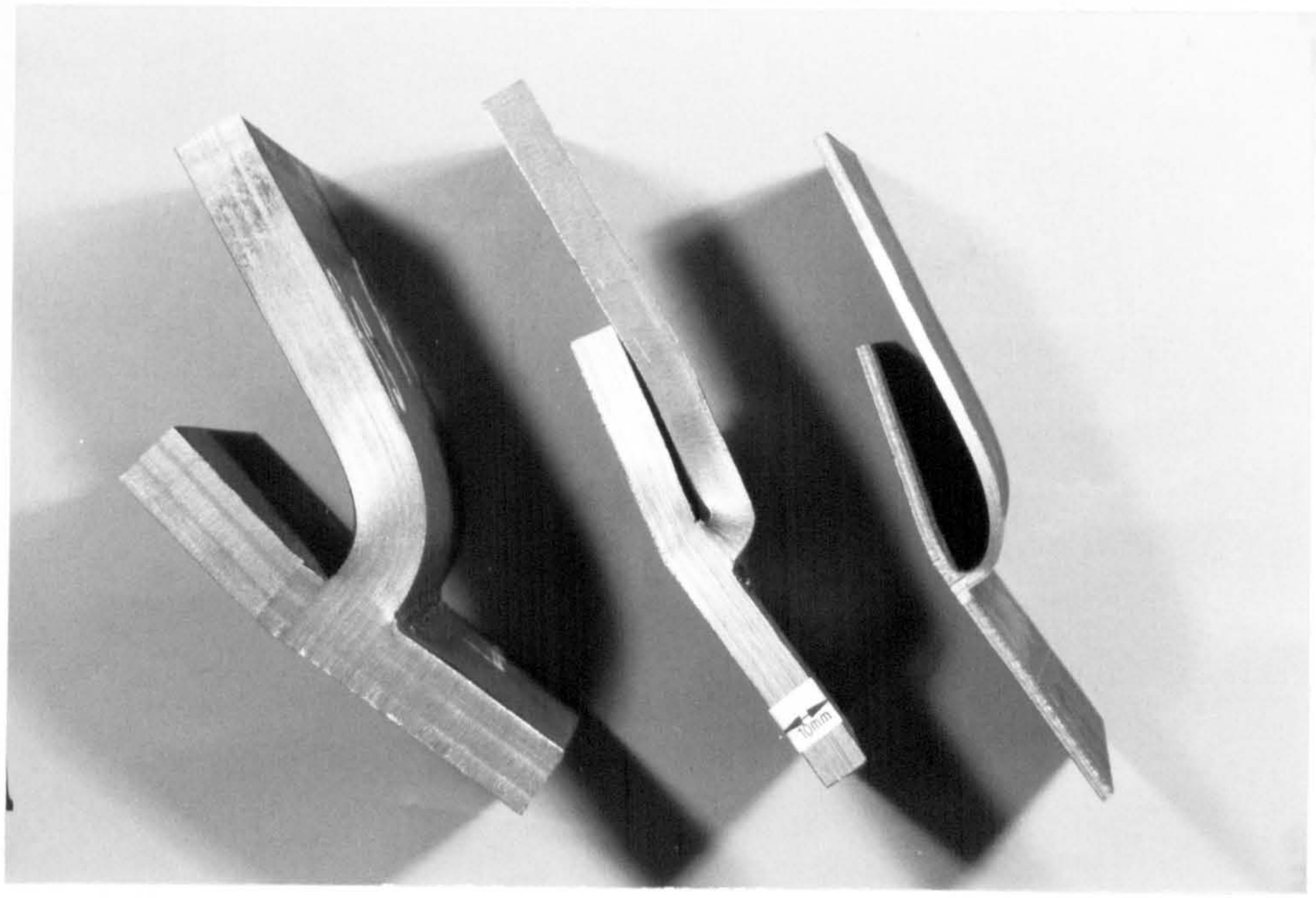

Figure 5.07 - Acceptable skid welds after a fillet fracture type test

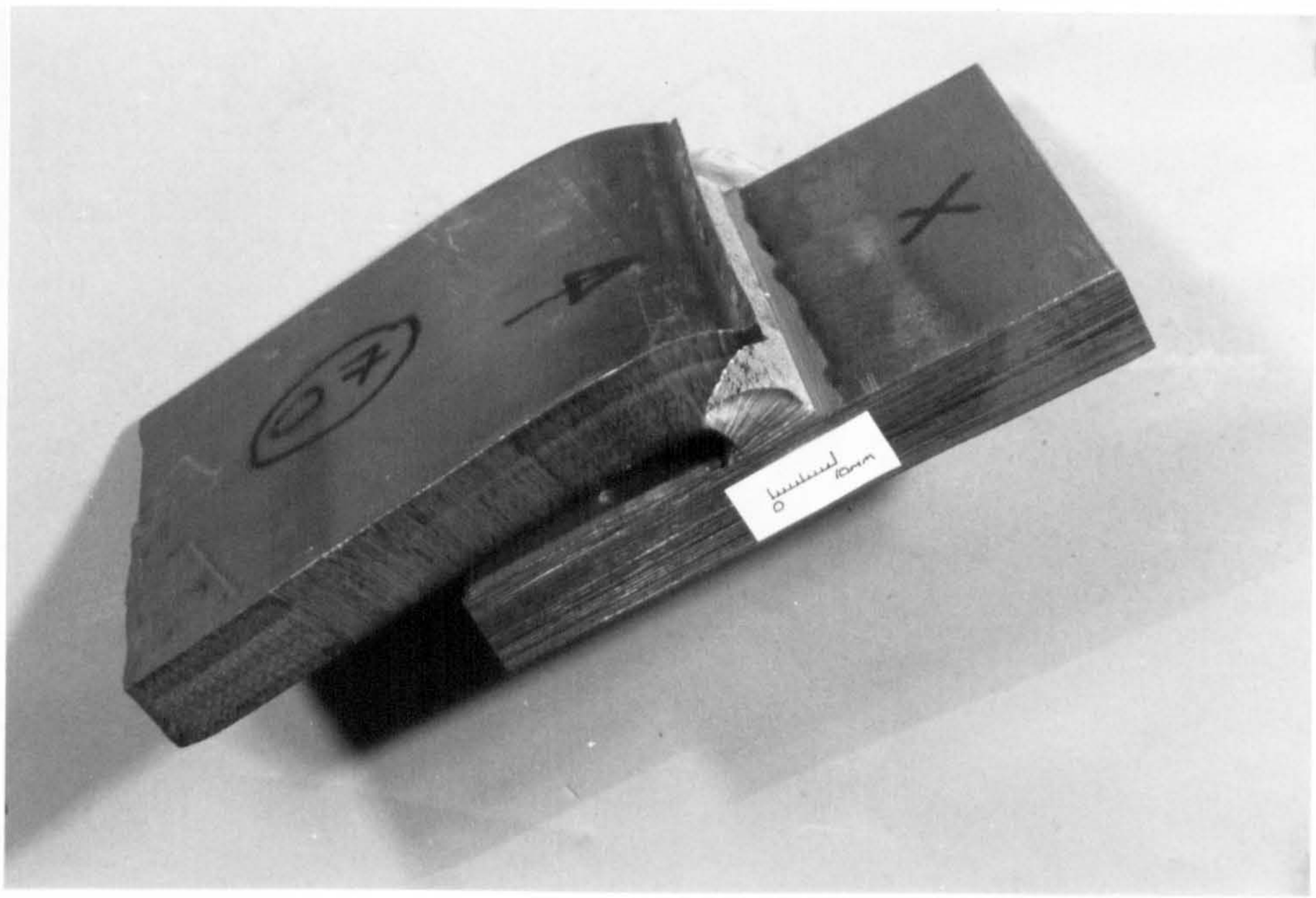

Figure 5.08a - Failure in a fillet fracture from a saw cut notch into the web plate

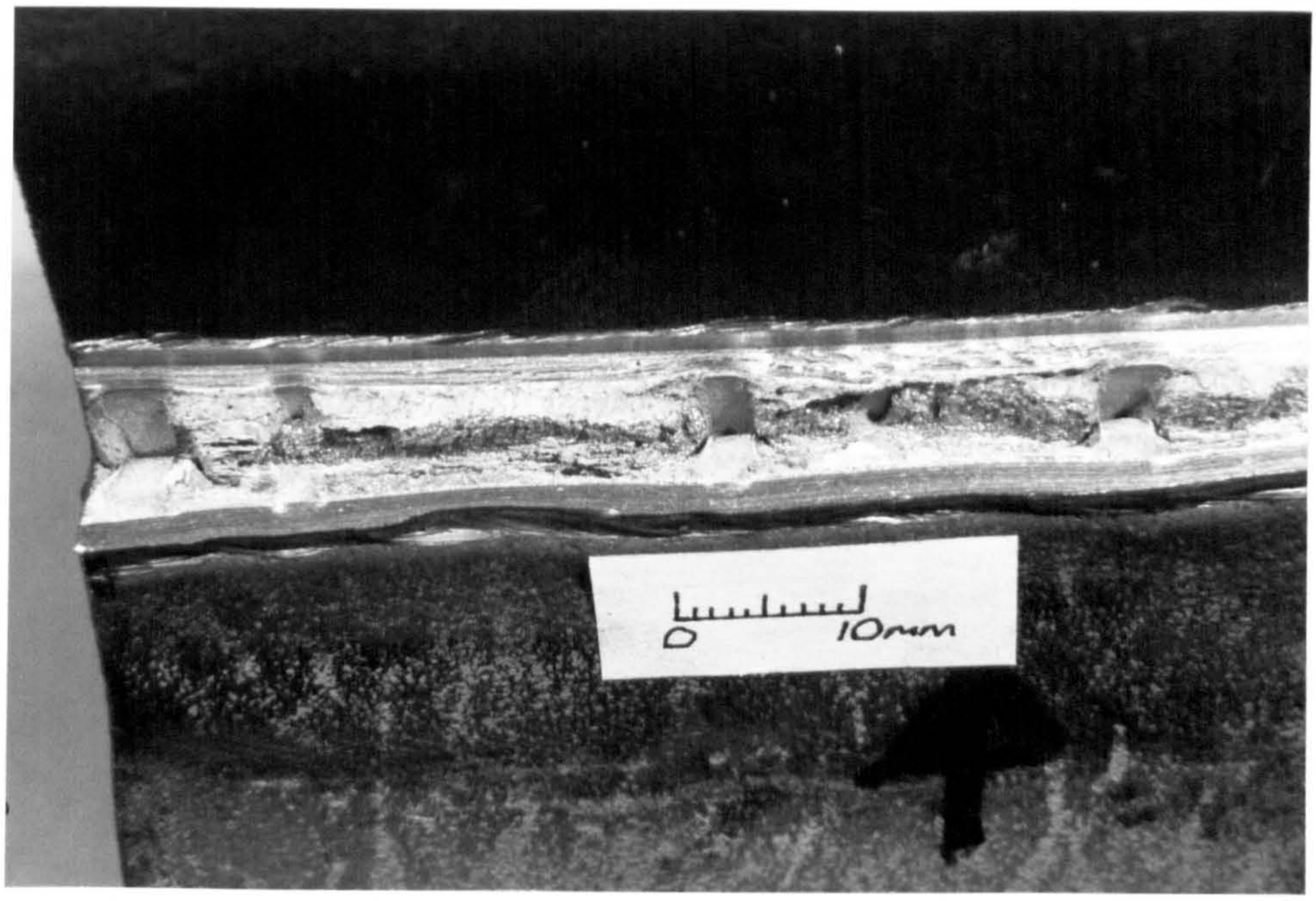

Figure 5.08b - Initial failure during fillet fracture testing due to zones of hot cracking

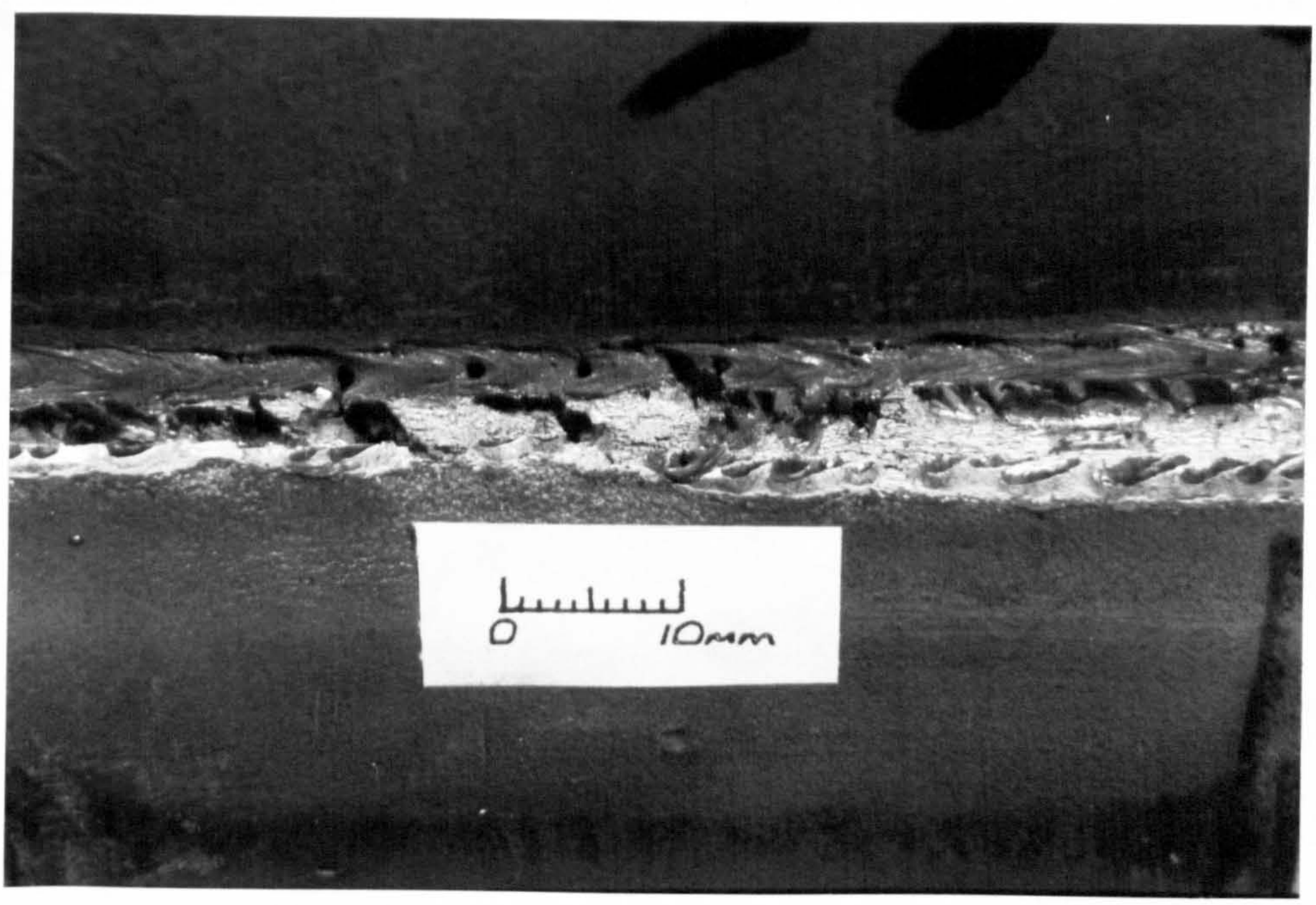

Figure 5.08c - Initial failure during fillet fracture testing due to porosity

scanning. However, without such a cut notch, some of the defects previously found did not necessarily cause failure.

The various types of failure observed are shown in figure 5.08 a to c.

The tests have shown that by applying an adapted fillet weld fracture test weld flaws, may be identified. Firstly a 1mm deep saw cut is made in the incident bead surface and a force applied in the web plate directed away from the cut position perpendicular to the web. Secondly the process is repeated on a different sample with a notch in the emergent bead. Then by repeating the process for the unnotched weld, the integrity of the weld beads and the ductility of the complete weld can be assessed.

Use of the test has emphasised the advantages to be gained from laser welding not only as a fully penetrating joint but also from the refined weld structure as discussed later in the chapter. This creates a strong yet ductile joint to give structural performance in excess of the twin fillet joint conventionally employed in shipbuilding.

5.4 IMPACT TESTING

For structural steels the usual reason for using an impact or toughness test is to provide data and checks to ensure that the material will not suffer from brittle fracture in service life [128] . In order to maintain total structural integrity the same criteria must be applied to the welds that join the steel piece parts. The toughness test most widely used in shipbuilding is the Charpy V-notch test as described by BS131 : Part 2 : 1972 [129] and Lloyds Rules [101]. The test determines the energy absorbed at a specific temperature in breaking a specimen, notched in the middle and supported at each end, from a single blow of a pendulum.

Normal procedural impact testing of arc welded butt joints for shipbuilding classification requires that triplicate test specimens are taken from a welded butt joint (or all-weld-metal sample in the case of welding consumables acceptance trials), with the average toughness value for a specific test temperature meeting a specified minimum. The values specified by MOD(N) and Lloyds are summarised in table 5.01.

However for fillet welded joints, so long as the weld fillets are of the correct size and the consumable material has been tested in an "all-weld-metal" test to the acceptance of classification societies, no direct testing of the actual joint configuration is normally required.

5.4.1 Use of Sub-sized Charpy specimens

The recommended cross section size of Charpy test specimens is 10x10mm, but if this cannot be achieved e.g. for welds in 6mm plate, "sub-size" specimens may be used. Various authors have provided factors to correlate the toughness values provided from full size and sub-size specimens [130] [128]. Generally the use of smaller specimens has the effect of lowering both the absorbed energy for any one test temperature and the transition temperature (the temperature at which the mode of failure changes from ductile to brittle). Towers [131] has recently summarised and assessed the adequacy of various classification codes for the use of sub-size Charpy specimens. For standards in the United Kingdom there is no modification to test temperature for sub-size specimens, this being taken into account when specifying the "modified energy".

The requirements for sub-size specimens are summarised, table 5.03 :

Whilst these correlation factors may be used to provide a reference for minimum acceptance standards, cross reference between results of varying sized specimens could be misleading when comparing detailed transition curves. Therefore in order that the results from nearly all the thicknesses of plate being skid welded could be tested, sub-sized specimens of 5x10mm were used throughout the present trials.

Code	Energy requirement as a function of that for a full size specimen (10x10mm)	
	7.5x10.0mm	5.0x10.0mm
BS4360 : 1979	0.77-0.78	0.66-0.68
Lloyd's Register 1981	0.77-0.78	0.66-0.68

Table 5.03 - Guidelines for sub-sized Charpy specimen impact requirements - after Towers [131]

Temperature (°C)	Standard size energy absorption (J)	Sub-sized (half) specimen absorption (J)
20	47	33
0	34	23
-20	27	18

Table 5.04 - Charpy acceptance criteria for skid weld toughness testing

The MOD(N) specify that for welds in mild steel plate of less than 25mm thick, the energy absorbed during Charpy testing at 20°C should not be less than 47J (33J for half size specimens). Lloyds give no toughness requirement for joint acceptance in Grade A plate. However normal shipbuilding practice is to accept the guidance of BS4870:1981[1] using BS5500:1982:"Specification for the design of unfired fusion welded pressure vessels" [132] to provide minimum requirements. Therefore, for the purpose of the test programme, acceptance levels specified using sub-sized specimens were adopted, table 5.04.

5.4.2 Alternative procedures to all-weld-metal consumable testing

For normal arc welding consumable classification, weld runs are deposited in a wide "V" prepared plane butt joint and "all-weld-metal" test specimens extracted. The welding consumable may then be classified to varying standards depending on the Charpy values achieved at a particular temperature for a certain welding process.

For the high aspect ratio single pass laser weld such a test would be misleading. Insufficient consumable material is run into a normal joint space during a single pass run to ensure that an "all-weld-metal" sample may be extracted. If a multi-run technique was employed not only would the weld material cooling rates far exceed those normally experienced in the single pass welds, but also subsequent runs would have a heat treating effect changing the weld properties.

All-weld-metal testing is conventionally highly relevant to the tee section joint. So long as the tests conducted on such samples give satisfactory results and fillet shapes are to the required size, no Charpy testing of the fillet joint material is required. In the absence of an immediate alternative to the "all-weld-metal" test of the consumable material, a programme of trials was designed, firstly to examine Charpy properties of skid welds themselves and secondly to show how properties of the weld metal could be improved.

In order that Charpy specimens could be removed from skid joints themselves, a secondary web plate was welded directly opposite to the first web joint to form cruciform samples. A small jig was designed and produced to ensure alignment of the two webs. Charpy test specimens were then machined from the two webs, containing two welds with the flange plate sandwiched in the middle, figure 5.09.

After testing the acceptability of welds taken from the skid welding configuration, comparative trials on butt type welds were then conducted to assess the effect of using various filler wires to improve potential weld toughness properties.

The latter butt welded tests were in keeping with the classification society dependence on butt joints for the setting of consumable acceptance standards for conventional weld classification. Also they were more akin to the requirements placed on the testing of fully penetrating tee joints as described by BS5400:1980,Part6 " Steel,

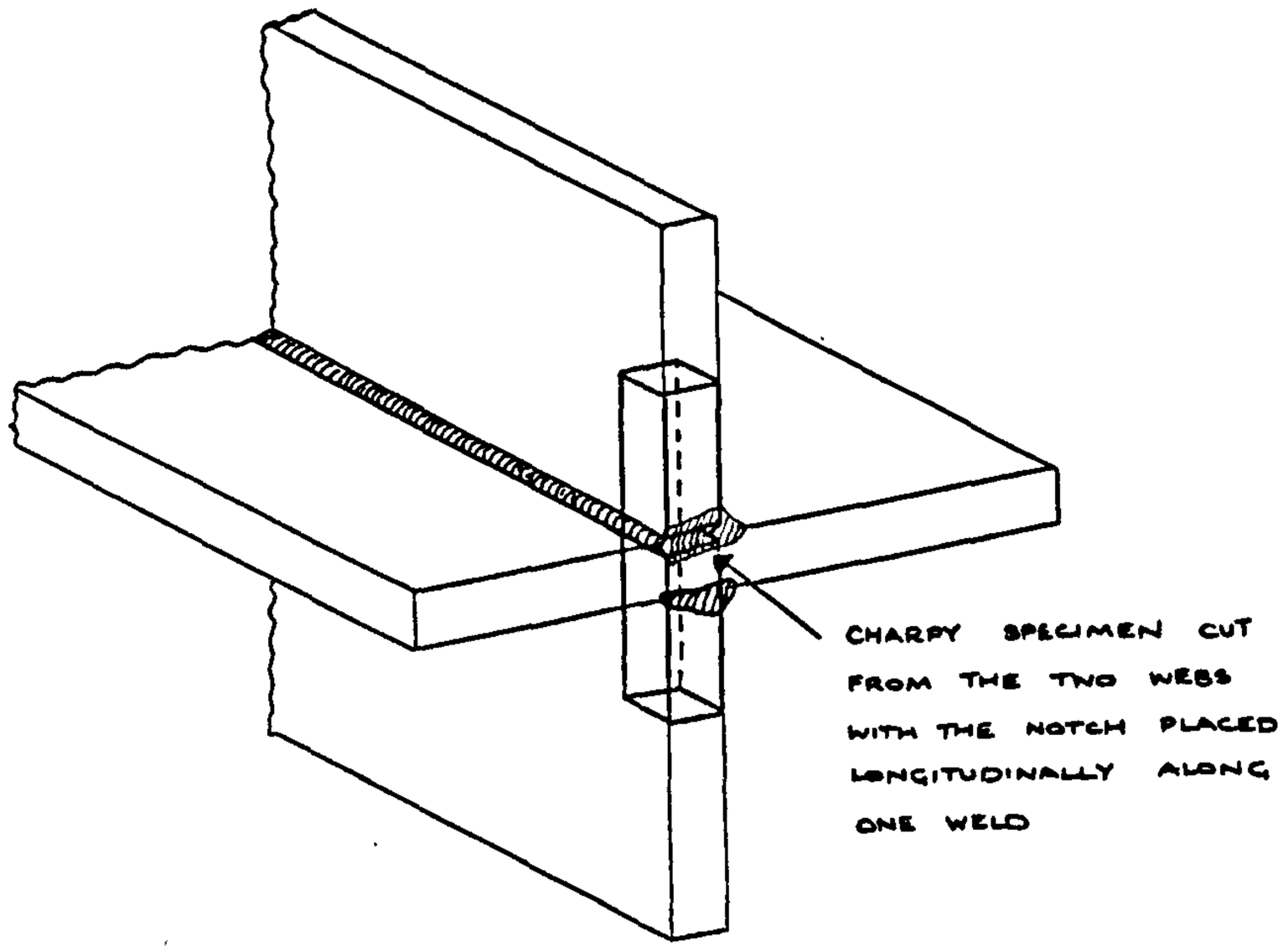

Figure 5.09 - Charpy test specimen extraction from a cruciform welded sample

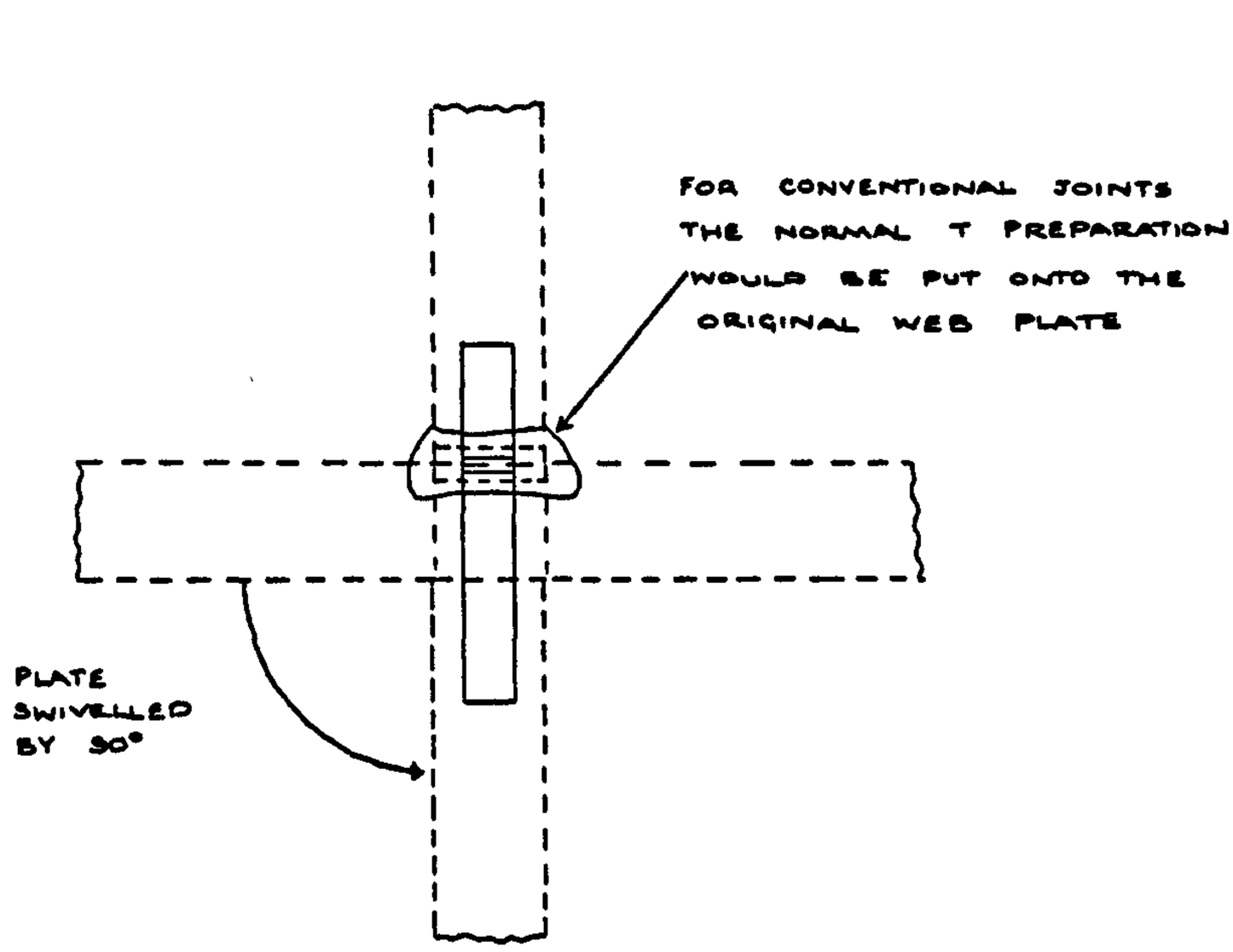

Figure 5.10 - Rotation of the face plate for an alternative configuration to Charpy test tee section joints

concrete and composite bridges, specification for materials and workmanship, steel" [133] . This describes how, instead of the direct toughness testing of tee joints, the flange plate may be rotated by 90° and butted to the web plate, figure 5.10. The web plate edge is prepared in the normal way for the tee joint. As there is no preparation necessary for a normal single pass laser skid weld, by following the guidance of BS5400 a butt joint configuration may be used instead for comparative experiments.

Although no specified acceptance criterion is defined for these tests by Lloyds or the MOD,(N) the results were compared against the toughness values stipulated for butt weld procedural acceptance. For each joint parent plate specimens were also tested in order that comparisons could be made between plate properties and those of the weld.

5.4.3 Charpy testing of narrow weld sections

The problem of applying the Charpy V notch test to welds with narrow fusion zones, both of laser and EB welds when there is a tendency for the fracture path to deviate out of the fusion zone into the HAZ or parent metal, has been noted by various authors, [134] [135] [3] [121] [136] [137]. However, this problem gives rise to misleading results unrepresentative of the weld metal itself and was first highlighted by Goldak and Nguyan [138] using the analogy of a "plastic hinge" failure mechanism.

They suggest that the problem is due to the stress field around the crack tip extending beyond the fusion line of the narrow weld into the parent plate. When the yield strength of the weld material is greater than that of the parent plate and the yield strength of the parent plate is reached before brittle or ductile fracture occurs in the weld, the parent plate will yield first thereby easing the strain around the crack tip. At the outside of the sample where stress concentrations are highest, the material then tears so deviating the fracture path into the parent plate. Because of this deviation, toughness values are often higher than would normally be expected, however this does not necessarily show that the weld metal has a higher toughness.

In practical service situations, with a larger structure (compared to the size of a Charpy specimen) it could be argued that the deviation mechanism would dominate because the applied stress fields would extend over a larger area compared with the normal striker geometry so that failure actually through the weld would only occur at a temperature low enough for brittle failure.

An indication of the validity of this argument is shown in some of the results of Metzbower [37] [140] [39]. Metzbower's tests were conducted to ASTM standards [141] where the striker geometry is notably flatter compared with the ISO striker geometry, figure 5.11, used for the British Standard measurements. The impact force will be distributed over a larger area similar to any impact on a larger structure. Not only are the weld toughness values in the apparently ductile section higher than

those for the parent plate, but also he describes how in nearly all samples the fracture path deviated into the base material.

However, authors using ISO Charpy test equipment, in addition to showing deviating fracture zones, have shown results where ductile fractures have stayed in the weld zone and occasionally, when from previous results a ductile failure was expected, a brittle fracture has occurred. Obviously if this type of failure is possible, results must be assessed with caution. To avoid confusion, only energy levels for fractures staying in the weld should be compared. However by examining the fracture properties further, the temperature and toughness noting of when fracture deviation actually occurred may enable the deviating specimens to be used in judging weld acceptance.

In addition alternative forms of Charpy samples have been proposed recently [142] where additional slots are made down the sides of the specimen. However, insufficient results are available to correlate standard and slotted samples for procedural classification.

5.4.4 Charpy specimen manufacture

Three sets of welds were produced for toughness testing. The initial tests were conducted on a butt sample produced during trial 1 to ensure compatibility of weld toughness properties to classification requirements, using the 10kW laser compared with Martyr's [3] results

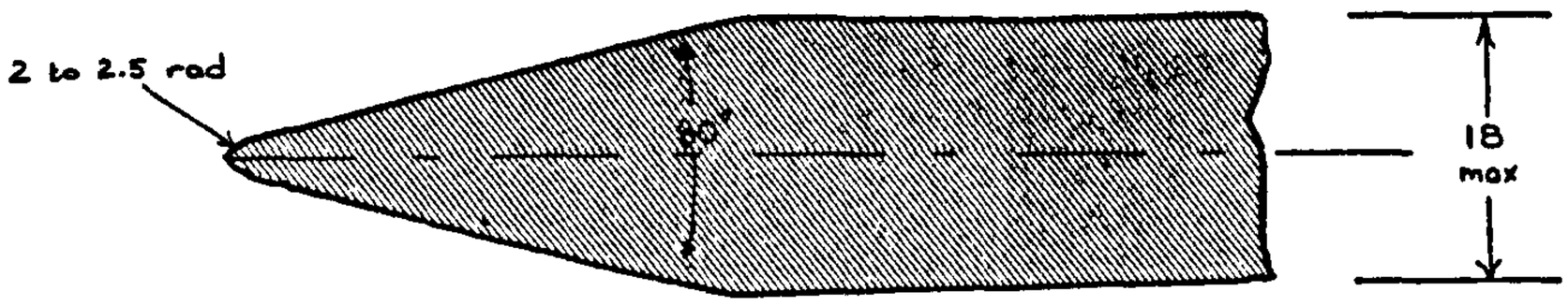

Figure 5.11a - I.S.O. standard stricker geometry for Charpy testing

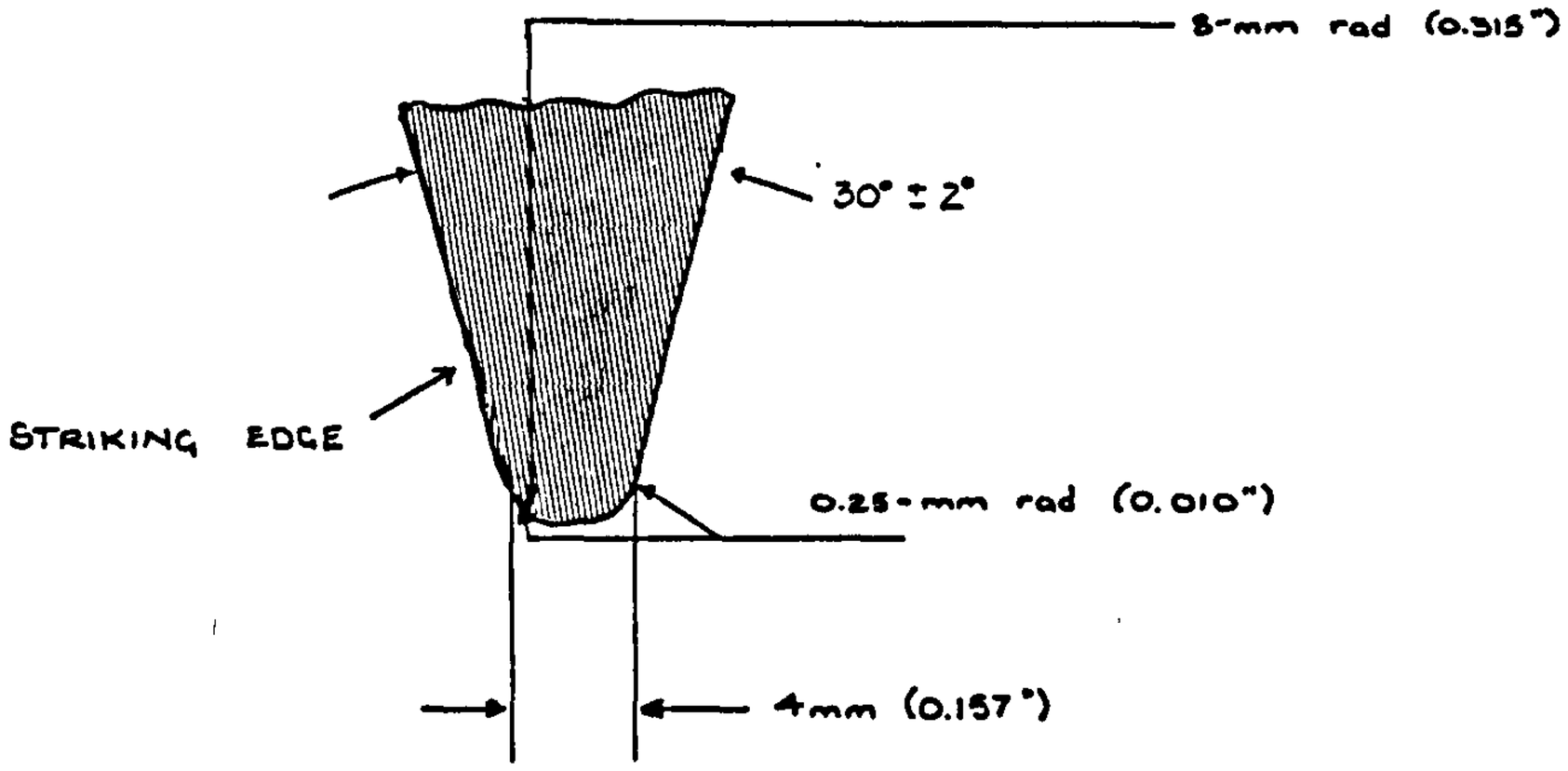

Figure 5.11b - A.S.T.M. striker geometry for Charpy testing

using the 5kW laser. The second set of tests were conducted on cruciform sections which were produced during trials 7 and 8 in each plate thickness, 6-15mm, at the "optimum" speeds to produce balanced beads using an alloyed double deoxidised, C-Mn-Si-Mo, wire to BS2901:1983: "Filler rods and wire for gas shielded arc welding, Part 1, ferritic steels":A31 (Bostrand 20).

The toughness values for the cruciform samples showed a similar range to those for the butt welded sample when compared against classification requirements. Whilst, in the majority of cases, values were marginally above the minimum requirements, some were below minimum and therefore a set of trials to assess the effect of using various filler wire types on Charpy properties was designed.

Five different filler wires were used for the butt weld comparative trials. In addition to the C-Mn-Si-Mo wire (the molybdenum normally associated with good tensile properties) another wire used in general structural applications for MIG welding an unalloyed double deoxident, C-Mn-Si wire to BS.2901(1983) Pt1:A18 (Bostrand LW1) was used.

The A31 and A18 wires had been used for the previous parameter assessment trials, being wires typically used in the shipyard for the MIG welding of mild steel plate and also used by Martyr for laser welding without any obvious difficulties. Watson [120] [135] , investigating the laser welding of niobium microalloyed structural steel showed improvements to impact properties by reducing the weld carbon content.

Therefore two SAW wires, to BS4165:1984:"Electrodes, wire and fluxes for submerged arc welding of carbon steel and medium tensile steel", an S2 and an SD3 wire were used. These wires had to be drawn from an initial diameter of 2.5mm to 1.6mm for the trial. Finally the use of an alloyed triple deoxidant, C-Mn-Si-Ti wire (Thyssen K-Nova) found to give improved toughness qualities in narrow welds made in pipe girth welds using the MIG welding process [143] and used for limited laser welding trials on an API 5L x 65 pipeline steel [144] .

In controlled amounts the presence of titanium di-oxide in the weld has been shown to aid the nucleation of acicular ferrite with a consequential increase in toughness, without any increase in weld hardness [145] [146] . A comparative compositional analysis of each wire is presented in table 5.05.

Butt welds were produced using each of the five wires in plate thickness of 6,10, and 15mm. A power of 9kW(WP) and the same traverse speed as used to produce balanced skid welds were used to produce the butt welds so that for each plate thickness the heat input would be the same.

Where possible a set of nine test specimens was machined from each sample as detailed by BS131:Part 2, 1972 [129] with the notch placed longitudinally to the welding direction in the weld metal. The first three test pieces of each batch were tested at -20, 0 and 20 degree Centigrade. Having obtained an indication of the transition temperature

	Bostrand 20	Bostrand LW1	S2	S3	Thyssen
CHEMICAL COMPOSITION					
C	0.1	0.08	0.09	0.09	0.09
Mn	1.1	0.90	1.05	1.7	1.48
Si	0.2	0.6	0.22	0.25	0.76
S	0.02	0.02	0.014	0.006	
P	0.03	0.02	0.011	0.007	0.013
Ti					0.059
Mo	0.3				
Al				0.025	
MECHANICAL PROPERTIES					
Yield Strength (N/mm^2)	550	530	410	490	440
Tensile Strength (N/mm^2)	690	620	520	550	570–630
Elongation (%)	25	22	28%	27%	30– 25
Charpy V notch (J) at +20°C	120	80			110
0°C	50	60	40		65
-20°C	50	50			
-30°C	40				
-50°C				60	

NOTES

Analysis taken from all weld metal test sample

Table 5.05 - Specification composition and mechanical properties of filler wires used during the skid welding trial

from these samples, test temperatures for the following 6 specimens were selected within the range -70 to +70 degree Centigrade to complete a transition curve and identify upper and lower shelf energy levels.

For procedural testing to classification society requirements, three samples should be tested at one temperature and the results averaged. At the most, results from only three set temperatures (-20, 0 and 20 degrees C) are required.

For research and development purposes this small number of results fail to provide enough information about the nature of the transition between ductile and brittle fracture, when at least six points are needed. However, within the project budget, provision of average values at each point was going to severely restrict the number of weld variables that could be tested. Therefore, following the convention of other recent authors [122] [121] [120] , tests have been made at up to nine separate temperatures with the transition curve drawn to form a visually averaged plot within any scatter of individual points. To clarify the graphs further the present Author has used solid points (as opposed to open points) to denote when fractures deviated and a dotted line (as opposed to a solid line) to show the continuation of the transition curve at temperatures above that at which fracture deviation was first identified (Tdv).

5.4.5 Charpy test results and discussion

Figure 5.12 shows the toughness transition curve obtained after testing the 8mm thick butt welded sample. No fracture deviation was visible and absorbed energy values were in excess of both the minimum values as detailed by classification societies and obtained from the parent plate. A surprisingly low value was found at a test temperature of +50 °C. However the fracture face showed large pores which will have reduced the sample's resistance to failure, reducing the absorbed energy.

Initially the results from the cruciform test samples, shown graphically in Appendix C-3 (figure C5.01 a-1) and summarised in table 5.06, appeared less clear than gained from the first butt welded sample results, as the onset of fracture deviation increased the amount of scatter in the measured energy levels. However, by plotting a curve and noting the temperature at which fracture deviation commenced, an assessment of the weld properties still could be made.

Plots for Charpy tests of the butt welds produced in the same material as the skid welds using the same filler wire and traverse speed are shown for plates of 6,10 and 15mm thickness, together with parent plate results.

In addition, for each specimen, the percentage area of crystallinity as detailed by BS131:Part5:"Notch Bar Tests" [129] has been determined and plotted in order to accurately calculate the Fracture Appearance

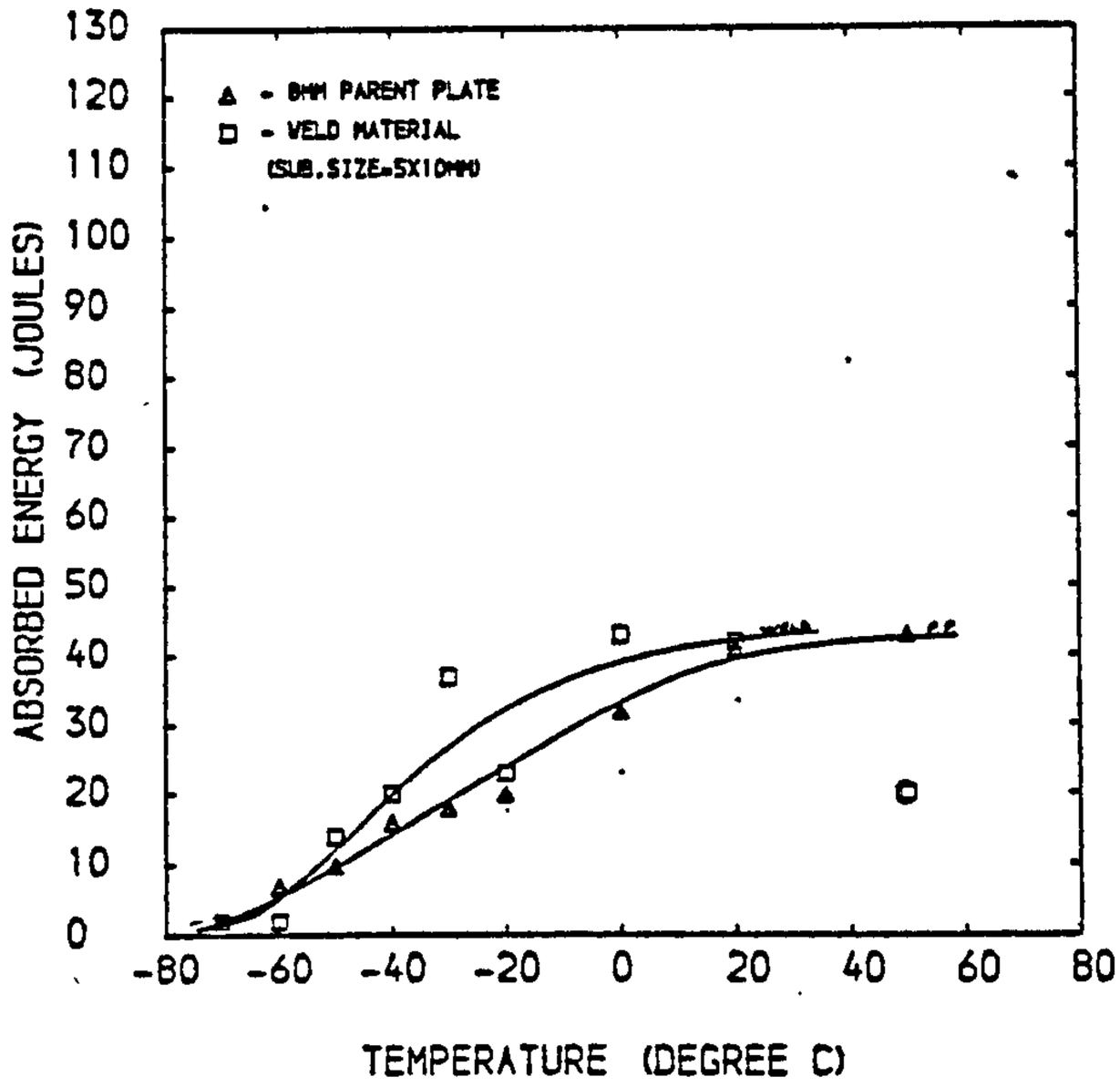

Figure 5.12a - Charpy transition curve for a laser butt weld : 8mm plate, 9kW laser power, A31 filler wire

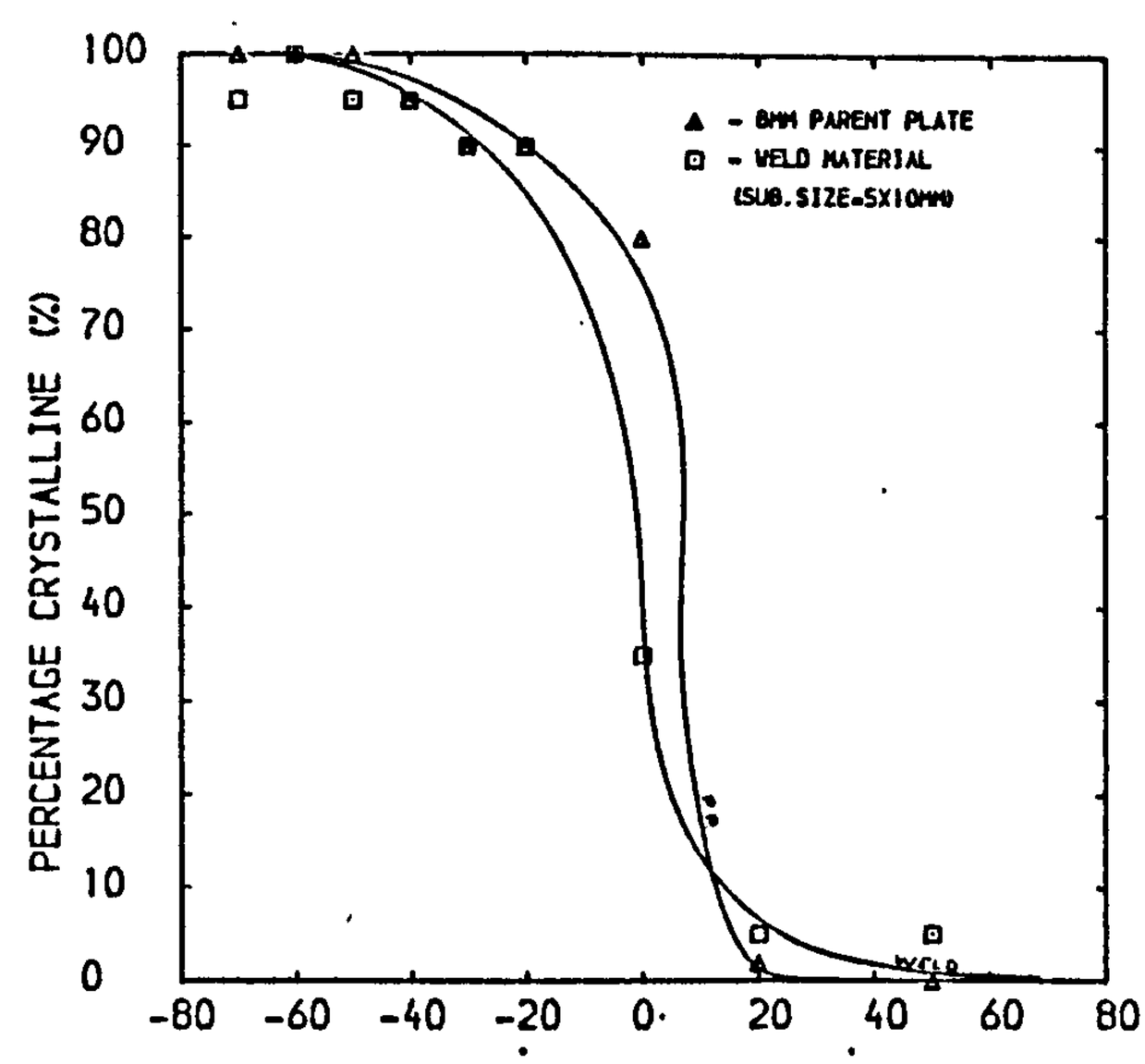

Figure 5.12b - Fracture appearance transition curve for the same weld as Fig. 12a

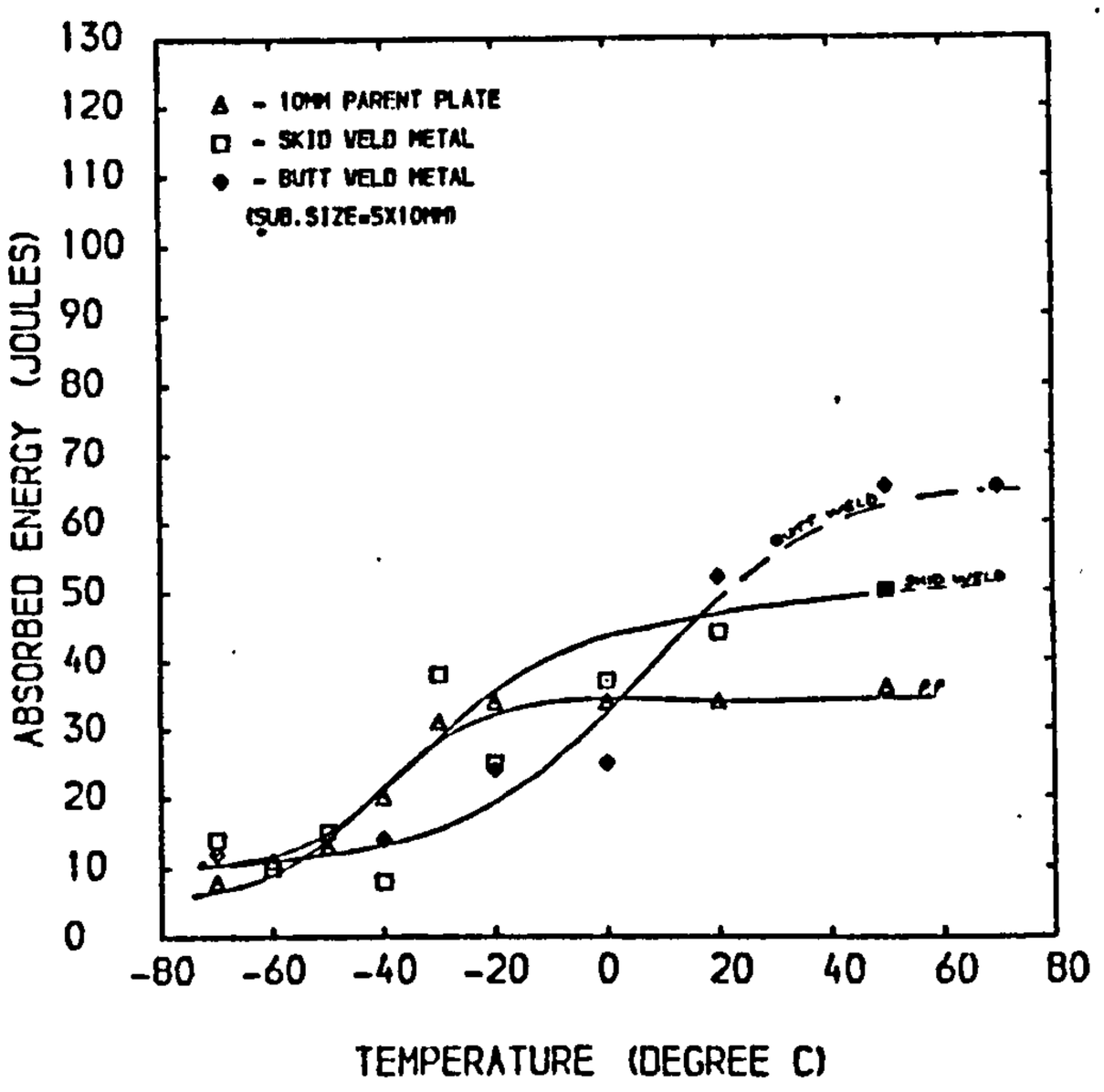

Figure 5.12c - Charpy transition curves for laser butt weld metal; 10mm plate, 9kW laser power, A31 filler wire

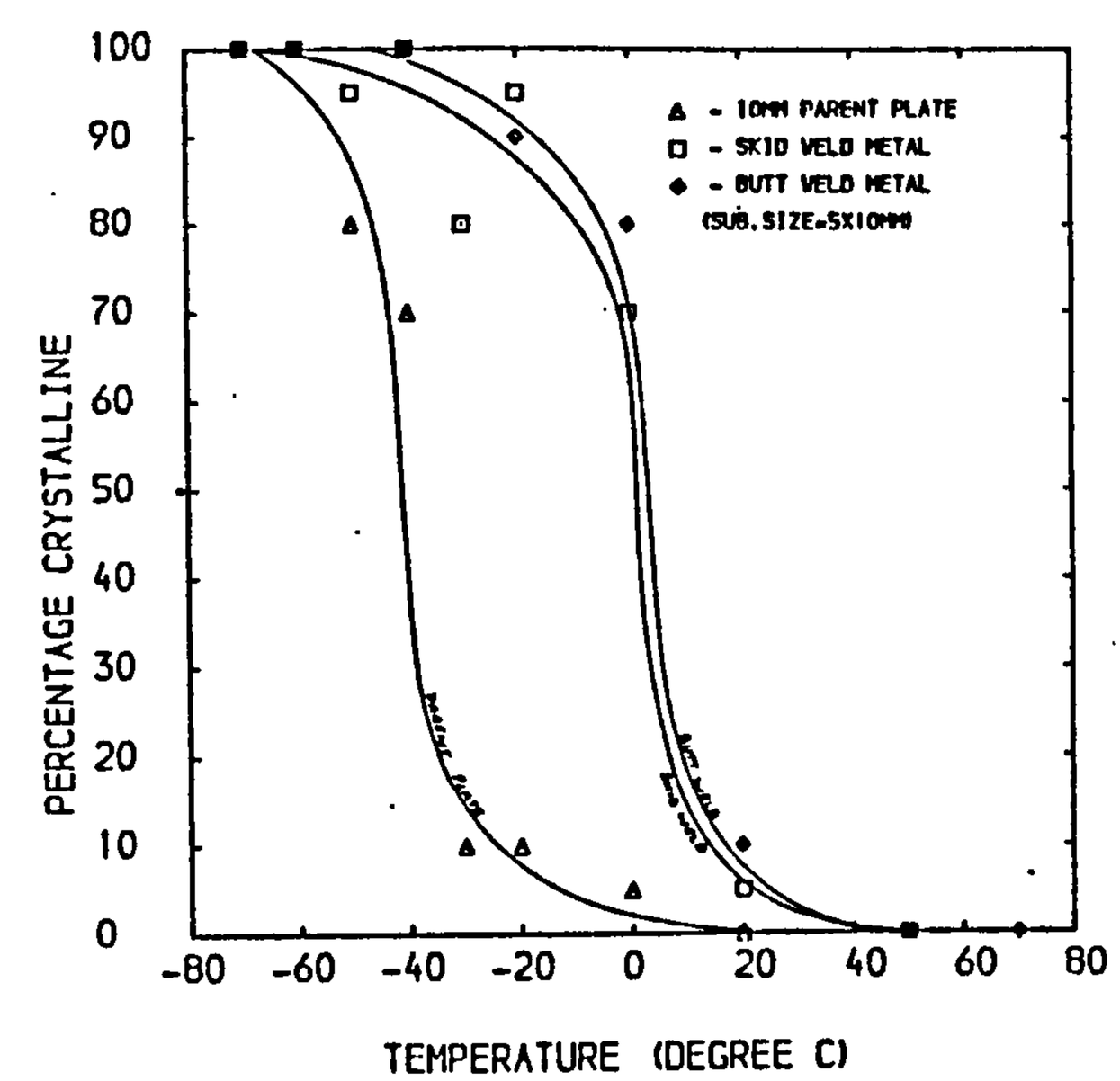

Figure 5.12d - Fracture appearance curves for welds detailed in Fig. 5.12c

PLATE THICKNESS	FATT °C		Tdv °C		18J TRANSITION		34J TRANSITION		UPPER SHELF ENERGY (J)	
(mm)	BUTT	SKID	BUTT	SKID	BUTT	SKID	BUTT	SKID	BUTT	SKID
6	6	(-35)	20	(-50)	(-20)	(-20)	9	(>20)	(50)	(>20)
8	-	-8	-	0	-	-20	-	(16)	-	(40)
10	9	4	20	50	-19	-33	0	-4	(65)	(50)
12	-	-10	-	20	-	-16	-	10	-	(40)
15	(14)	-20	20	20	-40	-34	-23	2	(85)	(60)
AVERAGE	10.3	-13.8	20.0	22.5	-26.3	-24.6	-5	12.8	65	42

NOTES: FATT = Fracture Appearance Transition Temperature (50% transition)
Tdv = Temperature at which fracture deviation initiates
( ) = Values directly influenced by fracture deviation

Table 5.06 - Summary of Charpy transition data for a comparison of the result for testing similar skid and butt weld metal.

Transition Temperature (FATT) ie the temperature at which the fracture surface shows 50% brittle failure.

For each graph, fracture deviation in a specimen has been noted by "solid" points and for results where subsequent inspection of the fracture face shows excessive defects eg large pores, the point plotted has been ringed.

Assessment of the transition curves produced for 8,10,12 and 15mm thick plate on the basis of non-deviating fracture specimens only, shows that the minimum requirements set by the classification societies were met. However, with the exception of welds in 10mm thick plate when values well in excess of the minimum have been achieved, acceptance margins were minimal.

The pattern of notch toughness and crystallinity results for 6mm plate is different. As noted in Table 5.06, fracture deviation started at a temperature of -60 °C, significantly lower than the average value found for the other plate thicknesses of -14 degrees C.

Visual examination of the fracture surfaces in the 6mm specimens showed that the fracture path had diverted to the fusion line which itself failed by brittle fracture as opposed to the the tearing action normally associated with the "plastic hinge" mechanism. This mode of failure continued to test temperature of +20 °C, so that a transition curve could not be produced.

Hardness traverses on these samples showed hardness in the HAZ adjacent to the fusion line in excess of 450Hv together with grain growth. This grain growth will have created a line of low cleavage resistance which, with the stress field at the notch tip extending into the HAZ and parent plate, failed before the weld material. Joint cooling rates for the butt welds are lower than for the cruciform joint due to the reduced combined thickness, so that the excessive fusion line hardness values were not encountered. Therefore, for the butt welds brittle fracture within the weld dominated until fracture deviation to the parent plate occurred.

The comparative results from the butt welded samples in 6, 10 and 15mm plate also showed higher apparent upper shelf energy levels where fracture deviation influenced results.

The third set of Charpy tests on samples produced using various filler wires was designed to investigate if the wire filler technique could be used for improving the laser weld toughness qualities. The prime objective was to reduce the 50% crystallinity transition temperature whilst maintaining or increasing the upper shelf energy level of the weld metal.

The individual curves produced are contained in Appendix C-4 (figure C5.02a-f) summarised in table 5.07 and show notch toughness and percentage crystallinity curves for the three plate thicknesses tested. No conclusion could be drawn to the general effect of each wire on upper

shelf energy levels as the results varied for each plate thickness, notably influenced by the effects of fracture diversion. Whilst the upper shelf toughness values for the 6mm plate show little variation for each wire the values for 10mm thick plate show improvements on the values found using the A31 wire. However by using the alternative wires the 15mm plate energy levels are reduced. These variations are possibly due to the joint effect of differing compositions and heat inputs for each plate thickness. Even so, all values are maintained well above the minimum set by classification societies.

However, the FATT results are more consistent for each wire used. While the transition temperature for welds produced using the A31 wire is maintained at an average of 10 degrees C welds produced using the other wires show lower values; the K-Nova wire showing an average transition temperature of as low as -35 °C. A similar trend is found when assessing the temperature at which fracture deviation commences (Tdv). Fracture deviation appears to commence at or below the 50% transition level for the butt welds in the normally ductile range.

Once the Tdv value was reached and the "plastic hinge" failure mechanism dominated, no single sample showed excessively low energy values. When unexpected low absorbed energy values were obtained below the FATT (1% of samples tested), sample macro examination showed a predominantly columnar weld structure grain growth, with grains interlocking in the weld centre as opposed to having a centre line zone of equiaxed grains for good welds. The interlocking structure provides a

TABLE 5 - CHARPY TRANSITION DATA FOR BUTT WELDS PRODUCED WITH VARIOUS WIRE INPUTS

PLATE THICKNESS (mm)	FATT °C					Tdv °C					18J TRANSITION °C					34J TRANSITION °C					UPPER SHELF ENERGY °C				
	A31	A18	S2	SD3	K-NOVA	A31	A18	S2	SD3	K-NOVA	A31	A18	S2	SD3	K-NOVA	A31	A18	S2	SD3	K-NOVA	A31	A18	S2	SD3	K-NOVA
6	6	-14	-20	-	- 60	20	-30	0	-	-50	-2	-48	-35	-	-73	9	(-13)	-9	-	-55	(50)	(48)	(46)	-	(48)
10	9	-13	(-2)	-17	-(50)	20	0	-20	0	-50	-19	-80	-52	-52	-74	0	-40	-15	-33	-64	(65)	(92)	(70)	(78)	(86)
15	(14)	(20)	(-2)	(0)	(5)	20	20	-20	0	-20	-40	-44	-70	-37	-39	-23	-4	-30	-23	-17	(85)	(55)	(85)	(75)	(60)
AVERAGE	10.3	-11.3	- 8.0	- 8.5	3.5	20	-3.3	-13.3	0	-40	-26.3	-57.3	-52.3	-44.5	-62	-5	-19.0	-18.0	-28	-45.3	66	65	67	76	65-

NOTES: FATT = Fracture Appearance Transition Temperature (50% transition)
Tdv = Temperature at which fracture deviation initiates
( ) = Values directly influenced by fracture deviation

Table 5.07 - Charpy transition data for butt weld metal to compare the effect of using various filler wires

centre-line cleavage path for the fracture to follow resulting in the low values.

The occurrence of such centre-line grain structures emphasises the need for special care to be taken in conducting Charpy testing of narrow welds. In order that potential crack initiation points are highlighted, the machined notch needs to be positioned directly on the weld centre-line.

The experiments using different wire filler types have shown that toughness properties can be improved by using alternative filler wires.

The molybdenum contained in the A31 wire for improving the tensile strength properties probably contributed to the marginal toughness values found in the second set of trials. Use of the non alloyed A18 wire wire would prove a better wire if a double deoxidant MIG wire is required. The S2 and SD3 wires showed similar properties for temperature transitions at 18J and 33J (27J and 47J for full size specimens) as the A18 wire.

Of greatest significance was the use of the C-Mn-Si-Ti wire. While upper shelf energy levels were similar to those experienced for the other wires, significantly lower transition temperatures were obtained. In addition to having a lower carbon level than the A18 and A31 wires the Ti acts as a grain refining agent thereby increasing the cleavage resistance without increasing the hardness.

5.4.6 Recommendations for Charpy value assessment

While Charpy testing remains a recognised and cost-effective method of assessing material toughness during procedure testing, an acceptance standard will need to be set by classification societies.

The results of the present study have shown that, while analysis of non-deviating fracture specimens would be preferred, if toughness properties well in excess of classification minimum requirements are to be produced, fracture deviation may start at test temperatures below those normally specified for procedural testing before classification societies formulate an alternative standard. Therefore, in order to accommodate such occurrences into acceptance standards the Author has proposed a revised procedure. This takes account of the fracture appearance in assessing the likelihood of brittle fracture. The procedure activities are shown in figure 5.13.

From a purely mechanical testing viewpoint the results obtained during the present trial have shown how the toughness of the laser skid welds tested by the Charpy V-notch test, will satisfy the existing requirements of classification societies.

By careful selection of the filler wire addition the weld properties may be improved also to give weld toughnesses associated with weld specifications required for service conditions to temperature of -20 °C whilst maintaining absorbed energies of 27J (full scale specimens) as

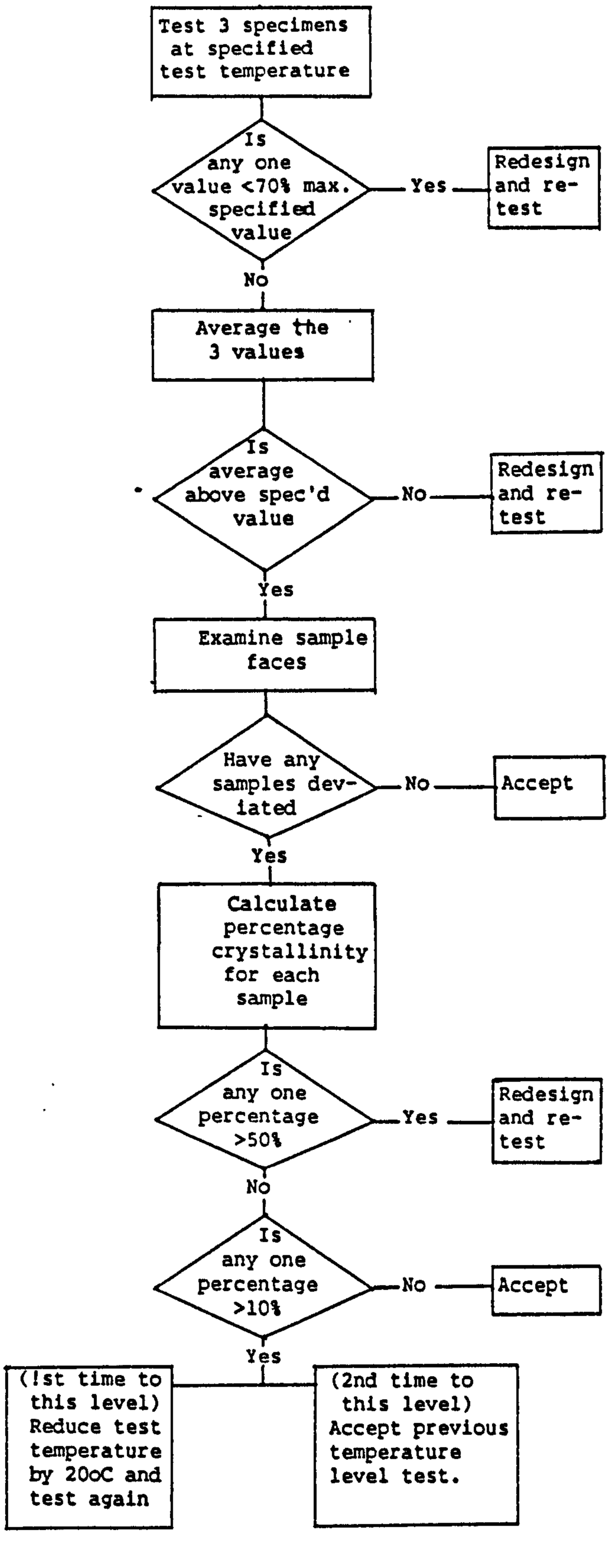

Figure 5.13 - Flow diagram for the proposed revised charpy testing schedule

defined by Lloyds to Grade 3Y.

Further analysis of the weld microstructure relating the weld mechanical properties to weld microstructure is conducted in Chapter 6. The present trials give enough evidence to show that further trials using a flux-cored type wire may be also of great value, to produce controlled additions of elements to control the weld microstructure and give the required mechanical properties [235].

5.5 FATIGUE TESTING

Fatigue failures in structures or components classified in a survey conducted by the International Institute of Welding [147] shows how, apart from failures in rotating shafts (36% of all failures) fatigue failures within ship structures had the next highest occurrence over the other, if somewhat subjective classes (engine parts, fatigue frames, cranes, pressure vessels, road vehicle axles, fans, bridges).

Yamaguchi [148] has categorised the various repeated loads acting on a ship's structure likely to cause fatigue failure:

1. Loads due to waves.
2. Loads due to the motion of liquid in tanks.
3. Loads due to vibration.
4. Other loads.

Most of the fatigue cracks observed in ship structures are caused by loading due to waves causing longitudinal bending of the ship and from repeated stress placed on transverse members due to changes in draught causing loading to side tanks. In addition there will be other repeated loads due to slamming and green seas. Under high frequency vibration the stress in the vicinity of the welded joint between stiffener and plate may be very high, creating a hazard for fatigue crack occurrence. Other loads could be due to changes of atmospheric temperature creating thermal stresses or for warships, recoil forces due to the firing of weapons.

Fatigue cracking will always initiate at a point of maximum stress concentration. Within a welded structure it is the geometric discontinuity caused by the presence of the weld itself which creates a stress concentration. Then, in the absence of any gross weld defects e.g cracks, lack of fusion, inclusions or porosity when crack initiation can take little time [149] the principal factors influencing the fatigue strength of the joint itself are the joint macro-geometry and the small slag inclusions at the weld toe which are inherent to most welding processes [150]. It is not surprising therefore that due to their shape and placing in a structure that the largest number of fatigue failures occur at fillet welds.

Appreciation of the consequences and necessary design considerations to minimise the likelihood of fatigue failure of marine structures has increased during the last decade. This is mainly due to the requirements being placed on the designers of structures for use in hostile offshore

environments. Joints or "nodes" in tubular constructed "jacket" type production and semi-submersibles platforms may give rise to particular problems of stress concentrations. These can result in dramatic failures and loss of life if undetected as occurred in the collapse of the accommodation platform Alexander L Kielland [85] in 1980.

Whilst the fatigue analysis of a tubular joint requires careful consideration in overall design, particularly for offshore operation, [151] fatigue resisting properties of welds themselves in a particular joint configuration, may be assessed in two ways - firstly by comparison with statistics of weld fatigue properties collected from various sources or secondly by conducting controlled tests to assess the specific joint in question.

As noted in the previous sections of this chapter, normal classification society rules concerning the testing of welds for surface vessels, require only the use of non-destructive or single cycle destructive tests. Therefore, to ensure minimal stress concentrations at the weld, the rules dictate shape and size criteria for the joint preparation and the weld material deposited. Ironically, structural failures often start from an unexpected discontinuity which can include slight faults from which a crack can easily propagate. The rules can only protect against such situations by ensuring good working practices.

As already stated the shape of the single-sided, skid weld does not conform to normal classification requirements. The leg length and throat

thickness of the smoothing beads is far smaller than a conventional fillet and the joint is in fact fully penetrating. This immediately reduces the potential number of crack initiation points.

With this background, discussions with classification societies [105] [106] [2] confirmed a need for some comparative fatigue testing of skid welded joints even though an exact ship-based, comparative specification was not available.

There have been only a few investigations of laser weld fatigue strength [32] [24] [25] [152] [70] [153] [154] [155] [156] , the majority being for laser butt welds. They all show the potential for forming compatible, if not superior joints when compared with coventional arc welded joints. Investigations have also been conducted on electron beam welds of similar shape [157] [20] [20] although again only on butt weld sections.

The only published reports of fatigue tests on laser welded tee section joints were conducted on twin fillet type welds by Hakansson [24] [25] . He reports such tests on double-sided weld joints to show the effect of varying edge preparation and parent plate composition on laser tee fillet joints. Fatigue experiments were conducted at a stress ratio of 1.3 for a loaded stiffener joint configuration, the joint being placed in plane tension. The results gained from the laser welds were compared against those found for twin fillet MMA welded control samples. Generally the laser weld fatigue life was greater than the control

samples. However shorter life resulted for joints made on primed plate or where the web edge had been flame cut as opposed to the shot blasted rolled flat stiffener type edges.

Fatigue strengths of steel joints made by conventional arc welding practice have been investigated by many organisations. A survey and statistical analysis of the results conducted by The Welding Institute [158] enabled design rules to be established in which joints are categorised according to their fatigue strengths [159] Subsequently these rules have been incorporated into the BS5400:1980:"Steel, concrete and composite bridges; Part 10 Code of Practice for Fatigue" [160] .

The standard presents a number of design "S-N" curves (of design stress against number of cycles fatigue life on a logarithmic scale) designated by the classifications B,C,S,D,E,F,F2,G and W. Each is representative of a "family" of joint types of reducing fatigue life. Therefore for a particular joint with an estimated number of cyclic loadings a limiting design stress range can be calculated.

The design curves correspond to the mean of the accummulated data minus two standard deviations and represent approximately 98% probability of survival. However for experimental comparison used in the present work the source data itself was used.

5.5.1 Tee Joint Classification within B.S.5400

The fatigue strength classification appropriate to a conventionally welded T-butt joint is shown in figure 5.14. Designated Modes 1 to 3 for the purpose of the experiments are as follows:

1. Mode 1 - Nonload-carrying stiffener; the oscillating force applied within the face plate perpendicular to the stiffener. Failure normally involves crack propagation from the weld toe through the face plate perpendicular to the applied stress. Consequently any undercutting in the weld toe will help to initiate the fatigue crack. Class "F" is assigned to this particular configuration.
2. Mode 2 - Load-carrying stiffener; the oscillating force being applied through the web perpendicular to the face plate. Classification is dependent on the source of crack initiation and the extent of weld penetration.

For the non-penetrating fillet weld, failure will occur either in the stiffener weld toe when class F2 applies, or, if the fillet size is too small, failure will initiate from the weld throat when class W, the lowest fatigue strength, applies.

For fully penetrating tee butt ("K" butt) welds there is no discontinuity in the middle of the joint from fillet roots so that the most likely failure position is again at the web toe and classified as class F.

3. Mode 3 - Load-carrying stiffener; the oscillating force was applied

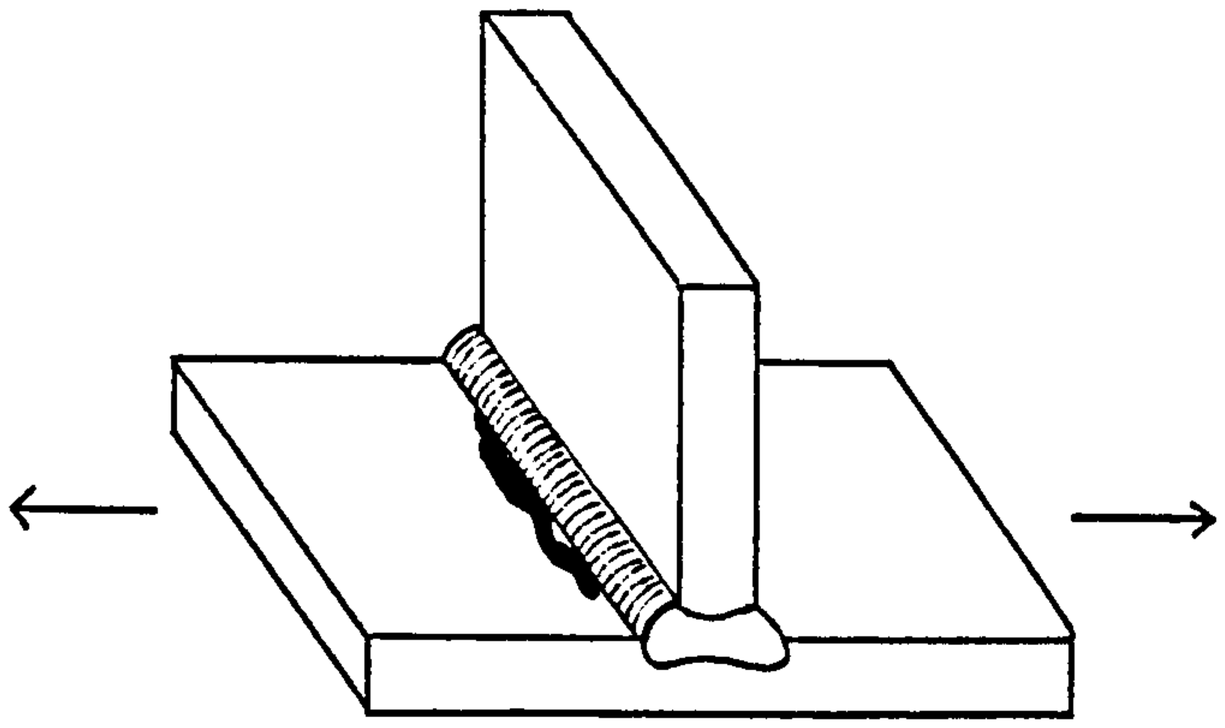

Mode 1 loading - failure at weld toe in load carrying plate, Class F.

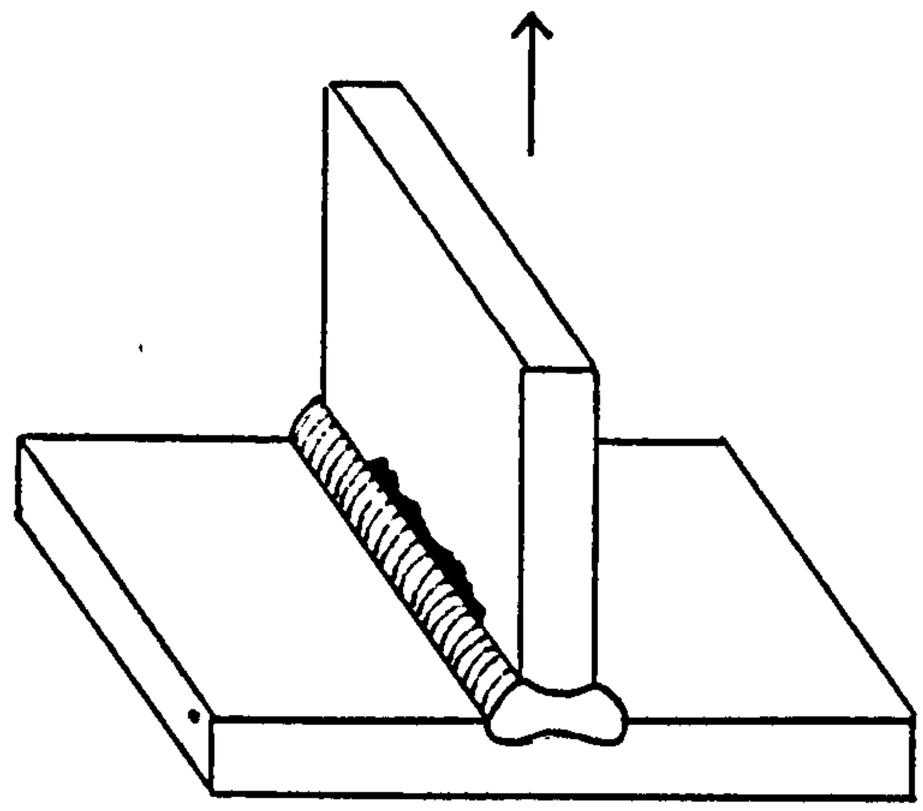

Mode 2 loading - failure at weld toe in stiffener for non-penetrating joint, Class F2; for fully penetrating joint, Class F; for failure at weld throat, Class W.

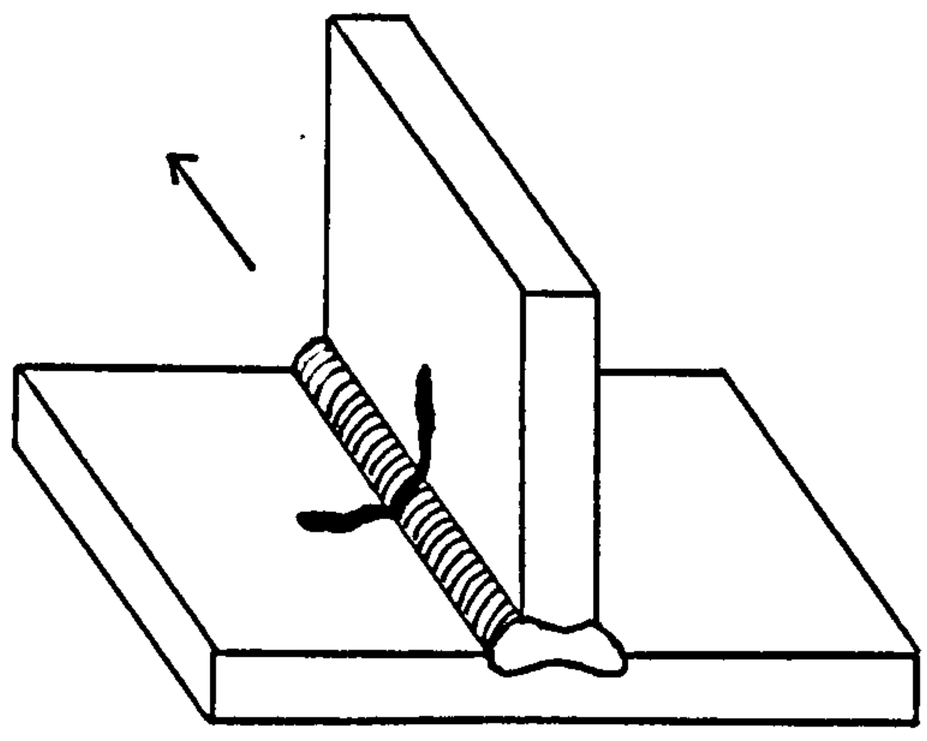

Mode 3 loading - failure from ripple on weld face, Class C or D.

Figure 5.14 - Three principal modes of fatigue loading for tee section joints and respective modes of failure

parallel to the joint within the face plate. Crack initiation would be at a surface discontinuity such as weld surface ripples or from an internal defect. The classification of C or D is the highest class of fatigue strength for the three modes and is therefore less critical to a design.

Because of the lower levels of the predicted failure strength for conventional welds, Modes 1 and 2 were selected as being the most suitable for a study of the laser weld fatigue strength properties.

The programme of fatigue trials was executed by The Welding Institute to ensure consistency of experimental standards between the present trials and those reported for the British Standard data base. Two sets of trials were commissioned and conducted to the requirements and using specimens provided by the Author. The first set of tests was conducted in Mode 1 and has subsequently been reported by Tubby [161] - Appendix C-5.

This mode was chosen because the most common defect in laser skid weld production had been the tendency for a small amount of undercutting (<0.5mm) at the emergent bead toe in the face plate. For conventional welds the maximum allowable depth of undercut as defined by British Shipbuilders Steelwork Standards [162] for fillet welds is 0.8mm and by BS4870:Part1:1981-"Approval testing of welding procedures" [126] is 0.5mm. Therefore in accepting some undercut in the skid welded samples to be fatigued to a maximum depth of 0.5mm and by firstly testing in the

Mode 1 configuration it was ensured that the weld profile would give practical weld fatigue properties.

Improvements in fatigue life compared with conventional fillet welds would be expected as a consequence of micro-geometry. Slag inclusions at the fillet toe, often extend 0.4mm into the weld surface [30] for conventional flux welding processes. This has a detrimental effect on fatigue life. The inclusions act as pre-existing cracks which start to propagate as soon as the cyclic loading commences, thereby shortening or eliminating the crack initiation period. In order to reduce this effect, processes such as grinding, shot peening [163] or plasma dressing [164] are often used. The laser skid weld should not require such post-welding treatments as the use of the inert gas shrouding precludes the possibility of ingress of any slag inclusions from the shielding mechanism.

After successful completion of the Mode 1 tests, comparing the results not only against the British Standard but also against control sample (MMA) results, tests were designed for Mode 2 testing.

Two alternative methods of testing were available as shown in Method "a", figure 5.15 a-b; applying an oscillating force to the web of a tee-shaped sample simply supported at the face plate surface, appeared to reproduce the types of loading expected of a ship's panel structure with bending stresses generated in the transverse plate, creating stress concentrations at the weld toe. However, in addition to the lack of

comparative information for testing conventional welds by this method, analysis of the distancing of the knife edge supports away from the web to ensure failure in the web (Appendix C-6) showed that they would have to be placed to within 2.6mm of the web centreline i.e. very little bending would actually occur.

Method "b"; applying an oscillating force between opposite webs in a cruciform configuration, while ensuring failure in the web also enabled direct comparisons with standard design data, mode 1 tests and fatigue tests conducted on double-sided laser tee welds [24] Therefore this method of testing was chosen for the second set of trials.

5.5.2 Fatigue test specimen manufacture

Test specimens were extracted from a number of weld samples produced in consecutive runs; firstly for the tee section mode 1 tests and secondly in a cruciform configuration for Mode 2 tests as shown in figure 5.16. The specimens were cold sawn from the parent samples then machined parallel and square. Sharp corners of the specimens were ground by hand to ensure cracking initiated within the joint zone.

During the welding of each parent sample, care was taken to ensure that distortion was minimised in the load carrying member.

Angular deflections of one and three degrees to the face plate member were pre-set in the mode 1 samples by cold flanging prior to laser and

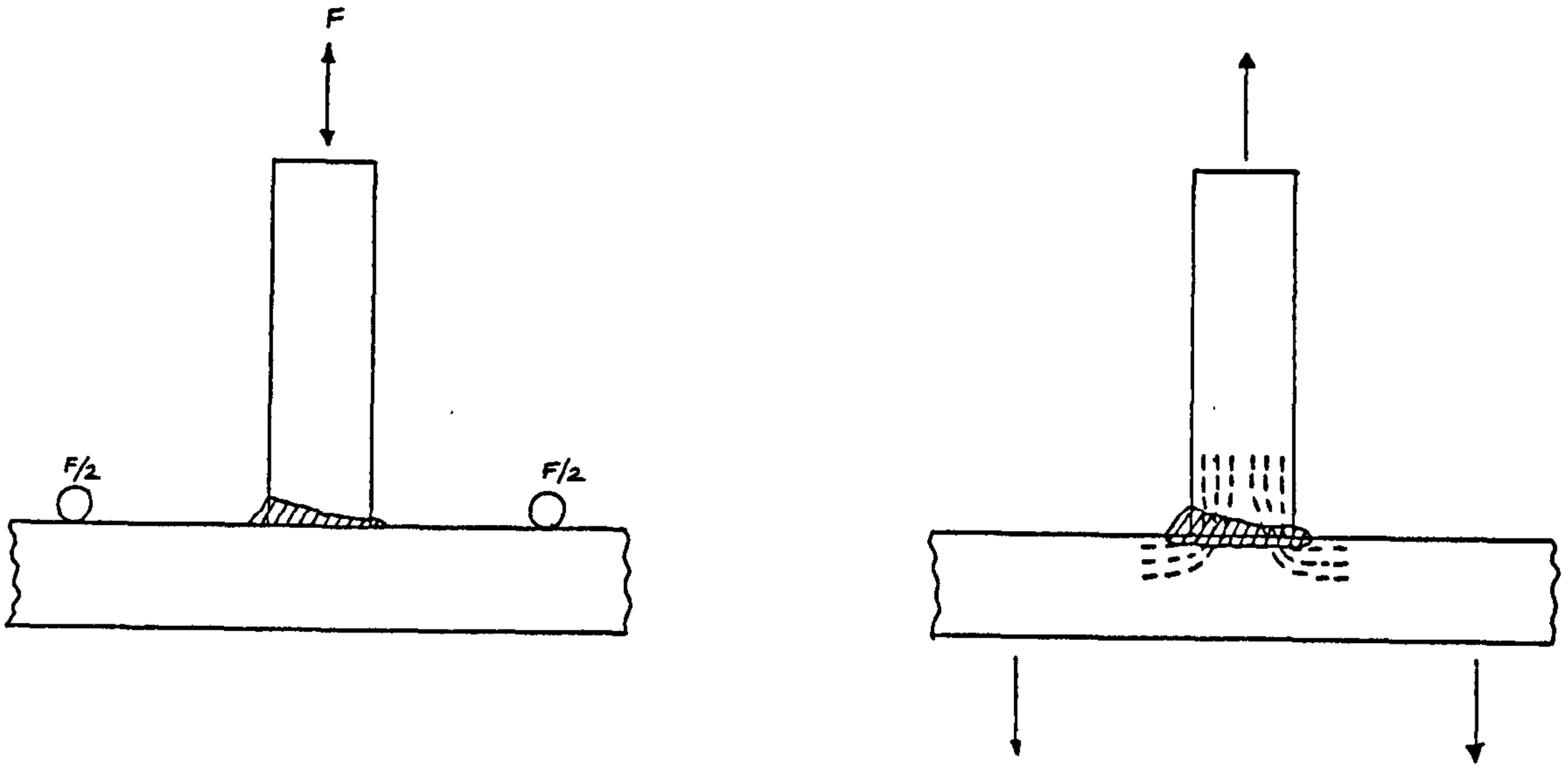

a) Tee section bending about simple supports

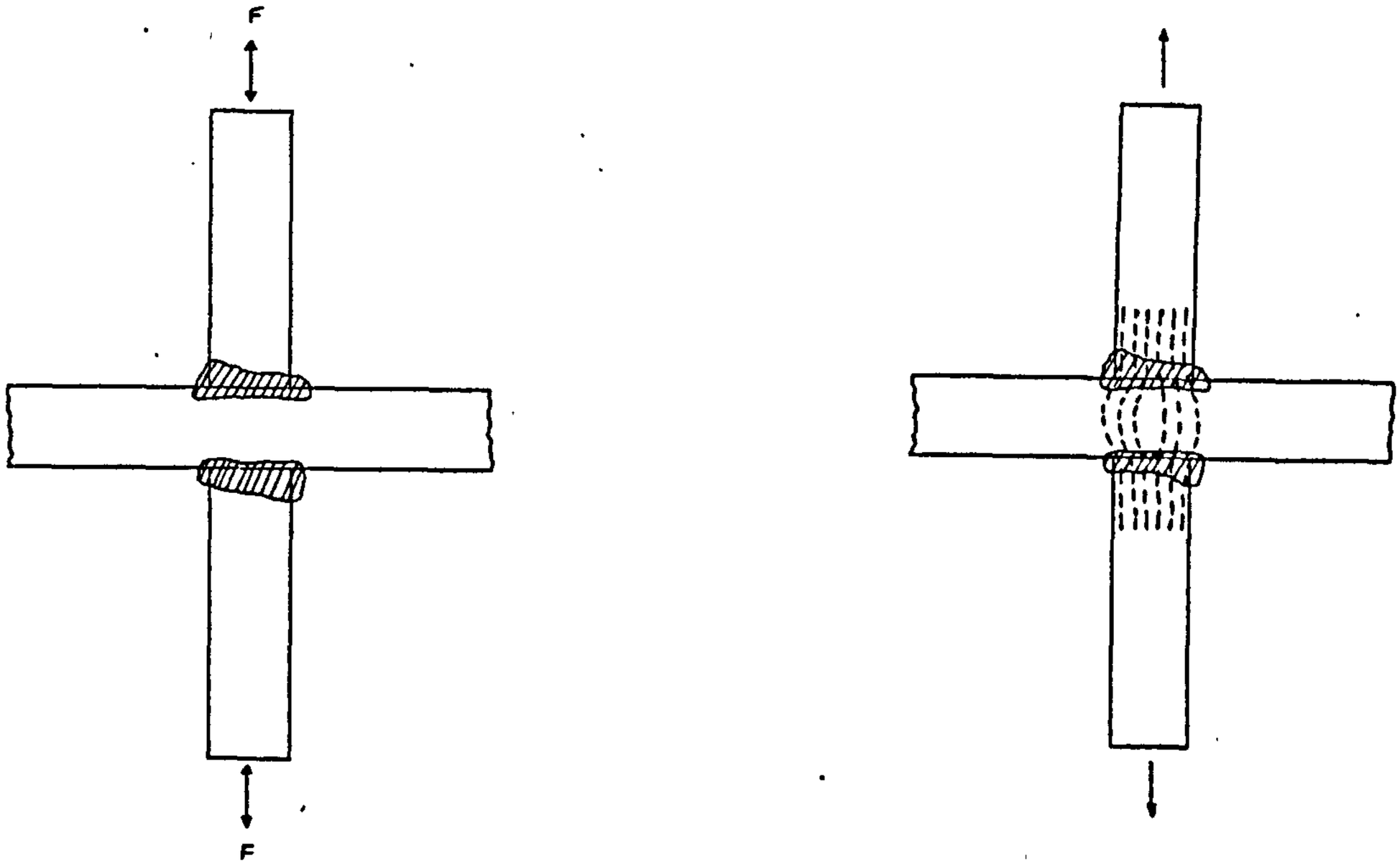

b) Cruciform section in tensile loading

Figure 5.15 - Two alternative arrangements for applying a fatigue load for the Mode 2 failure and associated stress flow lines

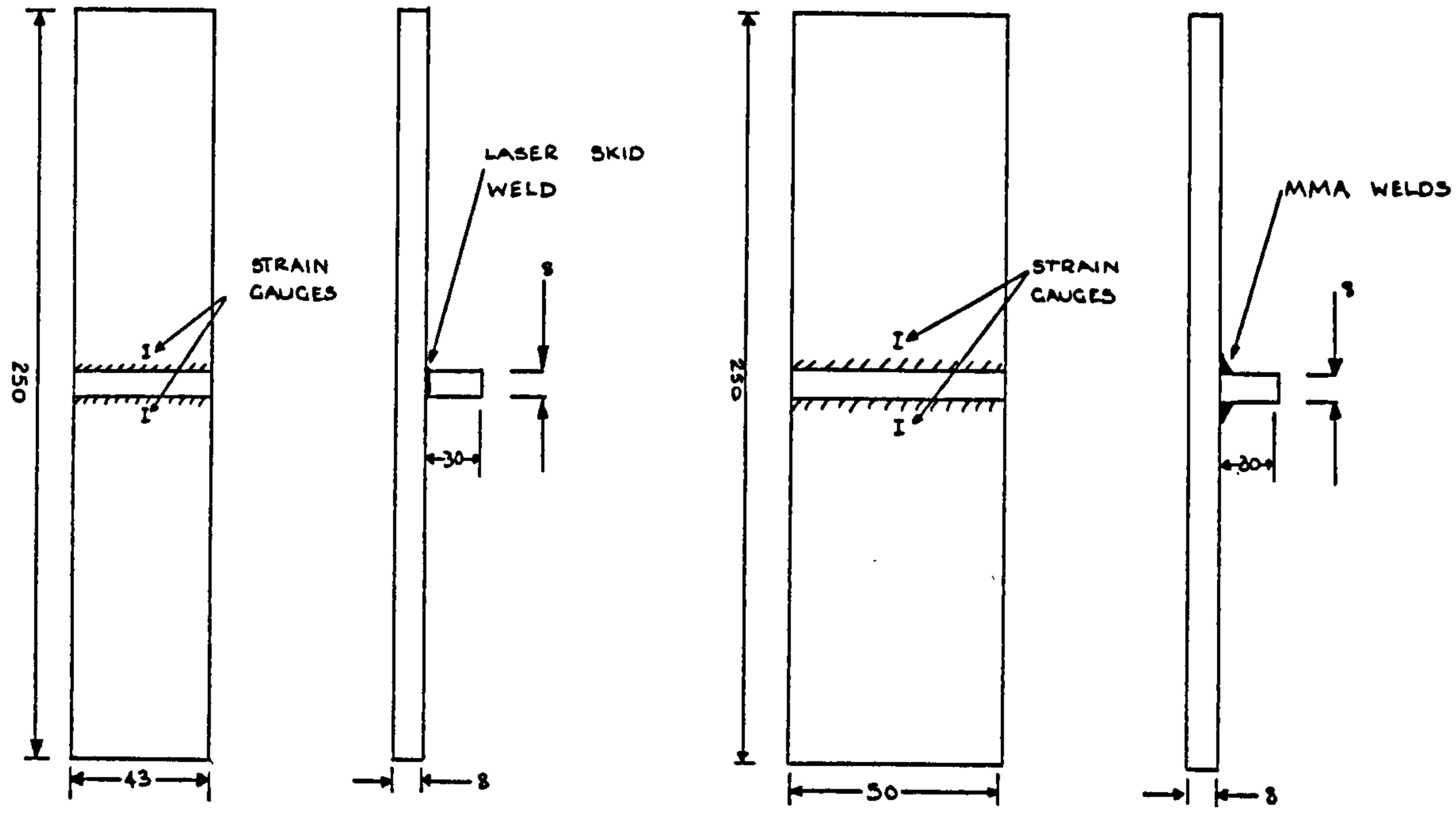

a) Test and control samples for Mode 1 testing

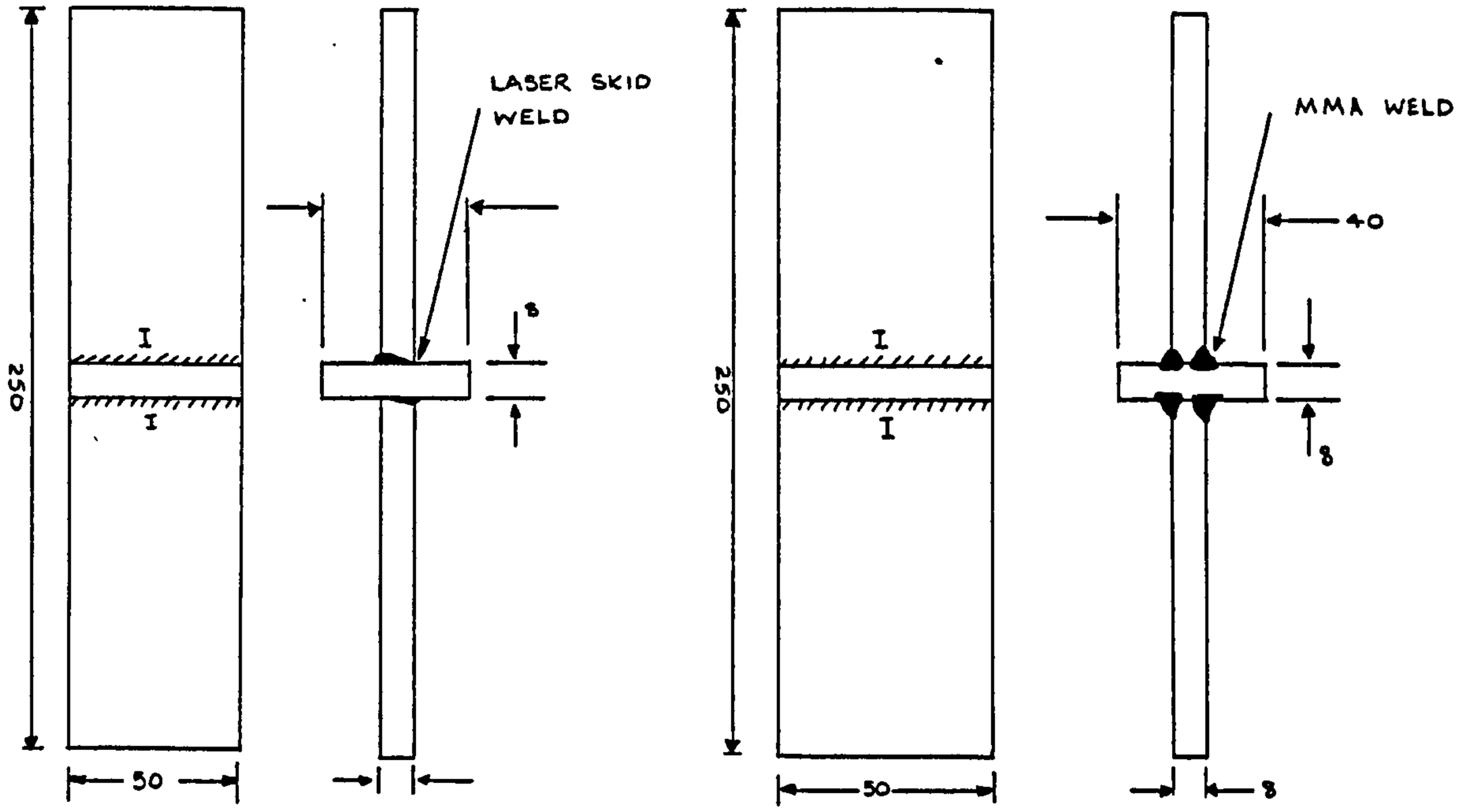

b) Test and control samples for Mode 2 testing

Figure 5.16 - Dimensions of fatigue test specimens

MMA welding respectively, in order to minimise distortion in the finished joint. These angles had been calculated from measurements taken on previous samples (Trial 5) to assess weld distortion. However, even though some samples still had small angular misalignment, no attempt was made to straighten the specimens so as to avoid modifying the residual stress distribution. Instead, 3mm gauge length foil resistance strain gauges were bonded on the sample centre-line close to the weld toe to measure the tensile stress at that point. This practice not only is sensible for research purposes but has also been advised in order to get an accurate measurement of ship loadings actually at a joint [149] .

Alignment of the cruciform web plates was assured by producing the pre-tacked sample in a specially designed jig and attaching this again during the final welding process. During the multi-run MMA welding of later control samples a conventional welding procedure was devised to ensure that the webs remained in line. Even so, strain gauges were again positioned to ensure consistency of results.

5.5.3 Fatigue Testing Details

All tests were conducted in laboratory air at room temperature. Test loads were varied between specimens to achieve fatigue lives in the range 10^5 to 10^7 cycles. The majority of tests were conducted in an electro-magnetic resonant test machine (Amsler Vibrophone) at a frequency of 100Hz. However, during Mode 1 testing at stress ranges above 240 N/mm2 a servo-hydraulic testing machine (Mayes) was used with frequencies

of 11Hz in order to achieve higher loads. This machine was used because the load that had to be applied in order to achieve the required tensile stress at the joint, was higher than expected due to the straightening necessary for the remaining slight distortion.

Compared with normal ship loadings the frequency of loading is very high, but it is consistent with the frequency used to produce data for the design codes. In comparison, Galsworthy [165] reports low frequency (0.008Hz) corrosion fatigue trials on narrow EB welds in marine environments. Satisfactory results have been obtained when compared with the properties of the parent plate. With the similarity of EB and laser welding processes, the present Author would expect the higher frequency results to be consistent with classification society requirements.

Compatibility between the electro-magnetic and hydraulic machines operation was checked by running both at similar stress ranges (223, 225 N/mm) resulting in similar fatigue lives (9.6×10^5 ; 9.68×10^5 N/mm^2). For both machines the stress ratio (i.e. minimum stress divided by maximum stress) while designed to be nominally 0 was maintained in the range 0 to 0.1.

Tests were continued until fracture sections either completely separated (in the hydraulic machine) or when failure through the major part of the test section led to an unstable running condition of the resonant testing machine. A life of 10^8 cycles was selected as the upper limit when machines were stopped.

5.5.4 Fatigue Testing Results

Mode 1

Figure 5.17 shows S-N curves produced from both laser and MMA control sample fatigue tests in mode 1 configuration. The 95% confidence limits for similar joints made by conventional arc welding practice [158] are also shown.

All the samples, both laser and control failed in the weld toe across the load-carrying flange member, figure 5.18a. From the laser samples, only one failed in the joint incident side; all the others failed in the emergent side

Fatigue fracture surfaces, figure 5.18b show similar crack development paths: multiple crack initiation at the weld toe followed by a semi-elliptical crack development through the plate thickness

Comparison of the experimental results show marginally superior laser results within the scatter of the test lives. Comparison with the confidence limits of the data used as a basis for the British Standard design curves show how all the results, including those for MMA welds, lie near the upper confidence limit in a band of shallower slope.

Three possible factors could contribute to this situation. Firstly, the standard data is taken from joints of a thickness range from 12.5 to

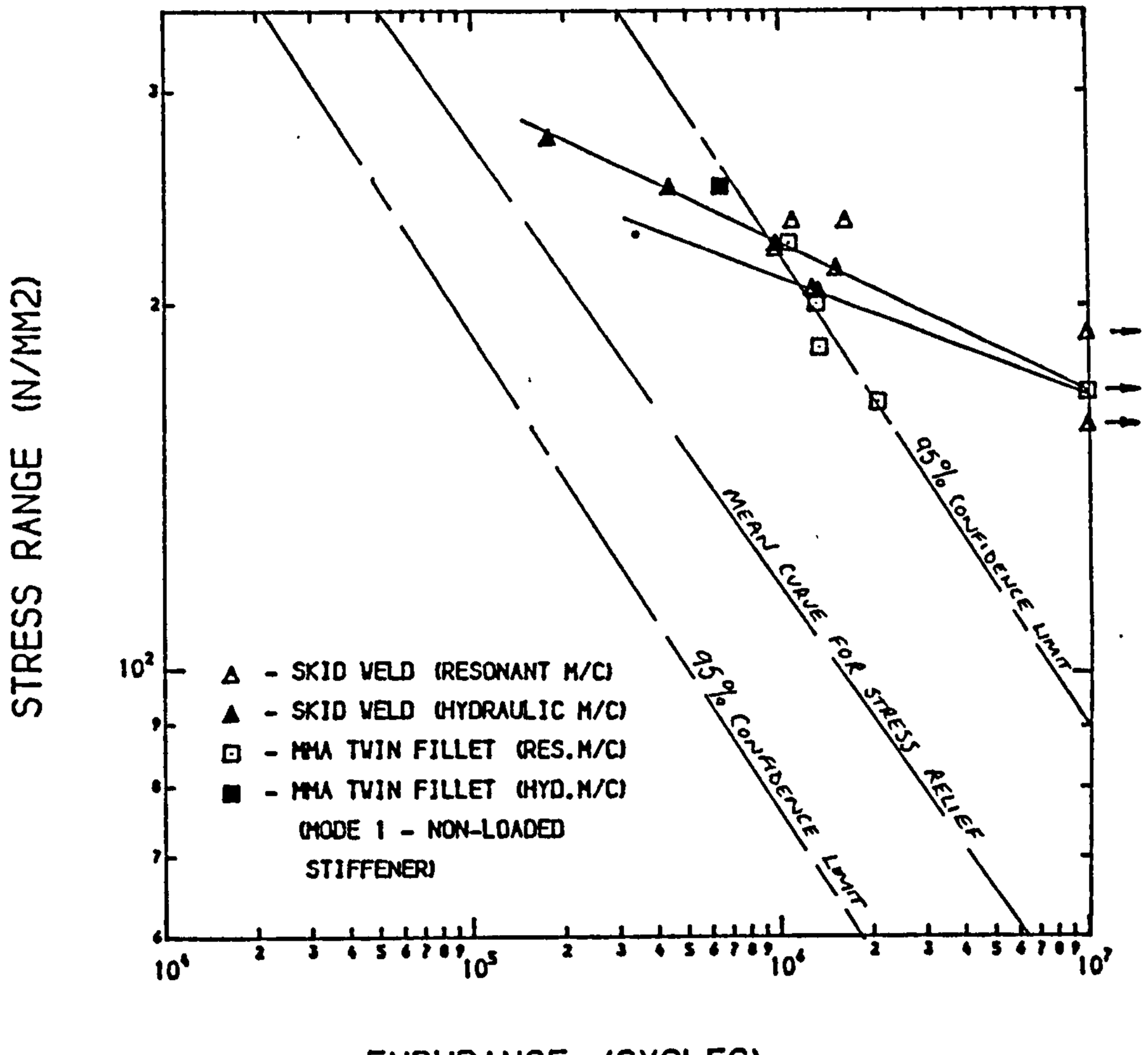

Figure 5.17 - Fatigue S-N curves results for Mode 1 loading - non-loaded stiffener

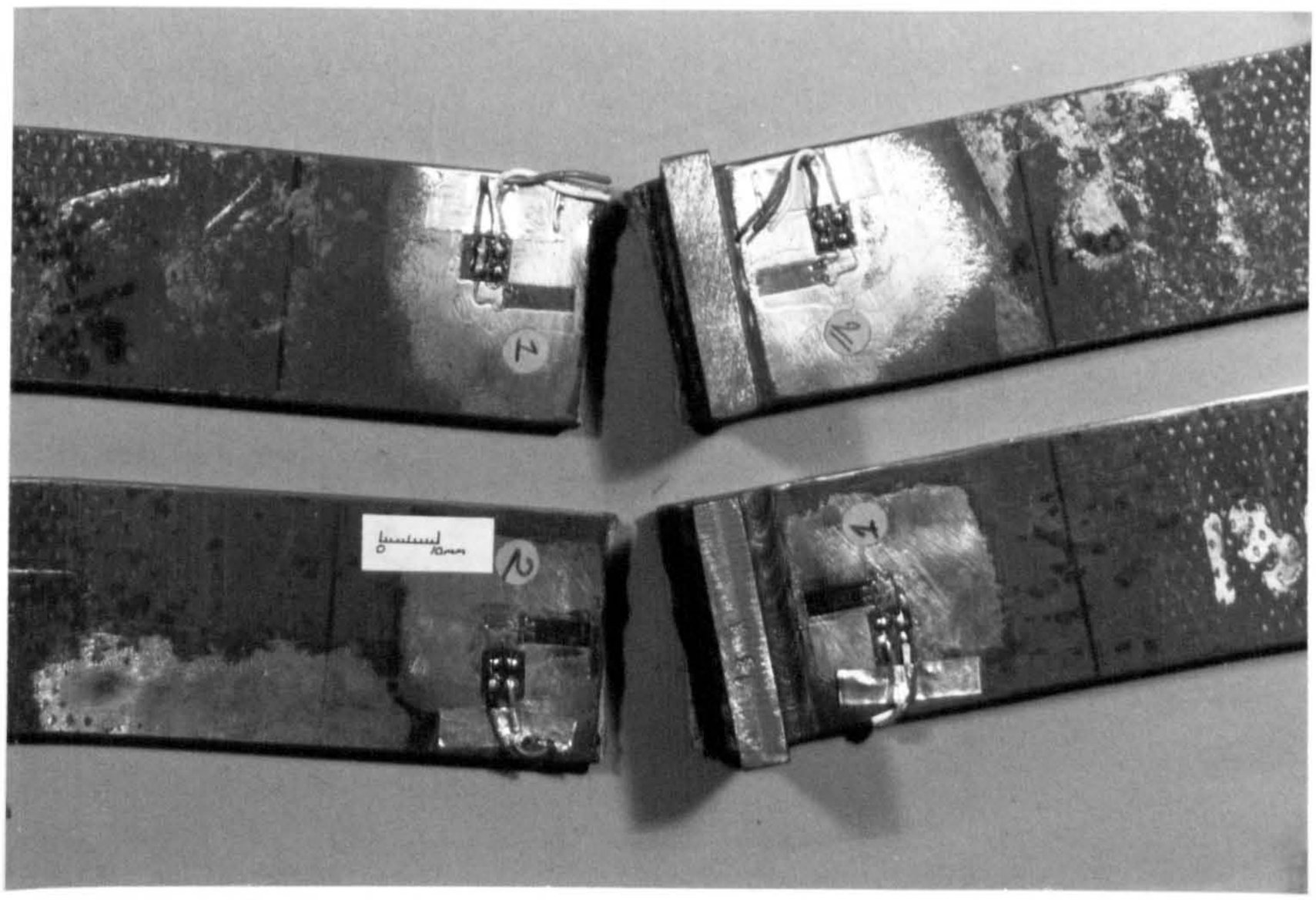

Figure 5.18a - Fatigue failure in the weld toe for non-loaded stiffeners, laser skid and MMA twin fillet welds

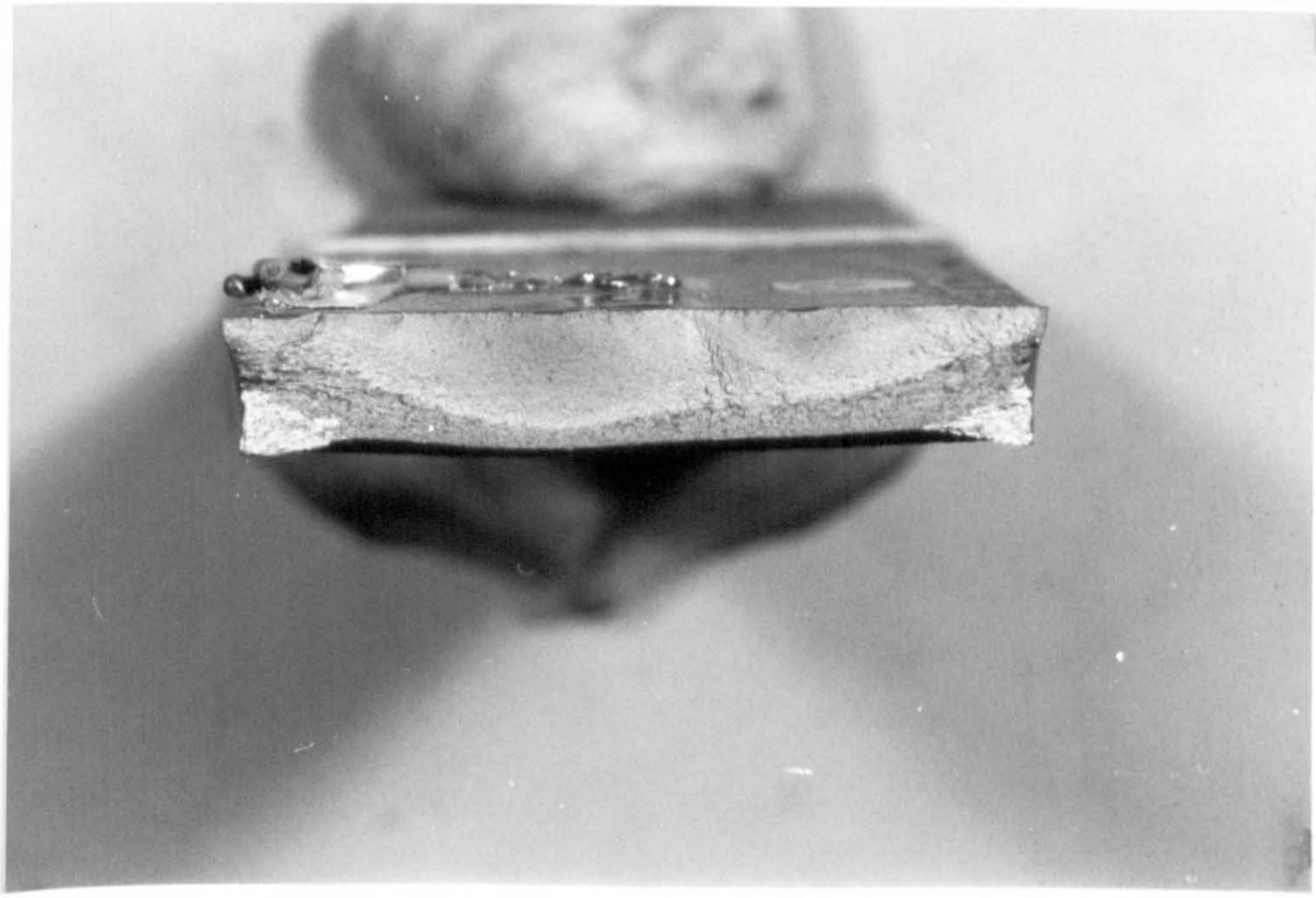

Figure 5.18b - Fatigue crack surface

16 mm while the Authors tests reported here were conducted using 8mm thick plate. Gurney [166] in studying fatigue in offshore structures, notes how higher fatigue strengths can be expected in thinner plates as a result of the reducing effect of stress concentrations at plate edges. A recent investigation into the effect of geometry changes upon predicted fatigue strength of welded joints [167] also concluded that increasing plate thickness decreased fatigue strength in geometrically similar joints, confirming the above views.

A second factor is the influence of bending. Figure 5.19 shows a comparison of the mode 1 data against S-N curves produced by The Welding Institute for joints in 6mm plate subject to both tensile and bending forces. The curve for bending is higher and slightly shallower than that for the axially loaded joint. However, the fact that the present data, for thicker plate, lies in a higher band and not, as predicted by the discussion above, in a lower band, leads to a need for further explanation.

Joint geometry is finally considered as a contributing factor. Gurney [168] notes how specimens with attachments on one side, as used for the present experiment, have often given higher fatigue strengths than those with attachments on both sides, as used for the comparative S-N curves. The difference in stress concentrations at the weld toe have been further demonstrated by Gurney by reference to photo elastic tests showing greater stress concentrations at the web toe for attachments on both sides.

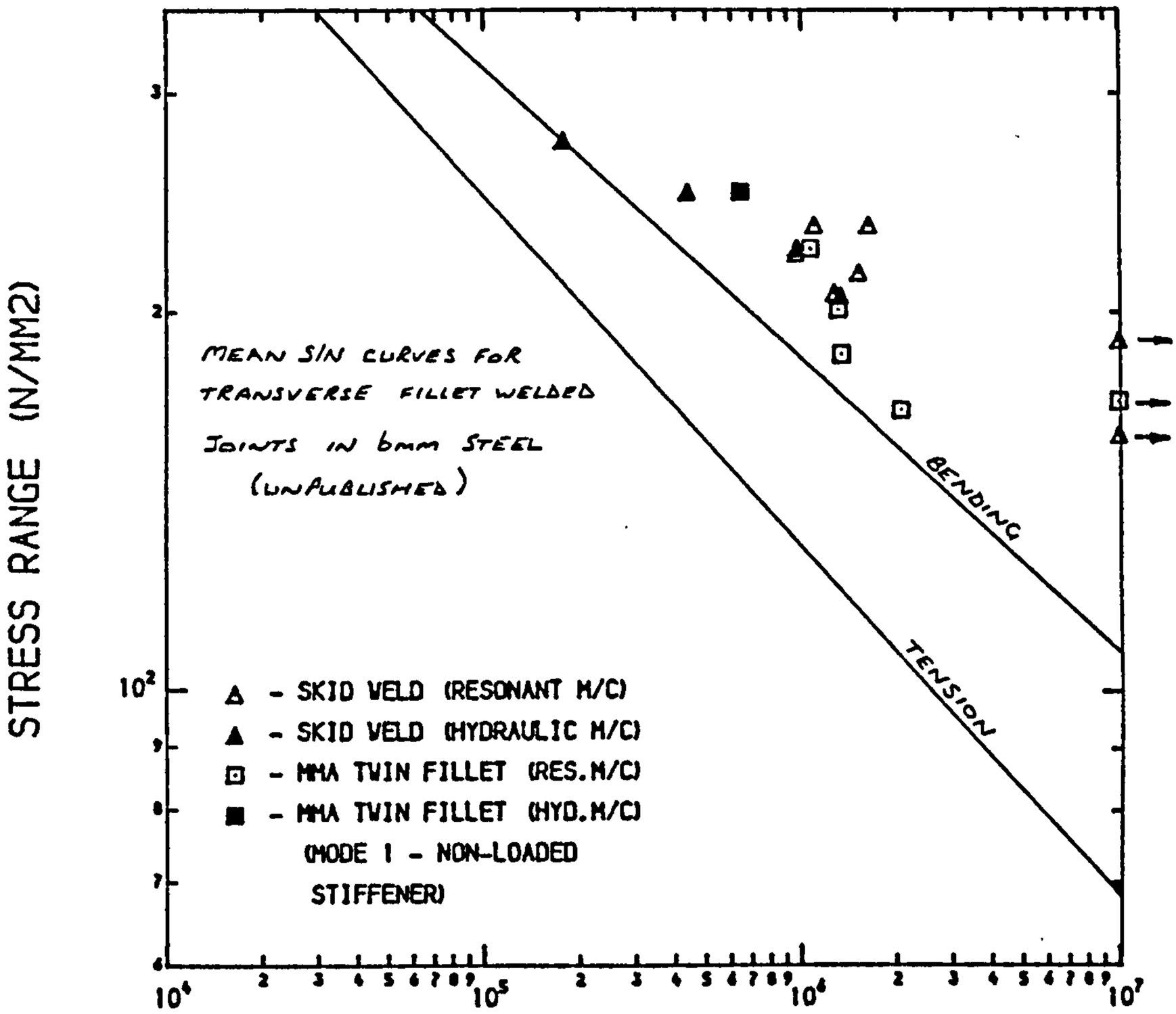

Figure 5.19 - Comparative results of a non-loaded stiffener for contol results in bending and tension

Notwithstanding the above discussion the testing of both laser welds and MMA samples under similar conditions has established comparability, if not marginal superiority, of the laser welded joint on the same basis as required by conventional design rules.

Mode 2

Figure 5.20 shows S-N curves produced from both laser and MMA control sample fatigue tests in the Mode 2 configuration. As detailed for the Mode 1 experiments, 95% confidence limits for similar joints (F and F2 design class) have been superimposed.

Out of three laser welds tested, two failed from the weld toe in the loaded plate and one, previously suspected of containing crack type defects found after dye penetrant checks, failed within the weld metal. The MMA samples produced with fillets as prescribed by the classification society rules (6mm leg) failed at the weld throat which under normal circumstances would place the weld within the lowest "W" design class. The Author was concerned to find that, contrary to fatigue test evidence, dynamically loaded ship structures are, often by default, being designed to this lowest class where failure is most likely to occur in the weld throat. Clearly this would be overcome by using the fully penetrating skid weld. To ensure failure in the weld toe as for class F or F2, a calculation, appendix D, showed that a leg length of greater than 8.5mm was required. The subsequent welds, using a 3-run welding procedure producing a 10mm leg joint, failed in the the weld toe as expected.

Fatigue fracture surfaces show characteristic semi-elliptical crack development. The fracture surface of the laser weld suspected of containing a crack defect showed a surface band of non affected fine granular structure adjacent to the weld edge. Interestingly, the other

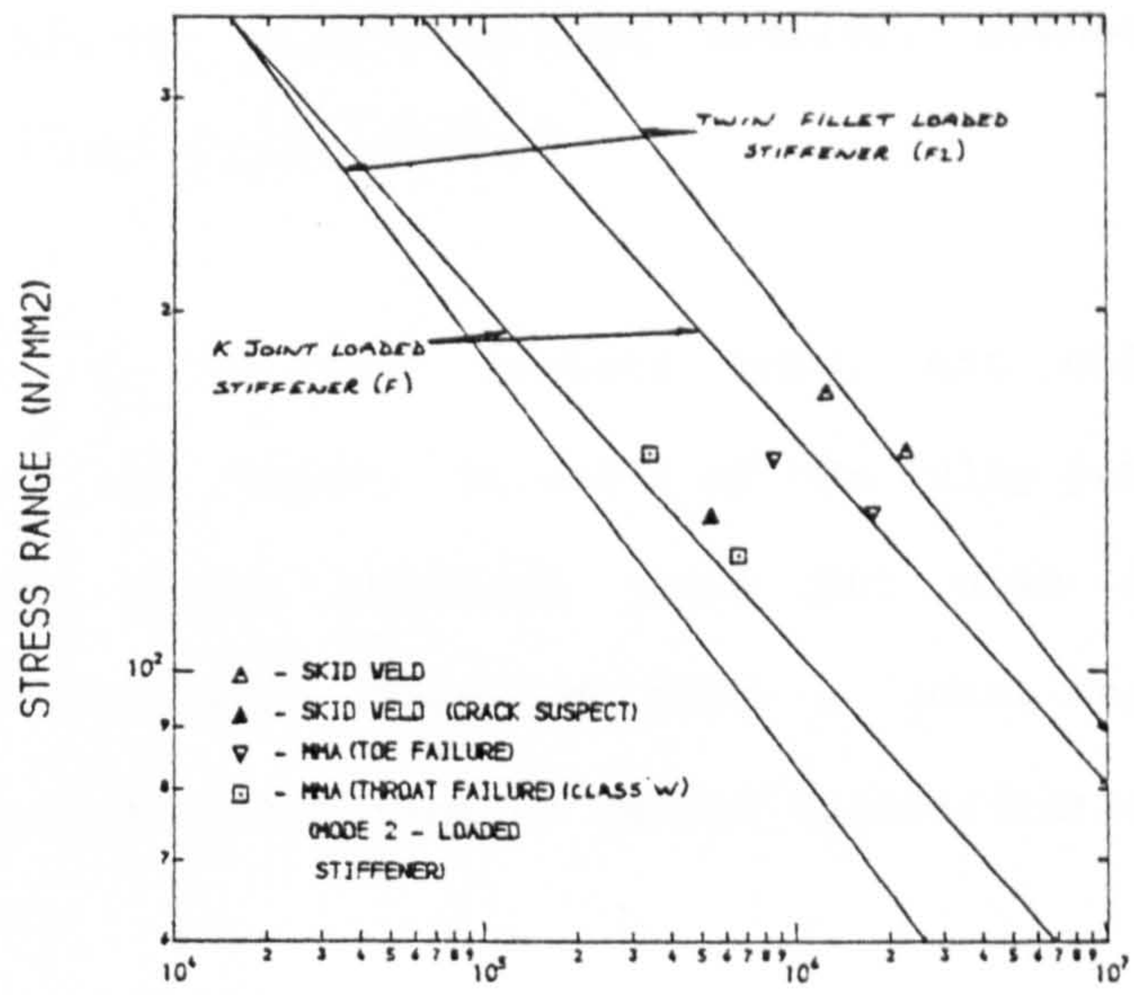

Figure 5.20 - Fatigue results for Mode 2 fatigue testing - loaded stiffener

Figure 5.21 - Fatigue crack surface showing areas of weld defects

laser welds fatigued in Mode 2 show similar, although less extensive features, as shown in figure 5.21.

Comparison of the test results show, not only the significant difference in the higher strength of the fully penetrating laser weld over the twin fillet standard joint but also other evidence of superiority, even when compared with a joint failing from a similar initiation point giving a similar design classification.

Comparison with the source data for the British Standard design rules shows the laser weld results lie on the upper 95% confidence limit for the twin fillet loaded stiffener and above that for the fully penetrating joint configuration even though defects were found within the same welds.

In view of the discussion about the high overall values obtained during Mode 1 testing, it should be noted that the results of the control MMA samples for Mode 2 (10mm leg) lie nearer the mean than the upper boundry. While both specimens had some undercut at the weld toe, which would have contributed to early crack initiation, the Mode 2 comparison compares the results of experiments on similar joints (i.e. both test and source data were for a cruciform joint configuration), increasing the probability that the joint configurations have a more significant relation with the fatigue strength in this particular case as opposed to any effect of thickness variations.

5.5.5 Alternative method for assessment of comparative fatigue properties

The use of conventional fatigue testing techniques have been described for tests in the Mode 1 and 2 stiffener loading configurations. However, such tests are expensive and time-consuming. Therefore, an alternative method of comparative assessment was selected for Mode 3 examination.

Just as weld surface and toe profiles have been considered as major contributing factors affecting the fatigue life of transverse loaded joints, so for continuous welds, loaded parallel to the joint line, it is ripples on the weld face or defects at the weld root which are most likely to initiate a fatigue crack. Therefore, for fully penetrating laser skid welds with the problems associated with root defects of twin fillet welds removed, a method of quantitatively comparing surface profiles was required to make a comparative assessment of the potential fatigue characteristics.

A direct comparison of surface roughness with fatigue strength was made by Goldberg [169] when assessing the effects of varying cut quality on fatigue strength for flat plate samples. He used a vertically-mounted needle, tip radius 0.25mm, resting on a sample which was traversed on the bed of a milling machine. The needle movements were transmitted from a transponder to a calibrated pen plotter. Measurements could then be made from the plot produced.

Although this method appeared to give roughness data that could be related to fatigue strength for cut edges, examination of Goldberg's profile measurements showed how the recording of the trough bottom shape could have been restricted by the size of the probe tip i.e. trough bottom profile is limited to a 0.25mm radius shape.

However, fatigue cracks are more likely to be initiated from sharp tipped discontinuities which will create a greater likelihood of stress concentration. Therefore, in the present experiments the Author has used a more sensitive device, with a stylus type probe (tip radius 0.3 um), figure 5.22, often employed for measuring the roughness of ship's hull surfaces [170] .

In order that this test could also be considered as a "non-destructive test", a replica was first made of the weld profile, figure 5.23. Firstly a 100mm length of weld in the horizontal position was isolated using plasticine "dams". Silicon rubber was then poured in between the dams to cover the weld surface. Once set this "male" plug was removed from the weld and placed in a compound of Solventless Flexible Polyurethane Elastomer. After 12 hours the plug was removed to leave a accurately cast replica of the weld surface.

Replicas of both laser skid weld incident and emergent beads were produced together with control replicas from MMA fillet welds. A number of traverses were made on each sample using a "Ferranti Surfcom" stylus machine incorporating a three micron truncated pyramid stylus. Each

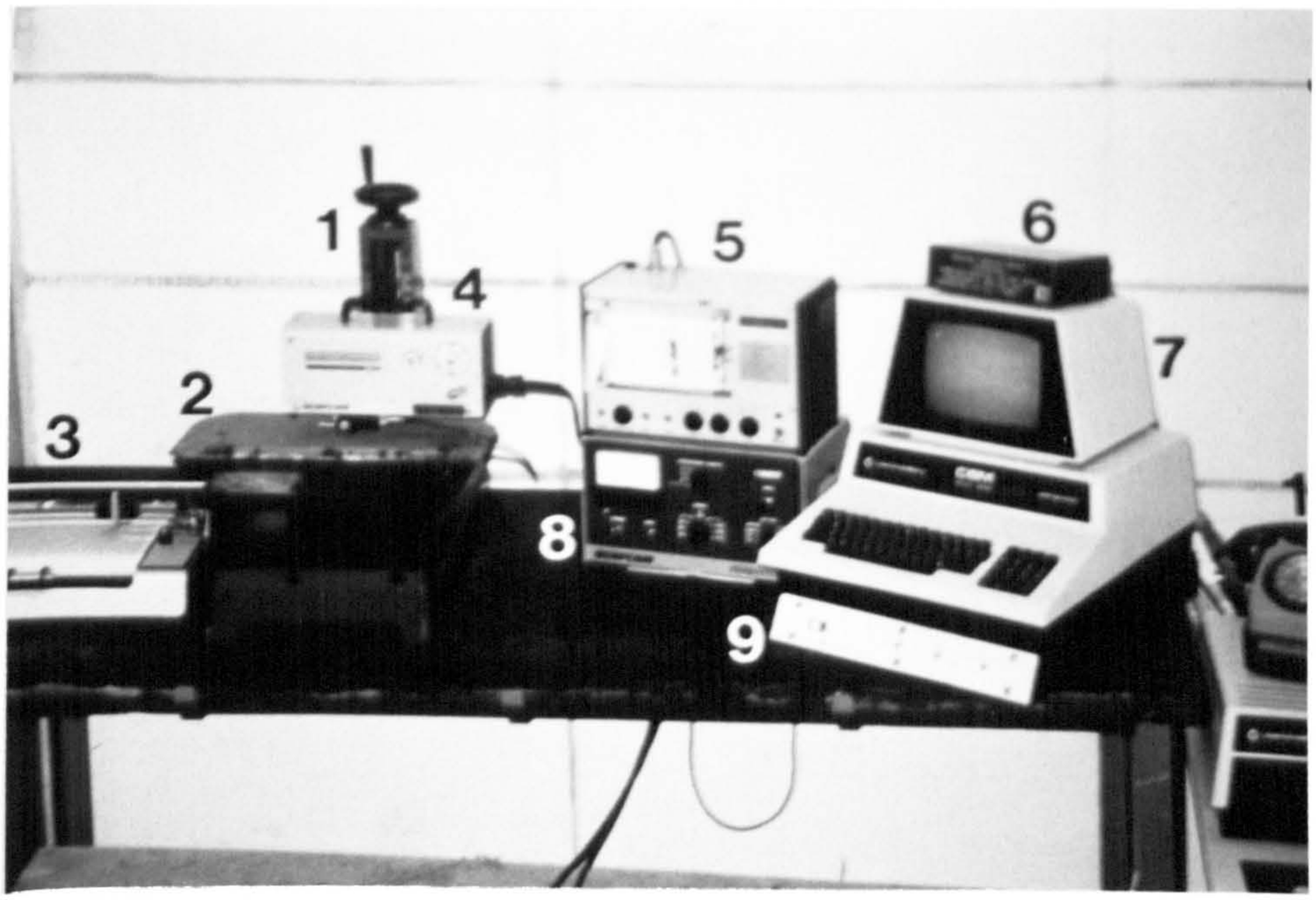

Figure 5.22 - Surface roughness measuring equipment - 1.Stylus unit,2.Weld mould, 3&5. hart recorder, 4.Stylus, 6&7.Microcomputer, 8&9.Control units

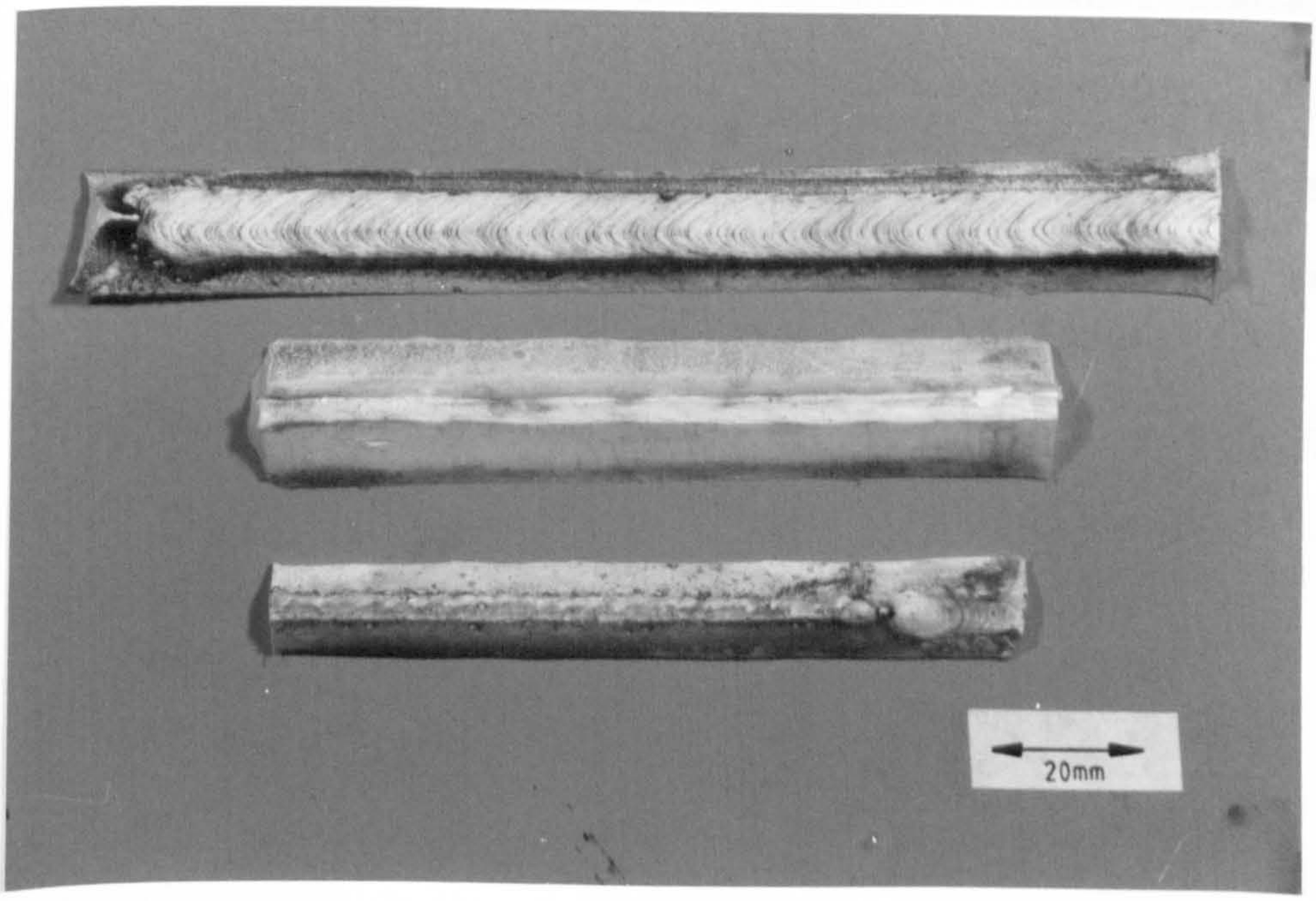

Figure 5.23 - Male replicas of the weld profile made in silicon rubber

traverse was controlled using the "Varicut 84" surface metrology program. Outputs were produced in the form of a direct pen plot profile or as a a statistical analysis of the surface roughness characteristics.

After a number of runs on each sample, the programme finally averages the data produced for each individual sample. A summary of these results is provided in table 5.08. They show not only similarity between the profile characteristics of the MMA and laser emergent bead surfaces, but also a reduction of 50% for the roughness of the incident bead surface compared with MMA.

The roughness values are within the range of maximum roughness found by Goldberg for cut edges (5um for high quality cut to 350um for low quality cut). However, while the more sensitive instrument used for these trials has shown mean valley radii of less than 0.25mm (i.e. the cut quality roughness is greater when measured with a reduced diameter probe) a direct comparison with Goldberg's results cannot be made.

Nevertheless the surface profile results indicate that if fatigue tests were conducted on laser welds in the Mode 3 loading it is likely that they would show similar, if not marginally better fatigue strengths compared with MMA fillet weld control samples. Similarly for twin fillet welds when the outside profile of both beads is characteristic of the incident bead profile, a far superior quality would be expected for the fully penetrating skid weld.

Weld surface type	Average roughness (mm)	RMS roughness (mm)	Peak-valley height (mm)	Mean valley radius (mm)
MMA fillet (4mm leg)	19.6	24.6	93.1	0.080
Laser skid incident bead (8mm plate)	8.1	12.1	49.5	0.10
Laser skid emergent bead (8mm plate)	19.9	23.9	81.9	0.07

Table 5.08 - Summary of the surface topography measurements of weld surfaces measured on 8mm plate joints

CHAPTER SIX

METALLURGICAL EXAMINATION AND CLASSIFICATION

In order that a definitive specification may be set for both design engineers and production engineers, classification rules state fixed requirements for the results of mechanical testing. The only traditional knowledge that may be gained by engineers of the weld structure and its composition i.e. the basis of the weld that actually determine the mechanical properties, is from hardness testing and examination of macrographic sections. However diagnosis is often very subjective.

Within this chapter the author has not only examined the hardness and macrographic characteristics of the laser skid weld but also, by the use of statistical evaluation of the weld microstructure, used a phase counting method to quantitatively compare welds and their characteristics.

For the present study such a method was used only on a selective basis but the results confirmed its potential as a diagnostic procedure. The author would therefore advise that, while at the outset shipyard weld procedure testing would be marginally more expensive, if statistical microstructure data was stored as part of a procedure data base then much more basic information could be collected. This would enable more effective and efficient procedure judgments and thus raise welding in shipyards from its often "black art" status to a more scientific one.

6.1 HARDNESS TESTING

Hardness testing provides a measure of a material's resistance to indentation from a specifically sized indenter, applied with a set force and is usually conducted at room temperature.

There are various alternative methods of hardness testing, but the most commonly used is the "Vickers Hardness Test" as defined by B.S.427: Part 1: 1961:"Method for Vickers Hardness Test", [171] which has a pyramid shaped diamond indenter applied with loads of from 1 to 100 kilogrammes force. A measure of the hardness is given by the "Vickers Hardness Value"(Hv), a ratio of the applied force in kilogrammes force and the sloping surface area of the indentation in millimetres square. In practice the ratio is interpolated from tables detailed for each applied load, given the mean of the diagonals across the top of the indentation.

Hardness in steels is related to the material's microstructure, which depends on chemical composition, cooling rate and any subsequent heat treatments. Therefore hardness values are used as an initial indicator to the types of properties which can be expected from a material. Also, if excessive e.g. above 350Hv for welding, it provides a warning to likely consequential properties such as a susceptibility to hydrogen cracking.

The difference between hardenability and hardness should be noted. For steel of "low hardenability" a rapid cooling rate will be required to produce a hardened microstructure whereas a material with high hardenability will give a hardened microstructure even at slow cooling rates.

Generally mild steels used in ship structures are of low hardenability but, with fast cooling rates found in laser welding, a change in "weldability" may have to be considered. Therefore the first section of this chapter studies the actual hardness found in the welds compared with classification requirements and in the second section an assessment of the "weldability", in terms of obtaining acceptable levels of weld hardness, is made for the skid welding process.

6.1.1 Classification Requirement for Hardness Testing

Hardness testing requirements of plate and weld material as specified by MOD(N) and Lloyds are rather subjective although each prescribe maximum limits for chemical composition and related equations for Carbon Equivalent (CE). Lloyds detail hardness test requirements for fillet weld test assemblies when examining welding consumables but then request "hardness of the weld metal, heat affected zone and base metal is to be reported" for an actual weld procedure test.

Although no upper limit is specified in the rules, a value of 350Hv was accepted as the nominal maximum - particularly with respect to the HAZ - by Lloyds and MOD(N) during discussions [105] [106] .

There are four areas of concern pertaining to criteria specified for the assessment of conventional welds when used with laser welds for shipyard classification:

1. Weld size - the narrowness of the weld and particularly the narrowness of the HAZ restrict the placing of hardness indentations especially when a gap of at least 2.5 times the diagonal of the indentation must be left between indentations. Figure 6.01 shows hardness traverse distribution to ensure non-interaction as detailed by Lloyds together with the author's proposed revised layout for laser skid welds.
2. Indentation size - Usually a 10kg load is applied to the indenter for weld hardness testing on conventional welds. For the most narrow laser welds it is likely that an indentation could be affected by more than one weld zone. However, use of microhardness testing would give an equally false indication of general hardness levels by only showing the hardness of individual grains. Therefore if there is concern for this situation occurring a smaller indenter load e.g.5kg, should be used.
3. HAZ sub-zone size - Within the HAZ the sub-zones may be very close together providing differing hardness values within a small width of material. If an "overheated" sub-zone (characterised by grain growth) has formed next to the weld fusion line, with rapid cooling a

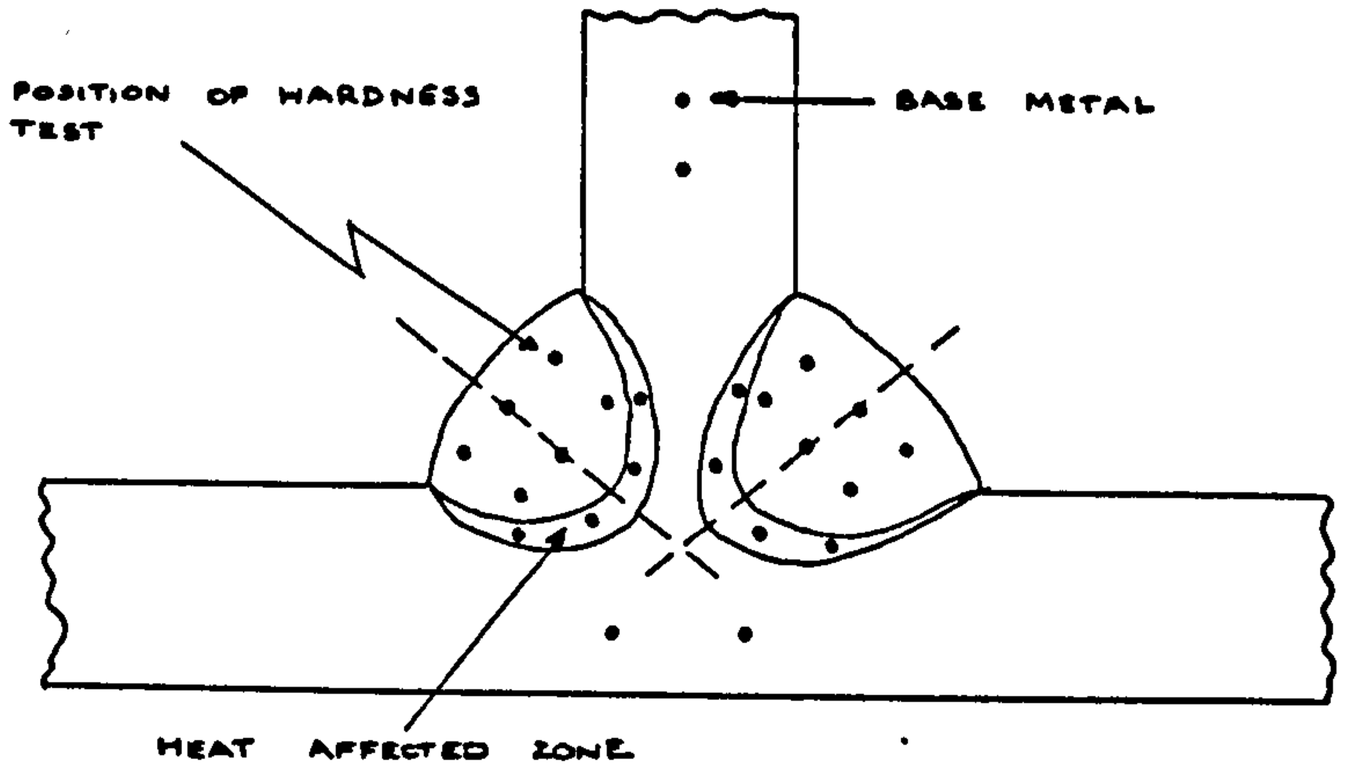

a - Conventional hardness test positions for a fillet weld test assembly

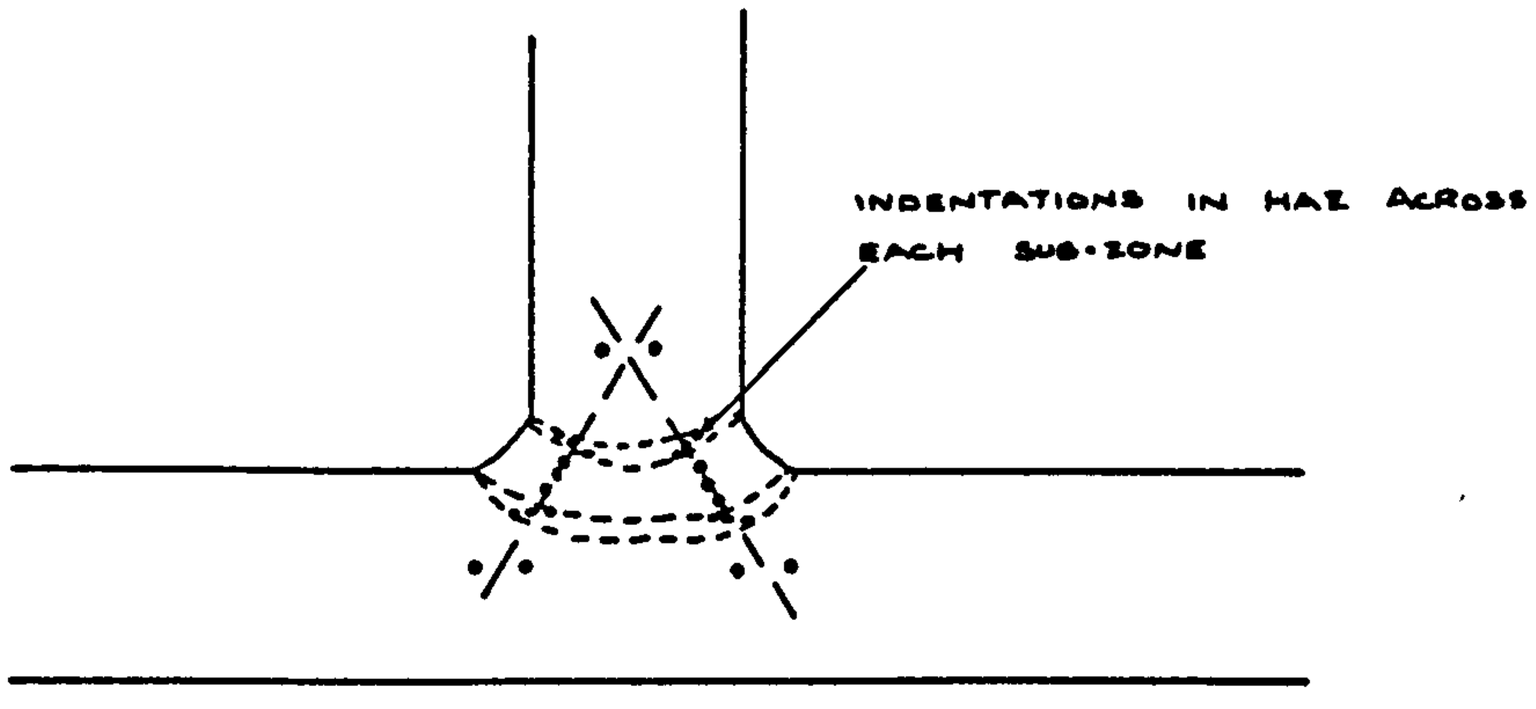

b - Proposed hardness test positions for laser skid weld assemblies

Figure 6.01 - Hardness traverse test positions for fillet and laser skid welds

very narrow zone of potentially martensitic microstructure may result giving the potential for hardness values well in excess of 350Hv. Within the "refining" sub-zone (characterised by a recrystallised microstructure) another characteristic hardness will result and similarly for the "transition" sub-zone characterised by partial recystallisation of the microstructure as shown in figure 6.02.

Therefore there is the potential for three distinct hardness values in a very small width, the one nearest the fusion line potentially being the highest. The proposed hardness mapping, figure 6.01 takes this into consideration, requiring greater precision on the part of the operator but giving a more accurate representation of potential effects of microstructural differences.

4. Use of micro-hardness testing - this method may be advised for analysing the hardness of individual grains using a spring loaded indenter with a load of between 1 and 100 grams. Although the Author has used this method as a means of confirming the hardness value of individual grains for microstructural characterisation, comparison for classification against conventional welds was made by using the Vickers Pyramid Hardness test using test loads of 5 and 10kgs. Although at times values will have been "averaged", as one indentation crossed a number of grain boundaries, the test not only enables direct comparison with classification requirements but also enables the use of equations relating to such tests. Of most importance is that it is satisfactory to the level required for shipyard approval testing if the above considerations are taken into

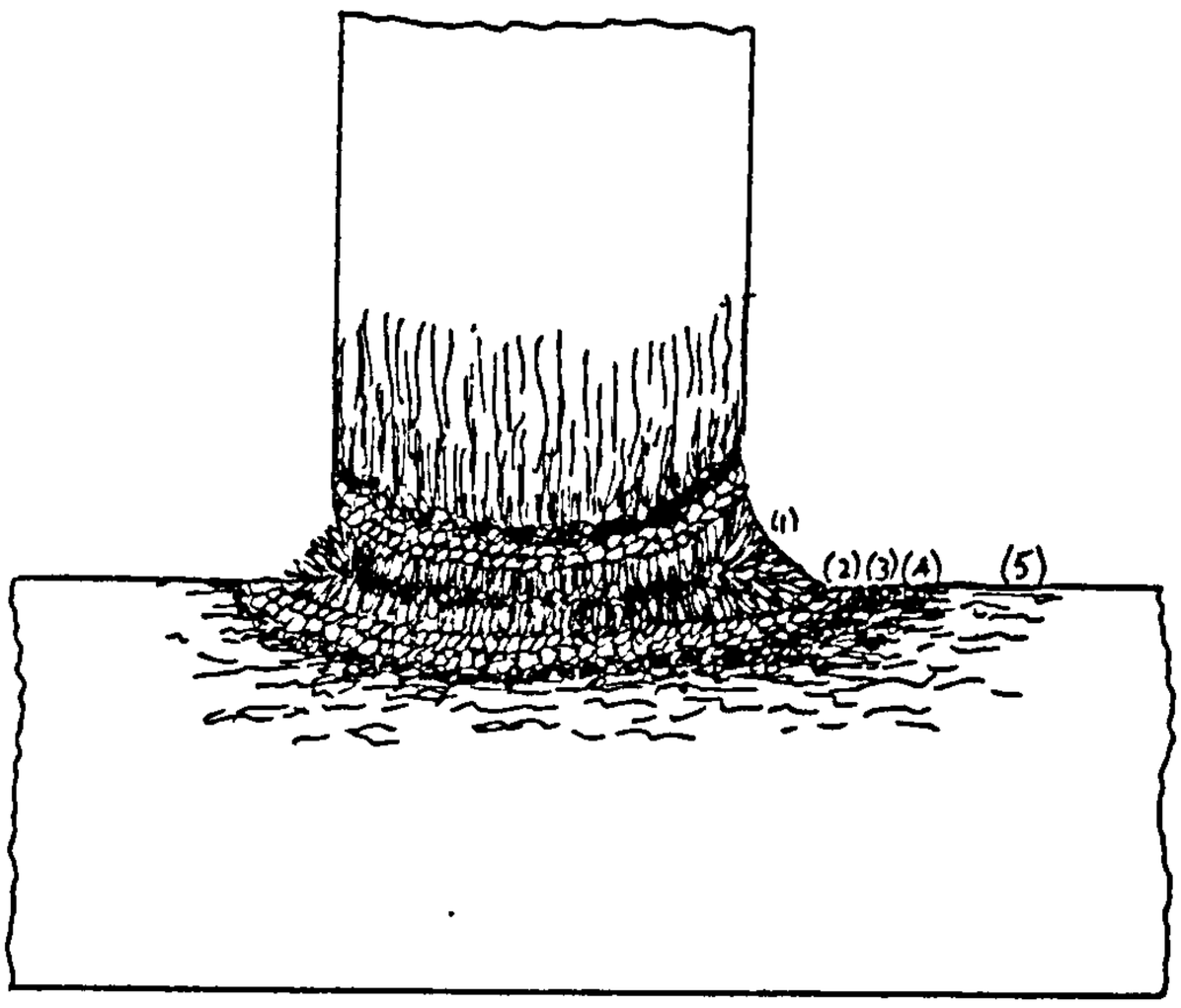

(1) Weld metal - Columnar/equiaxed crystal formation
(2) Parent metal - Overheated zone; grain growth
(3) Parent metal - Refining zone; complete recrystallisation
(4) Parent metal - Transition zone; partial recrystallisation
(5) Parent metal - Unaffected structure.

Figure 6.02 - Hardness traverse test positions for fillet and laser skid welds

account.

6.1.2 Hardness test specimen manufacture and testing

Sections were cut from the welds, mounted, polished and etched in 2% Nital as for macrographic samples. Hardness traverses were taken diagonally within the incident sector and again in the emergent sector. Three indentations were made in each parent plate, HAZ and weld material. Within the HAZ every care was taken in ensuring that one indentation was made as near as possible to the fusion line using the Vickers test.

6.1.3 Hardness Test Results and Discussion

Data from hardness tests is presented in figures 6.03 to 6.04 showing variations in hardness for welds in each plate thickness and their respective trial traverse speed ranges(at the "optimum" welding spot height). The effect of power changes for one particular plate thickness for two various plate compositions (plates P6/1/CS and P6/2/SHS), is also shown.

In order to simplify comparative interpretation of hardness traverses the three values measured in each sector were averaged, as were those between the incident and emergent sections. Typically hardness in the incident sectors was found to be 5% higher than that in the emergent side due to slightly higher cooling rates. Whilst appreciating the large

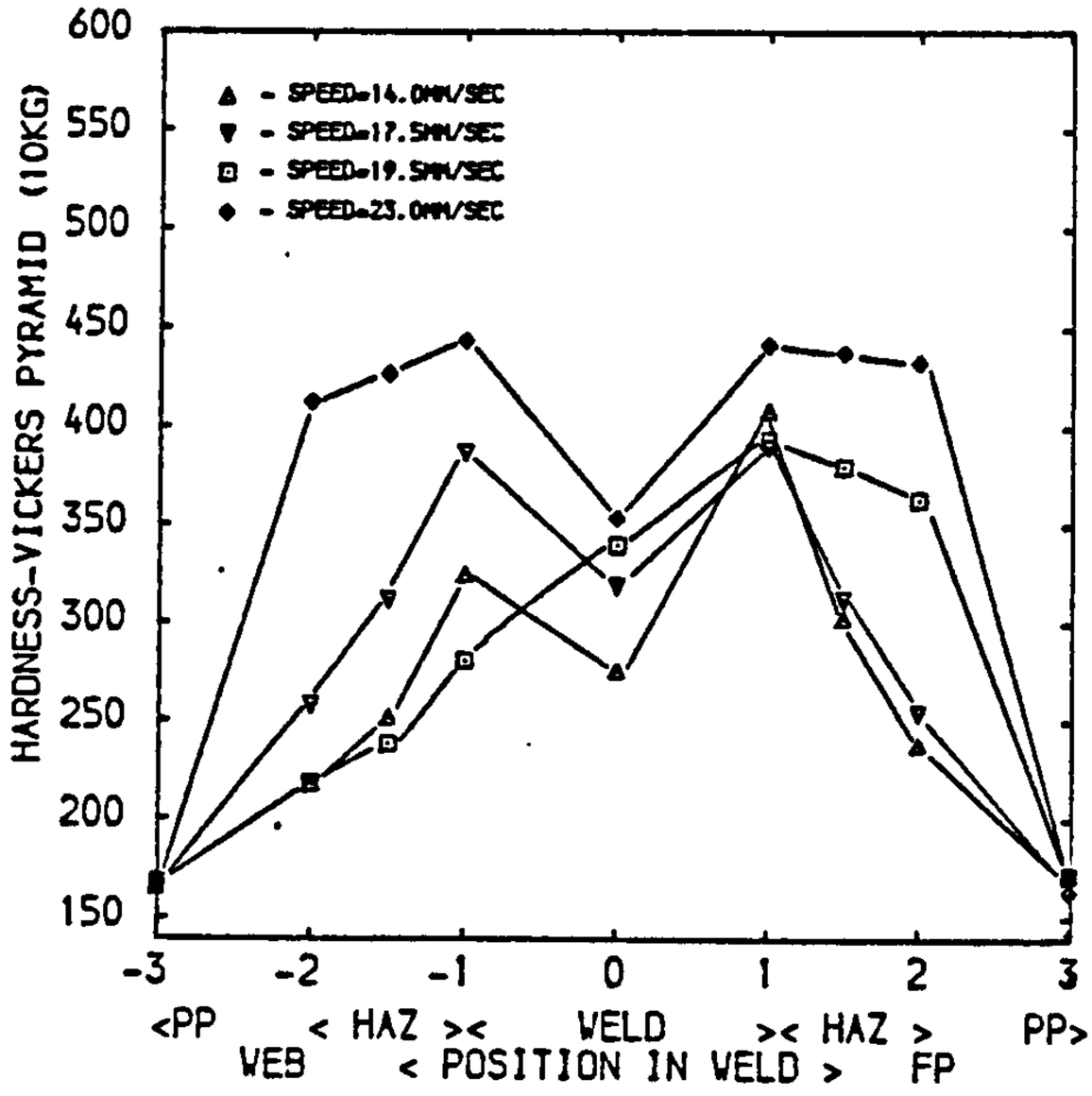

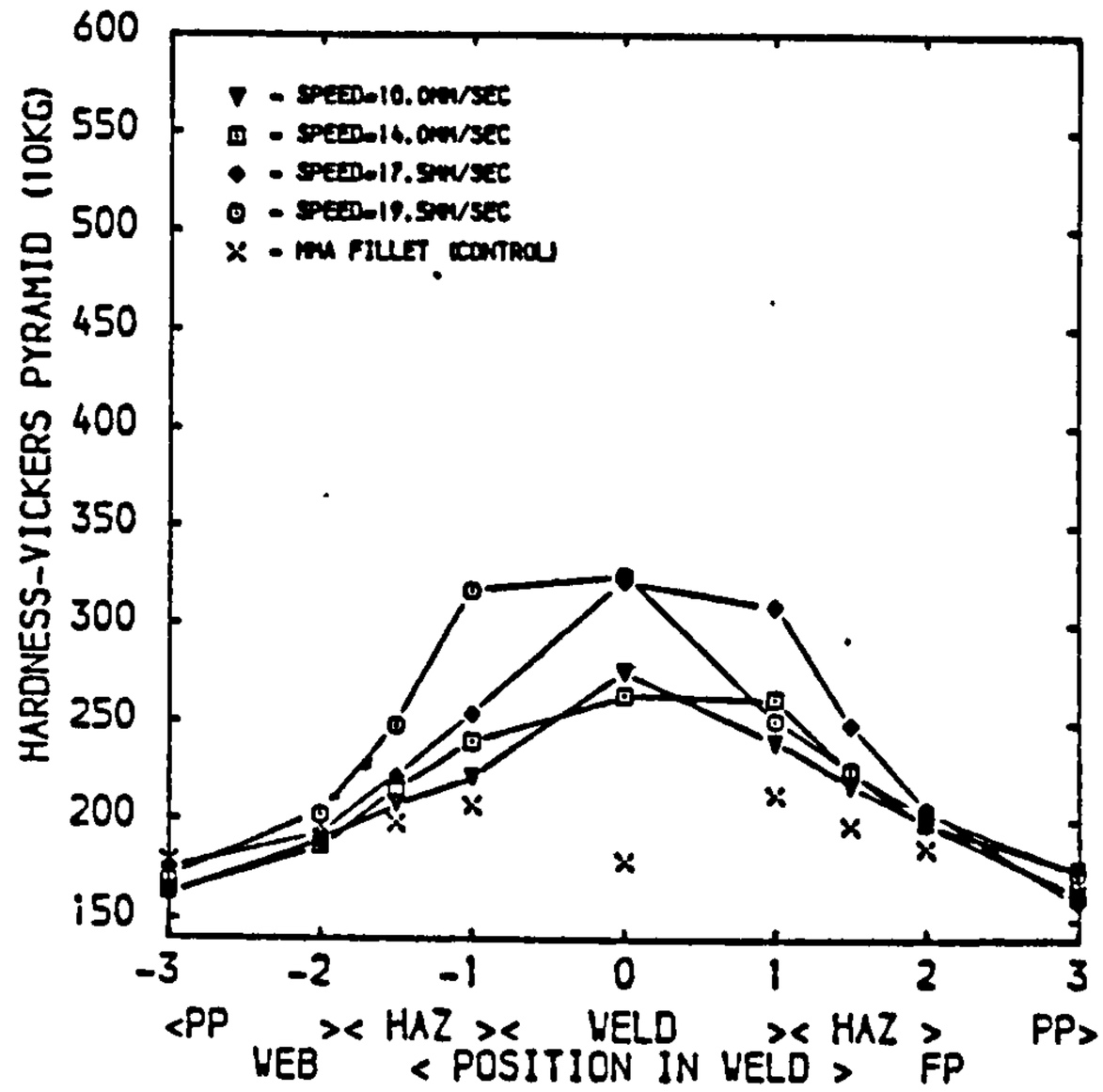

a) 6mm plate b)8mm plate

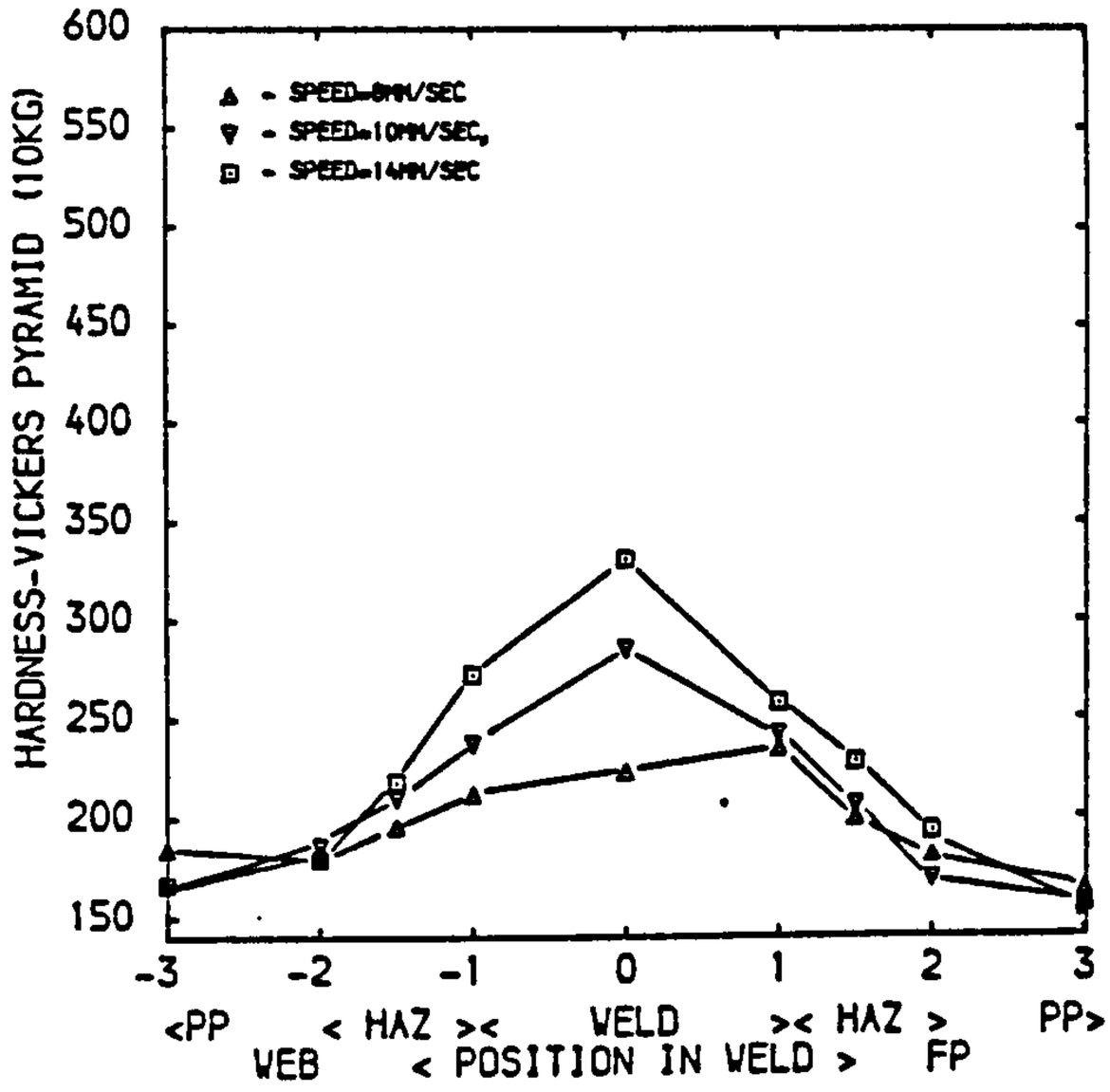

c) 10mm plate

Figure 6.03a-c Hardness traverse results for skid weld tee section joints in each plate thickness; 9kW laser power

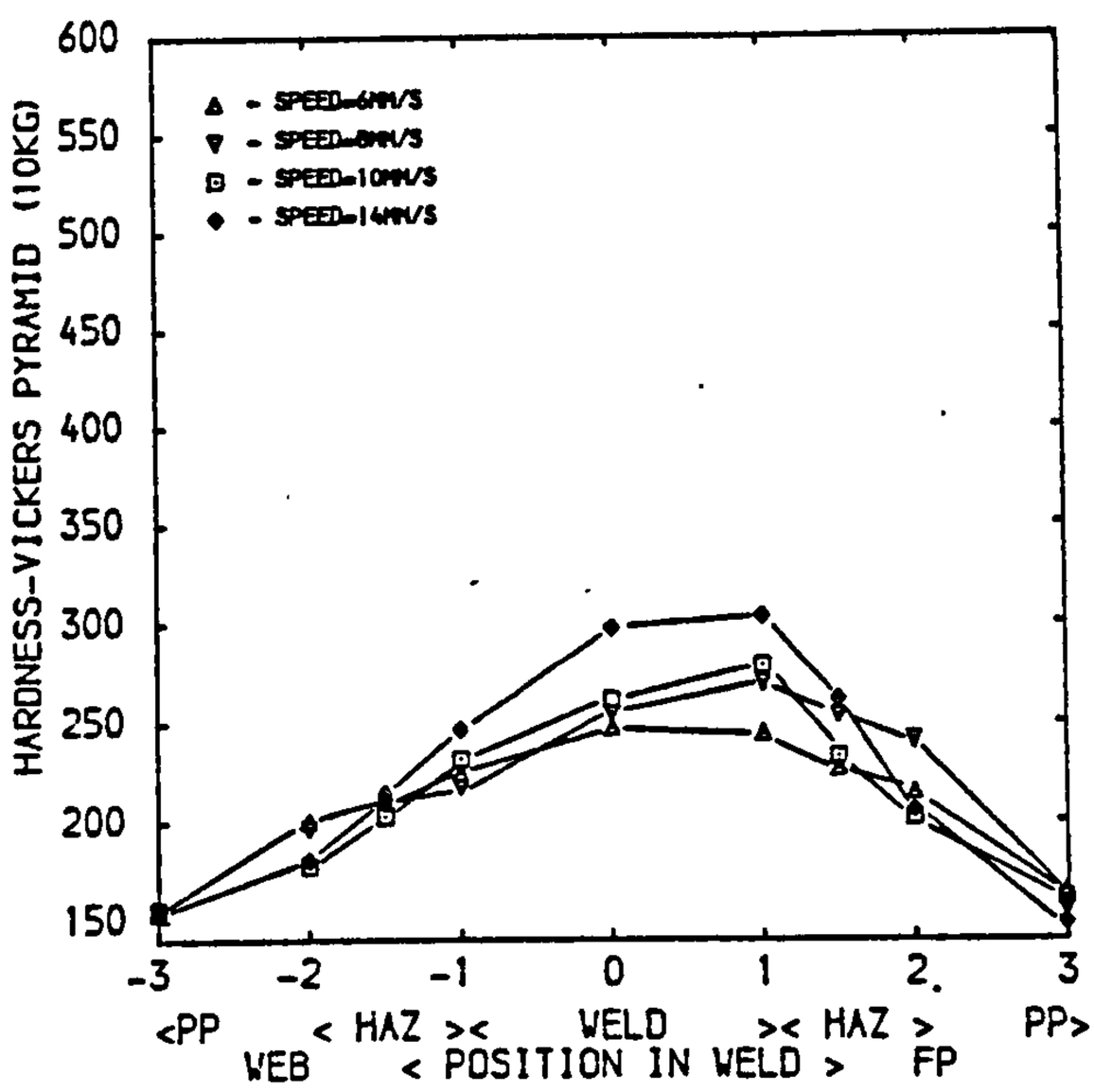

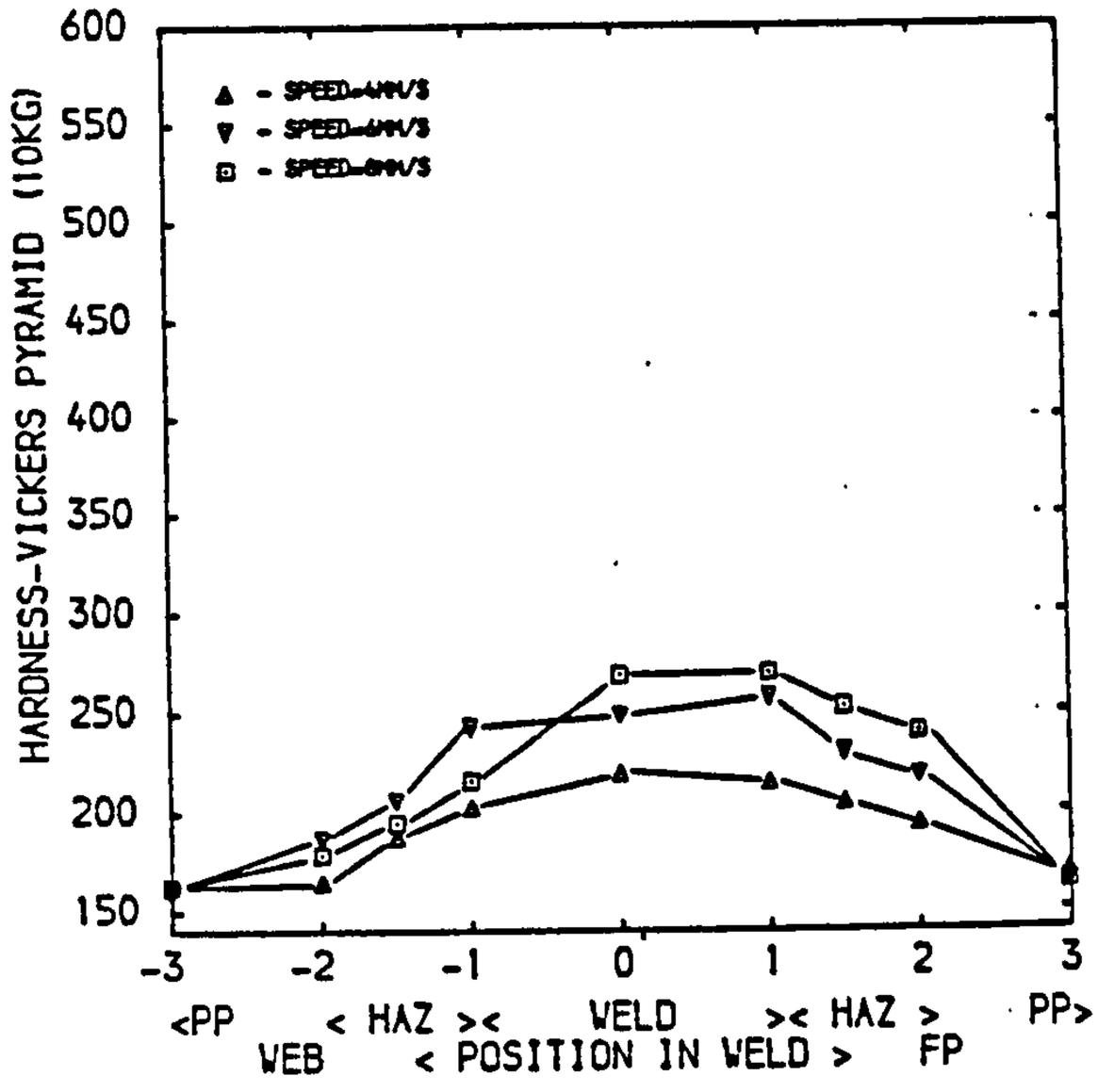

d) 12mm plate e)15mm plate

Figure 6.03d-e Hardness traverse results for skid weld tee section joints in each plate thickness; 9kW laser power

variation of results found in the HAZ the lowest found, usually associated with the structure nearest the parent plate, and the highest found, associated with the zone nearest the fusion line are plotted at respective positions (positions 1 and 2 on the diagrams).

Clearly these diagrams show that, while the power is kept constant at 9kW(WP), as plate thickness increased (using the speed range to actually form a satisfactory joint) or the traverse speed for any one plate thickness decreased, ie the heat input increased, so the resulting hardness both in the weld material and HAZ reduced.

It should be noted that a direct interpolation of results could not be made at this stage because of the variances in plate compositions for each plate thickness. This factor became particularly relevant when the first welds were made in 6mm plate (plate P6/1/CS) when traverse speeds of up to 23mm/second were combined with a plate composition of carbon content >0.19%. Hardness values in excess of 350Hv were measured in the HAZ adjacent to the fusion line.

The effect of material composition may also be observed by comparing the hardness measured in the weld metal to that in the HAZ. Whilst the variation in plate composition is reflected by a large variance in the HAZ hardness from 200 to 450Hv a smaller variance, from 200Hv to 350Hv, is noted in the weld material as the same wire composition is used for each thickness of weld. Consequently for fast welding speeds coupled with high carbon levels in the parent plate, HAZ hardness has shown

higher levels than that of the weld e.g for 6mm plate P6/1/CS, although for welds in plates of lower carbon levels e.g for 10mm plate P10/1/SHS, the weld material has the highest hardness. Whilst this trend is expected, hardness levels in the weld will be influenced by the dilution factor which will vary for each plate thickness and joint configuration.

Therefore to control the hardness in the weld material different filler wire compositions may be used. However for a set plate composition the only change that could be made to adjust the hardness of the HAZ would be to change the weld cooling rate. Variations in HAZ hardness for various heat inputs using various traverse speeds for laser powers of 9,8,7 and 6kW(WP) are shown in figure 6.04a-d. In each case, as heat input reduces and therefore cooling rate increases, so hardness values increase. Although, if heat input were to be increased (without changing the focal characteristics of the beam) whilst the hardness would reduce, unsatisfactory weld profiles would result.

Reductions in HAZ hardness were made by using a plate with a lower carbon equivalent (CE) i.e. increasing it's hardenability. The welds were repeated using the plate of C=0.13. The resulting hardness curves are shown in figure 6.05a-d. These show how control of plate composition had the effect of lowering the overall hardness levels within the joint to an acceptable level. Whilst this shows the result for one specific case, the concept of "weldability" is examined in more detail in the next section in order to derive general rules for the control of plate composition for the skid welding process.

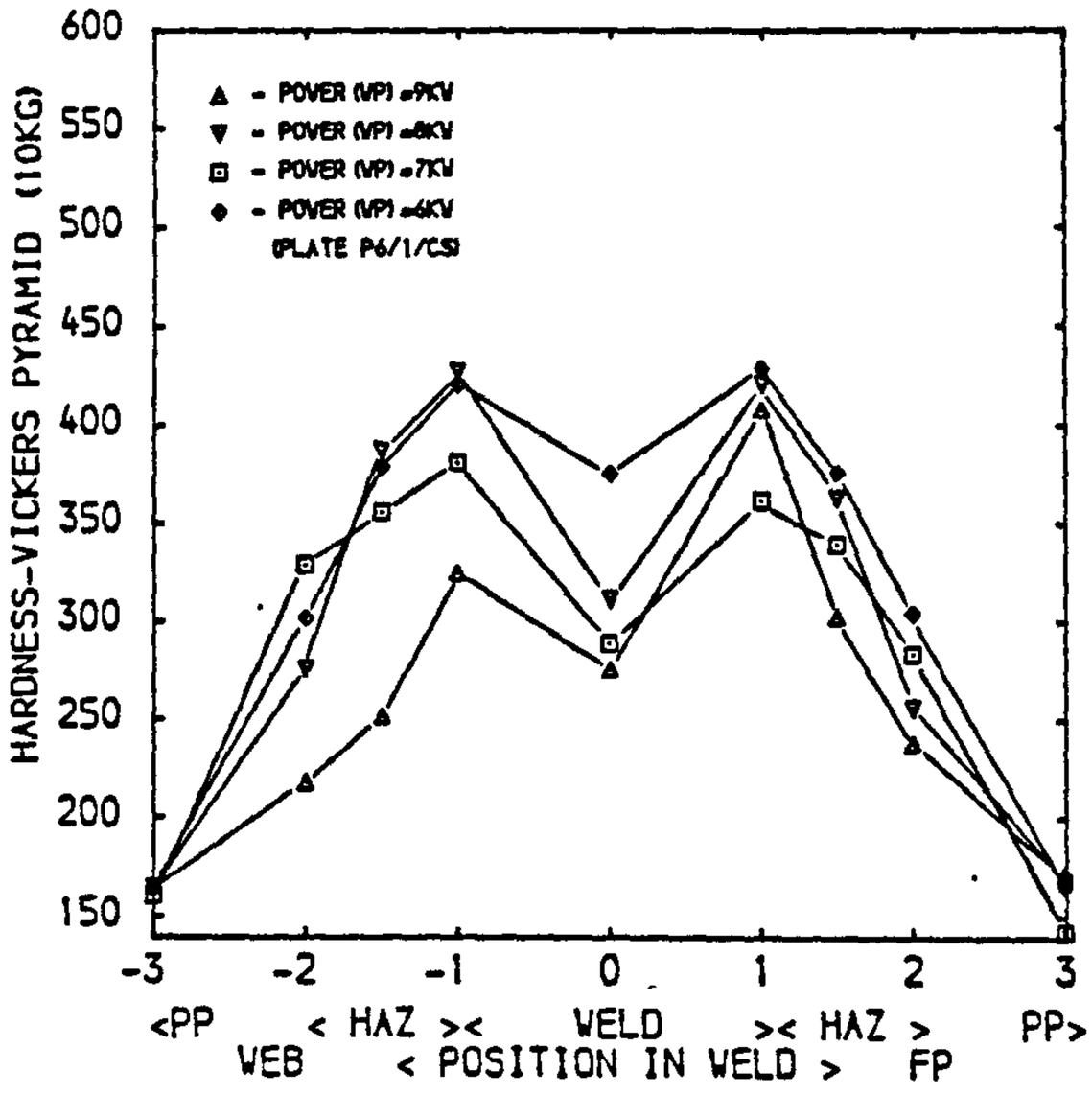

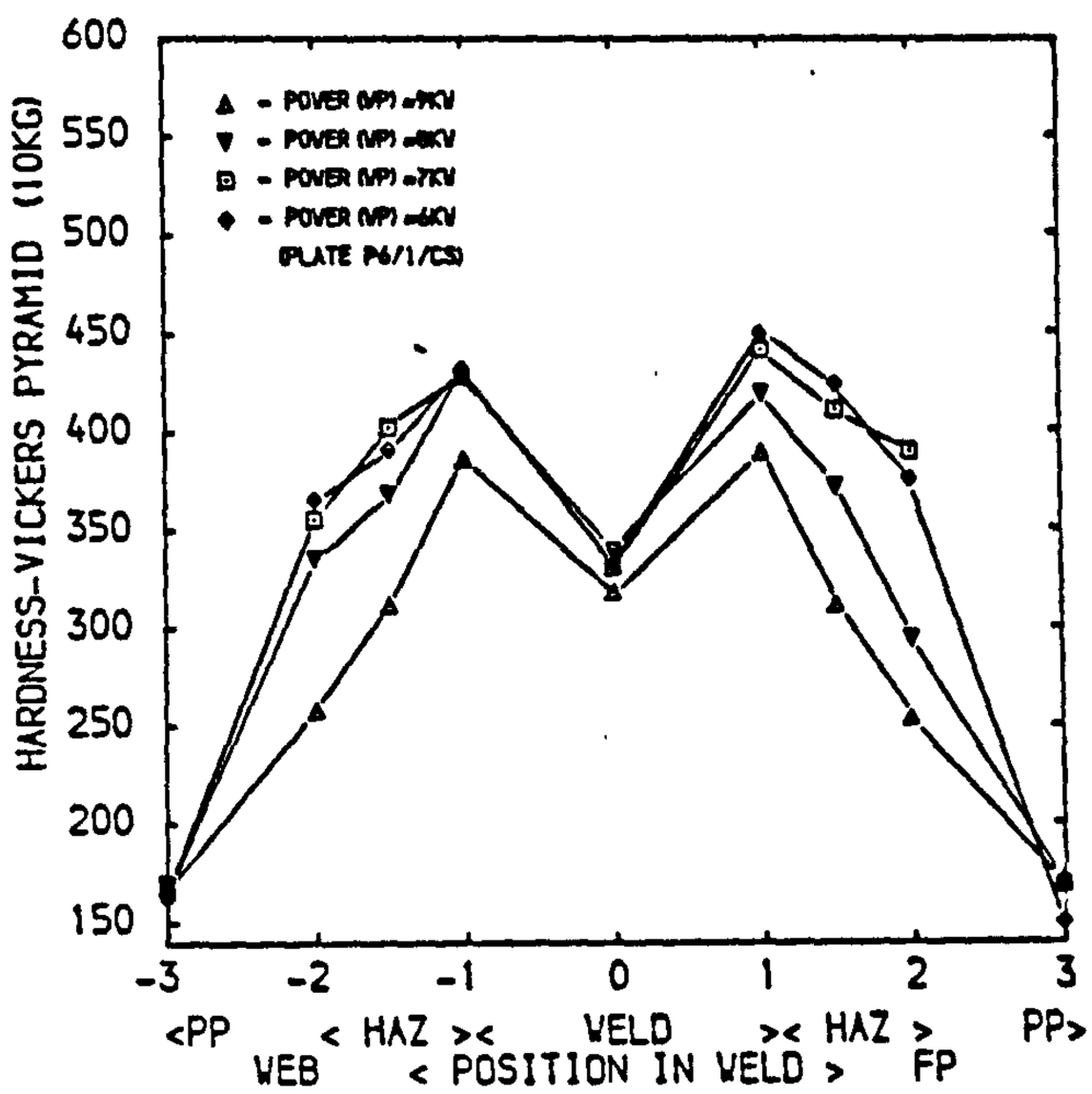

a) Speed = 14mm/sec. b) Speed = 17.5mm/sec.

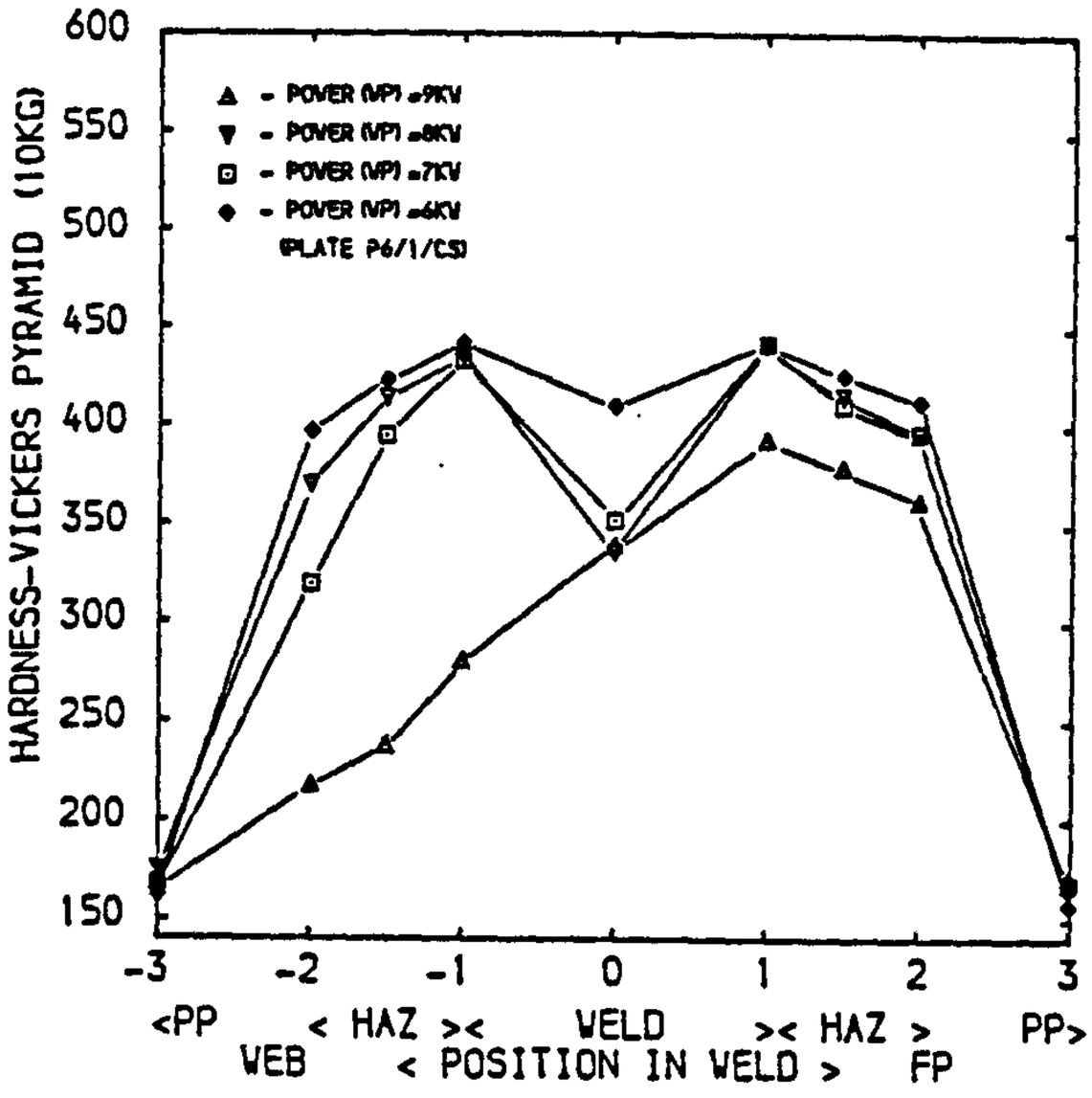

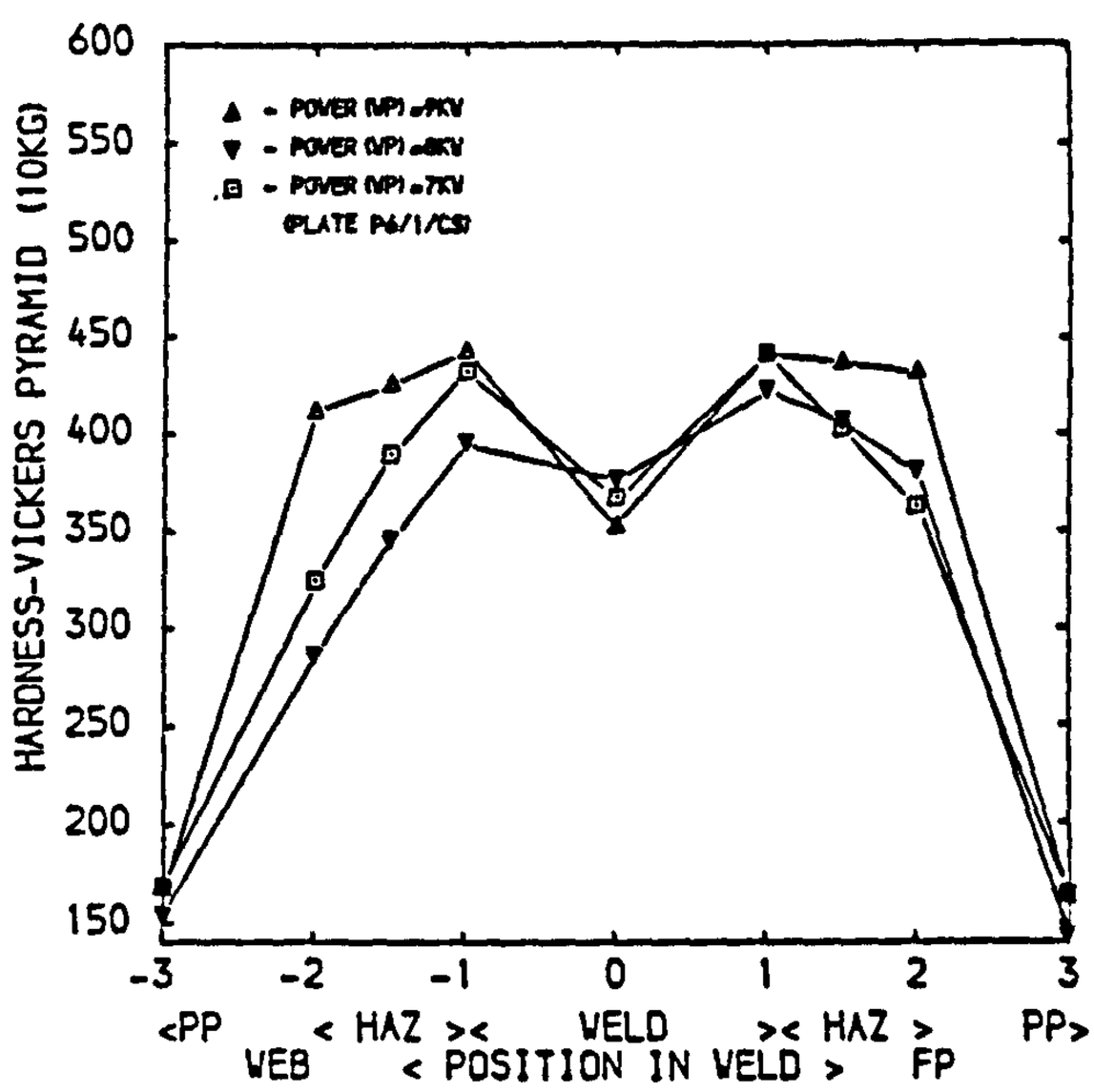

c) Speed = 19mm/sec. d) Speed = 23mm/sec.

Figure 6.04a-d Hardness traverse results for 6mm plate (P6/01/CS) skid welds; varying power.

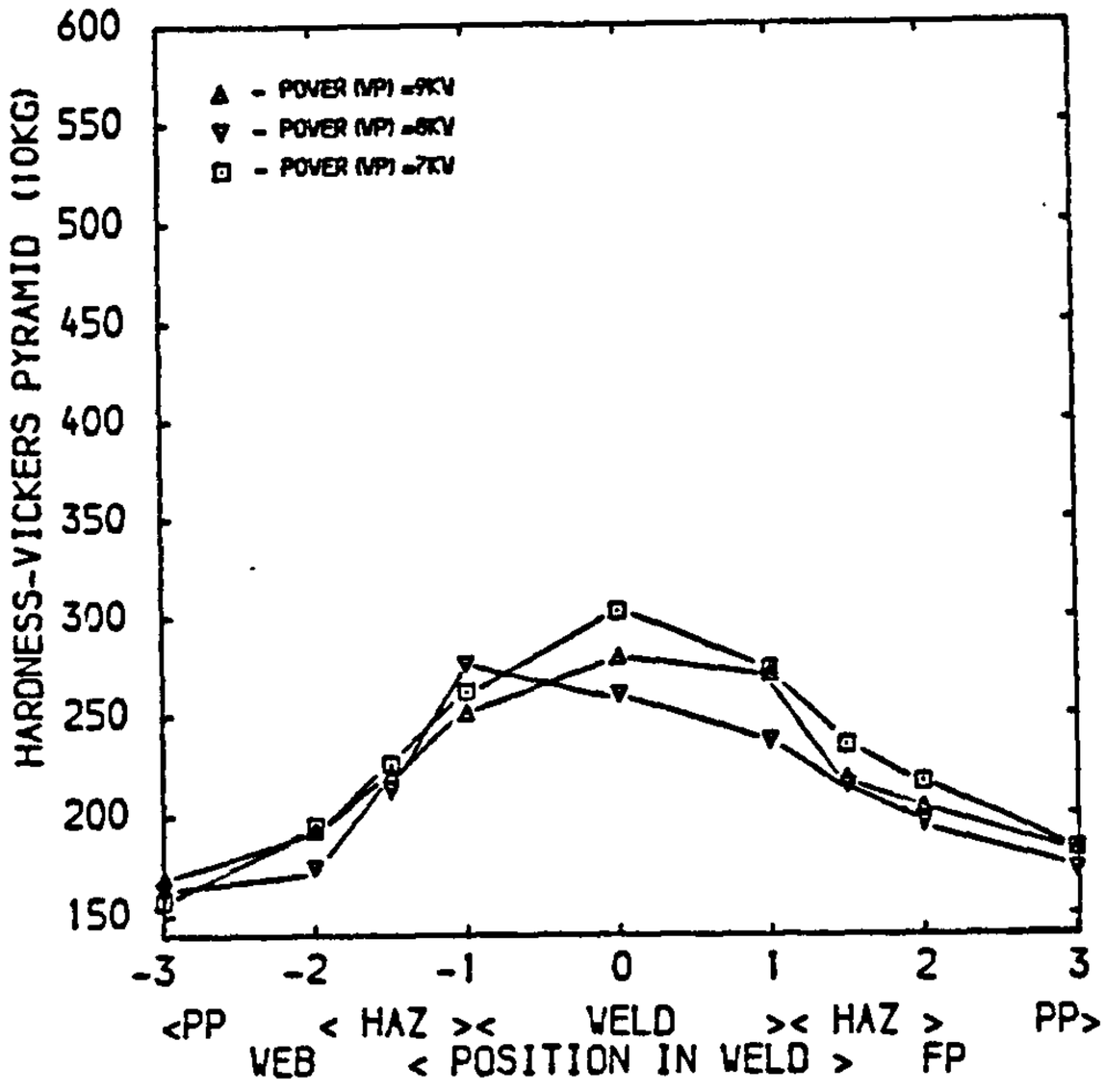

a) Speed = 14mm/sec.

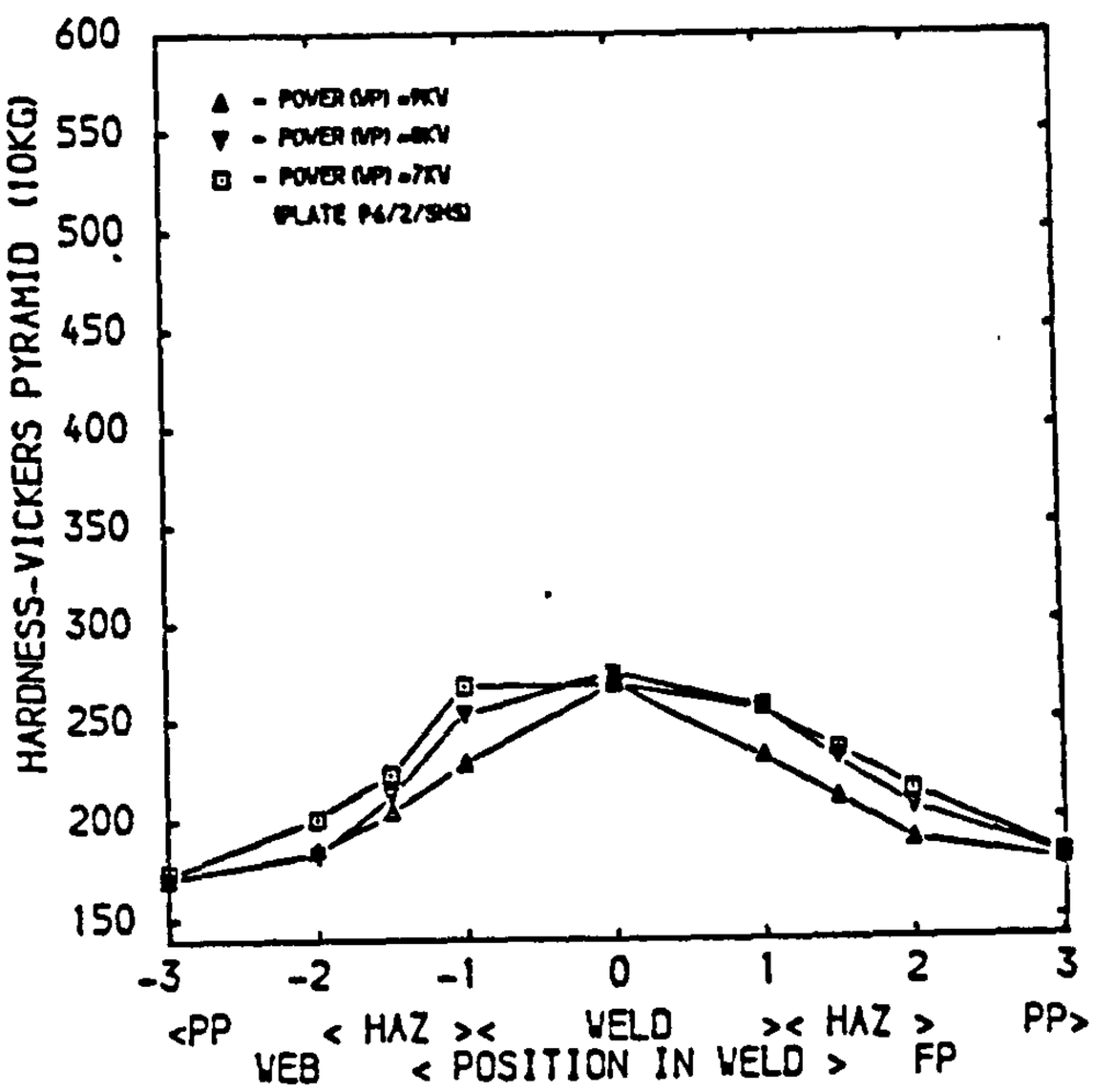

b) Speed = 17.5mm/sec.

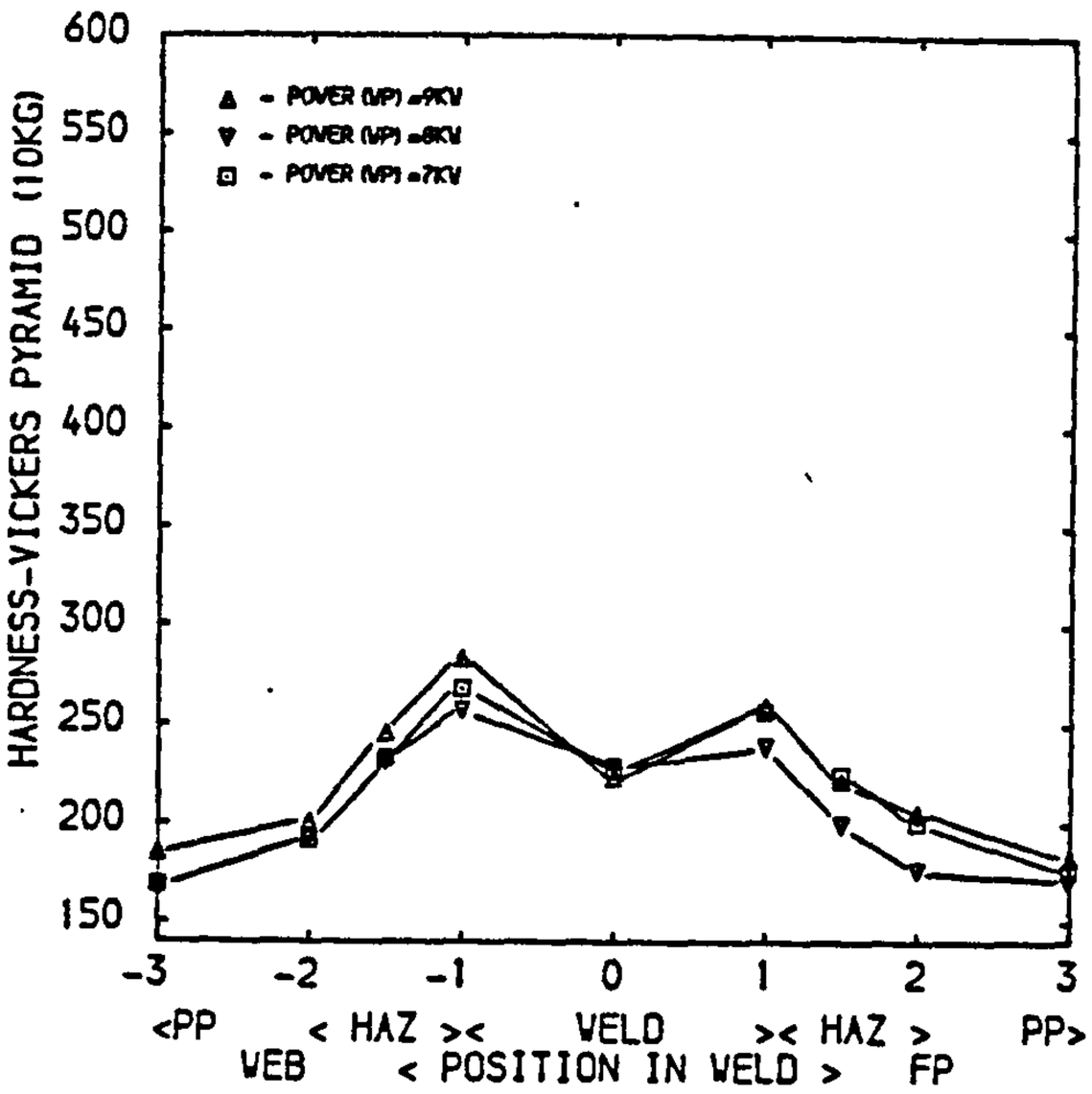

c) Speed = 19mm/sec.

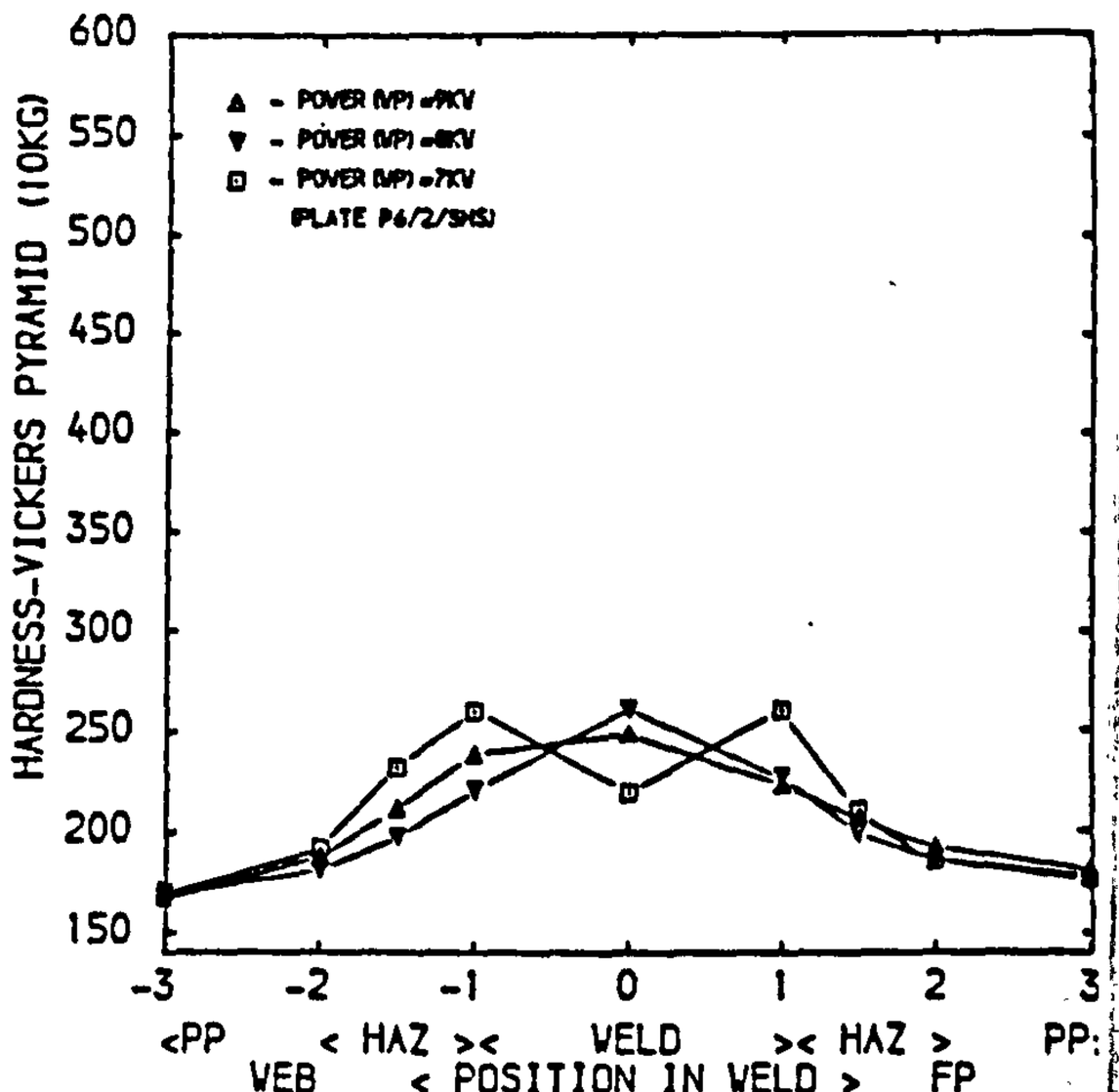

d) Speed = 23mm/sec.

Figure 6.05a-d Hardness traverse results for 6mm plate (P6/02/SHS) skid welds; varying power.

6.2 WELDABILITY OF SHIP STEEL FOR LASER SKID WELDING

An essential requirement of any structural material to be welded is that it has good "weldability". In terms of microstructure and hence mechanical properties this means that the post welding properties of the material will not adversely affect structural integrity. In this context the weldability of steel may be expressed in terms of a carbon-equivalent (CE) value. For conventional welding processes a mild steel is considered weldable if CE(IIW)<0.4 [172] .

Practically the CE values provide an indication of the type of microstructure to be expected in the weld heat affected zone as a function of the weld cooling rate. More specifically it provides an indication of whether or not martensite will form and consequently provides a basis for determining the hardness of the weld. In turn this provides an important measure for evaluating the susceptibility to cold cracking and stress corrosion cracking.

Various authors have proposed different equations to calculate CE each emphasising the affect of various alloying elements correlating specifically to certain structural properties. Cross reference to different CE values without knowledge of the source equation can often lead to confusion.

Lloyds use a calculation as defined by the International Institute of Welding (IIW) equation 6.01 primarily derived for use with C-Mn steels

but the MOD(N) use an alternative formulae directed more towards low-alloy steels, equation 6.02. Another similar formulae defining "Pcm" popular in Japan was proposed by Ito-Bessyo [173] , equation 6.03, and is able to reflect the use of micro-alloying agents typically found in modern steels.

$$C.E.(IIW) = C + \frac{Mn}{6} + \frac{Cu+Ni}{15} + \frac{Cr+Mo+V}{5} \qquad (6.01)$$

$$C.E.(MOD) = C + \frac{Mn}{6} + \frac{Ni}{40} + \frac{Cr}{.5} + \frac{Mo}{4} + \frac{Si}{24} \qquad (6.02)$$

$$Pcm = C + \frac{Si}{30} + \frac{Mn+Cu+Cr}{20} + \frac{Ni}{60} + \frac{Mo}{15} + \frac{V}{10} + 5B \qquad (6.03)$$

A useful comparison of both the IIW, Ito-Bessyo formula and others by Dueren has been compiled by Suzuki [174] . Using equations from this paper and by relating hardness found in sets of "standard" skid welding joints the present author has made estimates of weld cooling rates for the particular welds produced in order to predict HAZ characteristics, and determine "weldability" for the laser skid welding process.

For a given welding process, weld geometry and material, it is normally accepted that the coooling time through the range 800-500 degrees Centigrade (Dt8/5) is constant within the heat affected base metal and may therefore be used as a comparative cooling time indicator.

Suzuki [174] relates maximum hardness, (Hmax) measured by Vickers Pyramid indentation with 10kg load, carbon equivalent (Pcm), carbon content "C" to the cooling time in seconds Dt8/5 by the following equations:

$$Hmax = \varnothing_1 - (\varnothing_2 \times \arctan X) \qquad (6.04)$$

where:

$$X = \frac{\log Dt8/5}{\varnothing_4} + \varnothing_3 \qquad (6.05)$$

$$\varnothing_1 = (187 + 64.C + 485.Pcm)$$

$$\varnothing_2 = (97 + 680.C - 441.Pcm)$$

$$\varnothing_3 = (0.501 + 7.90.C - 11.01.Pcm)$$

$$\varnothing_4 = (0.543 + 0.55.C - 0.76.Pcm)$$

A formulae for cooling time may therefore be equated:

$$Dt8/5 = 10^{[(\varnothing_4 \times \tan((\varnothing_1 - Hmax) / \varnothing_2) - \varnothing_3]} \qquad (6.06)$$

Using equation 6.06 a computer program, "SKIDCOOL", Appendix D-1, was written to calculate the cooling times for each family of welds produced during trials using Hmax as measured in each weld. The results are summarised figure 6.06 with the cooling times plotted against welding speed for welds in each plate thickness made using 9kW (WP).

For 6,8, and 10mm thick joints the curves follow a similar base level as would be expected for joints where heat input is low enough relative to plate thickness for the combined thickness to have little effect on cooling rate. Then, for plates of greater thickness than 10mm with the

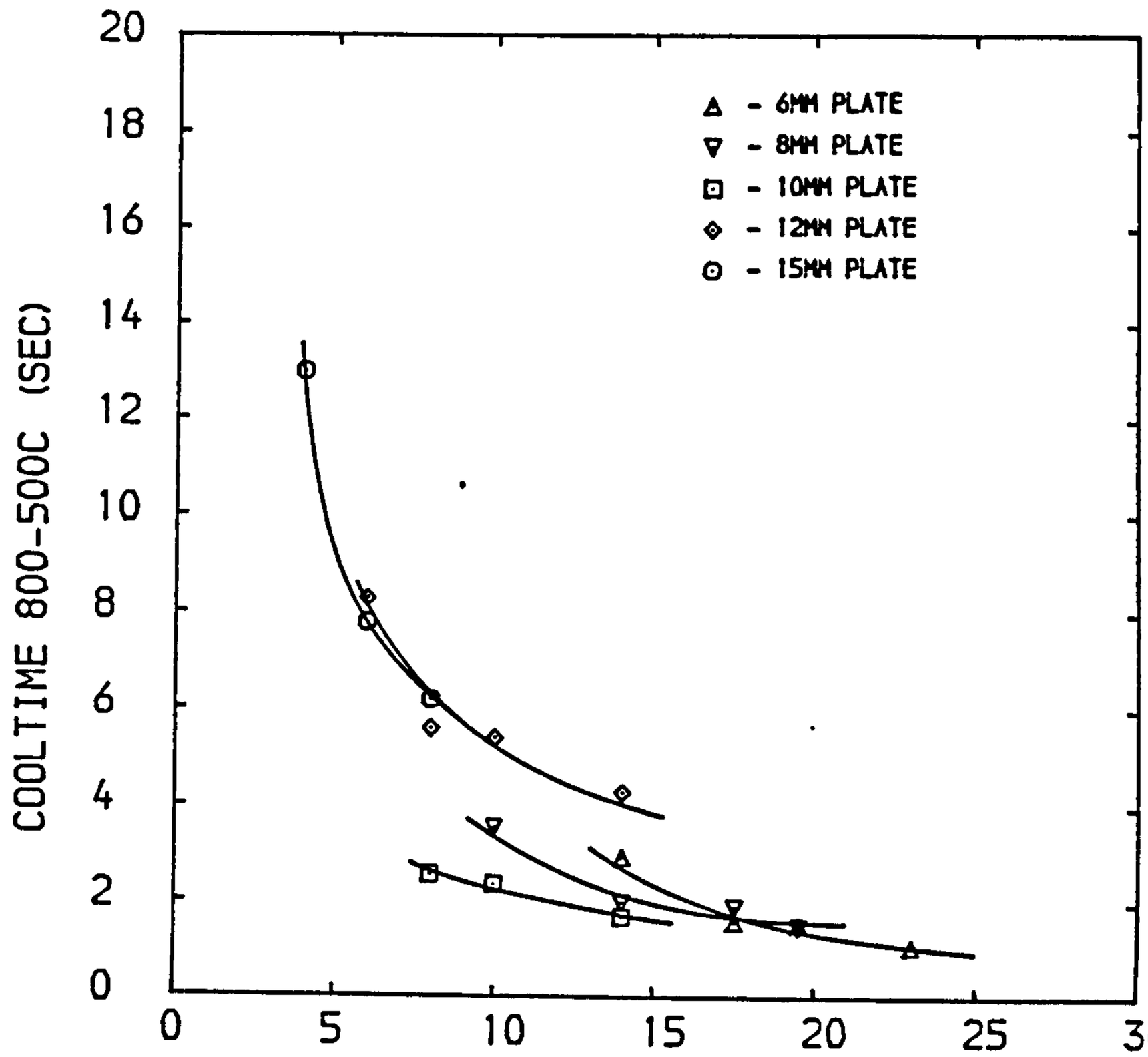

Figure 6.06 - Skid weld HAZ cooling times (800-500) for various traverse speeds as calculated from the max. hardness in the HAZ

slower traverse speeds, as heat input increases the cooling time increases as a function of combined plate thickness.

A difference is noticed for 12 and 15mm thick plate with a larger increase in cooling times, which also corresponds to the thickness of plate at which formation of the emergent bead becomes more difficult. This will have occurred as a result of increased heat energy being absorbed into the joint, as shown not only by the higher heat transfer efficiencies found for these thicknesses of plate, but also from observations during welding. The greatly reduced plasma at the emergent side when welding plate thickness was above 10mm meant that a larger proportion of the available power was entering the material. Also the subsequent increased plasma build-up on the incident side created an effective secondary heating to the joint so increasing the cooling time.

Cooling rates calculated for each plate thickness being welded at optimised traverse speeds for the joint configuration were then used with equation 6.04 (Suzuki) to predict the weld hardness for a given plate composition. It was also used to investigate the effect of plate compositional variances to ensure recommended hardness would not be exceeded.

The maximum possible hardness i.e. independent of heat input due to the formation of 100% martensitic transformation as proposed firstly by Dueren [175] and secondly by Coe [176] were also examined, equation 6.07 — and 6.08:

$$HvM(D) = 802C + 305 \qquad \text{(Dueren)} \qquad (6.07)$$

$$HvM(C) = 996.67C + 264.27 \quad \text{(Coe)} \qquad (6.08)$$

where HvM = Hardness once 100% martensite is formed.

A computer program "SKIDPROP" was designed and written by the Author in order to calculate the joint carbon equivalent values, tensile strength and hardness, appendix D-2.

An "average" plate composition was also defined by analysing all the plates used for the trials which were chosen at random from shipyard stockyards, table D6.01a-b, Appendix D-3.

Figure 6.07 has been designed to assess the relationship of maximum HAZ hardness in relation to plate carbon content when, as a result of a fast enough cooling rate, a fully martensitic state is reached. Hardness as predicted by both Coe and Duren are shown. From the graphs it can be seen that it is certainly possible to obtain hardness in excess of 350Hv for Grade A plate (C<0.23%) but only if welding speed is high and hence weld cooling time is sufficiently small.

Figure 6.08 has been plotted using the equation 6.06 to relate the weld cooling rate, predicted maximum hardness and plate composition (C and Pcm). From the average plate composition 95% confidence limits have been found for carbon levels - note that the upper 95% confidence limit

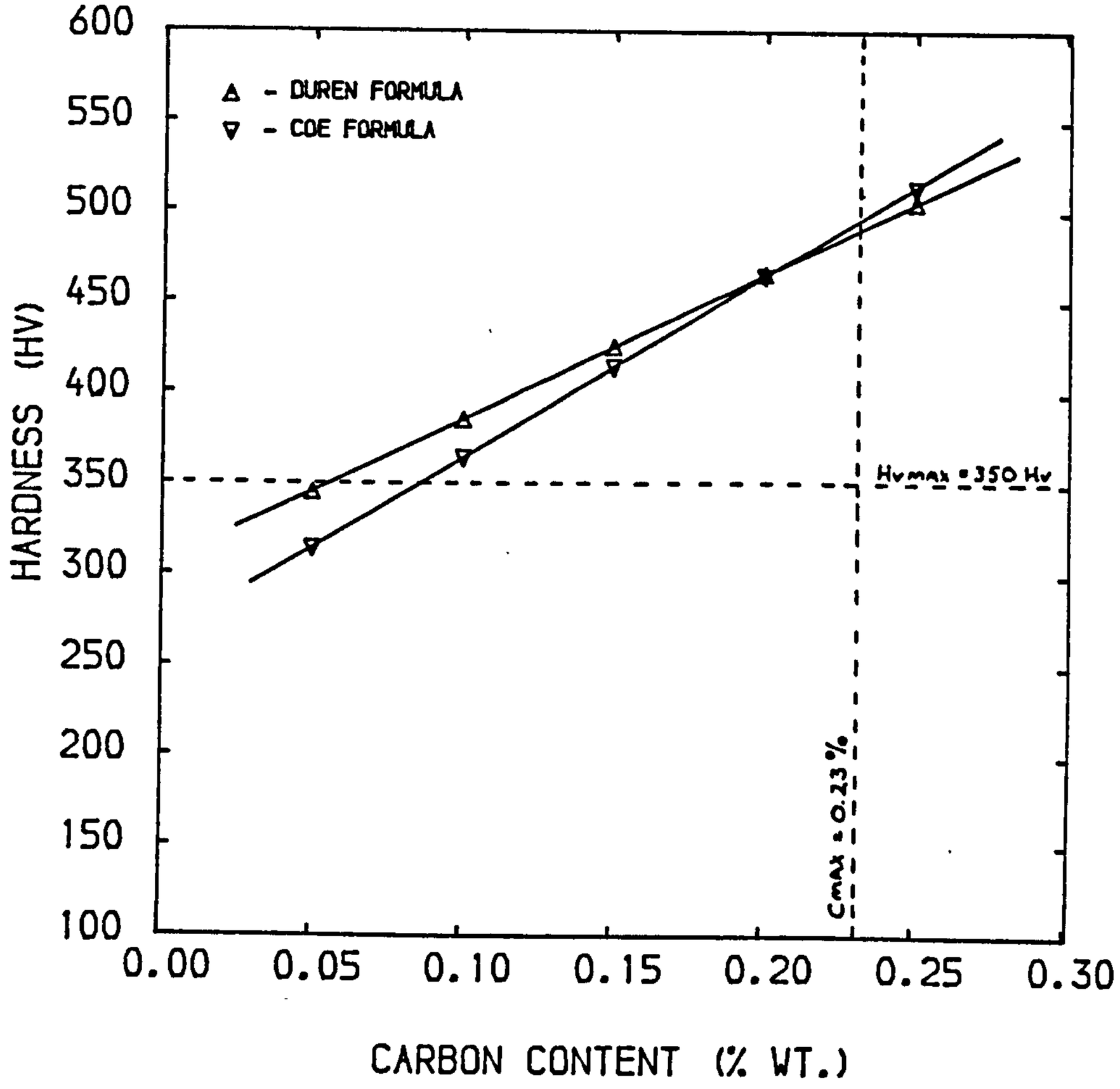

Figure 6.07 - Predictions of max. hardness in the HAZ assuming fully martensitic micro structure

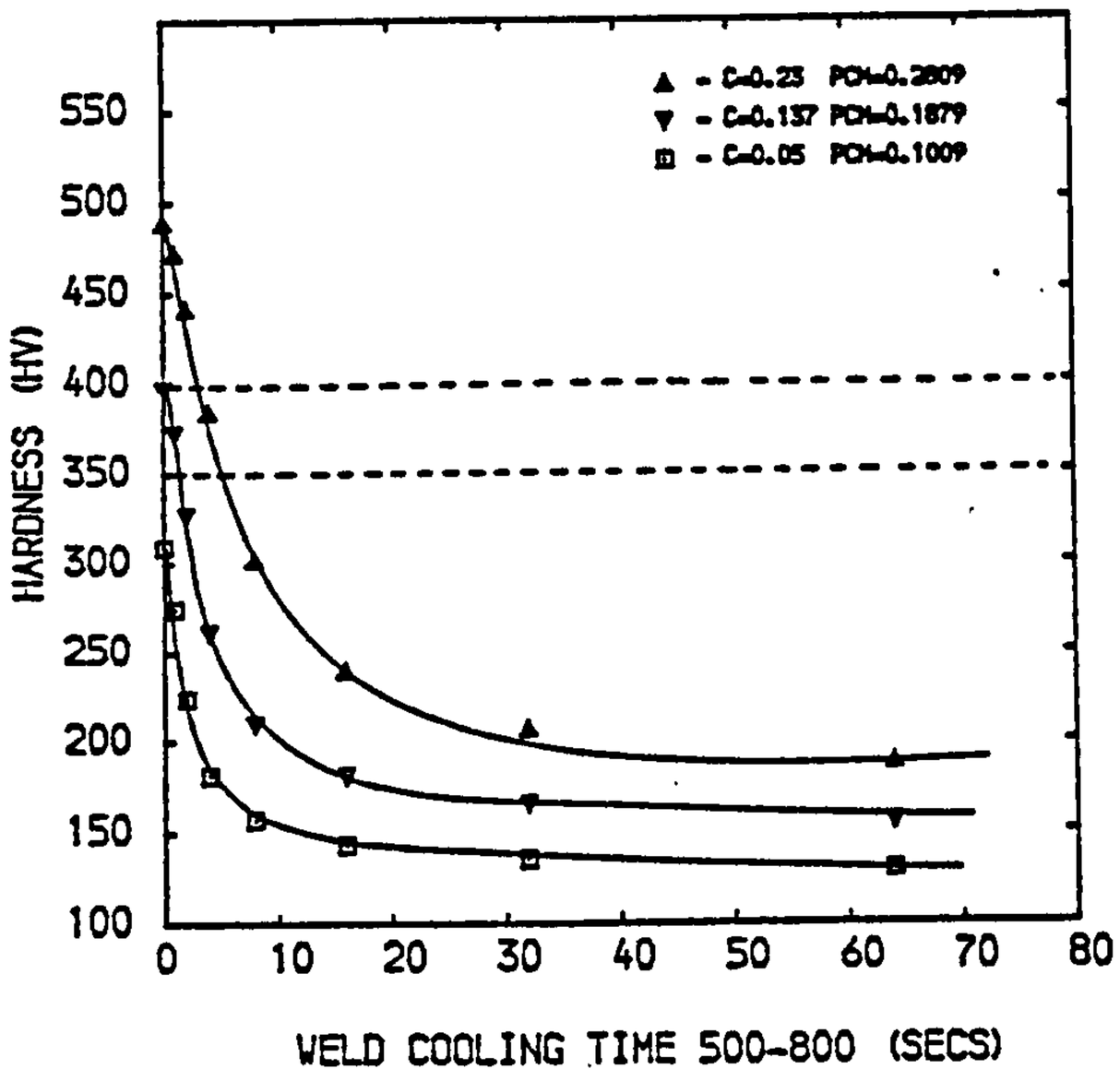

Figure 6.08 - Predictions of max. hardness in the HAZ for various weld cooling rates using equations of Suzuki

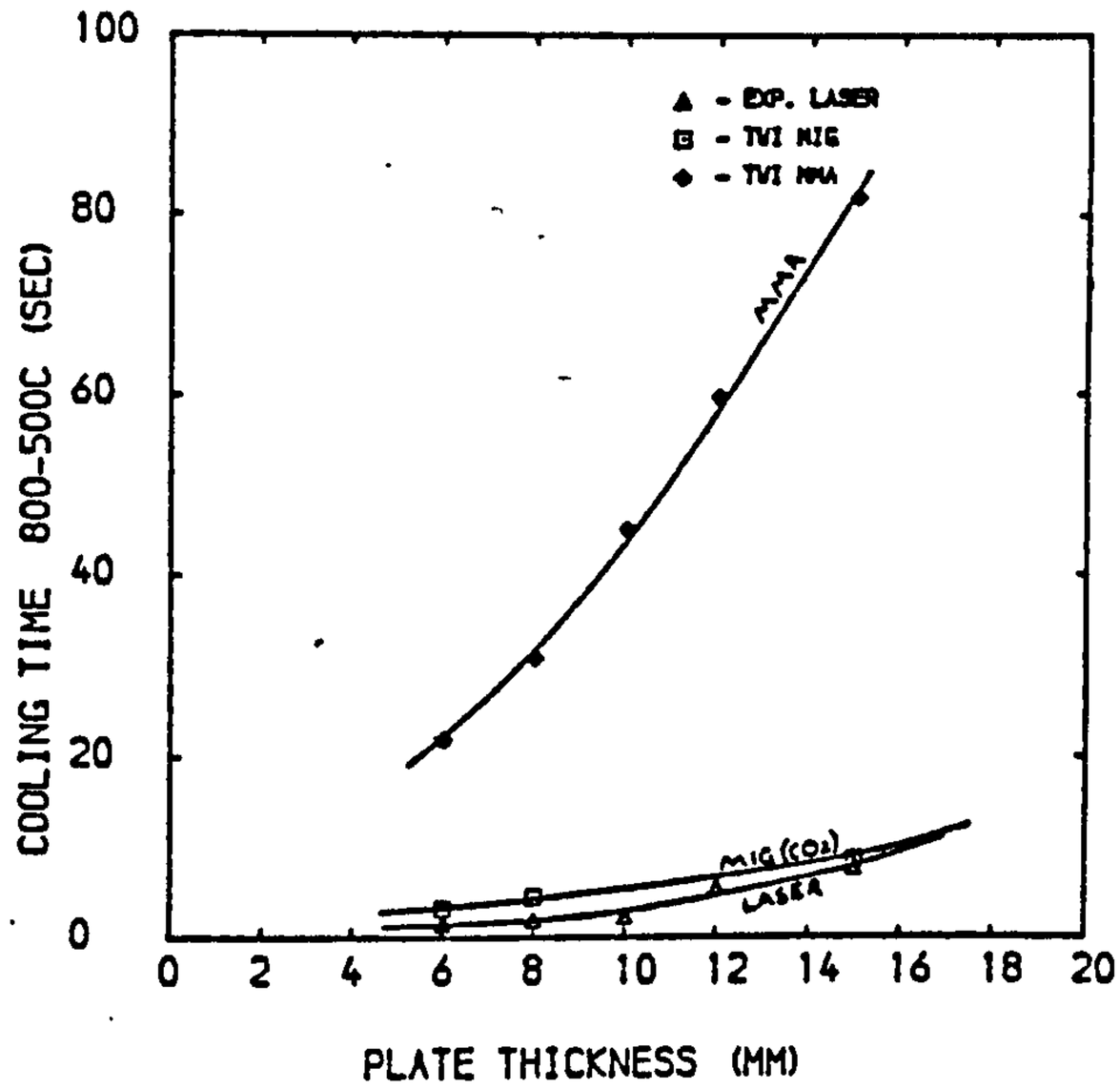

Figure 6.09 - HAZ cooling times (800-500) for laser skid welds, MMA and MIG fillet welds in the HAZ for various plate thickness

is in fact the maximum allowable level of 0.23% - with the average value of Pcm adjusted accordingly. The graph shows how for carbon levels of 0.05% , 0.137% and 0.23% minimum cooling times of 0.5, 1.5 and 5.5 seconds respectively would be necessary in order to ensure hardness values of less than 350Hv.

A comparison of likely cooling times for laser, MIG and MMA welds are shown in figure 6.09. For the conventional welds leg length of half material thickness has been assumed, arc energies estimated using standard data published by The Welding Institute [175] and then cooling times were calculated by a method developed by The Welding Institute and reported by Boothby [177] . Whilst good weldability would be expected for plate using MMA welds, in plate thicknesses of up to 15mm and carbon content of greater than 0.23% by comparing the curves for MIG welding and cross referencing to curves in figure 6.08, hardness levels greater than 350Hv would be expected at carbon levels above 0.23% if optimum MIG welding speeds are maintained in plate thicknesses below 9mm. This situation would apparently be more acute for laser welds. A comparison of relative hardness calculated from the cooling times for each process and based on average plate composition, figure 6.10 shows how hardness levels will just be maintained below 350Hv.

With this background a more detailed assessment was made of predicted hardness values for skid welds in each plate thickness produced with a constant power of 9kW(WP) at speeds optimised for production welding, figure 6.11. This showed that limits would have to be placed on carbon

level if hardness of 350Hv were not to be exceeded, table 6.01.

However, an alternative approach may be taken by assessing the validity of 350Hv as a maximum hardness level for the laser skid weld.

The maximum hardness level is selected in order to reduce the likelihood of either cold cracking - hydrogen cracking - or stress corrosion cracking. As a general rule for the former in both carbon-manganese steels and low alloy steels, the higher the hardness values detected in the weld zone, the more likely is the microstructure to be susceptible and the greater is the risk of cracking. Therefore if the welding process itself ensures that hydrogen levels are kept low and the ductility is acceptable then higher hardness levels may be tolerated.

Coe [178] tabularises various welding processes and related joint configurations. Whereas general MMA electrodes would be considered as having "high" hydrogen potential, MIG welding would be considered as a "low" hydrogen process. It is therefore expected that the laser process, using not only solid wire but also an inert gas shielding, would be classified as a low, if not "very low" hydrogen level process and as such is categorised for allowable hardness of 400Hv and possibly 450Hv.

Gooch [179] provides an appraisal of the link between hardness and stress corrosion cracking for ferritic steels. Like hydrogen embrittlement, service failure depends not only on microstructural, compositional variables and joint restraint but also on the amount of

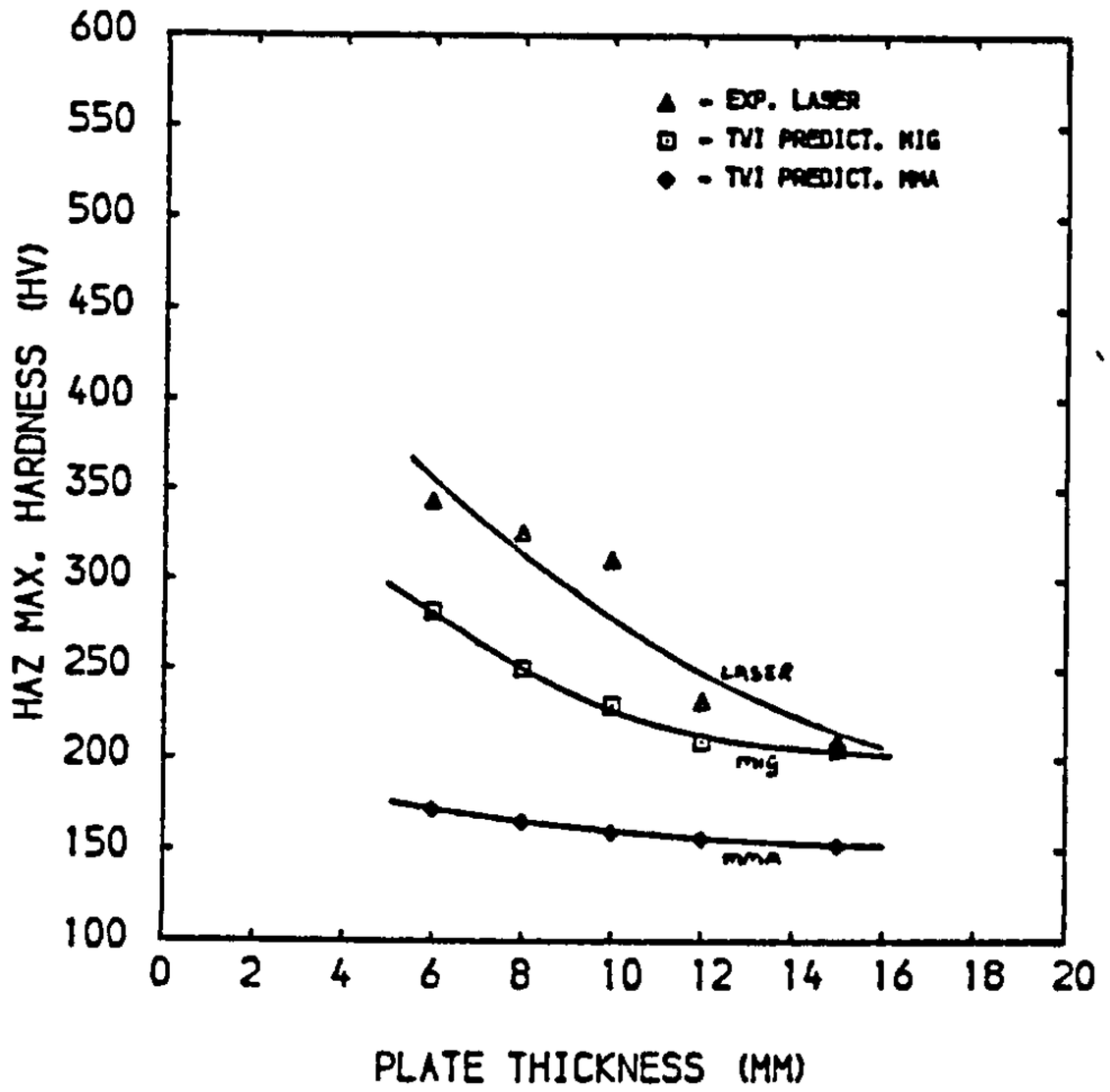

Figure 6.10 - Predictions of max. hardness in the HAZ for laser skid and MMA/MIG fillet welds assuming an average plate composition

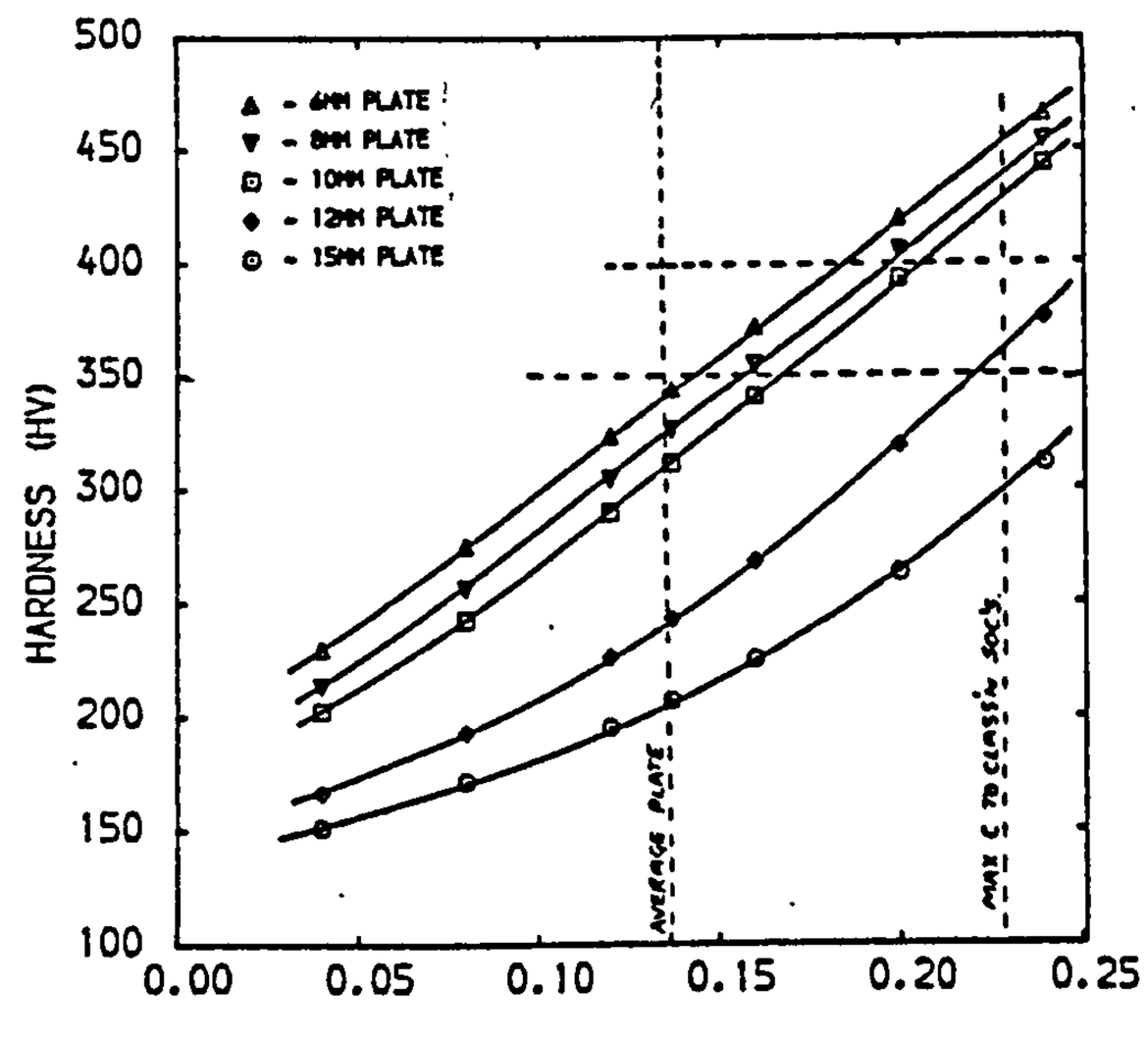

Figure 6.11 - Variation of hardness levels for varying plate compositions and skid weld plate thickness

Plate thickness	6	8	10	12	15
Max. C level for >350 Hv	0.15	0.16	0.17	0.22	>0.23

Table 6.01 - Maximum carbon levels so as not to exceed 350Hv (Optimum speed using a constant power of 9kW)

Plate thickness	6	8	10	12	15
Max. C level for >400 Hv	0.19	0.20	0.21	>0.23	>0.23

Table 6.02 - Maximum carbon levels so as not to exceed 400Hv (Optimum speed using a constant power of 9kW)

hydrogen capable of entering the material during service and acting to cause cracking.

One of the most practical situations of concern is therefore service in marine conditions. Gooch was unable to show stress corrosion failure developing for structural steels in salt water with hardness below 450Hv but he suggests a maximum hardness limit of 400Hv for practical design purposes.

Taking both factors into account its is seen that carbon contents higher than initially considered will now be acceptable, table 6.02.

These observations coincide with present investigations within British Shipbuilders to examine variations in the quality of steel entering the shipyards, with an aim of increasing the control of plate compositions. If this is achieved no further controls would be necessary for the skid welding process on mild steel plate, although post weld heat treatment would have to be considered for laser welding in higher tensile steels.

6.3 GENERAL ASSESSMENT OF WELD MICROSTRUCTURE

6.3.1 Classification of Laser Weld Microstructural Constituents

Descriptive classification of weld microstructural constituents can be very confusing, especially to the non-metallurgist. Nomenclature has depended on operator experience, equipment available, etching agents and familiarity with the types of microstructure to be examined e.g. homogeneous samples compared with welded samples.

In recent years attempts have been made to standardise classification procedures, simplifying the often historic names given to microstructural constituents and concentrating the operations on using the optical microscope. Hence a quantitative method of describing weld microstructure has been developed which can be easily understood by engineers.

Guidelines developed by the International Institute of Welding (IIW) [180] and an earlier scheme published by Abson and Dolby [181] give a method of point counting within weld constituents which can be defined with an optical microscope. This then enables a study of microstructural changes which are likely to accompany changes in strength, toughness and other mechanical properties; it aids comparisons of effects of changing welding parameters and it provides means of analysing microstructural changes caused by changes in consumable and parent material composition.

Point counting is conducted using an optical microscope, the weld area being viewed on a matrix basis at up to 1000 positions. The size, relative orientation and aspect ratio of the ferritic structure viewed at each position or "point" is then compared against a set number of comparative structures as listed by Dolby [181] . A statistical analysis can then be conducted on the points counted of each structure to establish the relative proportions of each.

Whilst the IIW document was only published in the middle of the project the Author used the nomenclature as defined by Abson and Dolby, but has provided a conversion table to compare both systems also noting the more traditional microstructural classification names, table 6.03. The author was encouraged that an international standard was available which could both be understood and actively compared by the metallurgist and engineer alike. Also the guidelines presented a method which could easily be used by follow-on researchers and related directly to the mechanical properties, providing a vital link between classification organisation requirements for laser welds against conventional welds.

Examination of the weld microstructure has been conducted on both "Grain growth microstructure" - the way in which the grains of prior austenite form during the weld cooling and "Transformed microstructure" - the constituent to which the prior austenite grains change during cooling. In addition to the weld material itself the HAZ, particularly material adjacent to the fusion line has been examined. During the examination defects in the weld structures which caused concern were

MAIN CATEGORY	SUB CATEGORY	ABBREVIATION (I.I.W.)	ABBREVIATION (DOLBY)	PREVIOUS DESCRIPTIONS
Primary Ferrite		* PF		
	Grain boundary ferrite	* PF(G)	GF	Proeutectoid ferrite, ferrite veins blocky ferrite, polygonal ferrite
	Intragranular polygonal	* PF(I)	PF	Polygonal ferrite, Ferrite islands
Ferrite with second phase		* FS		
	Ferrite with non-aligned second phase	FS(NA)		
	Ferrite with aligned second phase	* FS(A)	AC	Ferrite with aligned MAC Lamellar product
	Ferrite side plates	FS(SP)		Ferrite side plates
	Bainite	FS(B)		Feathery bainite
	Upper Bainite	FS(UB)		Upper bainite
	Lower Bainite	FS(LB)		
Acicular Ferrite		* AF	AF	Acicular Ferrite
Ferrite Carbide aggregate		* FC	FC	Ferrite and interphase carbide
	Pearlite	FC(P)		Pearlite
Martensite		* M	M	Martensite
	Lath Martensite	M(L)		
	Twin Martensite	M(I)		

Table 6.03 - Nomenclature for the classification of laser weld microstructural constituents

isolated and are discussed in the final section.

6.3.2 Grain Growth Microstructure

Columnar grain growth takes place away from the direction of heat flow resulting in two distinct orientations of columnar grain formation. Between the bounds of the web plate thickness and the face plate grain growth is mainly perpendicular to the web edge. Within the incident and emergent beads, as cooling takes place at an angle to the joint line, grains form from the bead surface. However, for plate thickness above 10mm when, because of reduced penetration, smoothing beads were smaller, there was little "fanning" of the columnar grains, as cooling through the plate surfaces dominated.

The centre line of the welds were characterised by a zone of equiaxed grains which formed during the final stages of solidification. The extent of this zone varied for plate thickness, heat input, position in the weld and would also be strongly influenced by weld pool chemical constituents.

Figure 6.12 shows how for reducing heat input (therefore shorter cooling times), the percentage equiaxed grains reduce in the 6mm plate example. This tends to a greater dominance of columnar crystals and subsequently, if highly restrained a likelihood of hot cracking along the joining line could exist. A similar trend is found by comparing the variation of equiaxed zone width to the variation of weld depth across

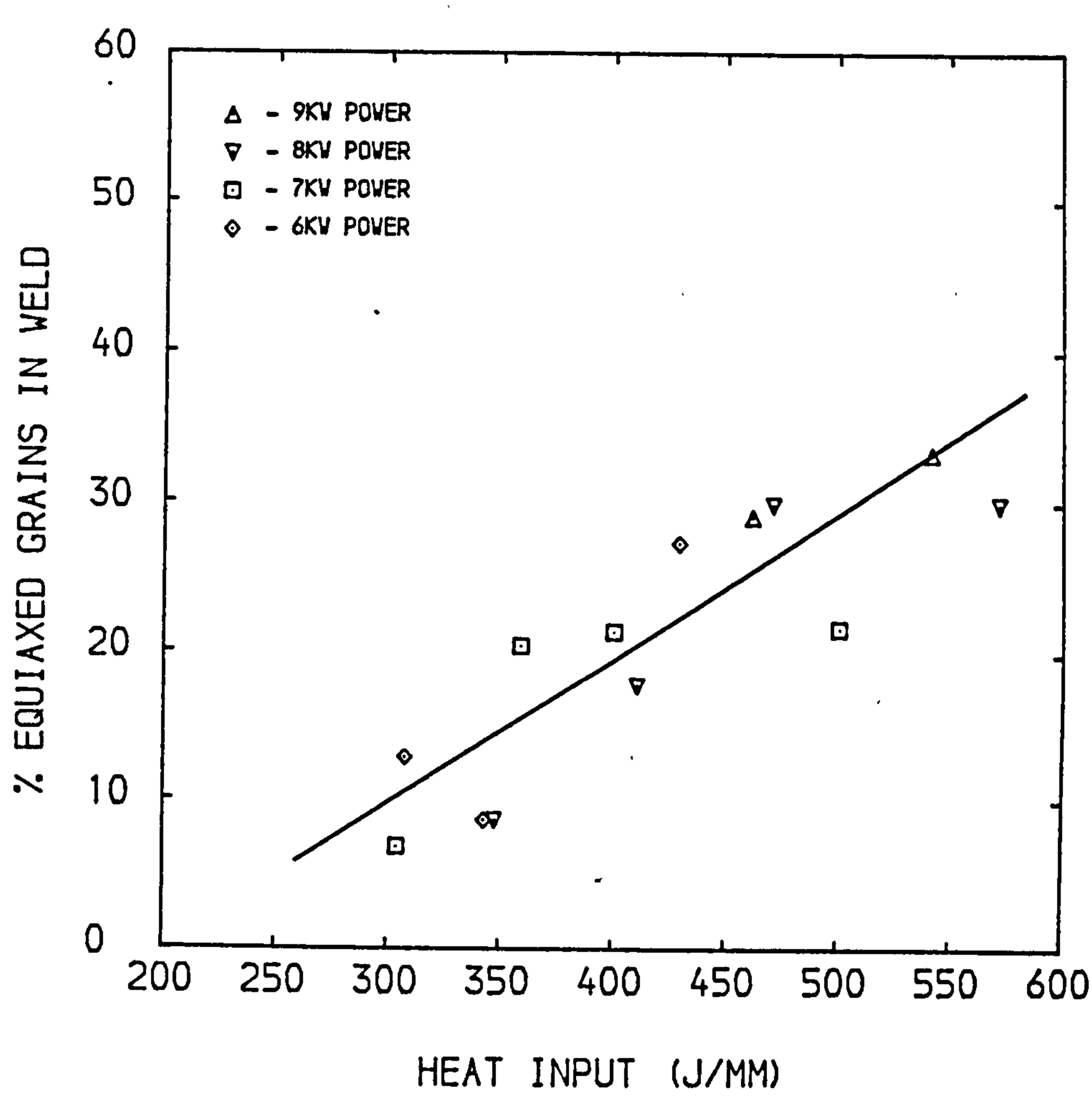

Figure 6.12 - Percentage of equiaxed grains to columnar grains for 6mm plate skid welds with varying heat input

its width, figure 6.13. Generally, as weld depth increases, so the percentage of equiaxed grains reduces. However, hot cracking has only been experienced where high restraint exists. This has been evident at the incident bead of joints in plate thickness above 12mm when cracking occasionally occurred in the middle of the bead when its size become excessive compared to the width of the weld at the emergent side.

Prior austenite grain size is of importance when assessing weld structural properties. Mean sizes found in 6, 10, and 15mm plate joints are plotted in figure 6.14 showing a range of from 35um to 55um compared to a typical range found for MMA fillet welds on similar joints of from 65um to 80um emphasising the finer, potentially stronger structure of the laser weld.

The majority of welds were microstructurally examined from transverse sections cut from the weld. In order to confirm certain grain orientations, centre line longitudinal sections were also removed for joints of 6mm,8mm and 15mm thick. For electron beam welds Komizo et al [182] had shown how at slow speeds (<4mm/second) with a large radius to the trailing edge of the weld pool elongated crystals could form along the weld centre line forming a "raft" structure, although when sectioned in transverse across these grains they appeared to be "equiaxed".

Whilst confirming that such a "raft" structure, normally associated with low toughness properties, was not present in the laser weld, the longitudinal section, Figure 6.15 a-b also showed how fluctuations were

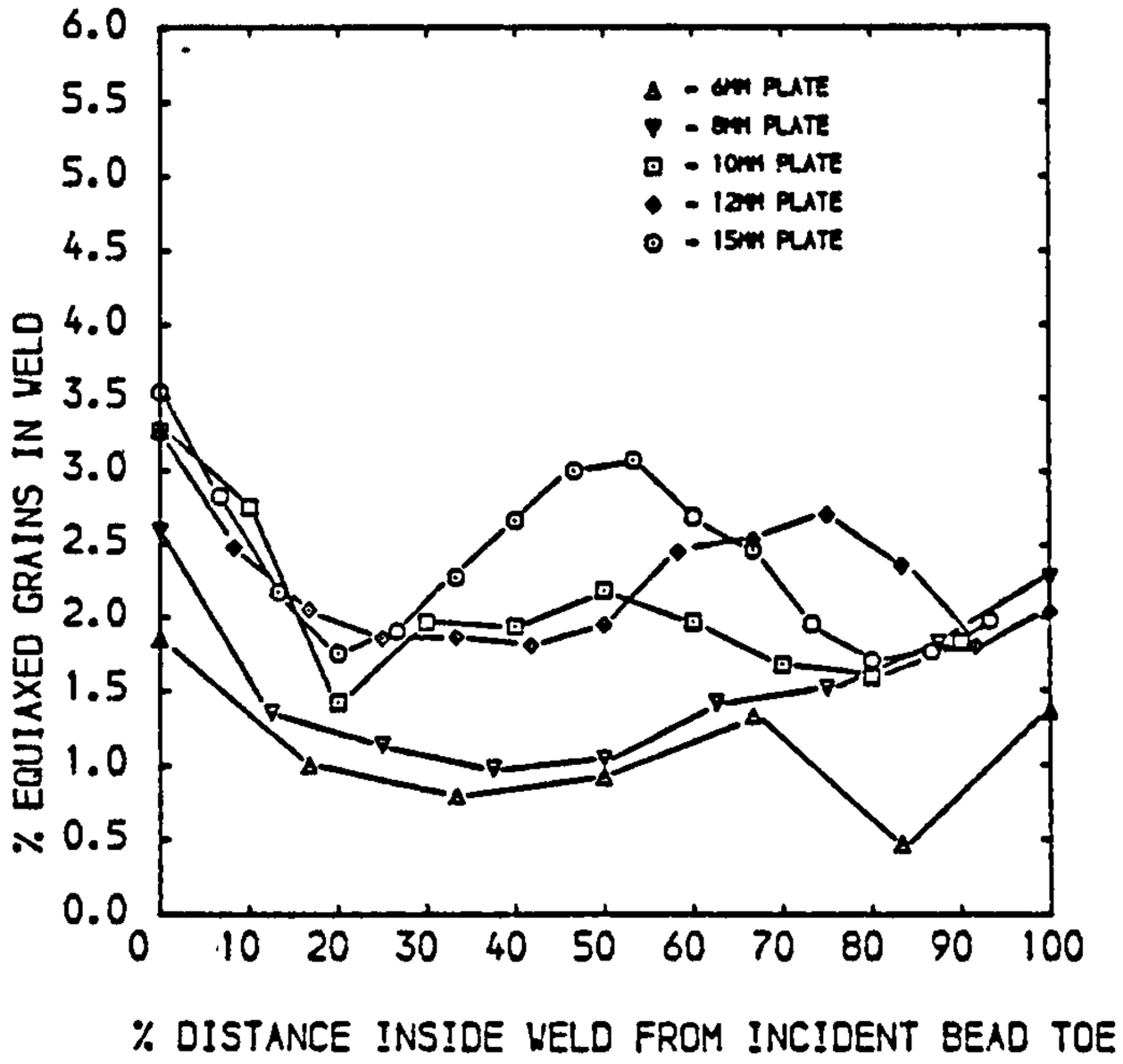

Figure 6.13a - Weld widths measured at various points across the weld transverse section

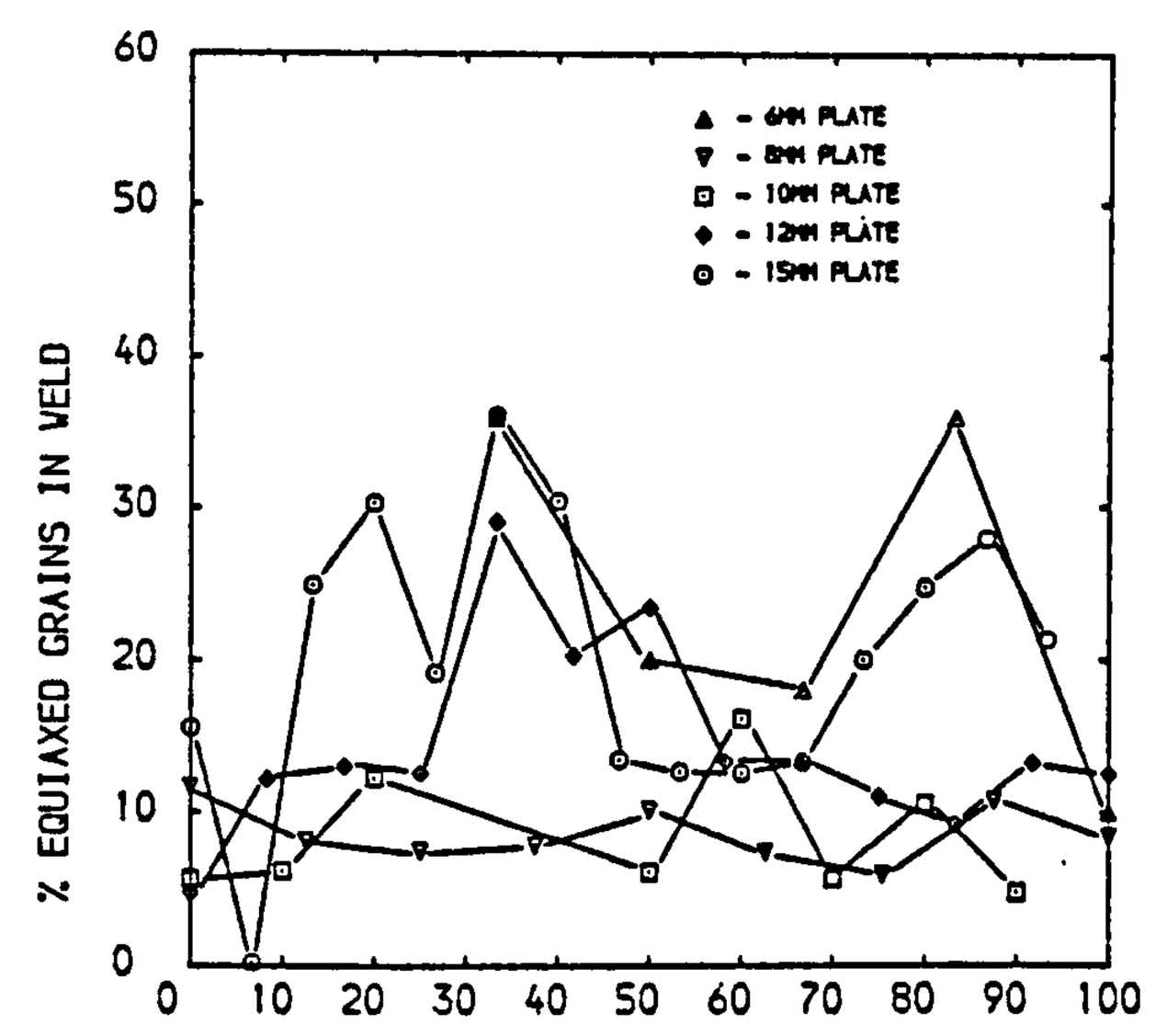

Figure 6.13b - Ratio of equiaxed/columnar grain zones corresponding to the measured width in (a)

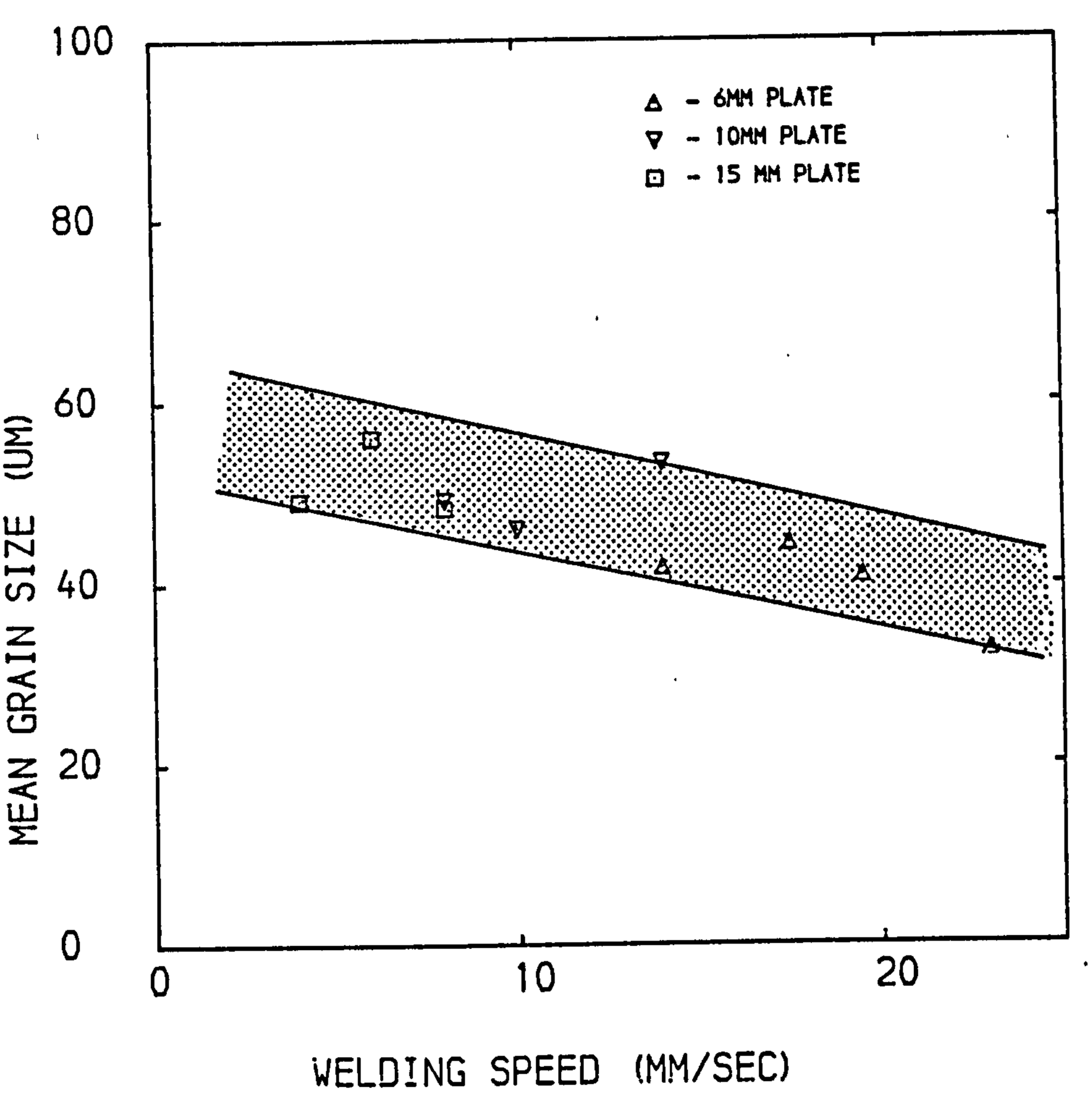

Figure 6.14 - Prior austenite grain sizes measured for skidwelds of various plate thickness

present in the weld profile along the weld length. At an average wavelength of 1.5mm between fluctuation peaks, this would represent a frequency of 9.3Hz for the 8 mm joint being produced at a traverse speed of 14 mm/second. Such regular fluctuations have also been shown in butt welds by Shinada et al [183] .

The effect of the fluctuations on the microstructure is to change the orientation of columnar grain growth slightly along the joint length so explaining a cutting-off effect sometimes noticed in columnar grains in transverse sections.

The pulsating effect could be due to cyclic power or modal fluctuations within the laser although these would be expected at higher frequencies. Extensive trials would be necessary to isolate laser affects from others e.g. those caused by mechanical vibration, wire feed vibration or inherent fluctuations within the keyhole, which could not be included within the scope of the present trials. Probably the most effective diagnostic means for investigating this further would be by the use of on-line radiography as used recently for examining weld pool stability [184] .

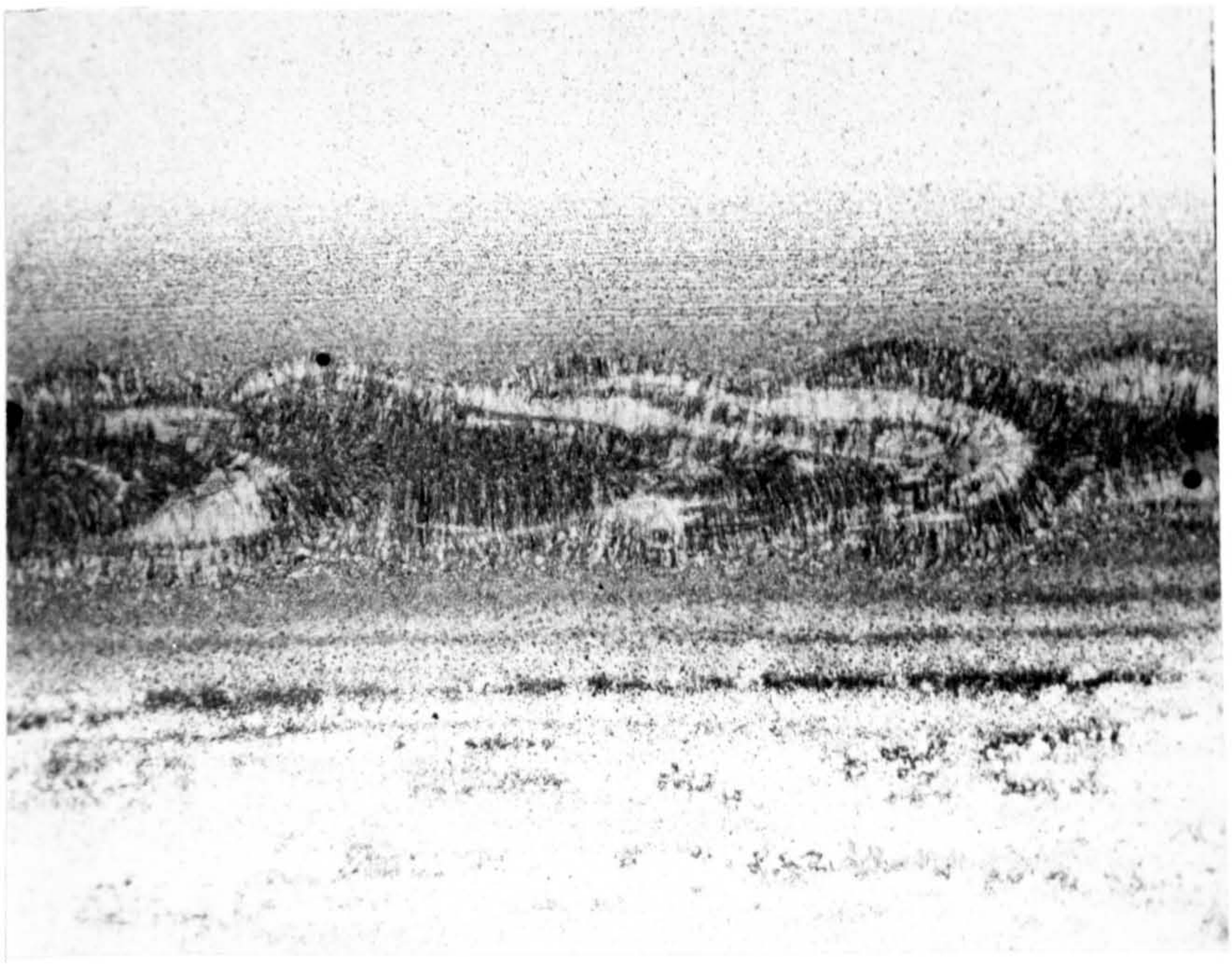

Figure 6.15a - Skid weld longitudinal section; 8mm plate (x12.8)

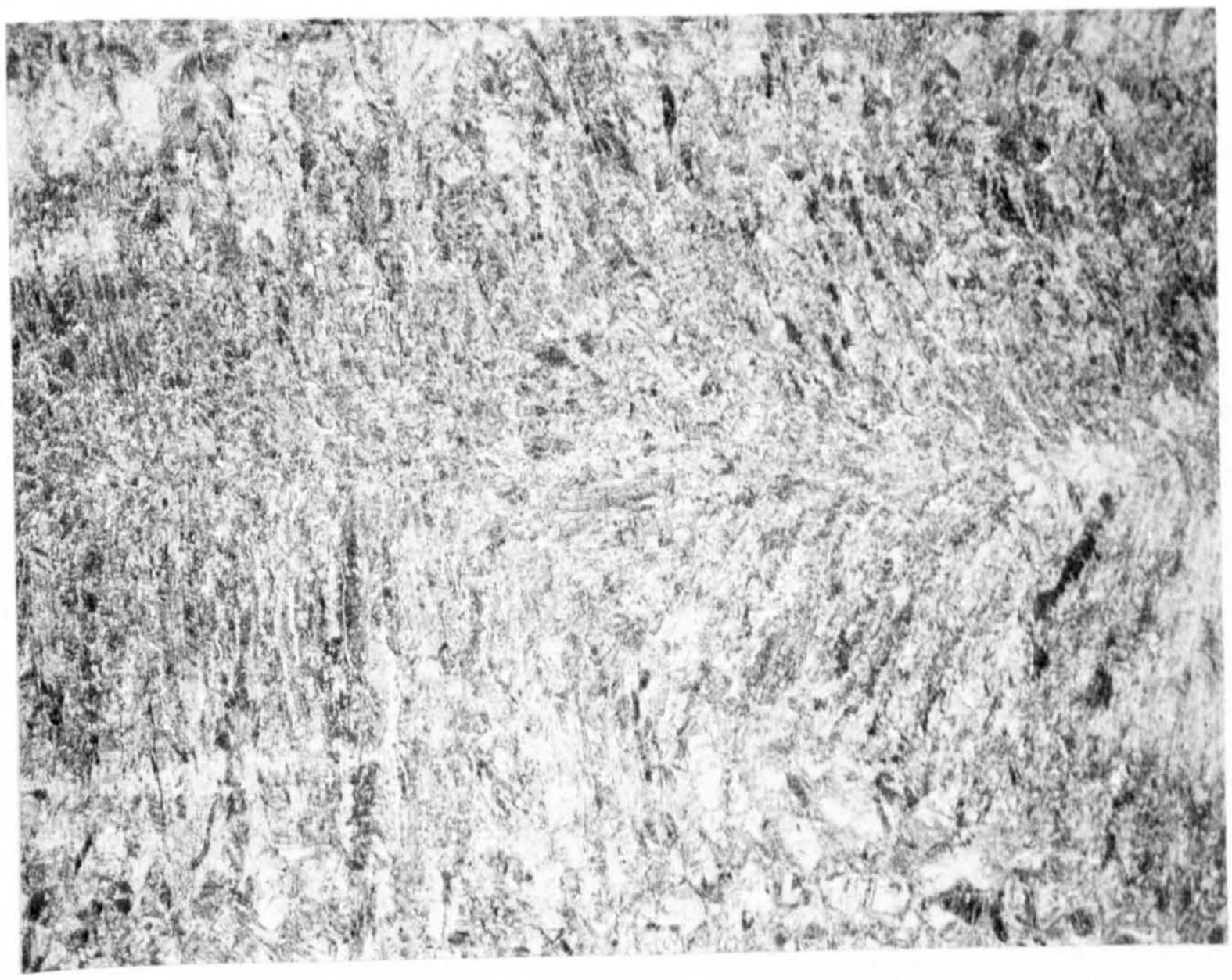

Figure 6.15b - Enlarged section of (a); (x64)

6.3.3 Transformed Microstructure

A statistical evaluation of transformed microstructure was made using transverse sections etched in 2% Nital. Using an optical microscope with a magnification of either x400 or X500 depending on the structural complexity, about 1000 points were classified and counted for each specimen. Transformed constituents were classified for welds in 6,10 and 15mm thick joints against the nomenclature as devised by Abson and Dolby [181] and shown in Table 6.03. In addition microphotographs were taken of representative weld areas. The statistical point counting was restricted to the weld material only. However, the fusion line and heat affected zone are also shown in microphotographs.

Figure 6.16a-d show the results of comparative microstructure phase counts for 6,10 and 15mm, each weld being produced at optimised production parameters to produce visually balanced beads. Two sets of counts are shown for joints produced in 6mm plate, the first being plate P6/1/CS and the second in plate P6/2/SHS. Due to the small range of individual speed fluctuations few conclusions may be drawn on the effect of speed changes on any one plate thickness. However, by comparing each joint thickness, particularly at the preferred welding speed the dominance of Acicular Ferrite (AF), Ferrite with aligned MAC-Martensite-austenite or carbide (AC), and Ferrite-carbide aggregate (FC), is evident.

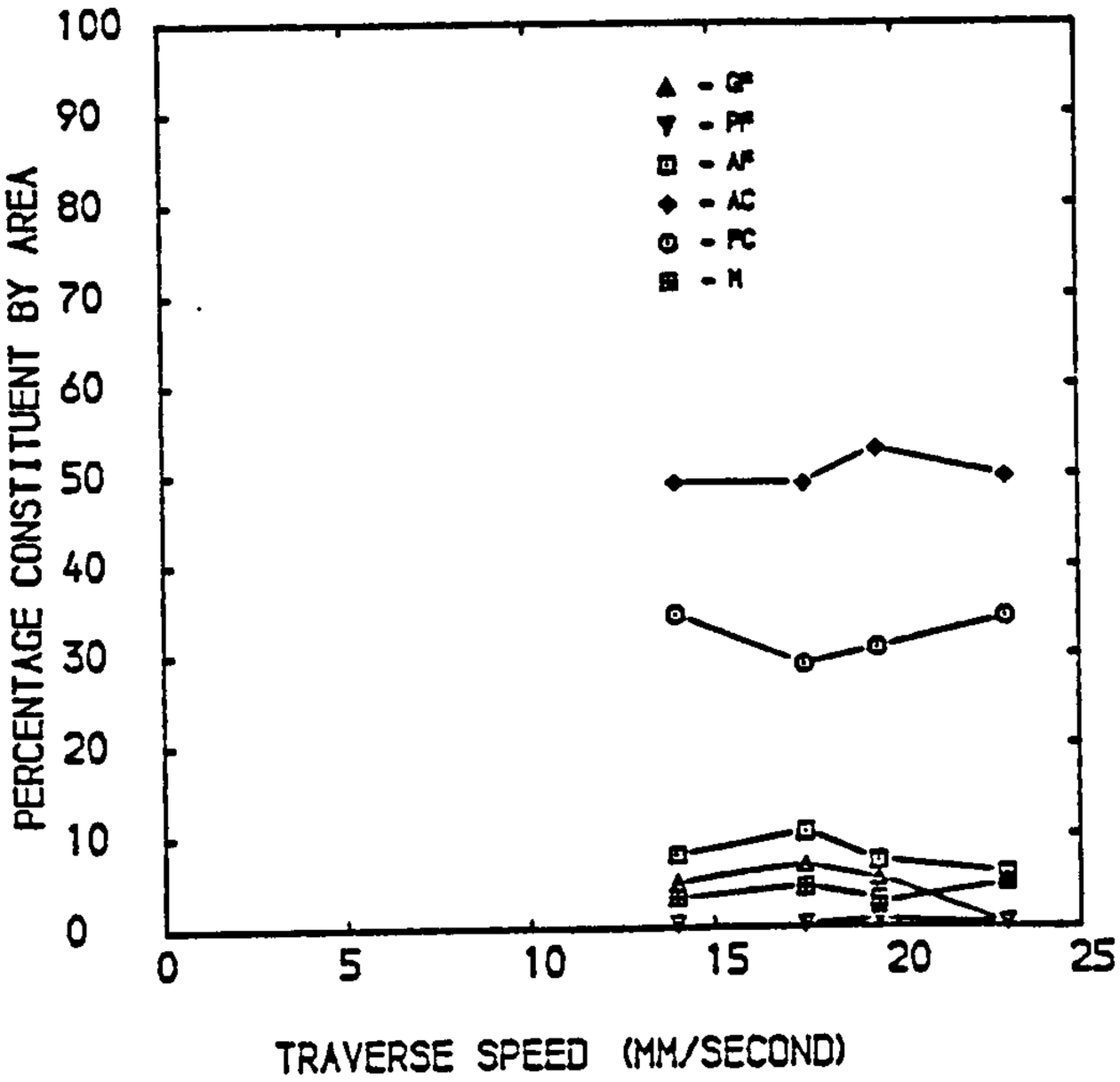

Figure 6.16a - Phase counts in 6mm plate skid weld, weld metal; plate P6/1/CS

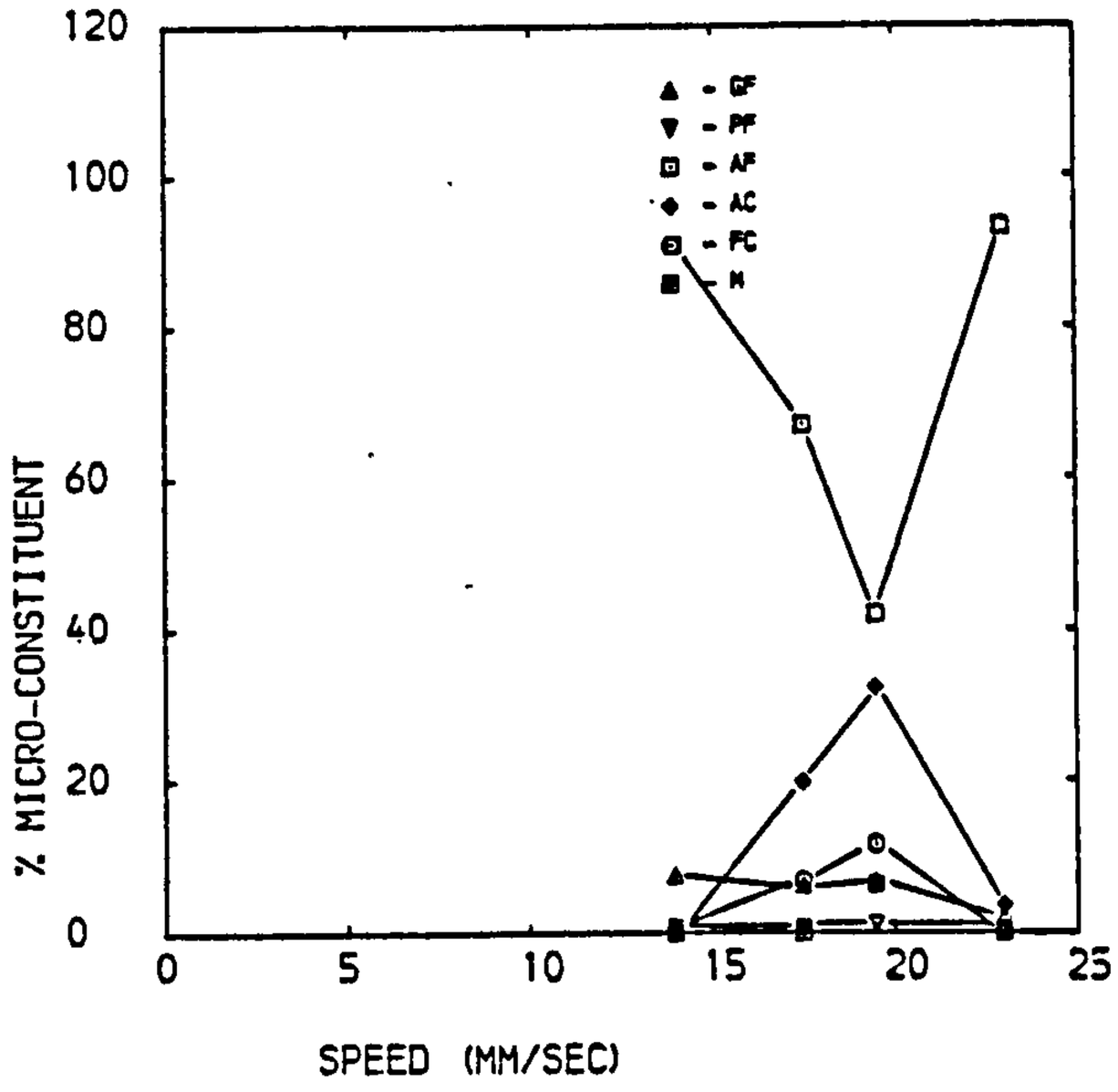

Figure 6.16b - Phase counts in 6mm plate skid weld, weld metal; plate P6/2/SHS

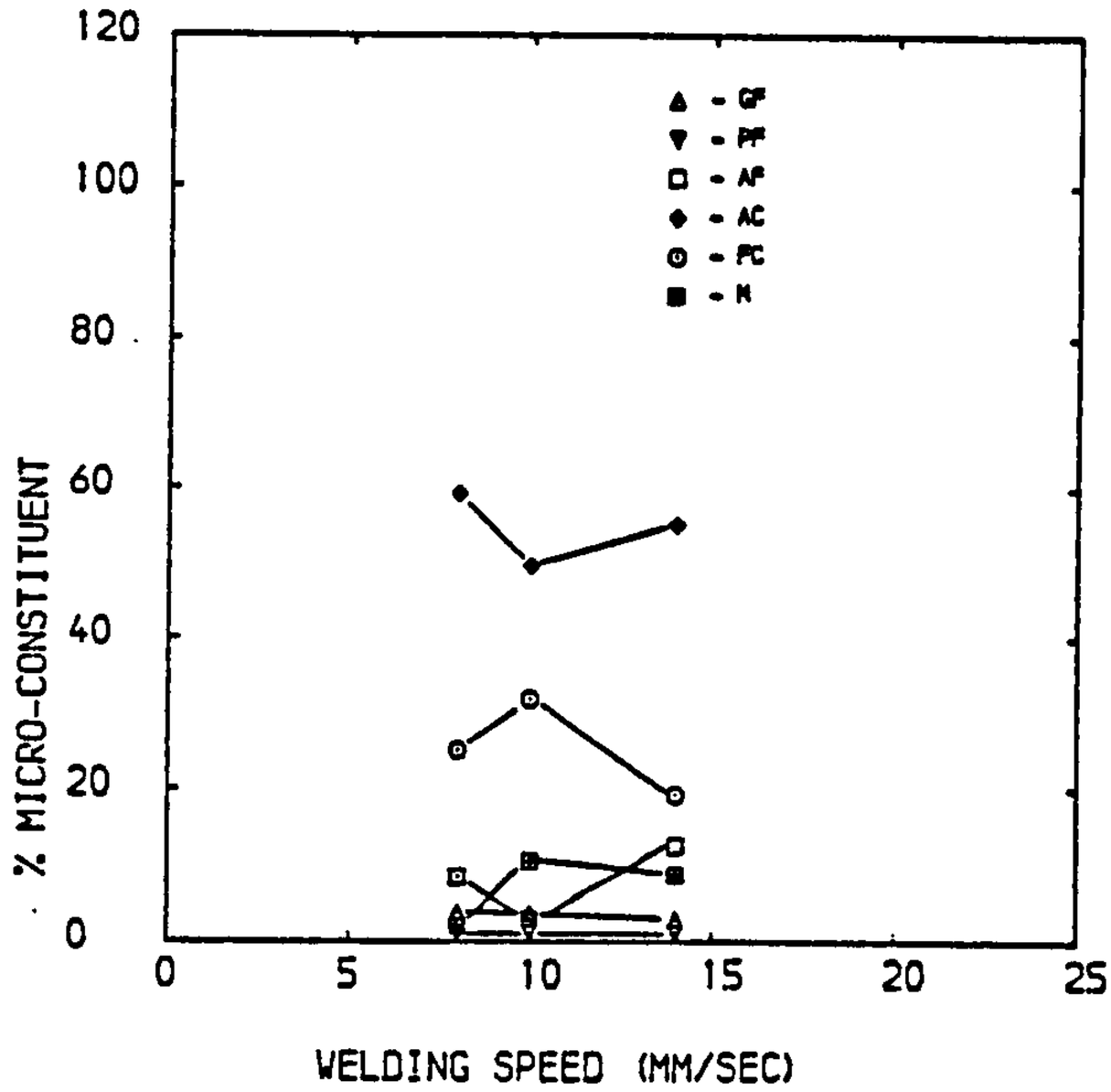

Figure 6.16c - Phase counts in 10mm plate skid weld, weld metal

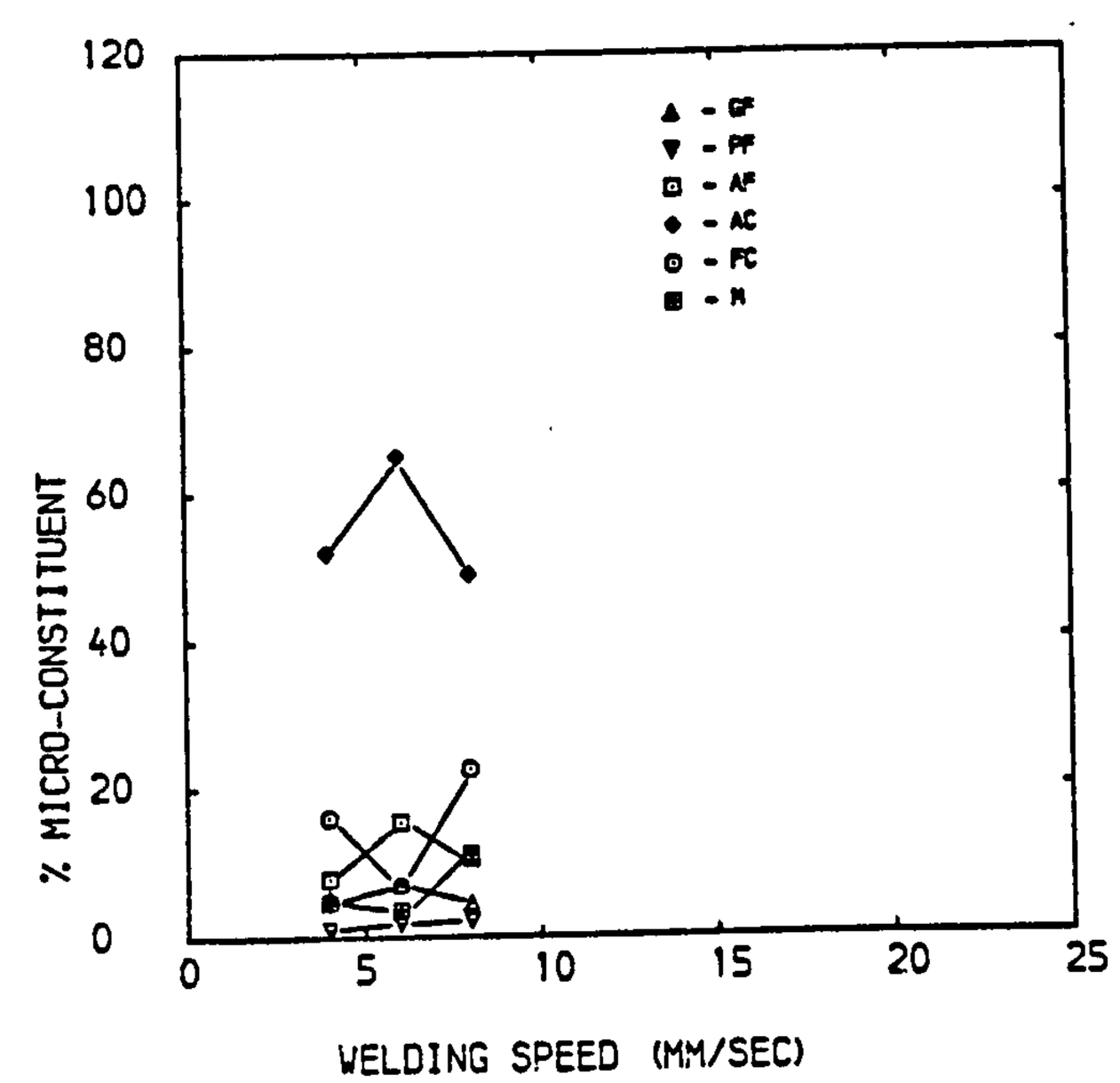

Figure 6.16d - Phase counts in 15mm plate skid weld, weld metal

In the majority of welds consistent levels of AC and FC have existed with proportions of between 55% and 65% and between 25% and 35% respectively, with the proportion of AF being 10%. However, for the first set of 6mm welds in plate P6/1/CS the levels of AF have dominated.

This apparent sudden change in structure is not however so surprising. Examination of a continuous cooling transformation diagram, figure 6.17 produced by Easterling [85] but with the nomenclature proposed by Abson and Dolby [181] added by the Author shows how the proportion associated with the formation of AF is relatively small. "Reaching" such an area is controlled not only by a relatively fast cooling rate but it is also affected by weld pool constituent and may also be controlled by optimising oxygen levels [139] and alloying elements.

A major proportion of the fine interlocking AF structure is preferred for weld microstructures [185] as, whilst providing a toughness characteristic similar to that of martensite, figure 6.18, hardness values can be maintained within acceptable limits. The lamellar AC structure, depending on its orientation to a fracture force, tends not to give such good cleavage resistance and is consequently less preferable within the weld.

A structure of fine grain boundary ferrite (GF) forming along prior austenite grain boundaries with AF forming in between, is most preferred for good structural properties. However, comparison of MMA control welds produced to normal shipbuilding practice showed that while proportions of

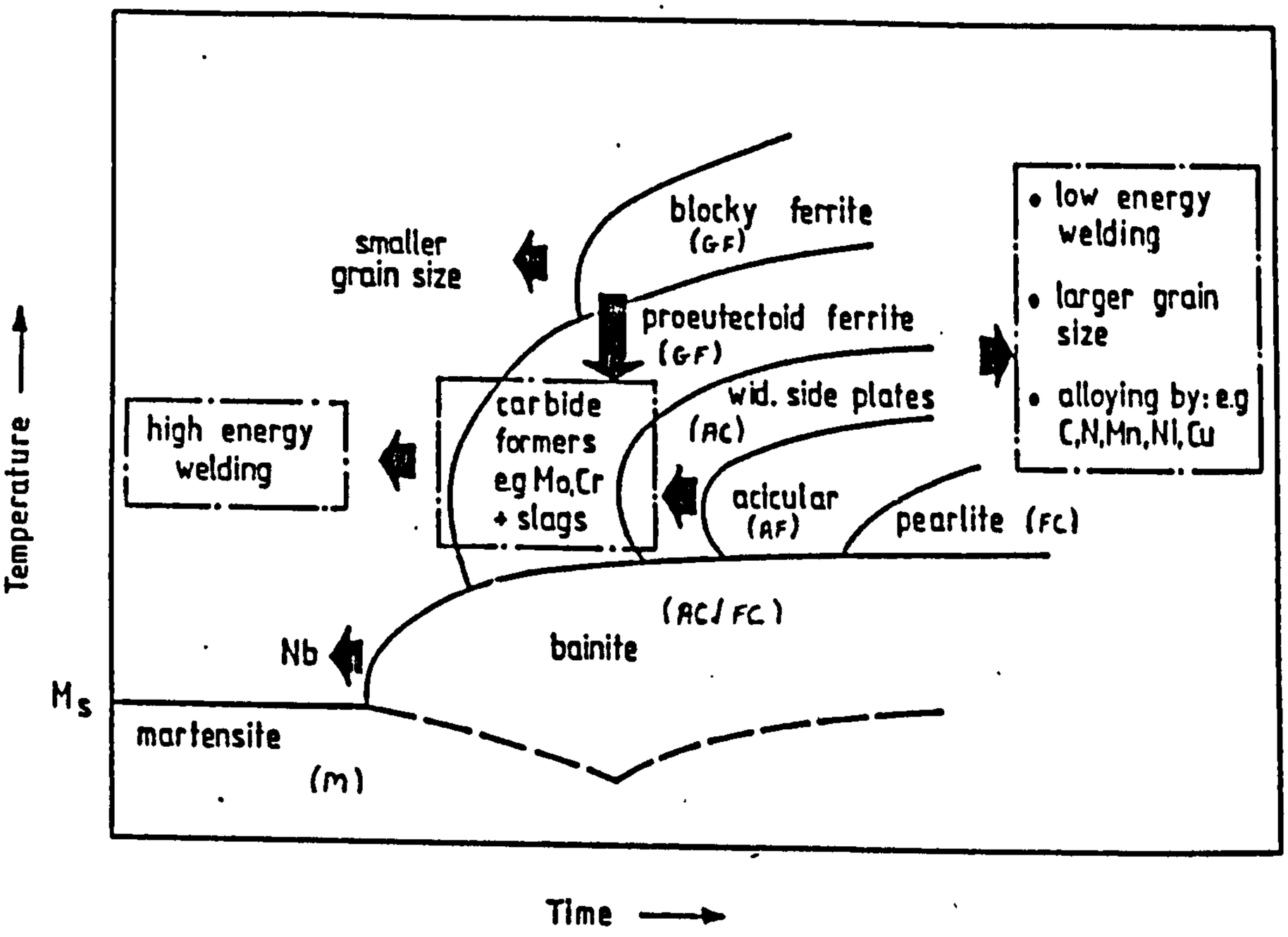

Figure 6.17 - Continuous cooling transformation curves and the influence of various parameters [85].

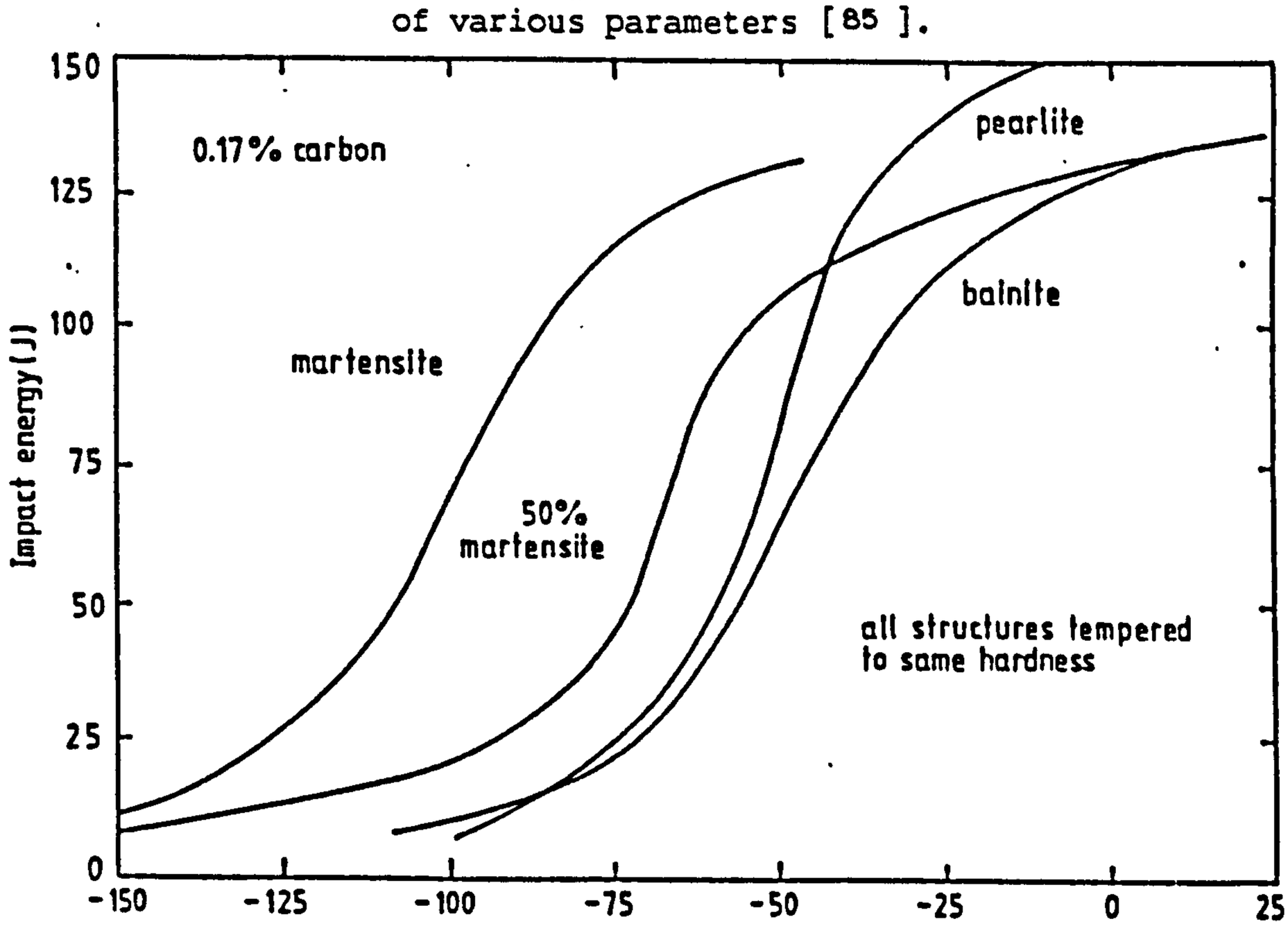

Figure 6.18 - Impact toughness of various microstructures [185].

AC and FC remained similar to that of the laser welds, there was a higher proportion of GF and Polygonal Ferrite (PF) to 10% and an AF level of only 5%. Combined with the presence of the larger grain size within the conventional weld, it is not surprising that the laser weld exhibited superior structural qualities during mechanical testing.

Visual comparisons may be made from the macrophotographs produced. Figure 6.19 shows typical microstructure found in the parent plate, HAZ and weld material. The fine grain structure of the laser weld may be compared to that in a typical shipyard welded MMA fillet weld, figure 6.20. Further microphotographs of welds in each plate thickness tested are produced in figures D6.01 to D6.05, Appendix D-4. Microphotographs have been produced of the majority of parent plates showing typically banded ferrite and pearlite structure of hot rolled mild steel plate, weld fusion line and weld metal to one side of the weld centre line. Magnifications of X200 and in particular cases to X500 and X1000 were used in order to highlight particular weld structures.

For the weld material, microstructural constituents follow the trend described from phase counting, however for 3mm plate a highly martensitic structure is found due to plates of high carbon content and short cooling times.

Whereas in the weld material, structure may be controlled by the choice of a consumable with a suitable carbon equivalent, examination of the fusion line necessarily relates to parent plate composition and

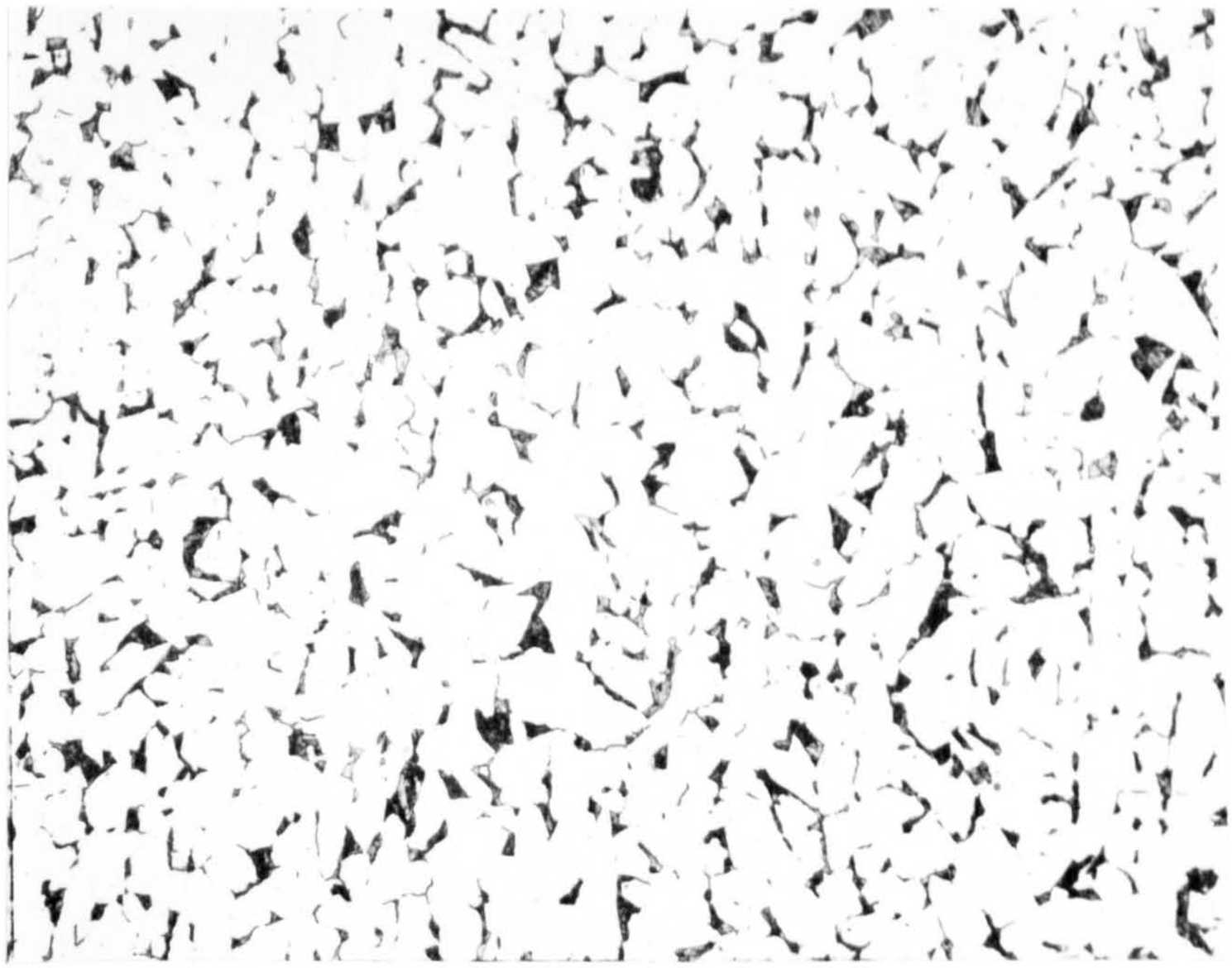

Figure 6.19a - 8mm skid weld, parent plate - banded ferrite and pearlite (x200).

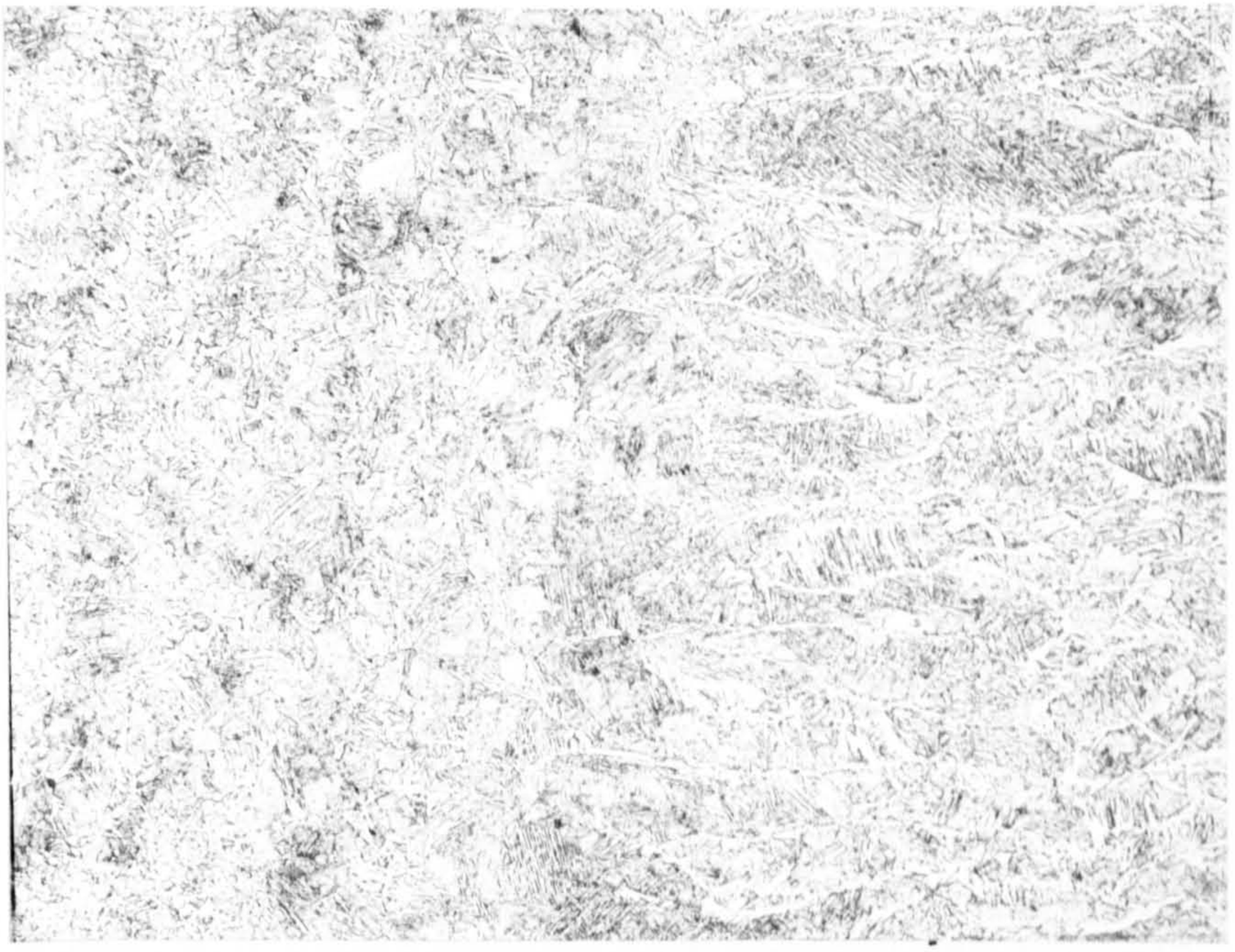

Figure 6.19b - 8mm skid weld, HAZ and fusion line (x200).

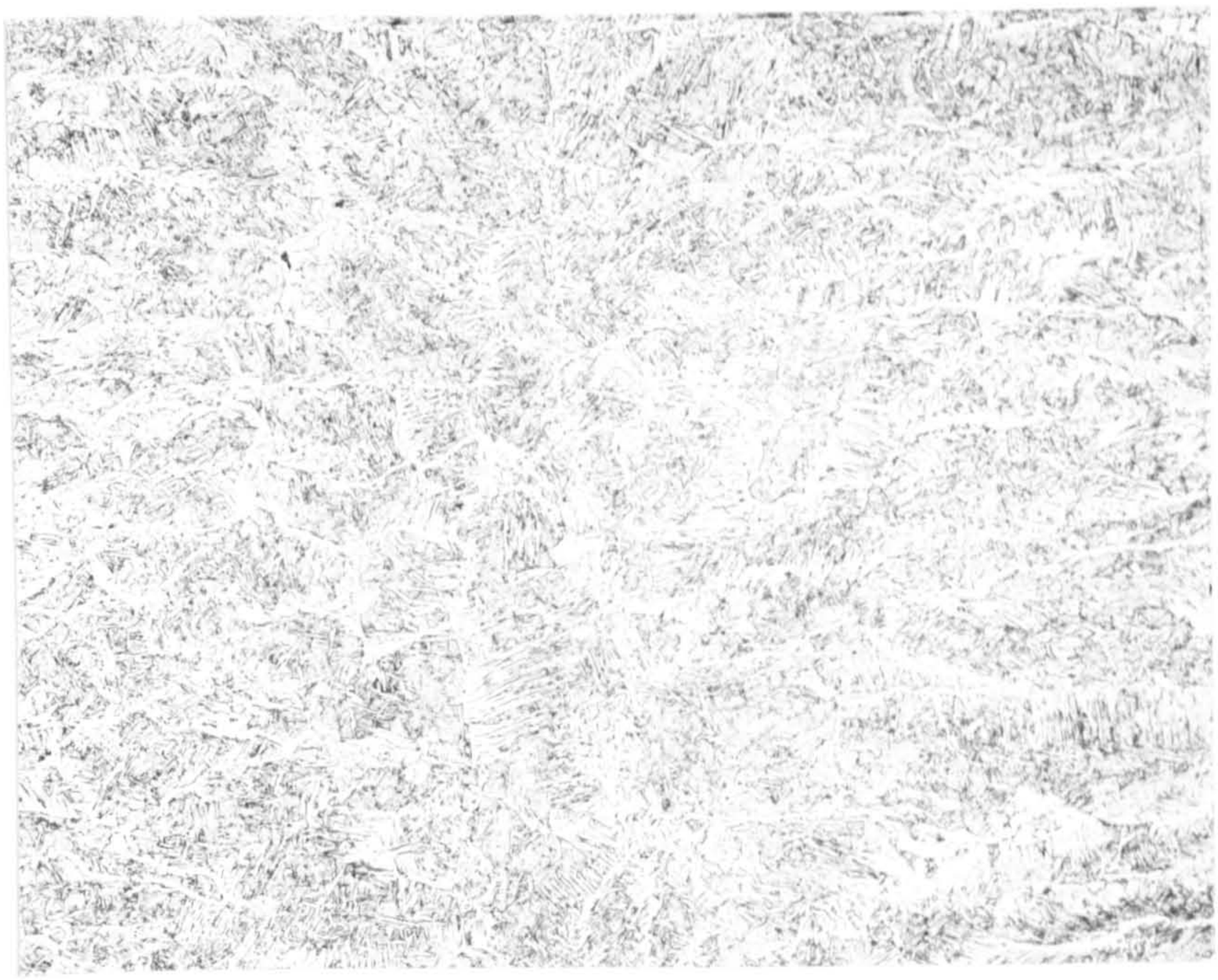

Figure 6.19c - 8mm skid weld, weld centre - fine GF and AC in FC, columnar grains extending in to central equiaxed grains (x200).

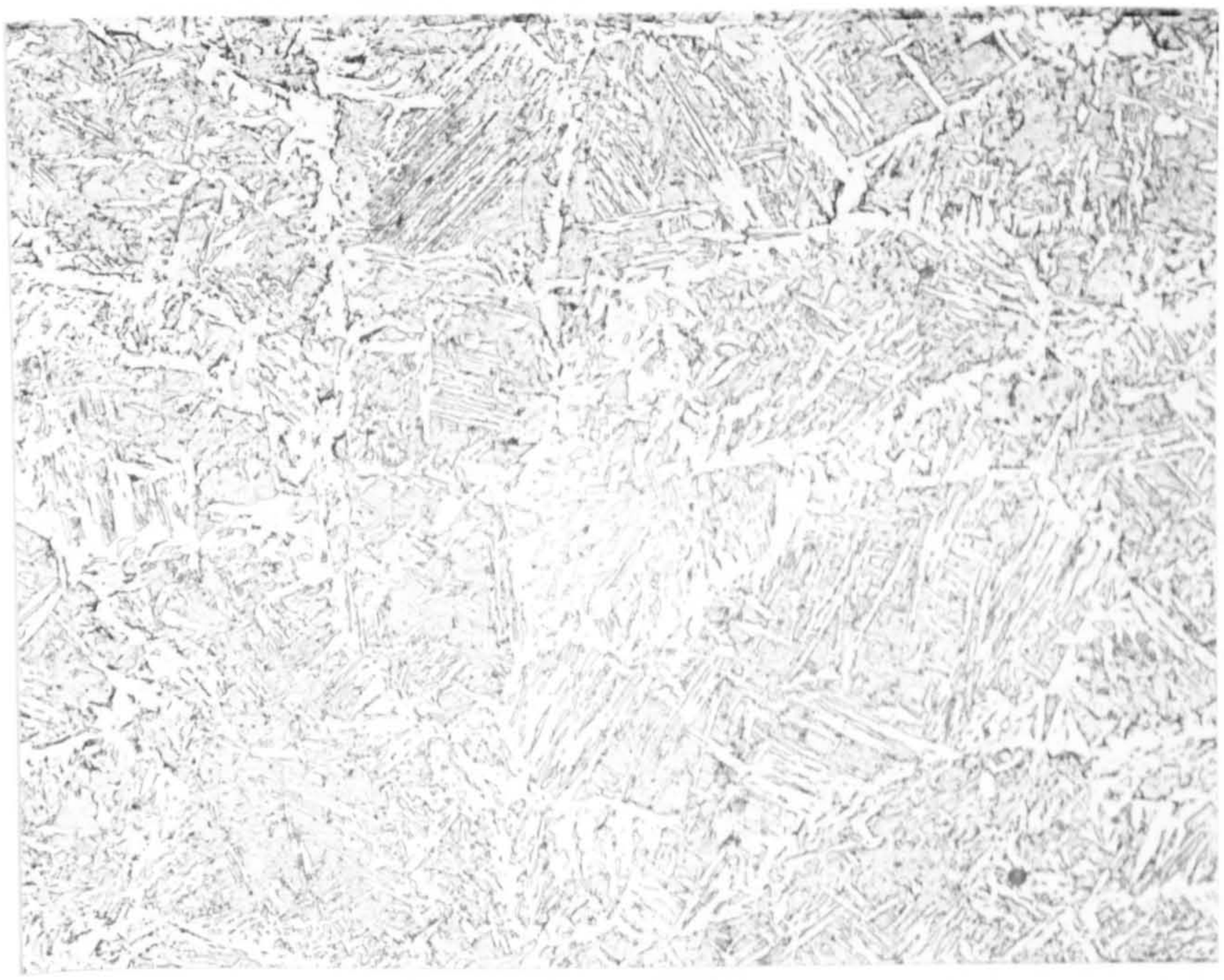

Figure 6.19d - 8mm skid weld, weld centre (x500).

Figure 6.20a - 8mm MMA weld fillet, fusion line - mainly AC in the HAZ. GF, PF and course AF in the weld (x200).

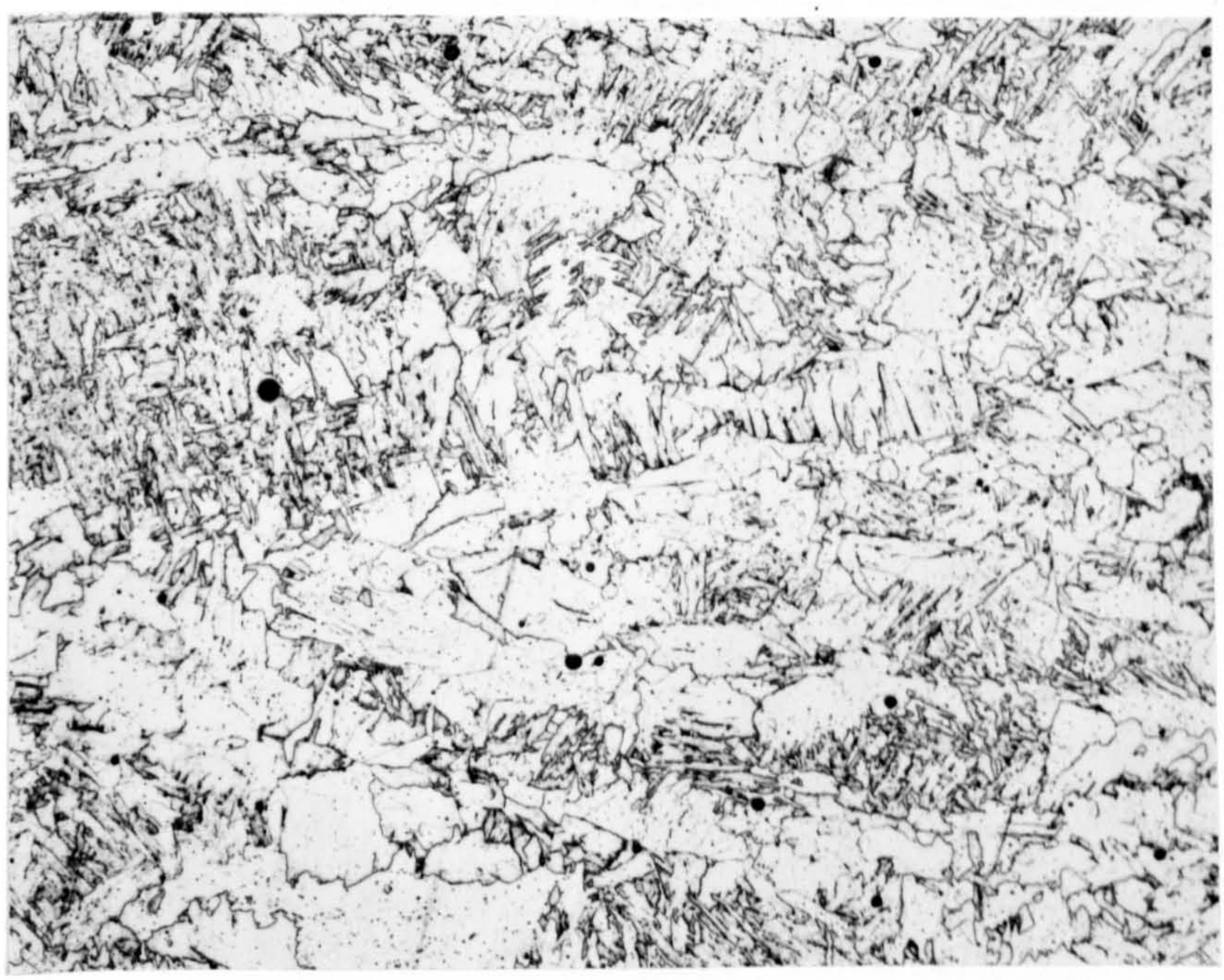

Figure 6.20b - 8mm MMA weld fillet - large areas of GF (x200).

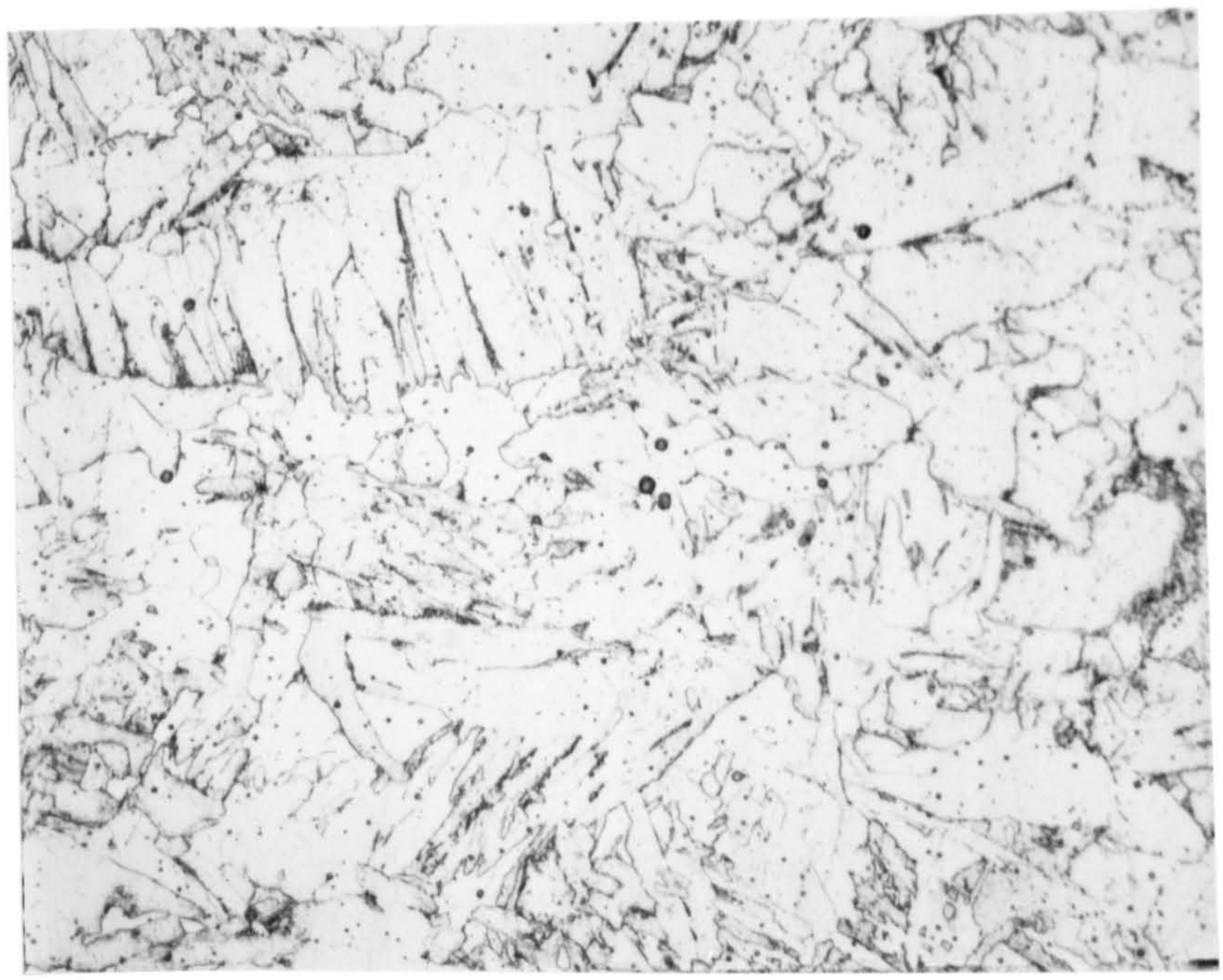

Figure 6.20c - 8mm MMA weld fillet - coarse grains of GF, also many slag inclusions (x500).

"hardenability". The fusion line is characterised in the parent plate by the super critical zone where grain growth has taken place. For plate thicknesses greater than 10mm this is less distinct as similar microstructural constituents have formed on both sides of the fusion line after cooling. For plate thicknesses below 10mm a marked difference is noticed particularly in the 6 and 3mm plate where a high proportion of martensite has formed at the fusion line, this being confirmed by the measurement of hardness values in excess of 400Hv in this region.

6.3.4 Relationship of microstructure to Charpy Values

Phase counts were also made on welds tested for toughness evaluation not only to compare the performance of butt welds to tee section skid welds but also to assess the effect of varying filler wire composition on the weld microstructure. Tabulation of phase counts, prior austenite grain size measurement and related hardness and toughness results is produced in table 6.04.

Firstly a comparison of butt and skid welds, produced using the same filler wire (A31) was made. Microstructural constituents (except for martensite) are generally of the same order, however, whilst there are negligible proportions of martensite for each of the butt welds, an average of 5% martensite is noted for skid welds. The difference is reflected in the 20% higher hardness found in the skid weld material. This will be due to the faster cooling rates as a result of the increased combined thickness of the tee section joint compared with the butt joint

Plate ThK	Joint Type	Phase Count (%)						Grain Size (um)		Charpy Testing (°C sub size)					Hardness (Hv)			
		GF	PF	AF	AC	FC	M	Mean	S	FATT	Tdv	18JE	34J	U.S.,	INC.	EMG.	AVE.	HMAX HAZ
6	Butt	3.4	1.0	24.6	40.6	30.4	-	46.9	18.7	6	20	-20	9	50J	267	288	278	330
	Skid	7.1	0.8	25.6	37.9	22.0	6.5	46.4	19.6	-35	-50	-20	>20	>20J	356	354	355	362
10	Butt	3.9	0.6	12.3	57.9	25.4	-	52.3	20.4	9	20	-19	0	(65J)	237	216	226	283
	Skid	4.1	2.1	12.1.	65.8	10.6	5.3	45.2	23.1	4	50	-33	-4	(50J)	284	283	283	287
15	Butt	4.1	1.1	13.6	62.1	18.2	0.9	51.7	23.1	(14)	20	-40	-23	85J	232	212	222	295
	Skid	4.0	1.2	8.1	60.5	20.4	5.8	52.1	21.9	-20	20	-34	2	60J	249	243	246	249

Table 6.04 - Microstructural/mechanical properties of butt and skid welds ; Balanced speeds, 9kW laser power

configuration. For mild steel, if increasing proportions of martensite result in high toughness an associated increase in hardness will be expected. This was found when comparing the butt and skid welds in 10mm thick plate. However in the 15mm thick plate the increase in toughness, but with lower hardness levels, can be associated with the increased AF levels measured.

For joints in 6mm plate the proportion of AF is double that of both 10mm and 15mm joints and hence good toughness properties would be expected. Produced partly as a result of the higher welding speeds this would normally be expected to give good toughness values but this has not occurred. Examination of the fusion line microstructure at a magnification of X1000 shows a line of inclusions just behind the fusion boundary, figure 6.21. The fracture, once diverted from the tough weld metal will have followed the path of least resistance along the inclusion lines.

Secondly a comparison of welds in 10mm thick plate using varying filler wire was conducted, table 6.05. From the examination of weld hardness values superior toughness values would be expected from the weld employing the A31 wire. However this is not the case due to the lower relative level of AF and higher proportion of AC produced . In fact the relationship of percentage AF is shown to have a direct relationship to toughness properties, figure 6.22. Projection of the curve would indicate that, in the absence of any martensite and while grain size remains constant, a minimum AF level of 8.5% would be required to ensure

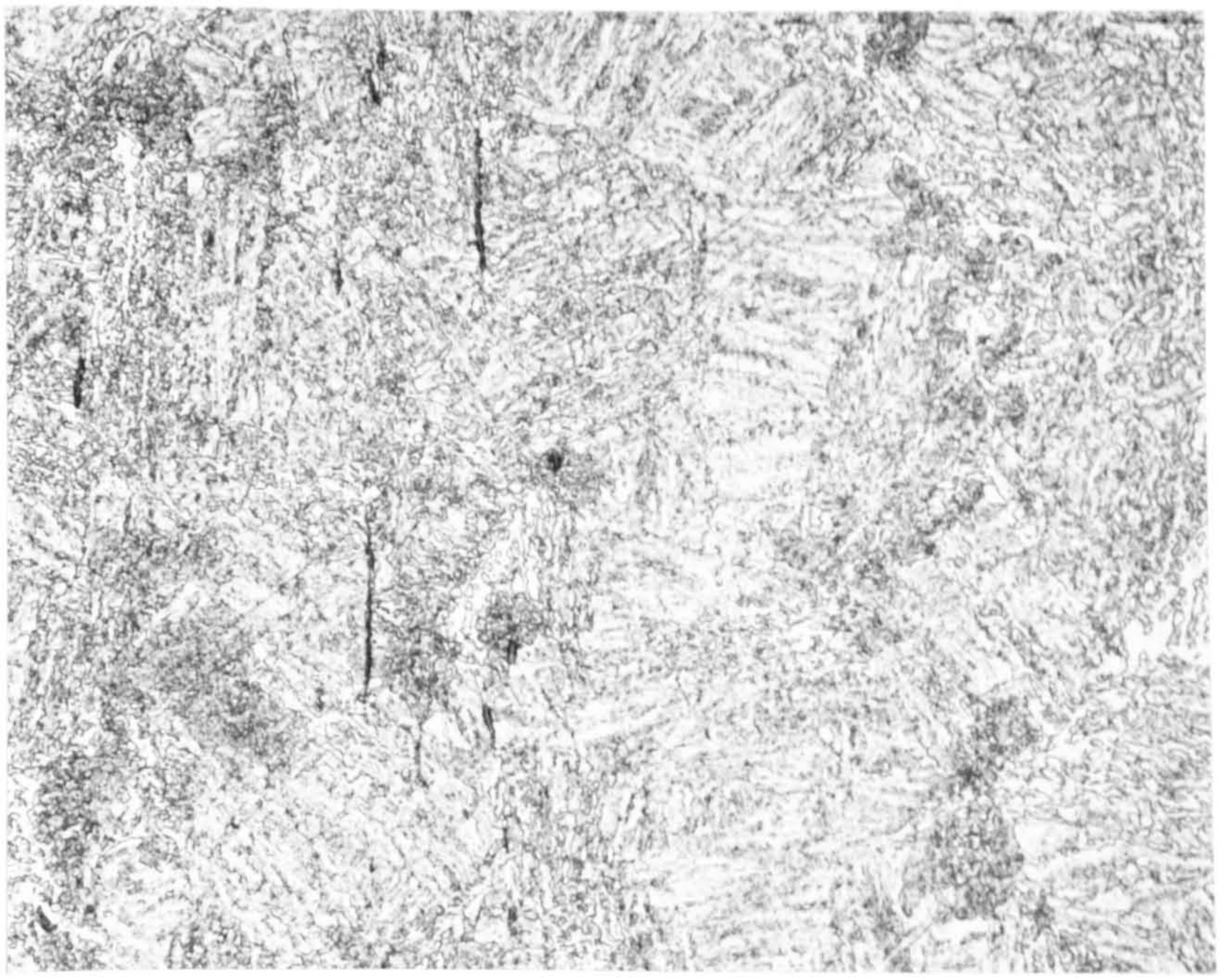

Figure 6.21 - Fusion line in 6mm skid weld (plate P6/01/CS) showing inclusions (x1000).

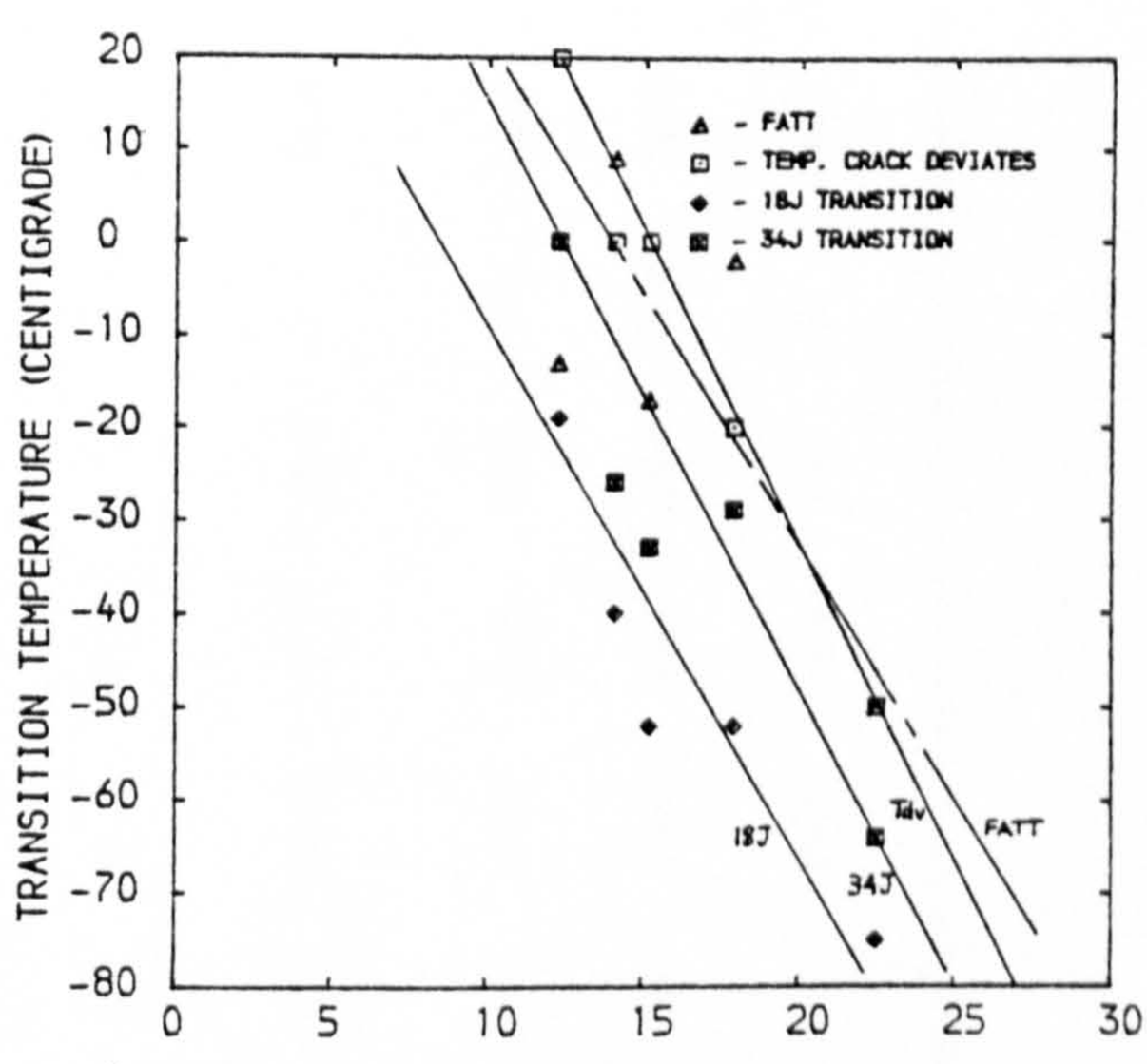

Figure 6.22 - Relationship of acicular ferrite levels and Charpy transition values for various wire feed compositions.

Wire Type	Phase Count (5)						Grain Size (um)		Charpy Testing (°C sub size)					Hardness (Hv)			
	GF	PF	AF	AC	FC	M	Mean	S	FATT	Tdv	18JE	34J	U.S.	INC.	EMG.	AVE.	HMAX HAZ
A18 (Bos.LW1)	4.9	1.4	14.1	67.3	11.9	0.3	57.2	25.3	9	0	-40	-26	92	193	208	203	191
A31 (BD20)	3.9	0.6	12.3	57.9	25.4	-	52.3	20.4	-13	20	-19	0	65	236	216	226	283
S2	9.3	0.8	17.9	60.8	11.2	-	45.6	18.3	(-2)	-20	-52	-29	70	193	208	200	191
SD3	6.8	0.6	15.2	60.4	16.8	0.3	52.2	22.5	-17	0	-52	-33	78	188	184	186	185
C-Mn-Ti (K-Nova)	5.0	1.1	22.5	51.8	19.7	-	45.6	19.9	(-50)	-50	-75	-64	86	198	235	217	230

Table 6.05 - Microstructural/mechanical properties of 10mm thick laser butt welds to compare the affect of varying filler wires

toughness properties to 33J(47J for full-size specimens) at 20 degrees as required by MOD(N) and 11.5% for 18J(34J for full size specimens) at -20 degrees centigrade as required by Lloyds.

The K-Nova wire was found to produce welds with the highest proportion of AF and, together with the S2 wire, the smallest grain size. This fact is reflected in the best Charpy results of all the wire while hardness values are maintained to satisfactory levels.

In practical terms, defining a tolerance envelope of chemical requirements is more complicated. However, by assessment of the results gained in the present trial programme together with observations of other authors' conclusions, certain guidelines can be given to the ship production-based welding engineer in order to optimise weld toughness, when initially assessing welding consumables:

1. Low carbon level - the use of low carbon equivalents and specifically low carbon levels themselves (<0.1%) in consumables in order to reduce the eventual carbon equivalent of the weld zone appears to aid the formation of AF. A similar observation was made by Watson (186) by directly comparing carbon equivalents of the weld material to the percentage AF , subsequently comparing these levels to the respective Charpy transition values. However, carbon levels also have to be considered with respect to the type of microstructure formed and a balance made between hardness and toughness within the weld material [186]
2. Oxygen levels - whilst no assessment has been made of oxygen levels

contained in the consumables and found in the welds for the present investigation, authors discussing both laser and electron beam welds emphasised its effect in promoting the nucleation of AF. Watson [120] shows how the level of AF is very susceptible to oxygen levels but is unable to provide any simple correlation. However from their work with EB welds O'Hara and Wallach [137] have recommended a level of 130ppm. A balance must obviously be made between having sufficient oxygen to provide sufficient oxide for inclusion sites for AF to nucleate without having excess oxygen which could induce porosity in the weld.

3. Micro alloying - the author has shown the advantage of the presence of a small proportion of titanium in the weld which precipitates AF nucleation. Similar effects have been found by Stares et al [121] using a nickel bearing filler wire. The advantage of weld treatment by this method is that the toughness may be increased without detrimental effects from excessive hardness levels.

6.4 WELD FLAWS HIGHLIGHTED BY MICRO EXAMINATION

Initial identification of flaws found in the welds was made during macrographic examination but the extent of such flaws was examined more fully at higher optical microscope magnification levels and described further in this section.

6.4.1 Solidification Cracking

Solidification cracks as described for conventional welds by Bailey and Jones [187] have been found to occur where a mainly columnar solidification structure has been coupled with a situation of high restraint. Typical results of such instances in laser skid welds are shown in figure 6.23 and 6.24.

The former occurred in a 12mm thick joint where a narrow emergent bead has solidified first thereby constraining the joint. Shrinkage of the large solidifying incident bead has then resulted in separation at the joint centreline. This could be avoided by using greater incident power to gain more penetration and form a nearer to parallel weld.

Whilst the cracks identified appeared mainly as a result of joint restraint, no comparison could be made for similar steel compositions in each joint thickness. However, the Author would expect that a test proposed for EB welds [188] may also apply for laser welds to derive a processing tolerance envelope.

The second form of solidification crack has occurred adjacent to a zone of lack of fusion between the weld and flange plate. This has resulted in increasing the residual stress in the weld, subsequently initiating the crack at the weakest point - the joining of columnar grains.

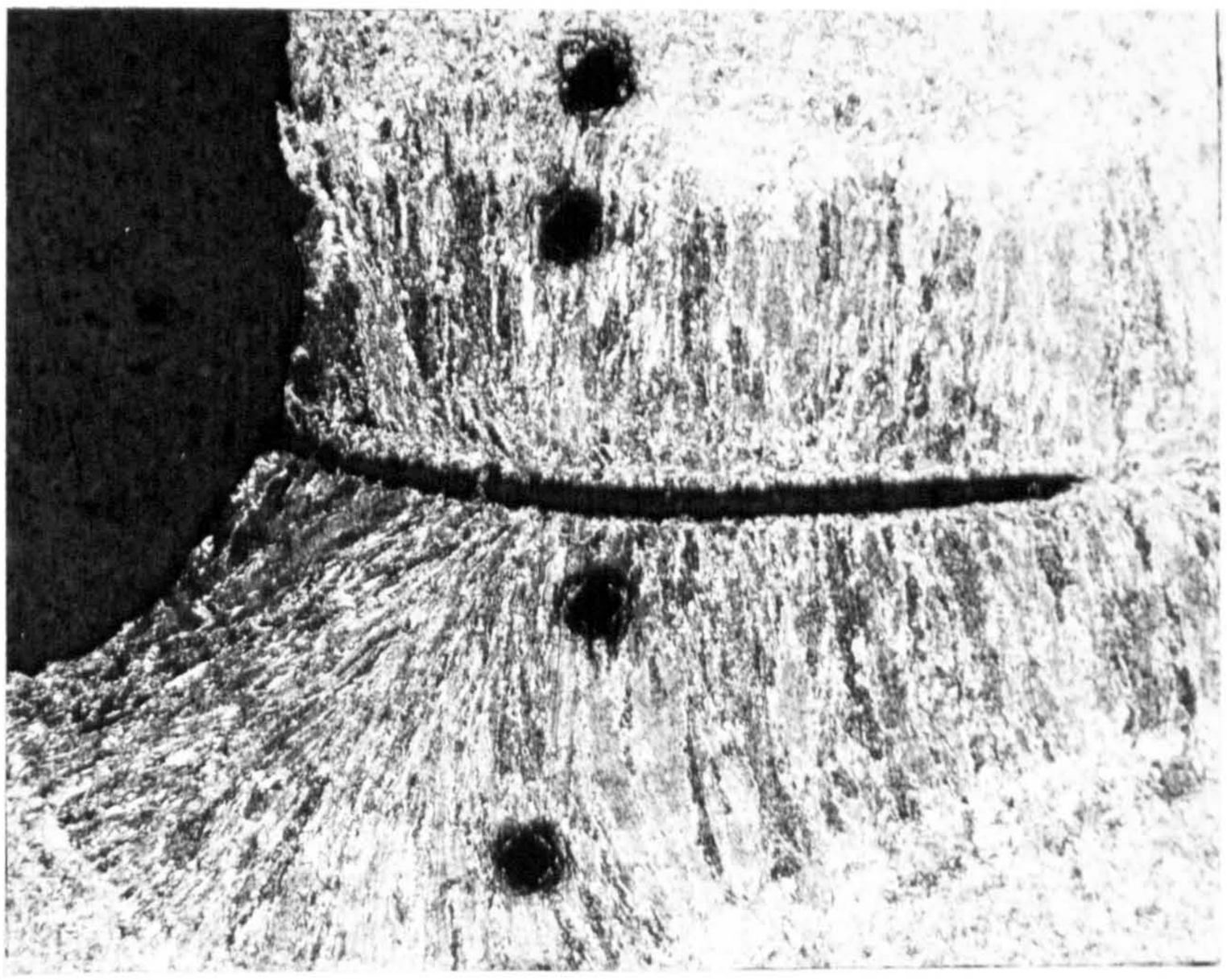

Figure 6.23 - Solidification crack in 12mm skid weld incident bead, columnar grains joining at weld centreline (x20).

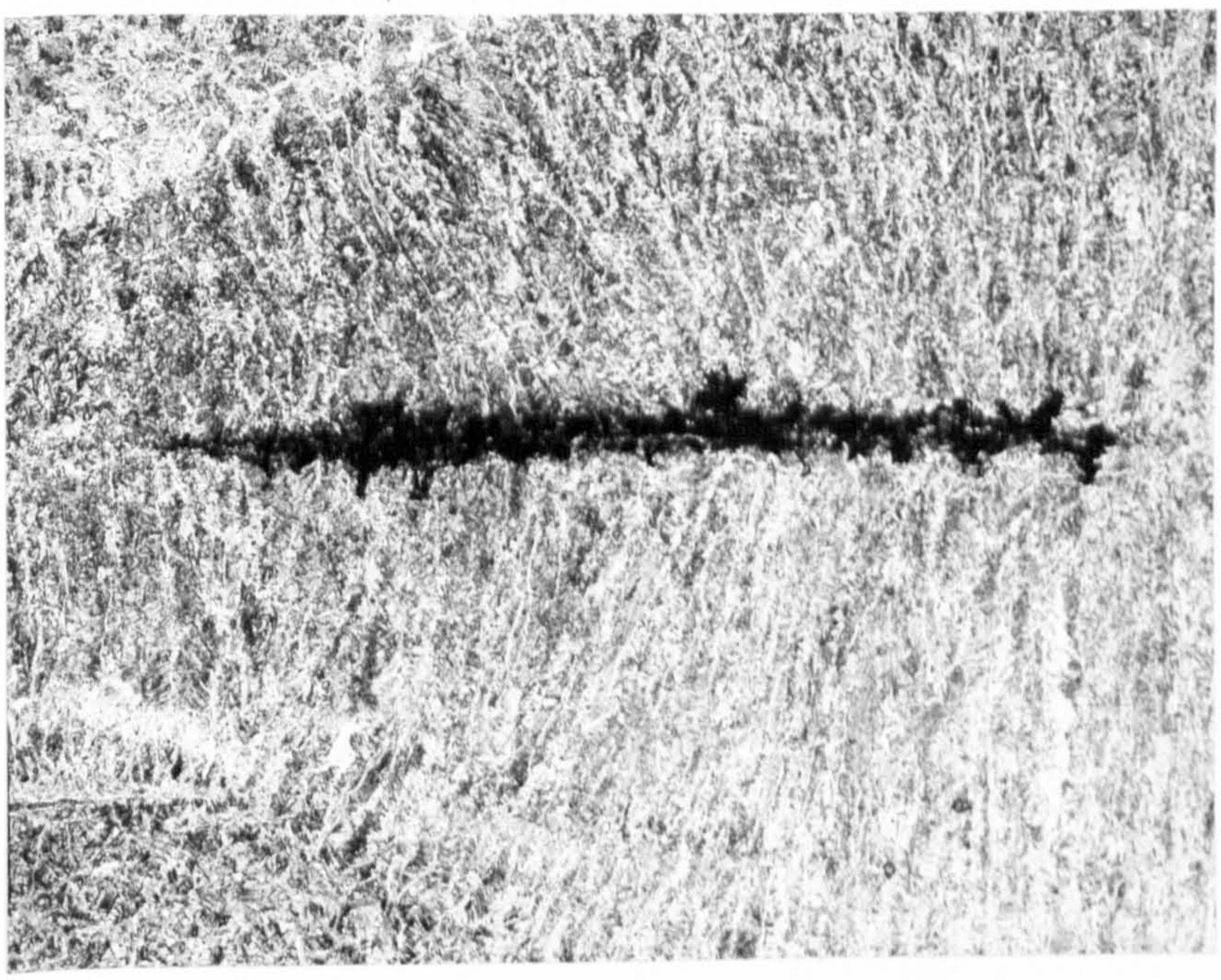

Figure 6.24 - Solidification crack in 12mm skid weld, formed in weld centre (x40).

6.4.2 Lack of Fusion

Figure 6.25 shows lack of fusion between the solidifying weld metal and flange plate. This occurred adjacent to the incident bead which from visual inspection of the weld surface appeared sound. Due to the higher heat intensity at the incident face caused by the plasma concentration, an enlarged area of fusion is formed at the keyhole mouth. This ensures fusion at the incident smoothing bead. However, further into the joint, if the laser beam is too high, lack of fusion may result.

The reverse happens if the laser beam is too low. Lack of fusion between the web plate and weld material occur, figure 6.26. The emerging material has failed to fuse with the web plate edge and cracks have then initiated.

Other types of lack of fusion have been investigated, mainly occurring at the emergent bead due to a failure of the beam to fully penetrate and produce a properly formed and fused smoothing bead.

The first type occurred with increasing joint thickness as the plasma balance became more dominant on the incident side. Molten material is only "forced" out at the emergent side by the pressure from within the keyhole rather than being formed as a result of the "extension" keyhole. In consequence the bead formed did not have sufficient heat energy to fully fuse with the plate sides, figure 6.27. This is undesirable as the notches formed would create corrosion positions and provide points for

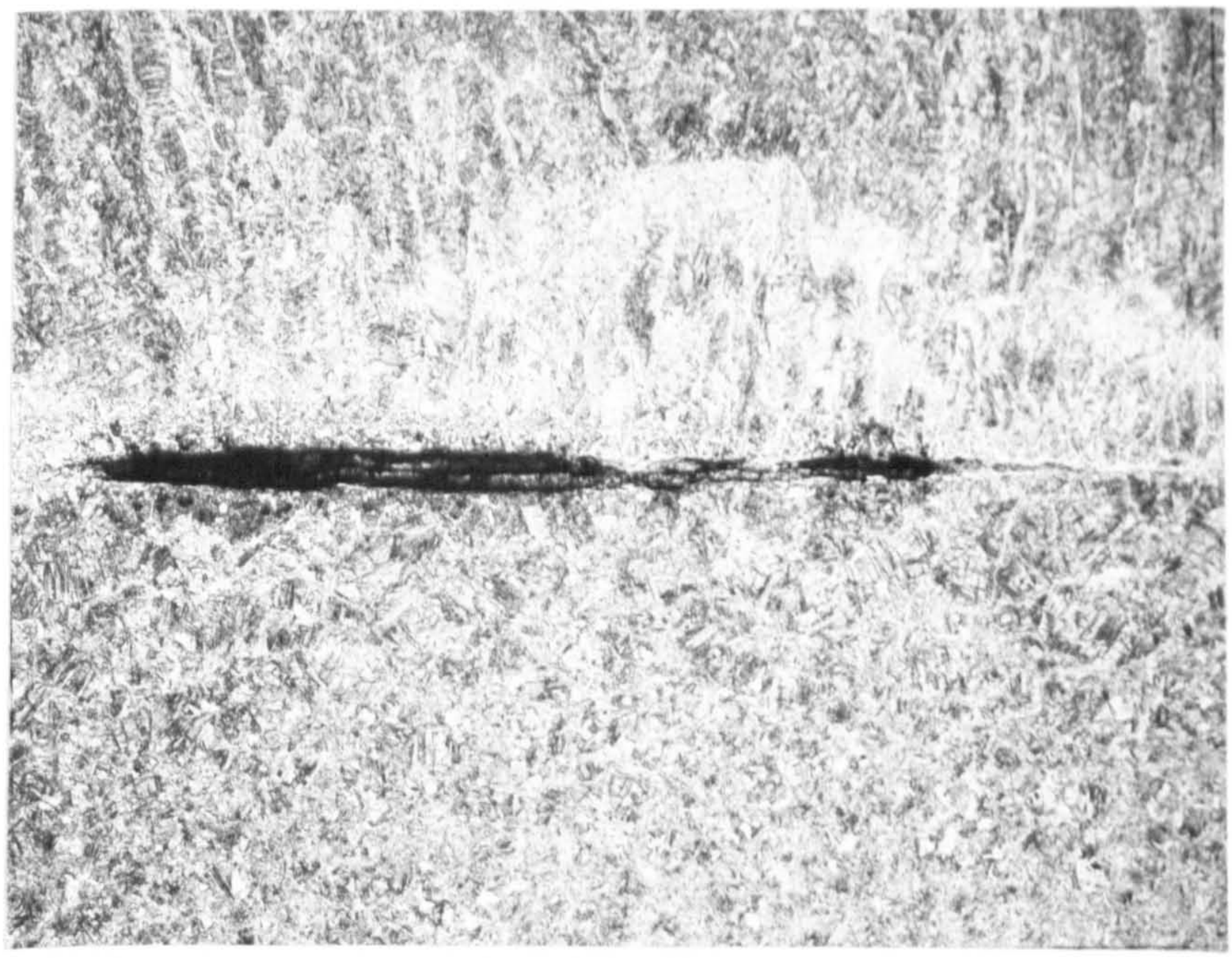

Figure 6.25 - Lack of fusion with the face plate due to too high laser beam height in a 12mm skid weld (x64).

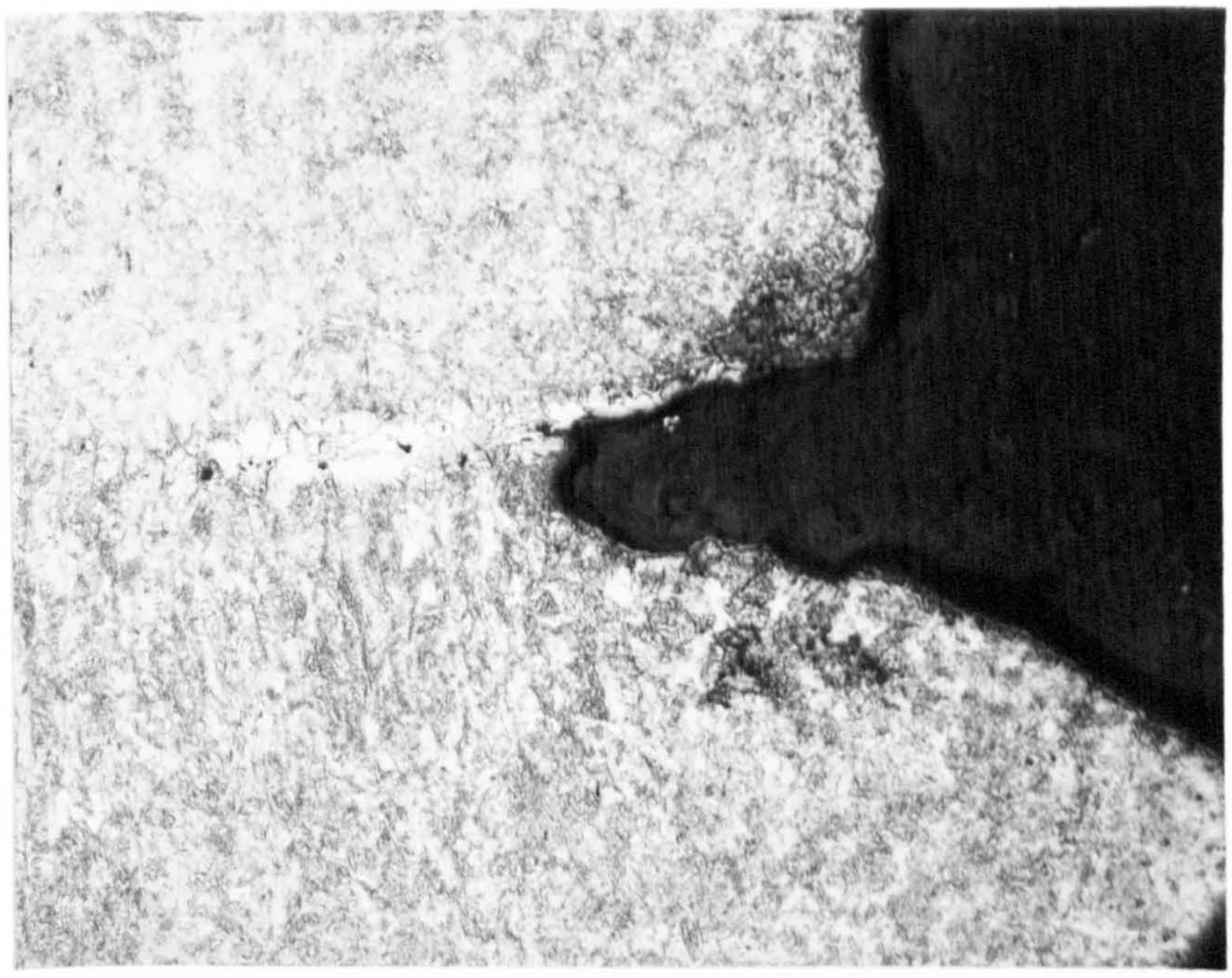

Figure 6.26 - Lack of fusion at the web plate edge due to too low laser beam height in a 10mm skid weld (x80).

crack initiation.

The second flaw of this type is similar but occurred with joints comprising a web plate of rolled section. With insufficient penetration insufficient material flows to the emergent side to compensate for the radius plate edge, leaving a notch between the solidified bead and plate section. As shown in figure 6.28 this may then result in secondary cracking from the notch. The effect is compounded when, if large quantities of filler material build-up at the incident side the emergent bead penetration reduces still further, figure 6.29.

6.4.3 Porosity

Various authors have described a number of alternative reasons for the generation of pores in laser welds [139] [184] [189] [183] . Typically they are associated with entrapped atmospheric gas due to bad shielding, entrapped shielding gas or trapped base metal vapour. However, there are further reasons associated specifically with both laser welding and keyhole welding.

Smith [139] notes how porosity changes for various types of steel together with the effect of changing focusing optics or plasma control methods but classifies two distinct types of pore:

1. "Fine" pores (less than 1mm in diameter or 0.33 of the weld width) which she attributes to inclusion breakdown

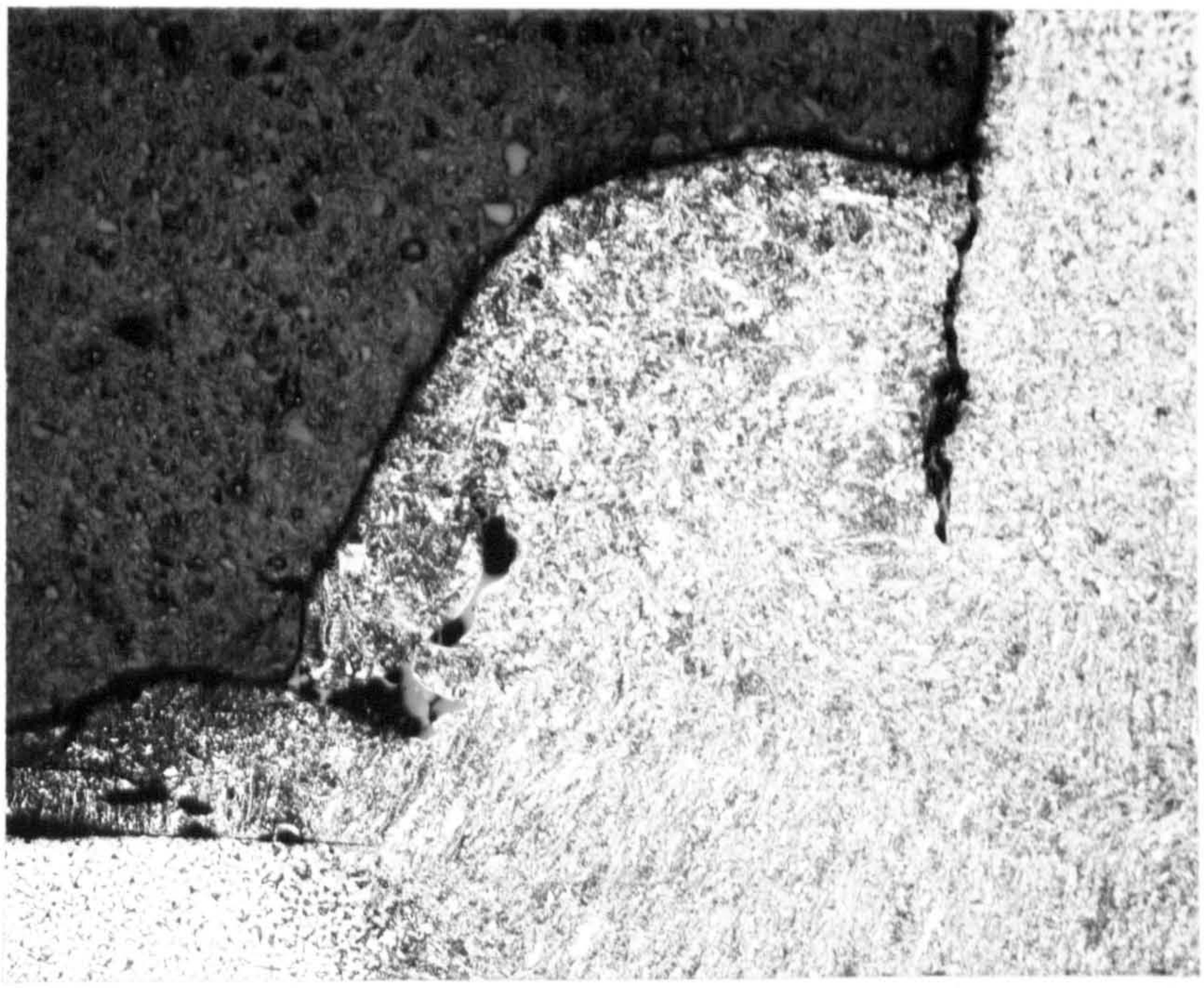

Figure 6.27 - Emergent bead of a 12mm skid weld. Molten material has been forced out at the molten zone without full fusion (x32).

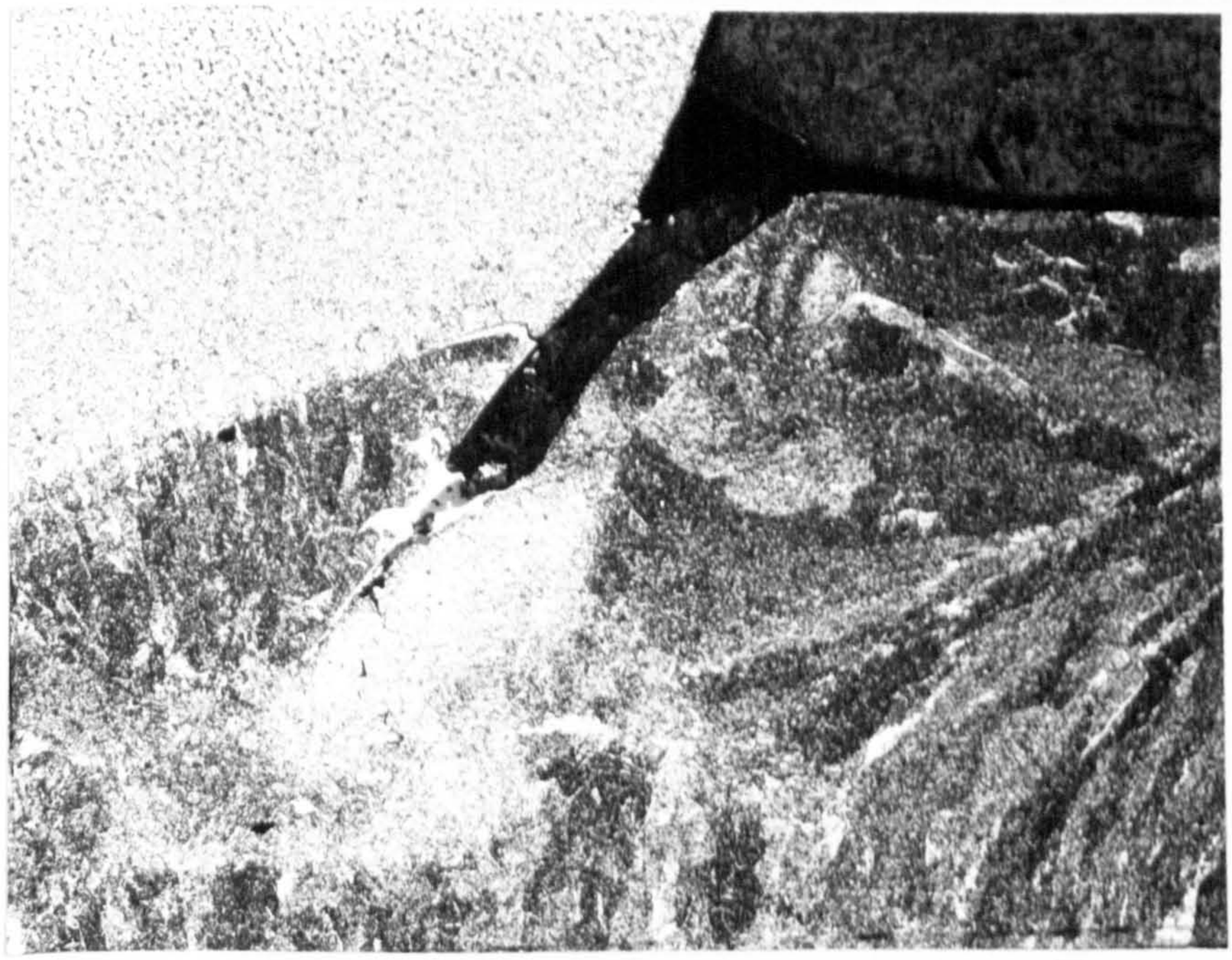

Figure 6.28 - Emergent bead of a 6mm skid weld with insufficient fusion with a rolled section web (x50).

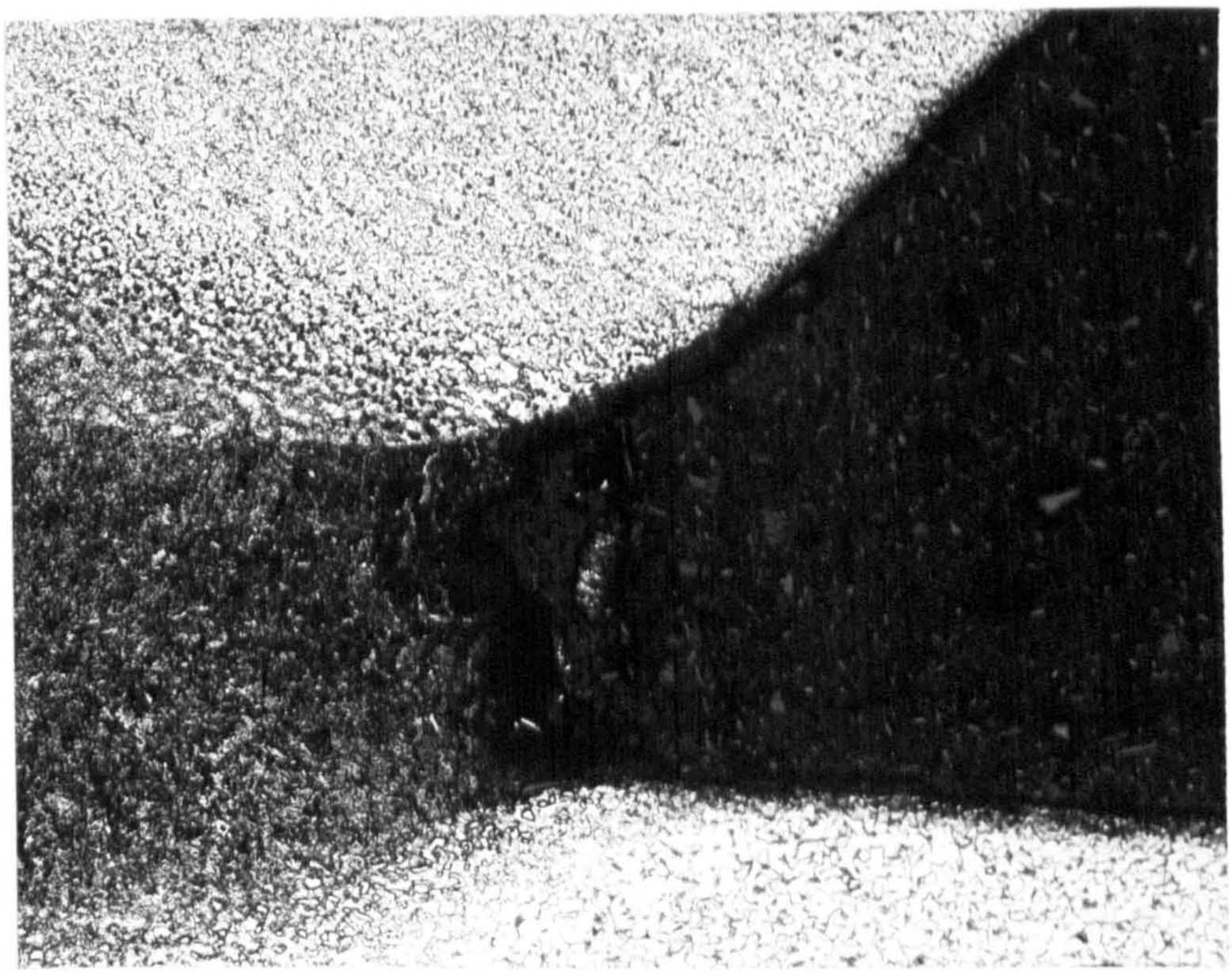

Figure 6.29 - 10mm skid weld joint emergent zone with a lack of flow of filler to a rolled section web edge (x50).

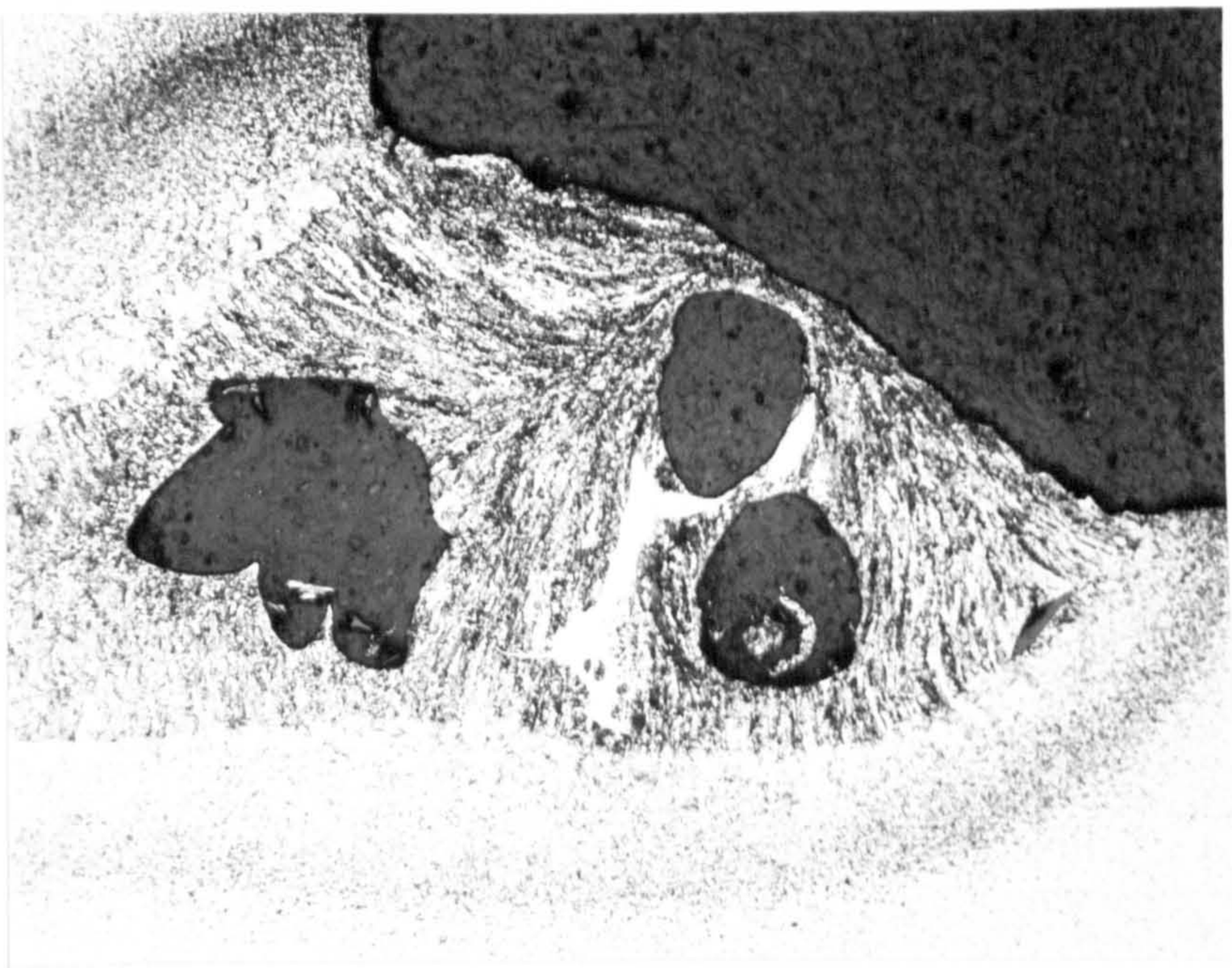

Figure 6.30 - Porous emergent bead in a 6mm skid weld (x20).

2. "Larger" pores related to keyhole behaviour.

The Author of the present work observed the formation of occasional "fine" pores, normally along the fusion boundary. Of greater significance and apparently peculiar to the skid weld was the formation of large pores in the emergent bead, figure 6.30. These often were unidentified at visual inspections but showed up as a lack of fusion during ultrasonic testing, mainly for plate of less than 6mm thick. Confined to the emergent bead and reducing in size with reducing heat input they are possibly a result of a "break-off" type effect as gaseous pockets release from the root of the keyhole . In the case of skid welds this effect coupled with turbulence caused by excess power being released at the keyhole "side-shoot". To stop such effects, power input was either reduced, thus reducing the excess power at the emergent bead, or increased, so increasing the size of the molten pool and allowing greater time for the escape of the enclosed gas before the weld solidified.

Pores obvious at visual inspection could usually be attributed to gas formation either because of surface coatings eg shop primers, or as in one instance, to dirty wire which had become excessively rusted after an escape of steam into the workstation. In these cases pores were of the "worm hole" type, initiating at the centre of the weld and extending to the surface of the emergent bead.

No pores were ever found to penetrate out from the incident bead as weld impurities appeared to be ejected mainly from the emergent zone.

CHAPTER SEVEN

EVALUATION OF SHIPYARD BASED FACILITIES EMPLOYING LASER SKID WELDING

The laser skid welding process applicable to single sided tee section skid welding has been assessed in terms of the potential for shipyard based machinery to produce structurally satisfactory tee section joints within typical ship production constraints. In the present chapter the Author has related issues raised while using the experimental workstation for the welding trials, visits to laser and equipment manufacturers [190] [191] [192], and surveys of the market for commercial lasers [193] to the design and operational requirements that would be placed on a production based workstation. Conceptual equipment configurations, practical operational constraints and the essentials for process monitoring are discussed together with proposals for safety procedural requirements, particularly to large high power laser based production equipment. Finally, facility design costing information and process parameters developed during the trials are utilised in an economic evaluation of an example of proposed laser based ship production facilities.

7.1 APPRAISAL OF LASER BASED EQUIPMENT FOR SKID WELDING IN SHIPYARDS

Although production equipment for laser processing with laser powers of up to 5kW is now becoming readily available to industry, this is not the case for production based processing using higher power lasers. Therefore in this section the Author discusses some of the more important issues which need to be addressed in the preliminary design and specification of equipment for a shipyard based laser welding workstation.

7.1.1 Production line laser generators

So far as shipyard based engineers are concerned, they will not necessarily want to become involved with the detailed physics of laser beam generation. They will require a "box" to do a job. However it is useful to examine some of the design requirements and pre-requisites involved in making machines suitable for ship production based machine integration:

1. Minimum downtime : Due to the high cost of laser based equipment, high equipment utilisation will be essential for facility cost effectiveness. Therefore hardware must be capable of virtually continuous operation to enable overall equipment utilisation of in excess of 75%. Clearly higher utilisations would be expected, but this level is at least compatible with typical utilisations for conventional equipment. In order to achieve these higher values the laser should be production engineered to minimise service times

providing well defined maintenance schedules. This is especially so if the design requires the changing of short life components e.g. the changing of cathodes on CL10 which become soiled with oxide deposit over a 100 hour period [107] .

To reduce the potential for system down-time if a laser breakdown should occur, the use of twin units, eg both of 10kW, would be advised. This would be preferable to the option of having a single unit of twice the power, eg 20kW and employ a beam splitter, so long as the majority of the processing only needed the lower power source. However, inter-links between the units to enable system flexibility would need to be carefully designed to ensure minimal power losses or the avoidance of detrimental influences on the beam quality.

2. Output stability: To enable processing consistency, a stable beam mode output will be required. Changes may alter the focal characteristics of the system and intensity distribution, resulting in changes to the weld, either affecting the penetration, weld shape or joint integrity.

Similarly to mode stability, directional stability (both in pointing direction and divergence) is especially important for large systems. Any small variation in the beam's projected angle at the laser will result in a large positional variation at a distant manipulator if uncompensated.

Prior to the selection of any one laser for integration into a facility, detailed trials should be done to assess beam stability in properly simulated shipyard conditions, e.g. in damp, cold and dusty environment running continuously over a period of many hours of

continuous unattended running.

Similarly, in order to achieve full utilisation, the machine should be designed to reach the specified stability within a sensible time period e.g. 5 minutes maximum from a cold start-up.

3. Environmental and operator protection: The production laser generator should have airtight and safety interlocked covers, not only to protect the machine from the environmental conditions within the shipyard but also to protect and prevent any unauthorised person from accidentally tampering with the equipment. Together with these operational requirements, provision of a unit enclosure which is seen to be built as a machine tool as opposed to a research tool, would greatly enhance the acceptability of the equipment.

4. Stable mounting : In order to achieve the stabilities noted, positional mounting of the laser should also be designed to isolate the equipment from vibrating influences.

5. Compactness : In addition to positioning the laser "head" (the unit in which the beam is actually generated) ancillary equipment such as power supplies, ballast units, gas supplies and any local control panels will need to be accommodated. Manufacturers will normally provide guidance on relative positions, not only to prevent any interference between units but also to ensure adequate access space for system maintenance. However, the equipment manufacturers should also be striving to minimise the size of the ancillary equipment, which, for laser powers greater than 5kW, may easily take more ground space than the laser head itself.

6. On-line system monitoring: To assess the state of the laser and

provide the data to manage the machine maintenance schedules, on-line machine operational maintenance should be applied. Sensors to measure temperatures, pressures, currents and voltages within the laser, should be set to indicate to the operator if a given operational range is being exceeded, automatically switching down equipment if necessary and alerting the operator to potential problems. Such microprocessor controlled devices are now becoming common-place for production machines of laser's up to 2kW power, figure 7.01.

A simple example of the operation of this is for the management of gas supplies. If gas is to be supplied from cylinders rather than bulk storage, remote change-over between bottles would be essential to enable continuous processing. Otherwise operator time would be required to change bottles in the middle of processing time. As the last bottle is started a warning should be shown or sounded at the operator's panel. Responses from such sensors may also be linked as a closed-circuit loop with responses from beam output sensors in order to correlate any consequential deterioration in beam quality.

7. Operator "friendliness": Operator awareness to equipment "state" on the control panel should also be presented in a manner that will be understood by a trained tradesman to a level expected of a skilled craftsman operating numerically controlled equipment. For situations that are beyond general operational requirements, control instructions should be designed to refer the operator to trained maintenance personnel, and in turn to the manufacturers if necessary. However, within the equipment the detailed operational conditions

Figure 7.01 - Microprocessor control unit attached to a 1.5kW laser

will need to be logged within the diagnostic memory for comparative assessment.

In summary, the laser generator selected must be safe, stable, reliable, user friendly and a cost effective machine tool which may be compared with any existing high technology machine tools.

7.1.2 Beam line transmission equipment

Although it is a fact that laser beams will propagate in air over long distances, in order to use the beam at the end of a long length of transmission, care must be taken to maintain the beam quality, direction and diameter and also to protect personnel from accidentally coming into contact with the beam. Therefore, whether the beam is to be transmitted along a fixed trunking, for which trials have shown that transmissions over 75m lengths are feasible, figure 7.02, or with a manipulative device as described in the next section, certain considerations need to be made when designing the beam line system.

Clearly the beam should not diverge excessively. By employing collimating optics between the laser and the beam line, figure 7.03, a near parallel (possibly with a focal point at mid length) beam path may be designed. A minimum beam diameter will need to be calculated, [14] to ensure optimum transmission of the beam for the particular beam line length.

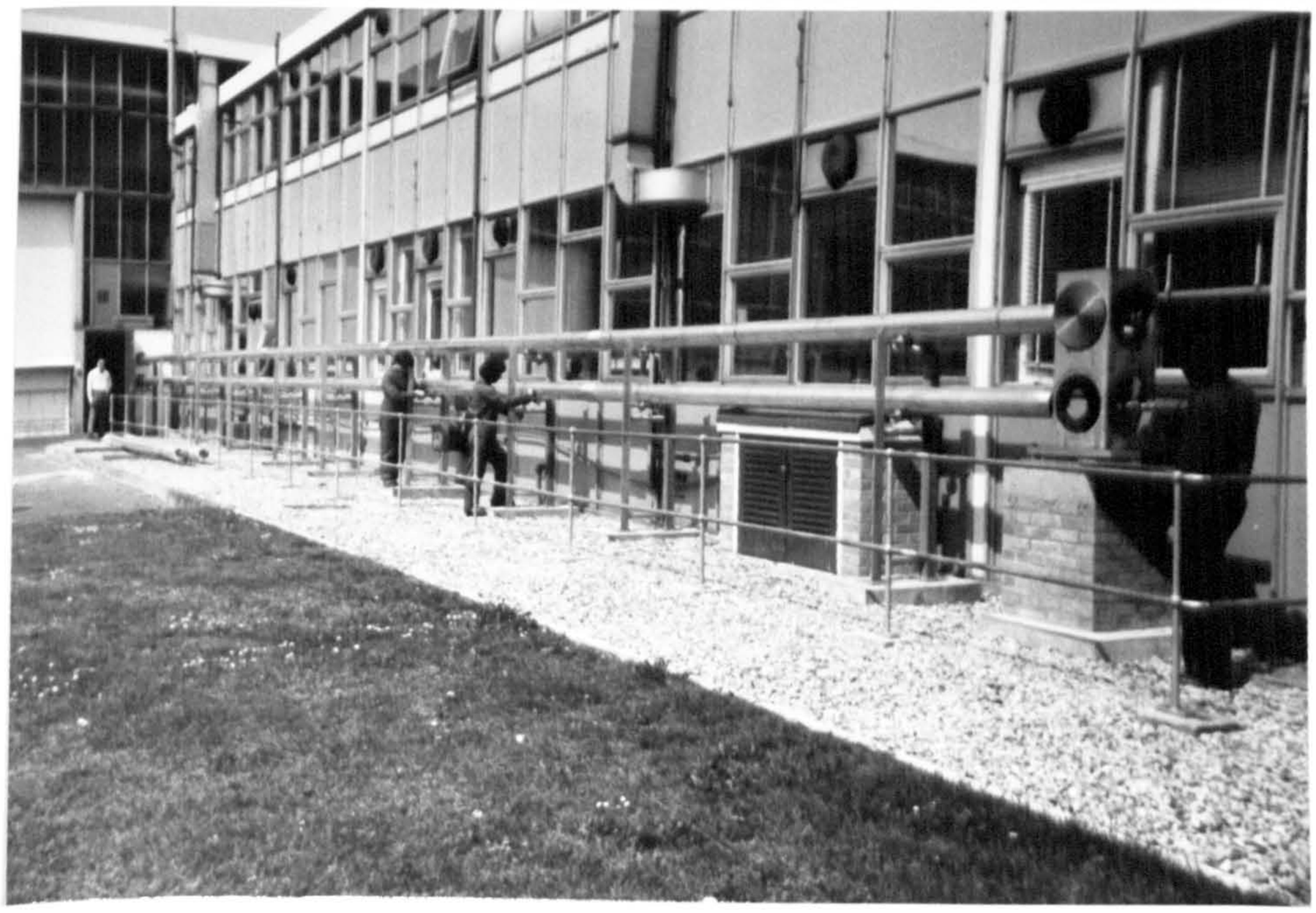

Figure 7.02 - 75m beam line for testing long beam path propogation

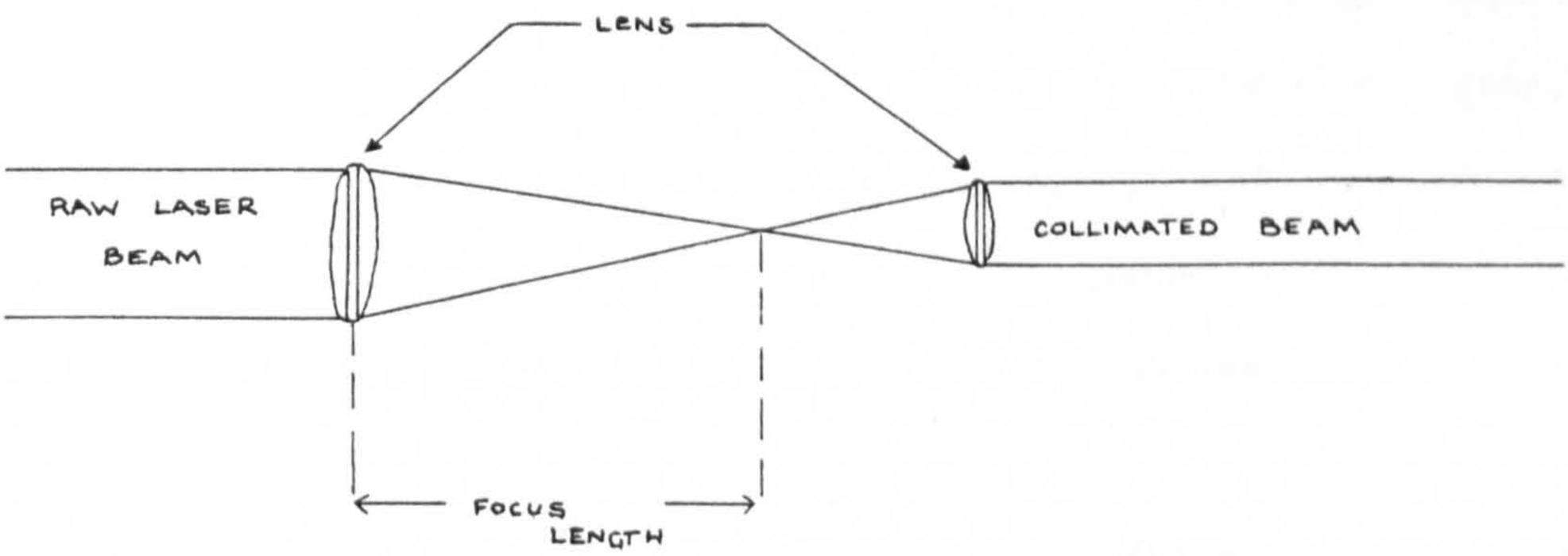

Figure 7.03 - Beam line optics for laser beam collimation

The control of the gas within the beam line is also important. Although dry air is normally employed, excessive levels of impurities may affect beam delivery due to thermal blooming. Similarly, turbulence in the gas may cause further disruptions to the power distribution.

Changes in temperature may also affect the line. Environmental temperature changes may cause distortional movements to the beam line causing a requirement that the beam line be insulated.

Vibration may also affect the beam line stability, particularly at any optical housings. Movement of any optical components due to the vibration would then affect the reflected angle of the beam. Although it is anticipated that servo driven beam control would be employed, minimising the possibility of vibration at each optic mounting would reduce the demand on any control system. Therefore, prior to setting up a system, vibration levels at a proposed site should be measured. Within the shipyard these may include vibration excited by crane or gantry movement, motors, ventilation fans, machine tools such as presses, guillotines. The natural frequency of the laser system must then be designed so as not to synchronise and thus avoid system resonance.

Research into the propagation of beams over long distances by other researchers has shown the need to ensure the positional accuracy of the beam along the beam line and particularly at any end-effect device prior to final focusing. For the majority of existing systems which are smaller than that being proposed for the shipyard application, this has

been ensured by the rigidity of the equipment itself and isolation from any external influences.

On large scale devices it is unlikely that the required tolerances of stiffness may be met. Therefore the use of servo-driven compensating optics [14] linked to a beam position monitor would be required. This would be required to ensure that the beam struck the final focusing mirror at the correct angle and position. Also to ensure that throughout the beam line length the beam did not get too close to the beam line walls creating the potential for overheating and breakdown of the structure. To date only simple devices have been used to protect the beam line from "beam wander" by employing sets of thermocouples in the beam line which simply shut-down the laser if an excessive temperature is recorded [194] .

7.1.3 Manipulation devices

The principal options that are generally considered as available to the laser system designer for linking the laser to the workpiece are a moving laser, moving optics, moving workpiece or by a combination. In more specific terms in linking a laser to a robotic device the options may be considered in terms of the following:

1. Static laser and a fixed position focusing head with a manipulated component.
2. Static laser connected to a jointed arm type robot via a flexible beam guide.

3. Static laser linked to a moving optic cartesian type robot.

4. Laser mounted on the end of a robot.

5. Laser linked into a conventional machine tool.

The first option, an example of which is shown in figure 7.04, was ideal for the trials programme when fixed parameters were used for each sample and the Boko machine table manipulated the sample alongside the fixed laser nozzle. However it could only be applied to welding relatively small components. A semi-continuous mode could be envisaged if the manipulation device was designed to continuously feed components to the laser nozzle, e.g. for welding flange plates to stiffener flat bars. Clearly, for the larger components found in the majority of ship structures considered for a skid welding workstation, this option could not be considered.

A number of the second type of devices are now incorporated into production facilities .They fall into three categories:

a. Fibre optic link type - for laser power systems (up to 500W) employing YAG lasers. The laser is linked to the robot end via a bundle of optical fibres [54] . While this is possible for the frequency of laser output involved, as power throughput is increased with present fibre optics technology, so the stiffness of the fibre optic bundle increases. Therefore there is likely to be an optimum power after which more mechanical means of transmission would be more "flexible". While the infrared frequency of CO2 laser light is not suited to such beam

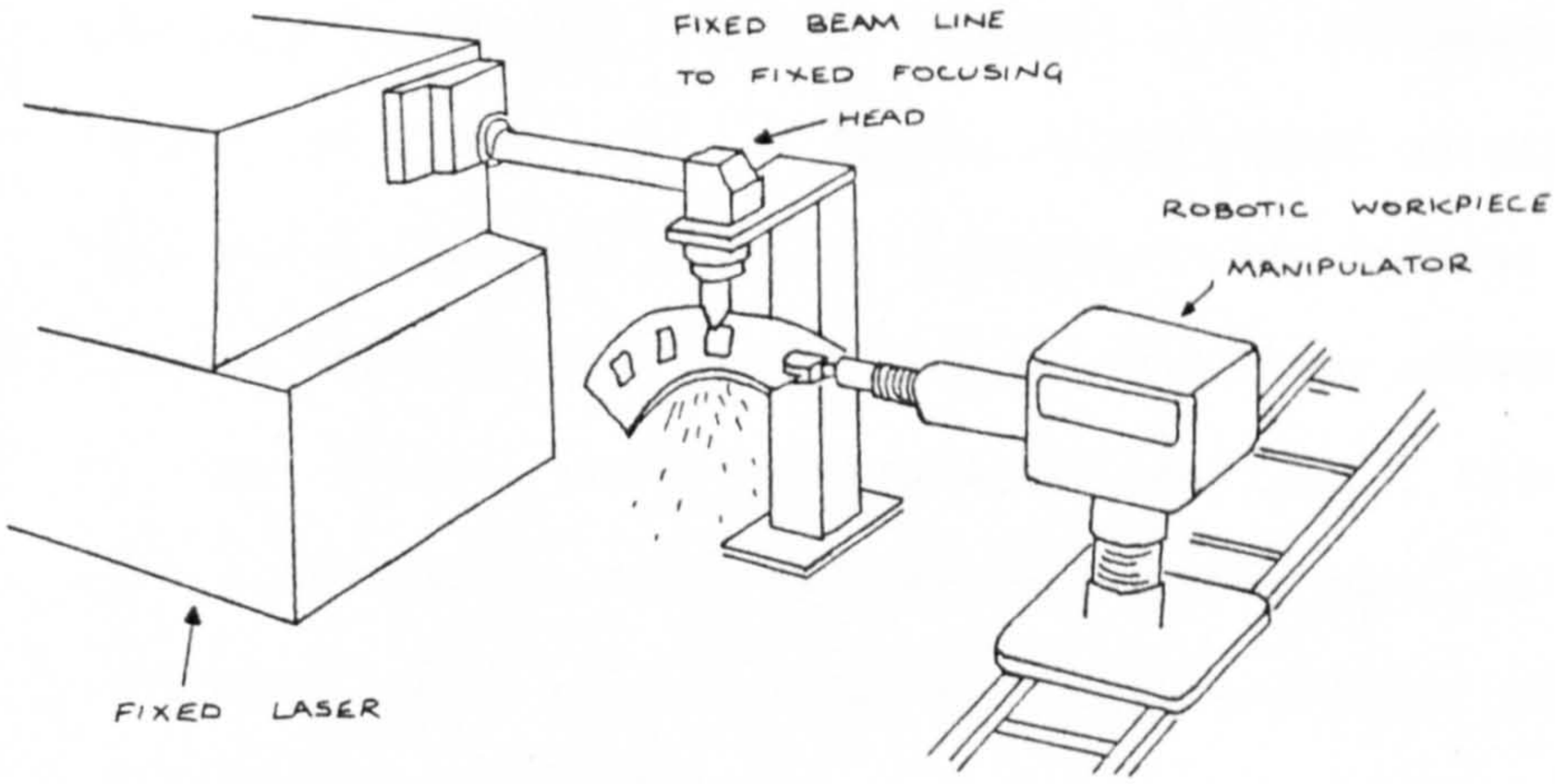

Figure 7.04 - Robot moves a part under a fixed laser nozzle

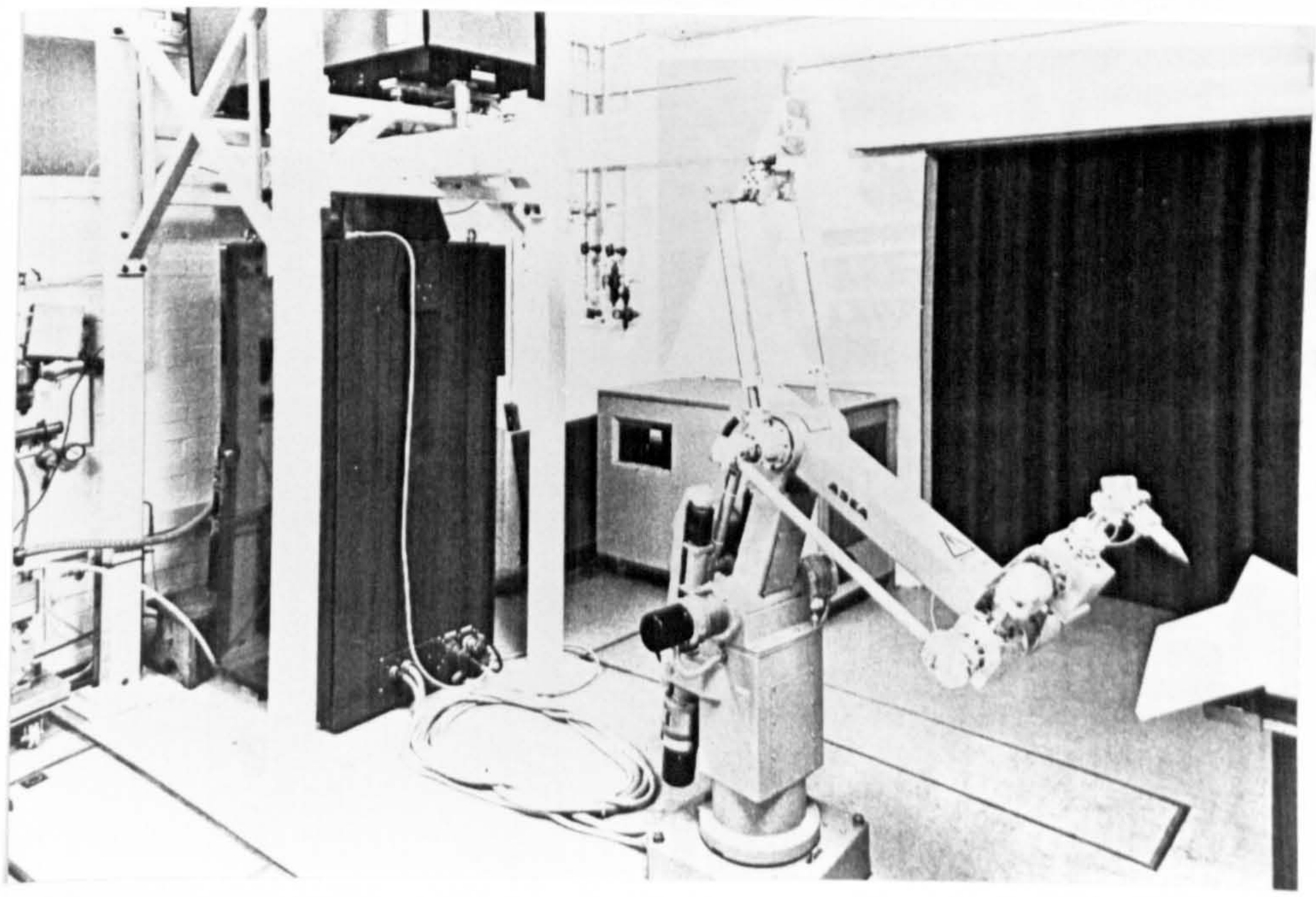

Figure 7.05 - Laser based articulating robot, the beam guide forms an integral part of the robot arm

transmission methods, (the present optical materials absorbing the laser beam power) further research with different types of optics or laser e.g. CO lasers, could result in utilisation of this means at higher processing powers in the future.

b. Integral beam guide - the beam guide, which may either be sited on the outside of the articulating arm [195] , figure 7.05, or within the robot's body, becomes an integral part of the robot following each articulating arm and therefore maintaining a relatively fixed length.

c. Independent "flexible" beam guide - a direct link is created between the laser and the robot end independent of the articulating parts of the robot, figure 7.06 a and b. This device has the inherent advantage that, not only does it enclose the beam path, but it can quickly be interchanged between robots if a particular articulating unit should fail.

Production based units of the latter two types have been restricted to powers of 2kW although system development companies note that they are intending to increase powering to such devices up to 5kW.

For existing production based multi-axis systems using powers of up to 2.5kW, the third option, an example of which is shown in figure 7.07a and b, is the most favoured for a number of reasons.

Because of the fewer number of cantilevered loaded connections, a gantry robot would be of stiffer construction, hence capable of carrying heavier loads e.g. optics necessary for beam transmission,

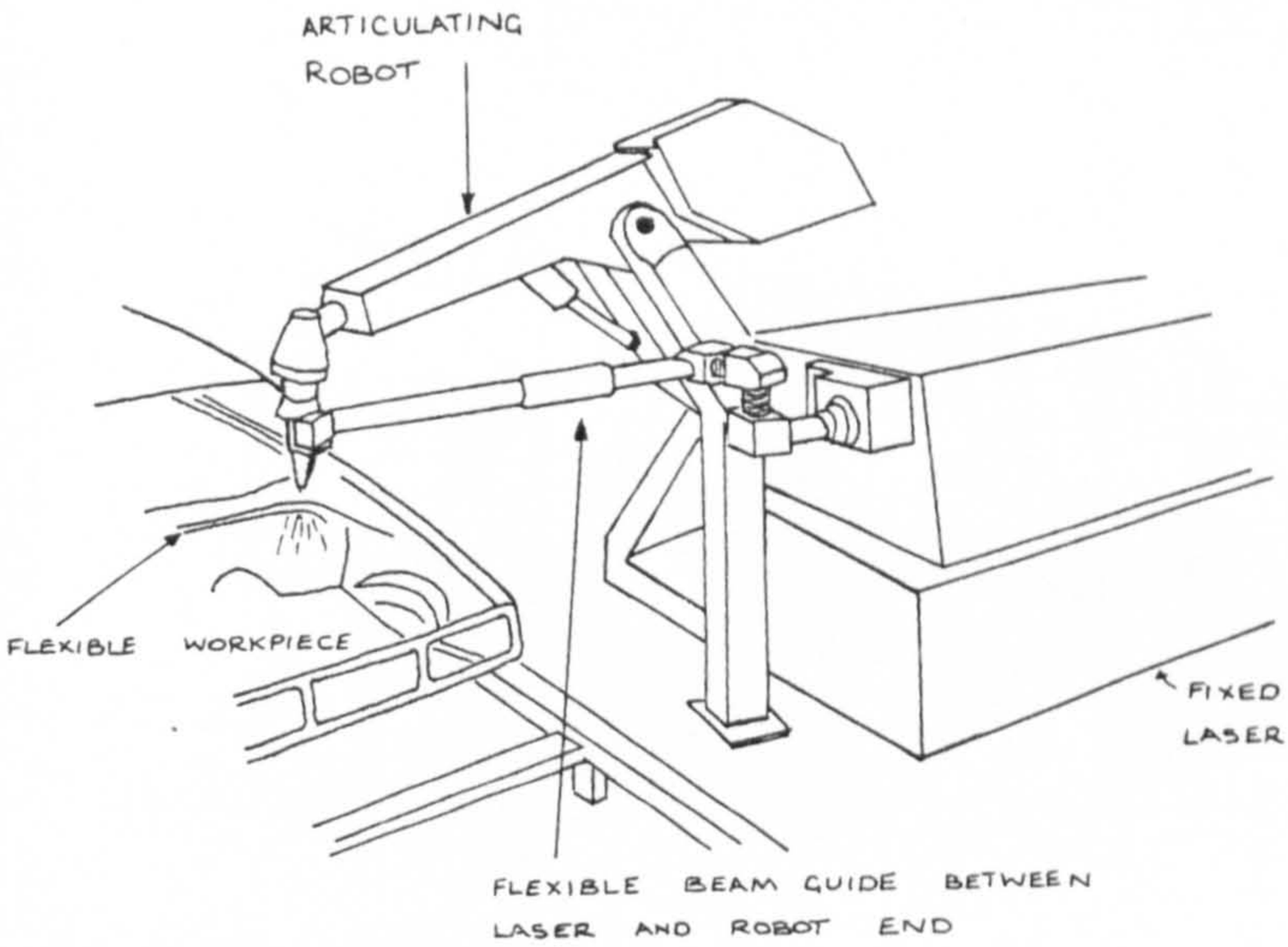

Figure 7.06a - Flexible beam guide linking the laser to the robots end

Figure 7.06b - Flexible beam guide production system

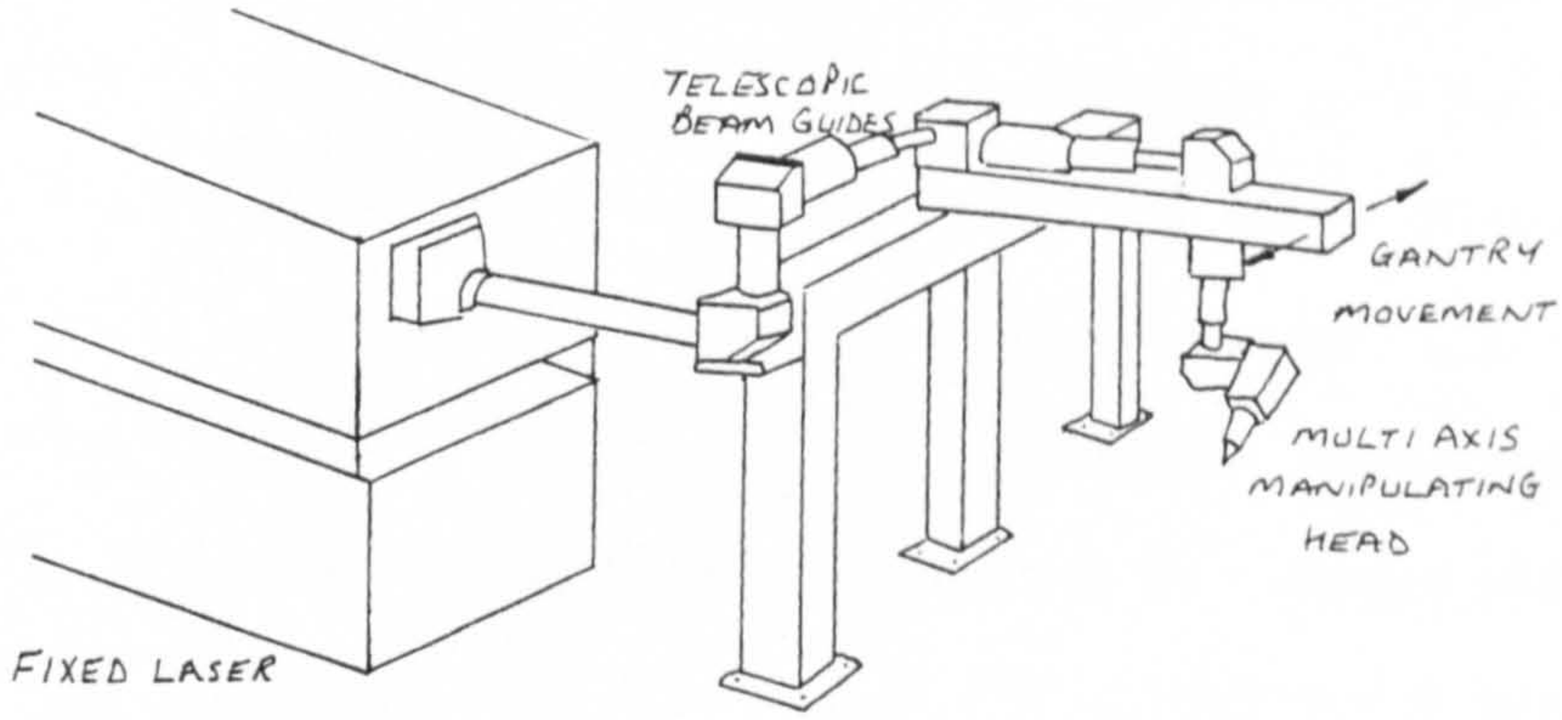

Figure 7.07a - Diagramatic view of a gantry mounted beam delivery and manipulation system

Figure 7.07b- Gantry mounted five axis production system

wire feeders, cameras, seam tracking devices. In an articulated robot, the precision and repeatibility of its motions vary significantly with the extension of its two primary arm components. In the dedicated gantry system only the "z" axis (the vertical axis) changes its length and it does so from a "stiffer" connection. The path of the laser beam is also different between articulated and rectilinear robotics. In an articulated system, each transition from one axis to another usually requires a pair of mirrors while only one mirror is required for each axis transition for a gantry mounted cartesian manipulator.

Lasers mounted on the end of robots, type four, are being built with the availability of very compact and light weight CO2 lasers, figure 7.08 and YAG lasers with output powers of up to 500W. For the powers required for the shipyard application, this is not a possibility with present laser designs.

One proposed shipyard based welding facility design [196] [197] incorporated a moving laser sited on a traversing gantry providing a moving laser in the Y axis, figure 7.09. While this option would be entirely feasible, it would depend on having a laser which had been designed to withstand the necessary movements and accelerations of the system [198] . At present no such laser of 5kW or higher power exists. Most laser manufacturers are preferring to spend their development resources on improving the reliability of their lasers for a static site.

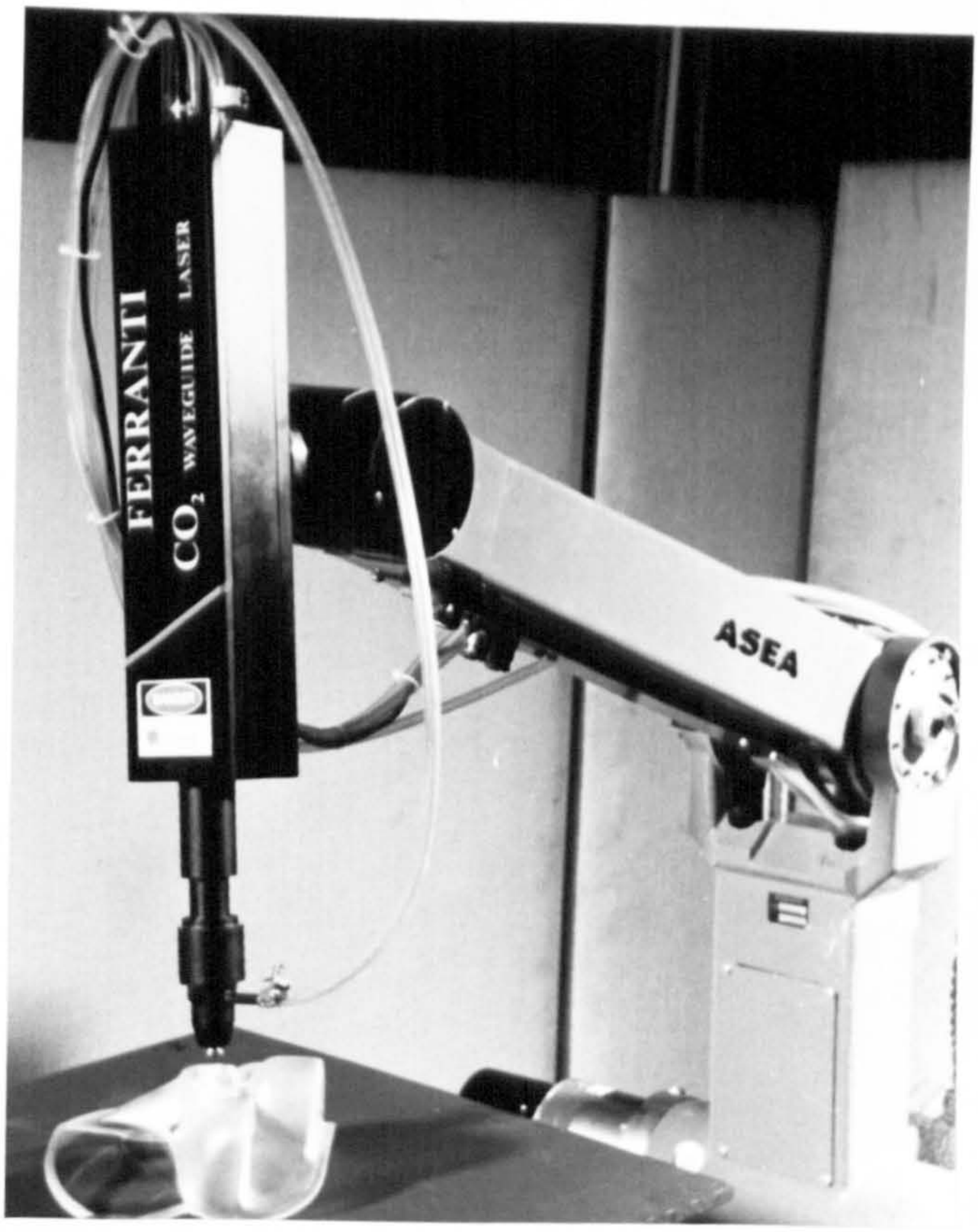

Figure 7.08 - CO2 laser connected to the end of a robot arm

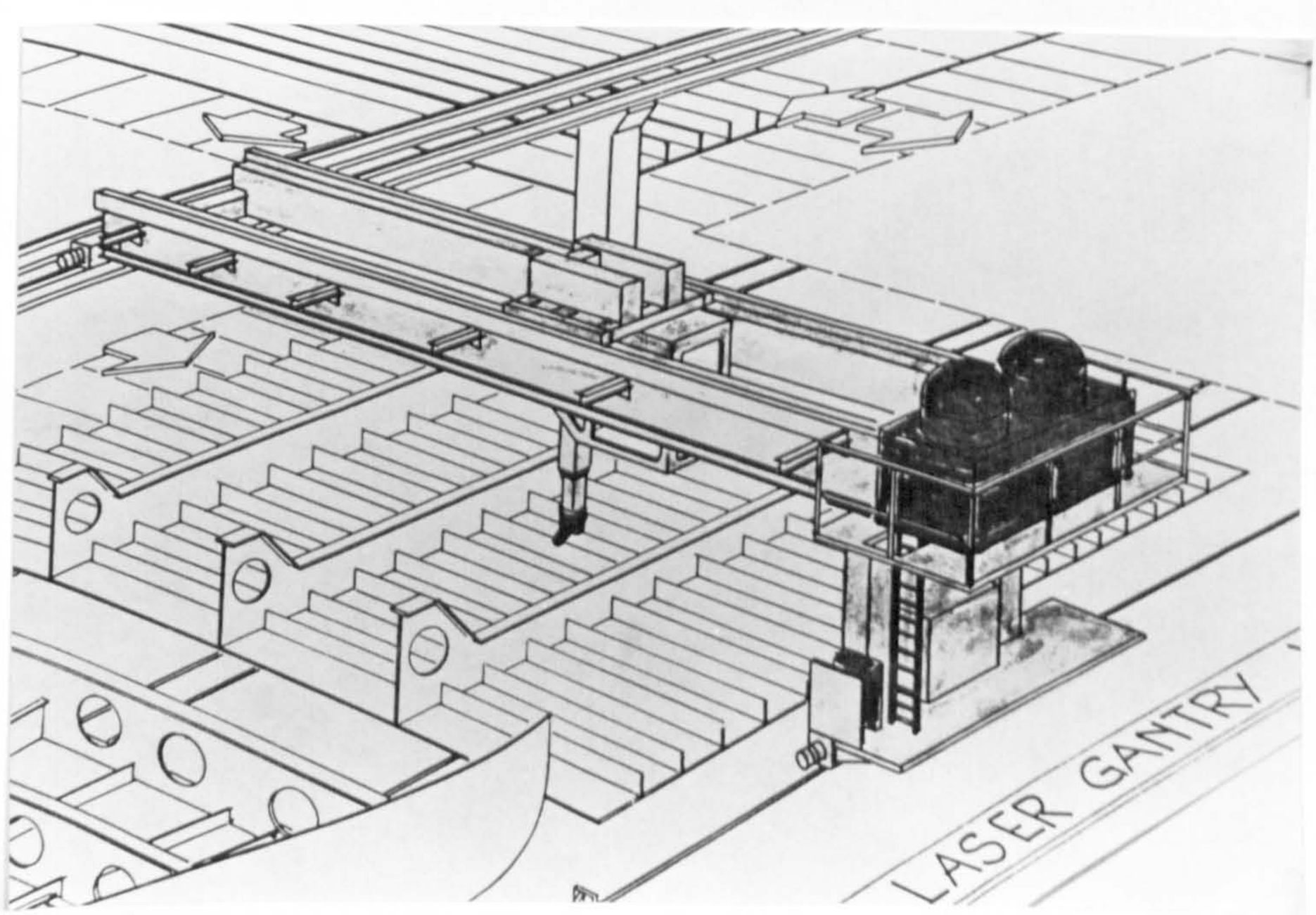

Figure 7.09 - Proposed gantry mounted laser [196]

The extent of multi-axis manipulation of the high power beam to the workpiece for skid welding will depend on the constraints of the product and the flexibility of the workstation.

There are a growing number of lasers integrated into conventional types of machine tools, but nearly all of them are used for cutting applications involving laser powers of less than 2kW. An example of such a machine is the integration of a laser to a woodworking tool, figure 7.10, so that the flexibility of the laser cutting process may be integrated with the high accuracies of the tool. The integration of a number of different types of laser and conventional machines with automated workhandling equipment then provides an opportunity for a laser based flexible manufacturing system. Such a system has been developed by the Japanese [199] in conjunction with a government sponsored laser development programme.

From the above discussion of some of the options available to the system designer for the manipulation of the laser beam to the workpiece, three types of multi-axis device have been identified as being particularly suited for shipyard based skid welding workstation applications:

1. Static laser connected to a stand-alone articulating robot or boom type device. While at present beam transmission to powers of 2.5kW have been employed in such laser based devices, it is considered only be a matter of time for higher powers to be utilised. Some shipyards have development programmes for using stand-alone robots with

Figure 7.10 - Laser integrated into an existing machine tool design

conventional welding heads. These are either at fixed workstations [200] for welding of flange bars, seatings, small minor assemblies, or in a more moveable mode, being positioned for the welding of web joints on panel line assemblies [201] . Since the justification for devices with conventional welding equipment can often only be achieved on the direct savings of manhours due to higher utilisations at the arc when compared to manual practices (as the welding process remains the same) consequential savings i.e. savings incurred in earlier or subsequent processes due to the use of a device or process at a particular workstation, also remain the same. Applying the laser to such devices would therefore fully optimise their capabilities to provide both direct, and of greater significance, consequential savings, eg reduced distortion, consistency of weld size due to a more consistent power source, constant welding speeds leading to greater predictability.

Column and boom type robots, figure 7.11, clearly have greater stiffness than the articulating type, giving potential for greater accuracies, although they are restricted in their flexibility in covering a large working envelope, they are essentialy side entry units for large enclosed structures to accommodate 2 dimensional or open top structures.

As fixed robots, the working envelope would be restricted to the extension of the robot arm. To extend this envelope the robot could be mounted on a moving trolley arrangement serving a number of working areas as has already been used for conventional robots [202]

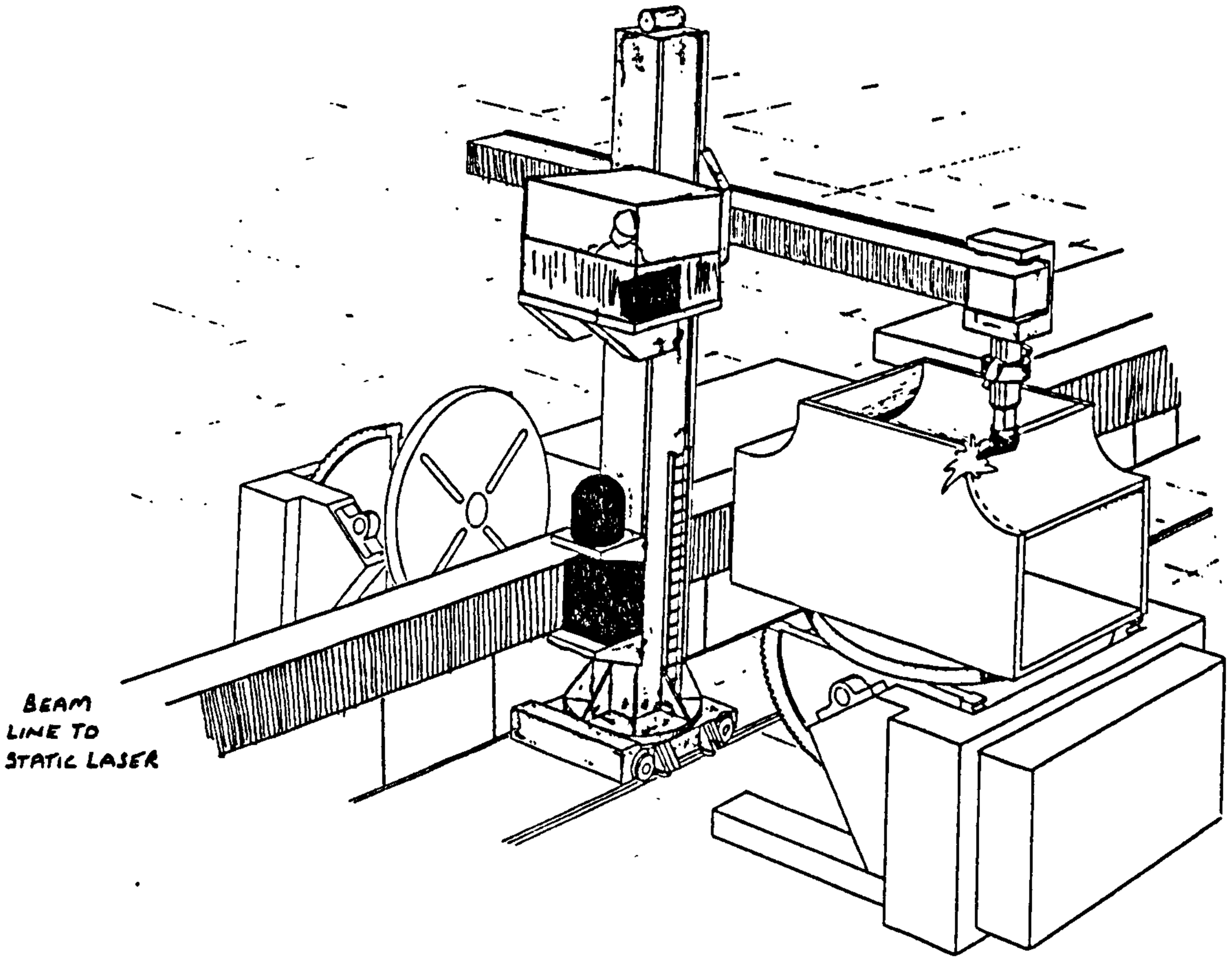

Figure 7.11 - Boom type robot attached to a static laser

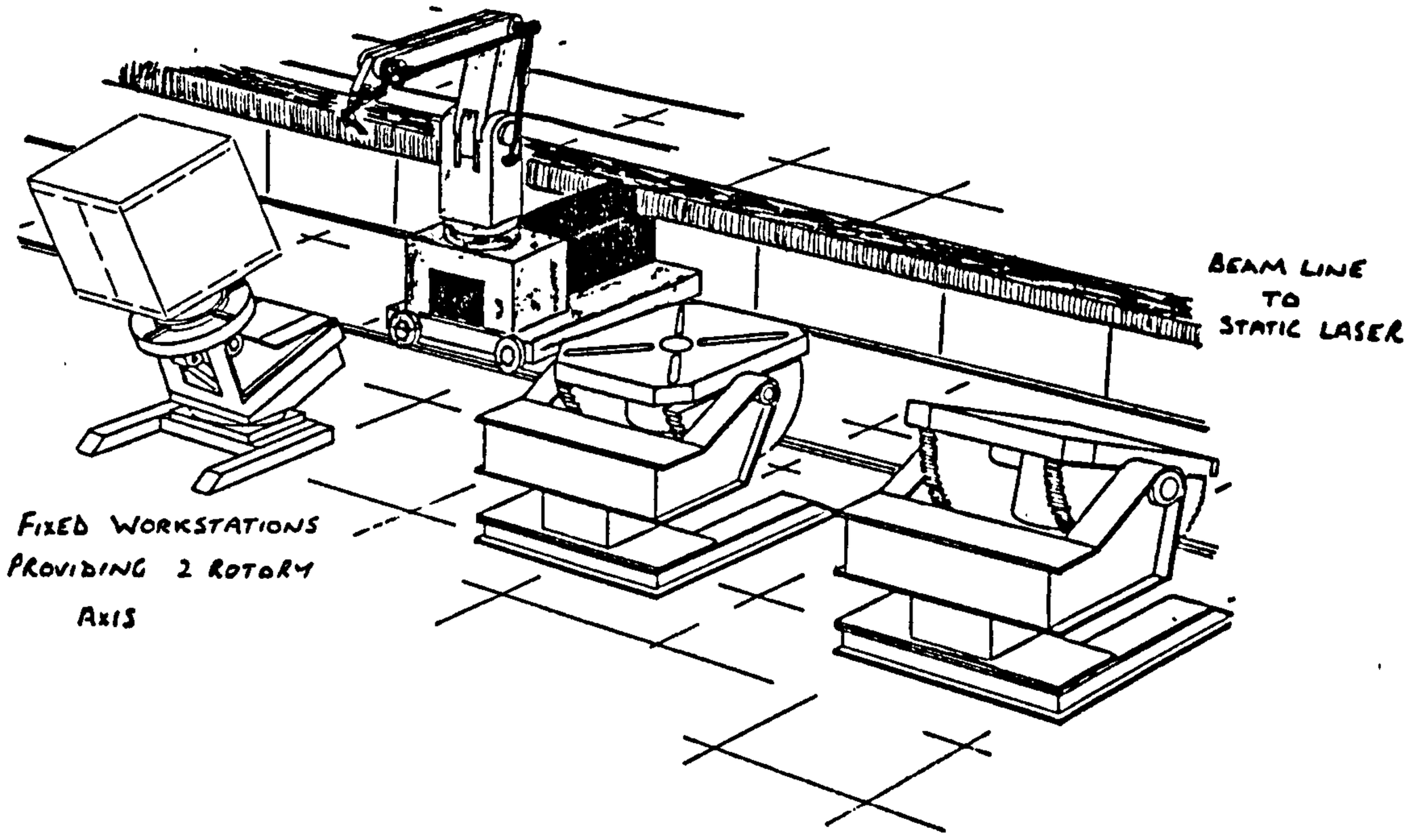

Figure 7.12 - Robot on rails serving a number of workstations

, with the laser fixed at the end of the line, figure 7.12.

2. Fixed laser connected to a dedicated gantry-mounted device. Such a device would take full advantage of having an increased working envelope over the articulated robot, covering a rectilinear volume rather than circular.

Some gantry mounted devices employing conventional welding heads have been developed over recent years. One example of this employs two welding heads on a rigid gantry system and is at present on evaluation trials in a Finnish shipyard [203] , figure 7.13. While production-based laser systems have been restricted to a powering level of 2.5kW, designs have been produced [192] [27] and systems built for prototype devices employing powers up to 15kW. Such a system is being developed in the USA known as LARS (Laser Articulated Robot System), [204] , figure 7.14.

In a European "BRITE" (Basic Research Into Industrial Technology) sponsored project titled Adaptive Control of Laser Processing [205] , constituent modules for such a gantry mounted device, with a multiaxis beam manipulator head, figure 7.15, resulting in a skid welding demonstrator gantry, are being researched. A major part of the project is directed to the research of the necessary adaptive control mechanisms needed to control such a system. From the demonstrator development work, system designers will have the required data to design a production gantry system suitable for shipyard skid welding applications.

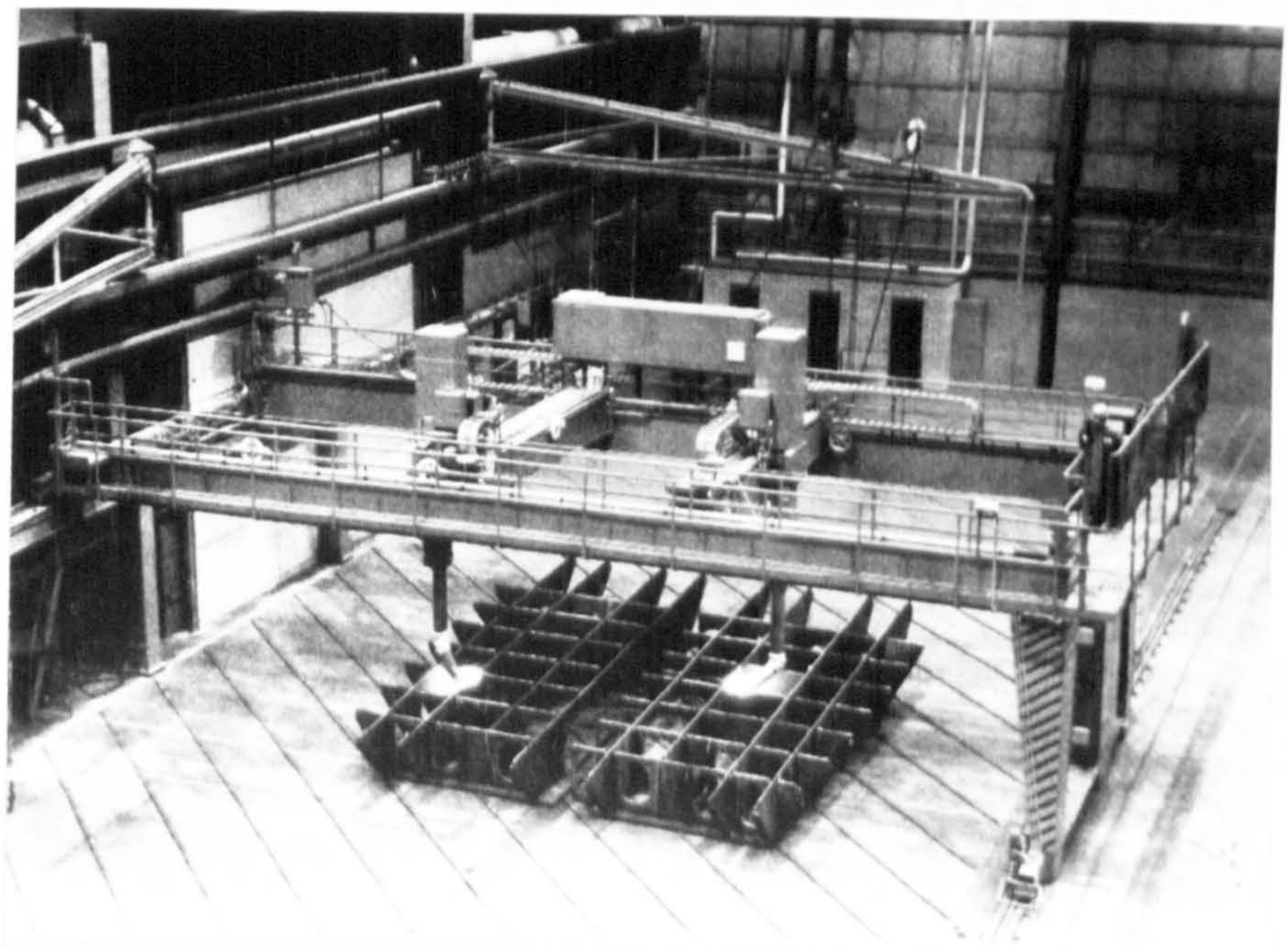

Figure 7.13 - Gantry based production welding robot using MIG welding

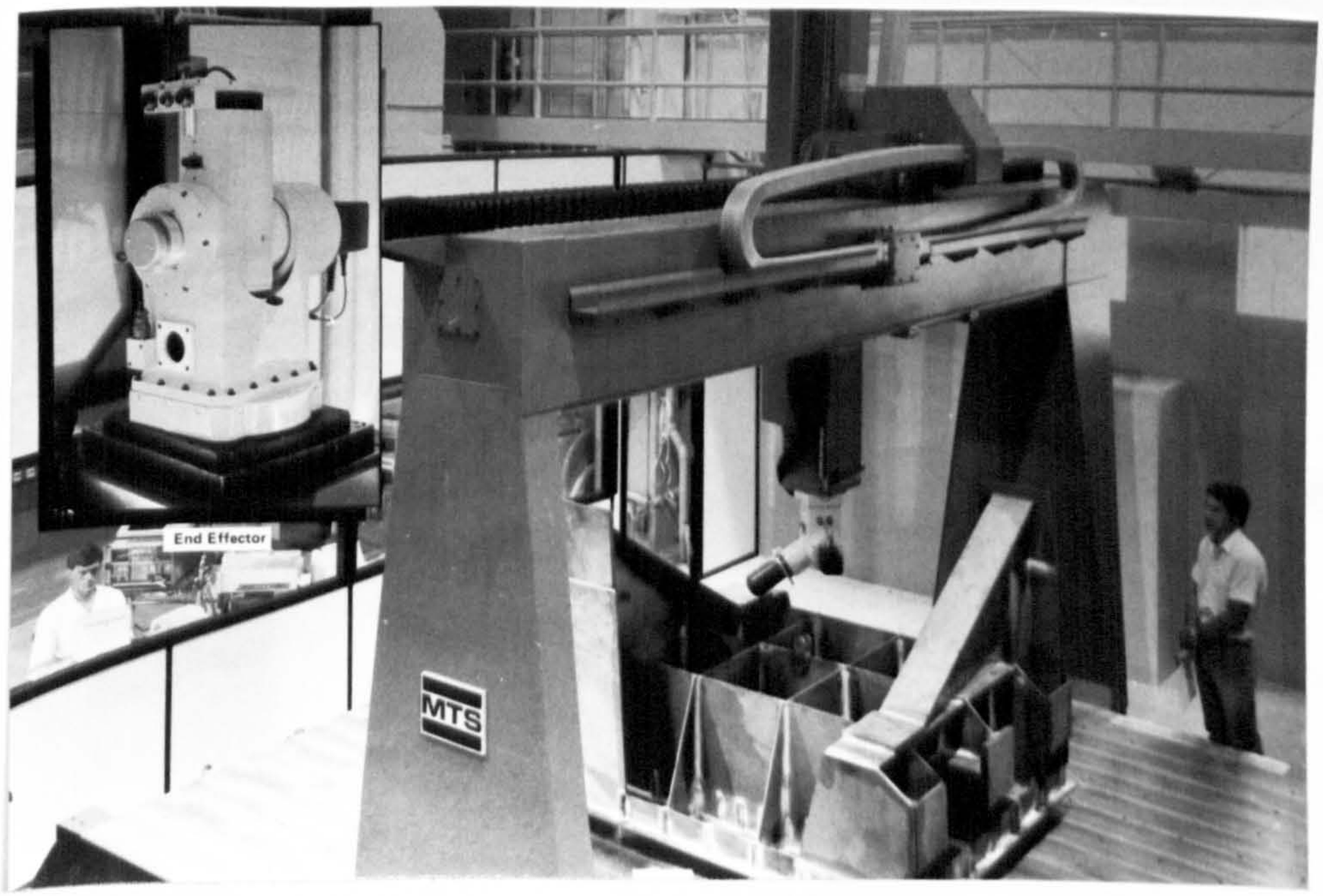

Figure 7.14 - Gantry based LARS laser processing system

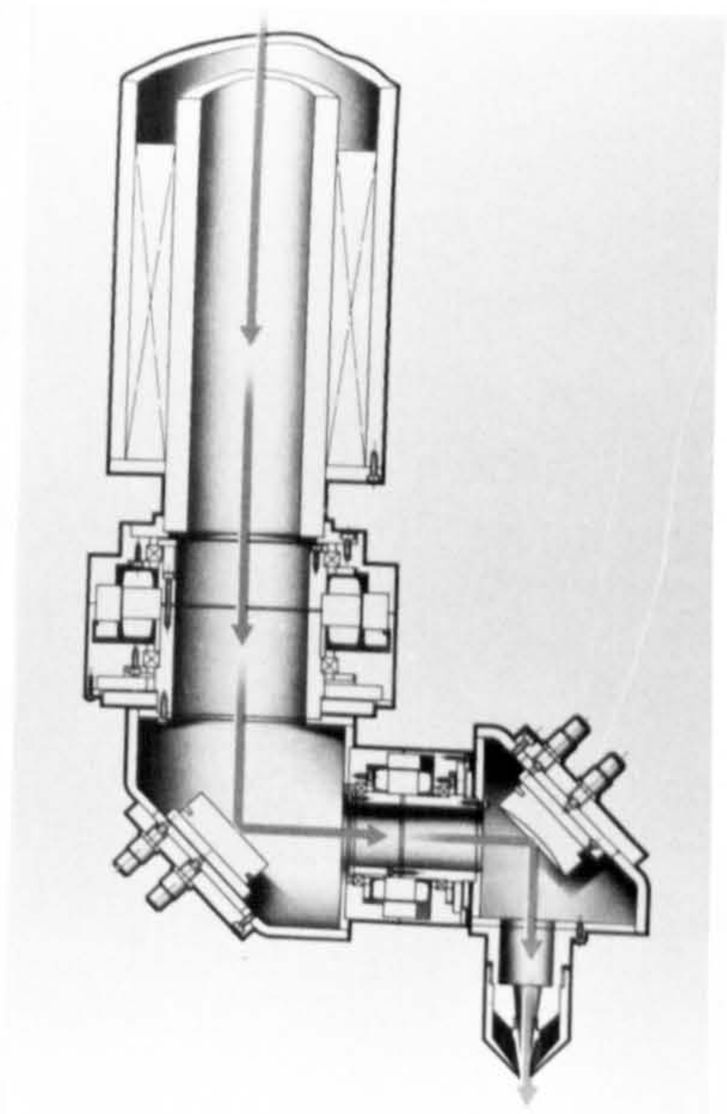

Figure 7.15 - Design of the multiaxis beam manipulator head to be incorporated into the European laser demonstrator

At present there may be doubts as to the accuracy achievable from conventional articulated robots to conduct laser processing to the required accuracies. The use of the stiffer gantry-mounted device should gain the tolerances and factors of reliability required for production based processing.

3. Fixed laser connected to a gantry-mounted articulating robot device. Such a device would not only be used to combine the higher speed of local movements achievable by articulating robots with the positional accuracy of a gantry-mounted system to give higher utilisation levels, but also to reach joints in the ship structure which are inaccessible to a dedicated cartesian device. However, to achieve the same positional accuracy of the dedicated gantry system, the robot itself would have to be built to a particularly high standard, taking tolerance requirements from the modular information of the cartesian system. To obtain such a balance the robotic system would probably have to be more refined than those envisaged for stand-alone operation so as to achieve adequate system stiffness.

Although a more detailed control and design specification would be necessary for the robot itself, the conceptual design of the beam delivery path components would be similar to those for the second option. Control of the system would take two forms:

a. Combined operation of gantry and robot - when the gantry and robot move together this option would provide the least accuracy and the greatest control requirements, but would result in the possibility of the highest utilisation factors.

b. Gantry moved and "locked" in specific positions prior to

operation of the robot ie indexing - utilisation would be lowered due to the movements and locking of the system, however it would probably be the option to obtain system accuracies for the requirements of the skid welding process.

7.2 APPRAISAL OF SKID WELDING FACILITY ON-LINE MONITORING AND ADAPTIVE CONTROL EQUIPMENT

As already noted, there are many factors that can degrade a laser beam's quality and stability between the laser and the workpiece. The beam's divergence will be influenced by the quality of the laser, the mirrors and the atmosphere. Once the beam has reached the end manipulator it must be focused with an intensity distribution appropriate to the process and directed to follow a defined seam or surface of a 3-dimensional workpiece to provide a perfectly reproducible result. In order to achieve this, sensors will be required to monitor and control the input variables and the process itself. Aspects of monitoring beam structure, its delivery, the joint path itself and the on-going process are discussed in the following three sections.

7.2.1 Beam structure and delivery monitoring

Comparisons of beam outputs from different lasers or from the same laser over a time period will show variations in quality and stability. Fluctuations in the gaseous medium density and modal differences may cause changes to the beam intensity and state of polarisation; thermal effects and extraneous vibration may cause variations in beam pointing and propagation thus influencing the beam between the laser and workpiece. Therefore, to ensure process quality and reliability the beam should be monitored. Correlation with process data may then be made to enable on-line control feedback. Various authors have summarised different laser beam diagnostic equipment and measuring devices [112] [206] for on-line measurements of intensity distributions in the "near field",(unfocused beam) and the "far field" (focused beam).

Computerised systems for recording beam profiles and polarisation states have been developed by research establishments but may be considered cumbersome to fit into a beam-line itself. Two alternative devices have been developed for beam line integration.

The spinning wire "laser beam analyser" [108] uses a thin reflective wire which is rotated through the beam. A fraction of the beam's power is reflected on to two detectors. The measured power intensity in two orthogonal directions is displayed on a oscilloscope screen, figure 7.16. The device is simple to use and practical for measuring near-field intensities but there is doubt as to its accuracy for far-field

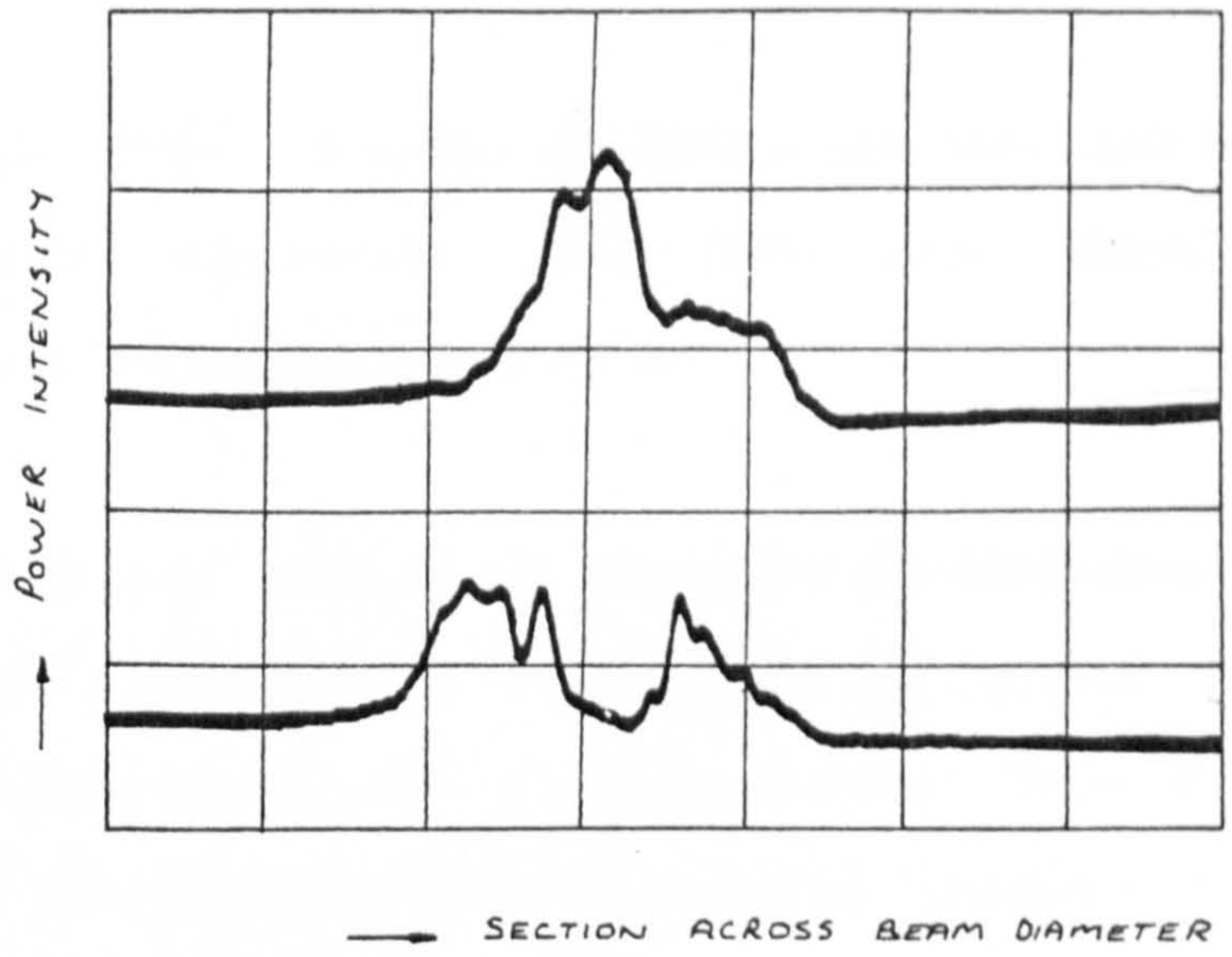

Figure 7.16 - Output from a laser beam analyser in orthogonal planes

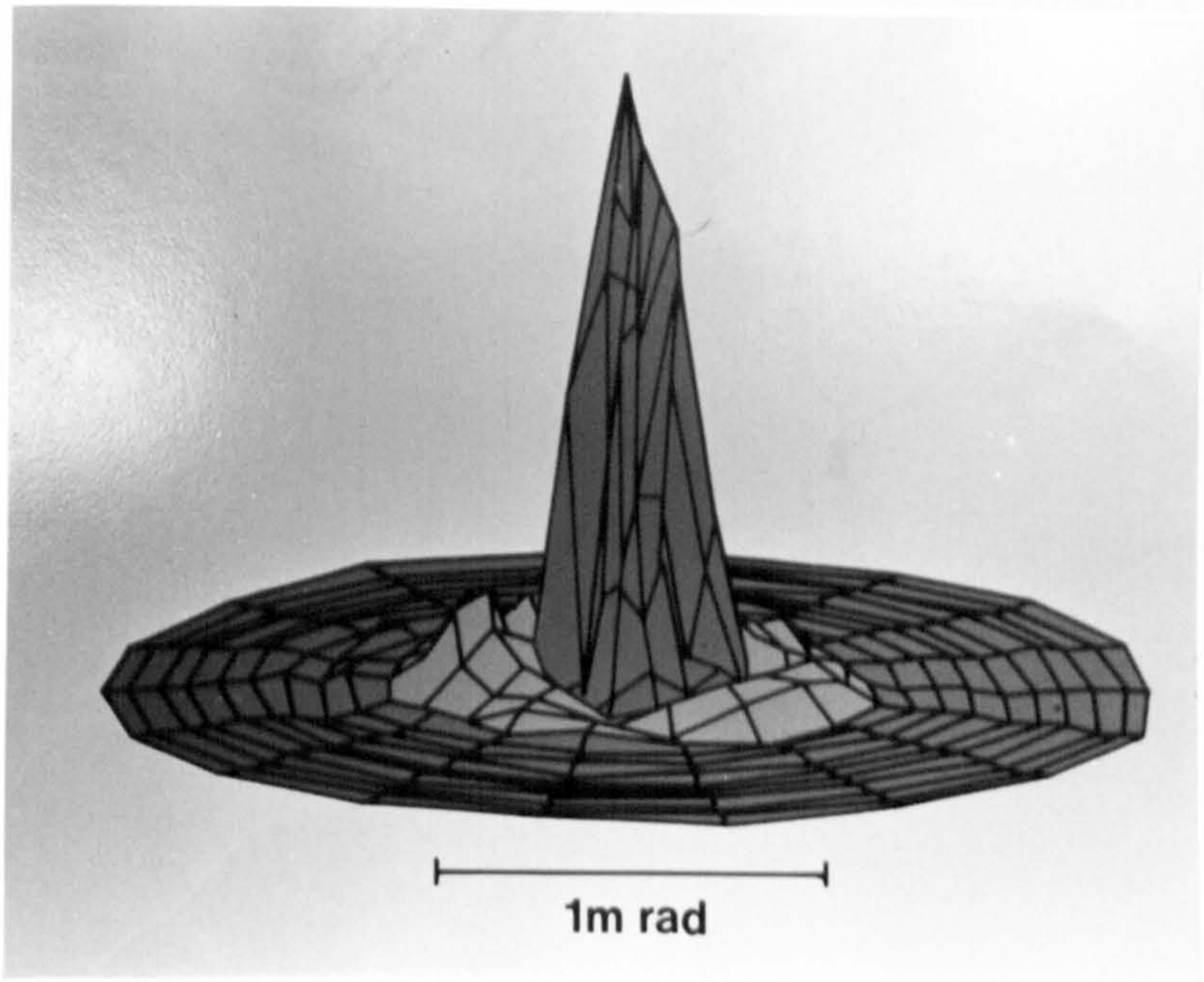

Figure 7.17 - 3D output from a beam analyser sensing through a hole matrix mirror

measurements [109] . Even so the device has been used in the field for system fault diagnostics [191] [207] after which faults have been isolated and subsequently rectified.

Far-field and near-field intensity distributions may be measured by the use of a "hole matrix mirror". This is a mirror with a matrix of small transmitting holes. The fraction of the beam transmitted by the holes may then be measured by a detector device, if required, in a 3-dimensional format, figure 7.17. The advantages of such a device are that the hole matrix mirror may be incorporated as one of the system optics rather than needing a separate insertion into the beam line appropriate to the laser beam analyser.

7.2.2 Process monitoring

One of the objectives of the present research was to determine and examine the tolerances of input parameters in order to achieve satisfactory skid welds. As already discussed, there are going to be fluctuations in laser output characteristics between different lasers and over time periods. Therefore to maintain process quality and achieve adaptability between different systems, while continually refining the process, the only approach is to achieve methods of automatically monitoring the process, not only to act as a means of process quality control but also to enable fine on-line adjustments to be made to the process itself.

Three approaches may be taken:

1. Monitor every process variable known to affect the weld and ensure that they do not deviate outside pre-set limits.
2. Monitor key parameters at the weld which are known to give reliable information on weld quality and ensure that they stay within certain tolerances.
3. Conduct immediate weld NDT e.g. by the use of real-time radiography, the results being digitised and compared with predetermined tolerance bands.

The complexity of process variables has been shown by the present trials programme. However, while most of them can be monitored, they could not easily take account of variations in workpiece compositions or imperfections in the joint surfaces. Therefore while basic parameters should be recorded, the first option could not be considered as an accurate method of determining process quality.

For the third method, while it is in principle feasible [184] , there could be many interrelated variables which could give rise to similar types of weld flaw formation so that information could not necessarily be fed back to make on-line process adjustments.

The second option may be compared with the natural way in which an experienced welder will know by "feel" the quality of the weld he is producing by, for instance, watching the arc (optical response monitoring) or listening to the process (acoustic monitoring). In

practical terms this was achieved by the author during the welding trials. As experience was gained, a good estimate of the weld quality could be made by viewing the balance of the plasma coming from the incident and emergent sides and listening for different types of "crackling" noises.

Many more options than just optical or acoustic monitoring are available for the automated skid welding process, most of which would assess weld penetration as the primary process variable. Ideally sensing of both incident and emergent sides would enable penetration points to be maintained,e.g.by measuring the infrared count at the emergent side as may be used for conventional welding.

However, for the single sided skid process, when sensing would be restricted to operating from the incident side of the joint, alternatives may include; probing of the weld keyhole by a HeNe laser and measuring the response of back reflections; measuring changes of the acoustic spectra associated with the plasma formation from the keyhole [208] ; analysis of the visible, infrared and ultraviolet [209] [210] radiation levels above the keyhole; measurements of the back reflections of the CO2 beam or close-circuit visual monitoring [209] [210] , real-time radiography [184] or ultrasonics.

Ultimately a means will be required to assess a particular process response, a comparison being made with known control parameter limits. The response may be used in two ways:

1. Closed-loop feed back - used to automatically adjust input parameters. For instance, suppose initial process settings have been computed to produce a balanced skid weld in a certain plate thickness, then if that thickness should increase without either reducing speed or increasing power, penetration would effectively reduce. If sensed, comparison with a comparative algorithm would then result in adjustments in the parameters to compensate.
2. Quality control record - recording of the responses in comparison with pre-determined limits would provide an on-line quality record of the process. If the response exceeds the limits, potential faults may be easily traced to the exact position within the joint and rectified immediately.

Early involvement of classification societies is very important for such a proposal to be accepted, both in understanding the process the potential flaws and also in setting sensible tolerance limits.

7.2.3 Seam Tracking

Although, as engineers, we may strive for perfection in product development and assembly techniques, at present we have to cope with inaccuracies. Just as manual processes rely on the "skill" of the operator to follow a seam, compensating for joint gaps and discontinuities, so also will any automated process.

Seam tracking for applying conventional welding to robotic devices will create a vital link to enable fully automated processing to be

perfected. This is the same for laser welding.

Mechanical methods of seam tracking have been used for many years in the form of tracked carriages, gravity welding frames [211] . Today microprocessor controlled methods of seam tracking are beginning to be implemented for conventional welding, primarily for MIG welding [212] including; tactile sensors with sensing rings which actually make contact with a joint surroundings; inductive sensors to measure the position of the joint relative to an inductive coil; vision systems which use optical viewing which is digitised and interpreted by a microprocessor [213] ; through-the-arc systems which measure the change in current in response to gun movements within a weld preparation and vision systems which employ laser scannning of the joint [214] [215] .

The method most preferred for the non-contact laser process is that of laser scanning the joint. Such a system is available for arc welding [214] and is currently under development for laser applications. The microprocessor based system uses a HeNe laser to scan the joint, figure 7.18. Analysis of the detected image allows measurement of seam positions, gaps and joint orientation. From this basis, welding speed, laser power, beam incident angle and feeder rates may be computed for continuous processing. The data derived in the present work of determining parameters for series of fixed parameter sets may now be used as an initial input to the correlation algorithm for the microprocessor based control loop.

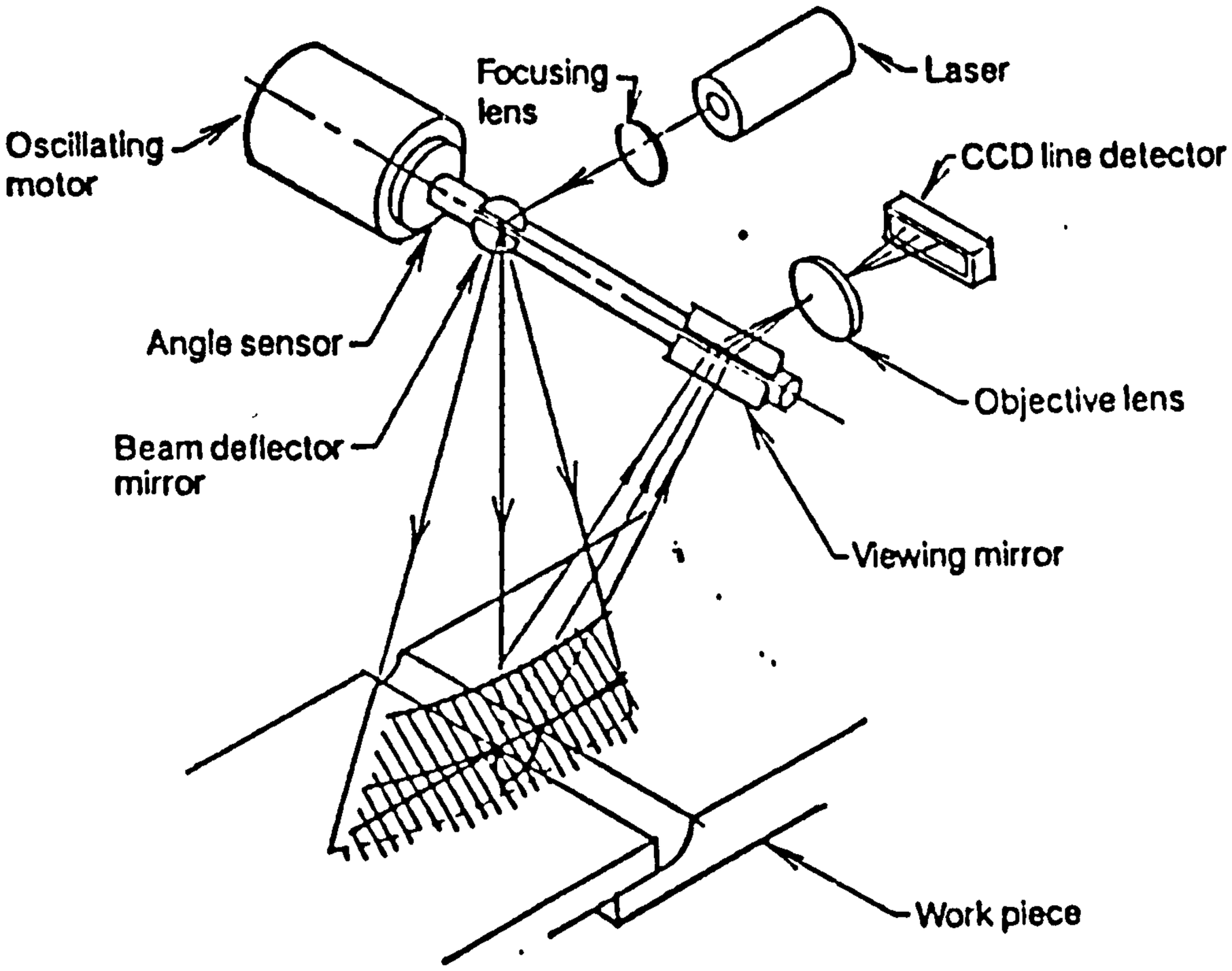

Figure 7.18 - Seam tracking using a scanning HeNe laser

It should be noted that many of the process control functions require feedback data analysis and high speed responses. These tasks could not be expected of the same controller which provides the robot motion control. Therefore a separate control system would be recommended providing also a data base for process monitoring and record keeping.

7.3 SAFETY REQUIREMENTS RELATING TO LARGE SHIPYARD BASED LASER SYSTEMS

At present safety guidance procedures for manufacturers and operators of lasers are presented in BS4803:1983:"Radiation safety of laser production and systems" [61] . However the standard is not specific when describing the safety requirements for high average power laser systems. The provision of a "protective enclosure", a physical barrier to stop personnel from being exposed to laser radiation levels above a prescribed level termed as the "Maximum Permitted Exposure" level (MPE), may be feasible for two dimensional operation eg for a cutting machine, or in the form of a cabinet for small multi-axis machines. But at an estimated cost of between £400 and £1000 per metre square [216] , to enclose a large system of the scale envisaged for shipyard-based skid welding e.g. to surround a panel line gantry workstation of dimensions 12m x 12m x 6m, including protection for overhead crane drivers at elevated levels in the shop, would strongly prejudice the viability of the facility.

Various investigations have been conducted by other authors to assess the requirements and potential demands to be made of physical enclosures [217] . However an alternative to having a physical enclosure as the sole

protection means has been investigated by the Author [218] for a working group assigned to producing an update for BS4803 in order to encompass practical safety considerations when employing high average power lasers in laser systems.

7.3.1 Operational Considerations

In addition to the increase in size, laser power and flexibility of the proposed multi-axis systems compared with existing smaller laser systems, a number of general and practical factors need to be taken into account. These may include:

1. The likelihood for work activities adjacent to the laser workstation, preparation work, or operation of adjacent machines in the production process require complete independence for the laser based workstation.
2. Ease of material flow between workstations - if large items are to enter the laser workstation an enclosure surrounding the area must be flexible enough to allow efficient movement i.e. a large physical protective door 12m x 12m would be totally impractical.
3. Free passage of personnel adjacent to the laser workstation - personnel not associated with the laser system but involved with associated machinery in a production line will require easy access to their particular operational areas.
4. Identification of "foreign" articles within the laser beamline or operational zone - presence of items not associated with the particular laser process could act as an influence on safety criteria

eg an unexpected surface acting as a focusing device.

7.3.2 Laser Affected Zone Monitoring

If, instead of a physical laser enclosure surrounding a laser aperture as required by the present standard, the volume enclosed was to be considered as a Laser Affected Zone (LAZ) and on-line zone monitoring devices were employed, monitoring within the zone would have to take account of the following operational modes:

1. LAZ Checking - Conducted prior to the high power beam being operated and would comprise:

   a. Beam line checking -use of HeNe devices to check alignments, beam line integrity.

   b. Workstation checking - scanning device checking for "foreign" items or personnel, similar to the infrared devices used as burglar alarms.

2. LAZ On-line Monitoring - Operated once the high power laser beam is in the beam line. Three operational situations need to be addressed:

   a. When there will be no errant beam - within this situation a beam monitoring device must ensure that the raw beam has travelled the length of the beam line and any manipulator, arriving at the workpiece in a pre-determined state. A similar comparative feed-back monitoring device may be used to show that reflective response within the beam line after commencing a particular job is correct. If any response is incorrect, the system would be

shut down within a pre-set time period. Beam line monitoring such as the "hole matrix" system or the "laser beam analyser" may facilitate a basis for such a monitoring device.

b. When there will be a possibility of an errant beam - within this situation, monitoring of the characteristics of the process itself should be examined. The optical or acoustic signature of a process may be compared against a specified tolerance envelope. The system would have to allow a certain time period for the process to stabilise then shut down if this stabilised state was not reached or the response signature failed to keep within specified limits. Such devices are already available for detecting potentially faulty welds by monitoring the ultraviolet radiation signature of the plasma [209] , but could be just as easily used in the safety role described.

c. When it is assumed that there will be an errant beam - with this situation, a monitoring device would have to respond to errant beams at any position within the laser affected zone. In addition such a device would be required to ensure that personnel and hardware were in accepted positions before the system is operated. A device to monitor the infrared radiation signature of a zone [216] would provide s basis for such development

7.3.3 System Shut-Down Time

If by having a monitoring system, safety levels were to be compatible with those for a physical enclosure, the monitoring system must be able to respond and shut down the system within the timescale dictated by the MPE levels. However, it was noted that the total time taken for a system to be made safe would have to include the following time periods:

1. Sensor response cycle interval - the cycle time within which a sensing device monitors a particular zone sector.
2. Feedback processing time delay - the time taken for the sensor signal to be compared against the prescribed tolerance envelope bounds.
3. Switching time - the time taken for the safety stop switch on the laser, or laser shutter to be activated.
4. "Switch to safe" time - the time taken after the safety switch has been activated for the system to be made safe.

For the laser power levels envisaged for the shipyard skid welding facility, calculations based on the present safety standards were made to assess the maximum exposure levels allowed and consequently the maximum exposure times, Appendix E-1. This showed that the allowable time of exposure, and hence the maximum total time required for the system to be shut down was less than 4.0 nanoseconds. Clearly this time scale is very short for any one of the switching time components, let alone the total shut down time. Therefore further alternatives have been considered.

7.3.4 Proposed safety procedures for the shipyard based skidwelding facility

From the present analysis, it is unlikely that the sole use of monitoring devices could be considered for primary safety protection within the present MPE limits as set by B.S. 4803. Although these values are being reassessed at present, safety procedures will have to make full use of administrative, mechanical and electronic control. Two levels of protection are proposed:

1. Non-authorised personnel - they would be restricted from entering the laser affected zone and kept at a safe distance (based on beam diffusion limits) from the operational area by physical barriers, similar to those required for any conventional operational robot. As a means of secondary protection only, a LAZ monitoring device would be installed to detect foreign articles and would facilitate system shutdown if the primary system was disregarded.
2. Operators and authorised personnel - they would be allowed into the LAZ while the laser was not operational in the beam line. Prior to opening a beam line shutter, such personnel would be required to enter into a cabin-type unit which may be sited in the LAZ and fully protected as a physical enclosure. A simple comparison of the procedure may be drawn from those used in hospital X-ray rooms. The general public being kept behind closed doors, but the operator remains in the room shielded when required by a protective cabin box.

7.4 ECONOMIC EVALUATION OF SKID WELDING FACILITIES

Previous authors [22] [3] [219] [21] have assessed the economic justification of laser based flat panel line systems. The earliest by Peters [21] noted the potential savings from both speed of processing and reduced distortion but the practical application of the work was constrained by the dependence on autogenous processing, thereby requiring impractical joint fit-up tolerances. Work by Martyr [3] and shipbuilding consultants [196] [219] , while taking account of the filler process, only used projected data for the welding parameters used. The most recent report by Peters [22] also relates projected feasibility comparisons for laser and electron beam processing. All the studies emphasise the need for a high equipment utilisation and dependence on an assessment of consequential savings eg from reduced rework, reduced distortion, reduced need for manually based quality control techniques, in order to use conventional costing methods.

Various methods have been proposed for evaluating welding or robotic equipment [220] [221] . These methods and other results of robotic equipment evaluations [222] emphasise the difficulty of justifying high technology equipment on a conventional basis. For the present study these have been used in conjunction with the standard equipment justification procedures as advised by British Shipbuilders.

Non of the laser-based shipyard studies so far break down the processing cost components in order to identify the prime influences on

cost savings nor do they reflect the sensitivity of the initial cost estimates on the overall cost effectiveness.

For the present analysis the author has selected three examples for comparative assessment. Every effort has been made to obtain accurate estimates of equipment costs. Consumable costs have been calculated for laser welding, based on parameters derived during the welding trials and for conventional processes by using statistcal data published by The Welding Institute and consumable manufacturers [175] [223] as summarised in tables E7.01a-e, Appendix E-2. Assumptions made during the analysis are listed in Appendix E-3.

The first is an idealised system devoted totally to tee section welding. This has been used to compare the cost for using the most commonly used arc welding process in shipbuilding with laser skid welding. In this example the costs have been categorised in order to examine the sensitivity of each category on the overall comparison. The second, a double bottom matrix line, uses the example of a production line where a large proportion of tee section welding is performed, often in very cramped conditions. An assembly of typical merchant vessel scantlings, average 12mm plate is used as an example product. The third, a minor assembly production line, is conventionally a labour intensive function using a lower dependence on capital equipment. In comparison to the matrix line, light scantling products are considered, based on average 8mm thick plate.

7.4.1 Analysis of welding facility and operational costs to compare laser skid and semi-automatic fillet welding

The economic evaluation of a shipyard based laser system, as should the assessment of any equipment being installed within a production line, needs to be made as part of its impact on the complete facility's ability to make a profit.

To make an assessment of the potential direct process savings which may be attributed to using laser skid welding, compared to a conventional welding technique, the Author has compared the operation of two idealised welding workstations. The first employs single sided laser skid welding and the second uses the semi-automatic MIG welding process to produce twin fillets. The latter was chosen for the example as being the most dominant welding process within shipbuilding worldwide.

The comparison is quantified by calculating the costs of welding a metre length of stiffener (a single pass for the laser skid welding, a twin pass to produce two fillets for MIG welding). It is based on comparative facilities capable of welding identical lengths of stiffener for plate thickness used in the present trials over a period of one year, calculated initially from the laser example based on a 75% utilisation factor then for higher and lower utilisations. The number of the slower MIG welding heads was then calculated in order to weld the same length of stiffener. A mean process time of 40% of arc time was used for this comparison. This is a higher level than is found at present in UK

shipyards (a more realistic figure is 25% for hand-held MIG welding) but it represents a mean between this lower level and a level to which shipyards should be aiming, particularly for robotic welding.

Where capital equipment costs are involved, maintenance charges are assumed as 1% of the capital cost and for this example depreciation is calculated over a five year period at 20% per annum. The author has devised four categories which best reflect potential process cost difference and may be applied to each process

1. Power source - for the laser system this includes the laser running consumable costs, maintenance and depreciation. For MIG welding it includes the electrical charges, maintenance and depreciation of the MIG units i.e. all costs related to producing the power input at the nozzle.
2. Nozzle consumables - this includes wire and shrouding gases consumed at the welding nozzle.
3. Labour - Calculated to enable the same length of stiffener to be welded for each system. The rate is based on typical basic wage rates currently used by British Shipbuilders at £4.03 per manhour. This may subsequently be affected by an overhead recovery rate of typically 143%. For accounting purposes, this may be included if, by the use of new equipment, surplus labour is still gainfully employed to a contract. One area of the production process which remains undermanned in virtually all British shipyards is that of Statistical Accuracy Control [224] to which the use of the low heat input laser processing is a direct contributor. Labour not utilised on the laser

based equipment would therefore be employed in this important but highly under utilised production function.

4. Operating equipment - the effect of the cost of the most recently designed equipment necessary to achieve efficient welding processing is often forgotten in process costing calculation because of its variability, even though its exclusion may make a nonsense of any costing exercise. For the present example basic workhandling and nozzle support equipment, as considered essential by shipyard welding engineers, has been included. For the laser facility this includes a gantry based manipulator, beam delivery, seam tracking, safety and operating equipment, total £500,000. For the MIG welding facility use of a twin gantry system for the suspension of MIG units is assumed, total £160,000.

The cost of electricity was given by the North Eastern Electricity Board based on the consumption of British Shipbuilders. Wire costs have been provided by welding consumable manufacturers. Gas prices differ considerably depending on a user's total gas consumption. For the examples, rates have been calculated based on British Shipbuilders present consumption plus a projected consumption for a 10kW laser.

The comparative costs for each category are shown in figure 7.19 a-d. Figure 7.20 a-b then shows the total cost and a comparison for different laser utilisation factors.

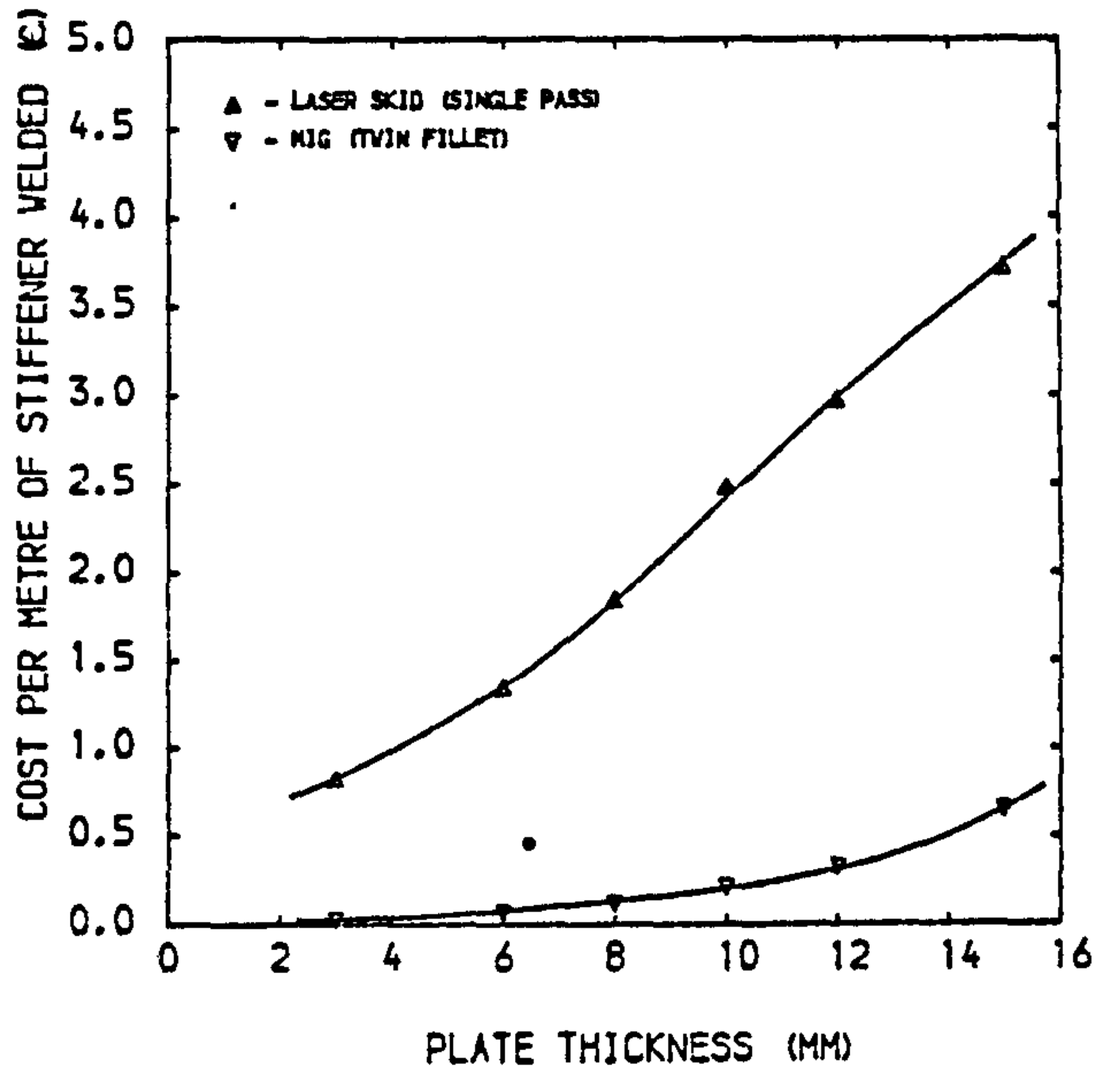

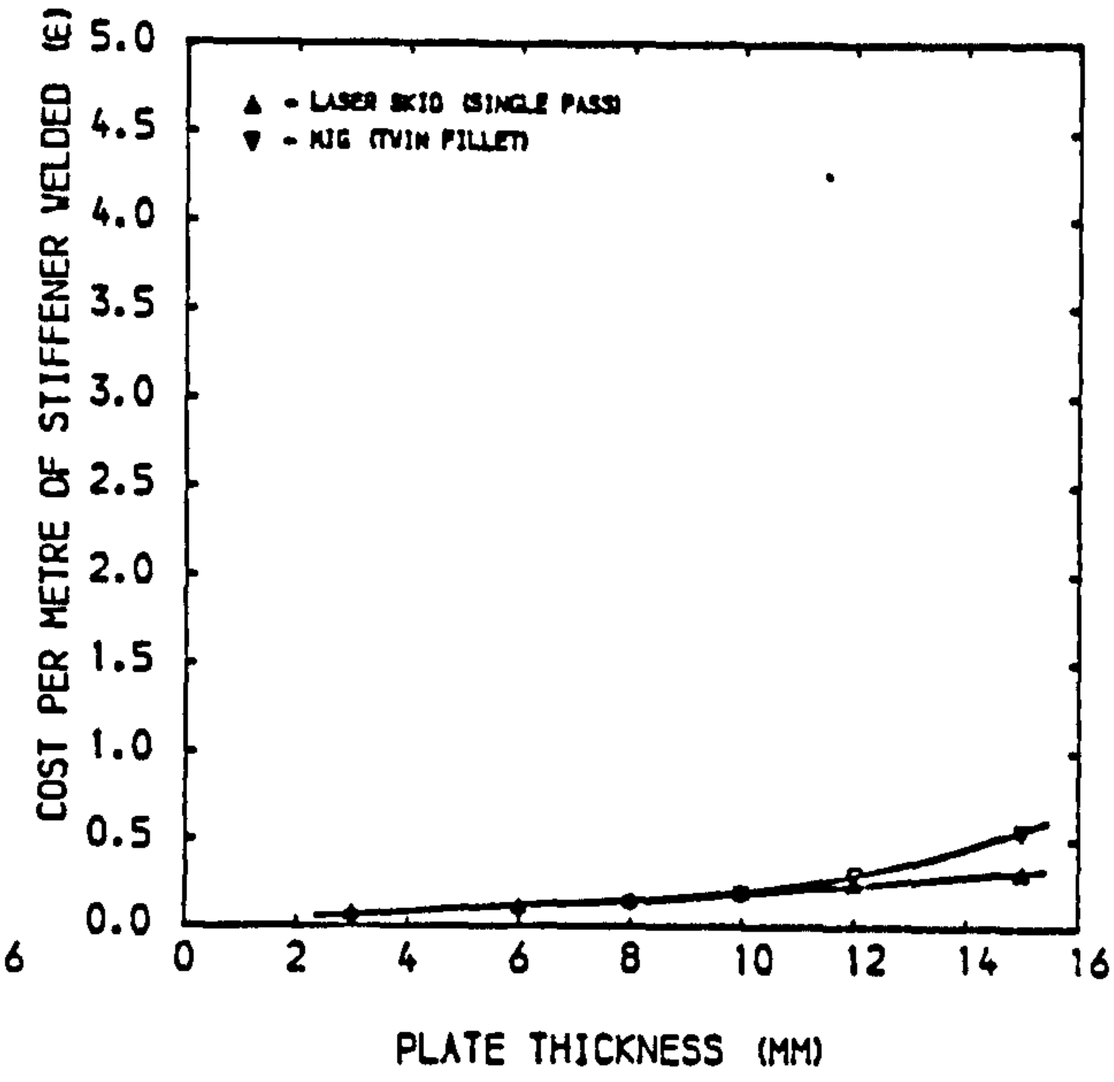

a)Power source b)Head consumables

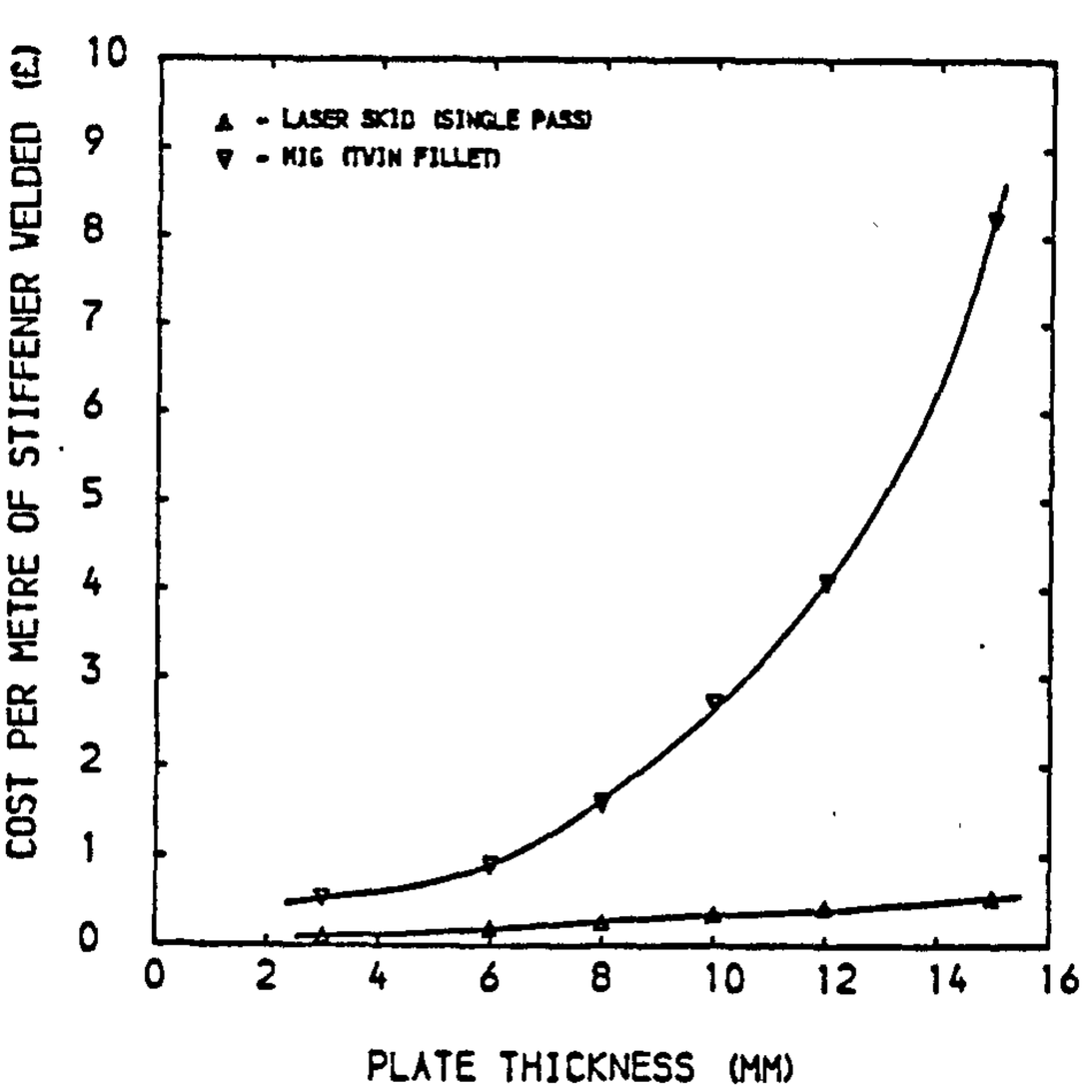

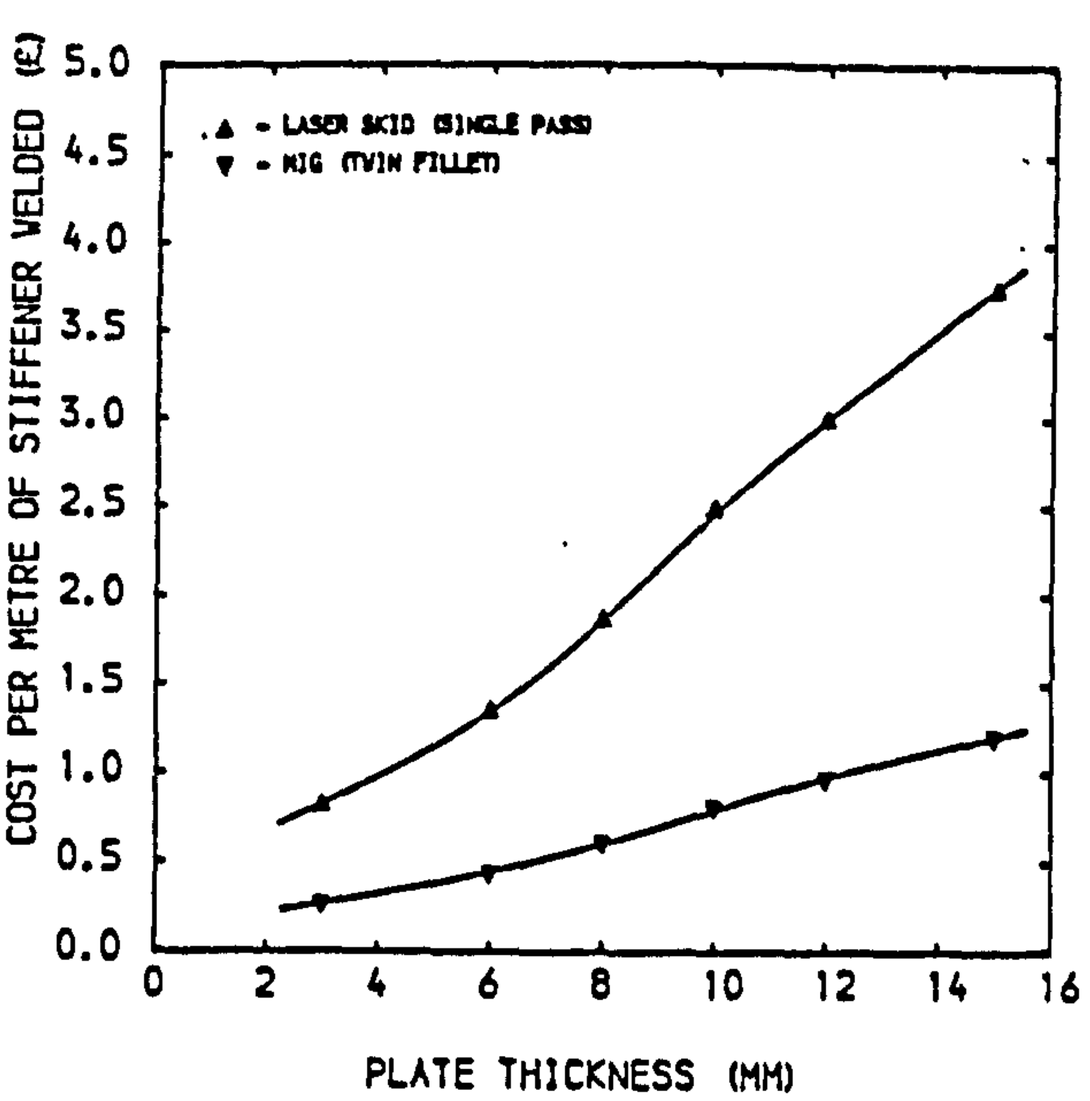

c)Labour d)Operating equipment

Figure 7.19a-d - Comparative costs for laser welding and MIG welding a continuous stiffener divided into four cost headings

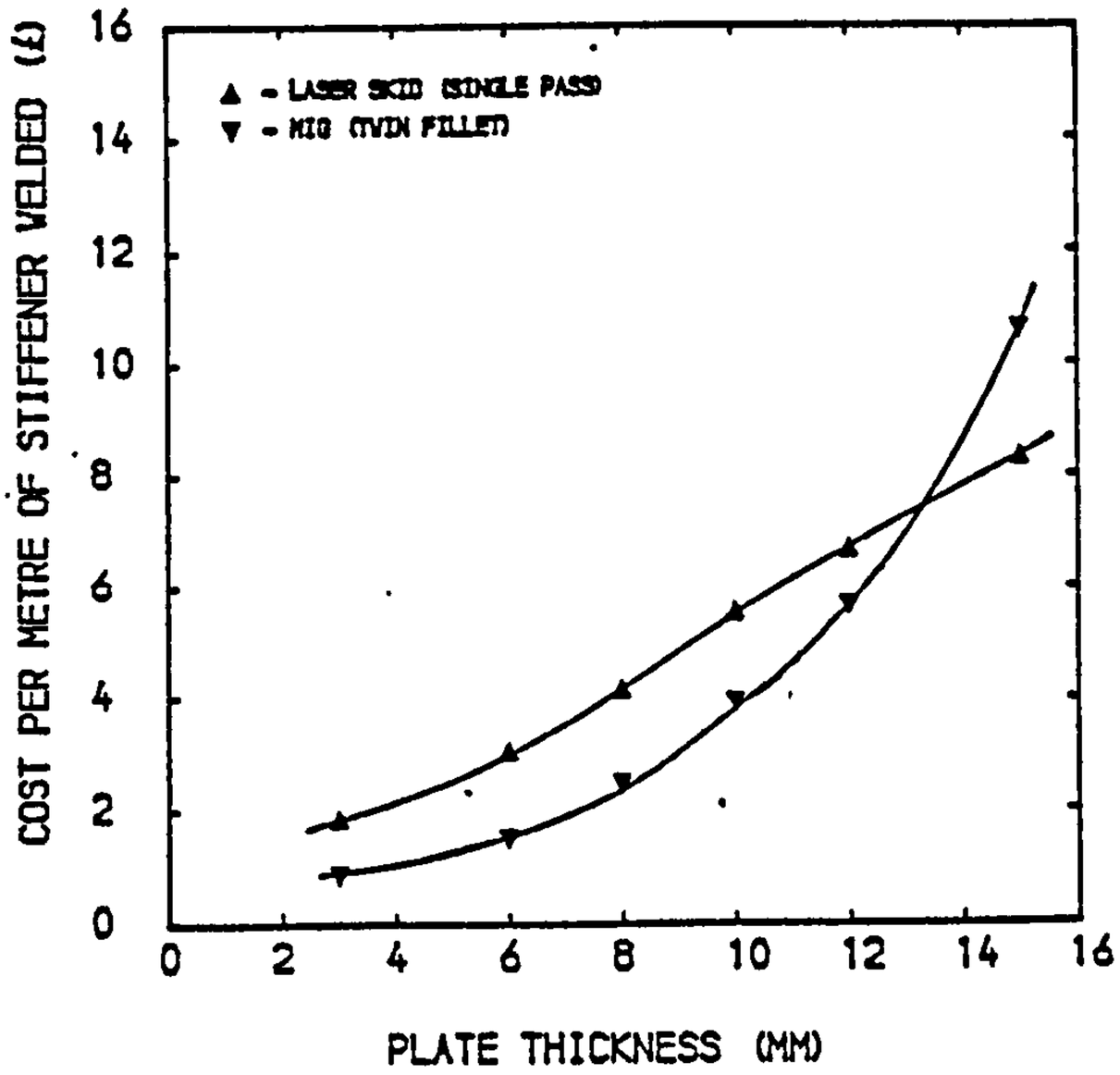

Figure 7.20a - Comparative total cost for laser or MIG welding a continuous stiffener, 75% laser utilisation

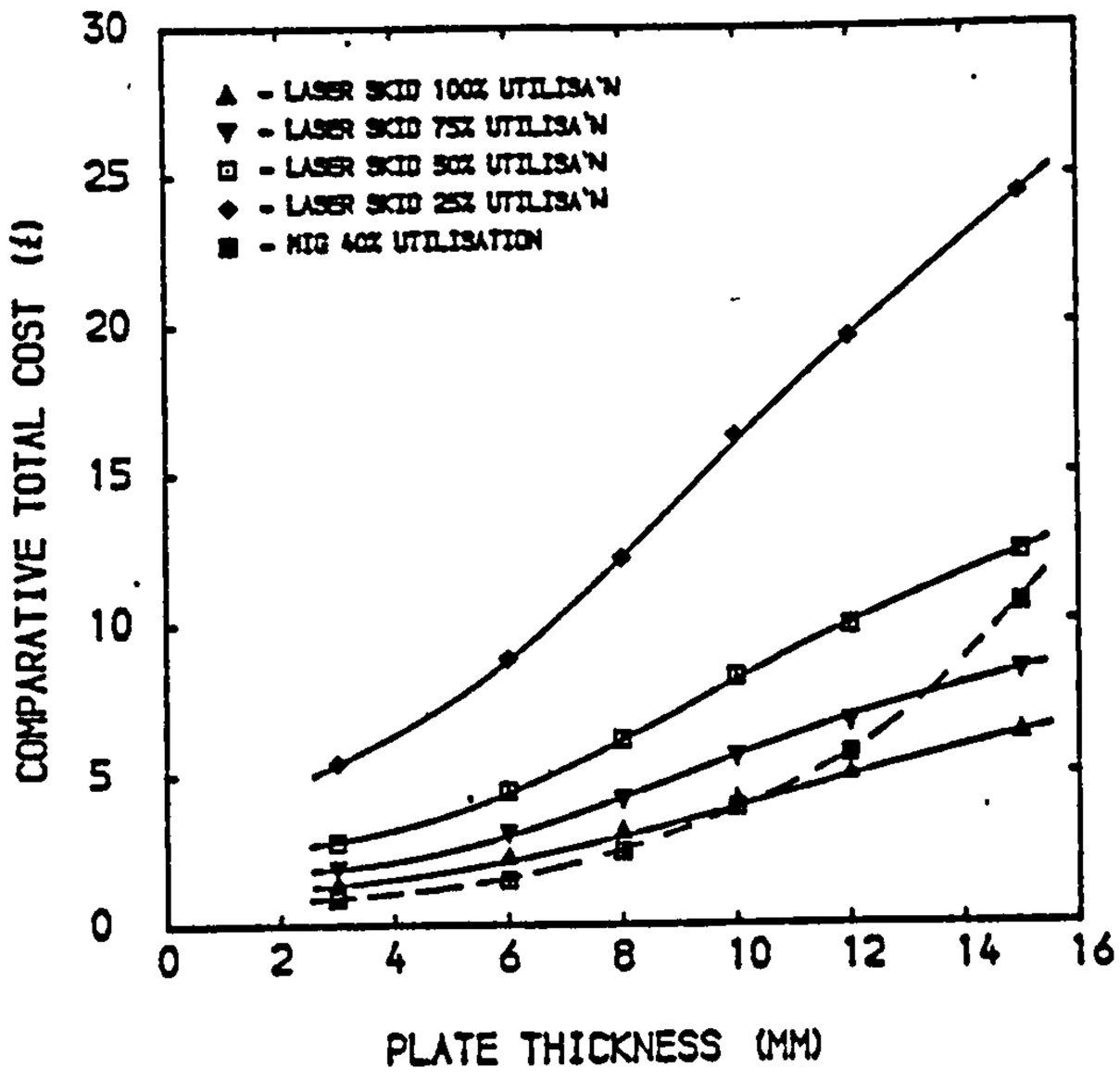

Figure 7.20b - Comparative total costs for laser or MIG welding showing the effect of varying laser utilisation

Power source costs for the laser are seen to be high compared to the MIG process. This is due to the high capital cost and low wall plug efficiency (5%) of the laser.

In contrast, head consumable costs are similar for both laser skid and MIG fillet welding. The higher cost of helium shielding for the laser welding compared with the carbon-dioxide or carbon-dioxide and argon mixtures for MIG welding is balanced by the reduced filler wire consumption found necessary for the single pass fully penetrating joint compared to that of the twin fillets. In future the Author would also expect more economical gas mixtures to be used for laser welding [69] , similarly for MIG welding recent authors [225] have shown how weld properties and weldability can be improved by the introduction of helium into conventional gas mixtures, ie consumable costs would increase.

The higher cost of labour for the MIG process reflects the lower utilisation, slower processing speeds and the doubling of the number of welding passes in order to produce the twin fillets. This requires a higher number of welding heads and operators to maintain a similar stiffener throughput.

The operating equipment cost is a direct function of the capital expenditure for the operational equipment. The laser cost is three times that of the conventional equipment due to the high unit cost of the laser itself and the associated robotic and beam delivery equipment necessary for the manipulation of the beam to the workpiece.

Although the total costs show a generally higher cost per metre stiffener welded for the laser system the large variances in cost differences for each category (apart from nozzle consumables) indicates that the calculation of the final total will be very sensitive to variations in the categories when examining a total system. This fact is emphasised by the reversal of cost trends when examining the cost of welding 15mm thick plate due to the ratio of traverse speeds for joint formation (laser welding being 8 times as fast as the MIG process).

Although this idealised, yet practical example, has enabled an examination of the relative constituent costs of comparative welding processes, it has not reflected the overall impact of a laser based skid welding facility as part of a ship production facility. This has been sought in the following two sections.

7.4.2 Synthesis and economic evaluation of a matrix line

Conventional methods of matrix panel construction vary according to facility mechanisation and the degree of confidence to which the shipyards are prepared to assemble pre-assembled parts. More recent shipyards designed for the United Kingdom [226] have followed Japanese trends where a matrix of stiffening components is produced on a jig then removed and sandwiched between two flat panels, figure 7.21. Inability to achieve a sufficient degree of accuracy in joining techniques is the main reason for a more conventional approach to persist in UK shipyards; two stiffened flat panels are produced, deep webs and girders are welded

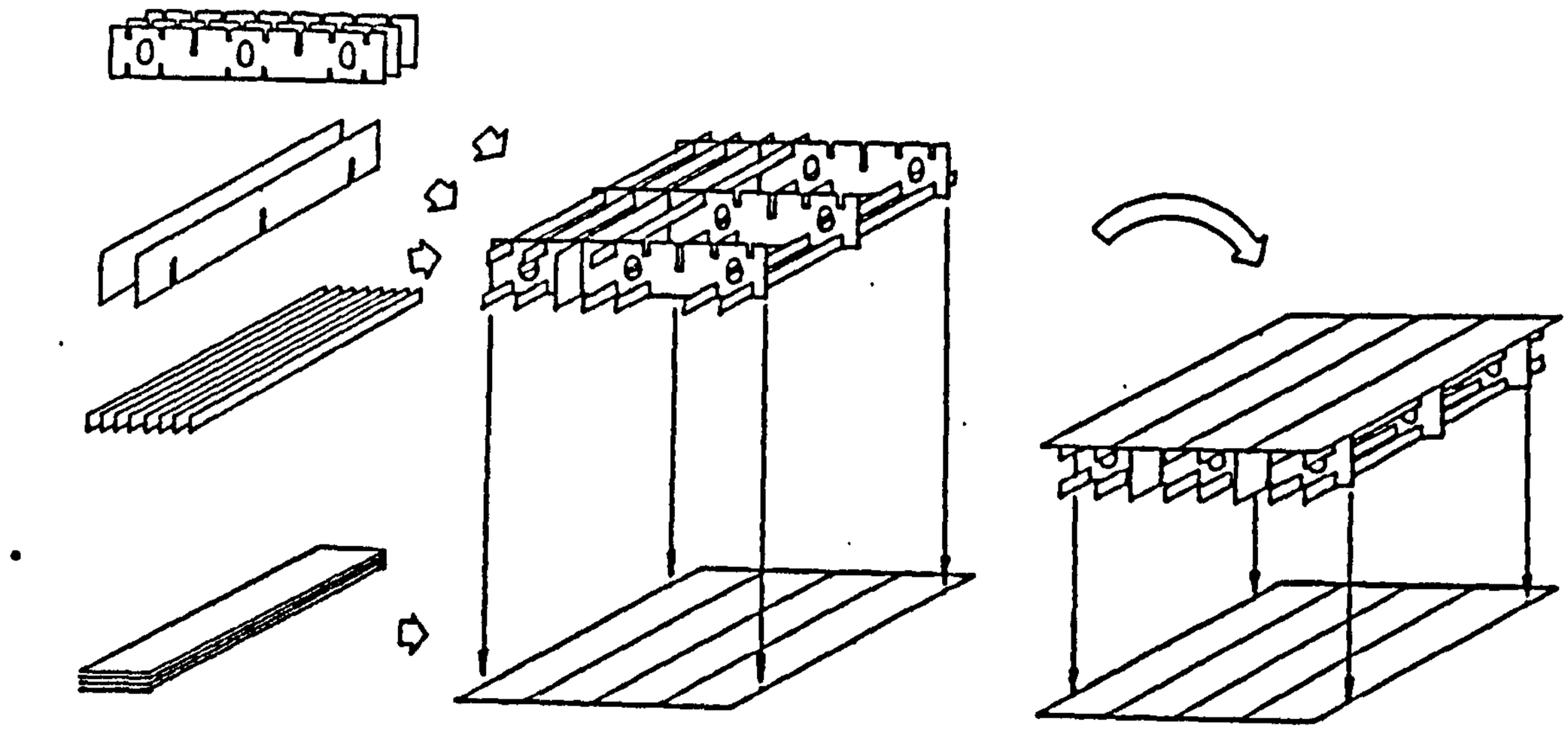

Figure 7.21 - Advanced method of assembling a matrix panel

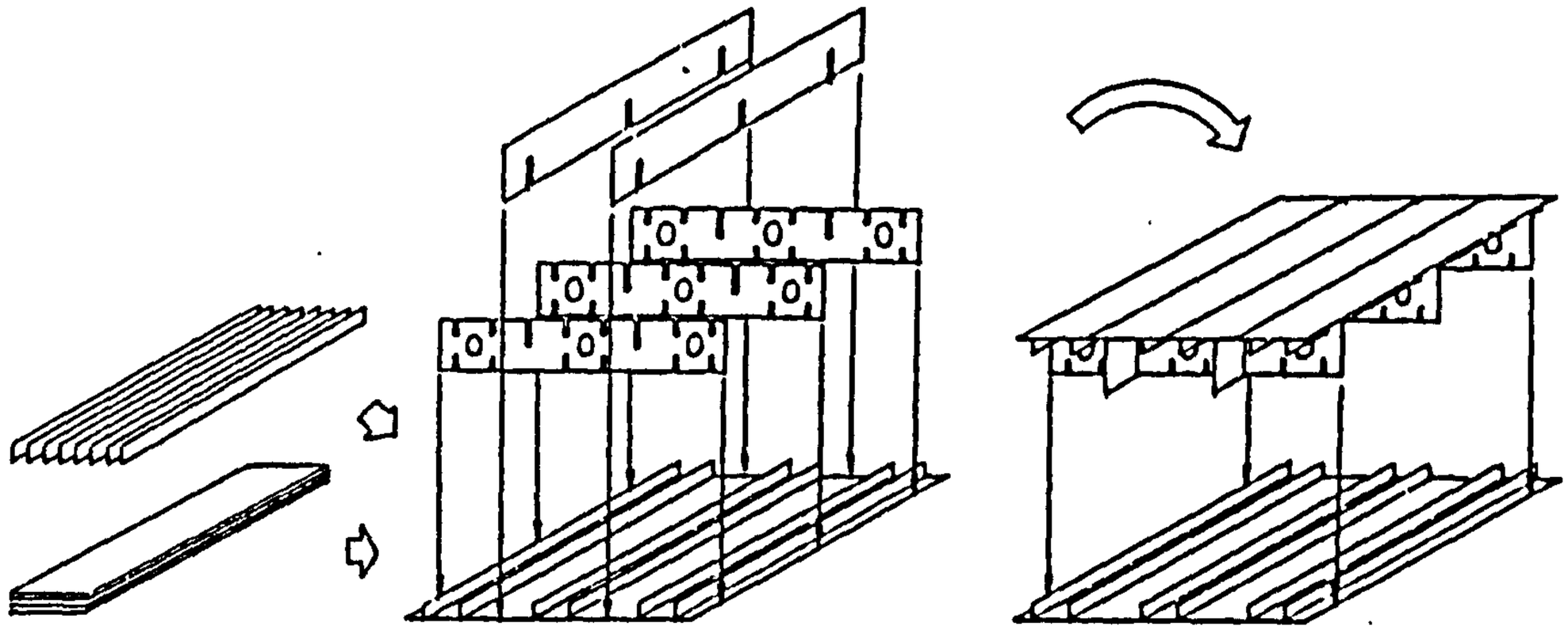

Figure 7.22 - Traditional method of assembling a matrix panel

on the first and the matrix is closed by joining the second stiffened panel, figure 7.22.

An example of such a line, figure 7.23, designed to produce a matrix by the later method has been sythesised in table 7.01 using typical production times as provided by shipyard based welding engineers and conventional welding statistical data [175] [223] . In order to optimise utilisation, the line has been "balanced" so that parts move between workstations at a regular time beat or "tact time" [227] of 5.5 hours.

The facility is designed to be capable of producing over 340 matrix assemblies per annum, a capacity which would be expected from the design philosophy of modern UK shipyards [226] . With a typical matrix assembly weight of 30 tonnes, this represents a yearly throughput of 10,470 tonnes of steel. As an alternative the line could also be fully utilised by a product mix of matrix and stiffened flat panel assemblies, the tact time for the panels being half that of the matrix assemblies. A laser-based matrix line was then designed to have the same output capacity as the conventional line but employing skid welding workstations. The synthesis of the laser line, figure 7.24, is shown in table 7.02.

For the conventional line, automated welding has been restricted to butt welding, employing a single sided SAW machine to combine plate clamping and welding, and the use of the particularly efficient gravity welding boom system for the welding of primary longitudinal stiffeners. However this precludes the fitting of any deep girders at this stage.

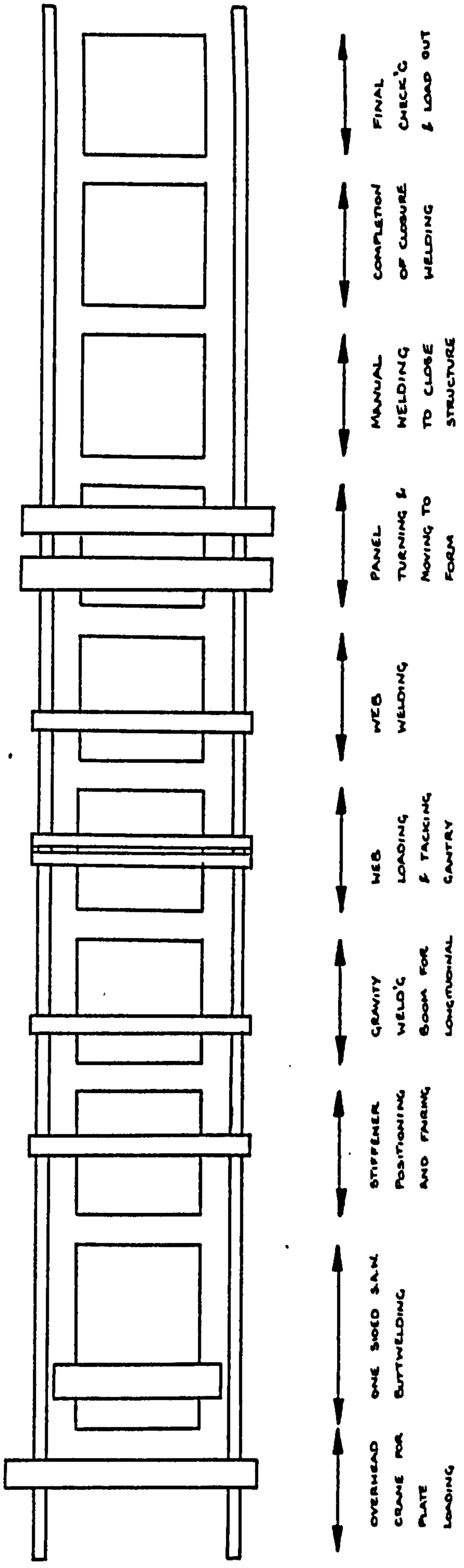

Figure 7.23 - Conventional matrix panel assembly flow line

Work St'n	Operation	Men	Ops. time (mins)	Tact time (mins)
1	1. Infeed and align plates		30	
	2. Align seams to gantry and apply backing strips.	2	20	130
	3. Attach run on/off plates		20	(x2)
	4. One side weld seams (0.4m/min)		50	
	Move panel forward		10	
2	1. Mark positions of stiffeners & webs	2	55	137
	2. Load and tack weld primary longitud'ls		72	(x2)
	Move panel forward		10	
3	1. Align gantry welding boom to each stiffener and weld (6x12min)	2	72	82
	Move panel forward		10	
4	1. Position and tack deep girders on first panel		36	
	2. Weld deep girders (0.4m/min arc time)	4	120	316
	3. Tack webs		36	
	4. Part fully weld webs		114	
	Move panel forward		10	
5	1. Complete web welding		126	
	2. Fillet weld longitudinal junctions and closing plates	4	26	
	3. Fillet weld junctions of deep sections		144	
	Move panel to turn		10	326
6	1. Turn panel; position on base panel in workstation 7	2	20	
	Move panel forward		10	
7	1. Assemble ventilation and lighting		60	330
	2. Part welding of longitudinals, girders and webs to base panel (0.4m/min)	4	260	
	Move matrix forward		10	
8	1. Complete welding of logitudinals, girders and webs to base panel.	4	260	330
	2. Dismantle ventilation, temporary lighting		60	
	Move matrix forward			

Table 7.01 - Synthesis of a conventional matrix panel line

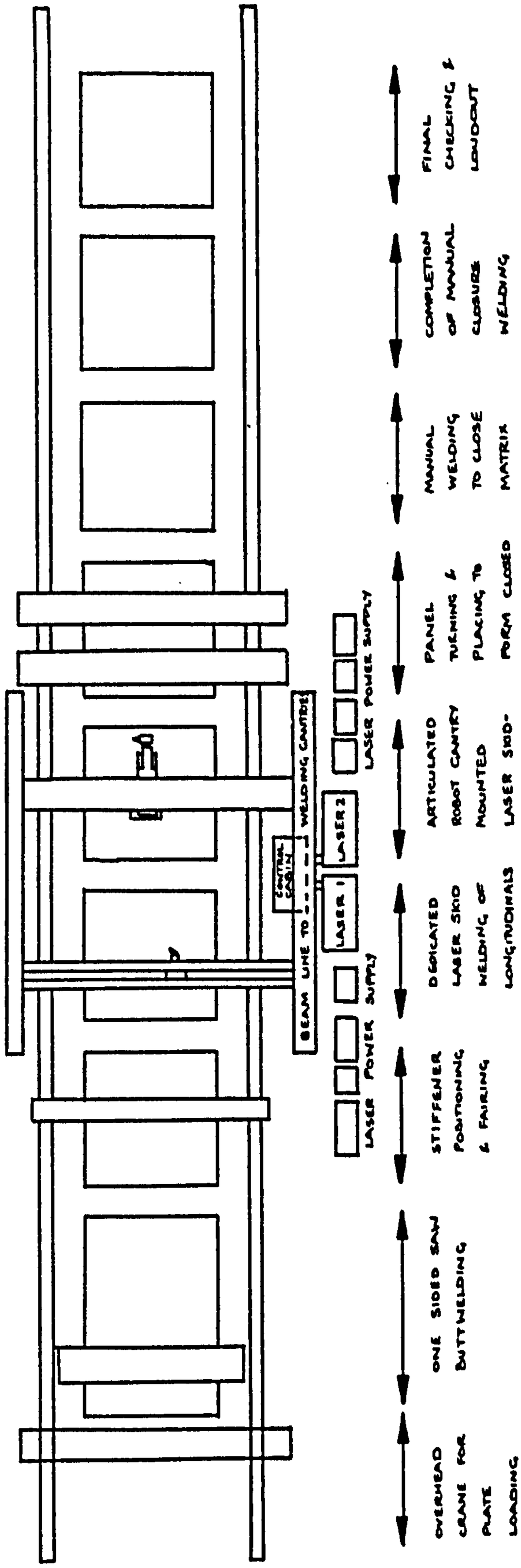

Figure 7.24 - Proposed flow line for a matrix panel line incorporating laser skid welding

Work St'n	Operation	Men	Ops. time (mins)	Tact time (mins)
1	1. Infeed and align plates		30	
	2. Align seams to gantry and apply backing strips.	2	20	130
	3. Attach run on/off plates		20	(x2)
	4. One side weld seams (0.4m/min)		50	
	Move panel forward		10	
2	1. Mark positions of stiffeners & webs	2	55	
	2. a) Mount and tack longitudinals and girders (Top panel)		a)96	a)161 b)137
	b) Mount and tack longitudinals (Base panel)		b)72	
	Move panel forward		10	
3	1. Skid weld of longitudinals	1	144	
	2. Reposition between stiffeners(8x2min)		16	180
	Move panel forward		10	
4	1. Skid weld deep girders (b)		48	
	2. Reposition between girder welds		4	
	3. Position and tack deep webs		36	
	4. Skid weld deep webs (0.5m/min laser time)		96	
	5. Skid weld junctions of webs and girders	1	58	297
	6. Skid weld webs to longitudinals		15	
	Move panel to turn		10	
6	1. Turn panel; position on base panel in workstation 7	2	20	
	Move panel forward		10	
7	1. Assemble ventilation and lighting		60	
	2. Part welding of longitudinals, girders and webs to base panel (0.4m/min)	4	260	330
	Move matrix forward		10	
8	1. Complete welding of logitudinals, girders and webs to base panel.	4	260	330
	2. Dismantle ventilation and temporary lighting, move matrix forward		70	330

Table 7.02 - Synthesis of a matrix panel line incorporating laser skid welding

All the deep sections are mounted tacked and manually welded using semi-automatic MIG units.

In contrast for the laser line all longitudinals (both primary stiffeners and deep girders) may be mounted, tacked and then skid welded together as the single sided process is not restricted by the depth of the deep girders as was the case when using the gravity welding boom. Once deep webs have been mounted and tacked, so segmenting the structure, the multiaxis laser skid welding head enables fast traverses of operation between each box section so increasing overall equipment utilisation.

After inversion of this partially completed matrix on to the bottom stiffened panel, conventional means have been employed for final matrix join-up. However, alternative means are available but at present are not being exploited. These could include the laser "through" welding, the use of a remote robotic device as proposed by Love [228] or the use of a specialised column and boom delivery device which may be inserted into the matrix sections through lightening holes to transmit a laser beam to an end-effect welding head within each double bottom chamber.

Application of the laser based tee welding has enabled the number of workstations to be reduced by one due to the higher processing speed, adaptability and multi-orientation capacity of the skid welding robotic head. By utilising numerical control and automated seam tracking line manning is also reduced from 24 to 16 persons.

Two 10kW lasers of the type used for the experimental trials are employed, both being interchangeable to each workstation, enabling utilisations of 75%, figure 7.25.

Costings for each matrix line are presented in table 7.03 and 7.04. Cost of the laser based line is dominated by the relative high cost of each laser (£575,000) and the multiaxis delivery systems. Costings of standard steel transport systems were obtained from shipyard consultants [229] [230] . Costs of multi-axis manipulators and beam delivery systems were based on data from laser and robotic system manufacturers [231] [232] . As a result of the laser based equipment, the laser line is 68% more expensive than the conventional line.

The Author would expect that such a high difference can only reduce as present prices of lasers and associated equipment for laser power ratings above 5kW are comparatively high because of development costs, low volume sales and as a result, few competing manufacturers. Table E7.03 (Appendix E-4) shows typical prices of production lasers of greater than 5kW output power for companies which responded to a survey initiated by the author. The way in which prices appear to be falling is shown in the example of one particular manufacturer for who, during late 1985 was quoting a price for a CL10 laser as £800,000. By mid-1986 the price had dropped to £650,000 and in late October 1986 the price dropped again to £575,000, this later price representing a cost per watt of power output of £65.

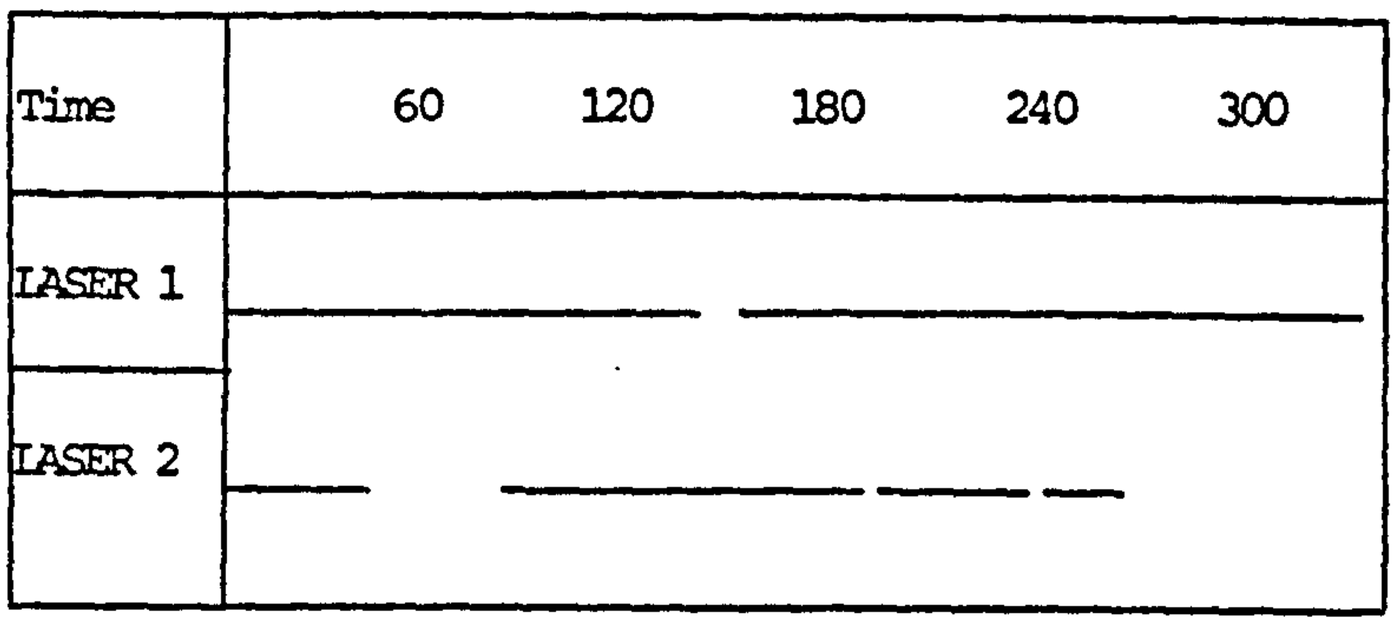

Figure 7.25 - Laser on times for the example matrix line; utilisation in total= 75%

Work St'n	Equipment details	Estimated cost 1986 (k&)
1	a) O/H crane for plate loading (15 tonne)	90
	b) Conveyor and rollers (35 tonnex12m)	35
	c) Magnetic clamping bed	40
	d) Positioning cam rollers	5
	e) One sided SAW gantry system	200
2	a) Conveyor and rollers (40 tonne x 12m)	40
	b) Panal alignment system.	50
	c) Stiffener fairing gantry	160
	d) Stiffener pallet and crane (55t x 12m)	90
	e) 2 MIG welding sets for tacking	10
3	a) Conveyor and rollers (55 tonne)	40
	b) Gantry and gravity welding boom	120
4	a) Conveyor and rollers (60 tonne x 12m)	45
	b) Deep girder and web mounting crane (share stn. 2)	-
	c) 4 MIG welding sets	20
	d) Fairing jigs	5
	e) Mobile welding sets	70
5	a) Conveyor and rollers (60 tonne x 12m)	45
	b) Mobile welding gantry	70
	c) 4 MIG welding sets	20
6	a) Conveyor and rollers (60 tonne x 12m)	45
	b) Panel turning cranes (2 x 45 tonnes)	200
7	a) Conveyor and rollers	45
	b) 4 MIG welding sets	20
	c) Ventillation and lighting systems	15
8	b) 4 MIG welding sets	20
	c) Ventillation and lighting sysytems	15
9	a) Loading-out jacking systems	200
	b) 2 MIG welding sets	10
	Capital equipment total	1770
	Installation and setting to work costs	177
	Building to cover 96 x 25m (&350/m2)	945
	Total cost for the facility	2892

Table 7.03 - Estimate of facility costs for a conventional matrix assembly line

Work St'n	Equipment details	Estimated cost,1986(k&)
1	a) O/H crane for plate loading (15 tonne)	90
	b) Conveyor and rollers (35 tonnex12m)	35
	c) Magnetic clamping bed & positioning rollers	45
	d) One sided S.A.W. gantry system	200
2	a) Conveyor and rollers (55 tonne) & alignment system	90
	b) Stiffener fairing gantry	160
	c) Stiffener pallet and crane (15t x 12m)	90
	d) 2 MIG welding sets	10
3	a) Conveyor and rollers (55 tonne)	40
	b) Gantry with dedicated cartesian skid welding manipulator for continuous skid welding.	250
	c) Seam tracking and gap sensing device	30
4	a) Conveyor and rollers (60 tonne x 12m)	45
	b) Web loading crane - share station 2	-
	c) 2 MIG welding sets & fairing jigs	15
	d) Gantry with multi-axis articulated beam manipulator	395
	e) Seam tracking and gap sensing device	30
5	a) Conveyor and rollers (60 tonne x 12m)	45
	b) Panel turning cranes (2 x 45 tonnes)	200
6	a) Conveyor and rollers	45
	b) 4 MIG welding sets	20
	c) Ventillation and lighting systems	15
7	a) Conveyor and rollers	45
	b) 4 MIG welding sets, ventillation and lighting.	35
8	a) Loading-out jacking systems	200
	b) 2 MIG welding sets	10
	a) 2 x 10kW lasers (&575,000 each)	1150
	b) Beam-line ducting, mirrors, servo mirror drives.	225
	c) Safety zone monitoring systems	60
	d) Systems diagnostics and monitoring	90
	Capital equipment total	3665
	Installation and setting to work costs	367
	Building to cover 96 x 25m (&350/m2)	840
	Total cost for the facility	4872

Table 7.04 - Estimates of facility costs for a laser based matrix assembly line

In a similar way, the same manufacturer is at present marketing a 5kW transverse flow laser for £350,000 and at the same time is selling a newly production-engineered modular type fast axial flow laser providing 5kW (TEM01*) or 6kW multimode for £200,000. This provides a pricing basis of £25 per Watt. Whilst each individual unit will have its own advantages, whether it be reliability or beam mode, clearly the trend is to higher levels of production engineering to produce reliable and more cost effective units.

On the basis of such examples, and while being cautious of the actual details of the eventual laser generating path, it would appear that by basing a prediction of future pricing regimes on the lowest "cost per Watt" figure would result in a 20kW laser power output for £600,000, thus halving the present cost.

In comparison to the high total line cost, savings, not only direct savings associated with the assembly line, but also those accruing as a consequence of using the low heat input laser process, must be examined to enable an overall comparison.

By comparison with the preliminary costings presented in the previous section, table 7.05 shows the cost of running the matrix lines per annum. As predicted, the final cost differences are very sensitive to the reduction in manning levels on the laser line to counteract the initial high capital related costs. The figures showed a direct savings on running cost for the laser system compared with the conventional line.

Consumable and operational costs	Conventional	Laser
1. Laser skid welding per unit (210m)	-	151
2. SAW butt welds (36m/36m)	25	25
3. MIG web fillet closing welds(96m/96m)	19	19
4. MIG fillet welds (180m)	35	-
5. Gravity welds (228m)	31	-
Total cost per unit	110	195
Total operational and consumable cost per year	38390	68055
Labour cost (24/16 persons)	451584	301056
Maintenance (1% capital)	28920	48720
Overall operational costs	518894	417831
Overall operational savings		101063

Table 7.05 - Operational costs of conventional and laser based matrix assembly lines

In order to ensure that no double accounting took place the "Discounted Cash Flow" calculations were made solely on the basis of the overall "consequential" savings which would be necessary for the laser system to be viable.

In addition to the direct influences on cost comparisons within the line, direct and "consequential" savings within the ship production facility may be listed as follows:

1. Reduction in edge preparation. The consistent requirement for square edge butting joints for the laser processing without the need for edge preparations to be either cut or machined on to plates for conventional processes.
2. Reduction in the requirement for quality control assessment as on-line quality control becomes accepted and parameter data bases become recognised as quality datums by classification societies.
3. Distortion is reduced to a level that may be considered negligible for built-up tolerances. Comparisons of distortion as measured by the Author, figure 7.26, for both laser skid and twin fillet MIG welds is shown in figure 7.27. Therefore post-weld fairing and rectification work may be eradicated. Also, with the minimised and controllable heat input, calculation of panel shrinkage will be made more reliable so providing more accurate and reliable data for statistical accuracy control methods.
4. Weight saving - reduction in welding wire consumables will result in a marginal reduction in steel mass therefore increasing the carrying capacity for a particular vessel design.

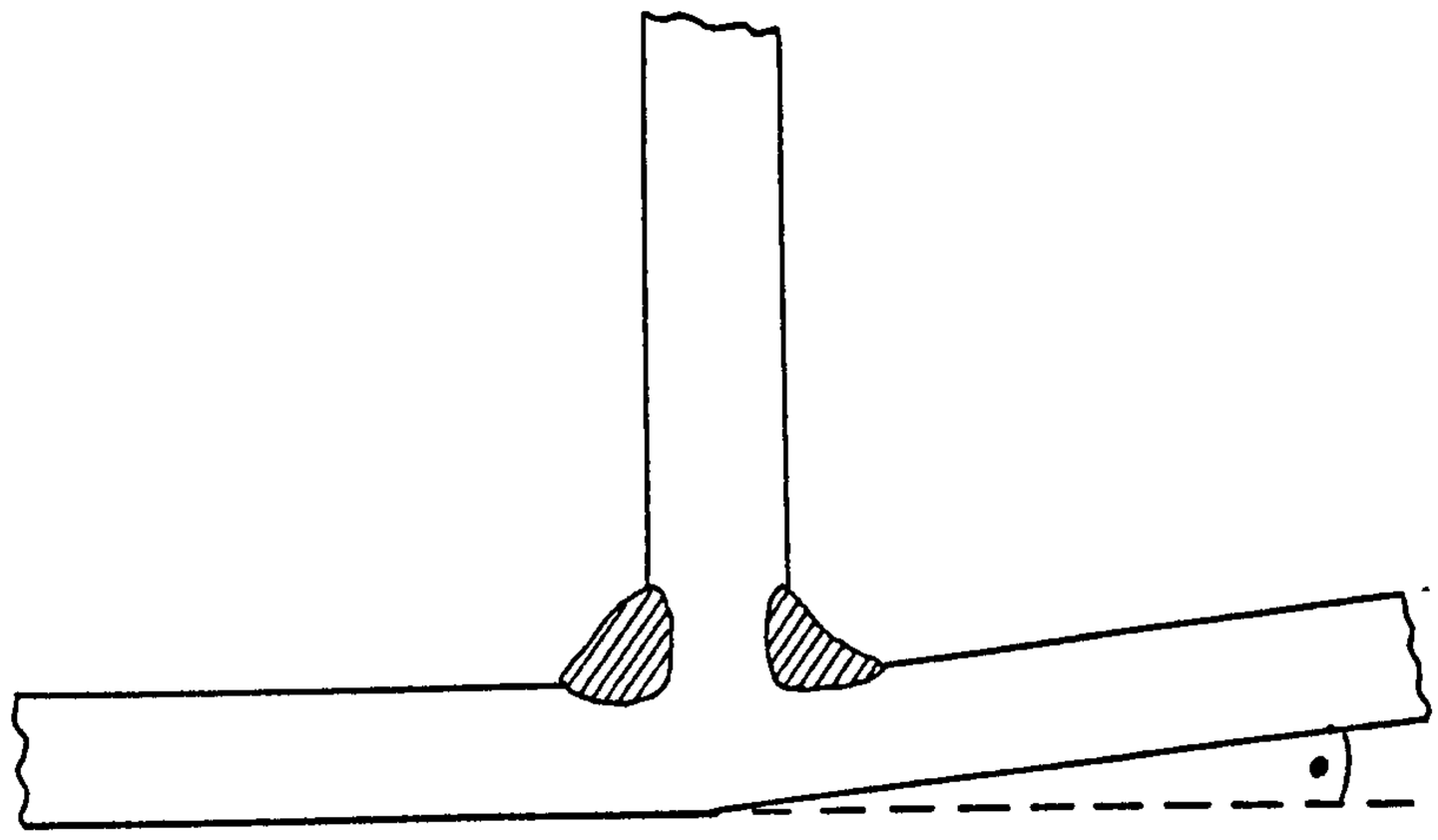

Figure 7.26 - Included angle distortion of welded tee joints

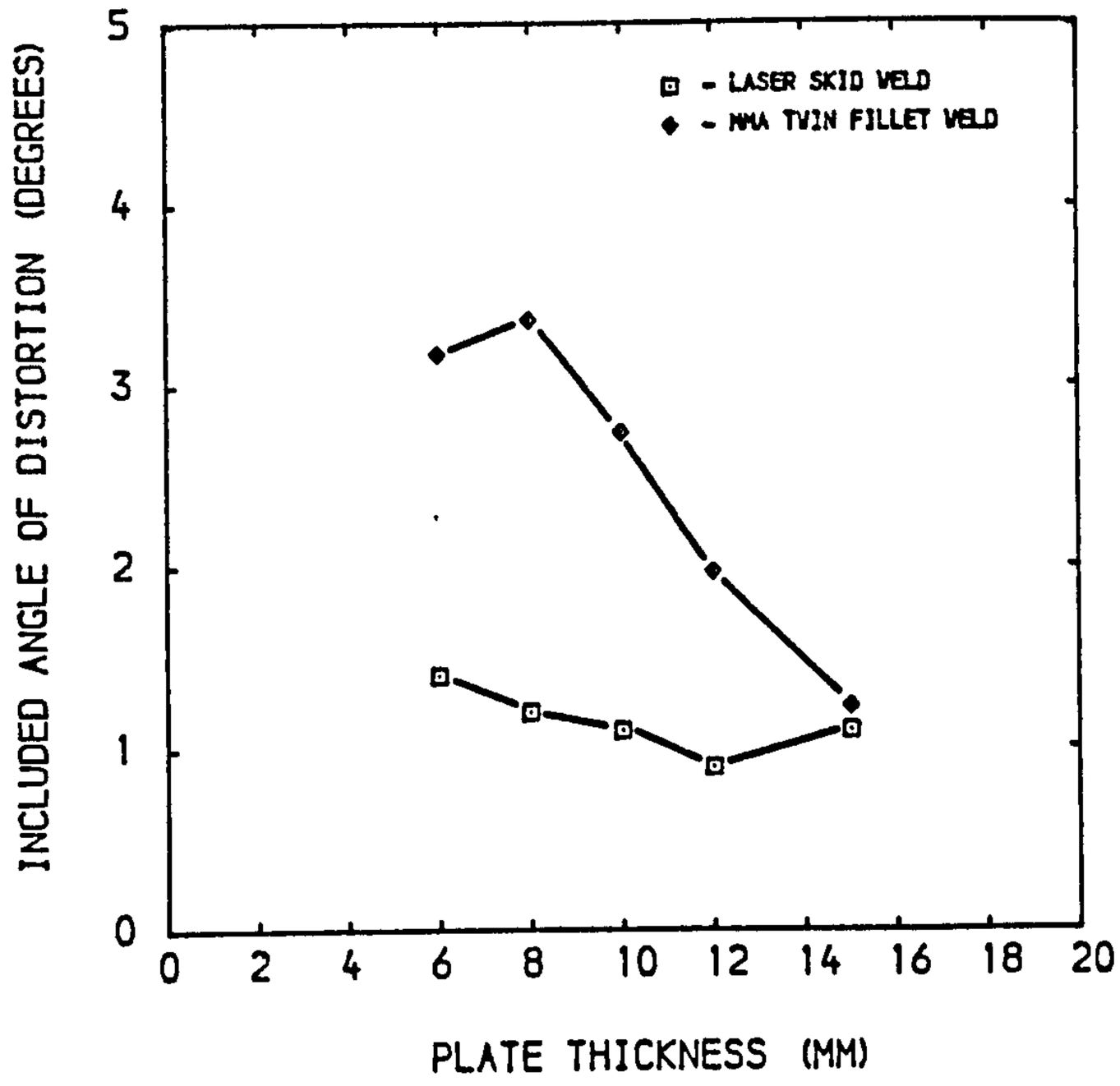

Figure 7.27 - Comparison of included angles of distortion measured for laser skid and MMA fillet welds in unconstrained joints

5. Production of joints where conventionally small fillets may not be easily obtainable. Shipyards building light scantling vessels find great difficulty in ensuring fillet leg sizes are kept to about half the plate thickness when this reduces below 8mm.
6. Increased material savings with reduced rework or scrapping.
7. Increased ability to plan and schedule work with the provision of more accurate manufacturing times and hence a reduced inventory requirement.
8. Further labour savings from the ability to communicate with other direct numerically controlled machines working further to Computer Integrated Manufacturing (CIM) systems.
9. Enhanced company image as users of new technology and up to date equipment but also by providing a better quality and consistency of product.
10. Increased safety of employees and consequential improvement in the quality of working life.
11. Increased technological development of employees and the potential enthusiasm which this can bring.

Together, these individual savings are very difficult to quantify by any global parameter. Probably the most recognised shipbuilding scale of costing and production related efficiency is "man-hours per tonne". That is, for steel, the average man-hours associated with processing each tonne of steel through a datum location eg steelshop or berth. Work content tends to vary inversely to component weight, but as a large variance is sometimes found when comparing production data [233] ,

concern is often shown when using the unit as an indicator of work content. However, because of the low reliability of the manhour figures actually kept for past contracts within most UK shipyards, it still remains the most accessible parameter for comparative studies.

Using this basis and relating savings only to the steel throughput associated with the matrix line, a scale of savings has been quantified, table 7.06:

By relating the above savings to the extra cost of the laser system, both for the present quotation of laser price and the authors prediction of future pricing trends, discounted cash flow calculations have been conducted. The calculations have been made in accordance with British Shipbuilders present accounting procedures.

Depreciation for tax purposes has been taken to be 25% of the outstanding balance of the capital expenditure and a tax rate of 35% has been applied. It has been assumed that tax is remitted in the year following that in which it was incurred

Curves of net present value when discounted at 15% for varying manhours per tonne savings is shown in figure 7.28. The basis of the calculations is shown for 5 manhours per tonne savings in table E7.04, Appendix E-5. This shows that for the present laser costs a return of 15% is realised for savings of greater than 4.3 manhours per tonne and for the projected costs this figure could be reduced to as small as 2.5

Productivity Improvement (Man-hours per tonne)	Annual Savings (Labour rate 9.80 &/hr)
2.0	205,800
4.0	411,600
6.0	617,400
8.0	823,200
10.0	1,029,000

Table 7.06 - Savings accruing to manhours/tonne savings for steelwork processing

Steelwork assembly zone	Shop	Berth	Total
Manhours per tonne (General cargo)	30	40	70

Table 7.07 - Manhours/tonne ratings for general cargo vessel steelwork manufacture

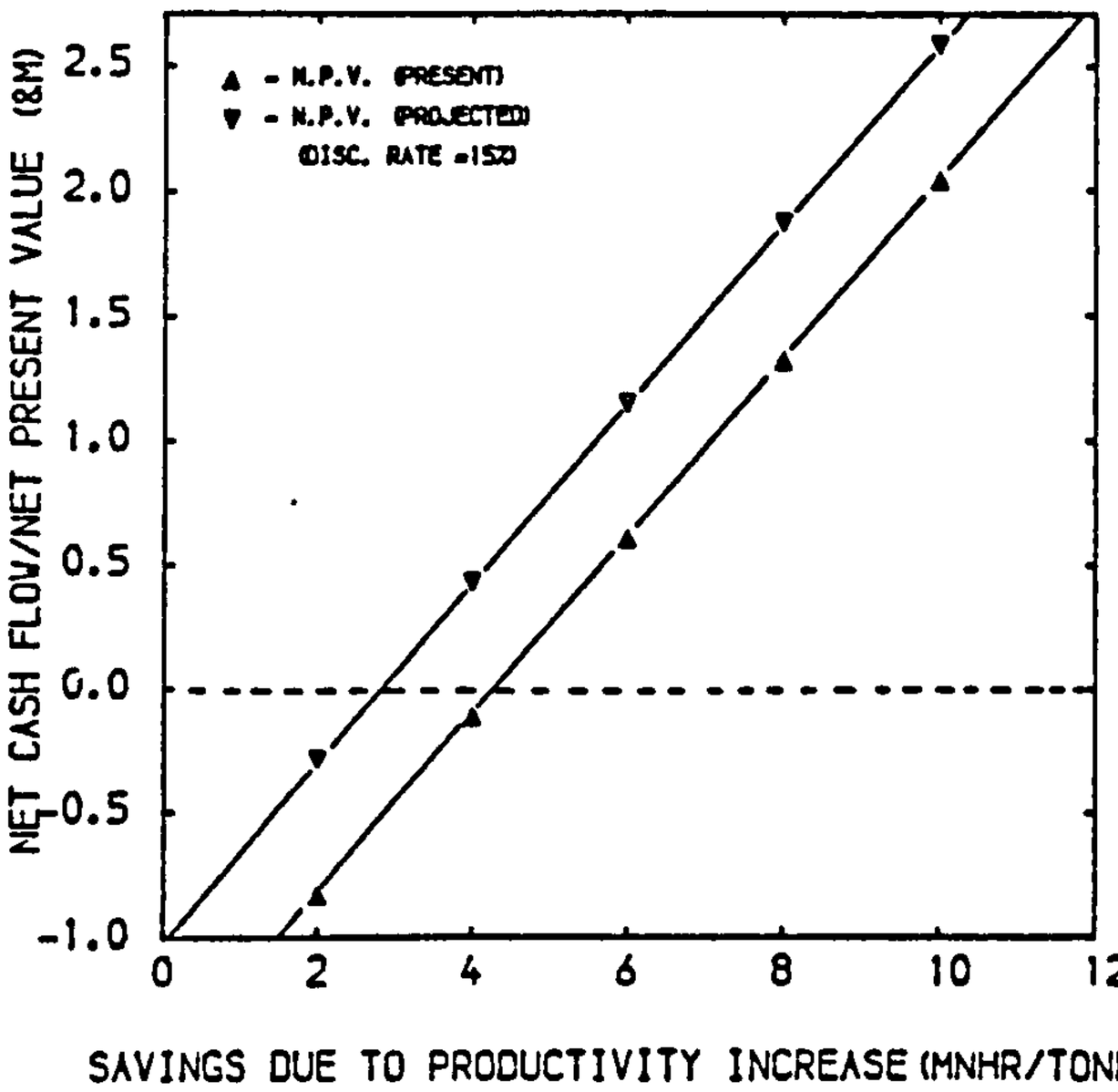

Figure 7.28 - N.P.V. for various levels of productivity savings when using a laser based matrix assembly line

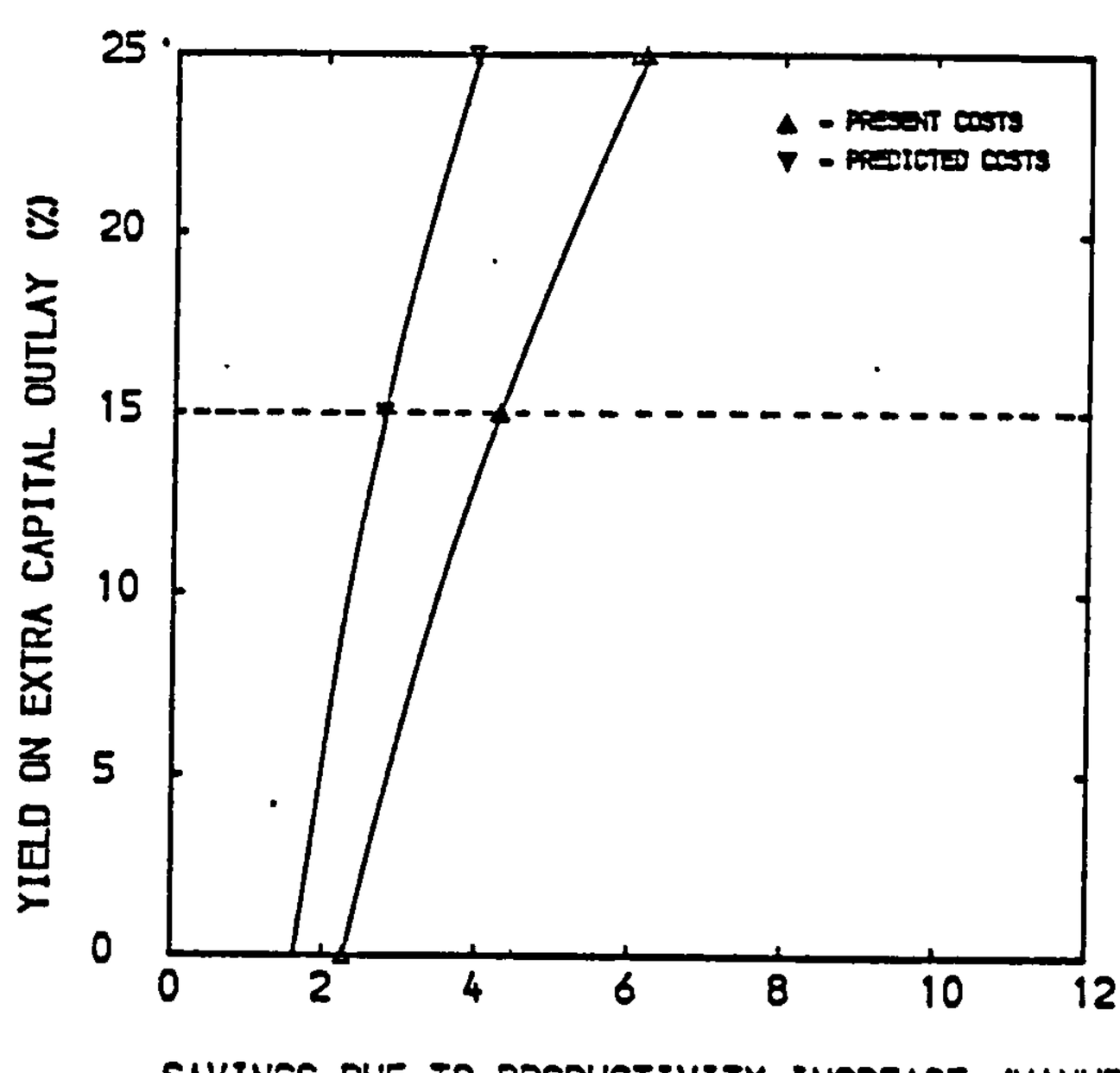

Figure 7.29 - Cost analysis of a laser matrix line; yield on extra capital as a result of increased productivity

manhours per tonne. From a series of such calculations figure 7.29 has been produced to show the yield on the extra capital for various consequential savings.

Example man-hours per tonne figures for steel shops and at the berth averaged from a number of British shipyards for the production of general cargo merchant vessels of scantlings typical to those used for the example matrix is shown in table 7.07.

With an average manhours per tonne of 40 at the berth the savings of 4.3 and 2.5 represents actual savings of 11% or 6% respectively over existing conventional practices. These seem to represent attainable results.

7.4.3 Synthesis and economic evaluation of a minor assembly line

In contrast to the capital intensive matrix line, the second case study was directed at a more labour intensive line producing minor assemblies [234] . In addition, a contrast is made by considering structures and plate thickness associated with the present prime product range to be found in UK merchant shipyards at present, that of light scantling ferries. The range of minor assemblies to be incorporated into a typical light weight ferry, 1500 tonne steel weight, was examined and specific groups of assemblies identified and quantified as shown in figure 7.30

1. FLOOR ASSEMBLY

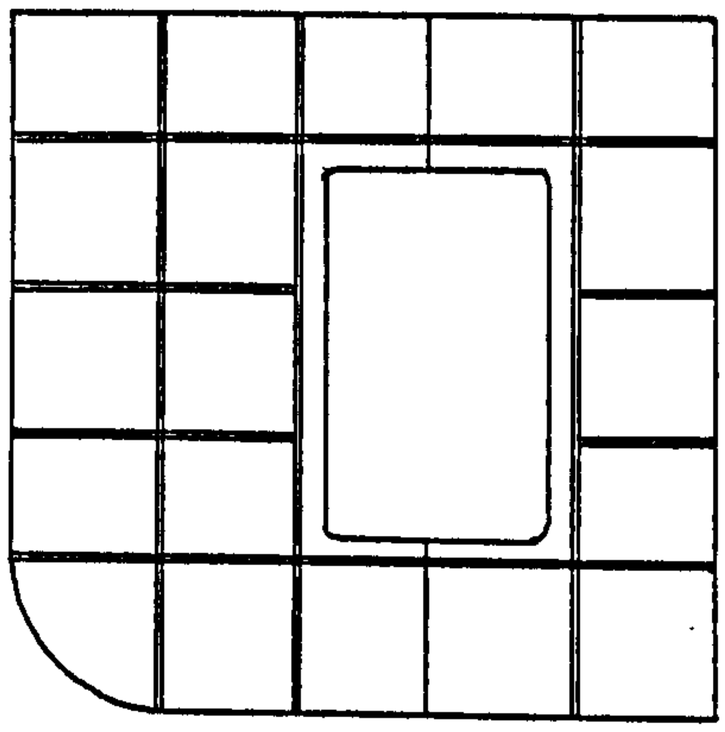

2. PANEL ASSEMBLY

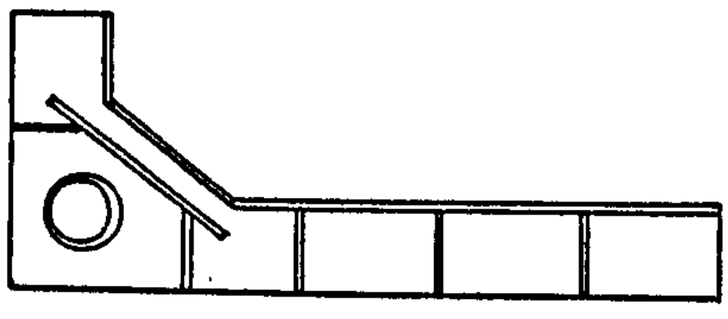

3. BRACKET ASSEMBLY

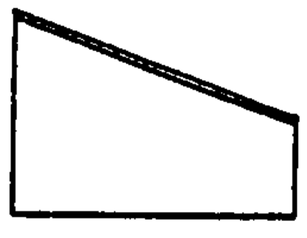

4. FLOOR ASSEMBLY

Figure 7.30 - Principal minor assembly structures identified within a design of lightweight ferries

To compare similar production philosophies, both laser and conventional methods were compared on a single flow line basis, figure 7.31a-b, with the respective functions at each workstation for each assembly being shown in table 7.08 and table 7.09. For each assembly type the lines have been balanced to provide a designed total batch time of 3.4 hours (a batch comprising; two units of type 1, one unit each of types 2 and 3 and four units of type 4). At 50 batches per vessel the line is designed for a throughput of 11.3 small ferries per annum. At 1500 tonne of steel weight for each ferry, total steelshop throughput of 17,000 tonne would be equivalent to that established over the past few years when between 5 and 6 standard design vessels (3,000 tonne steel weight) for which the shipyard was designed, were produced. With a minor assembly batch weight of 5 tonnes, this represents a line steel throughput of 2825 tonnes at a laser utilisation of 75%, figure 7.32.

Costs of the production facilities for each line are presented in table 7.10 and 7.11. As was the case for the matrix line, the additive cost of the laser and robotic related equipment dominates so that even with the extra workstation and cranage required in the conventional line, additive cost of the laser line is more than double the additive cost of the conventional line.

Running costs for the facilities are compared in Table 7.12 showing direct savings of £40,000 per annum. Relating consequential savings to manhours per tonne for the steel weight throughput of 2825 tonnes per annum in the line, potential savings have been calculated, table 7.13.

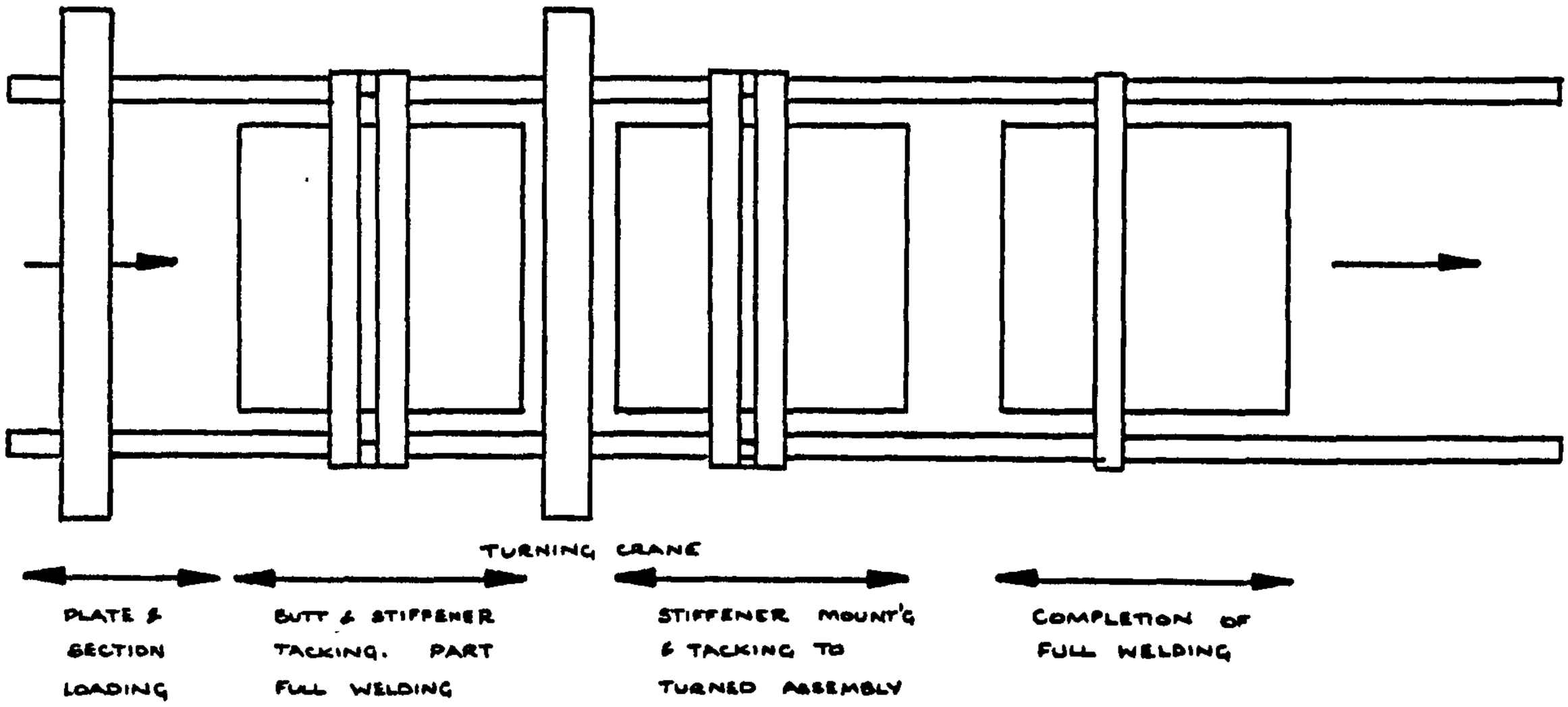

Figure 7.31a - Flow line for a minor assembly facility using conventional welding processes

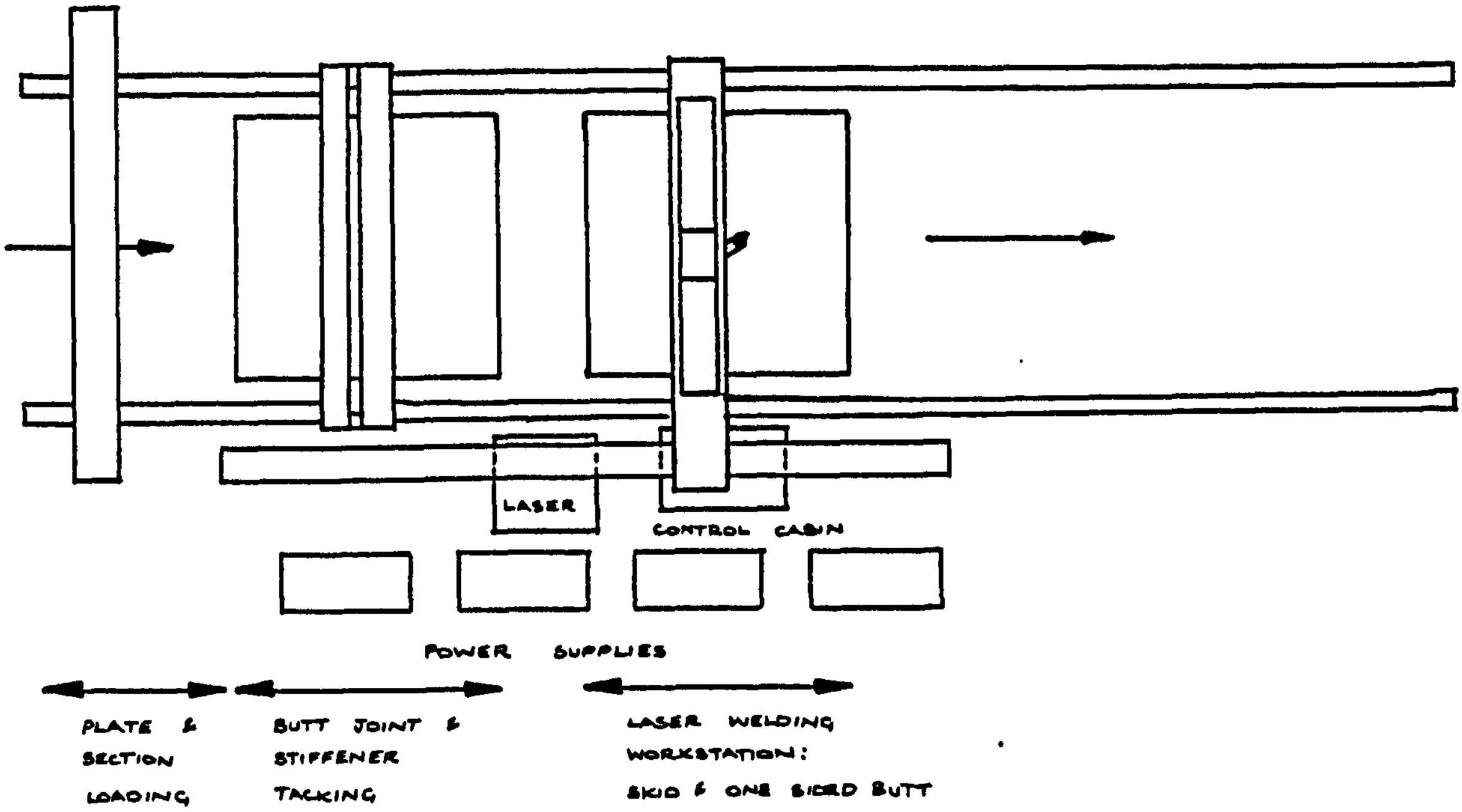

Figure 7.31b - Flow line for a minor assembly facility using laser skid welding

Ass'y type	Work St'n	Operation	Men	Ops. time (mins)	Tact time (mins)
1	1	1. Load plate to workstation		5	
		2. Mount and tack weld stiffeners	2	9	21
		Move tacked assembly forward and position		5	(x2)
	2	1. Skid weld stiffeners to plate (0.8m/min laser time)	1	14	21
		Move assembly forward		7	(x2)
2	1	1. Load plates to workstation	2	5	
		2. Position and tack weld butt joints		4	
		3. Position and tack weld stiffeners		48	64
		Move assembly forward and position		7	
	2	1. Laser weld butt joint (1.0m/min)	1	3	
		2. Skid weld stiffeners		80	90
		Move assembly forward		7	
3	1	1. Load plates to workstation		5	
		2. Position and tack stiffeners	2	6	
		3. Position and tack face plate		9	27
		Move assembly forward		7	
	2	1. Skid weld stiffeners and flats	1	25	32
		Move assembly forward		7	
4	1	1. Load plates to workstation		5	8
		2. Position and tack weld face plate	2	3	(x4)
		Move assembly forward		7	11
	2	2. Skid weld face flat (0.8m/min)	1	4	(x4)

Table 7.08 - Synthesis of an example laser line to produce minor assemblies

Ass'y type	Work St'n	Operation	Men	Ops. time (mins)	Tact time (mins)
1	1	1. Load plate to workstation		5	
		2. Mount and tack weld stiffeners	2	9	19
		Move tacked assembly forward		5	(x2)
	2	1. Fillet weld one side of stiffeners (0.8m/min arc time)	2	14	19
		Move assembly forward		5	(x2)
	3	1. Complete fillet welding of stiffeners	2	14	19
		Move assembly forward		5	(x2)
2	1	1. Load plates to workstation		5	
		2. Position and tack butt joint	2	4	
		3. Weld butt joint first side(0.8m/min)		13	
		4. Turn assembly		5	92
		5. Weld butt joint second side		13	
		6. Mount and tack stiffeners		48	
		Move tacked assembly forward		5	
	2	1. Fillet weld one side of stiffeners (0.8m/min)	4	80	85
		Move assembly forward		5	
	3	1. Complete fillet welding of stiffeners	4	80	85
		Move assembly forward		5	
3	1	1. Load plates to workstation	2	5	
		2. Tack face plates to plate(0.8m/min)		9	
		3. Fillet weld first side of face plates		15	29
		Turn and move assembly forward		10	
	2	1. Tack stiffeners to plate		6	
		2. Fillet weld second side of face plate	4	15	31
		Move assembly forward		5	
	3	1. Fillet weld stiffeners	4	20	25
4	1	1. Load plates to workstation	2	5	8
		2. Position and tackweld face plates		3	(x4)
		Move assembly forward		5	
	2	1. Fillet weld first side of face flat	2	6	11 (x4)
		Move assembly forward		5	
	3	1. Fillet weld second side of face flat	2	6	11 (x4)

MIN CON

Table 7.09 - Synthesis of a conventional line to produce minor assemblies

TIME (minutes)	0	60	120	180
LASER ON TIME	———	———	———	———

Figure 7.32 - Laser on times for the example minor assembly line for one batch; utilisation= 75%

Work St'n	Equipment details	Estimated cost 1986 (k&)
1	a) Plate and stiffener loading crane (15 tonne)	60
	b) Web mounting and tacking gantry	75
	c) 2xMIG welding sets and ventilation trunking	10
2	a) 10kW laser	575
	b) Gantry with multi axis dedicateed beam manipulator	305
	c) Beam line equipment, beam switching equipment	60
	d) System diagnostics and montioring	55
	e) Seam tracking and gap sensing device	30
	f) Safety zone monitoring and checking system	30
	Total capital costs	1200
	Installation and setting to work (+10%)	120
	Building costs to cover 20x20 sq. metres (&350/m2)	140
	Total cost of the installation	1460

Table 7.10 - Estimated costs for a laser based minor assembly line

Work St'n	Equipment details	Estimated cost 1986 (k&)
1	a) Plate and stiffener loading crane (15 tonne)	60
	b) Web mounting and tacking gantry	75
	c) 2xMIG welding sets and ventilation trunking	10
2	a) Web mounting and tacking gantry	75
	b) Assembly turning crane (15 tonne)	60
	c) 2xMIG welding sets and ventilation trunking	10
3	a) Mobile web welding gantry	55
	b) 2xMIG welding sets	10
	Total capital costs of equipment	355
	Installation costs and setting to work (+10%)	36
	Building to cover 30x20 metres (&350/m2)	210
	Total cost of installation	601

Table 7.11 -Estimated costs for a conventional minor assembly line

Consumable and operational costs	Conventional	Laser
1. Laser skid welds per assembly batch(67m)	-	23
2. Laser butt welds (2.5m)		1
3. MIG butt welds (5m)	2	-
4. MIG fillet welds (134m)	11	-
Total cost per assembly batch	13	24
Total operational and consumable cost per year	7345	13560
Labour cost (6/3 persons)	112896	56448
Maintenance (1% capital)	6010	14600
Overall operational costs	126251	84608
Overall operational savings		41643

Table 7.12 - Operational costs of a conventional and laser based minor assembly line

Productivity Improvement (Man-hours per tonne)	Annual Savings (Labour rate 9.80 &/hr)
2.0	55,370
4.0	110,740
6.0	166,110
8.0	221,480
10.0	276,850

Table 7.13 - Potential consequential savings as a function of manhours/tonne work improvement

Steelwork assembly zone	Shop	Berth	Total
Manhours per tonne (Light Warship)	120	140	260

Table 7.14 - Manhours/tonne ratings for light scantling warship steelwork construction

Using these figures as a basis for facility savings, discounted cash flow calculations have been conducted using the same accounting basis as for the matrix line. Net Present Values for a discounting rate of 15% are presented in figure 7.33 both for present and predicted laser costs. The basis of the calculations is shown in table E7.05, Appendix E-5. This shows that the laser system will be commercially viable with the realisation of consequential saving of 6.9 and 4.2 manhours per tonne respectively. Graphs of the yield on the extra capital expenditure for the laser line is shown in figure 7.34 for both situations.

Although the required improvements due to laser welding on the minor assembly line appear to be less in terms of manhours per tonne than the matrix line, a fair comparison may only be made on the improvement in overall productivity. No direct figures of manhours per tonne relating to lightweight ferry constructions were available. However, a comparison may be drawn to similar lightweight scantling structures used in warship construction, with the dominance of typically 8mm plate as used for the example. Manhours per tonne values were gained from warship builders, which, while influenced by the higher quality standards for MOD(N) vessels, when compared with the figures for merchant type scantlings, highlight the higher labour requirements to ensure quality products for the lighter scantlings as shown in figure 7.14.

Based on these figures a saving of 5% on todays laser prices and using predicted costings as little as 1% savings would be required at the berth in order for the laser facility to be cost effective. These seem to be

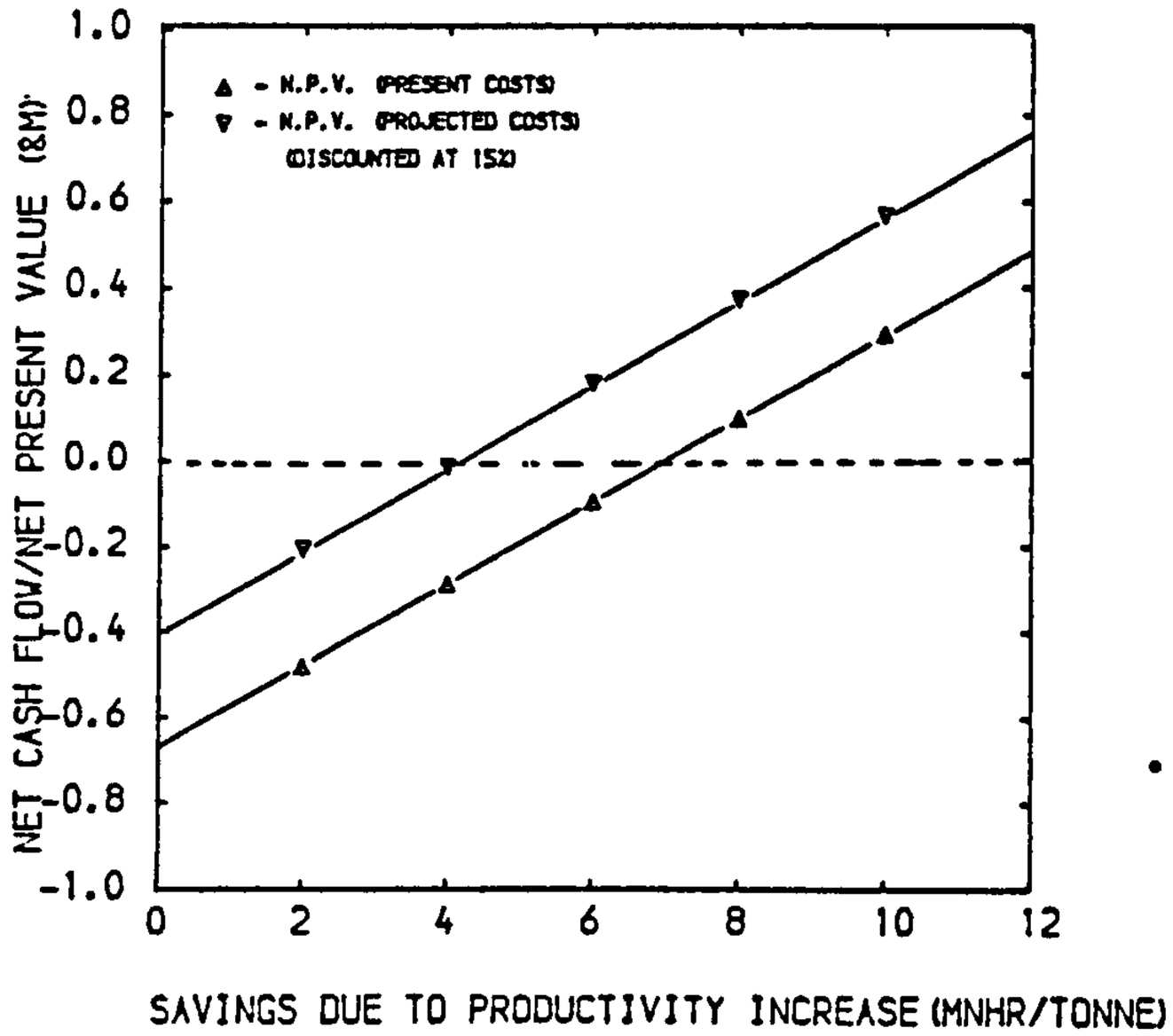

Figure 7.33 - N.P.V. for various productivity savings for a laser based minor assembly line

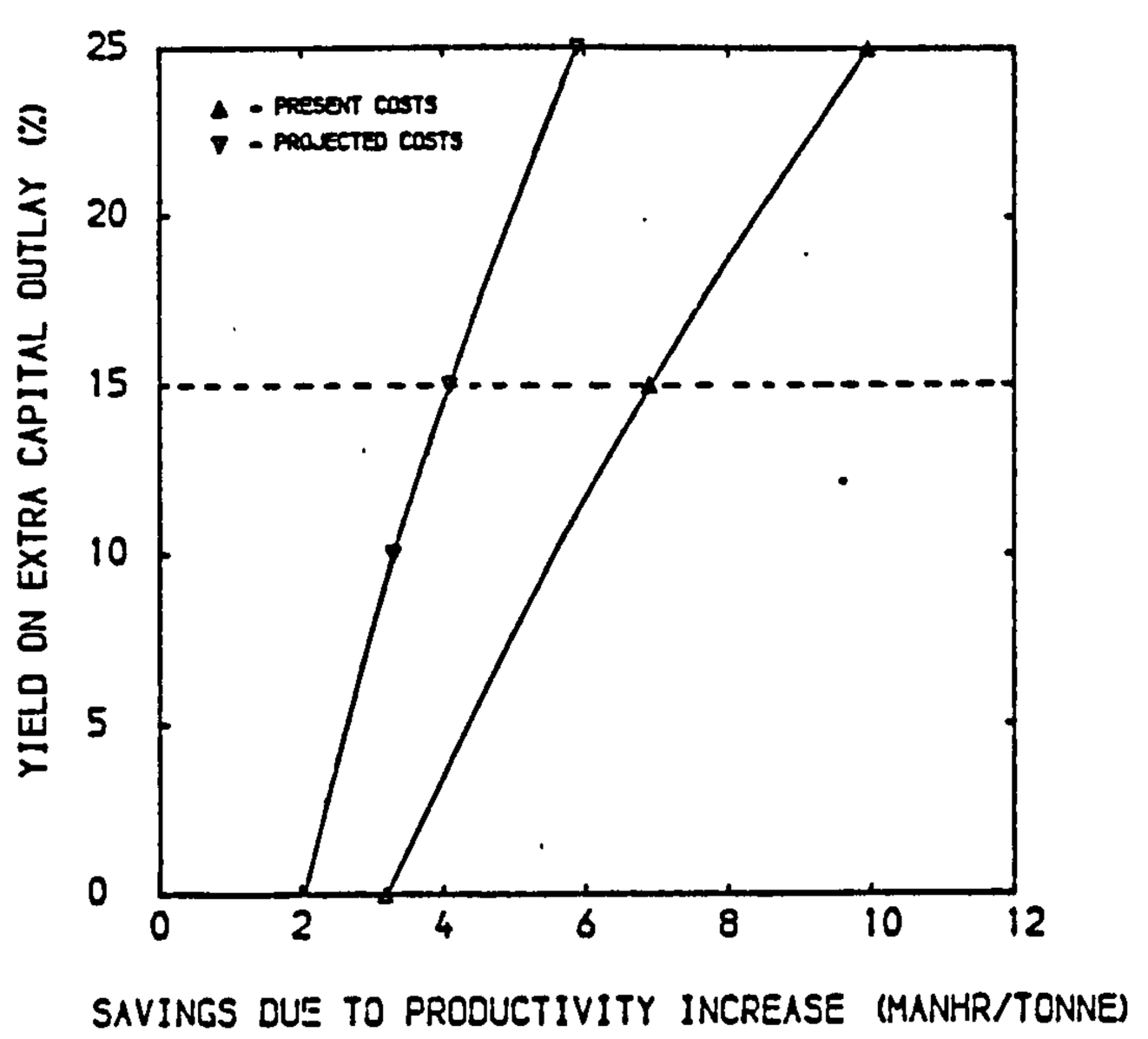

Figure 7.34 - Cost analysis for an example laser based minor assembly line; yield on extra capital as a result of increased productivity

very reasonably attainable

Comparison of the figures for both the heavier merchant scantling and lightweight scantlings shows the importance of examining the consequential savings of such a facility. The relative figures for productivity in terms of manhours per tonne show that the effect of lightweight structures results in a disproportionate increase in the manhours per tonne value. By comparing the figures for productivity, a 30% reduction in the plate thickness (12mm to 8mm) has resulted in a 350% decrease in productivity for conventional shipbuilding methods at the berth. Because of this, the potential savings of operating a system for lighter scantlings vessels using single laser welding techniques will have have much greater cost benefits.

CHAPTER EIGHT

SUMMARY, CONCLUSIONS AND RECOMMENDATIONS

8.1 SUMMARY

Few shipyard based authors or national shipbuilding institutions have examined the feasibility of laser welding, particularly tee section welding, to any great level of detail. Some evidence exists of the examination of double-sided tee section welding, but there are no reports of single-sided skid welding of tee section joints using filler wire for ship production.

An understanding of "point" and "line" heat source theory provided a basis to identify the primary processing variables in laser welding and an analogy to the dynamics of keyhole formation and associated heat flow patterns from a molten pool. The simplest form of laser welding could then be observed by the production of melt runs in a solid plate.

The presence of discontinuities e.g. joints, gaps, rough edges, plate mis-match, in practical joint configurations not only reduced the efficiency of the process but also made the inter-relationships of the variables required for precise modelling very complex.

A structured trials programme of experiments using a 10kW laser source was developed to examine the parameters needed to form visually and

structurally acceptable skid welded joints in plates of 3-15mm thick and to investigate process tolerances. A representative selection of shipyard stock plate, within the specifications of Lloyds Grade A and BS4360:43A, mild steel used in constructing surface vessel structures, was used in the experiments. Typical plate and edge preparations were used, both "as cut" and rolled section with variable pre-set gaps and surface preparations. A filler wire input provided both a means of laser beam interaction and of forming satisfactory bead profiles.

In excess of 30 prime processing variables were identified prior to the welding trials. Whilst this number was not exhaustive a set of priorities was selected to restrict the number of variable permutations to a manageable quantity. This enabled all the prime parameters of traverse speed; filler input; laser beam spot positioning and focus; and plasma control and shrouding to be investigated, although the number of permutations for each was naturally restricted.

Welding and classification rules as laid down by Lloyds Register of Shipping and the Ministry of Defence(Navy) were used as the initial basis of comparison of the joints produced. They normally provide few rules for fillet welded tee section joints compared with those for consumable material test pieces and butt joints. Having developed a fully penetrating joint with small smoothing beads instead of large fillets, an alternative set of test procedures was devised and then confirmed through discussions with the classification societies.

Tensile and toughness tests were made by producing cruciform samples, comparing the test results with the minimum requirements set for butt welded samples. Hardness traverses were made for each set of welds and compared not only with the normal upper value for conventional welds in mild steel of 350Hv, but also a revised upper limit of 400HV considered acceptable for the low hydrogen releasing laser skid welding process.

The author proposed the use of a revised version of the conventional fillet weld fracture test, the skid welded joint exhibiting great resistance to tearing through the weld.

A programme of fatigue tests was designed to satisfy any anxiety that the skid weld - a fully penetrating weld with smoothing beads - would be inferior to a twin fillet weld - non-penetrating with large external reinforcements - because of the proportionately small reinforcement.

A programme of metallurgical examinations was designed and conducted using the optical microscope; assessing grain growth and transformed microstructure to provide a link between the input welding parameters and the expected weld properties. In addition to categorising the welds by general views of micrographic sections, statistically-based grain size measurements and microstructural phase counting enabled quantitative judgements to be made of the expected skid weld material properties when compared with those of arc welded control samples.

Once satisfied that structurally sound skid welds could be produced on a repeatable basis, the Author examined in the final chapter some major considerations to be made when designing a shipyard based workstation. The requirements on, and the limitations of, the laser hardware, both presently available and being developed have been considered. This is in conjunction with a discussion of system monitoring, adaptive control and safety aspects, all an essential prerequisite to operating in a production environment. The economics of the system were then assessed to identify potential cost savings to be made by investing in a laser based skid welding facility.

8.2 CONCLUSIONS

The author has been able to compile the following conclusions from the work described:

1. Fully penetrating tee connections may be produced in thermally cut mild steel flat plate up to 15mm thick without gaps using a 9kW laser from a single side. Visually sound and balanced smoothing beads may be formed for joints of less than 10mm thick containing gaps of up to 2mm. For greater plate thickness the formation of emergent beads becomes less stable resulting in proportionately smaller and unbalanced bead profiles.
2. Skid welds may be produced using filler wire into tee section configurations assembled to typical ship production tolerances at up to 50% of the traverse speed used to gain the same penetration in a blind melt run.

3. Rolled section bars may be skid welded to a similar standard as square edge cut flat plate up to plates of 10mm thick. For greater thicknesses the increased volume of filler wire input necessary to compensate for the radiused edges, may fail to reach the emergent side of the joint resulting in unbalanced smoothing beads.

4. Iron epoxy shop primers on the joint surface caused disturbances within the welding process similar to those experienced with other semi-automatic welding processes and resulted in not only a large amount of sparks being ejected from the emergent side but also in high levels of porosity in the solidified weld. This was possibly a result of increased levels of combustion gas and weld pool viscosity. The effect may be reduced by slowing the traverse speed. Alternatively it may be eliminated by local grinding off of the primer or high speed laser etching.

5. In principle, wire feed rate may be equated to the volume of joint to be filled or reinforced. Unlike fully penetrating butt welds with no reinforcement the quantity calculated for skid welds should include a quantity to produce the smoothing beads. Their balanced sizes, particularly for the emergent bead, is dependent on keyhole penetration. This should be taken into account when using an on-line wire feed control. For rolled section joints the rate should also include a proportional volume in order to compensate for the plate edge radius sector.

6. To ensure balanced smoothing beads the wire is best positioned to interact with the laser beam in the centre of the joint. If the joint gap precludes this, the wire should be aimed to the leading

edge of the keyhole.

7. The angle of the incident beam to the face plate should be shallow enough to enable full penetration and complete fusion throughout the joint without either the focusing nozzle or the beam impinging on the plate prior to the joint line. While an angle of seven degrees may be adequate for plate thickness below 10mm a shallower angle would be preferred for greater thicknesses. The positioning of the beam interaction point above the face plate is critical to achieving the required bead profiles.

8. The mechanism by which the emergent beads are formed is dominated by heat flow from the keyhole through the molten pool formed at the emergent side and the formation of a keyhole "side-shoot" escaping through this pool. It is not formed by reflections of the beam inside the joint off the face plate surface.

9. A general flow of helium gas directed at the keyhole zone should provide a satisfactory level of plasma control. Therefore a plasma control device for multi-axis skid welding will not have to be constrained by the requirement for a directional jet as the joint shape appears to funnel the available gas across the beam interaction point.

10. Radiography of the skid weld only provides a good indication of the weld cleanliness when the web plate is cut off close to the weld. Ultrasonic testing using a narrow field probe provides a quick initial indication of intact weld quality.

11. Ultimate tensile strength of visually and ultrasonically tested sound joints should be greater than that for the parent plate. A good

estimate of the joint strength may be calculated based on the carbon equivalent of the parent plate.

12. When a steady sideways force is applied to a skid welded web plate, bending it parallel to the face plate, for visually sound joints the weld remained intact. By placing a notch in one of the smoothing beads failure either occurs through the line of principal stresses or through any line of flaws. The ductility of the weld is confirmed through this test which also provides an alternative to the conventional fillet fracture test.

13. Toughness values in excess of those required by classification societies have been achieved in skid welded joints. Toughness values may be improved further by careful choice of filler wire constituents to increase levels of tough acicular ferrite within the weld transformed microstructure.

14. Fatigue strengths of load carrying and non-load carrying laser skid welded stiffeners were established using 8mm thick plate and MMA twin fillet welded control samples. The fatigue strength of the non-loaded stiffener was marginally better than that of the arc welded joints. The loaded stiffener, having failed at the weld toe in the loaded stiffener, may be classed at a higher design rating than the inferior arc welds which, for equivalent sized fillets, failed from the weld throat. For a longitudinally stressed joint the laser weld, with a "smoother" weld profile surface is expected to have better fatigue performance when compared against the twin fillet joints.

15. Weld zone hardness will depend on the chemical composition of the

parent plate, filler wire, plate thickness and process heat input. For traverse speeds designed to produce visually balanced beads using 9kW laser power, material upper carbon levels may have to be restricted for plate of less than 10mm thick to maintain hardness levels below normal classification limits of 350Hv. However the Author considers that an upper limit of 400Hv is more appropriate for the skidwelding process, in which case the present material specification limits may be maintained.

16. A fine microstructural grain structure in laser skid welds may be expected, compared with arc welded twin fillet control samples. Columnar grains grow from the molten zone edges towards a zone of equiaxed grains along the joint centreline. With narrow zones of grain boundary ferrite and the potential for producing high levels of acicular ferrite there is every reason for the joint to be structurally superior to the conventional arc welds typically found in ship structures.

17. For the non-constrained joints tested, distortion levels, measured by included angular wrap-up, could be reduced by up to two thirds using the skid welding process compared with the MMA fillet welded control samples. While the author appreciates that as angular distortion will be less for joints constrained by surrounding structure, the secondary effects of reduced locked-in residual stresses should also reduce overall distortional effects.

18. To facilitate skid welding on a production basis will require adaptive control of the processing parameters to ensure consistent quality of product with minimal operator intervention. Monitoring of

the laser beam output, the workpiece and the on-going processing data will be necessary for input parameters to be controlled to the required tolerances.

19. Workstation hardware; lasers, beam delivery optics and lines and manipulative devices are at present under development for large multi-axis systems using in excess of 5kW laser power. Technically every indication is that a system suited to multi-axis processing on a large scale is both feasible and practical. An emphasis on encouraging value engineering, system reliability and high levels of utilisation from prototype workstations in the subsequent transition between development and production phases, should provide the potential for a high return to be made on invested capital.

20. Economic evaluations of skid welding laser systems are likely to be highly sensitive to the overall influence of processing at individual workstations on the total production cycle. Even though capital expenditure for laser-based equipment is at present high compared with conventional systems, direct labour savings and especially consequential savings are expected to provide a sufficiently high rate of return for a sound economic justification. As the availability of value engineered, laser based equipment increases the projected returns should increase proportionately.

21. Structurally and economically, for the 10kW laser power used in the present work, the process is ideally suited to the welding of ship plate to thicknesses of 10mm. This thickness range coincides with those where most production problems of gross distortion and rework occur conventionally and hence where levels of consequential savings

may be highest. The process is ideally suited to the welding of minor assemblies, sub assemblies and stiffened panels in the present light scantling product range of many UK shipbuilders.

8.3 RECOMMENDATIONS

1. Having proved both laser butt welding in previous authors' work and now laser skid welding in the present work, both structurally to classification societies and economically, the next stage, a development stage should necessitate establishing a prototype laser workstation within shipyard conditions. The following development projects would need to be considered:

   a. Process development encompassing all likely material, processes and configuration variables.

   b. Full procedural acceptance trials in the presence of classification societies, for the purpose of approval

   c. System development and acceptance to the shipyard environment.

   d. Production of trial assemblies for on-board ship acceptance trials.

   e. Research and development of further laser processing applications e.g cutting, heat-line bending, heat treatment.

   f. Development of structures designed to be optimised by the application of laser processing.

   g. Development of safety procedures for large scale laser systems.

2. While the thickness of joints produced in the present study has been

limited by the continuous power available from the power source being absorbed into the joint, single pass skid welding to greater thicknesses will require the development of higher powers of laser source and further research into the efficiency of laser/ keyhole interactions to run concurrently with research into multi-pass processing using contemporary powers.

3. Classification societies should consider making additions to their procedural requirements for the evaluation of tee section joints so that their rules may be appropriate to both twin fillet and skid weld type joints. Testing of existing consumables under typical cooling rates as estimated for laser welds would aid such a revision.
4. Development of a basis for on-line quality control whereby, through adaptive control of the process and the development of procedural data, weld quality (or the precise location of faults) may be defined from input parameters and control monitor surveys.
5. Tightening up the specification of plate composition, not only to ensure the control of hardness levels in laser welds that would normally be considered as high, but to specify more realistic limits to increase the quality of conventional welding processes.
6. Testing of skid welded samples produced with non-balanced beads to determine the acceptability threshold for joints previously considered as unsatisfactory after visual examination in the present study e.g. if only very small emergent beads are found to be acceptable then processing speed may be increased thereby increasing the viability of the process even further.

REFERENCES

[1] IRVING, R.R. The laser weld focus on steel plate structures. In: Iron Age, May.1976, pp 43-45.

[2] LEIDE, N.G. & JUNGLE, C. Prerequisite for advanced welding methods such as laser, electron beam and plasma welding in shipbuilding. Institute for Ship and Marine Technology, Copenhagen, BSRA Translation no.5003, Abs. 49035, 1977.

[3] MARTYR, D.R. Application of high power lasers to ship production. University of Newcastle upon Tyne, Department of Naval Architecture and Shipbuilding, Ph.D. thesis, Feb.1984.

[4] MAIMAN, T.H. Stimulated optical radiation in Ruby. In: Nature, vol.187, Aug.1960, p493.

[5] CHIRILLO, L. Shipbuilding alignment with lasers. Todd Shipyard Corporation, Seattle, Apr.1974.

[6] PATEL, C.K.N. High power carbon dioxide lasers. In: Lasers and Light, W.H. Freeman & Co. SBN 7167 0985-6, 1967.

[7] TABATA, N., NAGAI, H., YOSHIDA, H., HISHII, M., TANAKA, M., MYOI, Y. & AKIBA, T. High power CO2 lasers for FMS-10kW and 20kW-Class SAGE lasers. In: International Symposium, Materials Processing, Boston, Nov.1983.

[8] TABATA, N., YAGI, S., MORI, I., KIMBATA, Y. & HAYASHI, E. Silent-discharge carbon dioxide gas laser machining facility. Mitsubishi Denki Giho (company pulication), vol.56 no.5, 1982.

[9] BAKOWSKY, L. New CO2 lasers of 1-4 kilowatt power with fast axial gas flow. 2nd International Conference on Lasers in Manufacturing, Brighton, Proceedings vol.1, Mar.1985.

[10] HOFFMANN, P.", The start of new generation of CO2 lasers for industry. 2nd International Conference on Lasers in Manufacturing, Brighton, Proceedings vol.1, Mar.1985.

[11] BASS, M. Laser Materials Processing. North Holland Publishing Company, 1983, pp 67-68.

[12] WATSON, M.N. & STEEN, W.N. Desitech 2kW laser cutting machine - Interim report on trials conducted during period July-October 1983. Welding Institute Contract Report, LD23085, Nov.1983.

[13] GLENDINNING, A.D.,MEGAW, J.H.P.C. & HILL, M. An investigation of the possible effects of beam polarisation on laser welding. Laser Users Club Report CLM-RR-LUC7, Jun.1984.

[14] SELDON, A.C. & TRAVIS, A.J.B. Report on long beam path propogation experiments with a 10kW laser beam. Laser Users Club Report CLM-RR-LUC2, Nov.1984.

[15] SELDON, A.C., OSBORN, S.J., & BRAY, A.V. Report on the 75 metre beam-line experiment. Laser Users Club Report no. CLM-RR-LUC 15, Dec.1986.

[16] FORBES, N. Optical problems of beam delivery. 2nd International Conference on Lasers in Manufacturing, Brighton, Proceedings vol.1, Mar.1985.

[17] JENKINS, F.A. & WHITE, H.E. Fundamentals of optics, fourth edition. Mc Graw-Hill Inc., 1981.

[18] SANO, R., MIYATA, T., KAWATA, K., SAKURAGI, S., NANBA, H. & SUMIYA, M. R & D of optics for high power CO2 lasers. I.C.A.L.E.O. 1984.

[19] SANO, R., MIYATA, T. & KAWATA, K. R&D of optics for high power CO2 lasers. In: International Symposium, Materials Processing, Boston, Nov.1983.

[20] ELLIOT, S. & WYLDE, J.G. The fatigue strength of EB transverse butt joints in C-Mn steels. Welding Institute Members Report no.232/1984, Feb.1984.

[21] LONNING, K. & PETERS, G.T. Evaluation of laser welding in commercial ship construction United Technologies Research Centre, Report no. R76-150421-1, Mar.1976.

[22] DANKO, J.C., FERRELL, H.C., HOLSBERG, P.W. & PETERS, G.T. High energy beam welding in shipyard construction. 1984.

[23] BANAS, C.M. & PETERS, G.T. Application of laser welding to ship production - Vol. 1&2. Bethlehem Steel Corporation / US Marine Administration project report, BSRA Abs. 46965, vol.1-Aug.1974, vol.2-Dec.1979.

[24] HAKANSSON, K. High power laser beam welding of T sections with different edge preparation. In: International Conference on Joining of Metals, Helsingor. Proceedings vol.1, Aug.1981.

[25] HAKANSSON, K. High power laser beam welding of different steels,

Company report, Kockums Verkstader AB, Sweden, 1980.

[26] IRVING, R.R. The high powered laser welds carbon steel plate. In: Iron Age Aug.1982, pp 48-49.

[27] Industrial modernisation through advanced technical development. Manufacturers publicity document, M.T.S. Corporation, USA, 1984.

[28] WATSON, H. Laser articulated robot system. Notes taken during a lecture, Apr.1985.

[29] ANON. Naval Architects use lasers to shape ships. In: Lasers and Applications, Nov.1984 pp 38-40.

[30] IWASAKI, Y., TAURA, Y., SHIOTA, H., HIRABE, H. & TOOKURA, A. Study on the forming of hul plate by line heating method. In: Mitsubishi Technical Review, vol.12, pp 161-170, 1975.

[31] BORZECKI, T. & ROSOCHOWICZ, K. An effective method of straightening thin walled superstructures. In: 2nd International Symposium on Practical Design in Shipbuilding (PRADS 83), Tokyo, 1983.

[32] FRASER, F.N. & METZBOWER, E.A. Solidification structure and crack propogation in LB welds. International Conference on Lasers in Materials Processing, Los Angeles, Proceedings vol.1 Jan.1983.

[33] METZBOWER, E.A. & MOON, D.W. Mechanical properties, fracture toughness and microstructures of laser welds in high strength alloys. In: International conference on the Application of Lasers in Materials Processing, Washington, Apr.1979.

[34] DENNEY, P.E. & METZBOWER, E.A. H.S.L.A. steel laser beam weldments. I.C.A.L.E.O., Los Angeles, 1983.

[35] SALTER, G.R. Arc welding economics research. In: Metal Construction, vol.8 no.11, Nov.1976.

[36] METZBOWER, E.A. & STOOP, J. A metallurgical charactorisation of HY-130 steel welds. In: Welding Journal Research Supplement, Nov.1978, pp 345-353.

[37] METZBOWER, E.A., DENNEY, P.E., FRASER, F.W., & MOON, D.W. Mechanical properties of laser beam welds. Welding Journal, vol.63 no.7, Jul.1984.

[38] BANAS, C.M. Laser welding of navy ship construction materials. United Aircraft Research Labs., Connecticut, USA, Report no. AD-786-214, Aug.1973.

[39] METZBOWER, E.A. & MOON, D.W The effects of Inconel 600 on the

toughness of HY-Steel laser welds. In: Conference on Lasers in Materials Processing, O.H. USA, 1983, pp 248-253.

[40] KOBAYASHI, A. Recent progress in laser processing in Japan. 5th International Conference on Production Engineering, Tokyo, Proceedings vol.1, 1984, pp 459-465.

[41] FUJIWARA, S. & IKUTA, S. Cutting and marking machine system using 3kW CO2 laser Toshiba Corporation Publication, Japan, 1983.

[42] KIMURA, S., KINOSHITA, J., NAKAMURA, E. & ISHIKAWA, K. Thick mild steel cutting with high power CO2 laser. In: 2nd International Metal Cutting Conference, Wuhan, May.1985.

[43] KIMURA, S., NISHIO, M., SASAKI, M., NAKAMURA, E. & TAKAHASHI, T. Welding characteristics with high power CO2 lasers. In: 5th International Conference on Production Engineering, Tokyo, 1984.

[44] NAKAMURA, E., SASAKI, M., KINOSHITA, J. & SHIKAWA, K.I. Materials processing with a 10kW CO2 laser - metal welding. International Conference on Electron Beam Welding, Tokyo, 1986.

[45] SASAKI, H., NISHIYAMA, N. & KAMADA, A. Laser welding eith filler wire. 3rd International Colloquium on welding and melting by electrons and laser beam, Lyon, Proceedings, Sep.1983.

[46] LAUSCH, I.W. Laser hardened liners prolong cylinder life. In: The Motor Ship, Oct.1985, pp 32-36.

[47] BRANSDEN, A.S., GAZZARD, S.J., INWOOD, B.C. & MEGAW, J.H.P.C. The laser hardening of groves in medium-speed diesel engine pistons. 4th International Conference on Heat Treatment of Materials, Berlin, ; UKAEA Culham Lab. report no.CLM-P745, Jun.1985.

[48] MAIN, R.P. European Laser Companies: Small is Successful. In: Lasers and Applications, Mar.1984, pp 53-57.

[49] MARTYR, D.R. Laser applications within British Shipbuilders. In: Welding Institute Seminar on Lasers in Manufacturing, 1984.

[50] MARTYR D.R. The application of high power laser technology to ship production. In: NECIES Transactions, 1984-1985.

[51] TAYLOR, A.H. & WYLIE, F.S. Oxygen cutting of shipbuilding steel. BSRA Report no.323 1971.

[52] BROOKE, S.J. Visit to Ferranti (Dundee) for trials of Ferranti/Hancock laser cutting machine. University of Newcastle / British Shipbuilders trials report, Feb.1984.

[53] HAROUTEL, J. & LAGOUETTE, G. Welding metal sandwich structures by laser. In: Welding and Metal Fabrication, Oct,1983, pp 436-439.

[54] WEEDON, T.M.W. Flexible materials processing through fibre optics. International Conference on Power Beam Technology, Brighton, Sep.1986.

[55] SHIMOI, Y., HOSHINA, N. & USHINI, K. Laser welding in automatic assembly line for color CRT electron gun In: Toshiba - Annual CIRP vol.32/1/83 Jan.1983.

[56] WATSON, M.N. Microspot welding with a pulsed Nd-YAG laser. In: Welding Institute Research Bulletin, vol.24,no.10, Report no.R251/10/83, 1983.

[57] DAWES, C.J. & STOCKHAM, N.R. Resistance seam and laser welding of large hybrid metal packages. Welding Institute Research Bulletin, 1985.

[58] JANSSEN, M.G. Laser welding in heart pacemaker. In: Second Symposium on Exploiting the laser in Engineering Production, Coventry, Sep.1984.

[59] HOLDCROFT P.T. Welding Processes - Engineering Design Guides. Oxford University Press, p , 1979

[60] B.S.499: Part 1 1983: Welding terms and symbols - Pt.1 Glossary for welding, brazing and thermal cutting. British Standards Institution document, 1983.

[61] B.S.4803: Parts 1-3: 1983: Radiation safety of laser products and systems. British Standards Institution document, 1983.

[62] WILLGOSS, R.A., MEGAW, J.H.P.C. & CLARK, J.N. Assessing the laser for power plant welding. In: Welding and Metal fabrication, Mar.1979, pp 117-127.

[63] MAZUMBER, J. & STEEN, W.M. Heat transfer model for CW laser materials processing. In: Journal of Applied Physics, vol.51 no.2, Feb.1980.

[64] LUXON, J.T. & PARKER, D.E. Industrial lasers and their applications. Prentice-Hall Inc., 1985.

[65] ANDREWS, J.G. & ATTHEY, D.R. Hydrodynamic limit to penetration of a material by a high power beam. In: Journal of Physics D. Applied Physics, vol.9, 1976.

[66] KLEMENS, P.G. Heat balance and flow conditions for EB and laser

welding. In: Journal of Applied Physics, vol.47, May.1976.

[67] DOWDEN, J. .,DAVIES, M. & KAPADIA, P. Some aspects of the fluid dynamics of laser welding. In: Journal of Fluid Mechanics, vol.126, 1983, pp 123-146.

[68] WATSON, M.N. & DAWES, C.J. An assessment of the advantages of plasma control in laser welding of austenitic stainless steel. Welding Institute Members Report no.203/1983, Jan.1983.

[69] HILL, M., MEGAW, J.H.P.C. & STARES, I.J. Role of shielding gases in high power laser welding. Laser Users Club Report no.CLM-RR-LUC14, Apr.1986.

[70] MINAMIDA, K., YAMAGUCHI, S., SAKURAI, H. & TAKAFUJI, H. CO2 laser welding with plasma utilisation. In: I.C.A.L.E.O, Proceedings, 1982.

[71] PAULEY, J.T. & RUSSELL, J.D. US Patent Laser Welding. US Patent Office, US Patent no.4,127,761, 1977

[72] BANAS, C.M. & BREINAN, E.M. US Patent Fusion zone purification by controlled laser welding. US Patent Office, US Patent no.4,000,392, 1975

[73] SHARP, C.M. US Patent Laser Beam Welding. US Patent Office, US Patent no.4,128,753, 1977

[74] BANAS, C.M. US Patent relating to plasma control by pulsing. US Patent no. 4,152,575, May.1979.

[75] BREINAN, E.M. & BANAS, C.M. Laser welding - present state of the art. United Technologies Research Centre report, 1978,

[76] SWIFT-HOOK, D.T. & GICK, A.E. Penetration welding with lasers. Welding Institute Research Supplement, Nov.1973, pp 429-499.

[77] ANDREWS, J.G., ATTHEY, D.R. & BYATT-SMITH, J.G. Weld pool sag. In: Journal of Fluid Mechanics, vol.100 pt.4, 1980, pp 785-800.

[78] BLAKELEY, P.J. The measurement and prediction of thermal cycles in EB welding. Welding Institute Members Report no.198/1982, Nov.1982.

[79] MEYER, W.E., SCHEFFELS, W. & STEIGERWALD, K.H. A study of the formation and the energy balance of the capillary in electron beem deep penetration welding. 7th Electron and Laser Beam Symposium, Proceedings pp 531-539, 1965

[80] CHANDE, T. & MUZUMBER, J. Estimating effects of processing conditions and variables properties on pool and shape, cooling rates and absorption coefficients in laser welding, In: Journal

of Applied Physics, vol.56, no.7, Oct.1984.

[81] DOWDEN, J., DAVIS, M. & KAPADIA, P. The flow of heat and the motion of the weld pool in penetration welding. In: Journal of Applied Physics, vol.57 no.1, May.1985.

[82] CARSLAW, H.C. & JAEGAR, J.C. Conduction of heat in solids. Clarendon Press, Oxford, 1959, 360pp.

[83] ROSENTHAL, D. The theorey of moving sources of heat and its application to metal treatments. In: Transactions of ASME, vol.68, 1946, p849.

[84] School of Industrial Science, Cranfield, Course notes for the Diploma in Welding Engineering Course, School of Industrial Science Cranfield, Course notes no. P86, vol.1 and 2, 1986.

[85] EASTERLING, K. Introduction to the physical metallurgy of welding. Butterworths, 1984, 250pp.

[86] SALCUDEAN, M., CHOI, M. & GREIF, R. A study of heat transfer during arc welding. In: International Journal of Heat Mass Transfer, vol.29, no.2, 1986, pp 563-572.

[87] HABLANIAN, M.H. A correlation of welding variables. 5th Symposium on Electron Beam Technology, Proceedings, 1963.

[88] BARNES, T.A.L. The redesign of ships structures to facilitate automated methods of production. University of Newcastle upon Tyne, Department of Naval Architecture and Shipbuilding, M.Sc. Thesis, Mar.1985.

[89] BREIMAN, E.M., BANAS, C.M. & GREENFIELD, M.A. Laser welding - present state of the art. US Air Force Metallurgical Lab. Report no. AFML-TR-75-149, Nov.1975.

[90] CARSTENS, J.P. The future of high power laser welding United Technologies Research Centre report, 1983.

[91] DAWES, C.J. CO2 laser welding in low carbon steel sheet. Welding Institute Research Bulletin , Report no R248/8/83, 1983.

[92] JOHNSON, K.J. Fusion welding development for sheet metal fabrication - resistance, laser & MIAF techniques. In: Welding Institute Research Bulletin, Jul.1984, pp 218-226.

[93] DAWES, C.J. Laser welding of butt and T joints in deep drawing low carbon sheet steel. Welding Institute Members Report no.177/1982, Mar.1982.

[94] BELFORTE, D.A. High power lasers process complex shapes. Avco Everett reprint of paper, Industrial & Scientific Conference,

Chicargo,

[95] BELFORTE, D.A. High power laser applications in manufacturing. In: Laser Symposium, Moscow, USSR, Jun.1979.

[96] DAWES, C.J., WATSON, M.N. & SHARMAN, J.D. Laser welding of T joints in low carbon steel sheets - process tolerance data. Welding Institute Members Report no.209/1983, Jan.1983.

[97] LOCKE, E. Laser welding techniques for fabrication of naval vessels. Avco Everett Research Lab., Boston, USA, N.T.I.S. report no. AD-786-211, Jul.1973,

[98] BROOKE, S.J. Visit to UKAEA Culham Lab. to discuss arrangements for welding trials. University of Newcastle/ British Shipbuilders visit report, Aug.1983.

[99] Transmatic wire feed unit. Manufacturers documentation, British Oxygen Corporation, 1983.

[100] BROOKE, S.J. Steel requirements for first batch laser welding trials. University of Newcastle / British Shipbuilders internal report, Jul.1983.

[101] LLOYDS REGISTER OF SHIPPING. Rules and Regulations for the Classification of Ships, Part 2 - Materials for ship and machinery construction. Lloyds Register of Shipping, London, 1981.

[102] MOD(PE). NES 706: Welding and fabrication of ship structures. Naval Engineering Standard (NES) document, MOD(PE) Ship Department Section D191, Mar.1983.

[103] MOD(PE). NES 769: Welding consumables for structural steel approval system. Naval Engineering Standard (NES) document, MOD(PE) Ship Department Section D191, Mar.1982.

[104] MOD(PE). NES 791: Requirements for weldable structural steels - Pt.2 Notch tough mild steel plate. Naval Engineering Standard (NES) document, MOD(PE) Ship Department Section D191, Jul.1983.

[105] BROOKE, S.J. Visit to Lloyds Register of Shipping to discuss laser welding. University of Newcastle / British Shipbuilders visit report, Jul.1983.

[106] BROOKE, S.J. Visit to AMTE(Dunfermline) to discuss laser welding. University of Newcastle / British Shipbuilders visit report, Jun.1983.

[107] The CL10 Laser. Manufacturers specification, Ferranti plc, Dundee, Aug.1984.

[108] LIM, G.C. & STEEN, W.M. Laser beam analyser. In:International Conference on Lasers in Manufacturing, Brighton, Proceedings LIM-1, Nov.1983.

[109] WARD, B.A. Laser beam measurement and quality assurance. In: Second Symposium on Exploiting the laser in Engineering Production, Coventry, Sep.1984.

[110] Laser beam analyser. Manufacturers product information, Laser Technik GmB, 1983.

[111] ZIMMER, R.W. Basics of multikilowatt laser power measurement In: Lasers and Applications, Feb.1984, pp 77-79.

[112] CRAFER, R. & OAKLEY, P.J. Review of continuous wave CO2 laser beam measurement techniques, and the development of a high intensity beam scanner. Welding Institute Members Report no.165/1981, 1981.

[113] KONIG, W., MEIS, F.U. & WILLERSCHEID, I. Process monitoring of high power CO2 lasers in manufacturing. 2nd International Conference on Lasers in Manufacturing, Brighton, Proceedings vol.1, Mar.1985.

[114] BROOKE, S.J. Experimental log for high power laser skid welding trials conducted at UKAEA Culham Lab. 1983-1986. University of Newcastle / British Shipbuilders, 1986.

[115] BAARDSEN, E.L., SCHMATZ, D.J. & BISARO, R.E. High speed welding of sheet steel with a CO2 laser. In: Welding Journal, vol.52, Apr.1973.

[116] BANAS, C.M. Laser welding to 100kW. United Technologies Research Centre Report no.R76-912260-2, Feb.1977.

[117] KAYE, A.S., DELPH, A.G., HANLEY, E. & NICHOLSON, C.J. Improved welding penetration of a 10kW industrial laser. In: Applied Physics Letters, UKAEA Culham lab. preprint CLM-P705, Sep.1983.

[118] WATSON, M.N. Laser cutting trials in shipbuilding steel. Welding Institute Contract Report, LD23334, Jun.1984.

[119] MIDDLE, J.E. Welding pre-primed BS4360 constructional steel. In: International Conference on Joining of Metals, Copenhagen, Aug.1981.

[120] WATSON, M.N. Laser welding of structural steels with wire feed. Welding Institute Members Report no. 264/1985, Mar.1985.

[121] STARES, I.J., APPS, R.L., MEGAW, J.H.P.C. & SPURRIER, J. 10kW laser welding of 13mm pressure vessel steel using automatic wire feed. In: International Conference on Power Beam Technology,

Brighton, Proceedings, Sep.1986.

[122] HILL, M., MEGAW, J.H.P.C., NICHOLSON, C.J. & STARES, I.J. The use of filler in laser welding. Laser Users Club Report CLM-RR-LUC4, Jun.1984.

[123] HILL, M., MEGAW, J.H.P.C. & STARES, I.J. Role of shielding gases in high power laser welding. Laser Users Club Report no.CLM-RR-LUC14, Apr.1986.

[124] MOD(PE). Minimum acceptance standards for welds in HM ships and submarines. MOD(PE) design document: DG Ships G/10/1000B, Ship Department Section D191, Sep.1975.

[125] BENWELL, N. Laser Welding - Notes for discussion. Private correspondence and discussion notes, for the secretary, Lloyds Register of Shipping, Oct.1984.

[126] B.S.4870:1981: Specification for approval testing of welding procedures: Part 1 - Fusion welding of steels. British Standards Institution document, 1981.

[127] B.S.709:1971: Methods of testing fusion welded joints and weld metal in steel. British Standards Institution document, 1971.

[128] TOWERS, O.L. Charpy V-notch tests: Influences of stricker geometry and of specimen thickness. Welding Institute Members Report no.219/1983, Jul.1983.

[129] B.S.131:1972: Methods for notched bar tests. British Standards Institution document, 1972.

[130] CLARK, W. & CRACKNELL, A. Impact test requirements for subsidiary standard test pieces. Private corespondence, British Standard Institution, 1977.

[131] TOWERS, O.L. Testing sub-sized Charpy specimans. In: Metal Construction, vol.18, nos.3-5, 1986, pp 319-325.

[132] B.S.5500:1982: Unfired fusion welded pressure vessels. British Standards Institution document, 1982.

[133] B.S.5400:1980: Steel, concrete and composite bridges - Part 6: Specification for materials and workmanship. British Standards Institution document, 1980.

[134] ELLIOT, S. The effect of process parameters on the weld metal toughness of EB welds in a range of C and C-Mn steels. Welding Institute Members Report no.169/1981, Dec.1981.

[135] WATSON, M.N. Laser welding of a 12.5mm thick niobium microalloyed structural steel at powers up to 9kW. Welding

Institute Members Report no.243/1984, Jul.1984.

[136] SMITH, L.M. Pipelaying using laser welding: a comparison of weld properties in five pipeline steels. International Conference on Power Beam Technology, Brighton, Sep.1986.

[137] WALLACH, E.R., OHARA, M., HARRISON, P.L. & WATSON, M.N. Microstructures and toughness of electron beam welds in steels. International Conference on Power Beam Technology, Brighton, Sep.1986.

[138] GOLDAK, J.A. & NGUYEN, D.S. Fundamental difficulty in Charpy V-notch testing narrow zones in welds. In: Welding Research Suppliment, Apr.1977, pp 119-125.

[139] SMITH, L. Porosity in laser welding. Electron Beam and Laser Welding Technical Group Meeting, Minutes of meeting, The Welding Institute, London, Apr.1985.

[140] DENNEY, P.E. & METZBOWER, E.A. Laser beam welding of HSLA steels. International Conference on Power Beam Technology, Brighton, Sep.1986.

[141] Standard methods for notched bar impact testing of metallic materials. ASTM Mechanical Testing Code E28, Jul.1982.

[142] NORRIS, I.J. Preliminary investigation of a modified Charpy test for the assessment of narrow welds. Welding Institute Members Report no.308/1986, Nov.1986.

[143] KIRKWOOD, P.R.,PROSSER, K. & BOOTHBY, P.J The properties of pipeline girth welds produced by arc welding processes. International Conference on Welding in Energy Related Projects, Toronto, Proceedings, Sep.1983.

[144] BOOTHBY, P.J. & TINDLE, K. Laser welding trials in X65 linepipe staeel. British Gas plc internal reportno. R3577, Engineering Research Station, Jan.1987.

[145] BAILEY, N. Ferritic steel weld metal microstructures and toughness. In: Centenary Conference of Sheffield University Department of Metallurgy, Jul.1984.

[146] GARLAND, J.G. & KIRKWOOD, D.R. Towards improved submerged arc weld metal. In: Metal Construction, May-Jun.1975,

[147] HARRISON, J.D. Lessons from service fatigue failures. In: Welding Institute Research Bulletin, vol.21, R183/3/80, Mar.1980.

[148] YAMAGUCHI, I. Fatigue failure in ship structures and their countermeasures. International Institute of Welding Document XIII-504-68, 1968.

[149] NIBBERING, J.J.W. & SCHOLTE, H.G. The fatigue problem in shipbuilding in the light of new investigations. In: Trans. RINA, Apr.1975, pp121-144.

[150] GIGES, E.G., BAKER, R.G., HARRISON, J.D. & BURDEKIN, F.M. Factors affecting the fatigue strength of welded high strength steels. In: British Welding Journal Report, Mar.1967, pp 108-116.

[151] WYLDE, J.G., BOOTH, G.S., & IWAGAKI, T. Fatigue tests on welded tubular joints in air and sea water. Welding Institute Members Report no.251/1984, Nov.1984.

[152] CLISSON, J., MAS, C., GERBET, D. & BOUSSEAU, M. Comparison of results obtained in laser beam and electron beam welding of steel 15CDV6. In: 3rd Interternational Conference on Welding and Melting by Electrons and Laser Beams, Lyon, Sep.1983.

[153] GILL, S.J., MOON, D.W., METZBOWER, E.A. & CROOKER, T.W. Fatigue of A36 steel laser beam weldments. In: Welding Journal, vol.65 no.2, Feb.1986, pp 48-50.

[154] BLARASIN, A. Laser welding of high strength steels used in the transport industry. In: Rivista Italiana della Saldatuna, vol.33 no5-8, Sep.-Oct.1980.

[155] WIRTH, P., SARADY, I. & NILSSON, K. Latest trends in cutting and welding with CO2 lasers in the metal processing industry. In: 6th International Conference on Optoelectronics in Engineering, Munich, Proceedings, 1983.

[156] MAZUMBER, J. Laser welding of titanium and tin plate. University of London, Ph.D. Thesis, Apr.1978.

[157] ELLIOT, S. Electron beam welding of C-Mn steels - toughness and fatigue properties. In: 64th Annual AWS Convention, Philadelphia, Apr.1983.

[158] GURNEY, T.R. & MADDOX, S.J. A re-analysis of fatigue data for welded joints in steel. In: Welding Research International, vol.3 no.4, 1973.

[159] GURNEY, T.G. Fatigue design rules for welded steel joints. Welding Institute Research Bulletin, Vol.17, May 1976.

[160] B.S. 153: Part 3b & 4: 1972 - Specification for steel girder bridges - fatigue. British Standards Institution, 1972.

[161] TUBBY, P.J. The fatigue strength of non load carrying laser welded T-butt joints in steel. Welding Institute Contract Report no.23583/1/85, Apr.1985.

[162] Britsh Shipbuilders Steelwork Manufacturing Standards. British Shipbuilders, Newcastle upon Tyne, 1982.

[163] MADDOX, S.J. & FITZPATRICK, B.J. Investigation of factors which affect the fatigue strength of shot peened fillet welded joints. Welding Institute Members Report no.161/1981, Sep.1981.

[164] BAXTER, C.F.G., & BOOTH, G.S. Improved fatigue strength by plasma dressing. In: Welding Institute Research Bulletin, Sep.1979.

[165] GALSWORTHY, J.C. Low frequency corrosion fatigue of electron beam weldments in a marine steel. International Conference on Power Beam Technology, Brighton, Sep.1986.

[166] GURNEY, T.R. The influence of thickness on the fatigue strength of welded joints. In: 2nd International Conference on the Behaviour of Offshore Structures, London, Proceedings, 1979.

[167] SMITH, I. & HURWORTH, S. The effect of geometry changes upon the predicted fatigue strength of welded joints. Welding Institute Members Report no.224/1984, 1984.

[168] GURNEY, T.R. Fatigue of welded structures. Cambridge University Press, 1979.

[169] GOLDBERG, F. Influence of thermal cutting and its quality on the fatigue strength of steel. In: Welding Journal Research Supplement, Sep.1973.

[170] SVENSEN, T. The economics of hull and propeller maintenance in the face of uncertanty. In: Transactions NECIES, Oct.1983.

[171] B.S.427:1961: Methods for Vickers Hardness Testing. British Standards Institution document, 1961.

[172] HART, P.H.M. & MATHARU, I.S. Heat affected zone (HAZ) hydrogen cracking behaviour of low carbon equivalent C-Mn structural steels. Welding Institute Members Report no.290/1985, Mar.1985.

[173] ITO, Y. & BESSYO, K. Weldability formula of high strength steels related to HAZ cracking. International Institute of Welding document: IX-631-69-1969, 1969, pp 1-18.

[174] SUZUKI, H. Carbon equivalent and maximum hardness. International Institute of Welding document IX-1279-83, Feb.1983.

[175] LORENZ, K. & DUEREN, C. C-Equivalent for evaluation of weldability of large diameter pipe steels. International Institute of Welding document: IX-B-11-82, 1982, pp 1-36.

[176] DIXON, R.D. & LEWIS, G.K. Electron emission and plasma formation

during laser beam welding. In: Welding Journal Research Supplement, vol.64 no.3, 1985.

[177] BOOTHBY, P.J. Predicting hardness in steel HAZs. In: Metal Construction, vol.17 no.6, Jun.1985, pp 363-366.

[178] COE, F.R. Welding steels without hydrogen cracking. The Welding Institute, Abington, 1973.

[179] GOOCH, T.G. Hardness and stress corrosion cracking of ferritic steel. Welding Institute Research Bulletin, vol.23, pp241-246, Aug.1982.

[180] Guidelines for classification of ferritic steel weld metal micrstructual constituents using the light microscope. International Institute of Welding document no.IX-1377-85, 1985.

[181] ABSON, D.J. & DOLBY, R.E. A scheme for the quantitative description of ferritic weld metal microstructure. In: Welding Institute Research Bulletin, Vol.21, Apr.1980.

[182] KOMIZO, Y., PUNSHON, C.S., GOOCH, T.G. & BLAKELEY, P.J. Effect of process parameters on centre-line solidification structures of EB welds in steel. Welding Institute Members Report no.252/1984, Nov.1984.

[183] SHINADA, K., OHMAI, T., YOSHIDA, Y. & SUZUKI, S. Study of weld quality of CO2 laser welding. In: International Conference on Welding Research in the 1980s, 1980.

[184] HILL, M., MEGAW, J.H.P.C. & OSBORN, S.J. Real time radiography of laser welding - Parts 1&2. Laser Users Club Report no.CLM-RR-LUC11/16, Jun/Sep.1986.

[185] DOLBY, R.E. Factors controlling weld toughness. Welding Institute Members Report no.14/1976/M, May.1976.

[186] WATSON, M.N. Laser welding of some low C and low S C-Mn-Si-Al-Nb structural steels. Welding Institute Members Report no.271/1985, Apr.1985.

[187] BAILEY, N. & JONES, S.B. Solidification cracking of ferritic steels during submerged arc welding. The Welding Institute, Abington, 1977.

[188] RUSSEL, J.D. The development of an electron beam weld solidification cracking test. Welding Institute Members Report no.47/1977, 1984.

[189] WATSON M.N. Laser weld metal in a microalloyed steel: fracture toughness. Welding Institute Members Report no.176/1982, 1982.

[190] BROOKE, S.J. Visit to Ferranti(Dundee) plc to discuss development and build programme for the CL5/CL10 laser. University of Newcastle/ British Shipbuilders visit report, Feb.1984.

[191] BROOKE, S.J. Visit to Desitech(Welligborough)Ltd for fault finding trials of laser cutting machine. University of Newcastle/ British Shipbuilders visit report, Jan.1984.

[192] BROOKE, S.J. Visit to Fairey Engineering(Stockport) to discuss laser applications and workstation design. University of Newcastle/ British Shipbuilders visit report, Nov.1983.

[193] BROOKE, S.J. The application of lasers to shipbuilding - state of the art review. BMT report no. for the DTI, Mar.1986.

[194] Quotation for a laser system. Technical Proposal, United Technologies Research Centre, Connecticut, pp 86-32, Jan.1987.

[195] JOHNSON, T.A. Robot controlled Laser processing. In:International Conference on Lasers in Manufacturing, Brighton, Proceedings LIM-1, Nov.1983.

[196] Laser based workstation - Input to British Shipbuilders laser project. Total Transport Systems contract report for British Shipbuilders, Dec.1984.

[197] Shipbuilding Laser Application Project (SLAP). Total Transport Systems contract report for British Shipbuilders, Aug.1983.

[198] WARD, B.A. Feasibility of mounting the CL10 laser on a moving gantry. Private correspondence, UKAEA Culham Lab. Nov.1983.

[199] DAVIES, G.M., MARTYR, D.R., OAKLEY, P.J., SIMPKIN, R.C. & SPARHAM, D.T. Lasers in Japan. Welding Institute Report, sponsered by the DoTI, Mar.1986.

[200] KALOGERAKIS J.M. The use of robots in the shipbuilding industry. In: The Naval Architect Journal, Jul./Aug.1986, pp 266-276.

[201] Justification for two portable robots. British Shipbuilders capital justification approval document, 1985.

[202] ANON. Track mounted welding robot produces flexible manufacturing system. In: Welding Journal, vol.63 no.12, 1984.

[203] ANON. Shipbuilding world looks on as Finns pioneer robotic gantry. In: Metal Construction, vol.18 no.11, Nov.1986, pp 678-679.

[204] ANON. Laser robot performs seam tracking. In: Robotics World, Feb.1985.

[205] Adaptive Control of Laser processing. EEC BRITE Submission - UKAEA Culham Lab as contract coordinator, 1985.

[206] TRAVIS, A.J.B. Laser beam diagnostic equipment for on-line use with multikilowatt lasers. In: 5th International Symposium on Gas Flow and Chemical Lasers, Oxford. UKAEA Culham Lab. pre-print no. CLM-P751, Aug.1984.

[207] WATSON, M.N., WARD, B.A. & STEEN, W.M. Desitech 2kW laser cutting machine - Report on trials. Welding Institute Contract Report no. LD23085/1, Jan.1984.

[208] DIXON, R.D. & LEWIS, G.K. Plasma monitoring of laser beam welds. In: Welding Journal Research Supplement, vol.64 no.2, 1985.

[209] Opto-Electronics Welding Supervision System. Manufacturers manual, Lasertechnik GmbH, W. Germany, May.1986.

[210] BRANSDEN, A.S, HEATH, R., MEGAW, J.H.P.C. & STARES, I.J. An investigation of monitoring and feedback control of laser welding. Laser Users Club Report no. CLM-RR-LUC8, Jun.1984.

[211] HOLDER, S.J.,JONES, S.B. & WESTON, J. Mechanical approaches to seam tracking for arc welding. Welding Institute Members Report no.167/1981, Dec.1981.

[212] DREWS, P., STARKE, G. & WILLIAMS, K. The current state of development of sensors for gas-shielded welding robots. In: Welding and Cutting, 1984.

[213] DOHERTY, J., HOLDER, S.J. & BAKER, R. Computerised guidence and process control. In: 3rd International Conference on Robot Vision and Sensory Controls, Nov.1983.

[214] VERBECK, W.J. Arc welding process control by preview sensor. In: The Industrial Robot, Jun.1984, pp 86-88.

[215] BANGS, S. Laser vision robot guides welding arc. In: Welding and Fabrication, Nov.1984.

[216] EDWARDS, S.A. First steps towards a design standard for protective housings. British Standards EEL/28 laser safety working group paper, Feb.1986.

[217] WARD, B.A., BROWN, D.P.D. & WALKER, C.I. Case study-Safety aspects of a high power CO2 laser system for class 1 operation. UKAEA Culham Lab. report no.CLM-P664, Aug.1981.

[218] BROOKE, S.J. Alternatives to enclosures for high power laser

installations. British Standards/EEL 28 Laser safety working group paper, Jun.1986.

[219] BOOKER, D. Laser welding project - feasibility report. Hill Samuel & Co Ltd, contract report for British Shipbuilders, Mar.1985.

[220] AICHELE G. Counting the cost of welding operations. In: Welding and Fabrication, Oct.1983, pp 411-413.

[221] SALTER, G.R. An economic view of arc welding. In: Metal Construction, Feb.1984.

[222] KALOGERAKIS, J.M. & WIKENS, G.C. The automatic cutting, marking and processing of structural sections. In: SNAME Ship Production Symposium, Virginia, Aug.1986.

[223] The procedure handbook of arc welding. The Lincoln Electric Company, Cleveland, Ohio, Jun.1983.

[224] STORCH, R.L. Accuracy control variation - merging equations: A case study of their application in US shipyards. In: Journal of Ship Production, vol.1 no.2, May.1985, pp 133-144.

[225] HILTON, D.E. & McKEOWN, D. Improvements in mild steel weld properties by changing the shielding gas - theorey or practice? In: Metal Construction, vol.18 no.10, Oct.1986, pp 617-619.

[226] KIMBER, D. & HARGROVES, M. Creating a production facility for standard ship. In: Transactions RINA, Apr.1976.

[227] KIHORA, H. & YAMAMOTO, N. Recent developments in management and production methods in Japanese shipyards. In: Trans. SNAME, Jun.1968.

[228] LOVE, J.G. & HEWITT, R.J. The application of robotic welding technology to shipbuilding. 13th International Symposium on Industrial Robotics, Chicago, Proceedings, vol.1, Apr.1983.

[229] Modular Steel Fabrication Systems. Total Transportation System, Panel production line technical information, TTS, Norway, 1983.

[230] SOEVRE, A. Budget prices for panel line equipment. Private correspondence, TTS Norway, Oct.1986.

[231] CHADWICK, J. Multi-axis gantry system quotation. Privaye correspondence to British Shipbuilders, Integrated Laser Systems, Jan.1987.

[232] VERBECK, W.J.P.A. Seam pilot quotation. Private correspondence, Odelft, Holland, Nov.1986.

[233] WINKLE, I,E, & BAIRD, D. Towards more effective structural design through synthesis and optimisation. In: Trans. RINA, 1985.

[234] British Shipbuilders Assembly Standards, Interim product definitions, British Shipbuilders Standards Document, Jun.1983.

[235] STARES, I. J., APPS, R.L., MEGAW. J.H.P.C., & SPURRIER. J., Improved micro-structure and impact toughness of laser welds in a pressure vessel steel. In:— Metal Construction. March '87 pp. 123—6

Appendix A

APPENDICES ASSOCIATED WITH CHAPTER 3

A-1 VARIABLES OF MATERIAL AND EQUIPMENT AFFECTING SKID WELDING PERFORMANCE

Skid welding operational variables

Variable	Comments
Laser power	All initial welds were made at 9kW at the workpiece. This was only reduced either if a satisfactory joint was unobtainable or to affect a change to heat input at fixed speeds.
Traverse speed	Progressive to suit each plate thickness. Pitched with respect to the machine table settings at 4.0, 6.0, 8.0, 10.0, 14.0 17.5, 19.5 & 23.0 mm/second.
Filler rate	See Filler Variables.
Shroud gas flow	See Shroud Variables.
Laser incident spot height (above the face plate surface	Varied for each plate thickness at a pitch of 0.25mm from 0 to 1.50mm.
Laser incident angle measured from the face plate surface	Angle kept constant once a minimum determined to ensure non-interaction with the face plate

Table A3.01a - Laser skid welding operational variables

Variable	Comment
Plate thickness	Tests on 3,6,8,10,12,15 mm
Web	)Use same plate thickness
Face plate	)for each.
Joint gap	Nominal minimal gaps of 0.25-0.50mm and outsized gaps of 1mm to 2mm
Web edge condition	
Gas cut	*
Laser cut	
Machined	
Rolled section	*
Plasma cut	
Web edge preparation	
Wire brushed	*
Ground	*
Shot blast	
Painted	*
Oxidised	*
Face plate surface prep.	
Ground	*
Shot blast	
Painted	*
Web/flange angle	All tests conducted with the web perpendicular to the face plate.
Orientation	
Flat	
Horizontal	*
Vertical	
Plate rolling direction	All samples cut with the longest side in the rolling direction.
Plate grade	
Chemical composition	)Restricted to Lloyds Grade A and
Heat treatment	)BS4360:43A with representative)plates from shipyard stock
Sample temperature	Room temperature

* - selected as being in most common use in the shipyard

Table A3.01b - Tee joint configuration variables

Variable	Comment
Laser power (workpiece)	Attempt made to produce welds in each plate thickness using 9kW, adjusting speed to control heat input and penetration.
Power stability	As provided, assuring a typical output for an industrial laser unit.
Beam mode/Stability (at workpiece)	As provided.
System focal number	Selected to give a focal length for shallow incident angles.
Workstation dewpoint	As provided - with a large workshop type enclosure, a good simulation of a shipyard environment.

Table A3.01c - Laser beam line variables

Variable	Comments
Shroud type	Existing technology unit redesigned for high power tee section work.
Gas flows	
Jet	Changed until minimum - zero
Lense	Changed until minimum - 351/min.
General top	Used only for a clean finish
General back	Single sided welding therefore not used.
Stand off distances of shroud unit	Maintained at a nominal 2mm to avoid likely collisions with tack welds
Gas types	
Argon	* used as a constant as already proved successful for butt welds.
Helium	
CO2 & Mixes	

Table A3.01d - Laser welding shroud variables

Variables	Comments
Composition	Initially mild steel comparable to wire that geanerally used in the shipyard for MIG welding. Restricted trials on alternative compositions to improve properties.
Construction	
Solid	* Used as most conventional comparative data available.
Flux core	
Diameter	Mainly 1.6mm diameter; 0.9, 1.0, 1.2mm used for comparisons.
Input rate	Initially amount proportional to the joint gap, then with a factor for small reinforcing beads, then equated to account for relative penetration.
Input angles	
Angle to the laser	Starting point of 45 degree to each
angle	but lowered nearer to the face plate
Angle to the joint	as joint gap allowed joint access.
Interaction position	
Front) of the weld	* Used to ensure good mixing of the
Back) pool	wire in the molten pool.
Wire temperature	Room temperature.

Table A3.01e - Filler wire variables

A-2 TRIALS PROGRAMME LISTING

Trial no.	Date		Trial Listing
0	16/08/83 to 17/08/83	0.0	Familiarisation period to learn equipment operation techniques.
		0.1	Butt welding on 10mm plate to test continuity of operation between Martyrs trials using 5kW and present Authors work using 10kW.
1	27/09/83 to 28/09/83	1.1	Initial skid welding on 10mm thick plate; trial to assess optimum positioning for plasma control shoe.
		1.2	Beam incident angle trials, changing beam angle to face plate from 5-13 degrees.
		1.3	Filler welding using F0 wire rates to directly fill joint gap.
2	24/01/84 to 28/01/84	2.1	Parameter surveys on 8mm plate; spot height survey, no filler wire, constant speed.
		2.2	8mm plate; plasma control and gas shrouding survey, constant speed.
		2.3	8mm plate; filler survey with F2 wire rates.
		2.4	8mm plate; traverse speed survey, fault was found with the gas jet devise.
		2.5	8mm plate; plasma control and shrouding survey repeated using no plasma control jet.
		2.6	8mm plate; spot height survey on rolled section plate.
3	04/04/84 to 05/04/84	3.1	8mm plate; spot height/speed survey using F2 filler rate , no plasma control jet, and ground face plate surface.
		3.2	8mm plate; optimised height and speed used on coated plate parameter survey.

		3.3	Confirmation runs for coated plate joints.
		3.4	10mm plate; initial runs based on settings derived from 8mm plate tests.
4	22/05/84 to 23/05/84	4.1	8mm plate: parameter completion runs for spot height/ speed survey; shielding gas survey to assess optimum general shrouding; filler rate survey to assess the effect of filler rate above F2 rates; test sample completion.
		4.2	6mm plate: prliminary spot height/ speed survey to assess likely parameter ranges
		4.3	10mm plate: full spot height/ speed survey.
5	07/08/84 to 08/08/84	5.1	6mm plate: full spot height/ speed survey; filler rate confirmation using F2 rates; edge coating welding parameter survey; gap effect survey; cruciform test sample production.
		5.2	8mm plate: rolled section welding survey; plate wrap-up assessment; edge coating welding parameter survey; gap effect survey.
6	11/09/84 to 12/09/84	6.1	12mm plate; preliminary parameter survey.
		6.2	8mm plate; production of fatigue test samples (mode 1) overseen by Lloyds Register of Shipping.
7	24/10/84 to 25/10/84	7.1	6mm plate; power/ speed survey to assess the effect of heat input on hardness values; edge shape parameter survey; gap effect parameter survey.
		7.2	8mm plate; production of cruciform sample for Charpy testing.
		7.3	11mm plate; spot height/ speed parameter survey; filler rate survey above and below F2 rate; gap effect parameter survey.

8	09/01/85 to 11/01/85	8.1	6mm plate; production of cruciform samples for Charpy and tensile tests; coated plate parameter effect survey; edge shape survey; gap effect survey.
		8.2	8mm plate; coated plate surface effect confirmation runs; cruciform section production; gap effect parameter survey.
		8.3	12mm plate; spot height/ speed survey, filler rate varied 0-F1 as F2 rate found execcessive; coated plate parameter survey; edge shape parameter survey; gap effect parameter survey; production of cruciform samples for destructive testing.
		8.4	15mm plate: spot height/ speed parameter survey.
9	26/02/85 to 28/02/85	9.1	3mm plate: spot height/ speed survey; power reduction survey form 9kW; beam incident angle survey.
		9.2	6mm plate: coated plate effect parameter confirmation runs.
		9.3	8mm plate: edge shape parameter survey.
		9.4	10mm plate: production of cruciform; vertical weld shrinkage test samples; gap effect parameter survey; coated plate effect survey; rolled section effect survey; welding on tack effect.
		9.5	12mm plate: confirmation parameter runs; production of cruciform samples for destructive testing; gap effect parameter survey; coated effect survey.
		9.6	15mm plate; coated surface effect parameter survey; edge shape effect survey; production of cruciform samples for destructive tests gap effect parameter survey.
10	08/05/85 to 10/05/85	10.1	Butt weld samples in 6,10,15mm plate to compare various filler inputs for resulting toughness values.

		10.2 7mm plate: production of cruciform samples for fatigue (Mode 2) testing.
		10.3 7mm plate: survey to assess tolerance of focal positioning.
		10.4 7mm plate: production of cruciform samples for tensile testing.
		10.5 3mm plate: parameter survey using 5kW input power.
		10.6 3mm plate: gap effect survey; production of cruciform samples for destructive testing.
11	08/10/85 to 11/10/85	11.1 8mm plate: production of cruciform samples for fatigue testing (Mode 2) - 7mm samples failed in ultrasonic testing due to excess height parameter.
		11.2 Confirmation trials for the use of SKIDFILL filler rate program in 6,10,15mm plate.
		11.3 Comparative trials for welding 6mm plate using a different plate composition to change weld HAZ properties.
		11.4 Focus position tolerance survey on 6,12mm plate.
		11.5 Continuation of butt welding trials to assess different wire inputs.
		11.6 Melt run production for comparative melt ratio confirmation.

Appendix B

APPENDICES ASSOCIATED WITH CHAPTER 4

B-1 SURFACE PROFILES AND MACROPHOTOGRAPHS OF SKIDWELDS IN 3-15MM PLATE

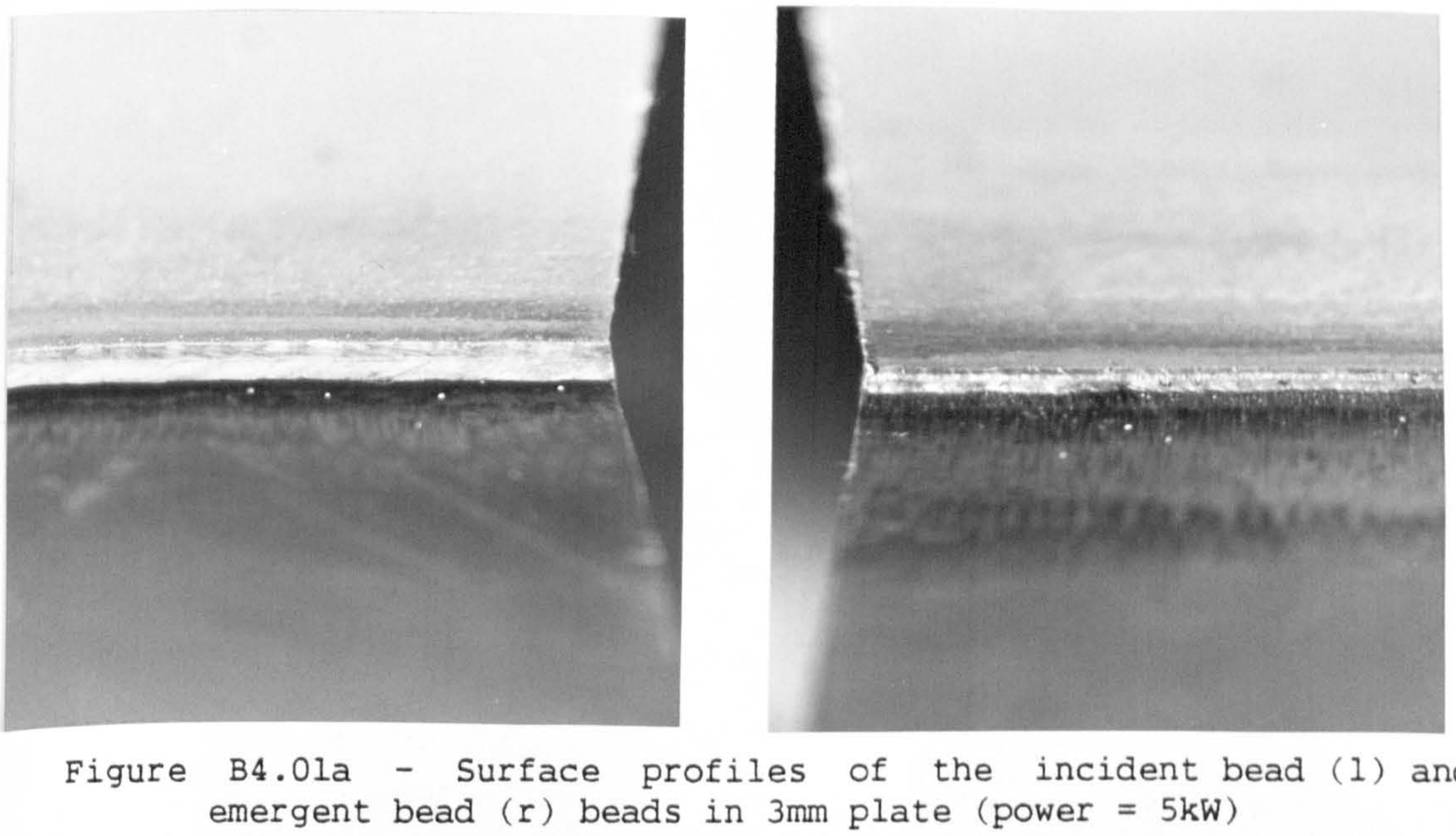

Figure B4.01a - Surface profiles of the incident bead (l) and emergent bead (r) beads in 3mm plate (power = 5kW)

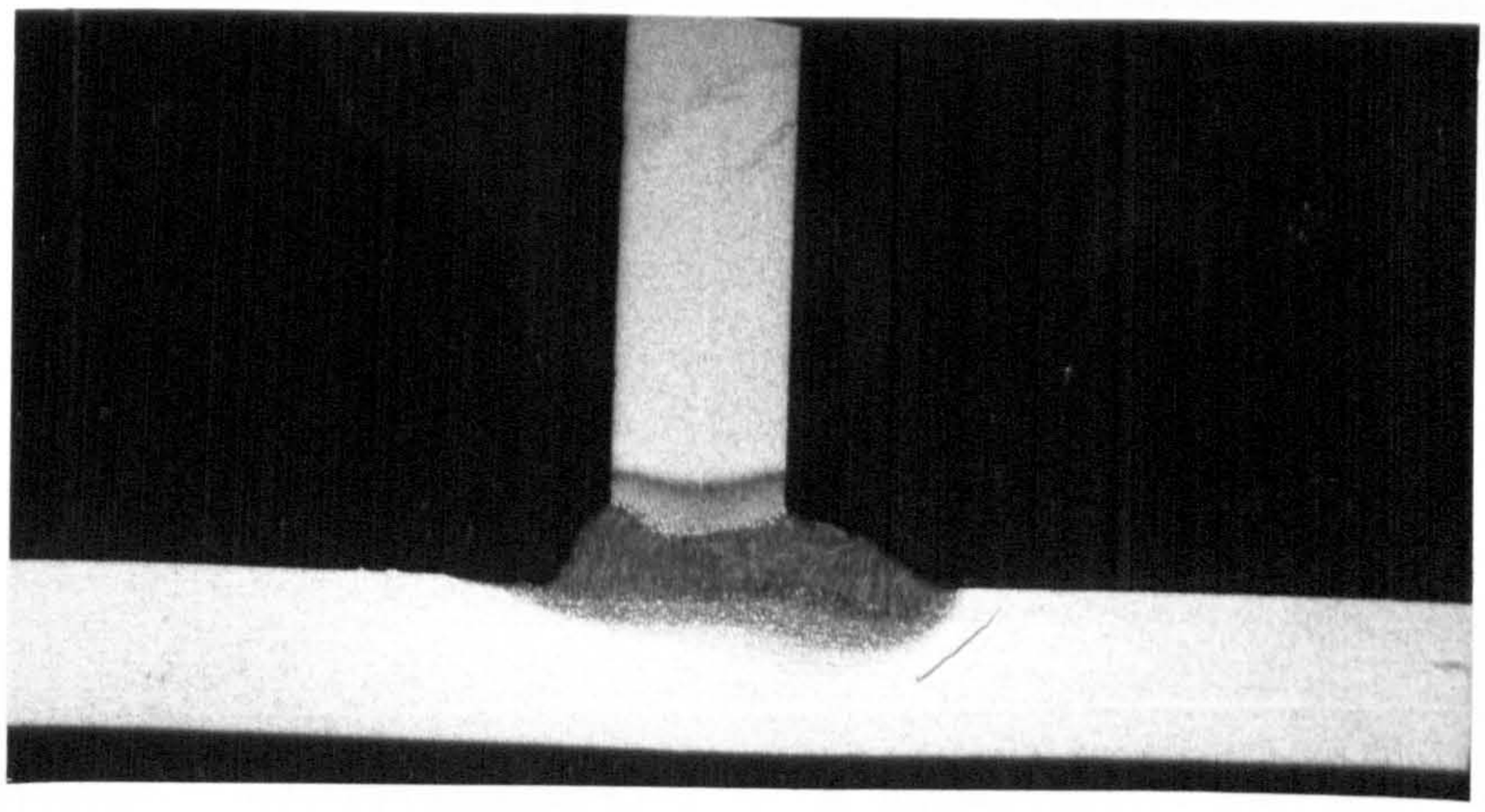

Figure B4.01b - Macrophoto (x4.8) of a skid weld in 3mm thick plate (power = 5kW)

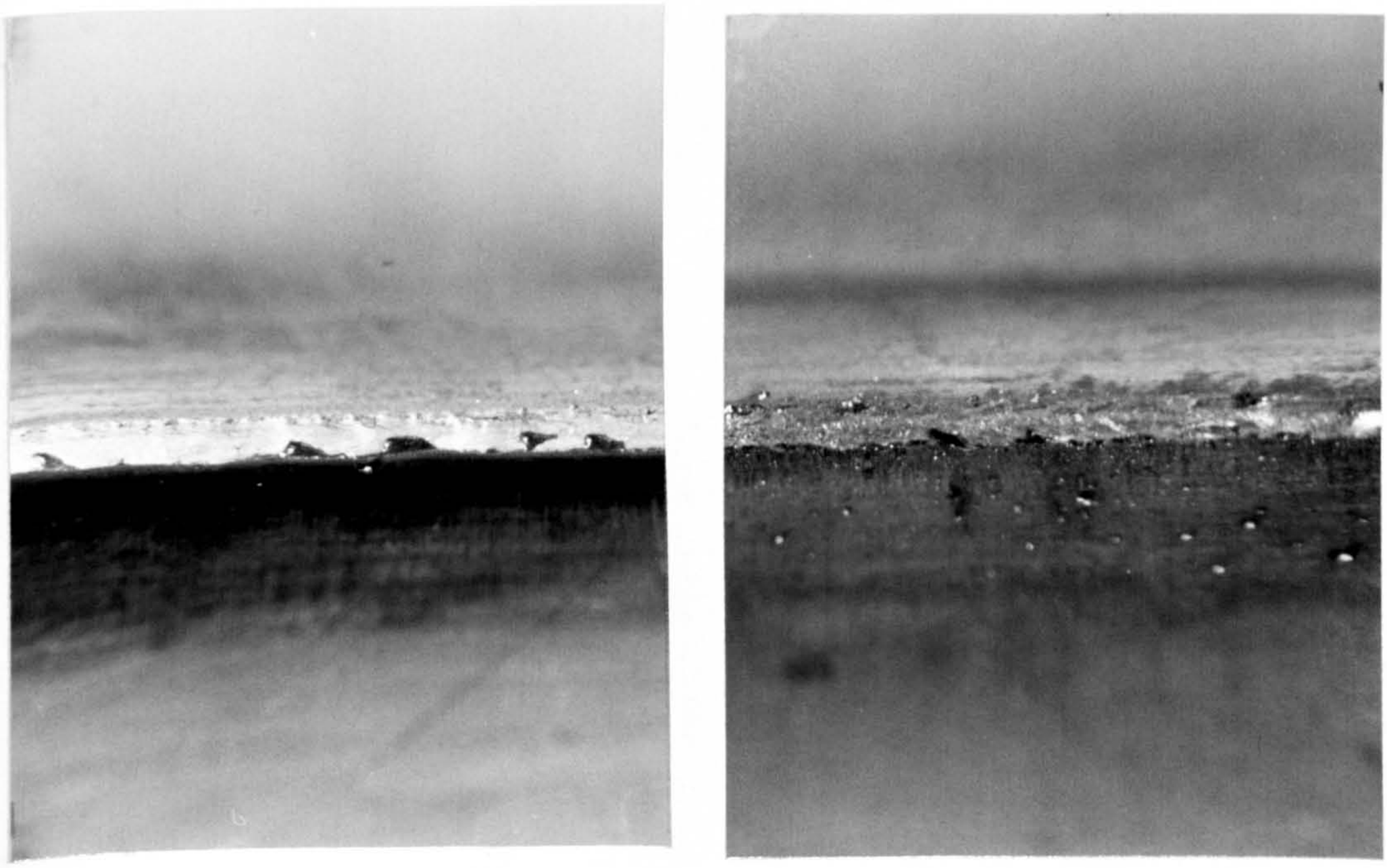

Figure B4.02a - Surface profiles of the incident bead (l) and emergent bead (r) beads in 6mm plate (power = 9kW)

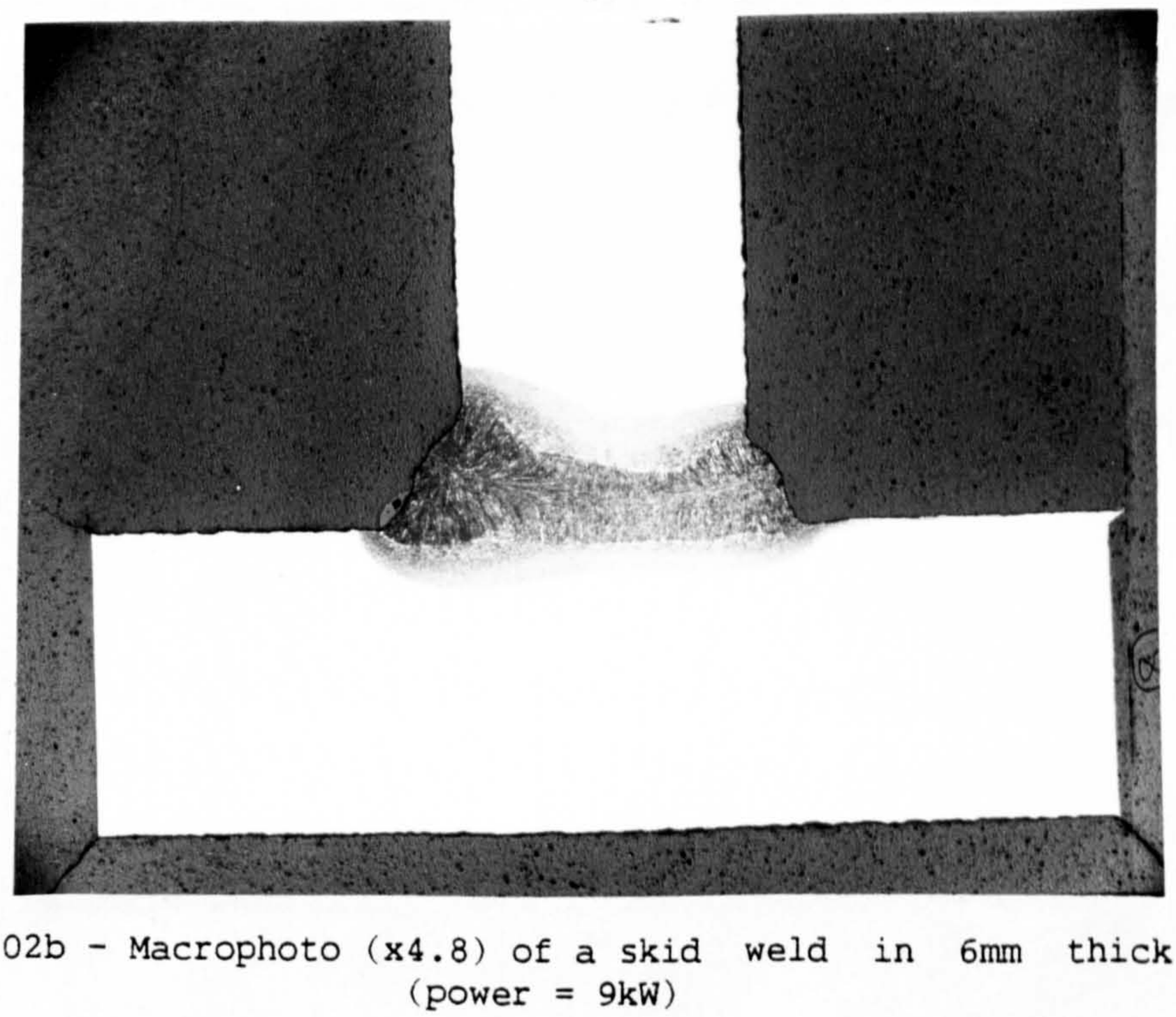

Figure B4.02b - Macrophoto (x4.8) of a skid weld in 6mm thick plate (power = 9kW)

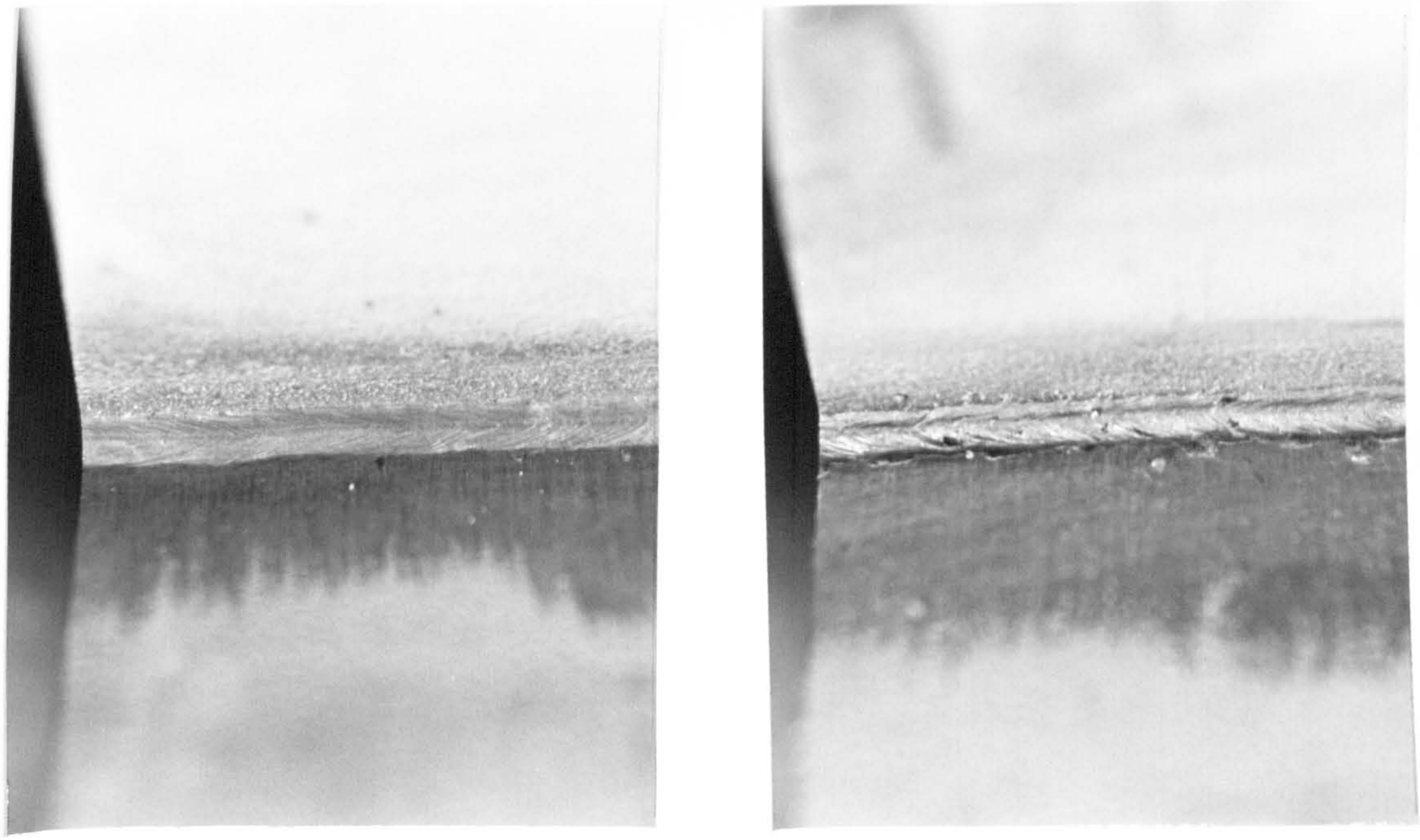

Figure B4.03a - Surface profiles of the incident bead (l) and emergent bead (r) beads in 8mm plate (power = 9kW)

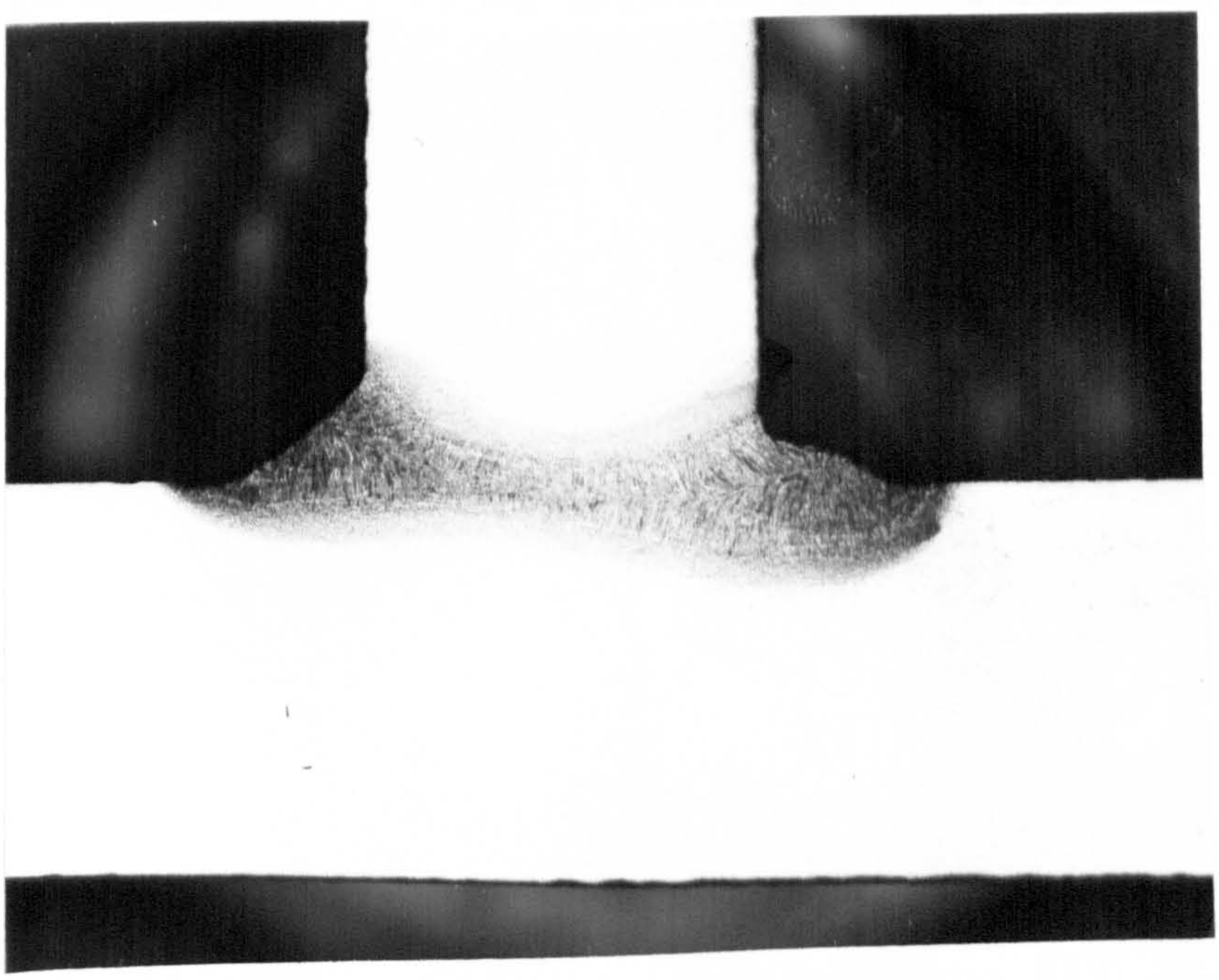

Figure B4.03b - Macrophoto (x4.8) of a skid weld in 8mm thick plate (power = 9kW)

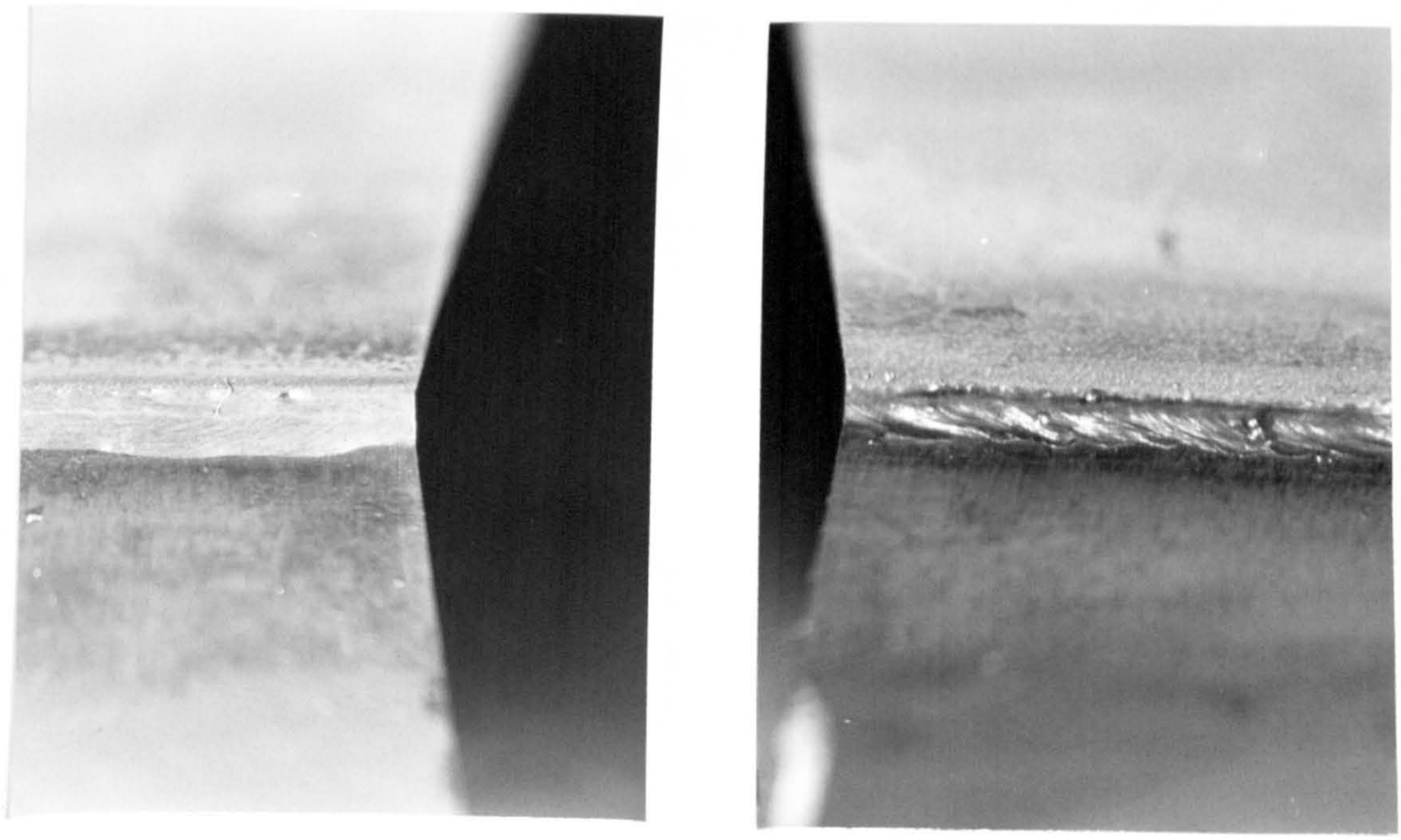

Figure B4.04a - Surface profiles of the incident bead (l) and emergent bead (r) beads in 10mm plate (power = 9kW)

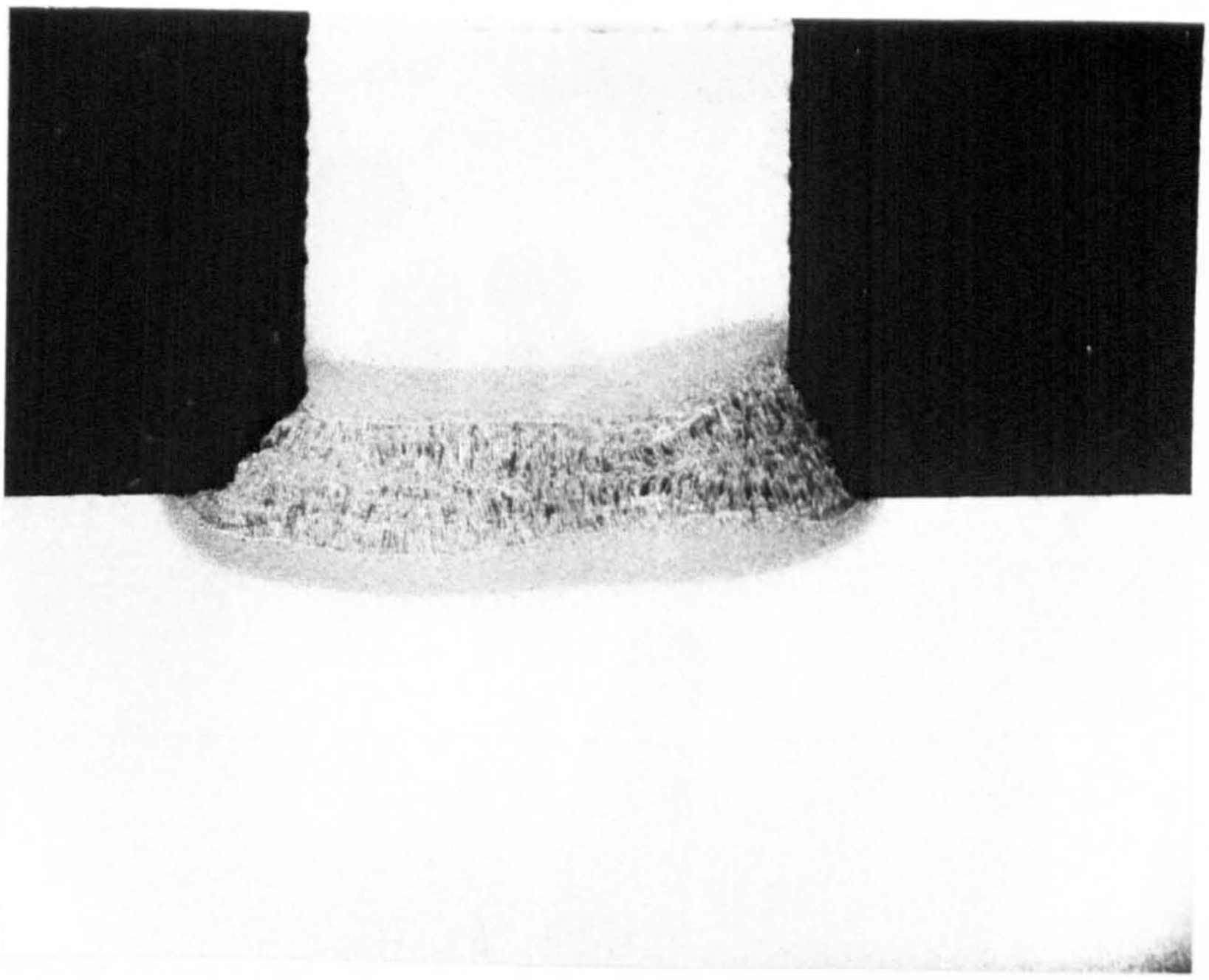

Figure B4.04b - Macrophoto (x4.8) of a skid weld in 10mm thick plate (power = 9kW)

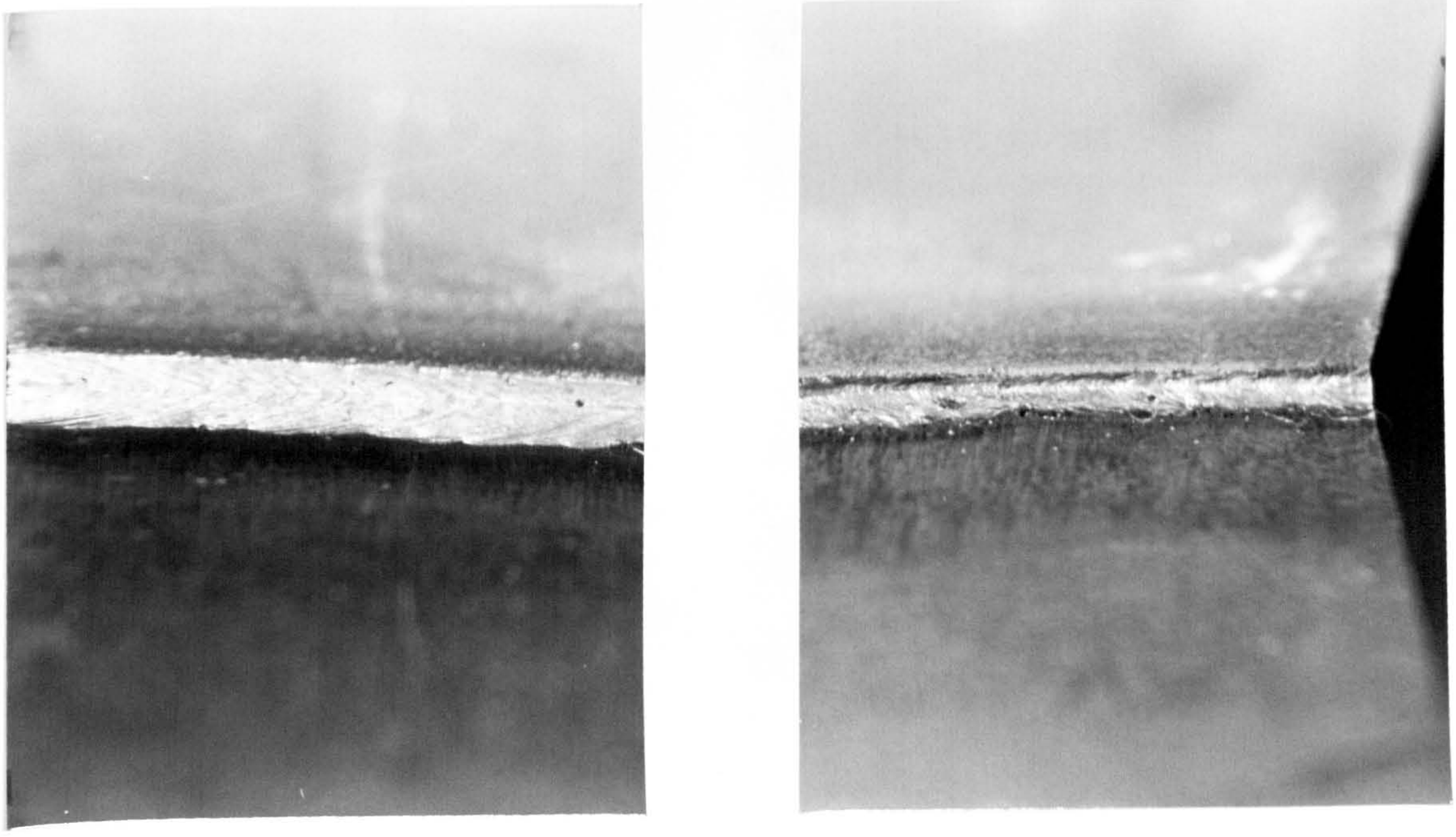

Figure B4.05a - Surface profiles of the incident bead (l) and emergent bead (r) beads in 12mm plate (power = 9kW)

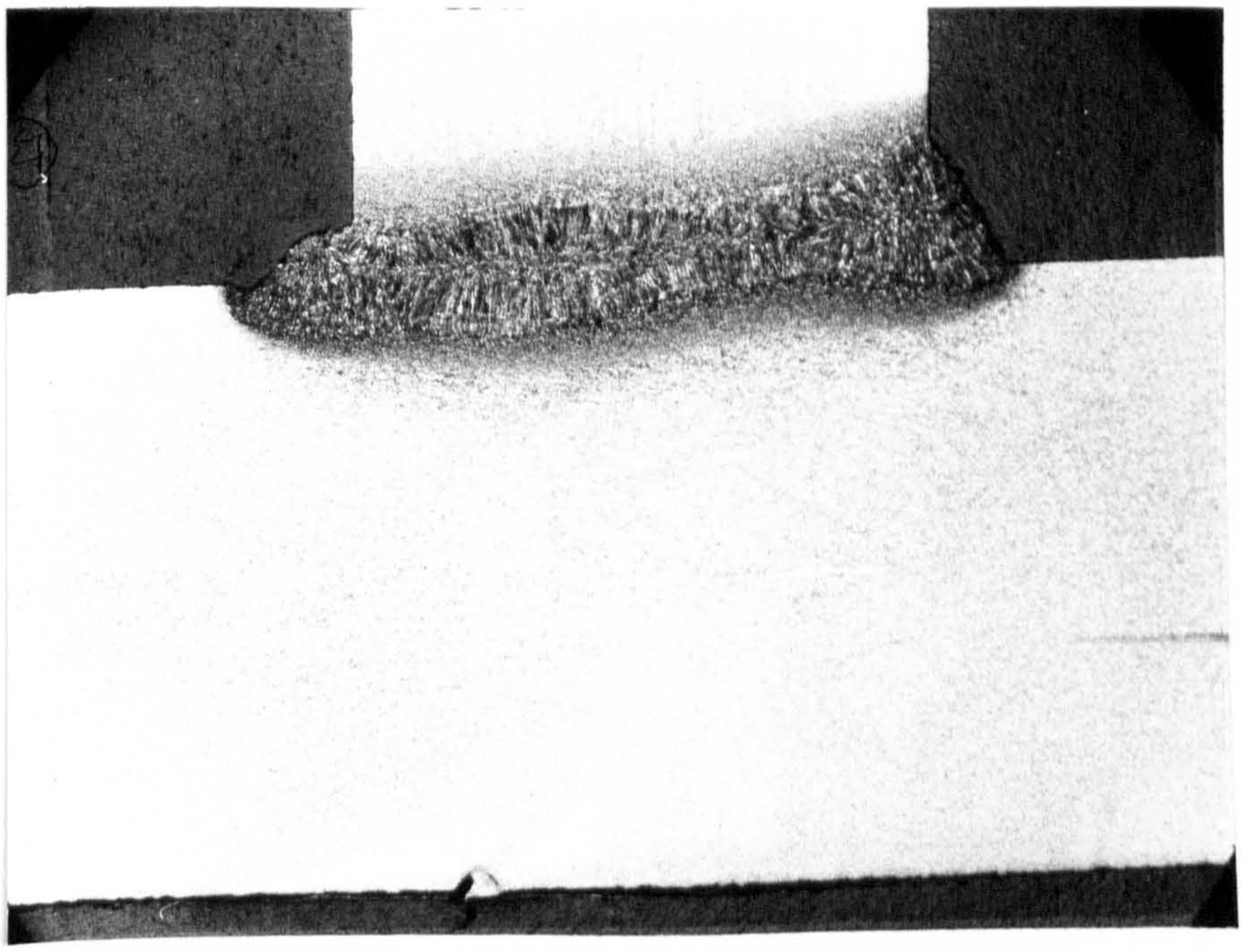

Figure B4.05b - Macrophoto (x4.8) of a skid weld in 12mm thick plate (power = 9kW)

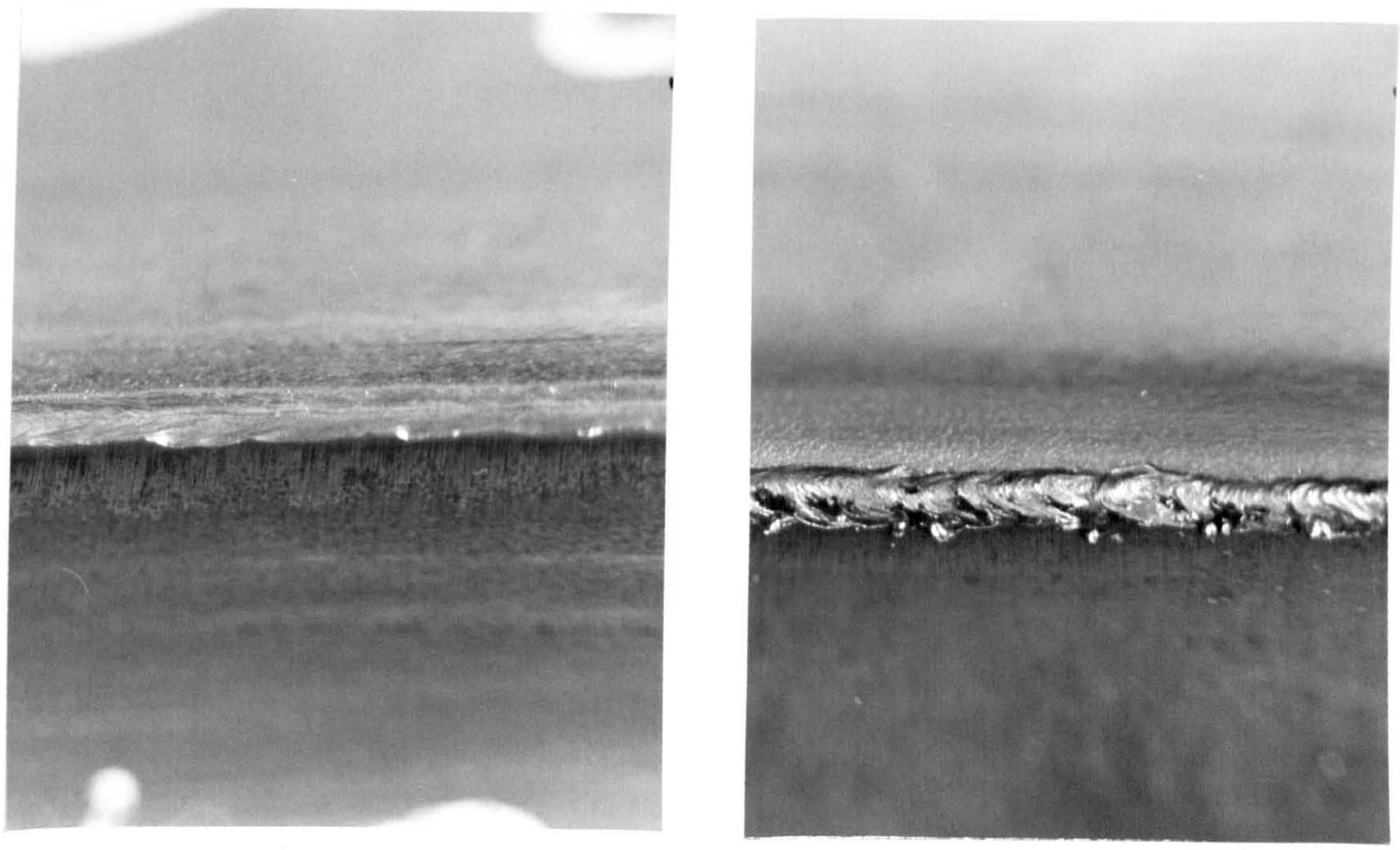

Figure B4.06a - Surface profiles of the incident bead (l) and emergent bead (r) beads in 15mm plate (power = 9kW)

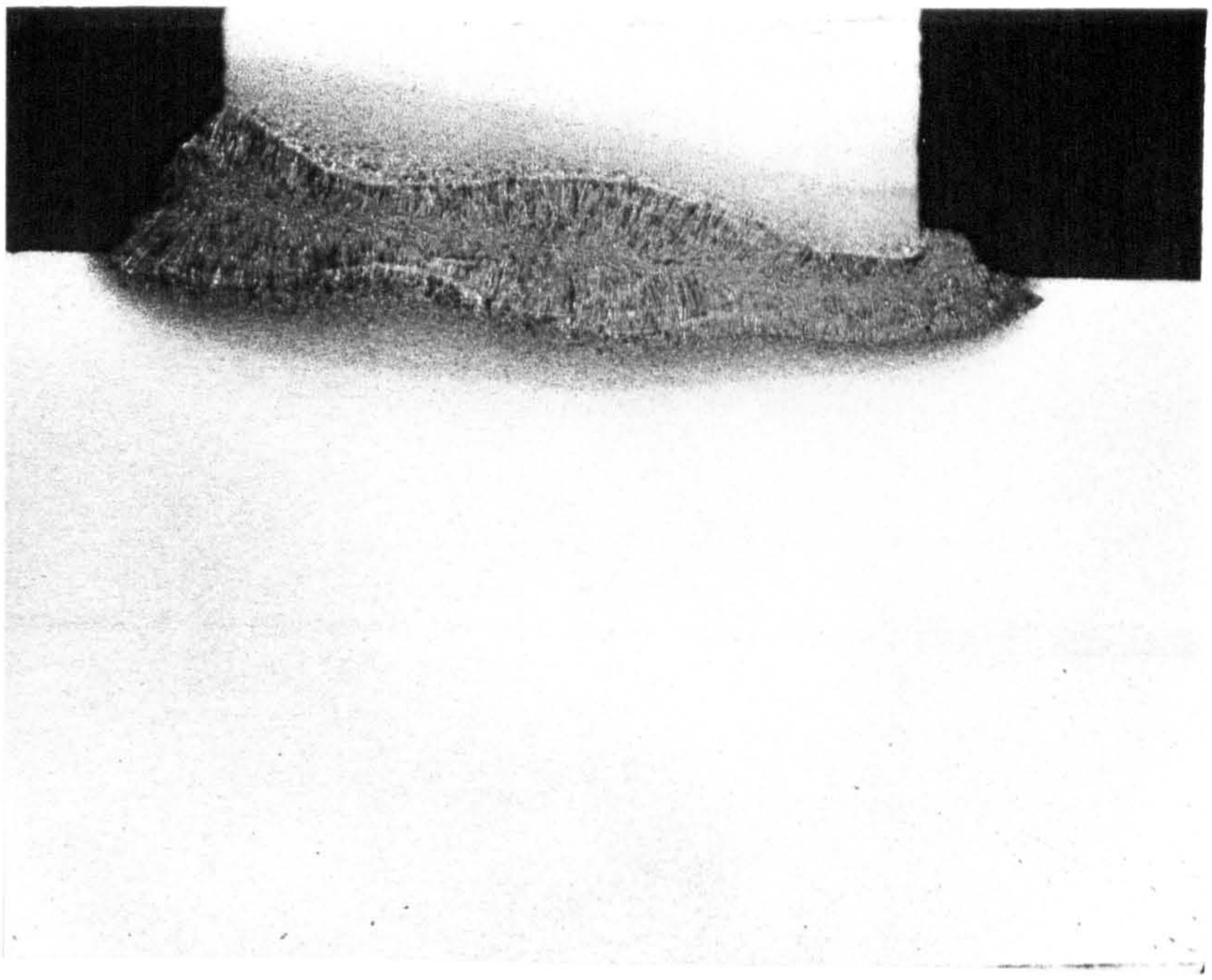

Figure B4.06b - Macrophoto (x4.8) of a skid weld in 15mm thick plate (power = 9kW)

B-2 COMPUTER PRINTOUT OF THE SKIDFILL SOURCE PROGRAM AND DATA

```
C ***************************************************************************
C *                  SOURCE CODE FOR THE LASER SKIDWELDING PROGRAM          *
C *                           - SKIDFILL -                                  *
C *                                        COPYRIGHT APRIL 1987 - SJB;UNUT;BS *
C ***************************************************************************
C
C     PROGRAM TO CALCULATE THE WIRE FILLER RATES REQUIRED FOR USE IN
C     LASER SKIDWELDING OF TEE SECTION JOINTS IN SHIPBUILDING
C
C     DATA IS INPUT FROM A DATA FILE LINKED TO CHANNEL 5 AND OUTPUT
C     VIA CHANNEL 6 TO A FILE OR SCREEN
C
C     DATA IS INPUT AND OUTPUT IN THE MOST WIDELY USED UNITS BUT
C     CONVERTED TO M,SEC,KG,W FOR CALCULATIONS.
C
C     MATERIAL THERMAL PROPERTIES ARE SET WITHIN THE PROGRAM AND IN
C     THIS VERSION ARE SET FOR APPLICATION IN MILD STEEL
C     ***************************************************************
C
      IMPLICIT REAL*8(A-H,O-Z)
      DIMENSION FW(10),GAP(10),WVOL(10),WMAS(10),TRAV(10),WDIA(5),POWP(5
     *),PLTHK(10)
C
CCC   ***************************************************************
CC    INPUT PLATE THICKNESSES(MM),LASER POWERS(KW),WELDING SPEEDS(MM/SEC)
CC    JOINT GAPS(MM),FILLER WIRE DIAMETERS(MM),PROJECTED WELD HEAT
CC    TRANSFER EFFICIENCY
CC    (%) AND THE RELEVENT NUMBERS OF EACH.
CC    ***************************************************************
C
      READ (5,1100)NPLTHK,PLTHK,RSR,NPOWP,POWP,NTRAV,TRAV,NGAP,GAP,NWDIA
     *,WDIA,EHT
1100  FORMAT (I2/10F6.2/F6.2/I2/5F6.2/I2/10F6.2/I2/10F6.2/I2/5F6.2/F6.2)
C
C
C
      WRITE (6,2090)
2090  FORMAT('1LASER SKID WELDING FILLER REQUIREMENT DATA CALCULATED USI
     *NG',/,' ***************************************************
     **')
      WRITE (6,2091)
2091  FORMAT(' THE SKIDFILL PROGRAM',/,' ************************')
C
      RSR=RSR/1000.0
C
      DO 3999 K=1,NPLTHK
      WRITE (6,2100) PLTHK(K)
2100  FORMAT(22HOPLATE THICKNESS (MM) ,F6.2)
      WRITE (6,2101)
2101  FORMAT(29HO****************************)
```

```
      IF (RSR .EQ. 0.0) GO TO 2105
      RSR=RSR*1000.0
      WRITE (6,2102) RSR
2102 FORMAT ('0ROLLED SECTION RADIUS (MM)',F6.2)
      RSR=RSR/10000.0
2105 CONTINUE
C
      DO 3999 I=1,NPOWP
C
      WRITE (6,2110) POWP(I)
2110 FORMAT(22H0LASER POWER-WP (KW)  ,F6.2)
      WRITE (6,2111)
2111 FORMAT(29H ============================)
C
C****SET MATERIAL THERMAL CONSTANTS FOR MILD STEEL PLATE
C
      POWP(I)=POWP(I)*1000.0
      PLTHK(K)=PLTHK(K)/1000.0
      TCON=41.0
      TDIF=9.1E-06
      VTC=4.5E 06
      AMTEMP=293.0
      DTEMP=1809.0

      DEN=7860.0
      SPHT=620.0
      LATF=250.0
      PI=22.0/7.0
C
C****CALCULATE THE BASE TEMPERATURE FUNCTION
C
      FTEMP3=1.0/(773.0-AMTEMP)+1.0/(1073.0-AMTEMP)
C
C****CALCULATE FUNCTION TO ACCOUNT FOR LATENT HEAT OF FUSION
C
      FLATF=1.0/(1-LATF/DTEMP)
C
C****CALCULATE MAXIMUM HEAT INPUT TO WELD
C
      DO 3900 J=1,NTRAV
      TRAV(J)=TRAV(J)/1000.0
      HI=POWP(I)/TRAV(J)
C
C****CALCULATE THE POTENTIAL WELD PENETRATION
C
      THKOP=DSQRT(HI*EHT*FTEMP3*FLATF/(2.0*VTC))
C
C****CALCULATE THE ASSOCIATED AREA OF THE MELT ZONE
C
      AM=POWP(I)*EHT*0.484*FLATF/(TRAV(J)*DEN*(SPHT*DTEMP+LATF))
C
C****CALCULATE THE AVERAGE WELD WIDTH(347)
C
      WID2=0.484*FLATF*TDIF*POWP(I)*EHT/(TRAV(J)*THKOP*TCON*DTEMP)
C
C****CALCULATE THE SIZE OF THE SMOOTHING BEADS WITH RESPECT OF THE AVAILABLE
C     PENETRATION
```

```
      WIDA=WID2
      BEDIN=WIDA
      BEDIN2=THKOP-PLTHK(K)
      IF (BEDIN2 .LT. BEDIN) BEDIN=BEDIN2
      IF (THKOP .GT. PLTHK(K)) GO TO 3400
      BEDIN=0.0
      BEDEM=0.0
      GO TO 3450
 3400 BEDEM=THKOP-PLTHK(K)-WIDA
      IF (BEDEM .LT. 0) BEDEM=0.0
      IF (BEDEM .GT. WIDA) BEDEM=WIDA
 3450 BEDTO=0.5*(BEDIN*BEDIN+BEDEM*BEDEM)
C
C****SET VARIABLES TO MM FOR PRINTING
C
      TRAV(J)=TRAV(J)*1000.0
      THKOP=THKOP*1000.0
      AM=AM*1000000.0
      WIDA=WIDA*1000.0
      BEDIN=BEDIN*1000.0
      BEDEM=BEDEM*1000.0
C
C****PRINT VARIABLES
C
      WRITE (6,2120) TRAV(J)
 2120 FORMAT(22H0TRAVERSE SPEED (MM/S),F6.2)
       WRITE (6,2121)
 121  FORMAT(29H ----------------------------)
      WRITE (6,2160) EHT
 2160 FORMAT(22H HEAT TRANS. EFF.     ,F6.2)
      WRITE (6,2170) AM
 2170 FORMAT(22H0MELT ZONE AREA (MM2) ,F6.2)
      WRITE (6,2180) THKOP
 2180 FORMAT(22H OPT. PENETRAT'N (MM) ,F6.2)
      WRITE (6,2190) WIDA
 2190 FORMAT(22H0AVE. MELT WIDTH (MM) ,F6.2)
      WRITE (6,2200) BEDIN
 2200 FORMAT(22H INCID.LEG LENGTH (MM),F6.2)
      WRITE (6,2210) BEDEM
 2210 FORMAT(22H EMERG.LEG LENGTH (MM),F6.2)
C
      TRAV(J)=TRAV(J)/1000.0
C
      DO 3800 M=1,NWDIA
      WRITE (6,2140) WDIA(M)
 2140 FORMAT(22H0WIRE DIAMETER (MM)   ,F6.2)
      WRITE (6,2141)
 2141 FORMAT(29H - - - - - - - - - - - - - )
      WDIA(M)=WDIA(M)/1000.0
C
C     ***************************************************************
C     CALCULATE THE FILLER RATE TACKING ACCOUNT OF THE JOINT GAP AREA,
C     PRODUCTION OF SMOOTHING BEADS FOR THE ASSOCIATED PLATE THICKNESS
C     AND THE POTENTIAL PENETRATION.
C     ***************************************************************
C                                  465
      DO 3700 N=1,NGAP
```

```
      GAP(N)=GAP(N)/1000.0
      FW(N)=0.0E+00
      WVOL(N)=0.0E00
      WMAS(N)=0.0E00
      FW(N)=4.0*TRAV(J)*(PLTHK(K)*GAP(N)+BEDTO+0.429*RSR*RSR)/(PI*WDIA(M
     *)*WDIA(M))
      WVOL(N)=FW(N)*(WDIA(M)*WDIA(M)/4.0)*60.0*60.0
      WMAS(N)=WVOL(N)*7850.0
C
      GAP(N)=GAP(N)*1000.0
      FW(N)=FW(N)*1000.0
C
3700 CONTINUE
C
C****PRINT FILLER RATES FOR RELEVENT JOINT GAPS
C
      WRITE (6,2130) (GAP(N),N=1,NGAP)
2130 FORMAT(22HOJOINT GAP  (MM)      ,10F7.2)
      WRITE (6,2215) (FW(N),N=1,NGAP)
2215 FORMAT(22H WIRE SPEED (MM/S)    ,10F7.2)
      WRITE (6,2220) (WMAS(N),N=1,NGAP)
2220 FORMAT(22H WIRE CONS'N   (KG/HR),10F7.2)
C
C****RESET DIMENSIONS FOR NEXT RUN
C
      WDIA(M)=WDIA(M)*1000.0
3800 CONTINUE
      TRAV(J)=TRAV(J)*1000.0
3900 CONTINUE
      PLTHK(K)=PLTHK(K)*1000.0
      POWP(I)=POWP(I)/1000.0
3999 CONTINUE
      STOP
      END
C*************************************************************************
```

Listing of SKIDFILLD at 12:49:13 on MAR 11, 1987 for CCid=NVC9

```
     1      01
     2      08.0
     3      1.0
     4      01
     5      09.00
     6      03
     7      10.00 14.00 17.50
     8      04
     9      00.25 00.50 01.00 02.00
    10      01
    11      1.6
    12      0.50
```

B-2.1 Computed printout of an example output of the SKIDFILL program

```
LASER SKID WELDING FILLER REQUIREMENT DATA CALCULATED USING
**********************************************************
THE SKIDFILL PROGRAM
**********************

PLATE THICKNESS (MM)    8.00

*********************************

ROLLED SECTION RADIUS (MM)  1.00

LASER POWER-WP (KW)     9.00
============================

TRAVERSE SPEED (MM/S) 10.00
---------------------------
HEAT TRANS. EFF.        0.50

MELT ZONE AREA (MM2)   28.66
OPT. PENETRAT'N (MM)   13.97

AVE. MELT WIDTH (MM)    2.22
INCID.LEG LENGTH (MM)   2.22
EMERG.LEG LENGTH (MM)   2.22

WIRE DIAMETER (MM)      1.60
- - - - - - - - - - - - - -

JOINT GAP  (MM)          0.25   0.50   1.00   2.00
WIRE SPEED (MM/S)       34.45  44.39  64.28 104.05
WIRE CONS'N   (KG/HR)    0.62   0.80   1.16   1.88

TRAVERSE SPEED (MM/S) 14.00
---------------------------
HEAT TRANS. EFF.        0.50

MELT ZONE AREA (MM2)   20.47
OPT. PENETRAT'N (MM)   11.81

AVE. MELT WIDTH (MM)    1.88
INCID.LEG LENGTH (MM)   1.88
EMERG.LEG LENGTH (MM)   1.88

WIRE DIAMETER (MM)      1.60
- - - - - - - - - - - - - -

JOINT GAP  (MM)          0.25   0.50   1.00   2.00
WIRE SPEED (MM/S)       38.43  52.35  80.19 135.87
WIRE CONS'N   (KG/HR)    0.70   0.95   1.45   2.46
```

B-3 COMPUTER PRINTOUT OF THE SKIDWELD SOURCE PROGRAM AND DATA

```
C ***************************************************************************
C *              SOURCE CODE FOR THE LASER SKIDWELDING PROGRAM              *
C *                                                                         *
C *                          - SKIDWELD -                                   *
C *                                                                         *
C *                                  COPYRIGHT APRIL 1987 - SJB;UNUT;BS*
C ***************************************************************************
C
C     PROGRAM TO PRESENT A GUIDE TO THE INITIAL PARAMETERS TO BE USED
C     FOR SKID WELDING ON SHIP PRODUCTION JOINT CONFIGURATIONS. IT
C     IS BASED ON INTERPOLATIONS FROM THE RESULTS OF SKID WELDING
C     TRIALS USING A CL10 10KW LASER
C     ***************************************************************
C
      IMPLICIT REAL*8 (A-H,O-Z)
      DIMENSION THK(6),TRAV0(9),TRAV5(9),TRAV1(9),TRAV2(9),POW(6),SPOT0(
     *6),HTE(6)
C
C     ***************************************************************
C     READ IN SOURCE DATA FROM DATA FILE CONNECTED TO CHANNEL 0
C     ***************************************************************
C
      READ (0,1100) THK,TRAV0,TRAV5,TRAV1,TRAV2,POW,SPOT0,HTE
1100  FORMAT (6F6.2/9F6.2/9F6.2/9F6.2/9F6.2/6F6.2/6F6.2/6F6.2)
C
C     ***************************************************************
C     INPUT ALL JOINT PARTICULARS AND TEST IF WITHIN PROGRAM LIMITS
C     ***************************************************************
C
      WRITE (6,1500)
1500  FORMAT('1**********************************************************
     **********')
      WRITE (6,1505)
1505  FORMAT('0                         SKIDWELD')
      WRITE (6,1506)
1506  FORMAT('                          ========')
      WRITE (6,1510)
1510  FORMAT('0INTERACTIVE PROGRAM TO DETERMINE THE INITIAL PROCESSING
     *PARAMETERS',/,' FOR HIGH POWER LASER SKID WELDING OF TEE SECTION
     *JOINTS IN SHIP',/,'PRODUCTION')
      WRITE (6,1520)
1520  FORMAT('0**********************************************************
     **********')
C
      WRITE (6,2050)
2050  FORMAT ('0AFTER EACH VARIABLE INPUT, PLEASE PRESS "RETURN"')
 300  WRITE (6,2055)
2055  FORMAT ('0JOINT SCANTLING AND CONFIGURATIONS>>>>>>>>')
      WRITE (6,2056)
2056  FORMAT (' ------------------------------------')
C
      WRITE (6,2100)
2100  FORMAT ('0ENTER WEB PLATE THICKNESS(MM)',/,'?')
      READ (6,*) TK
```

```
      IF ((TK .LT. 3.0) .OR. (TK .GT. 15.0)) GO TO 3500
C
      WRITE (6,2200)
2200 FORMAT ('0ENTER JOINT GAP(MM)',/,'?')
      READ (6,*) GAP
      IF (GAP .GT. 2.0) GO TO 3500
C
      PRIM=1.0
      WRITE (6,2220)
2220 FORMAT('0IF PRIMED PLATE ENTER  "1",  IF NOT ENTER  "0"',/,'?')
      READ (6,*)PR
      IF (PR .EQ. 1.0) PRIM=0.8
C
      ROL=0.0
      WRITE (6,2230)
2230 FORMAT('0IF R.S. WEB PLATE ENTER  "1", IF SQUARE EDGE FLAT PLATE E
     *NTER "0"',/,'?')
      READ (6,*) ROL
      IF (ROL .EQ. 0.0) GO TO 3200
      WRITE (6,2240)
2240 FORMAT ('0ENTER APPROX. RADIUS OF WEB PLATE EDGE CORNERS (MM)',/,'
     *?')
      READ (6,*) ROL
3200 CONTINUE
C
      PO=0.0
      WRITE (6,2255)
2255 FORMAT('1REQUIREMENTS OF LASER POWER (AT THE WORK PIECE)>>>>>>')
      WRITE (6,2256)
2256 FORMAT(' ------------------------------------------------')
      WRITE (6,2260)
2260 FORMAT('0IF 9KW ENTER "9", IF ADVISED POWER REQUIRED ENTER "0"',/,
     *'?')
      READ (6,*) PO
      IF (PO .EQ. 9.0) GO TO 3300
      CALL IPOL(THK,POW,TK,PO)
3300 CONTINUE
C
      CALL IPOL(THK,HTE,TK,HE)
C
      WRITE (6,2270)
2270 FORMAT ('1FILLER WIRE INPUT REQUIREMENTS>>>>')
      WRITE (6,2271)
2271 FORMAT (' ---------------------------------')
      WRITE (6,2275)
2275 FORMAT ('0ENTER FILLER WIRE DIAMETER (MM)',/,'?')
      READ (6,*) FILD
C
C     ****************************************************************
C     CALCULATION OF INTERPOLATED PARAMETER VALUES
C     ****************************************************************
C
      IF (GAP .GT. 0.5) GO TO 3400
      CALL IPOL(THK,TRAV0,TK,TR)
      TKL=TRAV5(7)
      TKRU=TRAV5(8)
```

```
      TKU=TRAV5(9)
      GO TO 3425
 3400 IF (GAP .GT. 1.0) GO TO 3420
      CALL IPOL(THK,TRAV5,TK,TR5)
      CALL IPOL(THK,TRAV1,TK,TR1)
      A=0.5
      B=1.0
      CALL IPOL2(A,B,TR5,TR1,GAP,TR)
      CALL IPOL2(A,B,TRAV5(7),TRAV1(7),GAP,TKL)
      CALL IPOL2(A,B,TRAV5(8),TRAV1(8),GAP,TKRU)
      CALL IPOL2(A,B,TRAV5(9),TRAV1(9),GAP,TKU)
      GO TO 3425
 3420 IF (GAP .GT. 2.0) GO TO 3500
      CALL IPOL(THK,TRAV1,TK,TR1)
      CALL IPOL(THK,TRAV2,TK,TR2)
      A=1.0
      B=2.0
      CALL IPOL2(A,B,TR1,TR2,GAP,TR)
      CALL IPOL2(A,B,TRAV1(7),TRAV2(7),GAP,TKL)
      CALL IPOL2(A,B,TRAV1(8),TRAV2(8),GAP,TKRU)
      CALL IPOL2(A,B,TRAV1(9),TRAV2(9),GAP,TKU)
 3425 CONTINUE
C
      IF  ((TK .LT. TKL) .OR. (TK .GT. TKU)) GO TO 3500
      IF  ((ROL .EQ. 1.0) .AND. (TK .GT. TKRU)) GO TO 3500
C
      IF (PRIM .EQ. 0.8) TR=TR*0.8
C
      IF (GAP .GT. FILD) GO TO 3430
      CALL IPOL(THK,SPOT0,TK,SH0)
      GO TO 3435
 3430 SH0=GAP*0.5
 3435 CONTINUE
C
      CALL FILLY(TK,PO,TR,GAP,ROL,FILD,HE,FR)
C
      ANG=7.0
C
      SJET=0.0
      SLEN=35.0
      STAL=0.0
C
C     **********************************************************************
C     OUTPUT - WELDING PARAMETERS
C     **********************************************************************
C
      WRITE (6,1500)
      WRITE (6,2500)
 2500 FORMAT('0             SKID WELDING PARAMETERS')
      WRITE (6,2501)
 2501 FORMAT('              ========================')
C
      WRITE (6,2510)
 2510 FORMAT('0SUMMARY OF INPUT VARIABLES',/,'==========================
     *==')
      WRITE (6,2520)
 2520 FORMAT('0 WEB PL.   JOINT    LASER   ROLL SEC. SURFACE    WIRE ')
```

```
      WRITE (6,2521)
 2521 FORMAT(' THICKNESS   GAP      POWER     RADIUS     COAT       DIA. ')
      WRITE (6,2522)
 2522 FORMAT('    (MM)       (MM)      (KW)      (MM)                (MM)')
      WRITE (6,2523)
 2523 FORMAT(' ------------------------------------------------------')
      IF (PRIM .NE. 1.0) GO TO 3450

      WRITE (6,2530) TK,GAP,PO,ROL,FILD
 2530 FORMAT (1H ,F6.2,4X,F6.2,3X,F6.2,3X,F6.2,5X,'CLEAN',3X,F6.2)
      GO TO 3451
 3450 WRITE (6,2535) TK,GAP,PO,ROL,FILD
 2535 FORMAT (1H ,F6.2,4X,F6.2,3X,F6.2,3X,F6.2,4X,'PRIMED',3X,F6.2)
 3451 CONTINUE

C
      WRITE (6,2550)
 2550 FORMAT('0INITIAL PARAMETERS REQUIRED FOR SKID WELDING')
      WRITE (6,2551)
 2551 FORMAT(' ========================================')
      WRITE (6,2560)
 2560 FORMAT ('0TRAVERSE   SPOT   INCIDENT   FILLER    PLASMA   LENSE
     *TRAIL')
      WRITE (6,2561)
 2561 FORMAT ('  SPEED    HEIGHT    ANGLE     RATE      JET     SHROUD
     *SHROUD')
      WRITE (6,2562)
 2562 FORMAT (' (MM/SEC)   (MM)    (DEGREE)  (MM/SEC)  (L/MIN)  (L/MIN)
     *(L/MIN)')
      WRITE (6,2565)
 2565 FORMAT (' ------------------------------------------------------
     *-------')
      WRITE (6,2670)TR,SHO,ANG,FR,SJET,SLEN,STAL
 2670 FORMAT (1H ,F6.2,3X,F6.2,2X,F6.2,7X,F6.2,2X,F6.2,4X,F6.2,2X,F6.2)
      GO TO 3800
C
C     ***************************************************************
C     OUTPUT - WARNINGS
C     ***************************************************************
C
 3500 WRITE (6,2800)
 2800 FORMAT('1WARNINGS OF POTENTIAL LIMITS TO THE SKID WELDING PROCESS'
     *,/,' ==========================================')
C
      IF ((TK .GE. 3.0) .AND. (TK .LE. 15.0)) GO TO 3520
      WRITE (6,2810)
 2810 FORMAT ('0FURTHER DEVELOPMENT WORK IS NECESSARY FOR WELDING WITH T
     *HE',/,' WEB PLATE THICKNESS REQUESTED')
      GO TO 3800
C
 3520 IF (GAP .LE. 2.0) GO TO 3580
      WRITE (6,2820)
 2820 FORMAT ('0FURTHER DEVELOPMENT WORK IS NECESSARY FOR WELDING WITH T
     *HE',/,' JOINT GAP REQUESTED')
      GO TO 3800
C
 3580 IF (PO .NE. 9.0) GO TO 3690
```

```
C
      IF (TK .GT. TKL) GO TO 3600
      WRITE (6,2850)
2850 FORMAT('0WEB PLATE TOO THIN FOR 9KW(W.P.), RE-RUN WITH "ADVISED" P
     *OWER')
      GO TO 3690
3600 IF ((ROL .EQ. 1.0) .AND. (TK .GT. TKRU)) GO TO 3610
      IF (TK .LT. TKU) GO TO 3690
3610 WRITE (6,2860)
2860 FORMAT('0WEB PLATE TOO THICK FOR 9KW(W.P.), RE-RUN WITH "ADVISED"
     *POWER')
3690 CONTINUE
C
3800 CONTINUE
      WRITE (6,2900)
2900 FORMAT ('1TO RE-RUN THE PROGRAM ENTER 1; TO EXIT , ENTER 0')
      READ (6,*) E
      IF (E .GT. 0.5) GO TO 300
C
      STOP
      END
C
C     ****************************************************************
C     *                        SUBROUTINES                           *
C     ****************************************************************
C
C
C     ****************************************************************
C     *                  SUBROUTINE - FILLY                          *
C     ****************************************************************
C
C     DATA IS INPUT AND OUTPUT USING THE MOST WIDELY USED UNITS BUT
C     CONVERTED TO M,KG,JOULES FOR THE CALCULATIONS.
C     INPUT PLATE THICKNESS(MM),LASER POWER(KW),WELDING SPEED(MM/SEC),
C     JOINT GAP(MM),FILLER WIRE DIAMETER(MM),PROJECTED WELD HEAT TRANSFER
C     EFFICIENCY(%).
C     ****************************************************************
C
      SUBROUTINE FILLY(PLTHK,POWP,TRAV,GAP,R,WDIA,EHT,FW)
      IMPLICIT REAL*8(A-H,O-Z)
C
C     SET MATERIAL THERMAL CONSTANTS
C
      POWP=POWP*1000.0
      PLTHK=PLTHK/1000.0
      R=R/1000.0
      TCON=41.0
      TDIF=9.1E-06
      VTC=4.5E 06
      AMTEMP=293.0
      DTEMP=1809.0
      DEN=7860.0
      SPHT=620.0
      LATF=250.0
      PI=22.0/7.0
```

```
C
C****CALCULATE THE BASE TEMPERATURE FUNCTION
C
      FTEMP3=1.0/(773.0-AMTEMP)+1.0/(1073.0-AMTEMP)
C
C****CALCULATE FUNCTION TO ACCOUNT FOR LATENT HEAT OF FUSION
C
      FLATF=1.0/(1-LATF/DTEMP)
C
C****CALCULATE MAXIMUM HEAT INPUT TO WELD
C
      TRAV=TRAV/1000.0
      HI=POWP/TRAV
C
C****CALCULATE THE POTENTIAL WELD PENETRATION
C
      THKOP=DSQRT(HI*EHT*FTEMP3*FLATF/(2.0*VTC))
C
C****CALCULATE THE ASSOCIATED AREA OF THE MELT ZONE
C
      AM=POWP*EHT*0.484*FLATF/(TRAV*DEN*(SPHT*DTEMP+LATF))
C
C****CALCULATE THE AVERAGE WELD WIDTH [347]
C
      WID2=0.484*FLATF*TDIF*POWP*EHT/(TRAV*THKOP*TCON*DTEMP)
C
C****CALCULATE THE SIZE OF THE SMOOTHING BEADS WITH RESPECT OF THE AVAILABLE
C     PENETRATION
C
      WIDA=WID2
      BEDIN=WIDA
      BEDIN2=THKOP-PLTHK
      IF (BEDIN2 .LT. BEDIN) BEDIN=BEDIN2
      IF (THKOP .GT. PLTHK) GO TO 3400
      BEDIN=0.0
      BEDEM=0.0
      GO TO 3450
3400  BEDEM=THKOP-PLTHK-WIDA
      IF (BEDEM .LT. 0) BEDEM=0.0
      IF (BEDEM .GT. WIDA) BEDEM=WIDA
3450  BEDTO=0.5*(BEDIN*BEDIN+BEDEM*BEDEM)
C
C****SET VARIABLES TO MM FOR PRINTING
C
      TRAV=TRAV*1000.0
      THKOP=THKOP*1000.0
      AM=AM*1000000.0
      WIDA=WIDA*1000.0
      BEDIN=BEDIN*1000.0
      BEDEM=BEDEM*1000.0
C
      TRAV=TRAV/1000.0
      WDIA=WDIA/1000.0
```

```
C
C****CALCULATE THE FILLER RATE
C
      GAP=GAP/1000.0
      FW=4.0*TRAV*(PLTHK*GAP+BEDTO+0.429*R*R)/(PI*WDIA*WDIA)
      WVOL=FW*(WDIA*WDIA/4.0)*60.0*60.0
      WMAS=WVOL*7850.0
C
      TRAV=TRAV*1000.0
      GAP=GAP*1000.0
      FW=FW*1000.0
      PLTHK=PLTHK*1000.0
      POWP=POWP/1000.0
      R=R*1000.0
      WDIA=WDIA*1000.0
C
      RETURN
      END
C*************************************************************************
```

Listing of SKIDWELD at 15:49:33 on FEB 13, 1987 for CCid=NVC9

1	3.0	6.0	8.00	10.0	12.0	15.0			
2	25.0	17.5	14.0	10.0	8.0	6.0	6.0	15.0	15.0
3	25.0	17.5	14.0	10.0	8.0	6.0	6.0	15.0	15.0
4	17.5	17.5	12.0	8.0	6.0	4.0	6.0	10.0	12.0
5	16.0	14.0	8.0	6.0	6.0	4.0	6.0	8.0	10.0
6	5.0	7.0	9.0	10.0	12.0	14.0			
7	0.50	0.75	0.88	1.00	1.13	1.13			
8	0.5	0.5	0.5	0.5	0.5	0.5			

Appendix C

APPENDICES ASSOCIATED WITH CHAPTER 5

C-1 DISCUSSION NOTES SUBMITTED BY LLOYDS REGISTER OF SHIPPING

Lloyd's Register of Shipping

71 Fenchurch Street, London, EC3M 4BS

Telephone 01-709 9166 Telex 888379 Cables Committee, London EC3

Please address further communications to The Secretary, and quote

Our Ref TSG/R/2344/PHRL

Your Ref SJB/KL

Date 18th October, 1984.

The University of Newcastle Upon Tyne,
Department of Naval Architecture
& Shipbuilding,
Armstrong Building,
The University,
Newcastle Upon Tyne,
NE1 7RU.

Attention: Mr. S.J. Brooke.

Dear Sir,

Laser Welding.

During your visit to this office on 26th July, 1984 you asked for advice on the extent to which the Society would require additional tests to explore the influence of practical process variables. The enclosed notes are proposed as a basis for discussion.

Yours faithfully,

N. Bennell

For the Secretary.

LASER WELDING

Consideration of "Procedure Tests."

1. The factors which could be expected to vary, in a way to alter the significant properties of a joint between plating and stiffener are:

   - Fit-up, plate to stiffener. As a practical range this could vary from 0 to 2 mm.

   - Alignment of joint with laser beam. It is assumed that the laser and associated optical train are mounted in a suitably rigid manner. The joint could be subject to a similar tolerance to fit-up, but probably in both directions, say ±2 mm.

   - Wire feed speed. Presumably an adapted MIG unit is being used, variation on speed is probably around ±10% (The MIG process does not call for very precise wire feed speeds).

   - Laser power
   - Welding speed

) These two factors probably do not suffer from large random variations - only errors in setting up are likely to cause divergence from established values.

2. Variations in fit-up and in wire feed speed would have similar effects, both resulting in a change in the size, and perhaps consequentially in the shape, of the external weld beads. The influence of variations in these factors could be explored by making welds at maximum gap combined with minimum wire feed speed, and with no gap and maximum wire feed speed. Shape could be assessed at intervals along each side of the weld, measuring undercut on each leg, and the external angle between the plate surface and the tangent to the weld head at the toe. (Possible limiting values of these characteristics could be 0,5 mm undercut and min. 115° or 120° for the angle at the toe). Subsequently a fatigue S-N curve could be obtained for a weld showing the worst shape.

./..

3. Misalignment between the joint and the laser beam will result in a reduction in the proportion of the thickness of the stiffener that is actually welded. This could be checked either by sectioning, or probably an assessment of a length of weld could be obtained by knocking the stiffener off the plate by hammer blows in the direction against the laser beam. Partial penetration could be accepted only for a limited length for one defect, and for a limited proportion of the total weld length. The limits would have to be set in the light of further experience with the process, and test results. As a preliminary indication of order of magnitude, the following could be taken as a starting point: minimum penetration 60% of the plate thickness of the stiffener; maximum individual length of lack of penetration, exceeding 10% of the plate thickness of the stiffener, 10cm; maximum proportion of total length showing such lack of penetration 10%. In regard to the maximum individual length, the usual condition for two adjacent defects would apply, namely that two defects closer together than the length of the longer are to be considered as a single defect of length equal to the distance between the extremities of the two defects.

   Further consideration of the limits could be given in the light of fatigue and static test results on welds showing defects.

4. Static tests should be conducted to demonstrate that for a given lack of penetration the transverse bending strength of the laser skid weld is not less than the lower of that for a rule continuous double fillet weld, or the bending strength of the stiffener. These tests should be conducted at room temperature, and also preferably at reduced temperatures, and the specimens should be loaded such that the back side of the weld is in tension.

./..

5. There are some indications that the impact strength of laser welds of the type being considered is less than that required by the Society for welding consumables even of the lowest grade. A Charpy transition curve should be established. The specimens could be prepared from a cruciform weldment. If the stiffeners were 8mm thick a subsidiary standard specimen 5mm thick could be obtained. The notch root would be in the weld.

15th October 1984

C-2 TENSILE TEST RESULTS

Plate th'kness (mm)	Carbon equivalent (Kihara)	Ultimate tensile strength (N/mm2)	Failure position	Defects
3	0.434	435.2 363.4	Web/fusion line	)Non visible)excessive .misalignment of webs
6	0.370	486.0 382.4	Parent plate	
8	0.300	455.0 464.0 479.0 476.0 483.0 457.0	Parent plate	
	0.369	467.0		
	0.512	369.0	Web/fusion line	
10	0.267	452.0 450.0	Parent plate	
12	0.444	509.0 502.1	Parent plate	Tearing from a crack
	0.371	423.6		
15	0.337	405.0 422.9	Parent plate	Lack of fusion

Table C5.01 -Results of cruciform tensile tests on laser skid welds

C-3 CHARPY TESTING TRANSITION RESULTS - VARIOUS PLATE THICKNESS

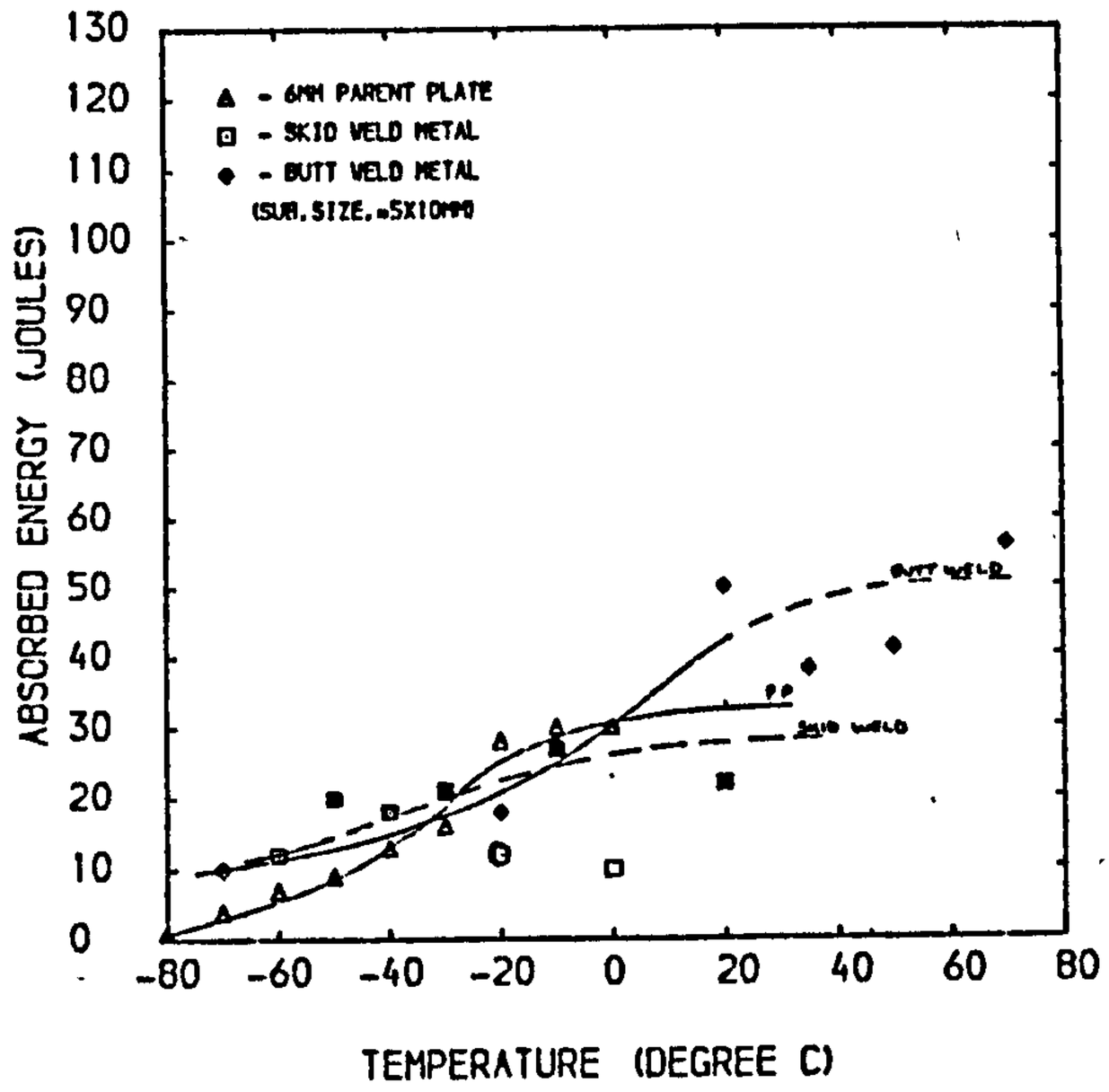

Figure C5.01a - Charpy transition curves for butt and skid weld metal : 6mm plate , A31 filler wire.

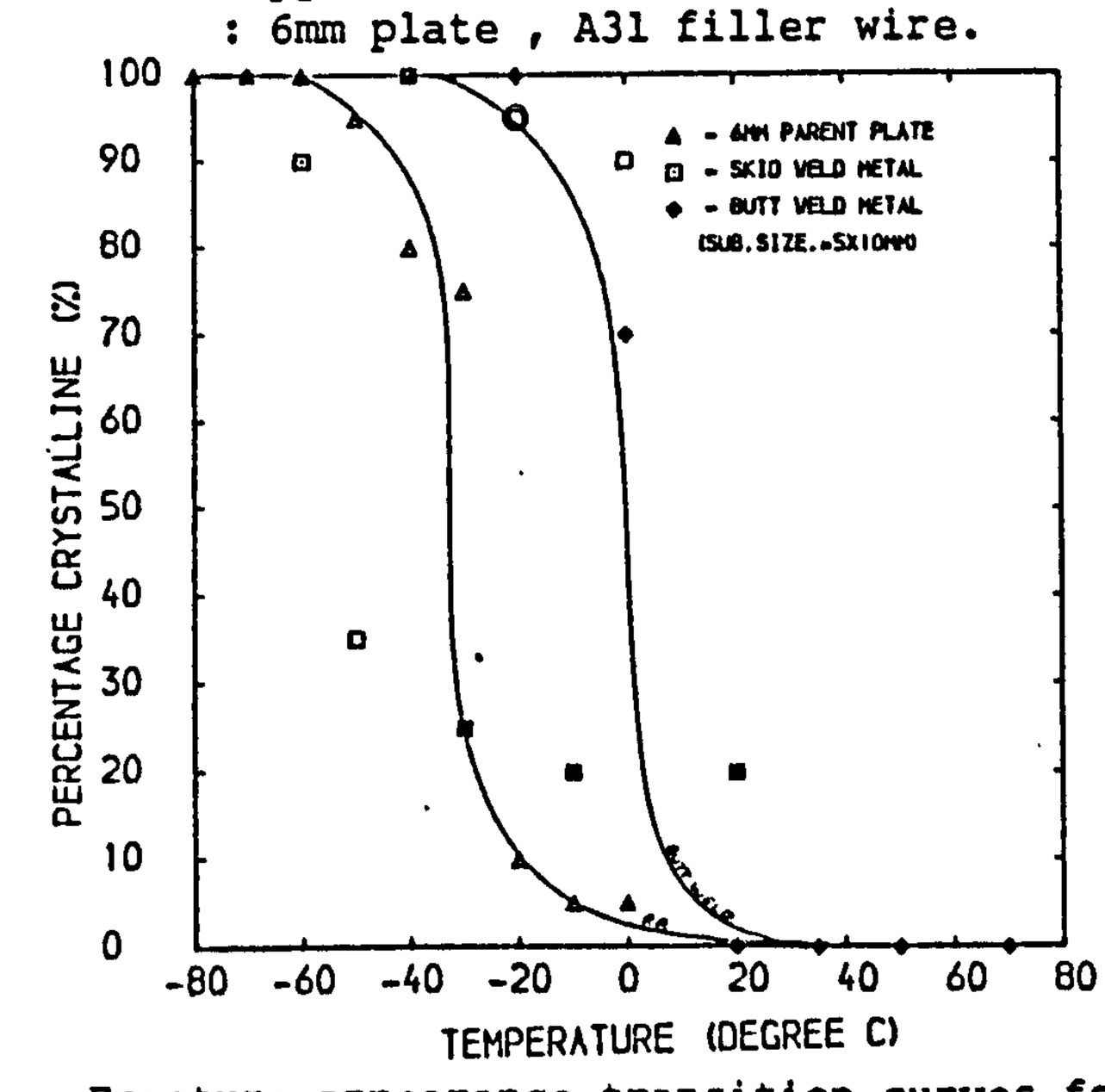

Figure C5.01b - Fracture appearance transition curves for butt and skid weld metal : 6mm plate, A31 filler wire

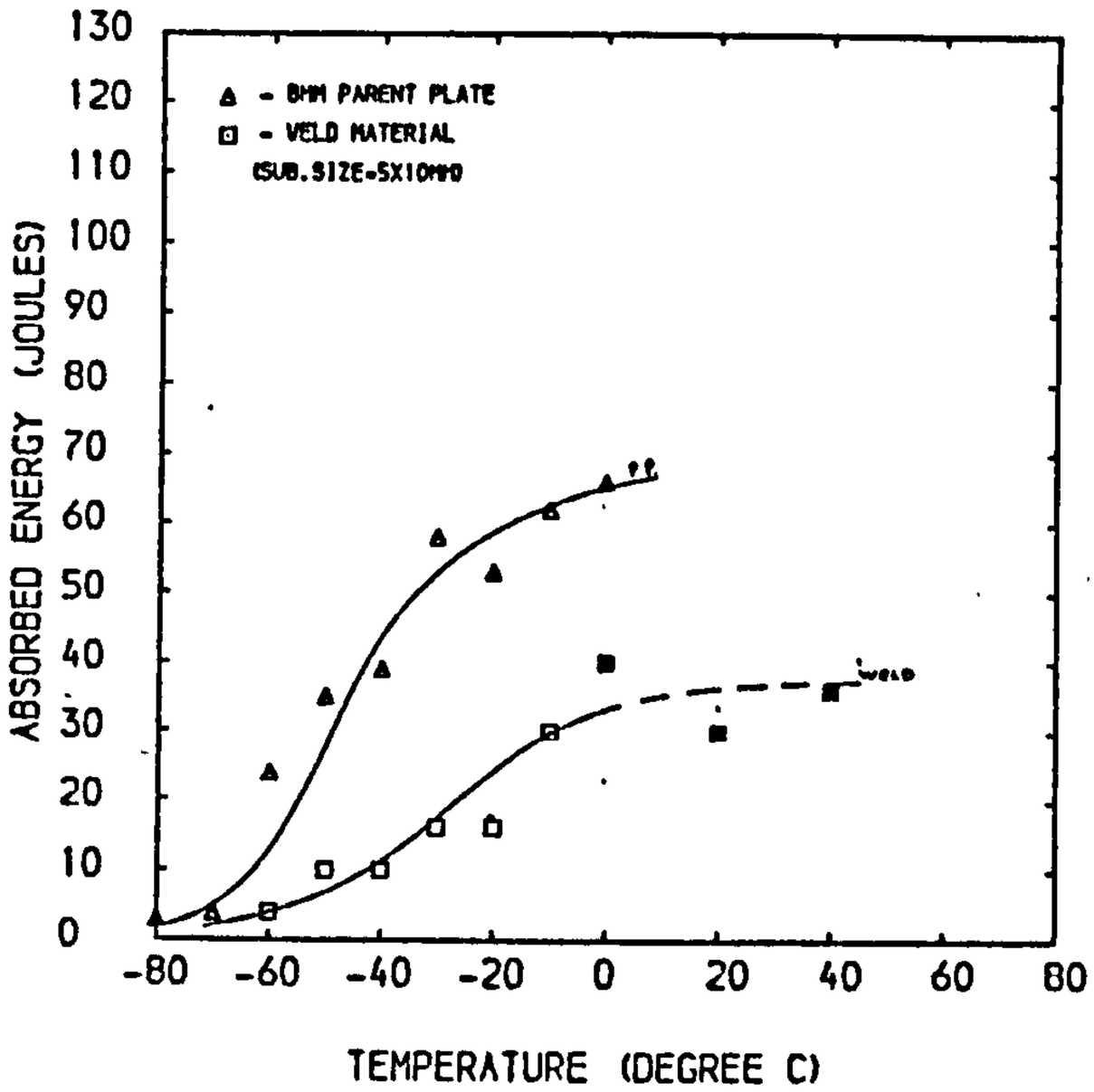

Figure C5.01c - Charpy transition curves for skid weld metal : 8mm plate, A31 filler wire.

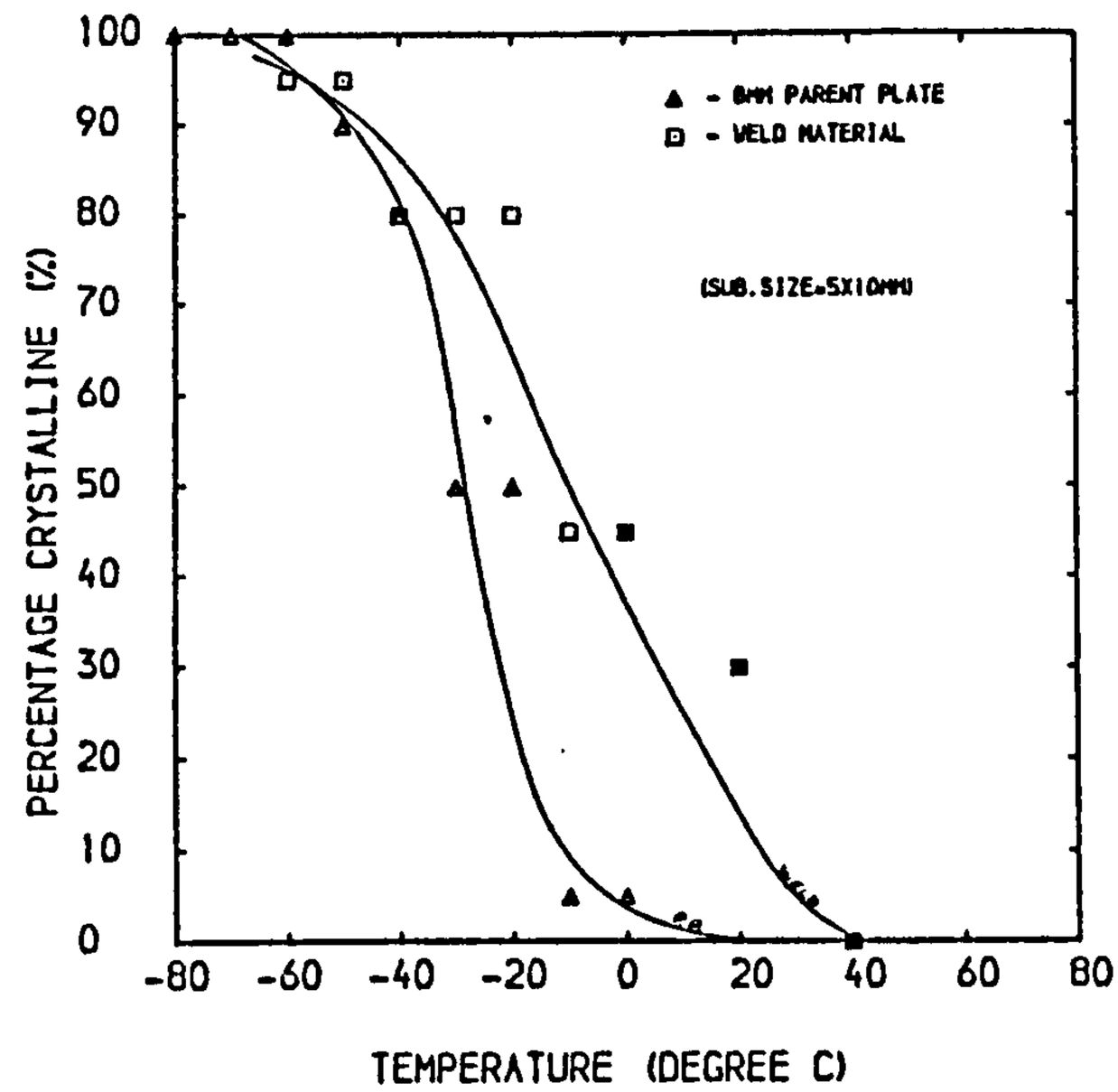

Figure C5.01d - Fracture appearance transition curves for skid weld metal : 8mm plate, A31 filler wire.

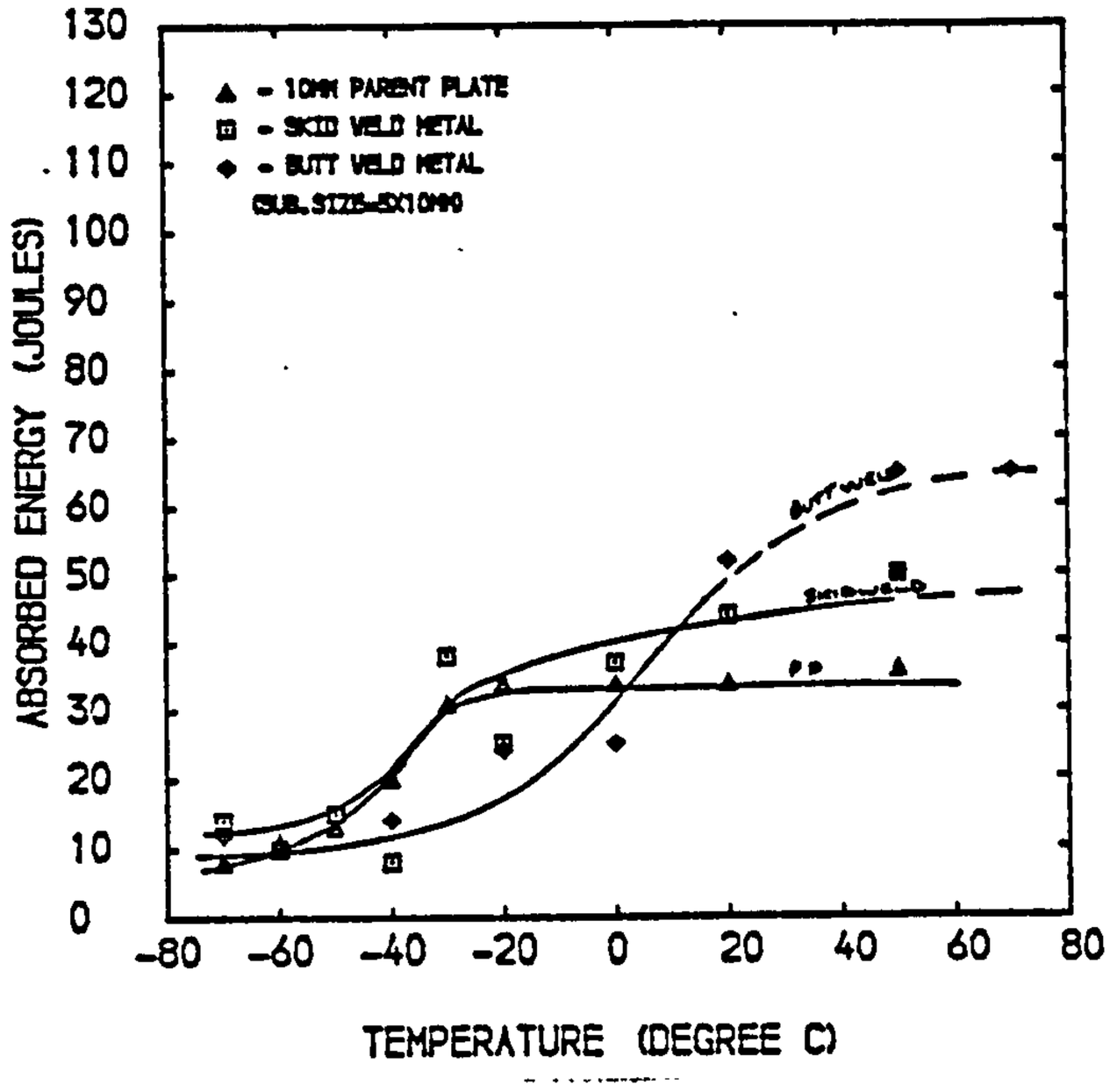

Figure C5.01e - Charpy transition curves for butt and skid weld metal :10mm plate , A31 filler wire.

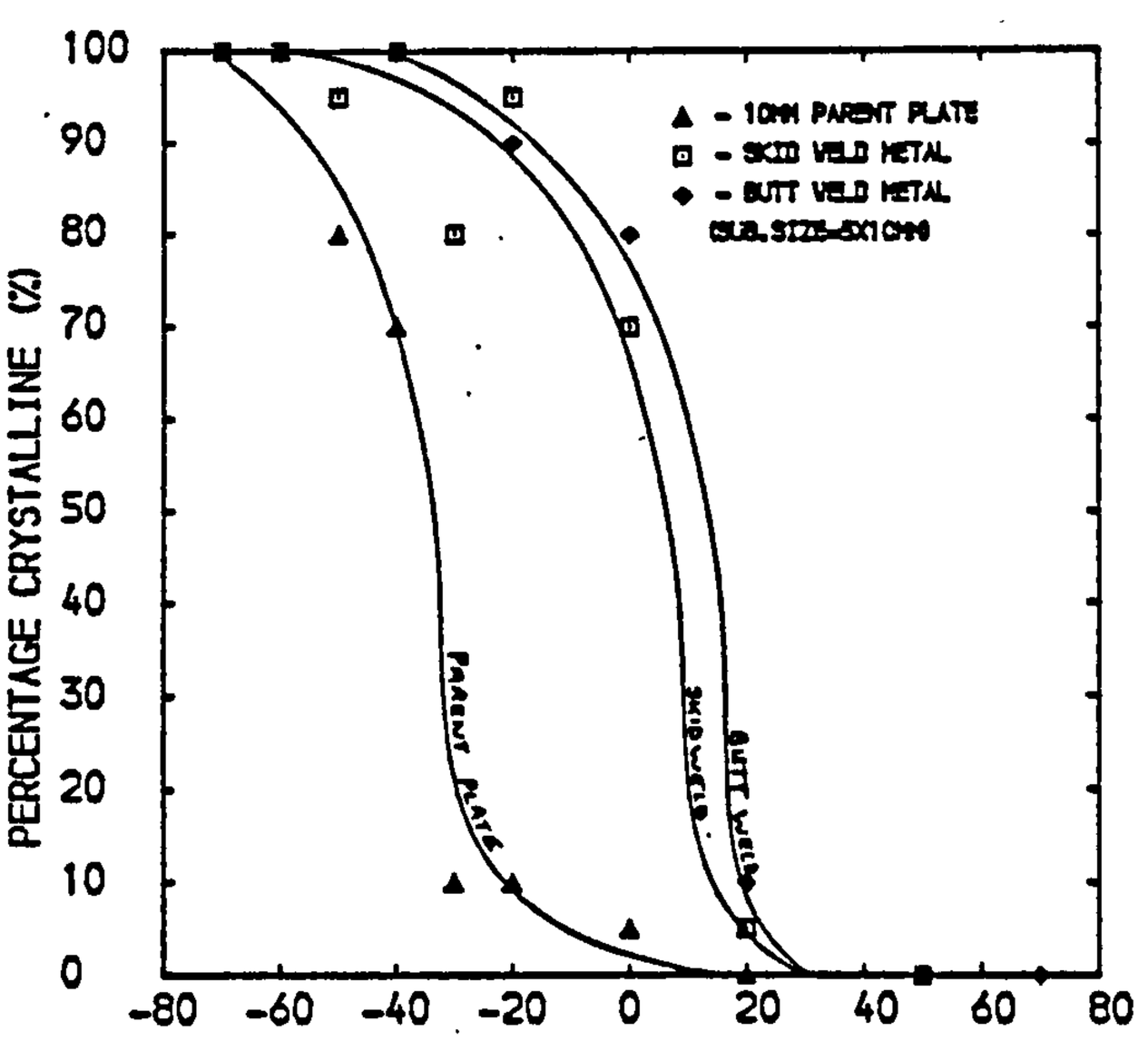

Figure C5.01f - Fracture appearance transition curves for butt and skid weld metal :10mm plate, A31 filler wire

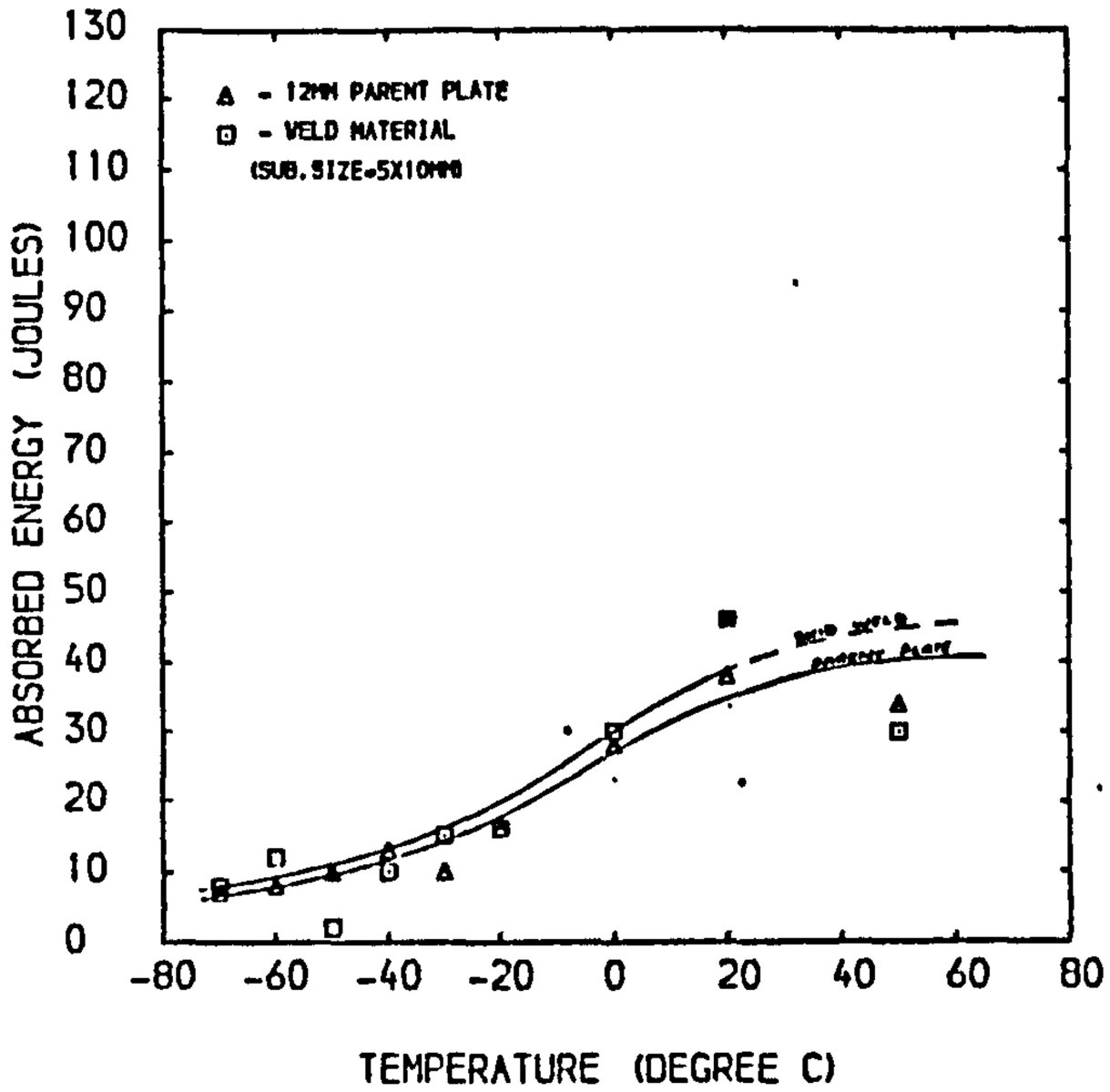

Figure C5.01g - Charpy transition curves for skid weld metal :12mm plate , A31 filler wire.

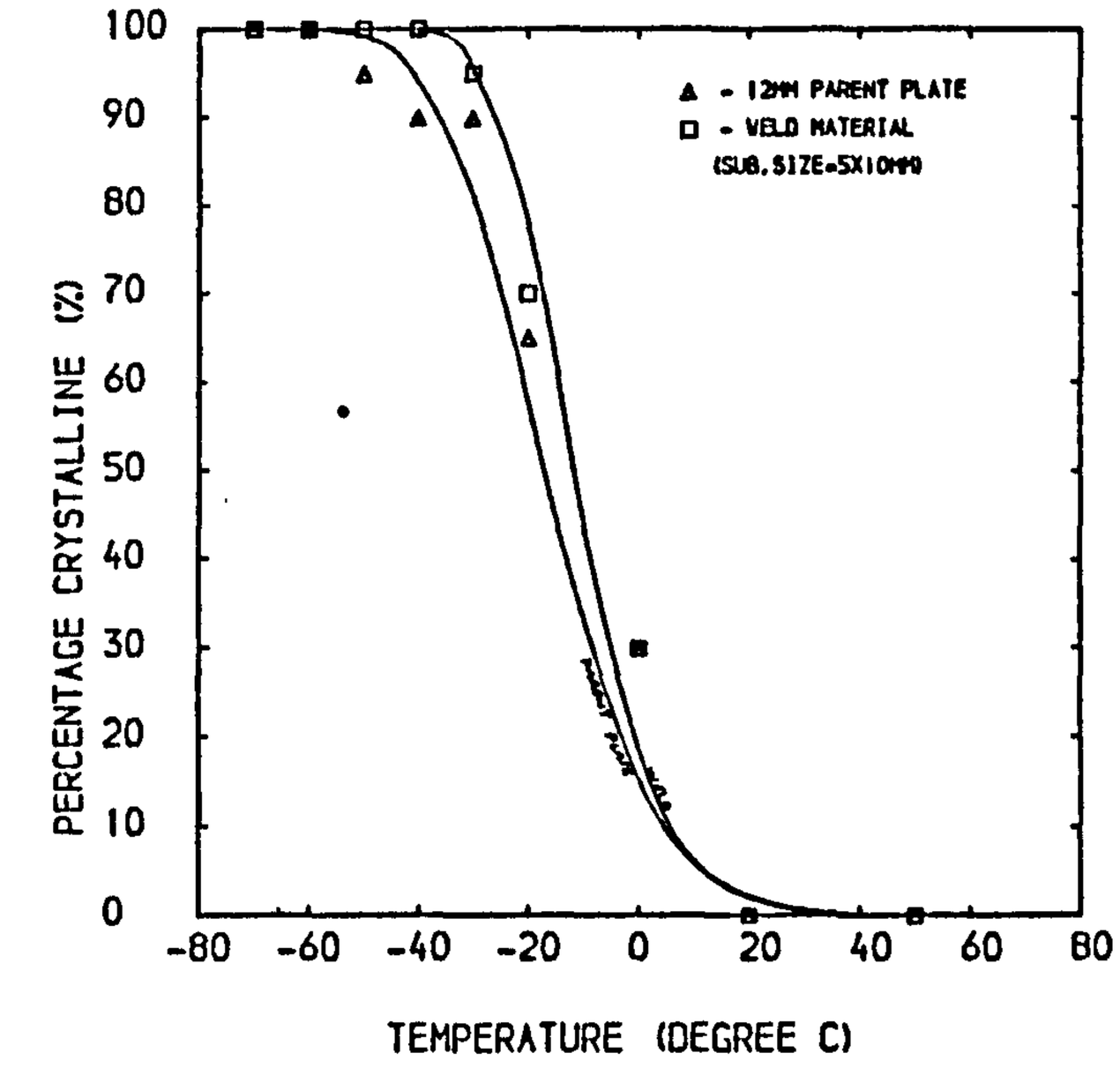

Figure C5.01h - Fracture appearance transition curves for skid weld metal :12mm plate, A31 filler wire

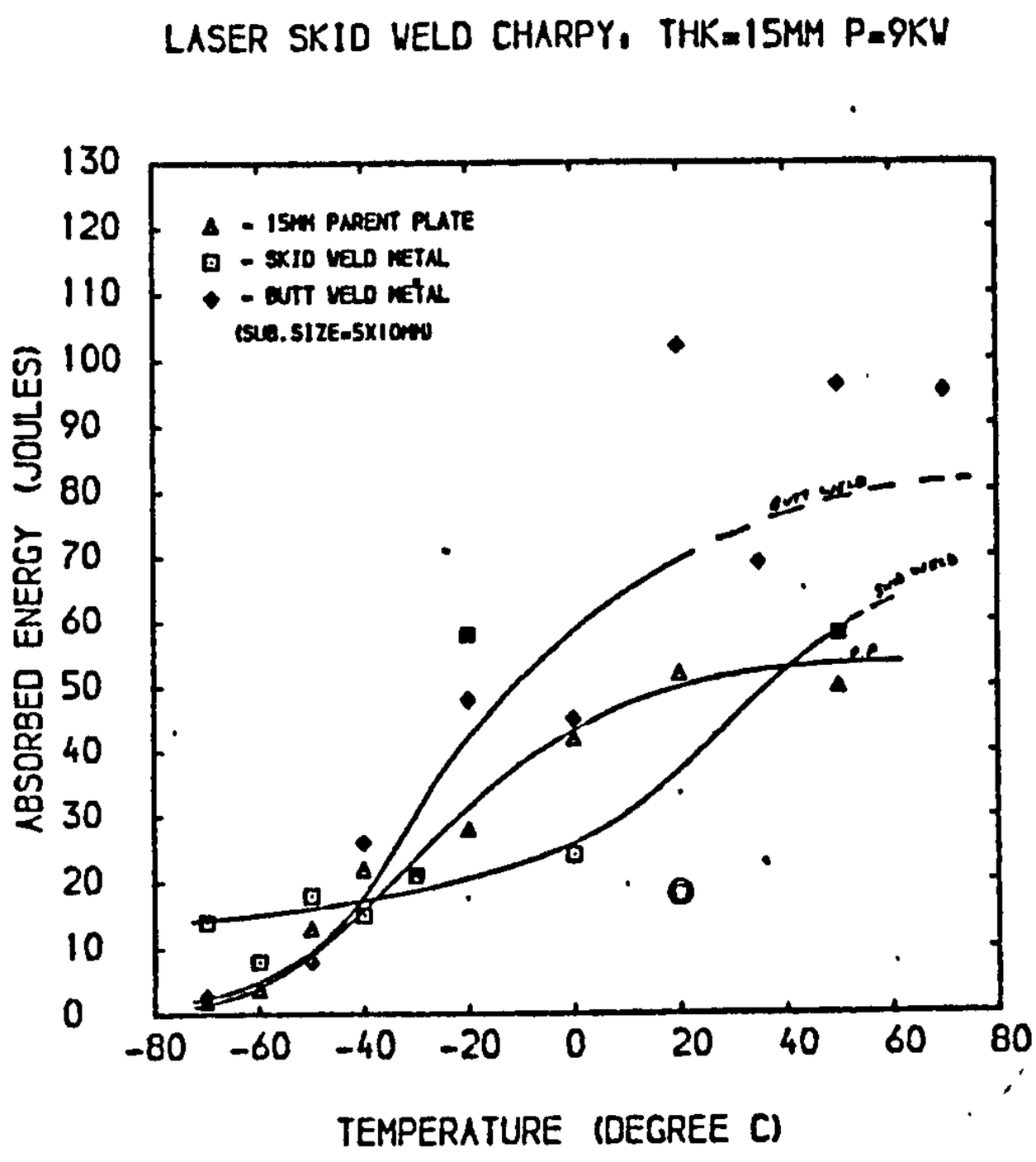

Figure C5.01i - Charpy transition curves for butt and skid weld metal :15mm plate , A31 filler wire.

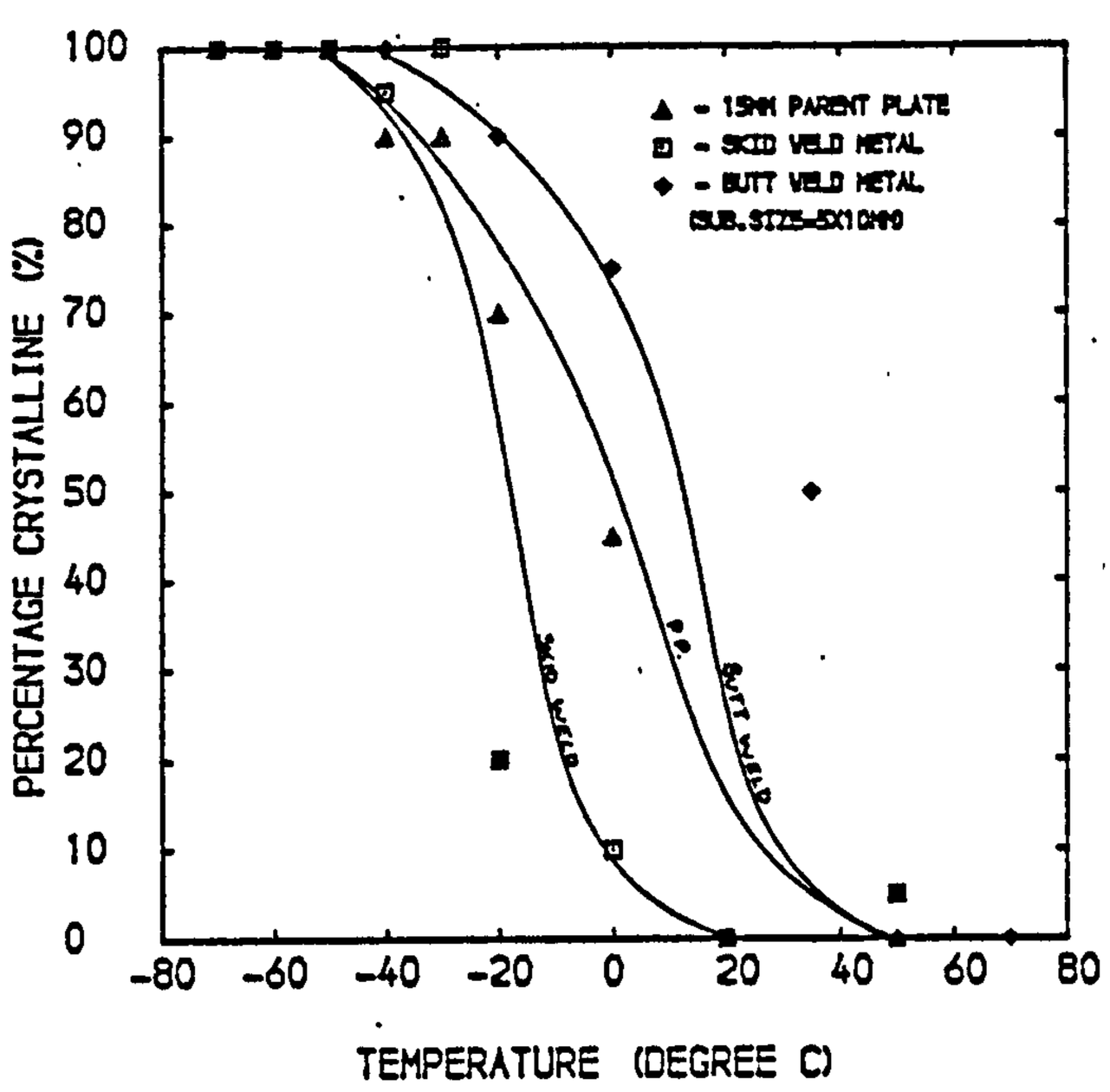

Figure C5.01j - Fracture appearance transition curves for butt and skid weld metal :15mm plate, A31 filler wire

C-4 CHARPY TESTING TRANSITION RESULTS - VARIOUS FILLER COMPOSITIONS

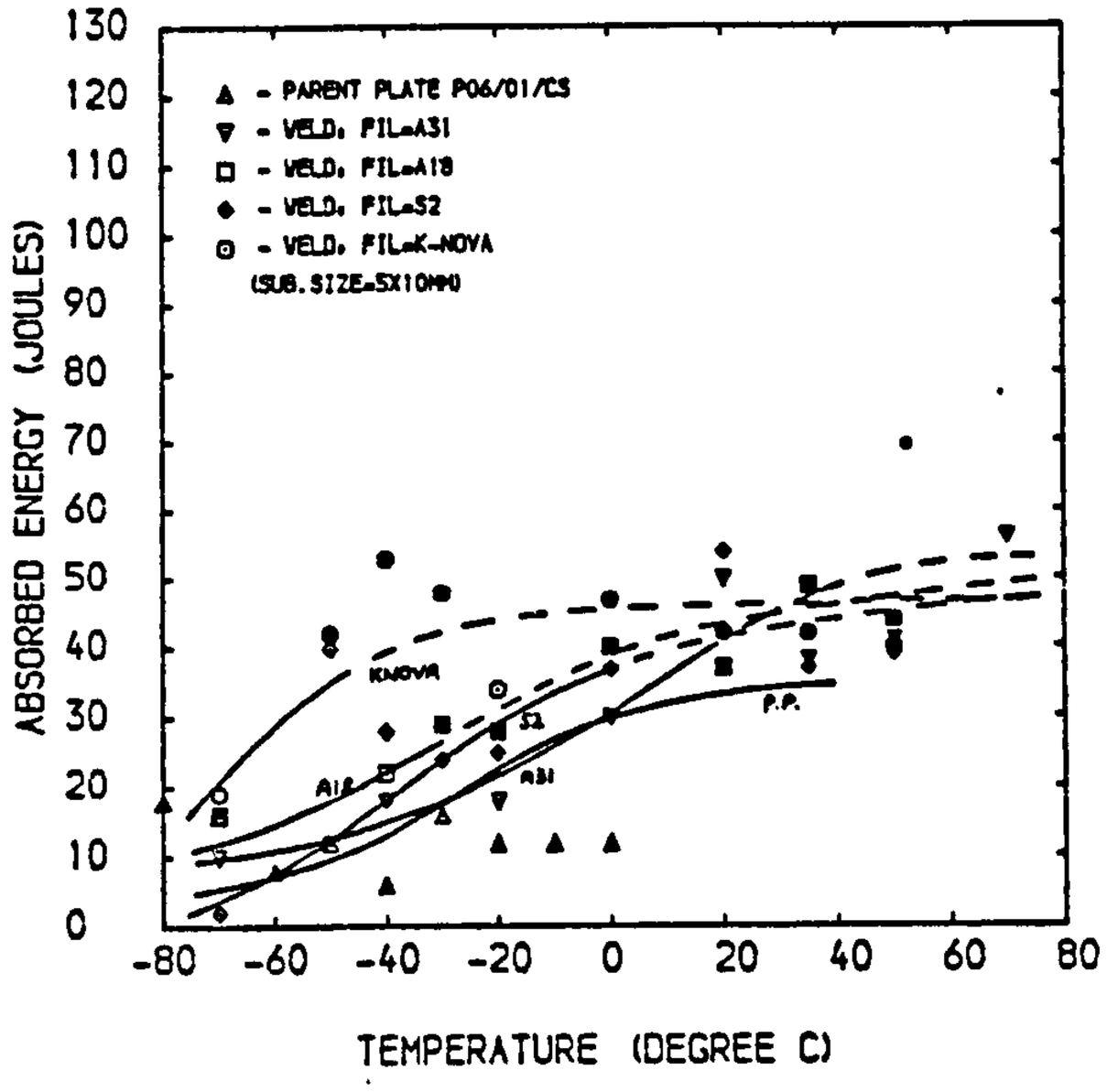

Figure C5.02a - Charpy transition curves for butt weld metal: 6mm plate, various filler wire compositions

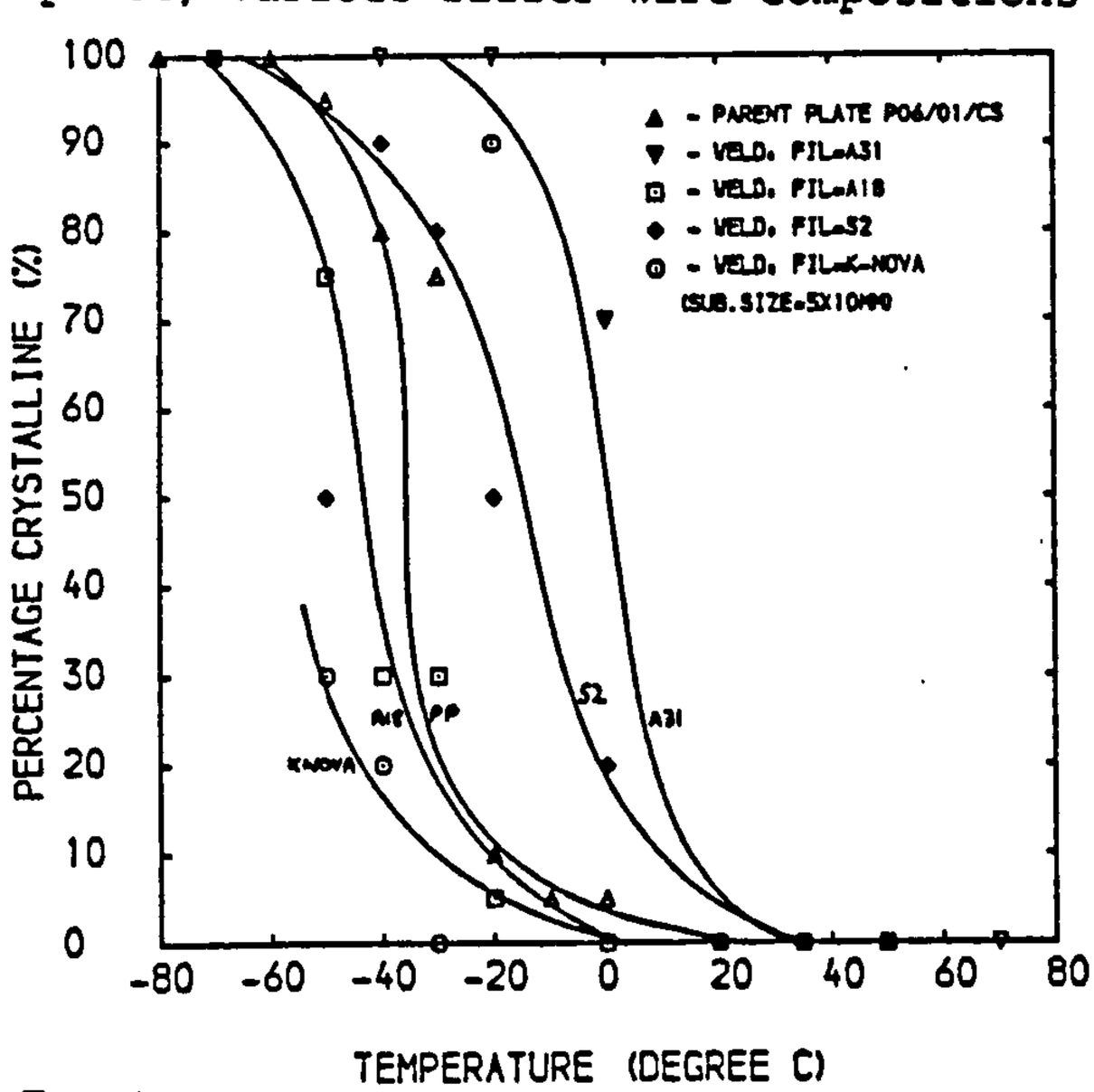

Figure C5.02b - Fracture appearance transition curves for butt weld metal: 6mm plate, various filler inputs

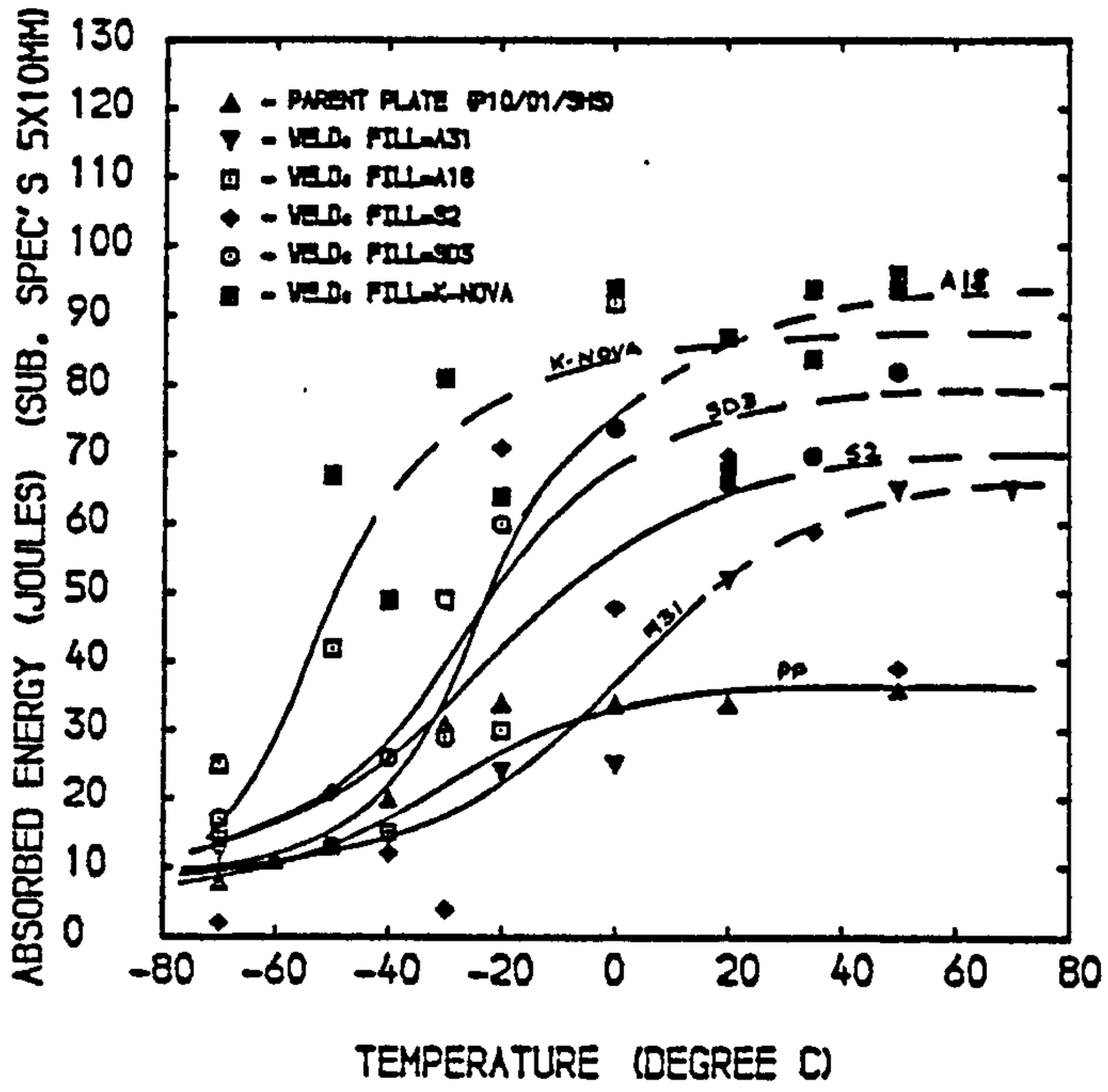

Figure C5.02c - Charpy transition curves for butt weld metal: 10mm plate, various filler wire compositions

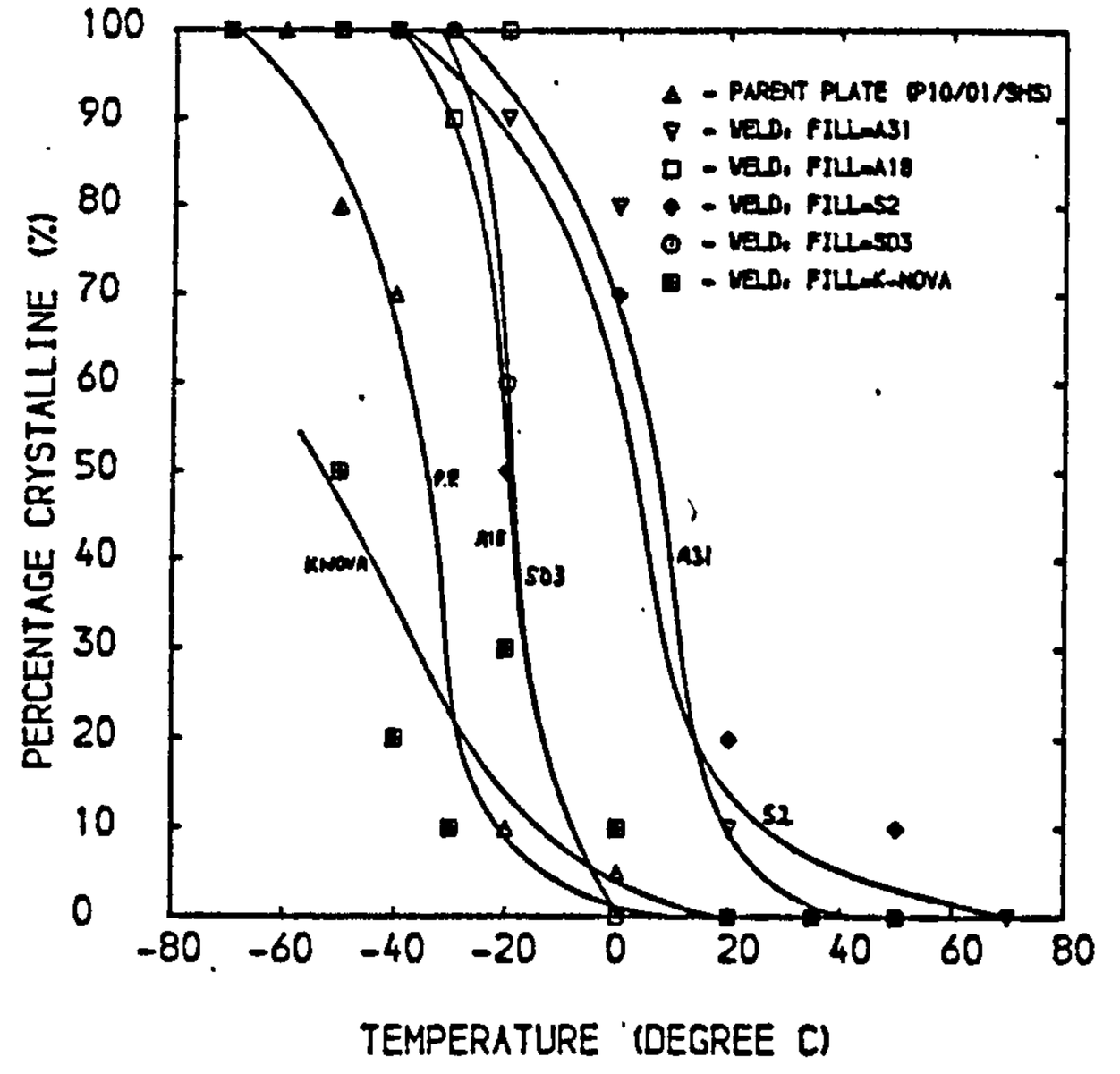

Figure C5.02d - Fracture appearance transition curves for butt weld metal: 10mm plate, various filler inputs

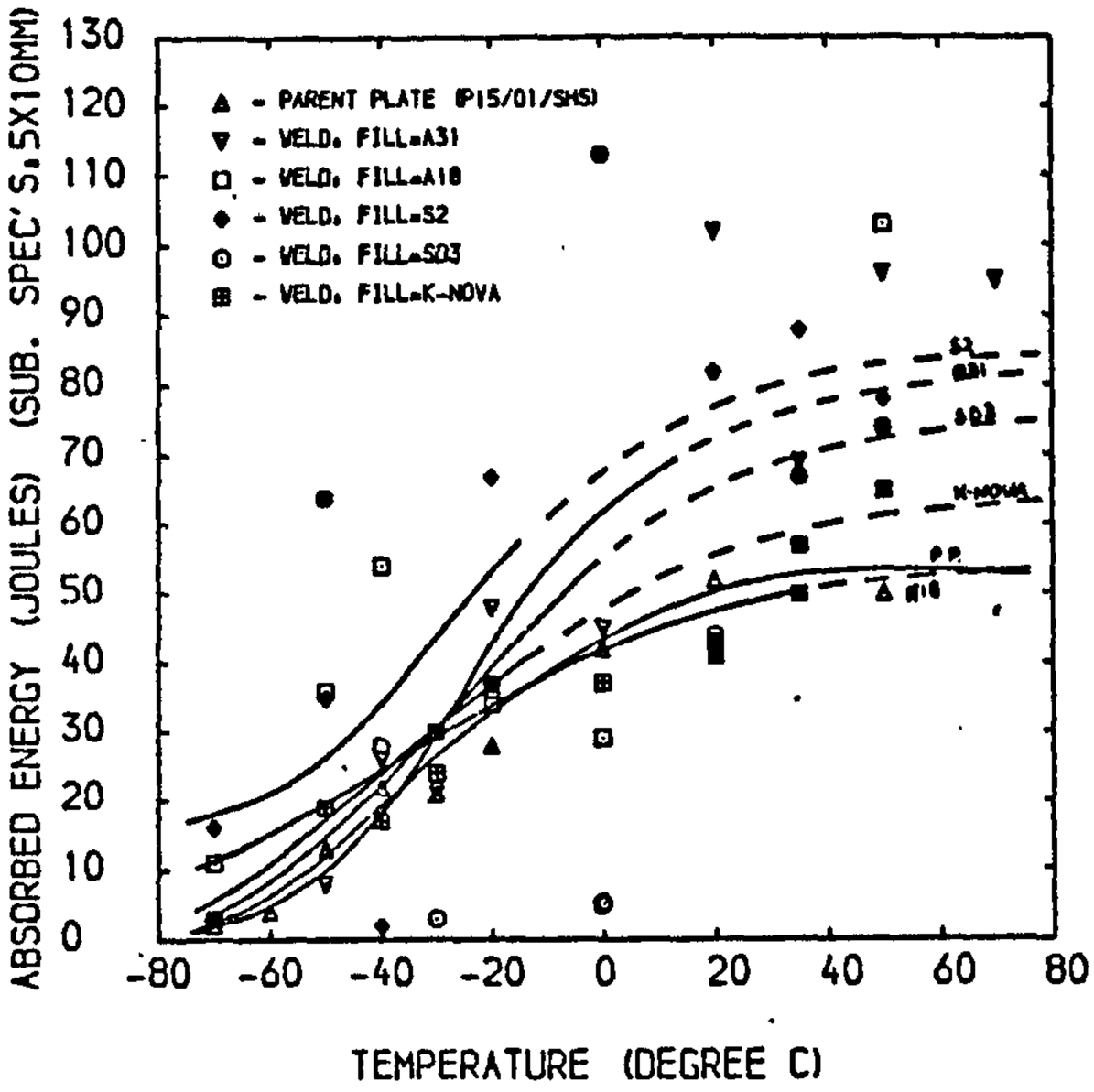

Figure C5.02e - Charpy transition curves for butt weld metal: 15mm plate, various filler wire compositions

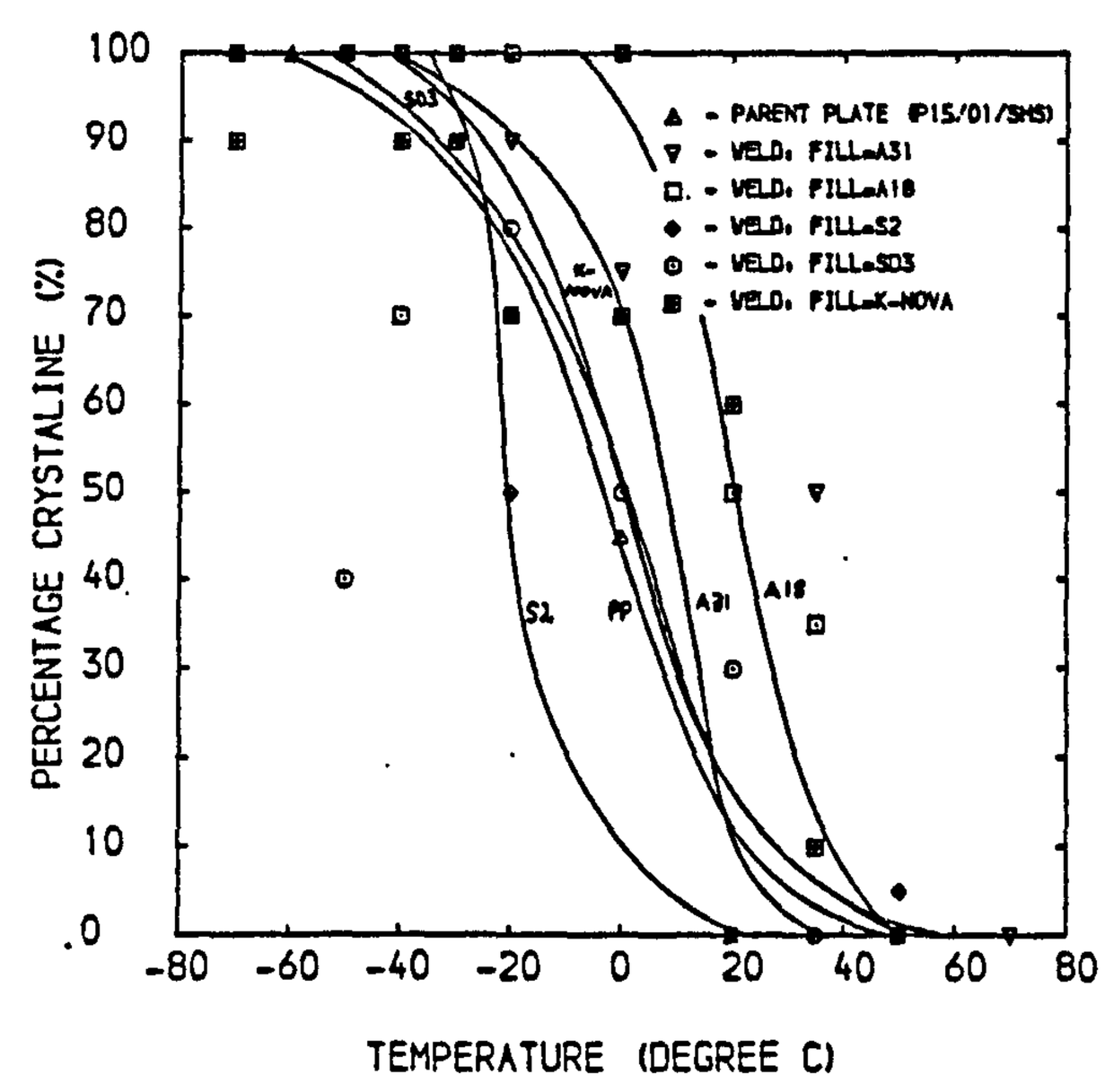

Figure C5.02f - Fracture appearance transition curves for butt weld metal: 15mm plate, various filler inputs

C-5 PROJECT REPORT OF NON-LOADED STIFFENER FATIGUE TRIALS SUBMITTED BY THE WELDING INSTITUTE

Project Report

23583/1/85
April 1985

THE FATIGUE STRENGTH OF NON-LOAD-CARRYING LASER WELDED T-BUTT JOINTS IN STEEL

For: British Shipbuilders

By: P.J. Tubby

THE WELDING INSTITUTE
Abington Hall, Abington, Cambridge. CB1 6AL

Telephone 0223 891162 Telex 81183

CONTENTS

23583/1/85
April 1985

THE FATIGUE STRENGTH OF NON-LOAD-CARRYING LASER WELDED T-BUTT JOINTS IN STEEL

For: British Shipbuilders

By: P.J. Tubby

1. INTRODUCTION

British Shipbuilders is investigating the possibility of using laser welding in ship construction. The process gives the potential for one sided operation using a unified energy source which can also be used for steel cutting. Superior weld quality and reduced heat input will minimise welding distortion leading to a reduction in the amount of rectification work needed to achieve good fit-up during assembly.

Practical work has been carried out by British Shipbuilders at the United Kingdom Atomic Energy Authority Culham Laboratory using a 10kW laser to weld full penetration T-butt joints in Grade A ship-building steel up to 15mm thick. Wire feed is used to ensure complete fusion. The process has been developed to the stage where sound joints can be produced with acceptable weld profiles at both the root and the incident weld face.

Ships hulls are subjected to fluctuating loads in service and must therefore be designed to resist fatigue failure. It is thus important to establish whether the fatigue strengths of the laser welded joints are adequate for their intended purpose.

The fatigue strengths of steel joints made by conventional arc welding practice have been extensively investigated by many organ-isations worldwide. A survey and statistical analysis of the results carried out by The Welding Institute in 1973 (1) allowed design rules to be established in which joints are categorised according to their fatigue strengths (2). Subsequently these rules have been incorporated in many design codes and standards. Investigations of the fatigue strengths of laser welds have been few (a number of abstracts are included in Appendix A) and no data relevant to the joint types, section sizes and materials currently considered are available. The objective of the present investigation was therefore to measure the fatigue strength of T-butt joints made by the laser welding process and to compare the results with those for conven-tional joints i.e. welds made by manual metal arc (mma) welding.

2. EXPERIMENTAL DETAILS

2.1. Specimen Geometry

As shown in Fig.1, there are three principal failure modes to be considered in a stiffened panel forming part of a ship structure which result from stresses acting in different directions relative to the joint. Failure modes 1 and 3 arise from stresses in the

plating, transverse and parallel to the joint. Mode 2 results from stresses transmitted across the joint, for example as a result of hydrostatic and hydrodynamic forces. For welds made by conventional techniques, failure modes 1 and 2 give the lowest fatigue strength, designated Class F in the fatigue design rules (2), and hence would govern the fatigue design of the structure. Failure mode 3 results in a higher fatigue strength, Class C or D, and is less critical to the design. Failure modes 1 and 2 were therefore selected as being the most suitable for study in laser welded joints, and mode 1, in which the stiffener acts as a transverse non-load-carrying attachment, was selected as the subject for this investigation. The specimen goemetries chosen to investigate both laser and manual metal arc welded joints are shown in Fig.2.

2.2. Materials and Specimen Manufacture

The specimens were manufactured by the sponsor from mild steel plate conforming to the requirements of Lloyds Grade A.

The welding consumables used were standard shipbuilding electrodes for the mma welds and double deoxidised MIG wire for the laser welds.

The specimens were manufactured separately rather than as a single panel. In order to minimise distortion the load carrying plates were preset before welding to a small angle previously established by trial and error; however both batches contained a small angular misalignment on completion. No attempt was made to straighten the specimens before testing since this would modify the residual stress distribution.

The specimens were cold sawn to the required width after welding. On receipt it was found that the laser welded specimens had been inaccurately cut so that the specimen edges were not straight or perpendicular to the stiffener. They were therefore machined parallel and square before testing, with the result that their widths were reduced to approximately 43mm, rather than 50mm as for the mma welded samples. Where necessary the specimens were ground by hand to prevent cracks initiating outside the test area.

2.3. Fatigue Testing Details

The specimens were tested axially in laboratory air at room temperature under load control. Test loads were varied from one specimen to another to achieve lives in the range 10^5 to 10^7 cycles. The majority of tests were conducted in an electro-magnetic resonant test machine (Amsler Vibrophore) of 100kN capacity at a frequency of approximately 100Hz. It proved difficult to achieve the higher loads required as a result of vibrations perpendicular to the loading direction caused by straightening of the distorted specimens. The high load tests were therefore performed in a servo-hydraulic testing machine (Mayes, 500kN) which does not suffer from this difficulty. The loading frequency in this machine was approximately 11Hz.

Since the degree of misalignment varied between specimens, local stresses at the weld toe were measured in each specimen using 3mm

gauge length foil resistance strain gauges bonded on the centre-line close to the weld toe as shown in Fig.2. Test loads were set to give the desired strain range at the joint which was taken as the average of the two gauge readings. A single specimen, in which the angular misalignment appeared to be the worst, had two additional gauges attached on the face opposite the joint to allow the bending distribution through the thickness to be assessed under static loading. The results indicate that the bending stress was approximately 6% of the total stress range. It was not considered that the degree of misalignment significantly affected the results obtained.

The stress ratio (i.e. minimum stress divided by maximum stress) varied slightly from one specimen to another but was always in the range 0 to 0.1.

Tests conducted in the hydraulic machine were continued until complete specimen separation. Those in the resonant testing machine were terminated at the point when the development of a fatigue crack led to an unstable machine running condition, which in all cases corresponded to cracking through the major part of the test section.

Eleven laser welds and six mma welds were tested.

3. RESULTS AND DISCUSSIONS

Both specimen types failed at the weld toe in the load carrying member (equivalent to the hull plating). Figure 3 shows macro-photographs of sections taken transverse to the joint, approximately on the specimen centre-line, for one specimen of each type. Failure occurred in the laser welded joint shown at a region of slight undercut at the weld toe on the root side of the joint. All the laser welded specimens failed at this position with the exception of specimen number 122 which failed at the toe on the incident side i.e. that nearer the laser during welding.

Figure 4 shows typical fatigue fracture surfaces produced in one specimen of each type. The fractures are entirely consistent with the expected mode of fatigue crack development viz. multiple crack initiation at the weld toe followed by propagation of a semi-elliptical crack through the plate thickness.

The fatigue test results are listed in Table 1 and are plotted in the form of an S-N curve on logarithmic axes in Fig.5. It is apparent that the two sets of results lie very close together. The results for the laser welds suggest a slightly higher fatigue strength at 10^7 cycles (approximately 200N/mm^2) than the mma welds (approximately 180N/mm^2), but in view of the scatter in test lives and the relatively few results, this difference cannot be regarded as significant. Thus it would appear that the characteristics of conventional arc welds which give rise to the severe weld toe stress concentration are also present in laser welds.

The 95% confidence limits for similar joints made by conventional arc-welding practice (from Ref.1) are also plotted in Fig.5 for comparison. All the results obtained in the present investigation lie near the upper confidence line on a band of shallower slope. A number of possible explanations may be put forward for this.

In the first instance the joints tested previously covered a range of thicknesses from 12.5 to 16mm, whilst the present specimens were only 8mm thick. It has been noted (3) that plate thickness affects the fatigue strength of welded joints, those in thicker plate having lower fatigue strengths, so results from 8mm thick plates might be expected to lie near the upper extreme of the scatterband in Fig.5.

A second factor is the influence of bending. In general it is found that joints tested in bending have higher and slightly shallower S-N curves than those tested axially, especially joints in thin material. For example, in Fig.6 mean S-N curves obtained at the Institute (in work as yet unpublished) for transverse fillet welded joints in 6mm thick steel tested in both four point bending and under axial loading are plotted for comparison with the data obtained in this investigation. It is apparent that the curve obtained under bending is significantly higher than that under axial loading. Although the joints tested here were subjected to only a relatively small bending component, as established by the strain gauge measurements, this factor may have contributed towards increasing their fatigue strength.

It is interesting to note that most of the data obtained in the present investigation lie above the upper curve in Fig.6, despite the fact that they are for joints in thicker material subjected to predominently axial stresses, so clearly the factors discussed above do not entirely account for the high fatigue strength. A third factor is specimen geometry. The confidence limits plotted in Fig.5 and the mean S-N curves in Fig.6 were obtained with specimens having attachments on both sides of the load carrying plate, whereas those tested in this study had attachments on one side only. As noted by Gurney (4) specimens with attachments on one side only have in some investigations been found to give higher fatigue strengths than those with attachments on both surfaces. Furthermore, Gurney cites photoelastic tests which have shown that the stress concentration at the weld toe is greater in specimens with attachments on both sides.

These factors go some way to explaining the high fatigue strengths obtained, however further investigation would be necessary to establish which is the most significant. For example, it would be instructive to conduct identical tests on specimens with attachments on both plate surfaces.

Having established that the laser welds give a satisfactory fatigue strength under this loading mode it is suggested that similar tests should be conducted on load carrying joints i.e. loading mode 2 in Fig.1. In tests under this mode the cyclic load carrying capacity of the joint itself is tested and hence surface or buried defects in the weld are potential failure origins.

4. CONCLUSIONS

The fatigue strengths of transverse non-load-carrying joints made by laser and mma welding in 8mm thick Grade A shipbuilding steel have been established. All the results were rather high compared with data for conventional arc-welded joints, however it was established that the fatigue stength of the laser welds was as good as if not marginally better than that of the mma welded control specimens.

Work carried out by Mr. G.W. Smith and Mr. D.J.H. Evans and reported by:

P.J. Tubby

REFERENCES

1. GURNEY, T.R. and MADDOX, S.J. 'A re-analysis of fatigue data for welded joints in steel'. Welding Institute Report E44, 1973.

2. GURNEY, T.R. 'Fatigue design rules for welded steel joints'. The Welding Institute Research Bulletin 17, May 1976.

3. GURNEY, T.R. 'The influence of thickness on the fatigue strength of welded joints'. 2nd Int. Conf. "Behaviour of Offshore Structures", Imperial College, London, August 1979.

4. GURNEY, T.R. 'Fatigue of welded structures'. 2nd Ed. Cambridge University Press, 1979.

Table 1. Fatigue test results

LASER WELDS

Specimen Number	Stress range* N/mm^2	Life Cycles	Comments
124	275	1.78×10^5	Toe failure
130	250	4.37×10^5	Toe failure
127	235	1.63×10^6	Toe failure
128A	235	1.1×10^6	Toe failure
123	225	9.68×10^5	Toe failure
125	223	9.66×10^5	Toe failure
121	215	1.52×10^6	Toe failure
122	207	1.27×10^6	Toe failure
129	206	1.33×10^6	Toe failure
128B	190	10^7	Unfailed
120	160	10^7	Unfailed

MMA WELDS

Specimen Number	Stress range N/mm^2	Life Cycles	Comments
13A	250	6.43×10^5	Toe failure
13B	225	1.07×10^6	Toe failure
01	201	1.31×10^6	Toe failure
15A	185	1.34×10^6	Toe failure
14B	170	1.97×10^7	Unfailed
14A	167	2.07×10^7	Unfailed

* Taken as the average of two strain measurements, one on either side of the attachment.

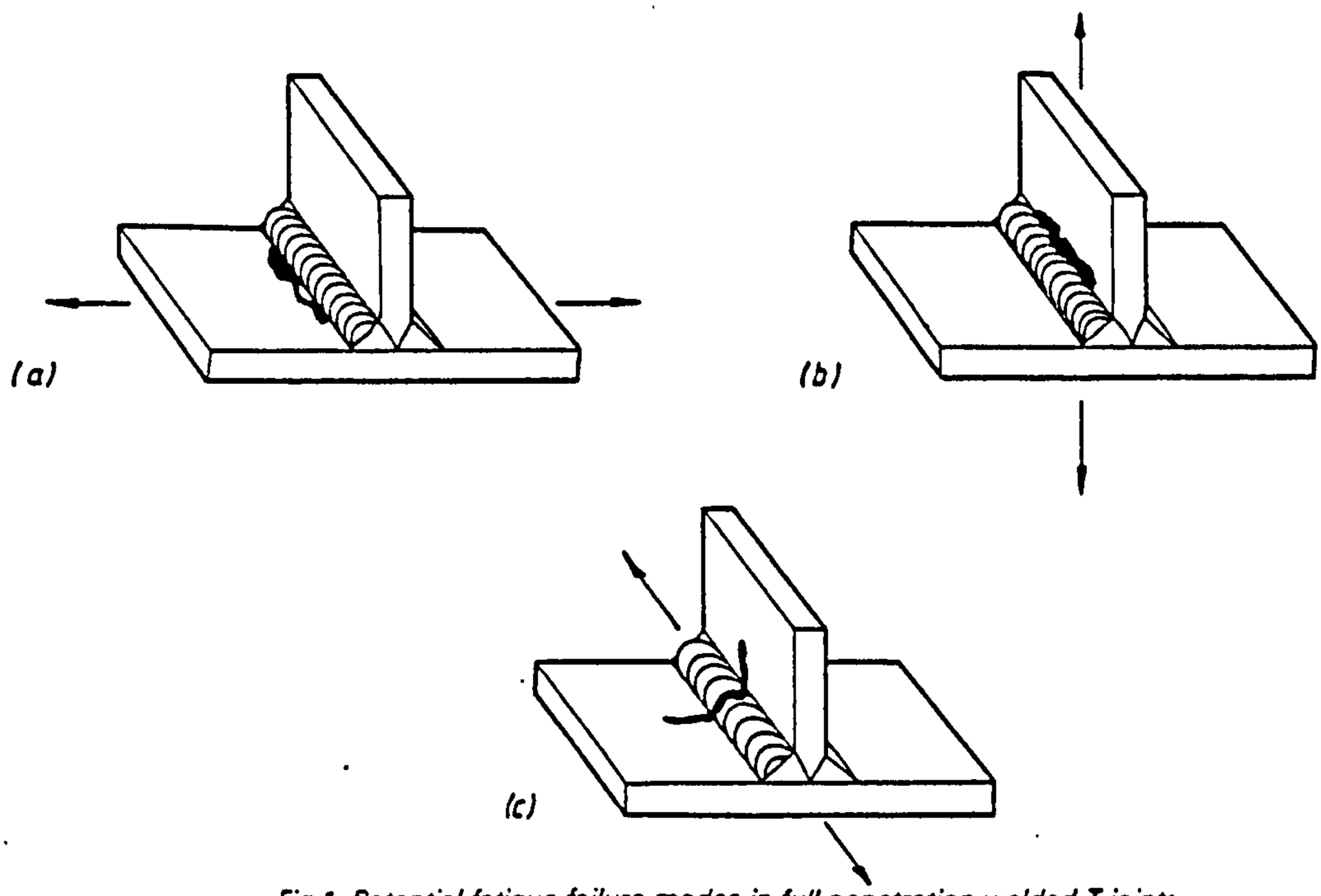

Fig.1. Potential fatigue failure modes in full penetration welded T joint:
a) mode 1 loading — failure at weld toe in load carrying plate, Class F
b) mode 2 loading — failure at weld toe in stiffener, Class F
c) mode 3 loading — failure from ripple on weld face, Class C or D

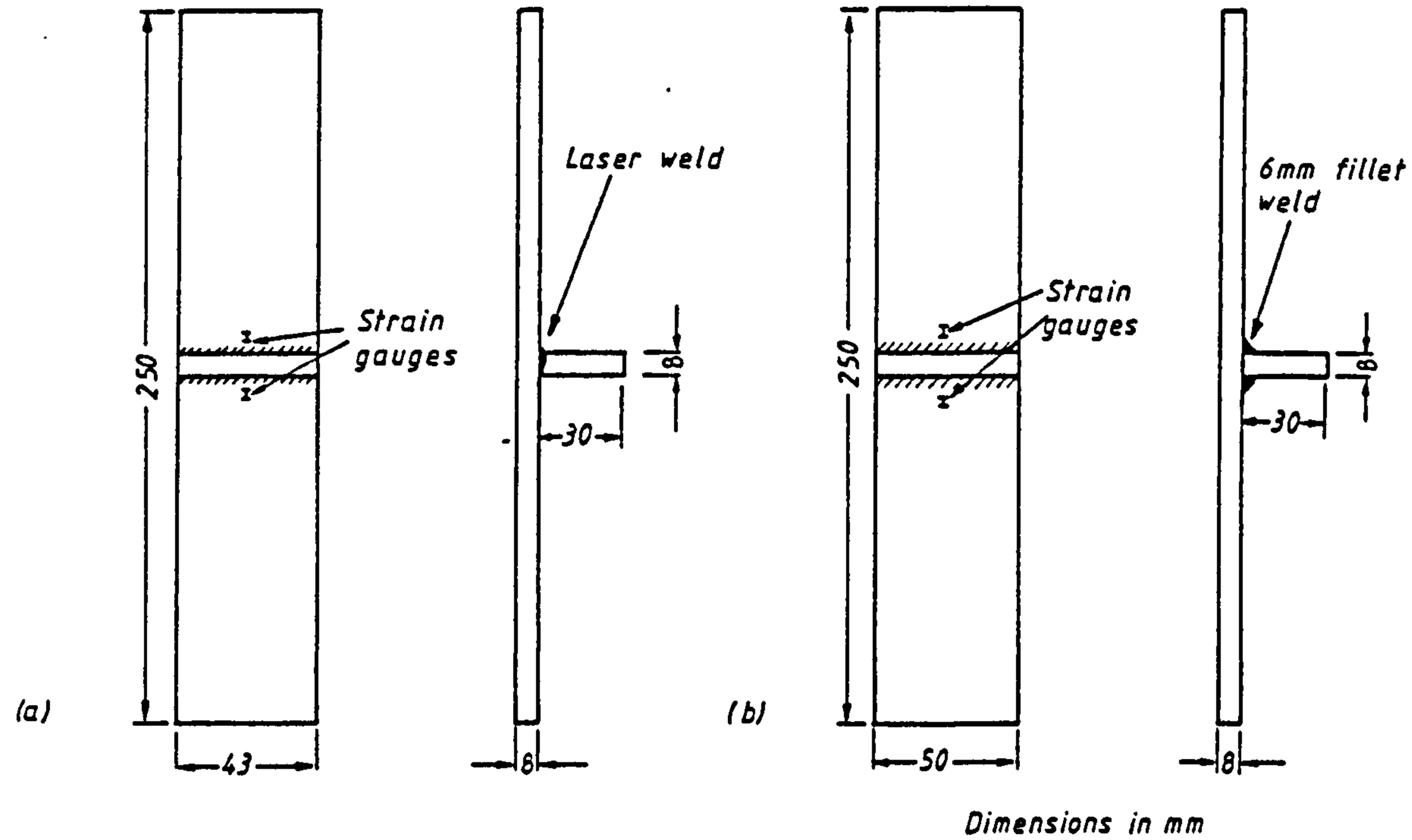

Fig.2. T joint specimen geometry:
a) laser welded b) fillet welded

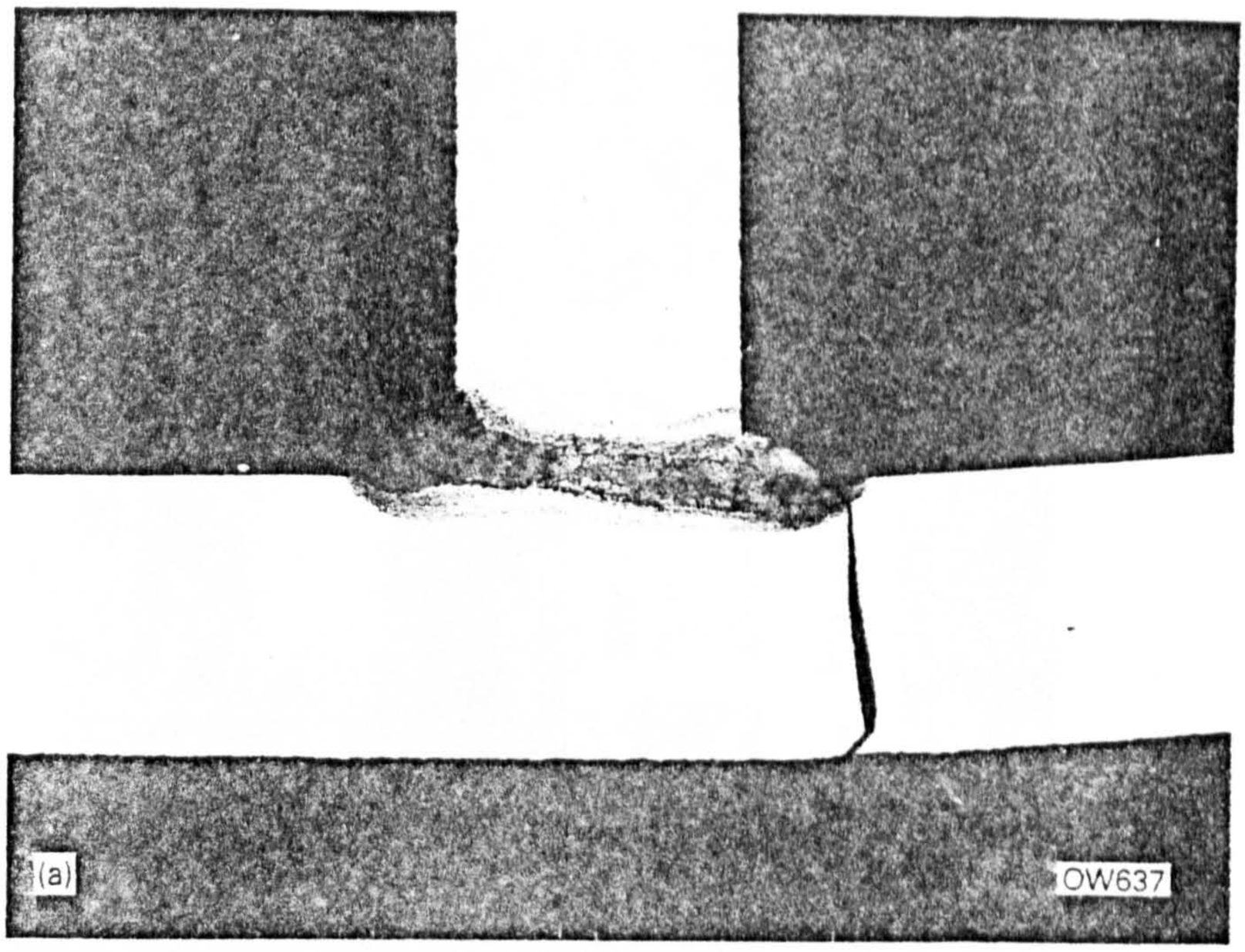

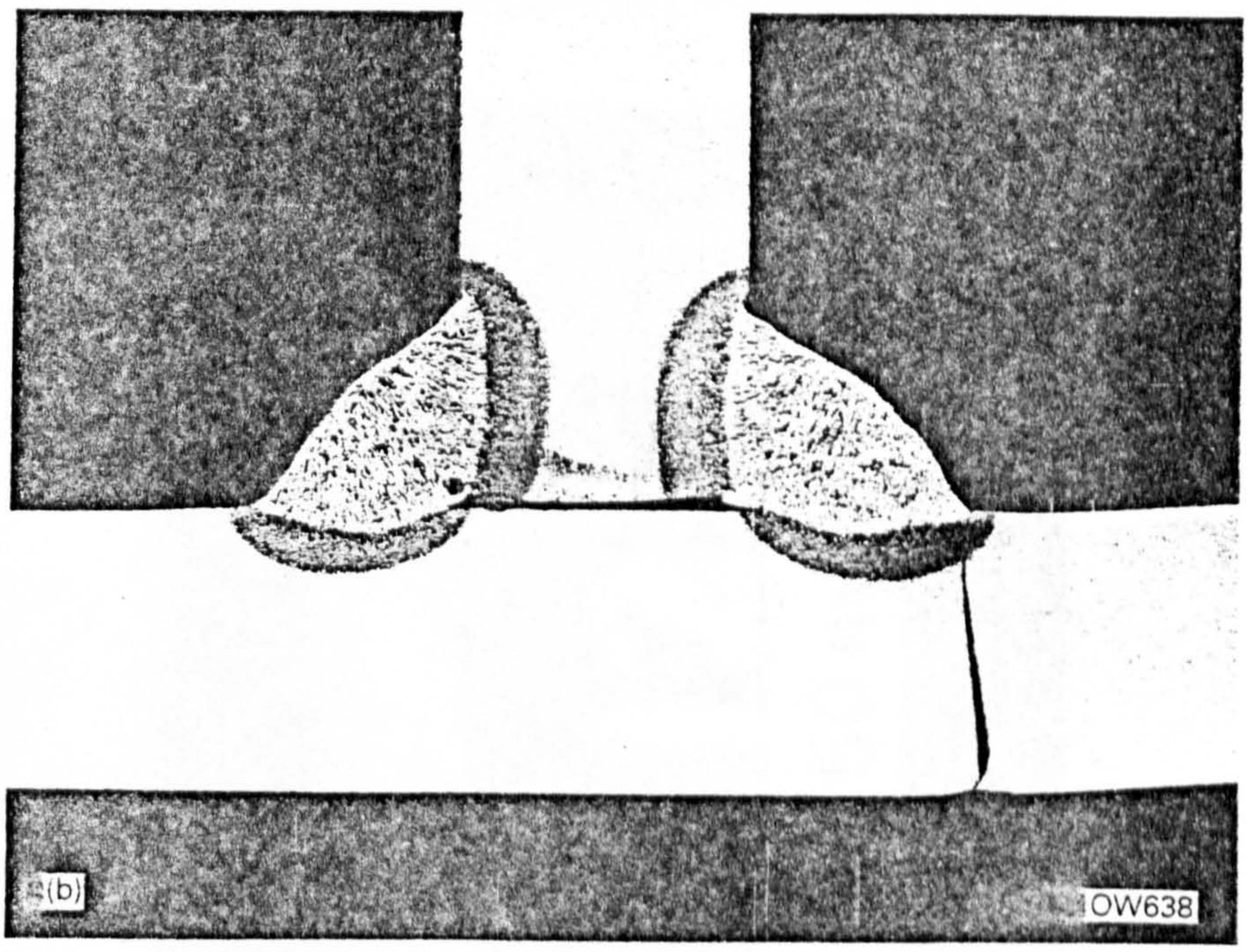

Fig.3. Macrophotographs of sections showing position of fatigue failure, ×4:
a) laser weld b) MMA weld

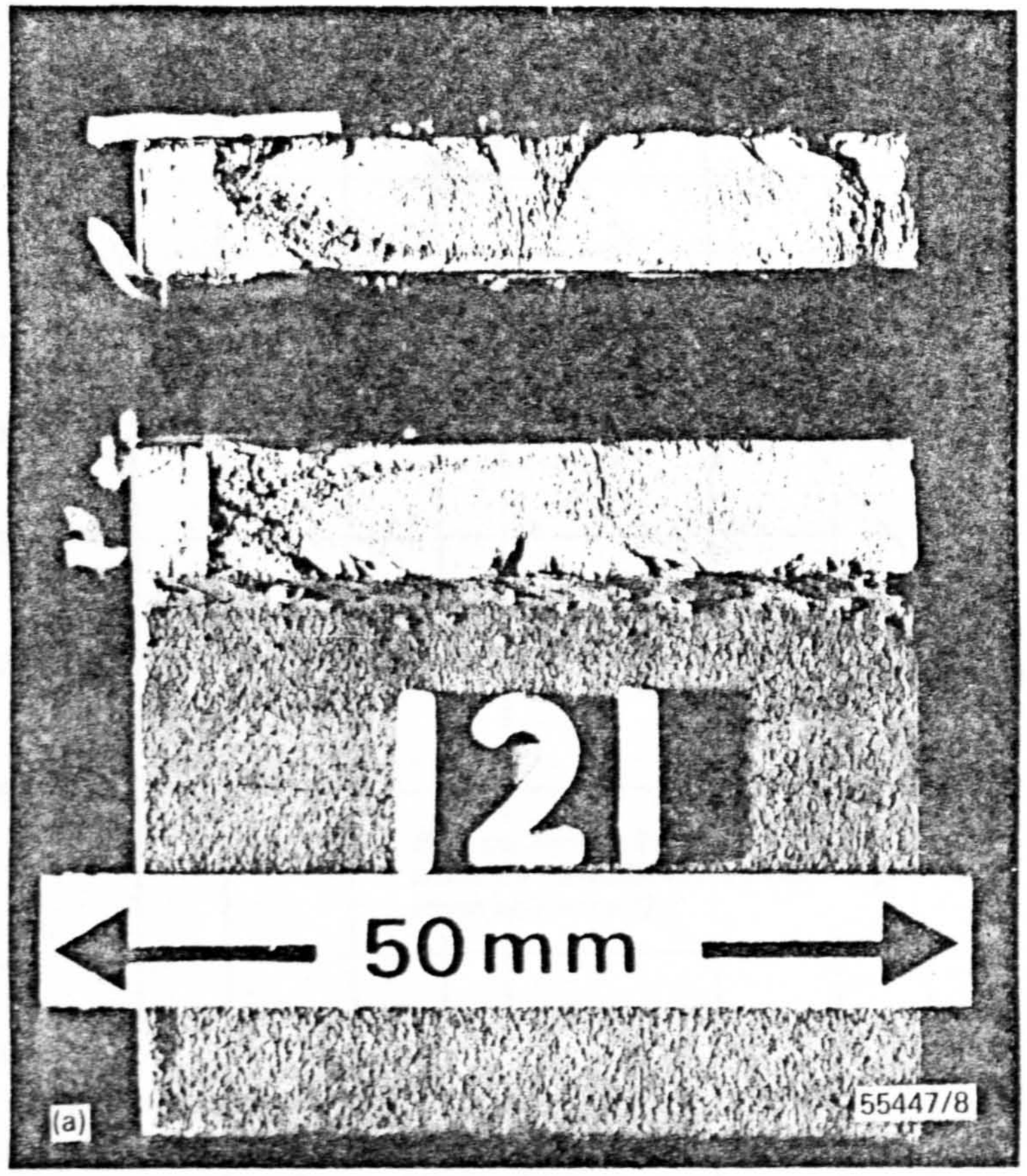

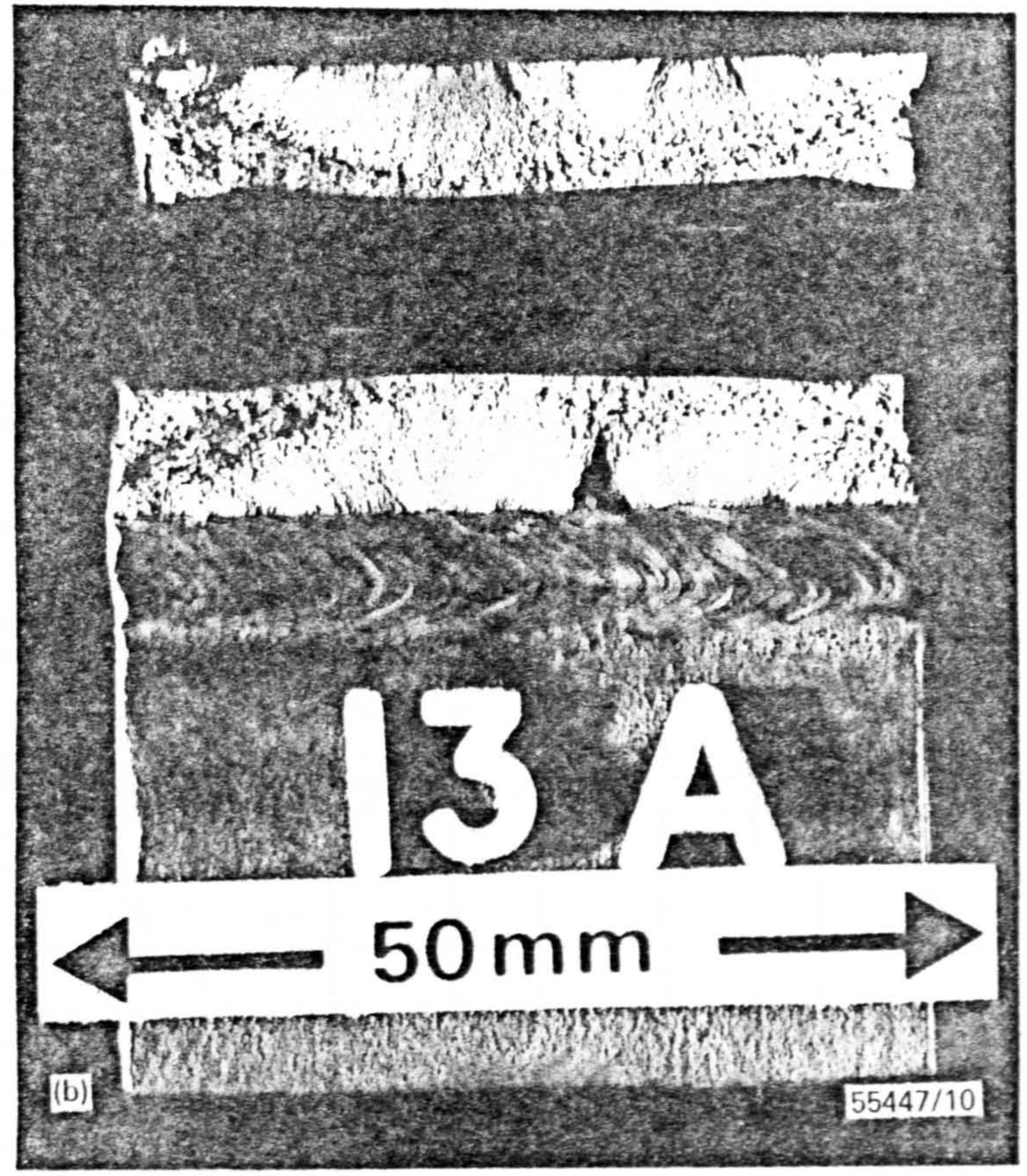

Fig.4. Fatigue fracture surfaces produced in:
a) laser welded specimen b) MMA welded specimen

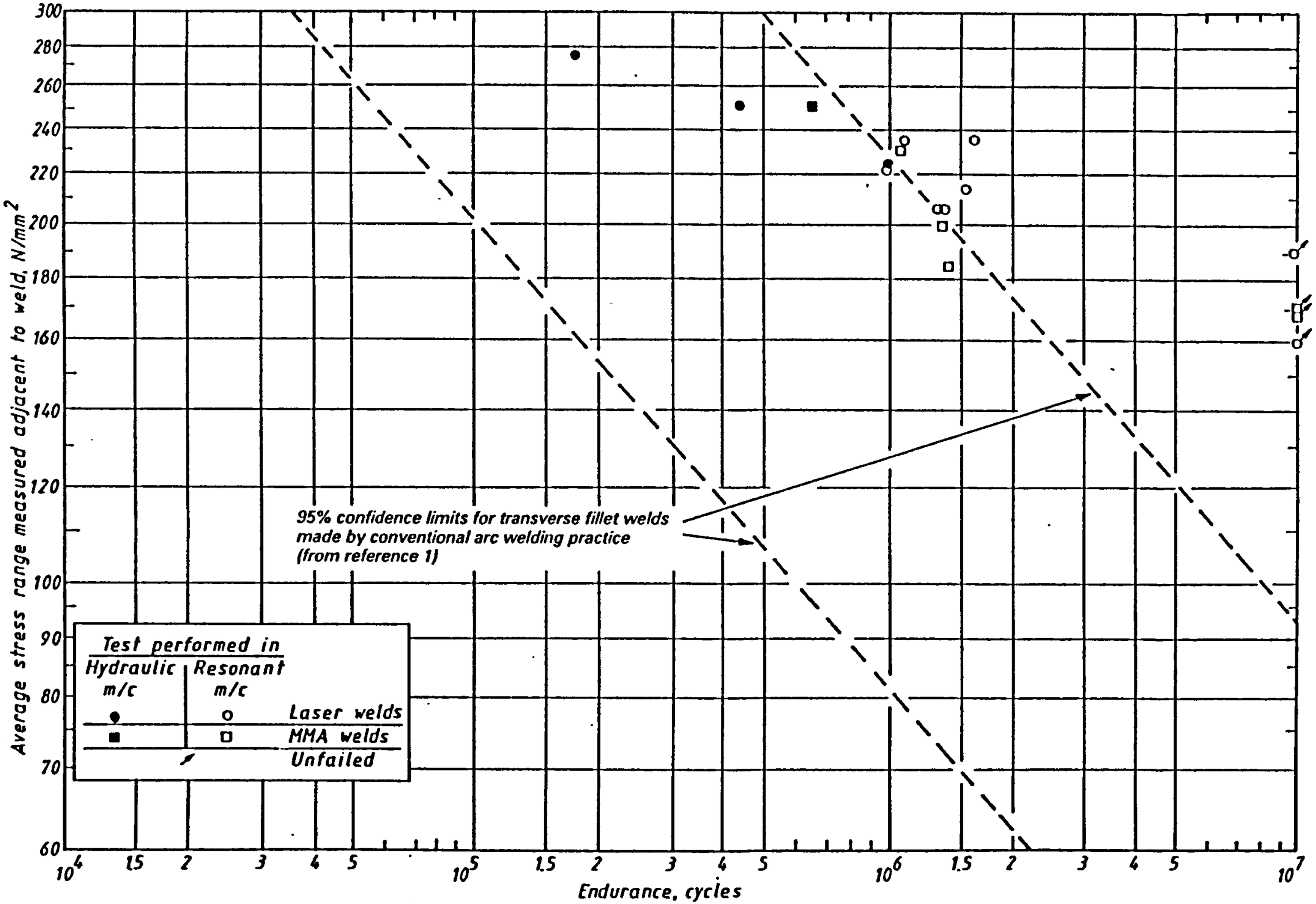

Fig.5. Fatigue test results.

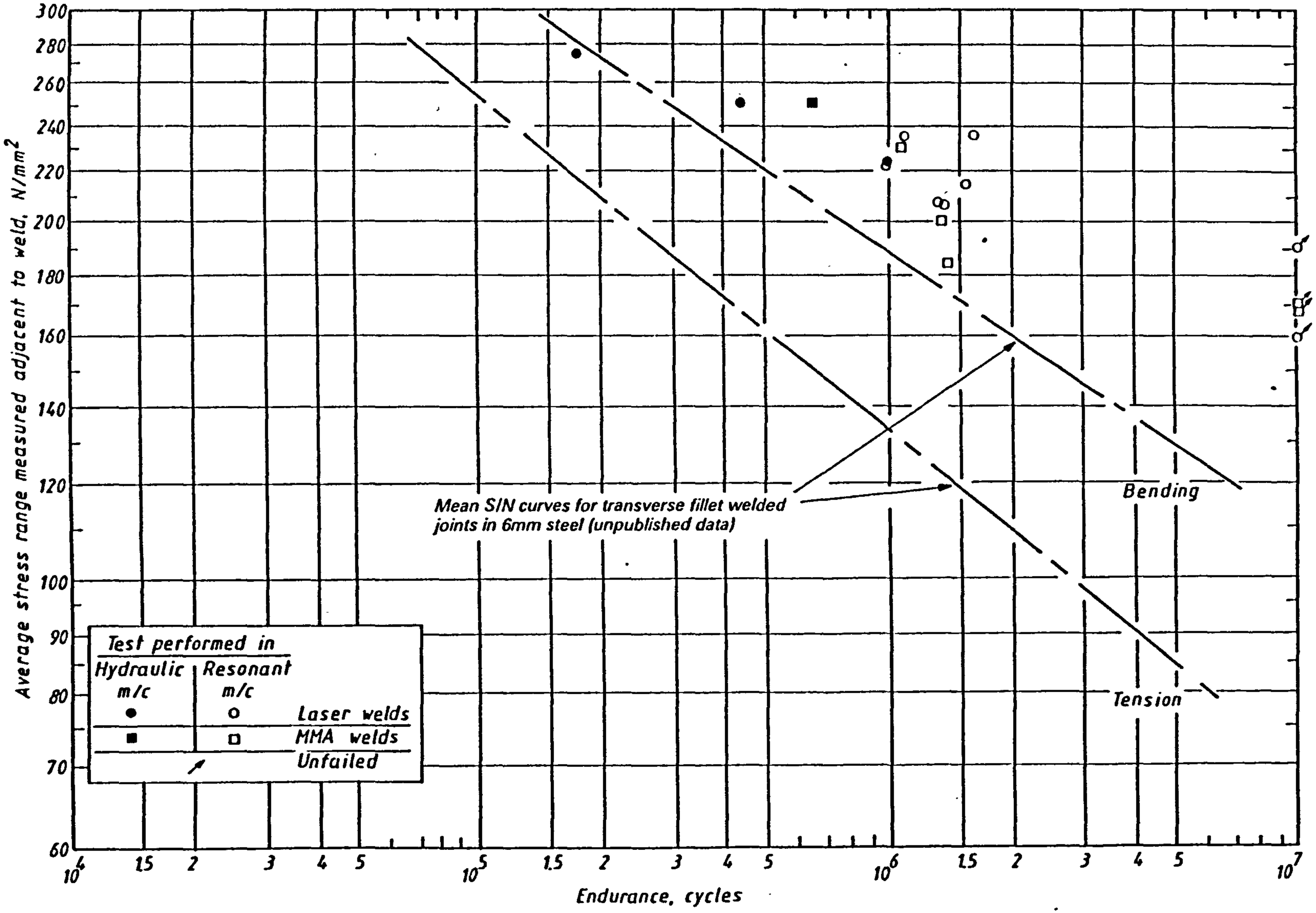

Fig.6. Comparison of fatigue test results with data for transverse fillet welds in 6mm steel tested in tension and bending.

C-6 ANALYSIS OF SAMPLE SCANTLINGS TO CALCULATE FATIGUE TEST A LOAD CARRYING WEB ARRANGEMENT (MODE 2)

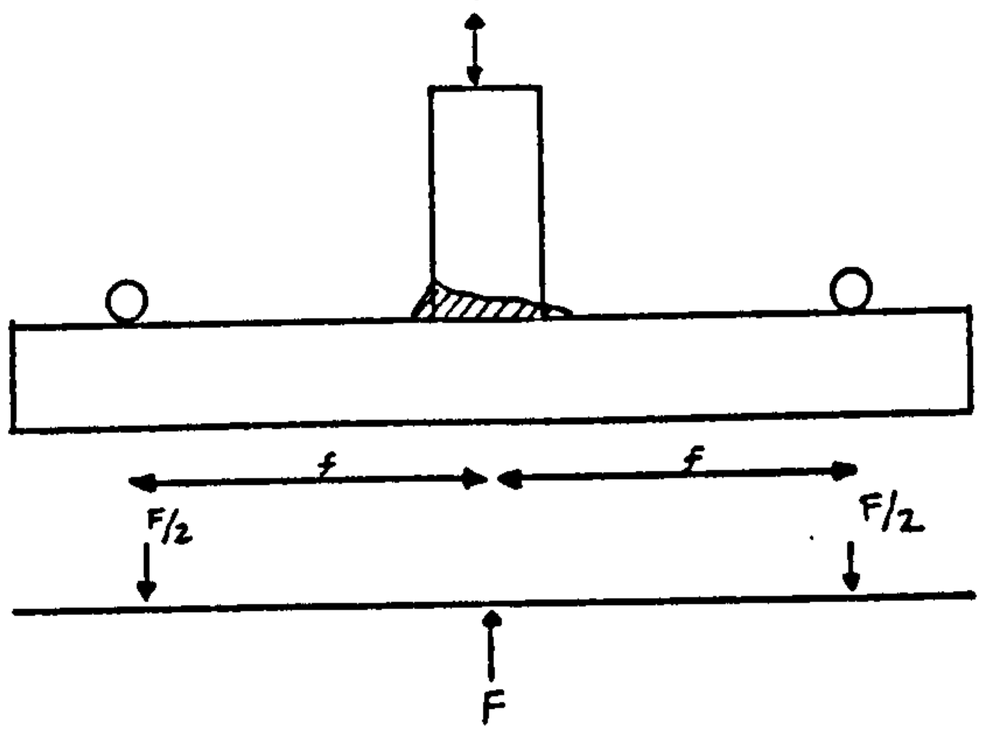

Equation of bending is $\frac{\sigma}{y_n} = \frac{E}{R} = \frac{M}{I}$

where : σ = bending stress ($N.m^{-2}$)

y_n = distance from the neutral axis (m)

E = Young's modulus ($N.m^{-2}$)

R = radius of gyration (m)

M = be nding moment (N.m)

I = second moment of area (m^4)

Greatest longitudinal bending stress in the face plate is given by:

$$\sigma_{fp} = \frac{M \cdot y_{max}}{I} \qquad (1)$$

Bending moment at mid length of the face plate is given by:

$$M = \frac{F}{2} \times f \qquad (2)$$

2nd moment of inertia of face plate of unit width given by:

$$I = \frac{1}{12} \times (1) \times (h^3) \qquad (3)$$

Also $$ymax = \frac{h}{2} \qquad (4)$$

Substituting 2,3 & 4 into 1:

$$\sigma_{fp} = F \times \frac{f}{h^2} \times 3$$

Direct stress in web (per unit width) given by:

$$\sigma_w = \frac{F}{h}$$

To ensure that the sample fails in the web rather than in the face plate:

$$\sigma_w > \sigma_{fp}$$

$$\therefore \quad \frac{F}{h} > \frac{F \times f \times 3}{h^2}$$

$$\therefore \quad f < \frac{h}{3}$$

But $h = 8mm$

$$\therefore \quad f < \frac{8}{3}$$

$$\therefore \quad f < 2.6mm$$

==========

C-7 CALCULATION OF TWIN FILLET WELD JOINT SCANTLINGS TO ENSURE FATIGUE FAILURE IN THE WELD TOE (MODE 2)

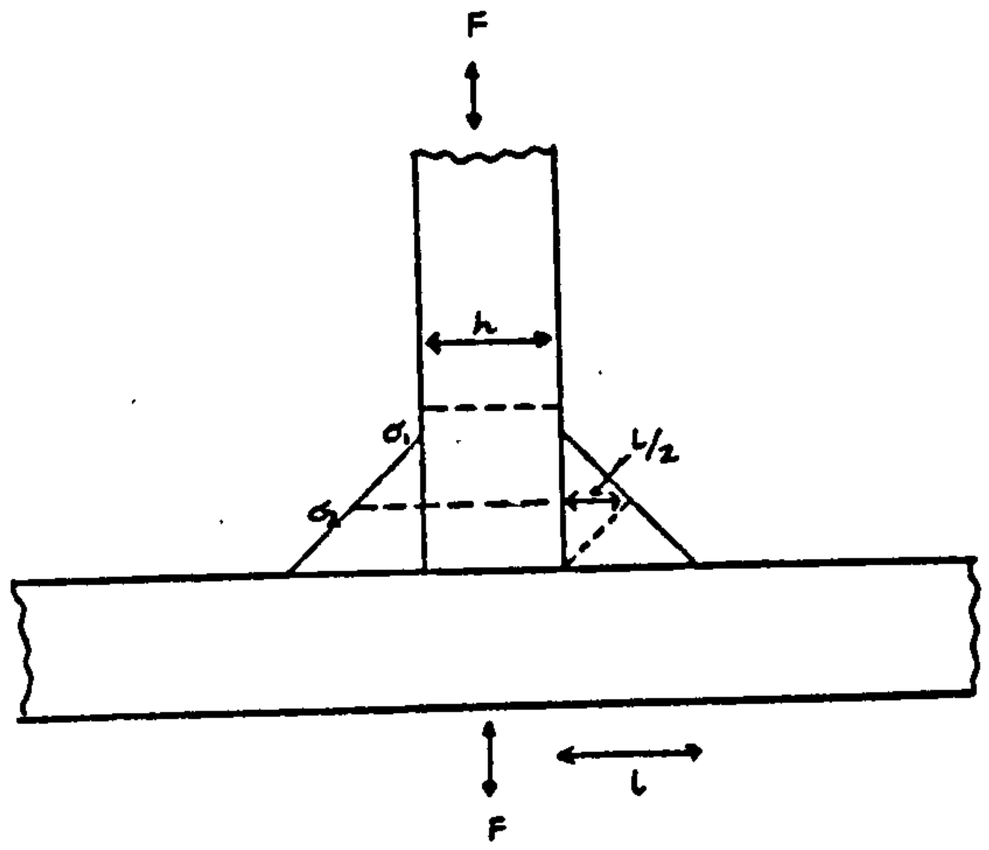

To calculate the stress to give equal potential of failure in the plate or in the weld throat, the "effective throat thickness" is used together with the relative stresses required for failure in each mode F2 and W from the design curves (BS 5400: Part 10,1980).

Stress at 10^6 cycles endurance:

F2 = 50 N/mm2

W = 33 N/mm2

Effective throat thickness for stress levels in weld σ_1 is:

$$2 \times \frac{1}{\sqrt{2}} = \sqrt{2} \times 1$$

Therefore, for an applied force F, the ratio of stresses for equal potential of failure is:

$$\frac{\sigma_1}{\sigma_2} = \frac{F \times \sqrt{2} \times 1}{h \times F}$$

$$\therefore \quad 1 = \frac{h \times \sigma_1}{\sqrt{2} \times \sigma_2}$$

Substituting for the given force ratio and plate thickness of 8mm:

$$1 = \frac{8 \times 50}{\sqrt{2} \times 33}$$

$$1 = 8.57\text{mm}$$

Therefore, allowing at least 10% factor of safety, the joint leg length should be at least 10mm to ensure failure in the web.

Appendix D

APPENDICES ASSOCIATED WITH CHAPTER 6

D-1 COMPUTER PRINTOUT OF THE SKIDCOOL SOURCE PROGRAM AND DATA FILE

```
C ***************************************************************************
C *          SOURCE CODE FOR THE LASER SKIDWELDING PROGRAM                  *
C *                                                                         *
C *                        - SKIDCOOL -                                     *
C *                                                                         *
C *                                   COPYRIGHT APRIL 1987 - SJB;UNUT;BS*
C ***************************************************************************
C
C    PROGRAM TO CALCULATE THE COOLING TIME OF A SKIDWELD AT THE HEAT
C    AFFECTED ZONE, BASED ON THE HIGHEST HARDNESS MEASURED WITHIN THE
C    HAZ MATERIAL,  BASED ON WORK BY SUZUKI
C
C    DATA IS INPUT FROM A DATAFILE CONNECTED TO CHANNEL 5
C    OUTPUT IS TO A DATAFILE OR SCREEN ON CHANNEL 6
C
C    UNITS OF INPUT OF MM,SEC  BUT CONVERTED TO M/S/KG FOR CALCULATIONS
C
C    ***************************************************************************

     REAL*8 C,PCM,CT,TRAVS,LTRAVS,HMAX,FA1,FB1,FC1,FD1
     INTEGER NDATA,PLTHK,PLCODE(20)
C
C    ***************************************************************************
C
C    READ IN SOURCE DATA FROM CANNEL 5
C    ***************************************************************************
C
     READ (5,101)C,PCM,NDATA,PLTHK
101  FORMAT (F8.4 / F8.4 / I2 / I2)
     READ (5,103)PLCODE
103  FORMAT(20A1)
C
C    ***************************************************************************
C    WRITE HEADINGS AND INPUT REQUIREMENTS
C    ***************************************************************************
C
     WRITE (6,201)
201  FORMAT(50H1PREDICTION OF COOL TIME IN LASER HAZ MAX HARDNESS)
     WRITE (6,202)
202  FORMAT(50H+__________________________________________________)
     WRITE (6,203) PLCODE,PLTHK
203  FORMAT(15HOPLATE CODE IS ,20A1,19HPLATE THICKNESS IS ,I2,2HMM)
     WRITE(6,204)C
```

```
204   FORMAT(17H0PLATE CARBON IS ,F4.2)
      WRITE(6,205)PCM
205   FORMAT(14H0PLATE PCM IS ,F6.4)
      WRITE (6,206)
206   FORMAT (24H0TRAVS  LTRAVS  HMAX  CT)
C
C     ***************************************************************
C     CALCULATE COOLING RATE FOR EACH HARDNESS VALUE AND PRINT
C     ***************************************************************
C
      DO 301 N=1,NDATA
      READ (5,102)TRAVS,HMAX
 102  FORMAT (2F8.4)
C
      LTRAVS=DLOG10(TRAVS)
C
      FA1=(187+64*C+485*PCM)
      FB1=(97+680*C-441*PCM)
      FC1=(0.501+7.9*C-11.01*PCM)
      FD1=(0.543+0.55*C-0.76*PCM)
      CT=10**(FD1*DTAN((FA1-HMAX)/FB1)-FC1)
C
      WRITE (6,207)TRAVS,LTRAVS,HMAX,CT
207   FORMAT (1H ,F4.1,1H ,F7.4,1H ,F5.1,1H ,F5.2)
301   CONTINUE
C
      STOP
      END
C ***************************************************************
```

```
Listing of HARDJOBD8.1 at 14:00:51 on FEB 13, 1987 for CCid=NVC9

     1      0.12
     2      0.1663
     3      11
     4      08
     5      P8/01/APS
     6      10.0     240.00
     7      14.0     262.00
     8      17.5     309.00
     9      19.5     317.00
    10      10.0     250.00
    11      08.0     209.00
    12      14.0     270.00
    13      14.0     272.00
    14      14.0     283.00
    15      14.0     266.00
    16      10.0     240.00
    17
    18
    19
```

D-1.1 Computer printout of the output from the SKIDCOOL program

PREDICTION OF COOL TIME IN LASER HAZ MAX HARDNESS

PLATE CODE IS P8/01/APS PLATE THICKNESS IS 8MM

PLATE CARBON IS 0.12

PLATE PCM IS 0.1663

TRAVS	LTRAVS	HMAX	CT
10.0	1.0000	240.0	3.55
14.0	1.1461	262.0	2.78
17.5	1.2430	309.0	1.67
19.5	1.2900	317.0	1.51
10.0	1.0000	250.0	3.17
8.0	0.9031	209.0	5.42
14.0	1.1461	270.0	2.55
14.0	1.1461	272.0	2.50
14.0	1.1461	283.0	2.22
14.0	1.1461	266.0	2.66
10.0	1.0000	240.0	3.55

D-2 COMPUTER PRINTOUT OF THE SKIDPROP SOURCE PROGRAM AND DATA FILE

```
C ***************************************************************************
C *              SOURCE CODE FOR THE LASER SKIDWELDING PROGRAM              *
C *                                                                         *
C *                          - SKIDPROP -                                   *
C *                                                                         *
C *                                  COPYRIGHT APRIL 1987 - SJB;UNUT;BS*
C ***************************************************************************
C
C     PROGRAM TO CALCULATE THE CARBON EQUIVALENTS FOR PLATES TO BE
C     SKID WELDED DURING EXPERIMENTAL TRIALS, FROM PREDICTED COOLING
C     RATES CALCULATE THE POTENTIAL WELD HARDNESS
C
C     DATA IS INPUT FROM A DATAFILE CONNECTED TO CHANNEL 5
C     OUTPUT IS EITHER TO A DATAFILE OR SCREEN CONNECTED TO CHANNEL 6

C     DATA INPUT AND OUTPUT IN UNITS OF MM,SECS,KG,KW BUT CONVERTED TO



C     M,KG,SECS,WATT  FOR CALCULATIONS
C     ***************************************************************************
C
      IMPLICIT REAL*8(A-H,O-Z)
      DIMENSION CHEML(24),ICHEMN(24),IPLCOD(15),TRAVS(10),COOLR(10)
C
C     ***************************************************************************
C     DATA IS INPUT FROM DATAFILE CONNECTED TO CHANNEL 5
C     ***************************************************************************
C
      READ (5,1001) IPLCOD,PLTHK
1001  FORMAT (15A1/F6.2)
C
      DO 3001 N=1,24
      READ (5,1002) ICHEMN(N),CHEML(N)
1002  FORMAT (A2,F8.5)
3001  CONTINUE
C
      READ (5,1003) POLO,FPOLO,AMTEMP,TRAVS,COOLR
1003  FORMAT (F6.2/F4.2/F6.2/10F6.2/10F6.2)
C
      CALL CHEM(IPLCOD,PLTHK,ICHEMN,CHEML,C,PCM,CEB,CEIMS)
      CALL HARD(C,PCM,CEB,TRAVS,COOLR)
C
      STOP
      END
C
```

```
C     ************************************************************************
C     *                        SUBROUTINES                                   **
C     ************************************************************************
C
C
C     ************************************************************************
C     *                  SUBROUTINE - CHEM                                   *
C     ************************************************************************
C
C     SUBROUTINE IS DESIGNED TO GIVE VARIOUS CHEMICAL PROPERTIES OF STEEL
C     PLATE. INPUT DATA IS THE CHEMICAL COMPOSITION OF THE PLATE.
C     ************************************************************************
C
      SUBROUTINE CHEM(IPLCOD,PLTHK,ICHEMN,CHEML,C,PCM,CEB,CEIMS)
C
      IMPLICIT REAL*8(A-H,O-Z)
      DIMENSION CHEML(24),ICHEMN(24),IPLCOD(15)
C
      WRITE (6,210)
210   FORMAT (50H1PLATE CHEMICAL COMPOSITION AND CARBON EQUIVALENTS)
      WRITE (6,211)
211   FORMAT (50H ==========================================)
C
      WRITE (6,221) IPLCOD,PLTHK
221   FORMAT (2H0 / 15H0Plate code is ,15A1,19HPlate thickness is ,F6.2,
     *2HMM)
      WRITE (6,216)
216   FORMAT (2H0 / 27H0Element  % Level by Weight)
      WRITE (6,217)
217   FORMAT (27H -------  ----------------)
C
C     ************************************************************************
C     CHEMICAL NAMES AND RESPECTIVE PERCENTAGE LEVELS ARE NOW  READ
C     AND PRINTED
C     ************************************************************************
C
      DO 301 N=1,24
      WRITE (6,201) ICHEMN(N),CHEML(N)
201   FORMAT(3X,A2,10X,F7.2)
301   CONTINUE
C
C****CARBON EQUIVALENTS BY VARIOUS AUTHORS CALCULATED
C
      C=CHEML(1)
C
      CEIM=CHEML(1)+CHEML(3)/6.0+(CHEML(7)+CHEML(8)+CHEML(9))*0.2+(CHEML
     *(6)+CHEML(15))/15.0
C
      CEIMS=CEIM+CHEML(2)/6.0
C
      CEMOD=CHEML(1)+CHEML(3)/6.0+CHEML(2)/24.0+CHEML(6)/40.0+CHEML(7)/5
     *.0+CHEML(8)/4.0
C
      CESEK=CEMOD+CHEML(9)/14.0
C
      CEBC=CHEML(1)+(CHEML(2)+CHEML(5))/3.0
```

```
      CEK=CHEML(1)+CHEML(3)/5.0+(CHEML(2)+CHEML(15))/7.0+CHEML(6)/20.0+C
     *HEML(7)/9.0+(CHEML(8)+CHEML(9))/2.0
C
      PCM=CHEML(1)+CHEML(2)/30.0+(CHEML(3)+CHEML(15)+CHEML(7))/20.0+CHEM
     *L(6)/60.0+CHEML(8)/15.0+CHEML(9)/10.0+CHEML(13)*5.0
C
      CEB=CHEML(1)+CHEML(2)/11.0+CHEML(3)/8.0+CHEML(15)/9.0+CHEML(7)/5.0
     *+CHEML(6)/17.0+CHEML(8)/6.0+CHEML(9)/3.0
C
C     **********************************************************
C     ULTIMATE TENSILE STRENGTH OF PLATE PREDICTED USING A REGRESSION
C     CURVE FROM THE EXPERIMENTAL RESULTS CE(K)
C     **********************************************************
C
      UTS=362.05+304.52*CEK
C
C****CARBON EQUIVALENTS NOW TO CHANNEL 6
C
      WRITE (6,1210)
1210  FORMAT (2H0 )
      WRITE (6,218)
218   FORMAT (52H0Carbon Equivalent    Reference    Carbon Equivalent)
      WRITE (6,219)
219   FORMAT (52H    Type                               Levels       )
      WRITE (6,220)
220   FORMAT (52H ---------------     ---------    -----------------)
C
      WRITE (6,202) CEIM
202   FORMAT (38H0  CE[IIW(M)]        LLOYDS/IIW       ,F6.2)
C
      WRITE (6,203) CEIMS
203   FORMAT (38H0  CE[IIW(M+S)]                       ,F6.2)
C
      WRITE (6,215) CEMOD
215   FORMAT (38H0  CE[MOD]           MOD(NAVY)        ,F6.2)
C
      WRITE (6,204) CESEK
204   FORMAT (38H0  CE[SEKIGUCHI]                      ,F6.2)
C
      WRITE (6,205) CEBC
205   FORMAT (38H0  CE[BCIRA]         BCIRA            ,F6.2)
C
      WRITE (6,206) CEK
206   FORMAT (38H0  CE[KIHARA]        KIHARA           ,F6.2)
C
      WRITE (6,207) PCM
207   FORMAT (38H0  PCM               ITO-BESSYO       ,F6.2)
C
      WRITE (6,230) CEB
230   FORMAT (38H0  CEB                                DUEREN       ,F6.2)
C
C****UTS NOW WRITTEN
C
      WRITE (6,240) UTS
240   FORMAT ('0ESTIMATED TENSILE STRENGTH=',F6.2,'(N/MM2)')
C
      RETURN
      END                                    510
```

```
C
C     ****************************************************************
C     *                    SUBROUTINE - HARD                         *
C     ****************************************************************
C
C
C     SUBROUTINE IS DESIGNED TO PREDICT MAXIMUM WELD HARDNESSES IN
C     THE HAZ FOR THE GIVEN PLATE CHEMICAL COMPOSITION, BOTH
C     DEPEDENTLY AND INDIPENDENTLY OF THE COOLING RATE
C     ****************************************************************
C
      SUBROUTINE HARD(C,PCM,CEB,TRAVS,COOLR)
C
      IMPLICIT REAL*8(A-H,O-Z)
      DIMENSION COOLR(10),TRAVS(10)
C
C     ****************************************************************
C     MAX.  HARNESS CALCULATED INDEPENDENT OF COOLING RATE AND PRINTED
C     ****************************************************************
C
      HVM=802.0*C+305
      HVMC=996.67*C+264.27
      HVB=350*CEB+101
C
      WRITE (6,220)
220   FORMAT (52H1HARDNESS FOR 100% MARTENSTIC AND BAINITIC STRUCTURE)
      WRITE (6,228)
228   FORMAT (52H ================================================)
C
      WRITE (6,221)
221   FORMAT (45H0Characteristic   Reference   Hardness [HV10])
      WRITE (6,222)
222   FORMAT (45H --------------   ---------   --------------)
      WRITE (6,223)HVM
223   FORMAT (32H0100% Martensite   Dueren       ,F6.1)
      WRITE (6,225)HVMC
225   FORMAT (32H0100% Martensite   Coe          ,F6.1)
      WRITE (6,224)HVB
224   FORMAT (32H0100% Bainite      Dueren       ,F6.1)
C     ****************************************************************
C     HARDNESS NOW CALCULATED FOR VARIOUS COOLING RATES FOR THE GIVEN
C     PLATE, AND PRINTED
C     ****************************************************************
C
C
      GA1=(187+64*C+485*PCM)
      GB1=(97+680*C-441*PCM)
      GC1=(0.501+7.9*C-11.01*PCM)
      GD1=(0.543+0.55*C-0.76*PCM)
C
      WRITE (6,1230)
1230  FORMAT (2H0 /2H0 /2H0 )
      WRITE (6,230)
230   FORMAT (46H0CALCULATED HARDNESS FOR VARIOUS COOLING RATES)
      WRITE (6,231)
231   FORMAT (46H ==============================================)
```

```
      WRITE (6,232)
 232  FORMAT (33H0Cooling Rate    Maximum Hardness)
      WRITE (6,233)
 233  FORMAT (33H ------------    ----------------)
C
      DO 300 N=1,10
      XCT=DLOG10(COOLR(N))
      HMAX=GA1-GB1*DATAN((XCT+GC1)/GD1)
C
      WRITE (6,234) COOLR(N),HMAX
 234  FORMAT (4H0   ,F4.1,12X,F8.2)
C
 300  CONTINUE
C
      CT=10**(GD1*DTAN((GA1-350.0)/GB1)-GC1)
C
      WRITE (6,235) CT
 235  FORMAT (37H0COOLING TIME AT WHICH HMAX>350HV IS ,F4.1,8H SECONDS)
C
      RETURN
      END
C*****************************************************************************
```

```
Listing of P082 at 15:49:13 on FEB 13, 1987 for CCid=NVC9

     1      P08/02/SHS
     2      8.0
     3      C 0.0750
     4      SI0.255
     5      MN0.812
     6      S 0.014
     7      P 0.015
     8      NI0.017
     9      CR0.025
    10      MO0.005
    11      V 0.0030
    12      AL0.026
    13      TI0.00000
    14      AR0.01200
    15      B 0.0004
    16      CO0.0040
    17      CU0.042
    18      NB0.0000
    19      PB0.00170
    20      SN0.00000
    21      TU0.0000
    22      BI0.000
    23      AN0.000
    24      ZI0.0010
    25      CE0.0000
    26      TA0.00000
    27      09.0
    28      0.5
    29      20.0
    30       04.00 06.00 08.00 10.00 12.00 14.00 17.50 19.50 23.00 30.00
    31       01.00 02.00 06.00 08.00 10.00 15.00 20.00 25.00 30.00 50.00
```

D-2.1 Computer printout of the output from the SKIDPROP program

PLATE CHEMICAL COMPOSITION AND CARBON EQUIVALENTS

PLATE CODE IS P08/02/SHS PLATE THICKNESS IS 8.00MM

ELEMENT	% LEVEL BY WEIGHT
C	0.07
SI	0.26
MN	0.81
S	0.01
P	0.02
NI	0.02
CR	0.02
MO	0.01
V	0.00
AL	0.03
TI	0.0
AR	0.01
B	0.00
CO	0.00
CU	0.04
NB	0.0
PB	0.00
SN	0.0
TU	0.0
BI	0.0
AN	0.0
ZI	0.00
CE	0.0
TA	0.0

CARBON EQUIVALENT TYPE	REFERENCE	CARBON EQUIVALENT LEVELS
CE[IIW(M)]	LLOYDS/IIW	0.22
CE[IIW(M+S)]		0.26
CE[MOD]	MOD(NAVY)	0.23
CE[SEKIGUCHI]		0.23

HARDNESS FOR 100% MARTENSTIC AND BAINITIC STRUCTURE

CHARACTERISTIC	REFERENCE	HARDNESS [HV10]
100% MARTENSITE	DUEREN	365.1
100% MARTENSITE	COE	339.0
100% BAINITE	DUEREN	175.3

CALCULATED HARDNESS FOR VARIOUS COOLING RATES

COOLING TIME (Sec)	MAXIMUM HARDNESS (Hv)
1.0	310.58
2.0	262.62
6.0	188.74
8.0	177.37
10.0	170.35
15.0	160.53
20.0	155.24
25.0	151.83
30.0	149.41
50.0	143.93

COOLING TIME AT WHICH HMAX>350HV IS 0.3 SECONDS

CE[BCIRA]	BCIRA	0.16
CE[KIHARA]	KIHARA	0.29
PCM	ITO-BESSYO	0.13
CEB	DUEREN	0.21

ESTIMATED TENSILE STRENGTH=449.59(N/MM2)

D-3 CHEMICAL ANALYSIS OF STEEL PLATES USED FOR THE WELDING TRIALS

TABLE - CHEMICAL ANALYSIS OF THE PLATE STEELS USED IN SKID WELDING TRIALS

Plate Thk (mm)	Plate No.	C	S	P	S_i	M_n	N_i	C_r	M_o	V	C_u	N_b	T_i	A_l	B	S_n	C_o	C.E. (IIW)	C.E. $IIW+\frac{S_i}{6}$	C.E. (MCD)	C.E. (KIHARA)	P_{cm}
3	P3/1/SMS	0.14	0.028	0.015	0.22	0.59	0.01	0.009	0.004	-	0.029	-	-	0.024	0.0004	-	0.001	0.24	0.28	0.25	0.29	0.20
6	P6/1/CS	0.19	0.010	0.014	0.20	0.68	0.06	0.020	0.016	-	0.014	-	-	0.023	0.0007	-	-	0.32	0.35	0.32	0.37	0.24
6	P6/2/SMS	0.10	0.010	0.014	0.23	0.50	0.06	0.020	0.016	-	0.014	-	-	0.023	0.0007	-	-	0.19	0.23	0.20	0.24	0.14
8	P8/1/APS	0.12	0.012	0.026	0.24	0.67	0.02	0.022	0.004	0.003	0.035	0.001	0.002	0.022	0.0002	0.007	0.007	0.24	0.28	0.25	0.30	0.17
8	P8/2/SMS	0.07	0.014	0.015	0.25	0.81	0.02	0.02	0.005	0.003	0.0042	-	-	0.026	0.0004	-	0.004	0.22	0.26	0.23	0.29	0.13
8	P8/3/SMS	0.12	0.011	0.010	0.13	0.57	0.17	0.11	0.031	0.004	0.453	0.001	0.001	0.034	0.0007	0.016	0.013	0.37	0.39	0.25	0.43	0.27
8	P8/4/SMS	0.11	0.018	0.016	0.24	0.85	0.04	0.03	0.007	-	0.046	0.001	-	0.011	0.0004	0.017	0.007	0.27	0.31	0.27	0.33	0.17
10	P10/1/SMS	0.10	0.008	0.020	0.27	0.51	-	0.05	0.01	0.030	0.003	-	0.005	0.06	0.0003	-	-	0.20	0.25	0.21	0.27	0.15
11	P12/1/SMS	0.20	0.022	0.024	0.31	0.93	0.04	0.03	0.006	-	0.055	-	-	0.023	0.0005	0.001	0.001	0.37	0.42	0.37	0.44	0.26
12	P12A/1/SMS	0.19	0.014	0.013	0.21	0.72	-	0.02	0.005	-	0.009	-	-	0.016	0.0002	-	0.006	0.32	0.35	0.32	0.37	0.24
15	P15/1/SMS	0.19	0.016	0.012	0.21	0.74	-	0.01	0.003	-	0.011	-	0.001	0.015	0.0002	-	0.007	0.32	0.36	0.33	0.38	0.24
Avc.	P.AVERAGE	0.14	0.015	0.016	0.23	0.70	0.04	0.03	0.009	0.003	0.065	0.0002	0.001	0.024	0.0004	0.003	0.004	0.27	0.31	0.27	0.33	0.19

Table D6.01a - Chemical analysis of the plate steels used in skid welding trials

TABLE – CHEMICAL ANALYSIS OF THE ROLLED SECTION STEELS USED IN SKID WELDING TRIALS

Plate Thk (mm)	Plate No.	C	S	P	S_i	M_n	N_i	C_r	M_o	V	C_u	N_b	T_i	A_l	B	S_n	C_o	C.E. (IIW)	C.E. $IIW+\frac{S_i}{6}$	C.E. (MCD)	C.E. (KIHARA)	P_{cm}
6	FB6/1/CS	0.17	0.027	0.026	0.27	0.69	0.14	0.14	0.024	0.002	0.290	–	–	0.012	0.0006	0.016	0.008	0.35	0.39	0.33	0.42	0.24
8	FB8/1/SHS	0.25	0.034	0.023	0.19	0.66	0.18	0.15	0.043	0.003	0.373	0.002	0.002	0.006	0.0002	0.022	0.016	0.44	0.55	0.41	0.51	0.32
10	FB/10/APS	0.13	0.019	0.019	0.15	0.58	0.16	0.12	0.024	0.005	0.340	0.001	–	0.013	0.0007	0.037	0.019	0.28	0.31	0.27	0.35	0.19
12	FB12/1/SHS	0.19	0.014	0.016	0.18	0.79	0.03	0.03	0.006	–	0.090	0.001	–	0.013	0.0003	0.019	0.007	0.33	0.36	0.33	0.39	0.24
15	FB15/1/SHS	0.16	0.020	0.016	0.24	0.83	0.12	0.09	0.020	–	0.280	0.002	–	0.007	0.0005	0.035	0.014	0.35	0.39	0.33	0.43	0.23

Table D6.02b – Chemical analysis of the rolled section steels used in skid welding trials

D-4 MICROPHOTOGRAPHS OF SKID WELD MICROSTRUCTURES

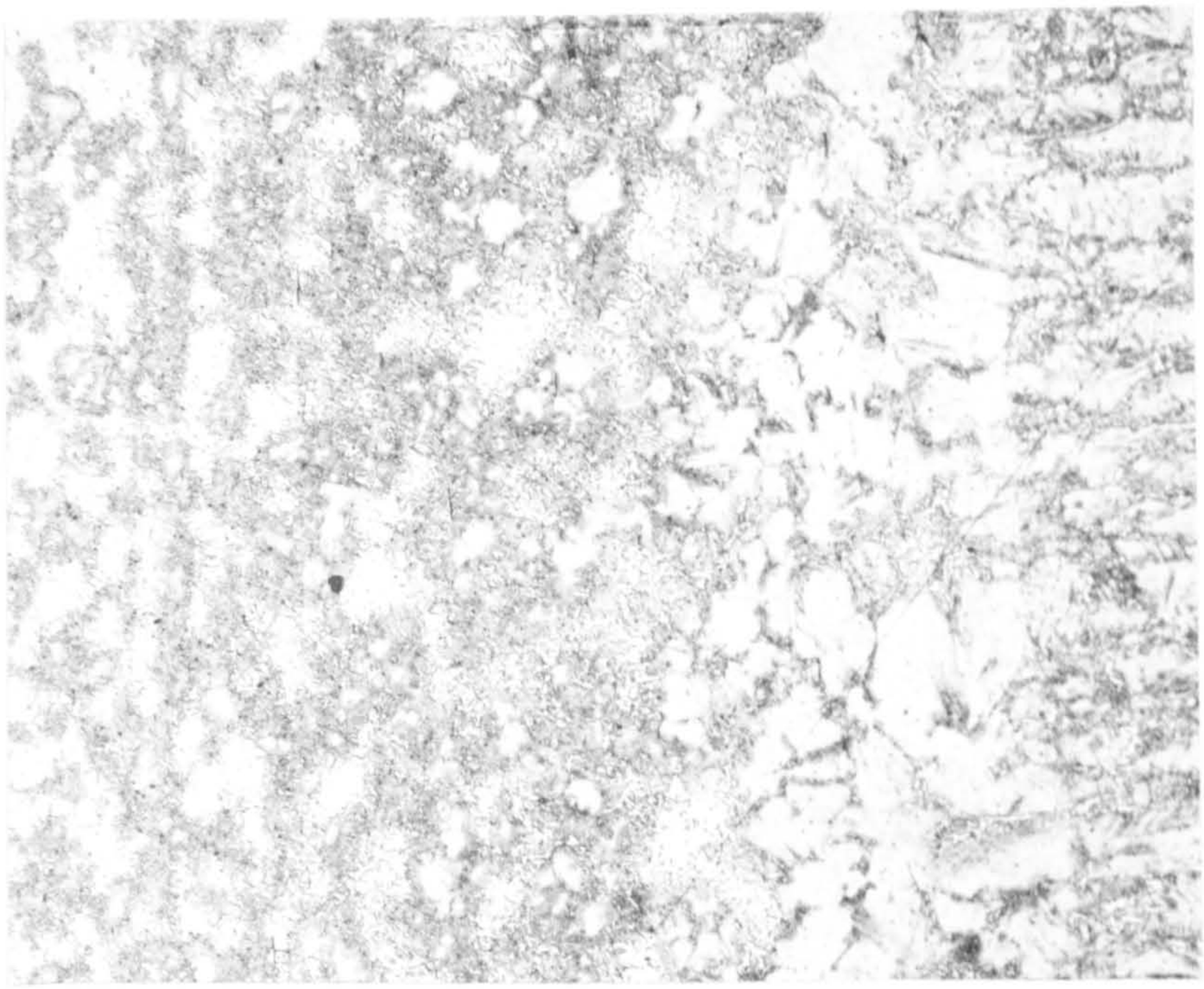

Figure D6.01a - HAZ and fusion line within a 3mm skid weld (x200)

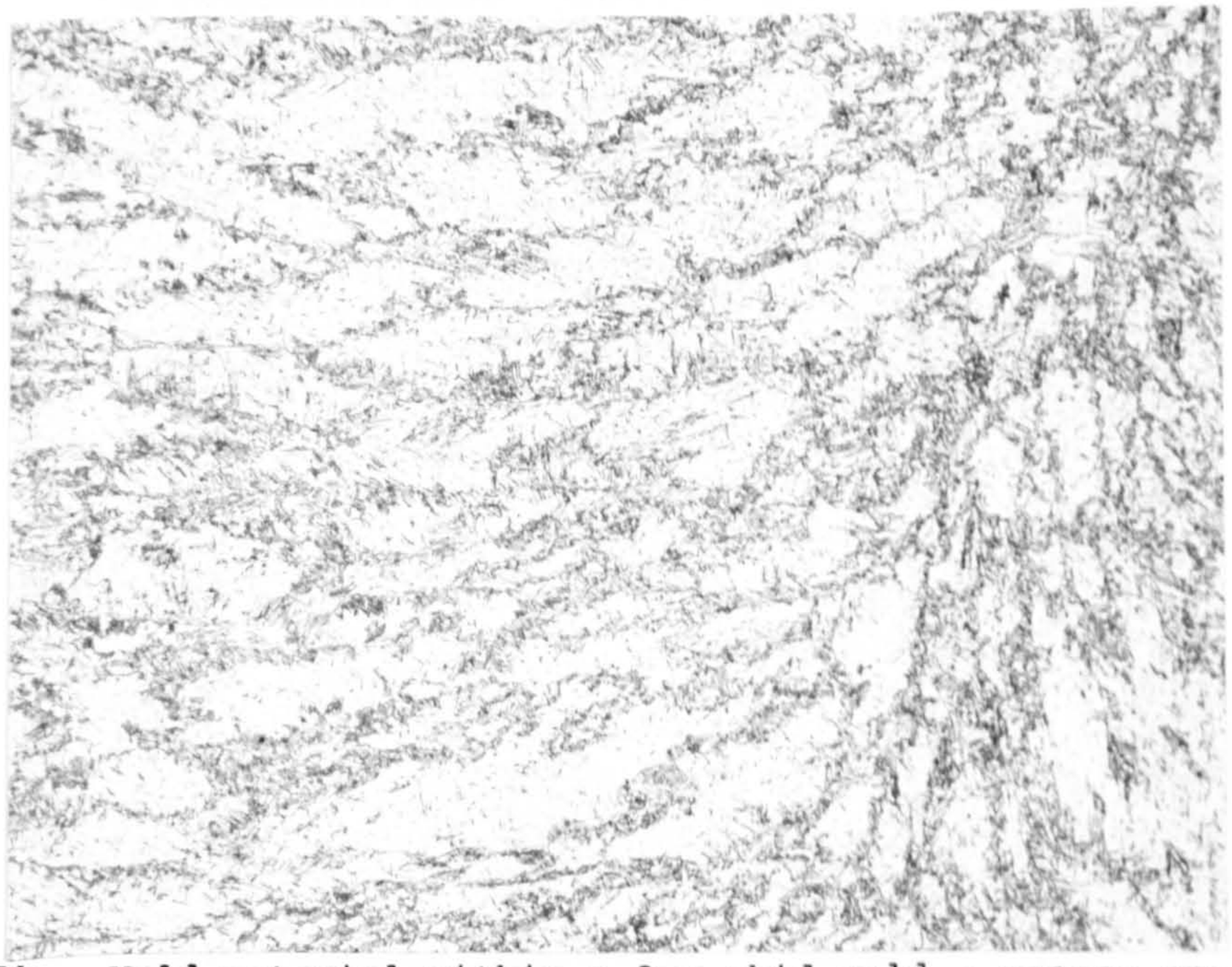

Figure D6.01b - Weld material within a 3mm skid weld ; coarse grains of transformed martensite (x200)

Figure D6.01c - Coarse martensite grains within a 3mm skid weld (x500)

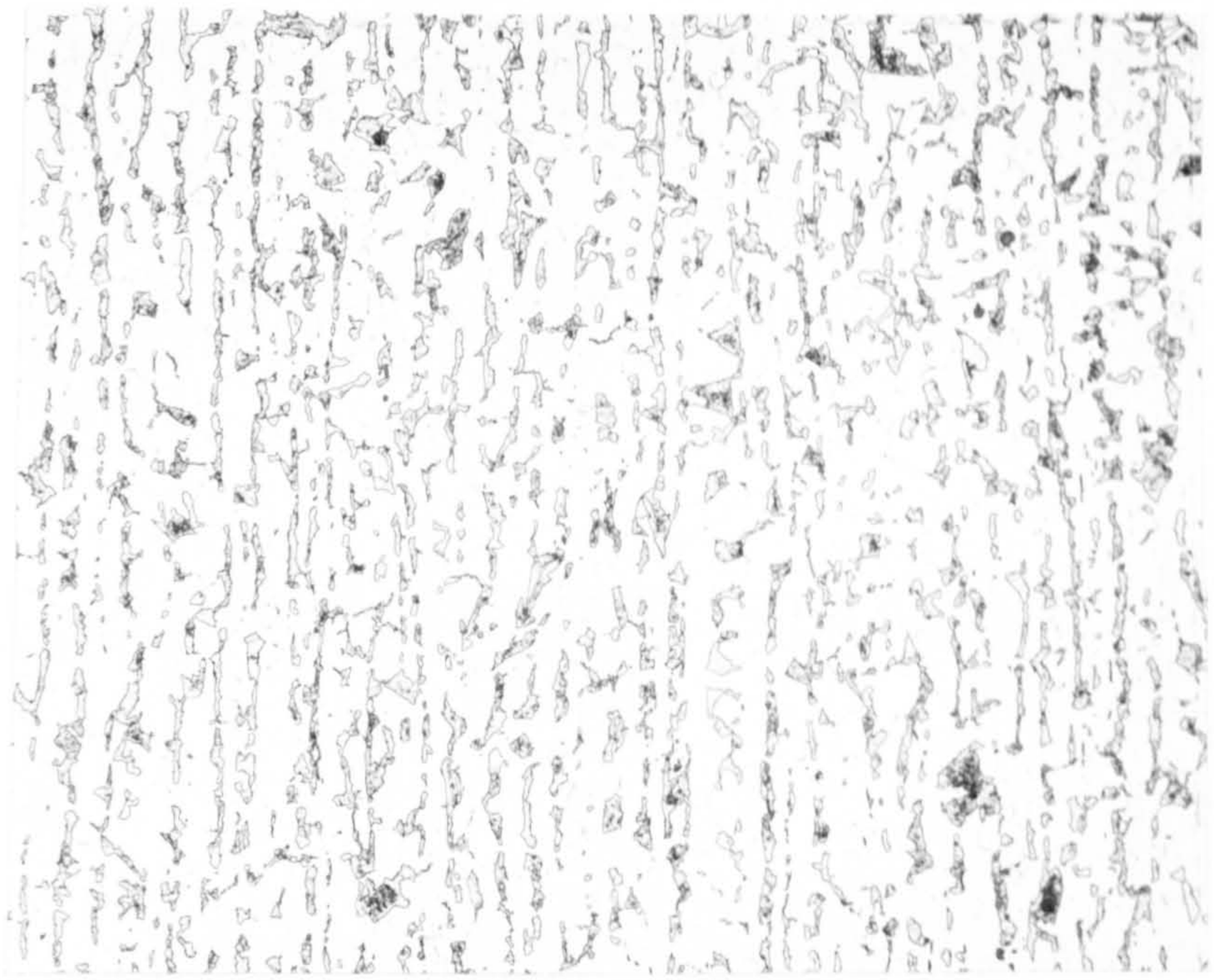

Figure D6.02a - Parent plate for a 6mm joint (x200)

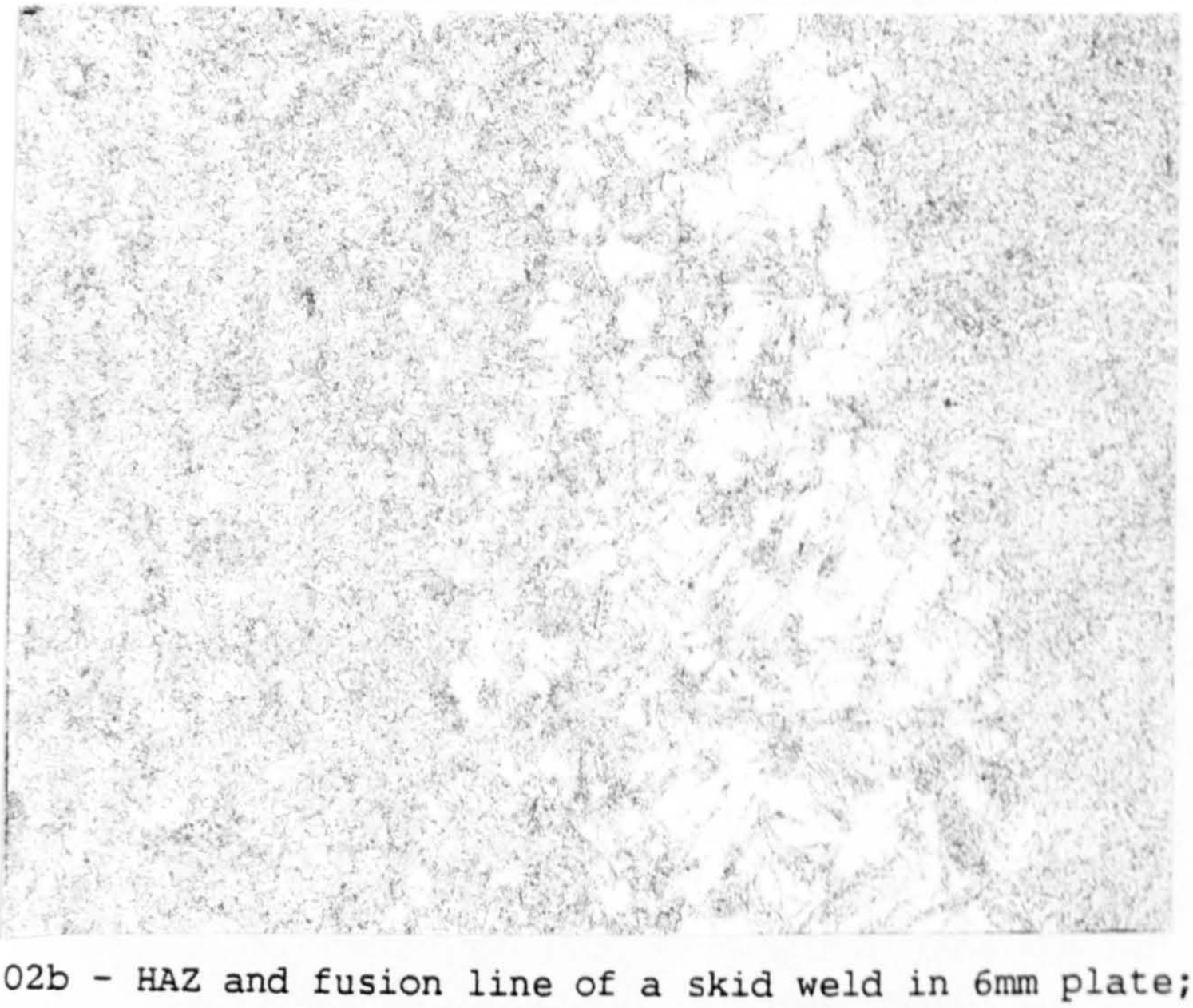

Figure D6.02b - HAZ and fusion line of a skid weld in 6mm plate; narrow zone of martensite at the fusion line

Figure D6.02c - Weld material in a 6mm plate joint; columnar grains solidifying into weld centreline

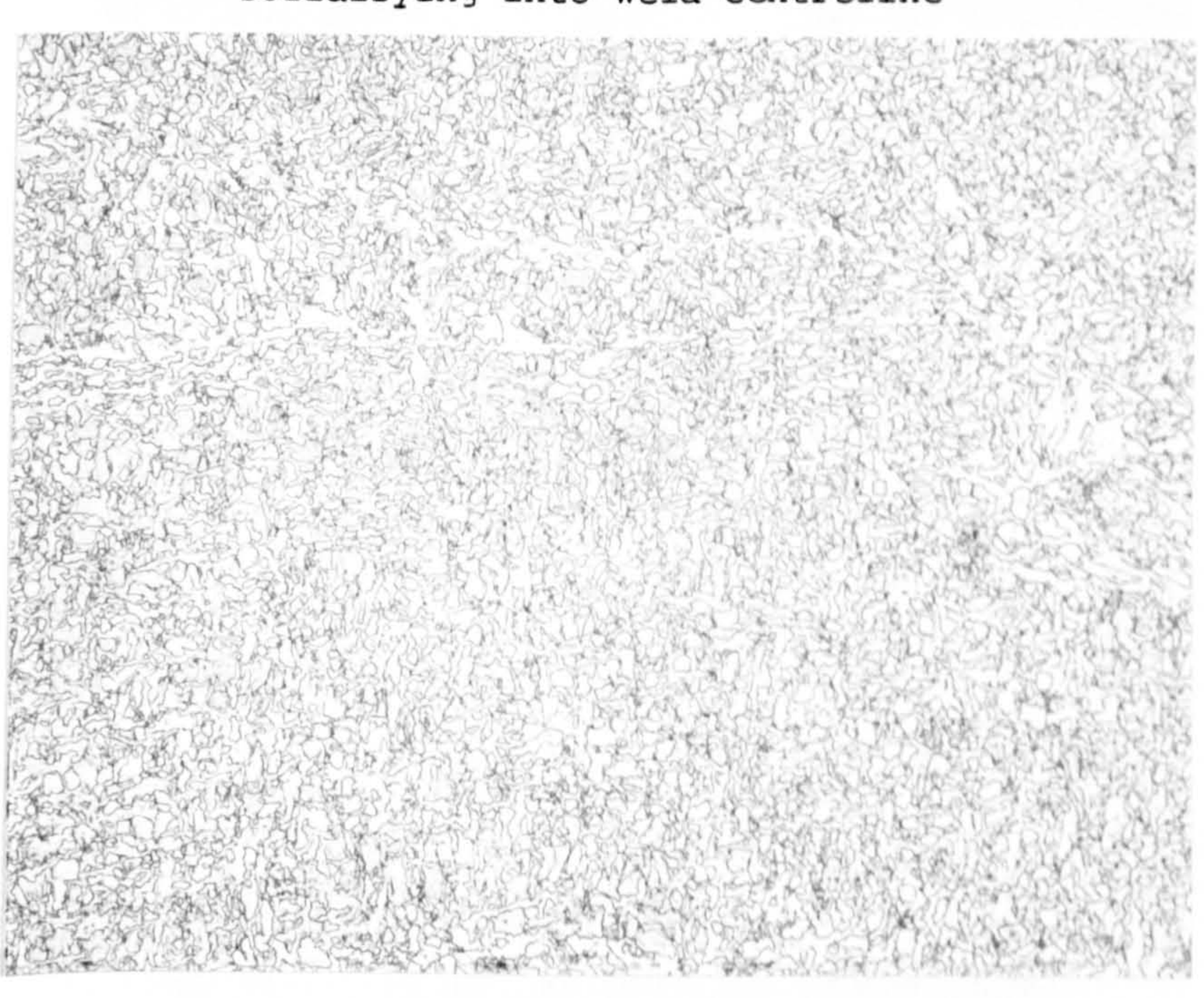

Figure D6.02d - Weld material in a 6mm plate joint; fine grains of acicular ferrite (x1000)

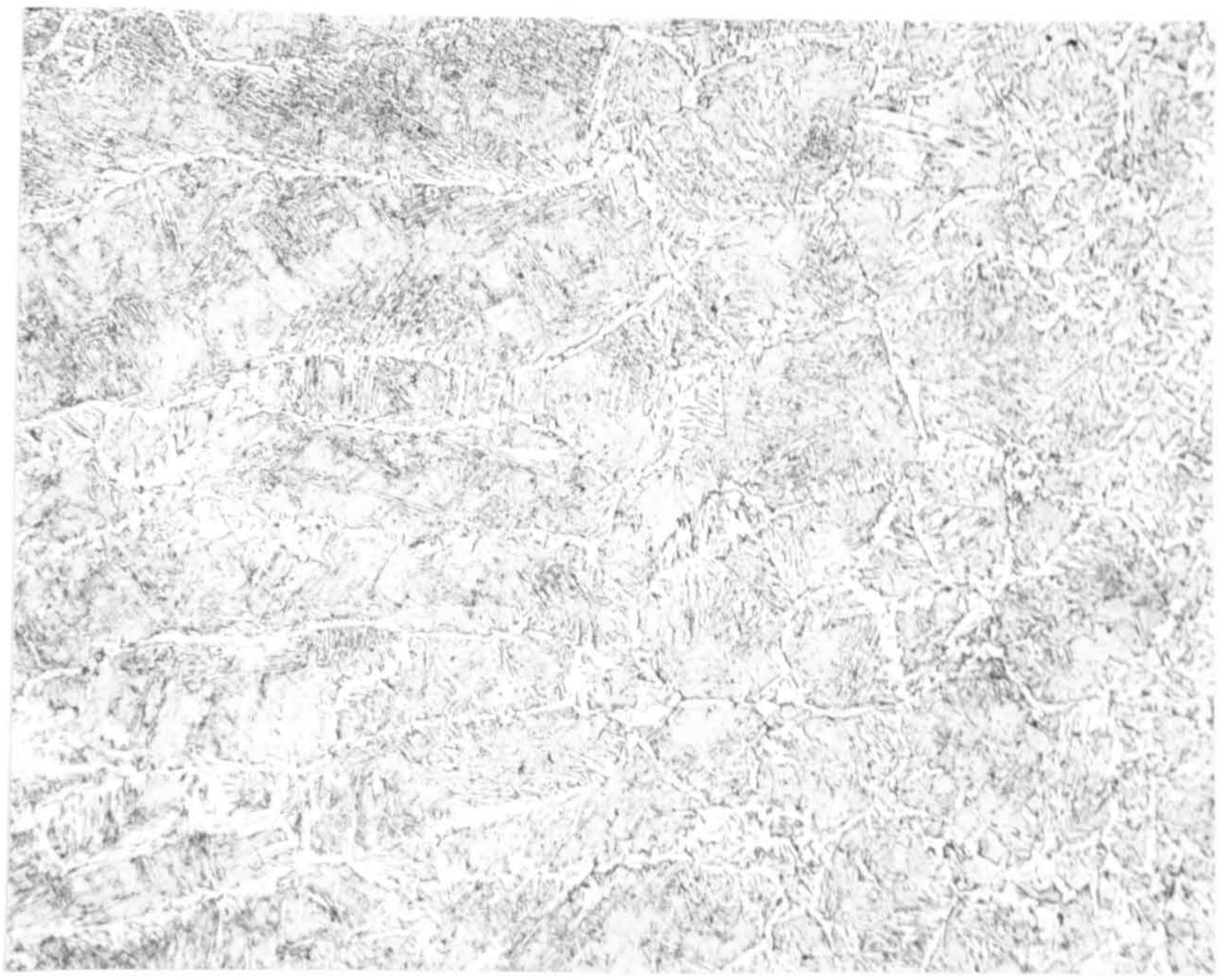

Figure D6.03a - Skid weld in 10mm plate; HAZ and fusion line (x200)

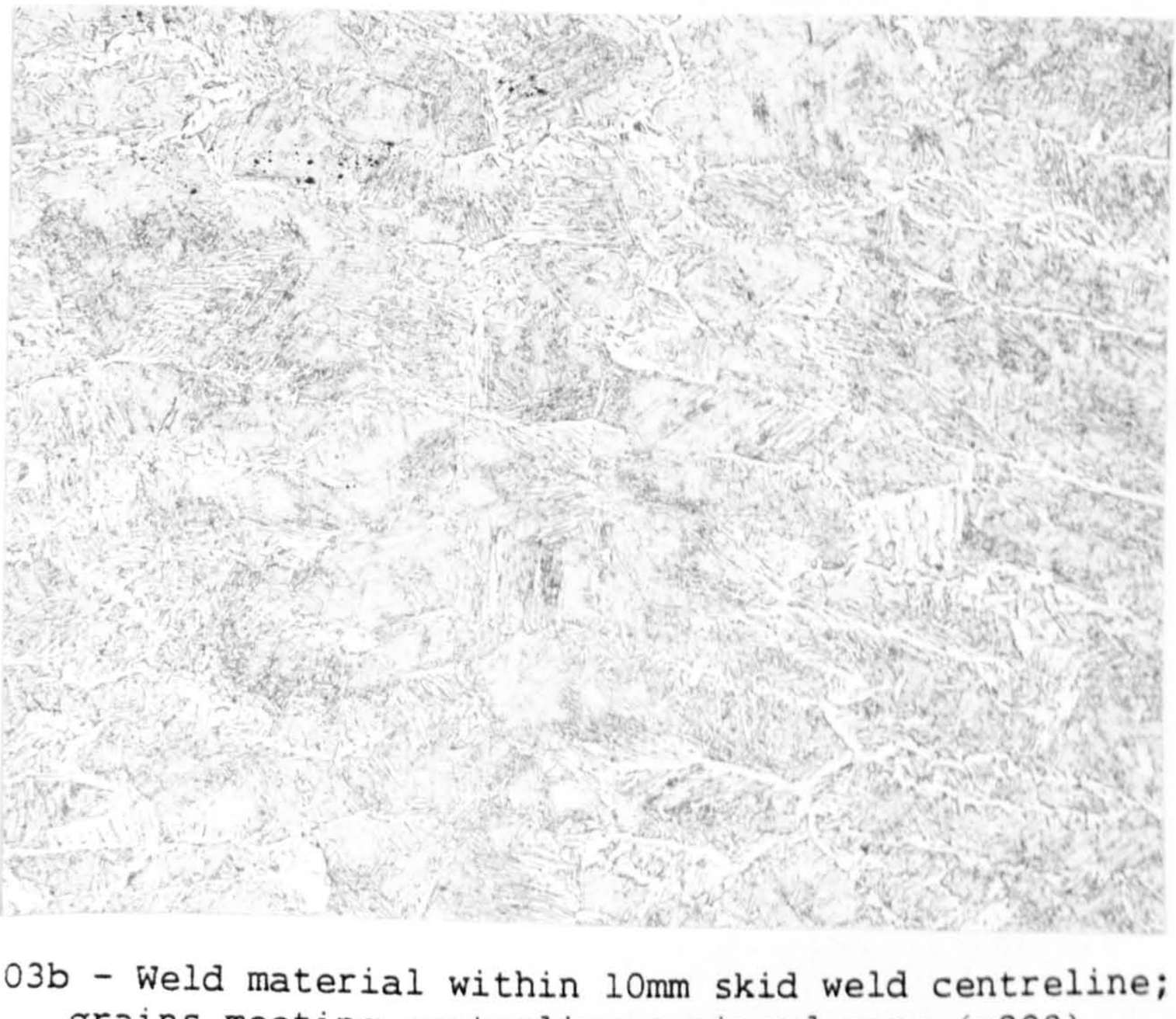

Figure D6.03b - Weld material within 10mm skid weld centreline; columnar grains meeting centreline equiaxed zone (x200)

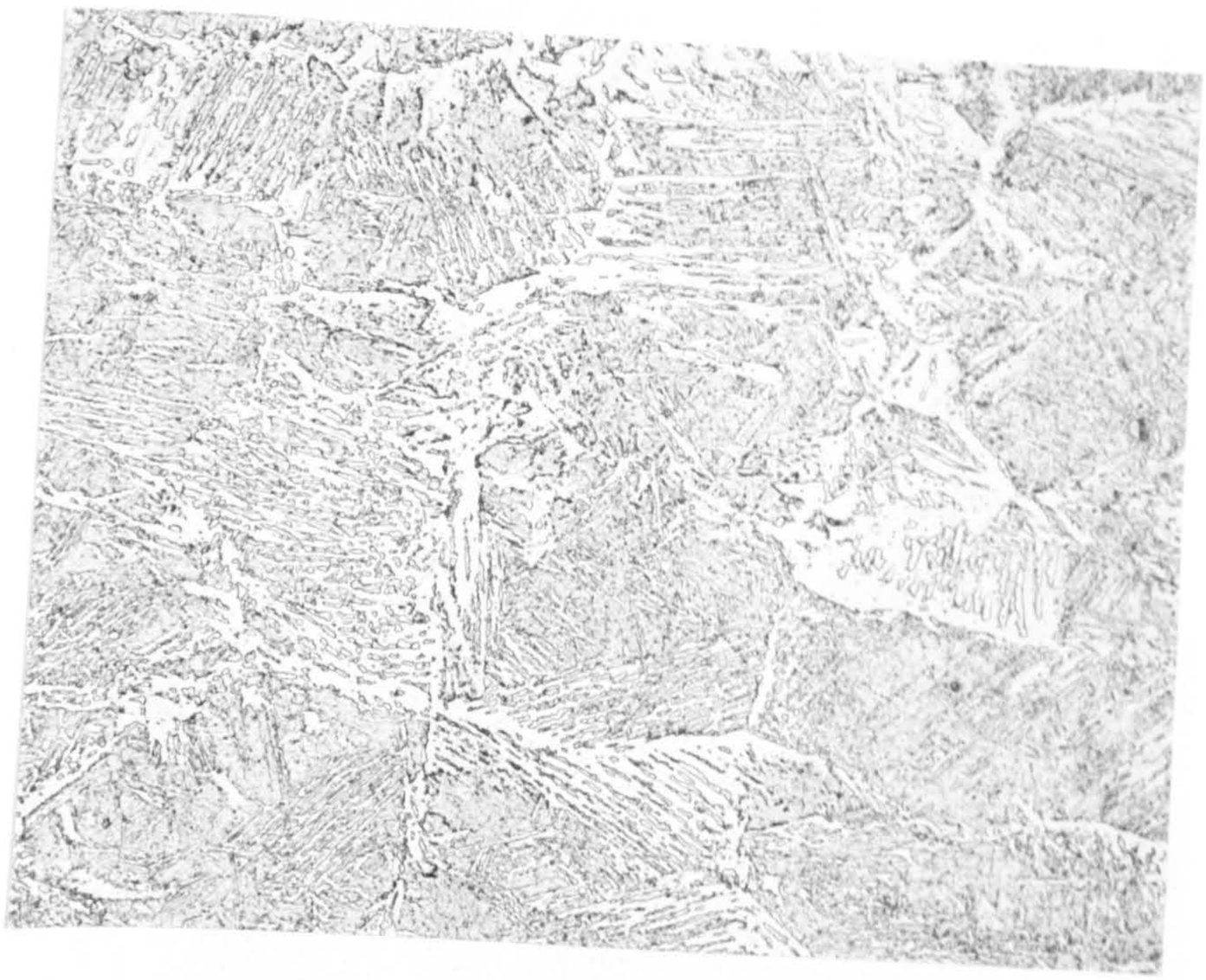

Figure D6.03c - Weld material of a 10mm skid weld; coarse zones of PF (x500)

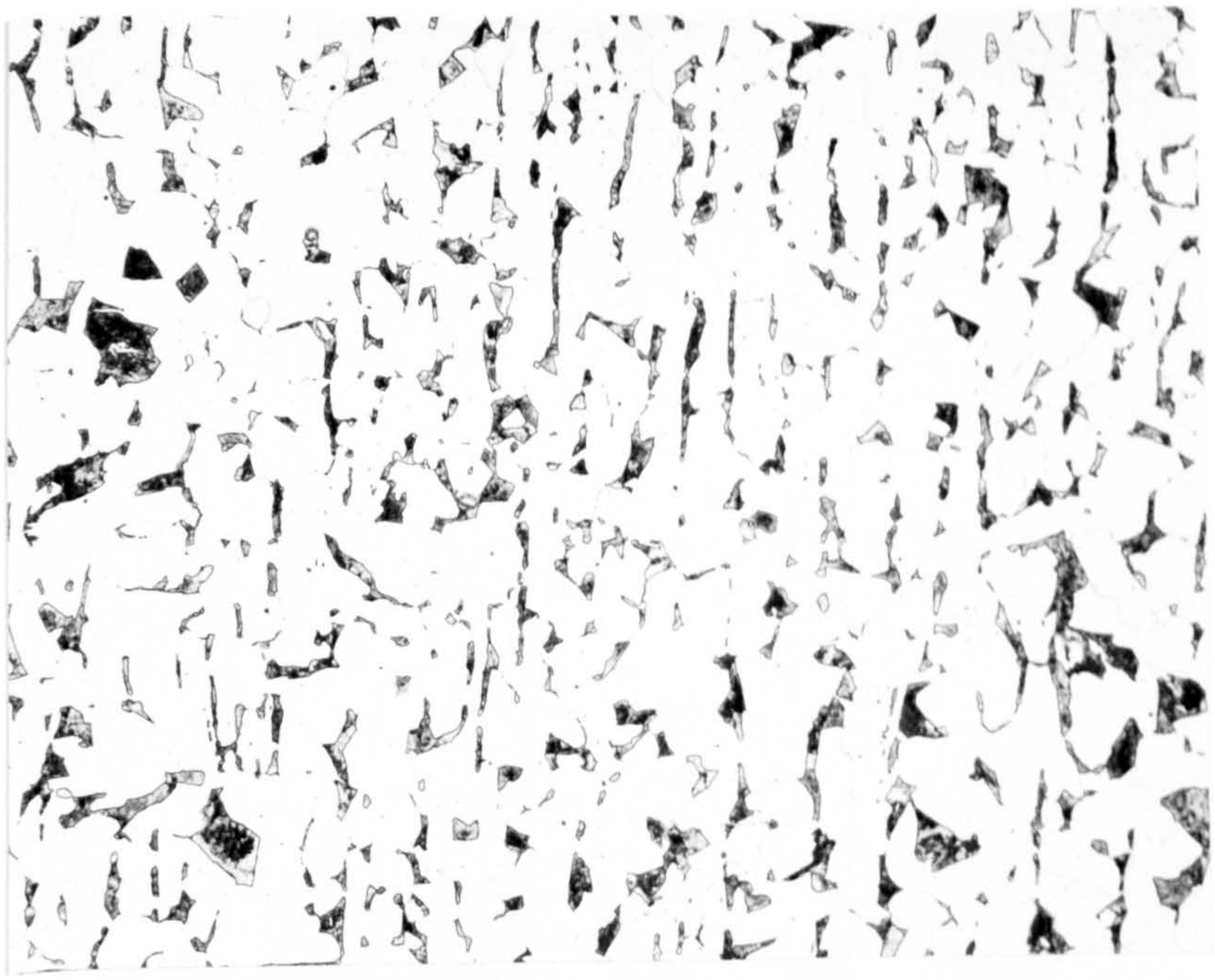

Figure D6.04a - 12mm thick parent plate (x200)

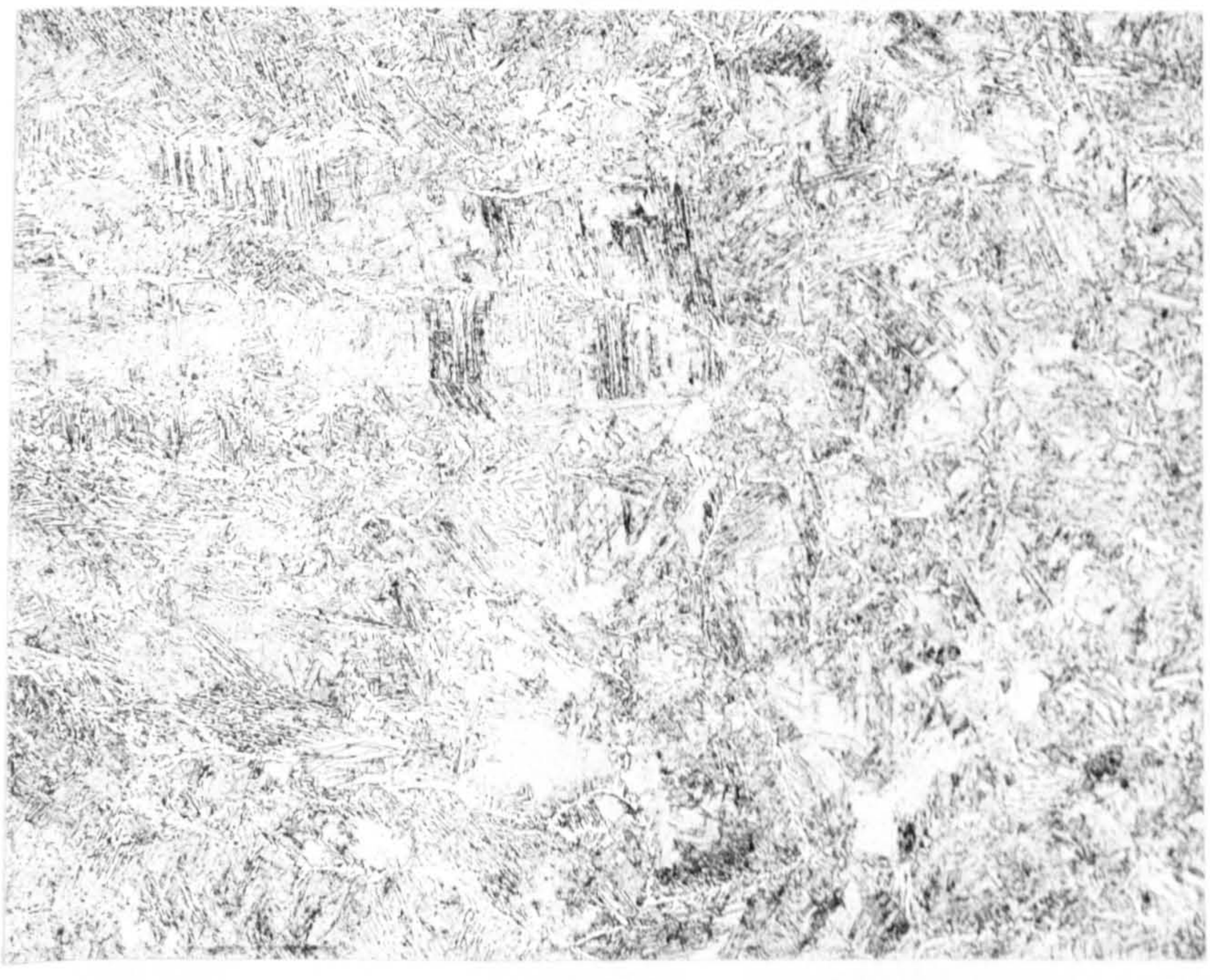

Figure D6.04b - Skid weld in 12mm plate; fusion line (x200)

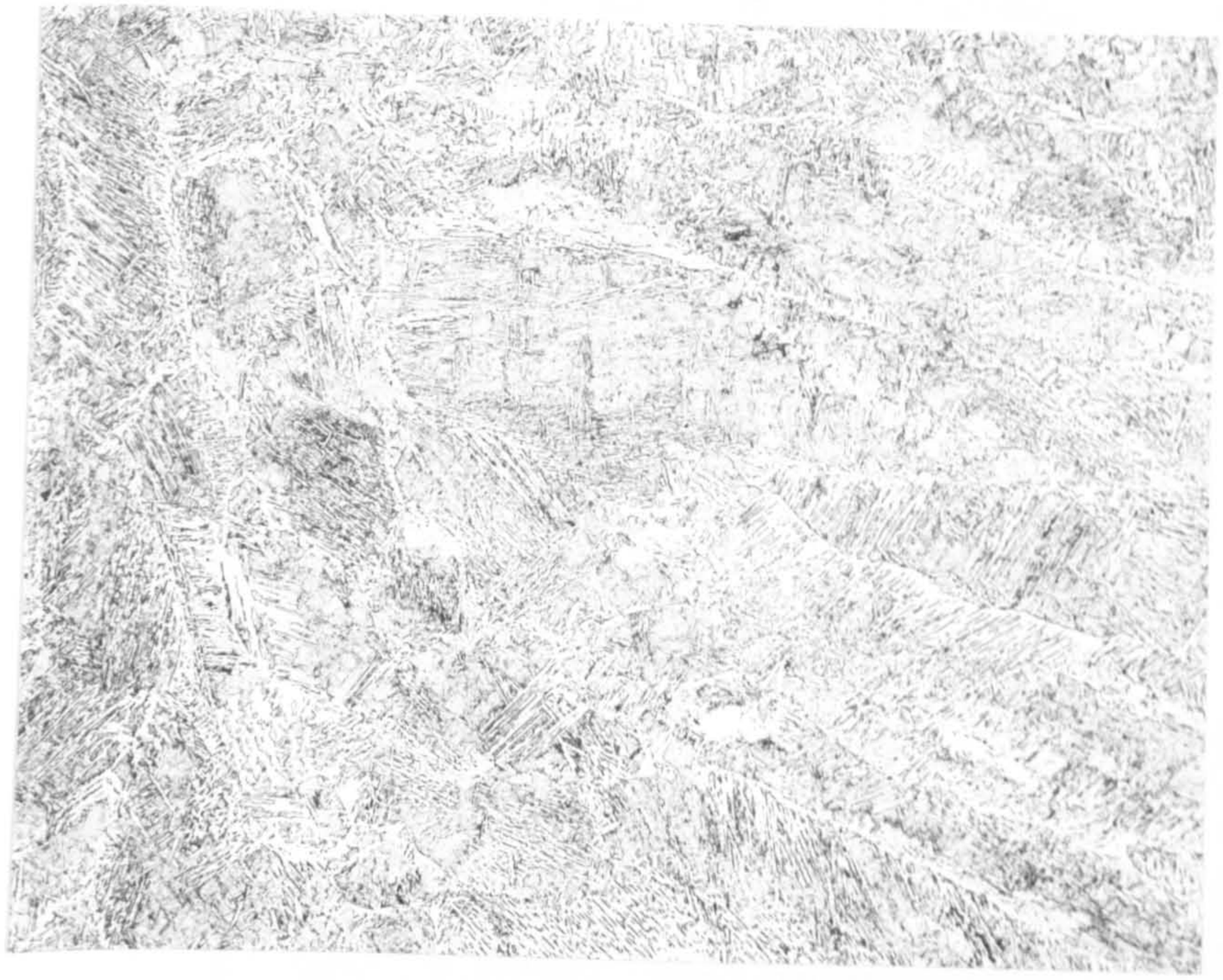

Figure D6.04c - Skid weld in 12mm plate, weld centre; course columnar grains join central equiaxed grains, fine AC and FC (x200)

Figure D6.05a - 15mm thick parent plate (x200)

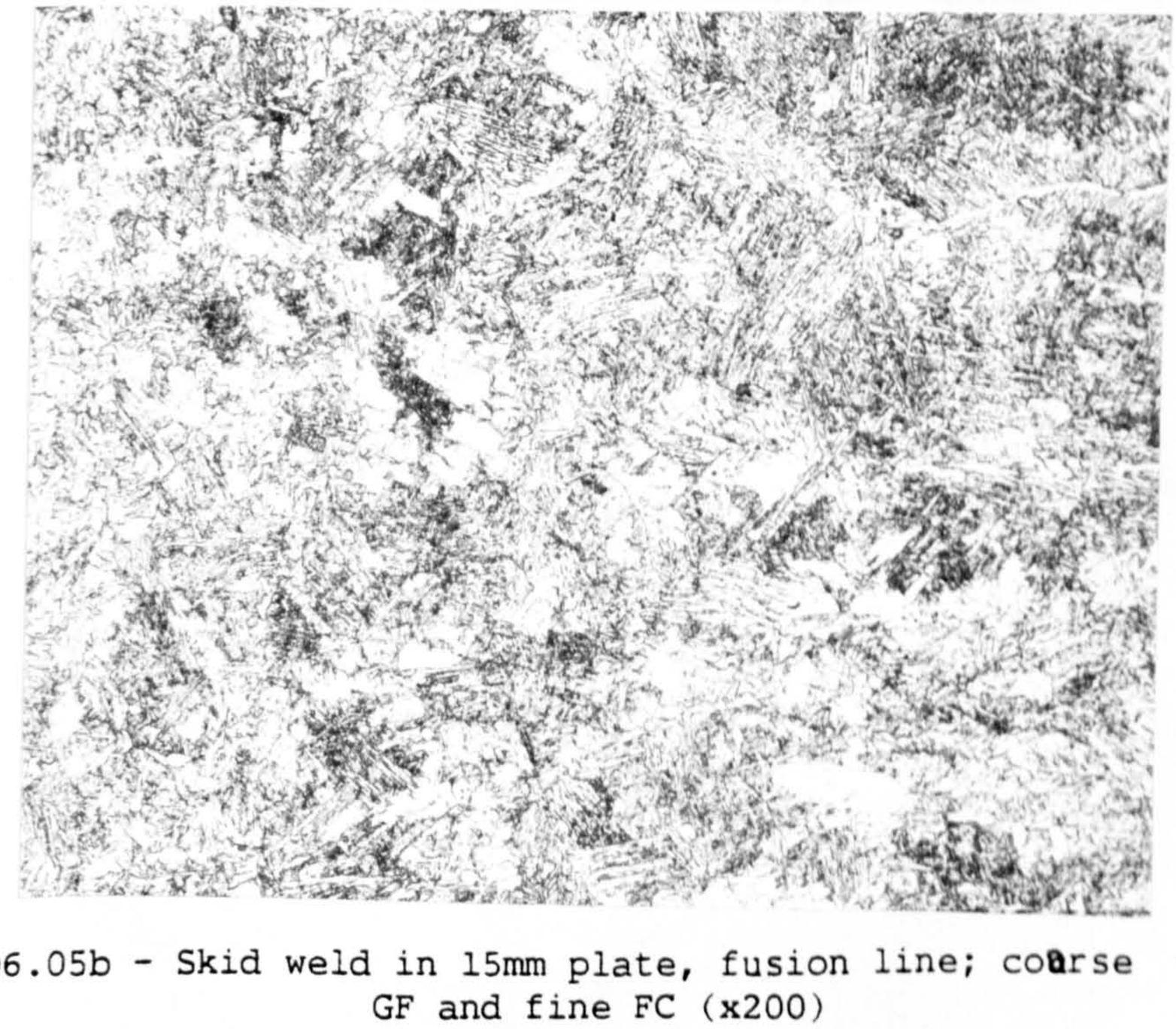

Figure D6.05b - Skid weld in 15mm plate, fusion line; coarse grains of GF and fine FC (x200)

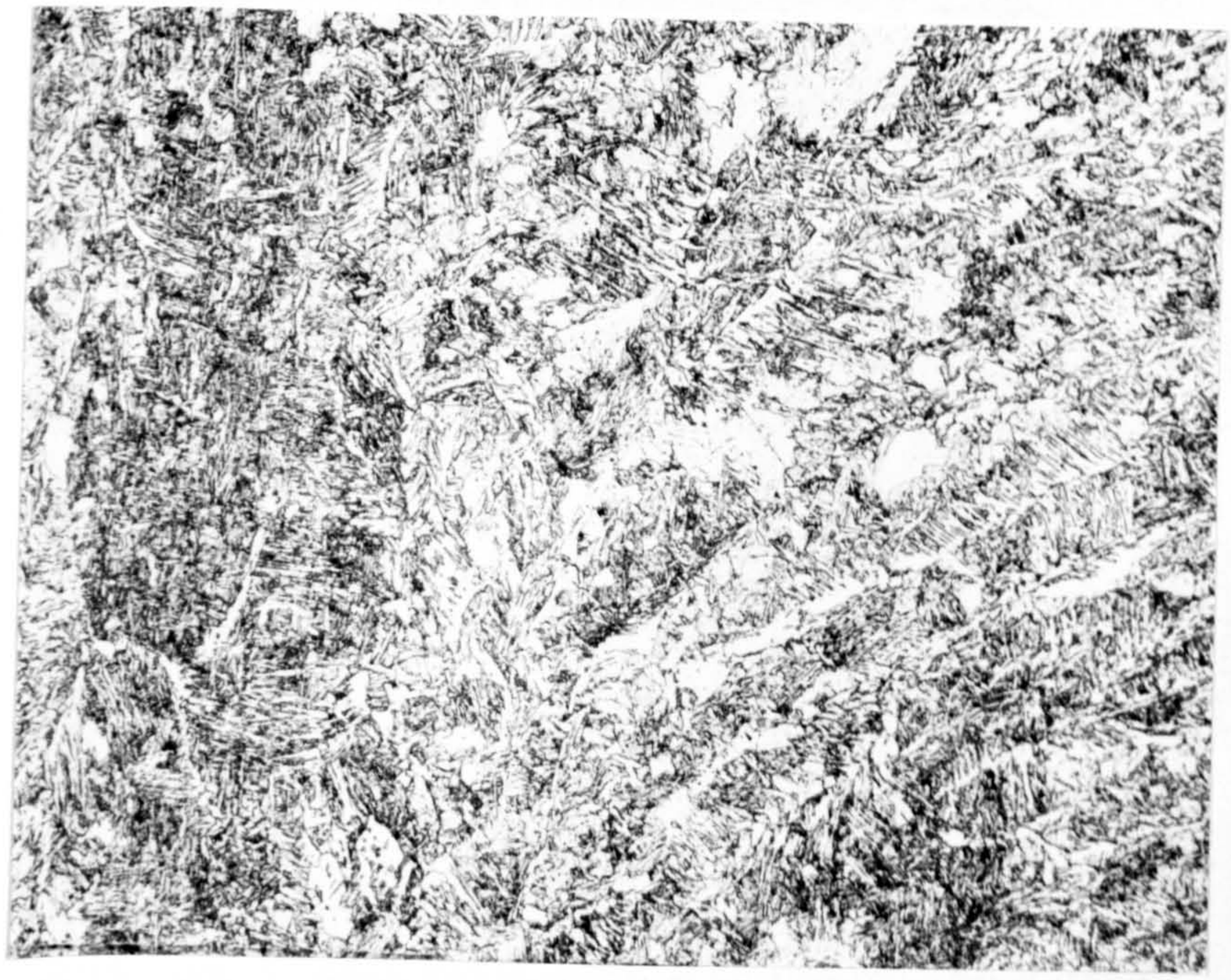

Figure D6.05c - Skid weld in 15mm plate, central weld; GF and AC (x200)

Appendix E

APPENDICES ASSOCIATED WITH CHAPTER 7

E-1 CALCULATION OF PERMISSIBLE TIMES OF EXPOSURE TO A 20KW LASER BEAM

Assuming a 20kW laser power with exposure levels restricted to

Class 1 as defined by BS4083:Pt1 and from BS4083:Pt2 Section 29
Measurement of laser radiation levels for classification purposes

(assuming an 80mm aperture):-- Measurement of laser radiation levels

Limiting energy value = 8×10^{-5} J

Laser power = 2×10^{4} J.sec-1

.. response time limit < 4.0×10^{-9} seconds

==========

From BS4803:Pt 2 section 30 - Classification of laser product classes

assuming a 1mm aperture:

Limiting radiant exposure = 100 $J.m^{-2}$

Aperture area = $0.52 \times \pi \times 10^{-6}$ m2

Laser power = 2×10^{4} $J.sec^{-1}$

.. response time limit < 3.9×10^{-9} seconds

==========

E-2 COMPARATIVE CONSUMABLE COSTS FOR CONVENTIONAL AND LASER WELDING

Plate thk. (mm)	Weld'g speed (mm/s)	Heat input (kJ/m)	Numb'r of ele'de	Weight dep'it (kg/m)	Power cost (£/m)	Elec'de cost (£/m)	Cons'le cost (£/m)
10	0.5	2352	2.3	0.114	0.026	0.09	0.116
12	0.3	3920	3.2	0.163	0.044	0.13	0.134
16	0.2	6240	5.3	0.285	0.069	0.23	0.299

Table E7.01a - Consumable costs for MMA gravity welding of fillet welds (Horizontal/Vertical), rutile rods, 140% recovery.

Plate thk. (mm)	Weld'g speed (mm/s)	Heat input (kJ/m)	Wire cons'd (kg/m)	Flux cons'd (kg/m)	Power cost (£/m)	W'e&F'x cost (£/m)	Cons'le cost (£/m)
9.5	1.22	3202	0.329	0.313	0.04	0.45	0.49
12.7	0.81	4815	0.479	0.461	0.05	0.66	0.72
15.9	0.51	7647	0.789	0.774	0.08	1.09	1.17

Table E7.01b - Consumable costs for single sided submerged arc butt welding (2 electrodes, copper backing)

Plate thk. (mm)	Weld'g speed (m/mi)	Heat input (kJ/m)	Wire cons'd (kg/m)	Shroud gas (l/m)	Power cost (£/m)	Wire cost (£/m)	Shroud cost (£/m)	Cons'le cost (£/m)
6	0.15	1439	0.22	133.3	0.016	0.165	0.03	0.211
8	0.09	2324	0.356	222.2	0.026	0.267	0.05	0.343
10	0.08	3918	0.568	250.0	0.044	0.426	0.06	0.530
15	0.05	8602	1.158	400.0	0.096	0.869	0.01	0.970

Table E7.01c - Consumable costs for MIG(CO2) butt welding (Downhand, unbacked).

Plate thk. (mm)	Weld'g speed (mm/s)	Heat input (kJ/m)	Wire cons'm (kg/m)	Shroud gas (l/m)	Power cost (£/m)	Wire cost (£/m)	Shroud cost (£/m)	Cons'le cost (£/m)
3	1.5	375	0.02	14.0	0.004	0.015	0.003	0.022
6	0.9	630	0.05	22.0	0.007	0.037	0.006	0.050
8	0.5	1139	0.08	40.0	0.013	0.06	0.010	0.083
10	0.3	1890	0.12	67.0	0.021	0.09	0.016	0.127
12	0.2	3545	0.17	100.0	0.039	0.13	0.025	0.194
15	0.1	6882	0.30	200.0	0.078	0.23	0.050	0.358

Table E7.01d - Consumable costs for MIG(CO2) fillet welding (horizontal (Horizontal/Vertical position).

Plate thk. (mm)	Weld'g speed (m/mi)	Heat input (kJ/m)	Wire cons'd (kg/m)	Shroud gas (l/m)	Wire cost (£/m)	Shroud cost (£/m)	Cons. & operation 25% (£/m)	50% (£/m)	75% (£/m)	cost 100% (£/m)
3	1.8	300	0.01	19.4	0.007	0.068	0.60	0.30	0.20	0.15
6	1.1	491	0.01	31.8	0.007	0.111	1.00	0.50	0.33	0.25
8	0.8	675	0.01	43.8	0.007	0.153	1.36	0.68	0.45	0.34
10	0.6	900	0.01	58.3	0.007	0.204	1.80	0.90	0.60	0.45
12	0.5	1080	0.01	70.0	0.007	0.245	2.16	1.08	0.72	0.54
15	0.4	1350	0.01	87.5	0.007	0.306	2.68	1.34	0.89	0.67

Table E7.01e - Consumable costs for laser skid welding, laser maximum power rating of 10kW, shrouding using helium.

E-3 ASSUMPTION USED FOR THE ECONOMIC EVALUATION

Details	Assumed value
1. Labour rates:	
Basic labour rate	£4.03 per manhour
Overhead recovery rate	143%
Fully recovered manhour rate	£9.80 per manhour
2. Gas costs	
Helium	£3.50 per 1000 L
Nitrogen	£0.55 per 1000 L
Carbon dioxide	£0.25 per 1000 L
Laser generation gas consumption (10kW) Total of 600 1/hour comprising 60% He; 25% N; 10% CO2; 5% O-N	
Overall cost	£2.29 per 1000 L
Overall cost/hour	£1.37 per hour
Shielding gas consumption rates	
Laser (Helium)	351/minute
MIG (CO2)	201/minute
3. Electricity costs	
Electricity cost (NEEB)	£00.04/kW.hour
4. Weld metal consumable costs:	
Solid welding wire	£0.75/kg
MMA rods	£0.81/kg
SAW wire	£0.70/kg
SAW flux	£0.70/kg
5. Processing efficiencies	
MMA arcing time as a % of process time	20%
MIG arcing time (manual) as % process time	25%
MIG arcing time (automated) for non-continuous welding	50%
Laser generation "wall plug" efficiency (ie cost of 9kW power = £7.2/hour)	5%
6. Conventional fillet size as ratio of plate thichness	50%
7. Working year: Consists 48 weeks, 5days per week, 8hours per day : total	1920 hours

E-4 COMMERCIAL LASER PRICES

Laser manufacture	Ref. name	Cont. laser output power (kW)	Beam mode	Beam gen. type	Beam output method	Price of unit (k£)	Price per Watt output (£)
Ferranti plc	CL10	10	MULTI	TF	AW	575	58
"	CL5	5	MULTI	TF	SW	300	60
"	FAFL	5	TEM01	FAF	SW	200	40
"	"	7	MULTI	FAF	SW	200	29
United Technologies Research Centre	TM 41-15	15	MULTI	TF	AW	672	43
	TM 31-9	9	MULTI	TF	AW	596	63
Toshiba	10	10	MULTI/ TEM01	TF	SW	440	44
	5	5	MULTI/ TEM01	TF	SW	236	47

Key:
- Multi - Multimode
- AW - Aerodynamic window
- SW - Solid window
- TF - Transverse flow
- FAF - Fast axial flow

Table E7.03 - Available prices of some commercial lasers of greater than 5kW noting respective generator configurations.

E-5 NET PRESENT VALUE CALCULATIONS FOR EXAMPLE SKID WELDING WORKSTATIONS

Yr	Remarks	Pre-Tax Cash Flow £	Tax Inflow (Outflow) £	Net Cash Flow £	P. W. Factor (15%)	Present Worth £	Cumul. P.W. £
0	Extra cost of line	(1980000)	0	(1980000)	1.0	(1980000)	(1980000)
1	Savings	513030					
	Tax on C.A.		173250	686280	0.87	596765	(1383235)
2	Savings	513030					
	Tax on C.A.		129938				
	Tax on sav'gs		(179560)	463407	0.756	350402	(1032833)
3	Savings	513030					
	Tax on C.A.		97453				
	Tax on sav'gs		(179560)	430923	0.658	283339	(749494)
4	Savings	513030					
	Savings		73090				
	Tax on sav'gs		(179560)	406559	0.572	232452	(517042)
5	Savings	513030					
	Tax on C.A.		54817				
	Tax on sav'gs		(179560)	388287	0.497	193047	(323995)
6	Savings	513030					
	Tax on C.A.		41113				
	Tax on sav'gs		(179560)	374583	0.432	161943	(162053)
7	Savings	513030					
	Tax on C.A.		30835				
	Tax on sav'gs		(179560)	364304	0.376	136955	(25097)
8	Savings	513030					
	Tax on C.A.		23126				
	Tax sav'gs		(179560)	356594	0.327	116572	91475
9	Savings	513030					
	Tax on C.A.		17345				
	Tax on sav'gs		(179560)	350814	0.284	99723	191198
10	Savings	513030					
	Tax on C.A		13008				
	Tax on sav'gs		(179560)	346478	0.247	85644	276842
11	Tax on C.A.		19756				
	Tax on sav'gs		(179560)	(169804)	0.215	(36498)	240343
	Total net cash flow			2018426			

Table E7.04 - Net present value calculations for the additional cost of a laser based matrix line, assuming 5 manhr/t savings.

Yr	Remarks	Pre-Tax Cash Flow £	Tax Inflow (Outflow) £	Net Cash Flow £	P. W. Factor (15%)	Present Worth £	Cumul. P.W. £
0	Extra cost of line	(859000)	0	(859000)	1.0	(859000)	(859000)
1	Savings	193795					
	Tax on C.A.		75162	268957	0.87	233876	(625124)
2	Savings	193795					
	Tax on C.A.		56372				
	Tax on sav'gs		(67828)	182339	0.756	137874	(487250)
3	Savings	193795					
	Tax on C.A.		42279				
	Tax on sav'gs		(67828)	168246	0.658	110624	(376625)
4	Savings	193795					
	Tax on C.A.		31709				
	Tax on sav'gs		(67828)	157676	0.572	90152	(286474)
5	Savings	193795					
	Tax on C.A.		23782				
	Tax on sav'gs		(67828)	149749	0.497	74452	(212022)
6	Savings	193795					
	Tax on C.A.		17836				
	Tax on sav'gs		(67828)	143803	0.432	62170	(149852)
7	Savings	193795					
	Tax on C.A.		13377				
	Tax on sav'gs		(67828)	139344	0.376	52385	(97468)
8	Savings	193795					
	Tax on C.A.		10033				
	Tax on sav'gs		(67828)	135999	0.327	44459	(53009)
9	Savings	193795					
	Tax on C.A.		7525				
	Tax on sav'gs		(67828)	133491	0.284	37947	(15062)
10	Savings	193795					
	Tax on C.A.		5644				
	Tax on sav'gs		(67828)	131610	0.247	32532	17470
11	Tax on C.A.		4233				
	Tax on sav'gs		(67828)	(63596)	0.215	13669	3800
	Total net cash flow			688619			

Table E7.05 - Net present value calculations for the additional cost of a laser based minor assemly line, assuming 7 manhr/t savings.